FRIEDRICH-SCHILLER-
UNIVERSITÄT
JENA

Structural investigations of Salicaceae-derived salicylates and their metabolic transformation in the lepidopteran herbivore *Cerura vinula*

Dissertation

(kumulativ)

Zur Erlangung des akademischen Grades doctor rerum naturalium

(Dr. rer. nat.)

vorgelegt dem Rat der Chemisch-Geowissenschaftlichen Fakultät der Friedrich-Schiller-Universität Jena

von *Dipl. Chem. Felix Feistel*

geboren am *26.06.1989* in *Stollberg, Erzgebirge*

Reviewers:

1. Prof. Dr. Georg Pohnert	Chair in Instrumental Analytics/Bioorganic Analytics, Institute for Inorganic and Analytical Chemistry, Friedrich-Schiller-University, Jena
2. PD Dr. Bernd Schneider	Research group Biosynthesis/NMR, Max-Planck-Institute for Chemical Ecology, Jena

Date of Public defense: July 4th, 2018

Table of Contents

List of Abbreviations

6-HCH	6-hydroxy-2-cyclohexenone
ADH	alcohol dehydrogenase
ALDH	aldehyde dehydrogenase
BA	benzoic acid
BAld	benzaldehyde
CD	circular dichroism
COEs	carboxylesterases
CYPs	cytochrome P450 monooxygenases
DIMBOA	2,4-dihydroxy-7-methoxy-1,4-benzoxazin-3-one
d.w.	dry weight; based on dry weight
e.g.	(lat.) *exempli gratia*, "for example"
GC	gas chromatography
GSTs	glutathione S-transferases
HCC	1-hydroxy-6-oxocyclohex-2-en-1-carboxylic acid
HCH	1-hydroxy-6-oxocyclohex-2-en-1-oyl
HCN	hydrogen cyanide
HRMS	high resolution mass spectrometry
HDMBOA	2-hydroxy-4,7-dimethoxy-1,4-benzoxazin-3-one
i.e.	(lat.) *id est*, "that is to say"
IR	infrared spectroscopy
MS	mass spectrometry
NMR	nuclear magnetic resonance
NOESY	nuclear Overhauser effect spectroscopy
PAL	phenylalanine ammonia lyase
PIs	protease inhibitors
PPOs	polyphenol oxidases
ROESY	rotating frame Overhauser effect spectroscopy
sp.	species
UDP	uridine diphosphate
UGTs	UDP-glycosyltransferases

List of Figures

1. Introduction

1.1 Chemical Ecology: Motivation

> *"Ours is a world of sights and sounds. We live by our eyes and ears and tend generally to be oblivious to the chemical happenings in our surrounds. Such happenings are ubiquitous. All organisms engender chemical signals, and all, in their respective ways, respond to the chemical emission of others. The result is a vast communicative interplay, fundamental to the fabric of life. Organisms use chemicals to lure their mates, associate with symbionts, deter enemies, and fend off pathogens. Chemical ecology is the discipline that is opening our "eyes" to these interactions"* THOMAS EISNER AND JERROLD MEINWALD (EISNER AND MEINWALD, 1995)

Chemical ecology is the product of a partnership between virtually any fields of chemical and biological sciences (Eisner, 2003). These include the fields of analytical and synthetic chemistry, genetics, ecology, neurobiology, evolution, molecular biology as well as bioinformatics (Meinwald and Eisner, 2008). Generally speaking, chemical ecology refers to chemically mediated interactions between organisms and their biotic as well as abiotic environment (Hartmann, 2008). The range of interactions (e.g. nutrition, reproduction and defense) is a result of pure self-preservation and relies completely on signaling molecules. The production and characterization of these signaling molecules, the mechanisms of their emission and transmission, their detection in recipient organisms along with the transduction of these signals within the recipient's nervous system and the behavioral or developmental response they evoke, all interest the chemical ecologist (Meinwald and Eisner, 2008).

Nature is an extremely complex system. So far 1.2 to 1.9 million eukaryotic species have been named with approximately half of these being insects (Hamilton et al., 2010; Mora et al., 2011). However, most recent estimates put global biodiversity at roughly 8.7 million eukaryotic taxa including approximately 2.2 million marine, 7.8 million animal, 298,000 plant species and 611,000 fungi (Mora et al., 2011).

1. Introduction

Even though scientists would like to understand every process underlying chemical ecological interactions in our world, it is impossible to explore all signaling pathways, defense mechanisms, biosynthetic processes (e.g. metabolism, catabolism) etc., within and between those organisms. Although eukaryotic cells share the same primary metabolism, the differences in their secondary metabolites are striking (Croteau et al., 2000). These organic compounds, sometimes also referred to as specialized metabolites (Croteau et al., 2000), are not directly involved in the growth, development and reproduction of an organism (Pichersky and Gang, 2000). Hence, their absence is *per se* not lethal, unlike the absence of primary metabolites (Croteau et al., 2000). But individual secondary metabolites support the survivability of organisms, shape their survival strategies and thus are the driving force behind chemical interactions.

In order to most efficiently study these interactions, chemical ecologists rely on established model organisms. It is expected that discoveries achieved using these extensively studied model systems will be transferable to other organisms and will thus provide a foundation for understanding, enabling the conception of scientific predictions (Fields and Johnston, 2005). The list of established model organisms is still small, including famous "traditional" species like the bacterium *Escherichia coli* (Blount, 2015), the fruit fly *Drosophila melanogaster* (Markow, 2015), baker's yeast *Saccharomyces cerevisiae* (Liti, 2015) and *Arabidopsis thaliana* (Krämer, 2015), the mustard plant (Fields and Johnston, 2005). All share similar characteristics qualifying them as suitable model systems for scientific laboratory investigations. These properties include fast reproduction cycles and thus short generation times, few requirements for their habitats, small condensed genomes as well as simple morphology (Alfred and Baldwin, 2015). In a nutshell: Model organisms must be as "uncomplicated" as possible. Nonetheless, in addition, they must also be able to generate experimental populations under laboratory conditions, allowing reliable replicates to be obtained. However, in nature species must adapt to selection pressures imposed by their environment such as limited resources, predators and competitors. But due to their short life cycles classical model organisms may be avoiding rather than confronting these environmental influences, and thus they may not accurately reflect an ecological

system. Since awareness of this conflict has grown over recent decades, scientists have focused on non-traditional model organisms. Poplar trees are a good example of such a species because their characteristics (growth size, longevity, complexity) differ from those of their predecessors (Fields and Johnston, 2005; Goldstein and King, 2016).

Because of their rapid growth as well as the moderate size of their genomes (~485 to 550 Mbp) (Bradshaw and Stettler, 1993; Tuskan et al., 2006), they fit the requirements for traditional model organisms. Additionally, their extreme tolerance for poor soil quality as well as for crowded conditions makes them useful trees to cultivate for laboratory experiments (Marmiroli et al., 2011). Even more important, however, is the long lifespan that characterizes these trees, in contrast to short-lived classic organisms. Since poplars may live for centuries (e.g. *Populus nigra* can reach 300 years of age)(Weisgerber, 1999), they remain in fixed locations that are subject to constantly changing abiotic and biotic stresses. To understand the role of trees in natural and managed ecosystems, it is essential to investigate these systems with representative species. Therefore, poplars have emerged as versatile experimental plant for the research of tree physiology, ecology as well as genetics (Benyó et al., 2016; Bradshaw et al., 2000). Since forests cover 30 % of earth's terrestrial surface (3.8 billion ha), and 25 % of all industrial feedstocks have their origins in forest-based resources, the knowledge gained from model tree systems may be of great value for the protection of forest ecosystems. In addition, such knowledge will also assist the study of trees grown in planation cultures for economic benefit (Bradshaw et al., 2000; Food and Agricultural Organization of the United Nations, 2003).

1.2 Poplar: The forest model organism

Poplar trees belong to the genus *Populus*. Together with its close relatives from the genus *Salix*, they represent the majority of species from the traditional Salicaceae family *"Salicaceae sensu stricto"* (Dickmann and Kuzovkina, 2014). Since evidence was obtained of a common ancestry with the tropical

family of Flacourtiaceae, around 50 members of the genus *Populus* were re-classified as Salicaceae, due to a revision recommended by the Angiosperm Phylogeny Group in 2003 (The Angiosperm Phylogeny Group, 2003).

Figure 1 – *Populus trichocarpa* located in Zuiderpark, 's-Hertogenbosch, NLD (Kaandorp, N. 2011).

The species *Idesia polycarpa*, belonging to the monotypic genus *Idesia*, is one such member (Chase et al., 2002; The Angiosperm Phylogeny Group, 2003). The greatly expanded new Salicaceae family contains 55 genera; once called *"Salicaceae sensu lato,"* nowadays it is simply referred to as the Salicaceae family (Dickmann and Kuzovkina, 2014).

Populus and *Salix* consist of around 400 to 500 species; most belong to *Salix* but at least 30 species are poplars. While *Salix* species appear in variable forms and sizes, from short-lived trees to tree-like shrubs, the genus *Populus* exclusively refers to single-trunked, deciduous trees (Eckenwalder, 1996; Julkunen-Tiito and Virjamo, 2016).

As mentioned above, *Populus* shows high tolerance for a variety of habitats. Furthermore, members of this genus are amongst the fastest growing trees on earth, with some species reaching 40 m within just 20 years (Bradshaw et al., 2000; Weisgerber, 1999). They are able to rapidly invade disturbed sites and thus have managed to adapt to many geographical regions of our planet. Poplar species are found between extreme cold zones and warmer latitudes of the northern hemisphere including Europe, Asia, and North America as well as a few regions in tropical Africa (Bradshaw et al., 2000).

Traditionally used as windbreaks and shelterbelts between agricultural lands, and in erosion control, e.g. next to streams and rivers, poplars are a very attractive economic investment because of the high quality of their wood (e.g. light, elastic, very resilient)(Benyó et al., 2016). Accordingly, they are valuable resources in the forestry and paper industries where high-quality fiber and wood are essential for pulp and paper, veneer, packing materials, lumber and engineered wood products (e.g. matches, snowboards, sauna interiors)(Benyó et al., 2016; Bradshaw et al., 2000; Tuskan et al., 2006).

As the demand for renewable energies rises, poplars are being cultivated more and more in high biomass plantations for the production of fuel, since they reach maturity after 4 to 6 years (Benyó et al., 2016; Tuskan et al., 2006). In addition to their economical usage, poplars are of increasing interest for the regeneration of environmental damage caused by humans. Therefore they are used in forest restoration programs in order to mitigate climate change (Bradshaw et al., 2000; Isebrands and Richardson, 2014). Additionally, poplar trees are also used as bio-indicators for air pollutants like ozone and sulfur dioxide, by scientists monitoring concentrations of leaf constituents (e.g. carotenoids, chlorophyll, starch), the accumulation rates of pollutants (e.g. heavy metals), growth and optical appearance (e.g. leaf damage, premature leaf loss)(Ballach, 1997). Because of their excellent ability to take up water, poplar species may also be useful for removing high levels of salinity from waste water (Marmiroli et al., 2011). Furthermore, their effectiveness for the phytoremediation of environmental toxins from water and soils has recently been shown. Among those toxins were heavy metals and organic pollutants like Cu, Cd, Pb, Ni and Zn (Baycu et al., 2006; Bissonnette et al., 2010) as well as nitrobenzenes (e.g. TNT)(Thompson and Polebitski, 2010; Thompson et al., 1998), atrazine (triazine class herbicide)(Burken and Schnoor, 1997), carbon tetrachloride (Wang et al., 2004) and 1,4-dioxane (Aitchison et al., 2000).

A deeper understanding of the *Populus* model system will likely improve our understanding of forest ecosystems. In the future, this knowledge may allow us to develop more reliable predictions and interpretations of changing processes in forest tree communities caused by variations of environmental parameters, e.g. the increase of atmospheric CO_2 or the occurrence of invading species. Furthermore, such knowledge may also be transferable to other similar ecological systems.

So far, numerous metabolites of *Populus* have been identified (Boeckler et al., 2011), the species' molecular physiology (Bradshaw et al., 2000) has been characterized and the genome of one of its species (*P. trichocarpa*) has been explored (Tuskan et al., 2006).These results may tempt us to call the *Populus* model system "well-studied," but in fact we know far more about *Arabidopsis*. Our knowledge of the biosynthesis networks of poplar trees is limited (Babst et al., 2010), details of the distribution of

defense chemicals within the plant remain unknown, and the ecological interactions of these defenses with different herbivores has yet to be studied. In the next section, we will explore what is known about the defense systems of *Populus*.

1.3 Plant-insect interactions and anti-herbivore defense

1.3.1 Plant secondary metabolites

In this section, a general overview of plant defense chemistry is provided before the defense system of Salicaceae species is presented. In order to survive, plants are forced to cope with competitors from their own or other species; they must defend themselves against herbivores and pathogens; and they have to endure natural catastrophes (droughts, storms, etc.). Although plants lack the ability to move, they have developed strategies to successfully adapt to their circumstances. Many of these strategies, which are based on distinctive chemicals, involve inter- and intraspecies communication, defense against herbivores and the up- and down-regulation of biochemical processes that are involved in all kinds of environmental interactions (Howe and Jander, 2008).

The defense chemicals belong to plant secondary metabolites also referred to as secondary products, natural products or specialized metabolites (Croteau et al., 2000). Unlike primary metabolites (sugars, organic acids, acyl lipids, nucleotides and amino acids), which are found in almost every organism and cell, secondary metabolites are not directly involved in growth and/or reproduction (Croteau et al., 2000). Thus, a pool of secondary metabolites often belongs to – and in some cases, is unique to – a specific plant linage. These defense chemicals, which are composed of more than 200.000 substances (Hartmann, 2007), can be divided roughly into four major groups (Fig. 2)(Croteau et al., 2000; Howe and Jander, 2008). The first group contains nitrogen-containing compounds, including alkaloids, glucosinolates, benzoxazinoids, etc. (Fig. 2A)(Adhikari et al., 2015; Bulduk et al., 2015; Whitney and Mortimore, 1959). The second group, which contains phenolics, comprises

phenylpropanoids, flavonoids and polyketides (Fig. 2B)(Corse et al., 1970; Iwashina, 2000; van der Vijver, 1972). The third class consists of all types of terpenoids such as mono-, di-, tri-, tetra-, sesqui-, polyterpens, etc. (Fig. 2D)(Anderson et al., 1969; de Kraker et al., 2001; Woo et al., 2010). Fatty acid derivatives form the fourth group: oleic or sterculic acids; long-chain aliphatics, such as alkanes and

polyacetylenes; and so-called green leaf volatiles like n-hexanol, (*Z*)-3-hexenal and (*E*)-2-nonenal (Fig. 2C)(Anderson et al., 1969; Drake and Lam, 1974; Razon et al., 2013).

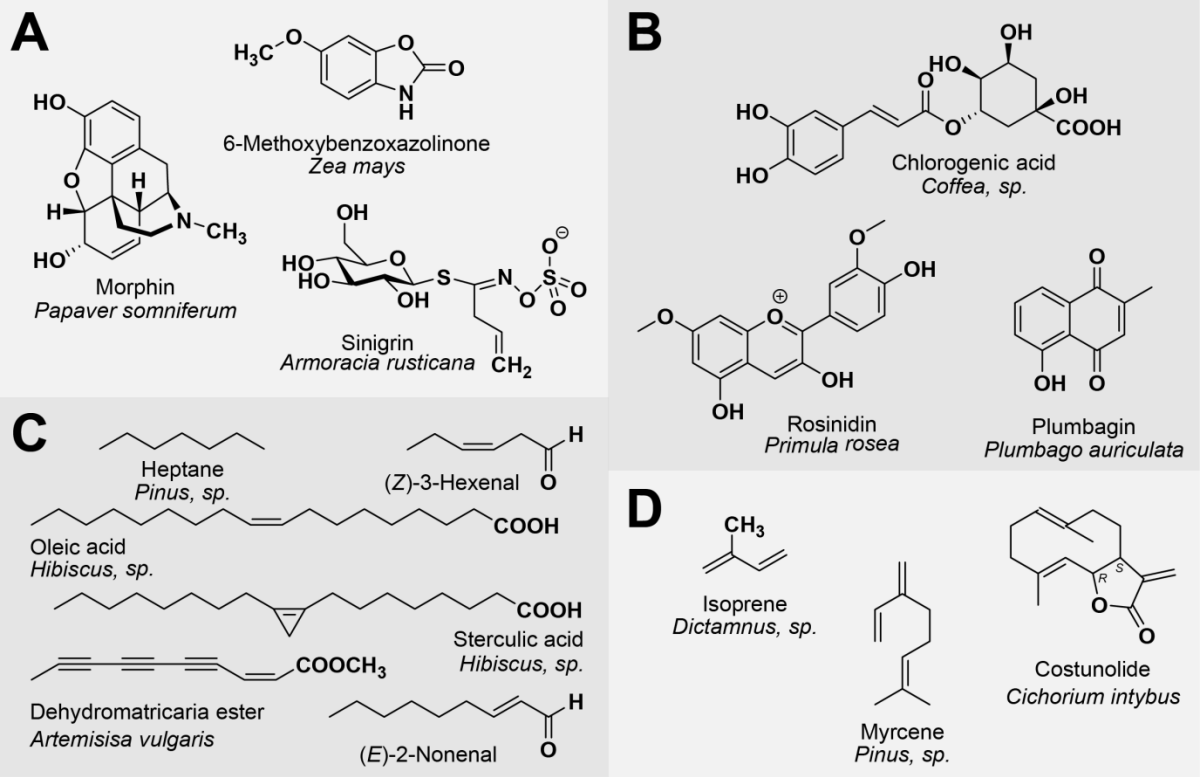

Figure 2 – Various examples of secondary metabolite structures from the four principal substance groups**: (A)** N-containing compounds, **(B)** phenolics, **(C)** fatty acid derivatives and **(D)** terpenoids. The originating species are written in italics but do not necessarily represent the only natural source of the given compound.

1.3.2 Secondary metabolites in plant defense

Plant defense is either direct or indirect. Direct defenses are immediately harmful to the attacker and theoretically possess the potential to harm all types of animals. In contrast, indirect defenses are used mostly against arthropods and consist of a third trophic level, that is, they attract the natural enemies of herbivores. Secondary metabolites involved in direct defense are generally toxic to

herbivores. The chemicals responsible for indirect defense are typically volatile molecules that advertise the presence of herbivores to their natural enemies.

However, a few compounds are immediately toxic to herbivores in their natural form. They are highly selective to specific targets only occurring in herbivores. For example, alkaloids such as morphine, nicotine or caffeine are harmful to herbivores but not plants. Pyrethrins, which occur in several *Chrysanthemum* species, interfere with specific ion channels located in the nervous system of both insects and higher animals (Wolansky and Harrill, 2008). However, because these compounds are not very toxic to mammals, the application of pyrethroids as agricultural and residential pesticides has increased during recent decades (Casida and Quistad, 1998).

In many cases, direct defense compounds are stored as inactive forms and activated only if there is tissue damage. The inactive structures of these substances are called "protoxins" the term "toxicokinetics" refers to the route from their uptake to the site of action. The process, which ultimately leads to the toxic metabolites, is called bioactivation, and usually involves several steps of a reaction cascade (Dekant, 2009). Quite often bioactivation is achieved when enzymes form a binary defense system; such a system comprises two factors, the protoxin and its activating agent. Since protoxins are typically β-glycosides, their bioactivation is initiated by the process known as "glucosidase-catalyzed deglycosylation". The protoxins are typically deposited in storage compartments (e.g. vacuoles) that are separated from their activation agent to prevent an undesired reaction. Hence, minimizing the protoxins' potential for auto-toxicity which is crucial for a plants' ability to protect itself. If plant's tissue is damaged, as happens, e.g., during herbivory, the protoxin and the activating agent come into contact, which leads to the release of a bioactivated toxic metabolite (Bennett and Wallsgrove, 1994; Pentzold et al., 2014).

However, not all bioactivating enzymes are plant-derived. They can also be endogenous to the herbivore. For instance, digestive or detoxification enzymes in the gut of the herbivore have been known to accidently transform a non-toxic precursor into a toxin (Dekant, 2009).

In plants, various examples report herbivore-derived β-glycosidases that are responsible for the toxification of plant-derived protoxins. In the broad bean (*Vicia faba*), the main chemical defense is represented by the alkaloid glycosides vicine and convicine. After being ingested by the bruchid beetle larvae (*Callosobruchus maculatus*), both compounds are activated by endogenous β-glucosidases; the result is the formation of the highly reactive and free-radical-generating aglycons divicine and isouramil (Fig. 3A). Both products were reported to inhibit glucose-6-phosphate dehydrogenases, causing adverse metabolic effects that result in the high mortality rates observed for *C. maculatus* feeding on *V. faba* (Desroches et al., 1995; Desroches et al., 1997).

A well-studied, classical example of defenses that are activated by these two components is the glucosinolate-myrosinase system, also known as the "mustard oil bomb," which can be found in the order Brassicales, including important crops such as cabbage, canola and mustard (Jeschke et al., 2016). Within the plant tissue, glucosinolates are spatially separated from myrosinases (a myrosinase is a β-thioglucosidase located in special myrosin cells)(Pentzold et al., 2014). After the enzymatic cleavage of the glucose moiety from the glucosinolate, an unstable aglycon is formed, which spontaneously rearranges to isothiocyanates, nitriles and thionitriles, amongst others (Fig. 3B). Because of their ability to irreversibly bind to amino and sulfhydryl groups of proteins, isothiocyanates are regarded as the most toxic of the glucosinolate hydrolysis products. The damage caused due to this mechanism may delay insect growth and development or even lead to insect death (Wittstock et al., 2003).

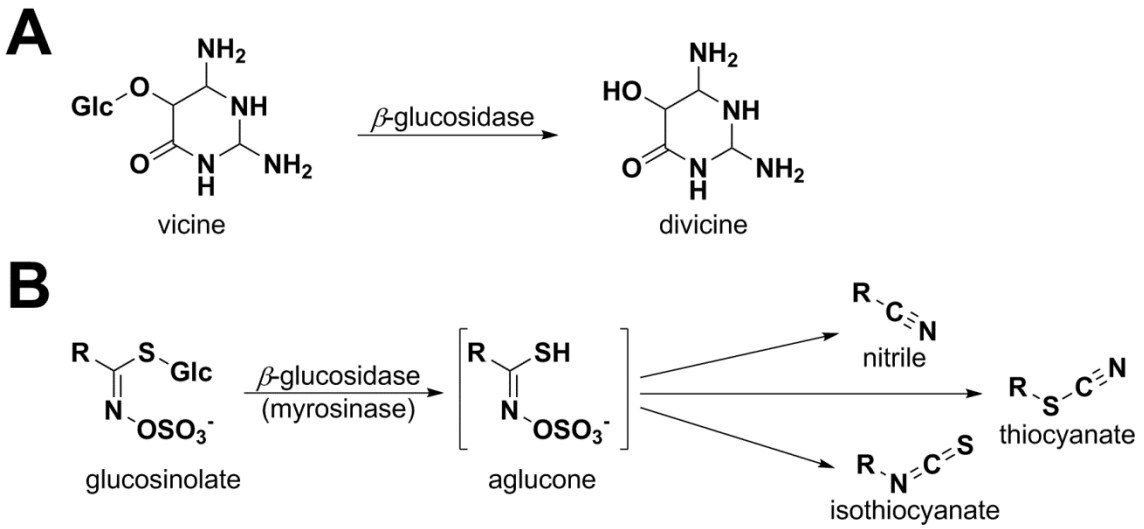

Figure 3 – Bioactivation cascade of vicine by endogenous *β*-glucosidase of *C. maculatus* (**A**) and the glucosinolate-myrosinase ("mustard oil bomb") defense system occurring in Brassicales species (**B**).

Benzoxazinoid glycosides are found in numerous species of the monocot family Poaceae. This includes major crops like maize (*Zea mays*), wheat (*Triticum aestivum*) and rye (*Secale cereal*)(Pentzold et al., 2014). A common benzoxazinoid glucoside in this plant family is 2,4-dihydroxy-7-methoxy-1,4-benzoxazin-3-glucoside (DIMBOA-glucoside), which is typically stored in vacuoles. Its electrophilic aglycon DIMBOA (Fig. 4A) is released after enzymatic hydrolysis by plant-derived *β*-glucosidases and has the potential to modify nucleophilic organic compounds, which may negatively influence insect development. Furthermore, the formation of stable thioether bonds with the thiol function of glutathione has been shown for DIMBOA; these bonds may lead to the irreversible inactivation of enzymes that contain cysteine residues (Dixon et al., 2012). In several aphid species, this effect was demonstrated by a much lower body mass, decreased rates of reproduction and increased rates of mortality (Escobar et al., 1999). Additionally, quick deaths (within three days) were observed for larvae of the domestic silkmoth (*Bombyx mori*; Lepidoptera)(Sasai et al., 2009). Furthermore, 2-hydroxy-4,7-dimethoxy-1,4-benzoxazin-3-one (HDMBOA), another benzoxazinoid glycoside from maize, has been shown to strongly deter two other lepidopteran species, the Egyptian armyworm (*Spodoptera littoralis*) and the fall armyworm (*Spodoptera frugiperda*)(Glauser et al., 2011).

Another large group of direct defense compounds are the cyanogenic glycosides. They are present in more than 2650 plant species distributed among 130 families within ferns, gymnosperms and angiosperms (Pentzold et al., 2014). In plants, the cyanogenic glycosides are stored in vacuoles (Vetter, 2000). The bioactivation of these compounds, also called cyanogenesis, proceeds according to a two-step mechanism (Fig. 4B)(Zagrobelny et al., 2008). After contact with plant β-glucosidases, an unstable α-hydroxynitrile is released, which, at pH-values above 6, spontaneously dissociates into a sugar, a keto compound and hydrogen cyanide (HCN). At low pH-values, the dissociation is enzymatically mediated by an α-hydroxynitrile lyase (Zagrobelny et al., 2008; Zagrobelny et al., 2004). The toxicity of HCN is caused by its affinity to cytochrome *c* oxidase, a key enzyme in the mitochondrial respiratory pathway (Blom et al., 2011). The inhibition of this enzyme leads to cell and tissue death within a short period of time and is therefore a strong deterrent to non-adapted herbivores (Moller, 2010; Pentzold et al., 2014).

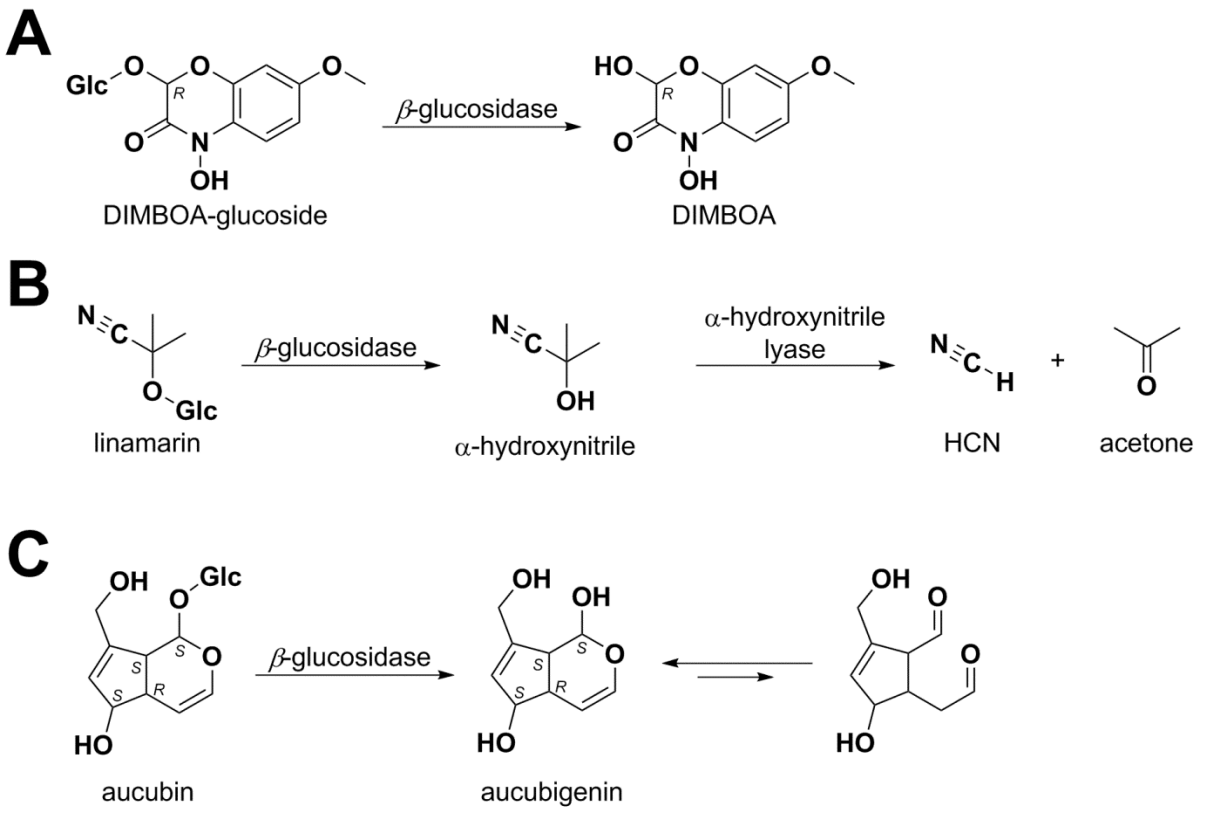

Figure 4 – The bioactivation systems: DIMBOA from *Zea mays* (**A**), the cyanogenesis of linamarin from *Manihot esculenta* (**B**) and Aucubin from *Plantago lanceolata* (**C**).

Iridoid glycosides are an example of defense compounds from the large group of terpene derivatives. Widespread in the Asterids, they occur in more than 50 plant families. They all have a monoterpene skeleton, comprising a cyclopentane ring that is connected to an oxygenated heterocyclohexene with an β-D-glucose attached at the C-1 carbon. Iridoid glycosides have a high structural diversity due to various aglycon decorations with epoxy and/or sugar groups (Dobler et al., 2011). They taste bitter to humans and have been shown to be unpalatable to other mammals, e.g. bats (Bowers, 1991). An even stronger response was reported for vertebrate predators like birds: to them, iridoid glycosides appeared highly distasteful (Bowers and Farley, 1990). In invertebrates, however, their toxic effect is induced mainly by enzymatic hydrolysis via plant-derived or endogenous β-glucosidases in the insect gut (Fig. 4C)(Pankoke et al., 2012). After deglycosylation, the pyran ring resonates with a dialdehyde structure, and the resulting compound tends to react with free amino groups and form the imine connections that are typically observed for Schiff' bases (Davini et al., 1986; Kim et al., 2000). Hence, iridoid aglycons denature amino acids, proteins and nucleic acids, causing unspecific cross-linking. Protein inhibition and a decrease in nutritive value of dietary proteins result, and, as a consequence, insect herbivores are deterred (Kim et al., 2000).

Phenolic salicinoids offer an example of successful defense compounds. They are found only in Salicaceae (including *Populus*) species, where they serve as direct defense compounds against insect herbivory (Boeckler et al., 2011; Chedgy et al., 2015). During the course of this dissertation the salicinoids and their biochemistry was studied. Therefore, the following paragraph will focus in more detail on the direct plant defense system of *Populus* species employing salicinoid compounds.

1.4 Herbivore defense in Populus *species*

1.4.1 Salicinoids: Phenolic glycosides from Salicaceae species

All members of the Salicaceae family (including *Populus*) defend themselves against leaf-chewing herbivores (referred to from here on out as herbivores) using phenolic glycosides (Boeckler et al., 2011; Palo, 1984). In poplars, two groups of these compounds, condensed tannins and salicinoids, are found. These compounds may account for up to 30 % of leaf dry weight. Due to their ability to precipitate dietary proteins, condensed tannins are considered to be broad-spectrum defense compounds, while salicinoids most likely play the major role against insect herbivory in *Populus* (Barbehenn et al., 2009; Hemming and Lindroth, 1995; Hemming and Lindroth, 2000; Lindroth, 1991).

Salicinoids are phenolic glycosides and belong to phenolic secondary metabolites (section 1.3.1). The Salicin molecule – a salicylic alcohol β-D-glucopyranoside – resembles the core structure of these compounds and is the name giving compound for the entire substance class (Fig. 5).

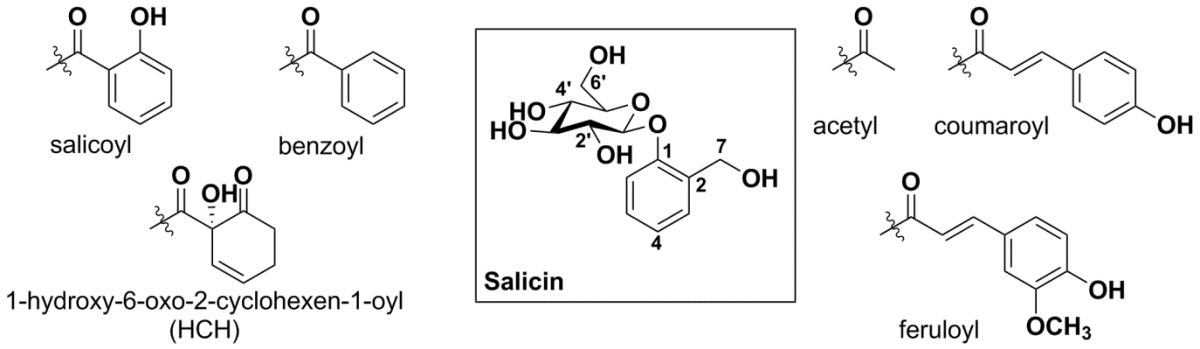

Figure 5 – Salicin is the core structure and eponymous compound for phenolic glycosides from Salicaceae species. The diversity of salicinoid derivatives results from the esterification of different organic acid moieties, which is shown next to the salicin structure.

Populus species (as well as other Salicaceae plants) produce almost 30 different salicinoids (Boeckler et al., 2011; Feistel et al., 2017). They are formed through ester connections between at least one of the salicin's hydroxyle functions and an organic acid moiety (Fig. 5). For salicinoid derivatives from *Populus* species, esterification typically appears at the primary alcohol function located at position

7 in the aglycon (salicylic alcohol) and at positions 2' and 6' in the glucose moiety. Possible substituents are salicylic, benzoic, acetic, cinnamic, caffeic, coumaric and ferulic acid. Additionally, a 1-hydroxy-6-oxocyclohex-2-en-1-carboxylic acid (HCC) is observed as a characteristic subunit for some of the most abundant salicinoids in *Populus* species (Boeckler et al., 2011). Some examples of important salicinoids are given in Figure 6. Out of this group, tremulacin and salicortin are the most well-known examples of 1-hydroxy-6-oxocyclohex-2-en-1-oyl (HCH)-bearing salicinoid derivatives, with up to 4 % of leaf dry mass from clonal aspen (*Populus temuloides*)(Donaldson et al., 2006).

Given that salicortin has a massive natural abundance and was observed in most of the *Populus* and *Salix* species investigated so far, it is unsurprisingly the most representative compound within the salicinoid substance class. Therefore, salicortin is one of the compounds investigated most intensively in this thesis.

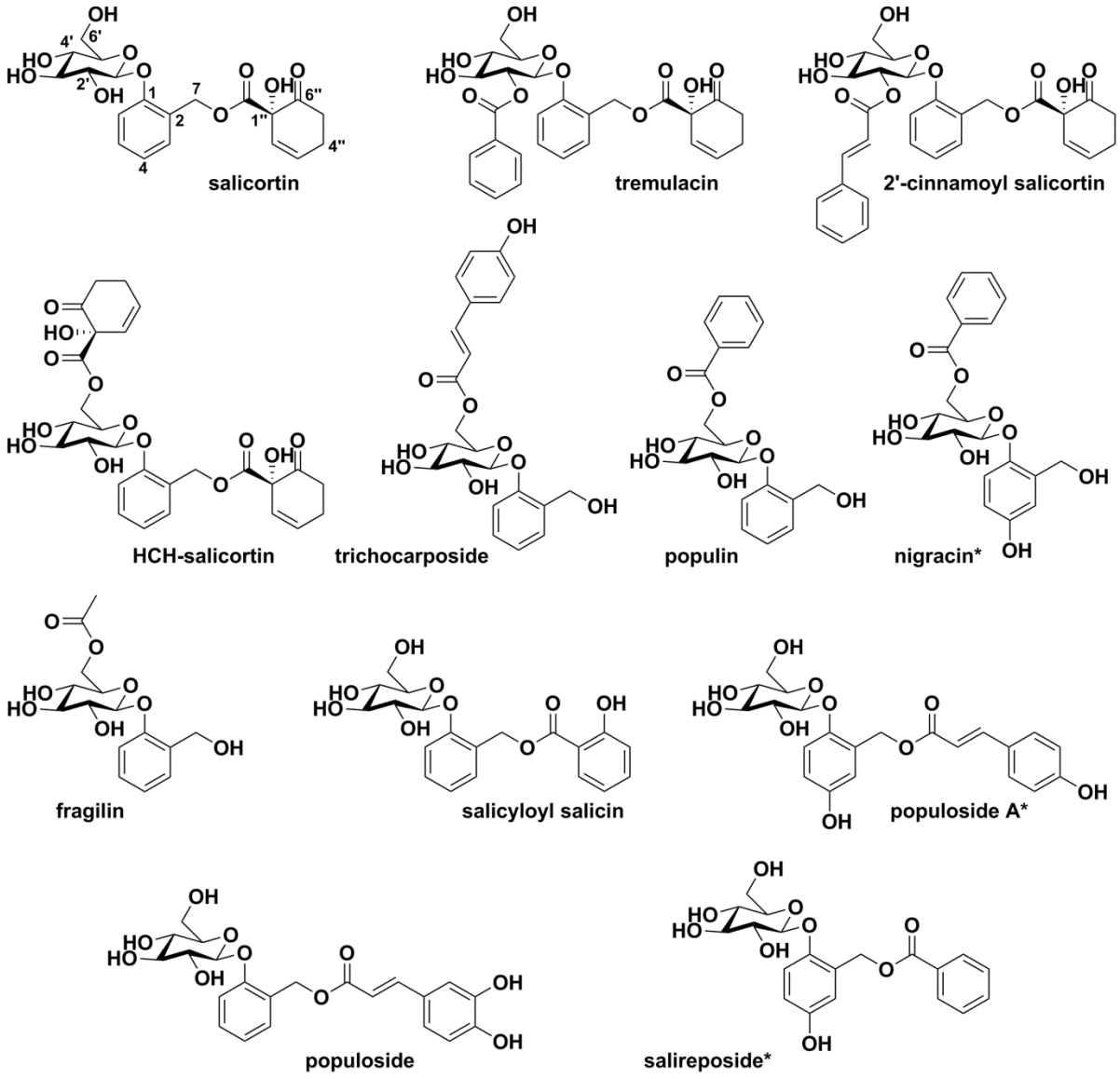

Figure 6 – Various salicyl- and gentisyl(*)-based salicinoids found in Salicaceae species.

However, in addition to the classical salicyl alcohol-based phenolic glycosides, there are also a few examples derived from a gentisyl alcohol (4-hydroxysalicyl alcohol) core molecule. These are listed as salicinoids: nigracin, populoside and salireposide, which are present in Figure 6, are just a few examples. Furthermore, non-salicinoid phenolics are also found in Salicaceae species. They can be glycosylated derivatives of salicylic acid (e.g. trichorcarpin), glycosylated phenylpropanoids (e.g. vimalin), phenylethanoids (e.g. salidroside) and benzenoids (Fig. 7). Even though these compounds are

not mentioned again in this thesis, they may also be specific defense-related compounds from the Salicaceae family (Boeckler et al., 2011).

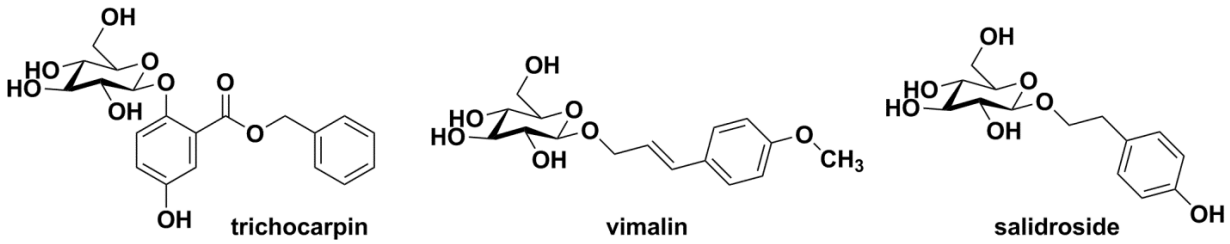

Figure 7 – Examples of non-salicinoid phenolic defense compounds from Salicaceae species.

Despite the longstanding interest in salicinoid compounds, detailed knowledge of their biosynthesis is not available. The inhibition of phenylalanine ammonia lyase enzyme (PAL) by the addition of 2-aminoindan-2-phosphonic acid drastically reduced the accumulation of salicinoids in shoots of *Salix pentandra,* confirming the biosynthetic origin of the plant phenylpropanoid pathway (Ruuhola and Julkunen-Tiitto, 2003; Vogt, 2010). Furthermore, various investigations using *in vivo* feeding experiments of isotope-labeled precursors (^{13}C, ^{14}C and ^{2}H) administered to poplar leaves led to the outline of a basic framework that proposes cinnamic acid as the potential precursor for the salicyl moiety (Fig. 8)(Zenk, 1967). The HCH moiety was also shown to likely derive from phenylpropanoids (Babst et al., 2010). Additionally, benzoates – especially benzoyl-CoA and benzaldehyde (BAld) – probably participate in the formation process (Babst et al., 2010). However, there are still conflicting hypotheses about the proposed biosynthesis pathway. Babst et al. (2010) showed that saligenin is converted into salicin but not into salicortin. Contrary to the assumption that salicin is a precursor for salicortin, these findings suggested no direct conversion (Babst et al., 2010; Ruuhola and Julkunen-Tiitto, 2003). This result is in accordance with a recent study which identified two specific acyl transferases (PtSABT an PtBEBT) within *Populus trichocarpa* and suggested an alternative biosynthetic route to salicortin and other more complex salicinoids (Chedgy et al., 2015). *In vitro* functional characterization showed these particular enzymes played an important role in the production

of salicyl benzoate (by PtSABT) or benzyl benzoate (by PtBEBT). Both are hypothetical precursors for salicyloyl- and benzyl-HCH, each of which then ultimately leads to salicortin (Fig. 8) (Chedgy et al., 2015).

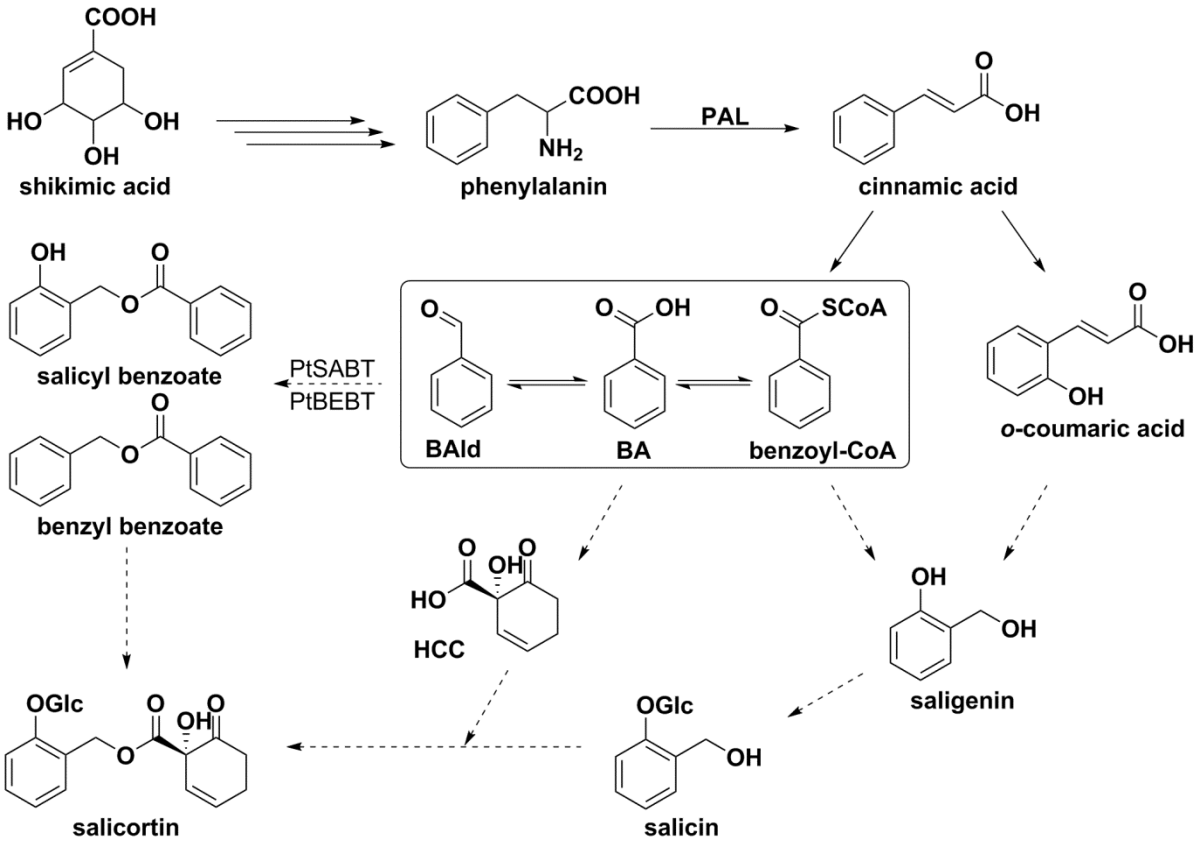

Figure 8 – Simplified biosynthetic pathway to salicortin. Conversions illustrated with dashed lines are still hypothetical.

Salicortin is not accessible by chemical synthesis. Although a stereoselective method yielding 1-hydroxy-6-oxocyclohex-2-en-1-carboxylic acid methyl ester (Me-HCC) has been established, further attempts to couple salicin did not succeed (Nagasawa et al., 2010; Richardson et al., 2007; Yamakoshi et al., 2010). Since chemical synthesis is not an option and other salicortin sources are not commercially available, we had to rely on the *in vivo* production and isolation of the desired compounds.

1.4.2 Salicinoid activity: The two-component direct defense system of Populus

Numerous studies have demonstrated the strong effect of salicinoids on the performance of both generalist and specialist insect herbivores. However, their mode of action against these herbivores is not yet fully understood; the effects of these compounds are described as "feeding deterring" and "fitness reducing" (Boeckler et al., 2011; Clausen et al., 1989; Julkunen-Tiitto et al., 1994; Ruuhola et al., 2001). Feeding (Kolehmainen et al., 1995) as well as oviposition stimulating effects (Roininen et al., 1999) have been observed for a few specialists; performance measurements from these insects after they ingested salicinoid-rich diets also increased (Matsuki and MacLean, 1994; Rank et al., 1998). The larva of the poplar leaf beetle (*Chrysomela populi*) is one of these examples. It incorporates salicin from the leaves of its *Populus* food plants (Pasteels et al., 1983). After being transported into the reservoir of the larva's defensive glands, salicin is metabolized into salicylaldehyde, a compound which deters predators (Michalski et al., 2008; Strauss et al., 2013). Interestingly, salicinoids also show anti-adipogenic (Lee et al., 2013) and anti-oxidative activity (Si et al., 2011; Si et al., 2009), inhibition of melanin biosynthesis (Baek et al., 2006) and inhibition of nitric oxide production (Kim et al., 2007).

Possible metabolic reactions have been postulated on the basis of *in vitro* approaches (Boeckler et al., 2011; Julkunen-Tiitto and Meier, 1992). For example, these are two ways that enzymatic breakdown may occur in salicortin. The glycosidic bond between glucose moiety and saligenin is a potential target for β-glucosidases, and the ester bond between the salicin core structure and the HCH moiety is susceptible to hydrolytic decomposition by an esterase. Generally, the toxicity of salicinoids results from the occurrence of saligenin and HCH which emerge through these reactions. The toxicity of saligenin was proven in tests with insects (Pentzold et al., 2014; Ruuhola et al., 2001). It has been hypothesized that, like salicylic acid, saligenin acts as an uncoupler of cell respiration (Boeckler et al., 2016; Terada, 1990).

After hydrolysis, the HCH is oxidized, releasing toxic pyrocatechol and *o*-quinone species (Clausen et al., 1990). This pathway was confirmed by *in vitro* experiments conducted under different pH values

and using enzymes (Julkunen-Tiitto and Meier, 1992; Pearl and Darling, 1970). Salicortin was shown to degrade into salicin and 6-hydroxy-2-cyclohexenone (6-HCH) in alkaline environments after it had been incubated with fresh leaves in buffer solution (Ruuhola et al., 2003). Furthermore, the possibility of a spontaneous reaction of 6-HCH to pyrocatechol was described (Ruuhola et al., 2003). As mentioned, the formation of *o*-quinones from pyrocatechol is likely due to further oxidation (Appel, 1993; Haruta et al., 2001; Pourcel et al., 2007). The toxicity of *o*-quinones, however, is deduced from their electrophilic nature (Clausen et al., 1989). Accordingly, their ability to bind to nucleophilic amino and thiol groups enables *o*-quinones to attack and alkylate a variety of biologically important molecules, including amino acids, peptides and proteins, by cross-linking and polymerization (Haruta et al., 2001; Ruuhola et al., 2001). These reactions are commonly known to cause food browning after of long term storage or browning of injured plant tissue and extracts (Friedman, 1996; Joslyn and Ponting, 1951). In insects, this reaction will inhibit digestion due to the precipitation of dietary proteins or digestive enzymes within the herbivore gut, which in turn impairs the nutritive value of the ingested plant material. Furthermore, covalent binding with epidermal proteins may not only disturb the digestive process but also harm the gut lumen and hence the organism (Appel, 1993; Boeckler et al., 2011). In addition, oxygen radicals, which can form during almost any oxidation of phenolics, are thought to disrupt membrane integrity and metabolism in the gut epithelium (Appel, 1993; Smith, 1985).

How exactly does the bioactivation of salicinoids take place in living herbivores? For lepidopteran herbivores, salicinoid bioactivation is thought to be driven by deglucosylation that is mediated by β-glucosidase; the process yields an unstable aglycon (Fig. 9). This HCH-saligenin aglycon is then directly hydrolyzed by an esterase or degraded spontaneously in the insect's alkaline mid gut environment (Appel and Martin, 1990). Since, foliar β-glucosidases and esterases from trembling aspen (*Populus tremuloides*) have been shown to degrade salicinoids *in vitro,* both enzymes are expected to be plant derived (Ruuhola et al., 2003). However, the involvement of an endogenous β-glucosidase cannot be excluded (Boeckler et al., 2011; Pentzold et al., 2014). Furthermore, high levels of polyphenol oxidases (PPOs) were shown in the leaves of trembling aspen. PPOs likely catalyze the

oxidation of *o*-diphenols (i.e. pyrocatechol) to *o*-quinone and thus also drive the salicinoid bioactivation in the insect gut (Barbehenn et al., 2010; Haruta et al., 2001).

Interestingly, in some generalist herbivore larvae like those of the gypsy moth (*Lymantria dispar*) (Lindroth and Hemming, 1990) and the eastern tiger swallowtail (*Papilio glaucus canadensis*) (Lindroth, 1988), the *β*-glucosidase activity has reportedly decreased after salicinoid ingestion. If abundance of toxic aglycon in the gut of the swallowtail and gypsy moth is reduced, as it is suspected, the insects may better tolerate the salicinoids (Lindroth, 1988). However, this tolerance is limited. *L. dispar* larvae stayed unaffected by a dietary salicinoid concentration up to 3 % (Lindroth and Bloomer, 1991; Lindroth and Hemming, 1990). This finding implies that, by avoiding the production of saligenin, the insect improves its survivability (Ruuhola et al., 2001). However, since ester hydrolysis of more complex salicinoids (salicortin, tremulacin) may release toxic *o*-quinone, these compounds may still harm the insect larvae and reduce their performance (Fig. 9).

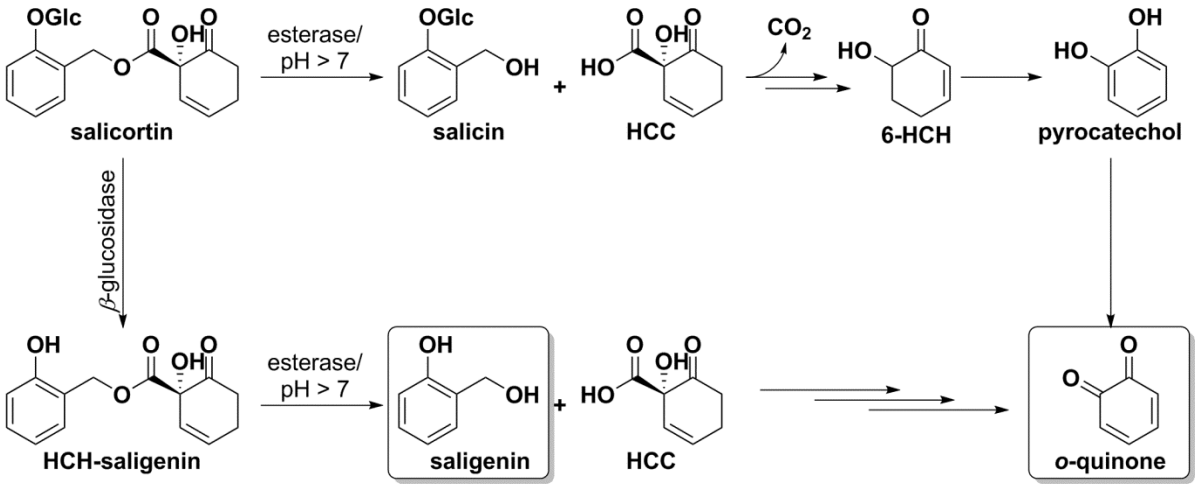

Figure 9 – Suggested bioactivation mechanism of salicortin yielding the toxic species (framed) saligenin and *o*-quinone (Boeckler et al., 2011; Lindroth and Hemming, 1990; Lindroth et al., 1988).

In order to avoid ingesting lethal doses of salicinoid, the insect may try to switch its host plant. This feeding behavior (dietary mixing) is mainly exhibited by generalists that are adapted to low or medium levels of defense compounds (Pentzold et al., 2014). Although selective feeding on plant tissue with

low levels of defense may minimize an insect's uptake of direct plant defense compounds, total avoidance of salicinoids is unrealistic.

1.5 How do herbivores act against chemical direct defense systems?

It is commonly believed that herbivores are compelled to adapt to direct defenses in order to ensure their survival. But considering the enormous diversity of compounds used in direct defense systems (chapter 1.3), a universal adaption is obviously impossible. As a consequence, herbivores have specialized in various ways. Accordingly, they can be roughly divided into two major groups, i.e. specialists and generalists (Ali and Agrawal, 2012; Pentzold et al., 2014). The specialists are highly adapted and thus immune to certain direct defense compounds; some may be even able to exploit these substances for their own purpose (see *C. populi*). The diets of specialists are restricted to a narrow host range. In contrast, generalists, which have the low degree of specialization, may only moderately adapt to a greater diversity of defense compounds but are able to choose from a large group of different hosts (Li et al., 2004).

Little is known about the mechanisms evolved by insects to overcome chemical defenses. But according to our recent knowledge, these mechanisms can be summarized as resistance by avoidance, sequestration and detoxification (Després et al., 2007).

1.5.1 Resistance by avoidance

Avoidance strategies are useful early in the interaction of herbivores with their host plants and are supposed to prevent protoxic defense compounds from becoming toxins. The innate oviposition behavior of female insects prevents eggs from being laid on unsuitable plants (Fox et al., 2004). Furthermore, insect larvae can also choose to eat plant organs that do not produce toxic compounds or to ingest plants at early developmental stages, when the toxins are present only at low concentrations or are completely absent (Nealis and Nault, 2005).

Another aspect of avoidance can involve the physical manipulation of a plant's chemical defense (Després et al., 2007). A striking example of an insect deactivating a plant's defense before feeding was reported for some lepidopteran larvae of both the monarch butterfly (*Danaus plexippus*)(Helmus and Dussourd, 2005) and the cabbage looper (*Trichoplusia ni*)(Dussourd, 2003). Larvae cut trenches across the leaves of their host plants, which caused the secretory channels to depressurize, thus preventing toxic exudations at the feeding site (Becerra, 2003). Furthermore, the oral secretions of several lepidopteran species have been said to suppress or reduce host-plant defenses. A glucose oxidase in the saliva of the tobacco earworm (*Helicoverpa zea*), for instance, decreases the level of nicotine induced in the leaves of cultivated tobacco (*Nicotiana tabacum*)(Musser et al., 2002). In *Aspen* (Salicaceae family), gall-inducing sawflies are able to decrease the phenolic content inside the gall where larvae develops (Nyman and Julkunen-Tiitto, 2000).

In order to increase their tolerance of chemical plant defenses, some insects have adapted their gut lumen chemistry. See, for example, the previously mentioned example of *L. dispar* larvae, which are capable of decreasing the expression of their own β-glucosidase after salicinoid ingestion (Lindroth, 1991; Lindroth and Hemming, 1990). Furthermore, it has been assumed that the alkaline gut environment of lepidopteran larvae blocks the activity of plant-derived β-glucosidases and thus also suppresses the bioactivation of glycosidic protoxins (Fitzgerald, 2008).

1.5.2 Resistance by sequestration

Sequestration addresses the ability of herbivores to assimilate plant-synthesized compounds (secondary metabolites) by ingestion and storage in their body tissue with the aim of avoiding toxicity and possibly enhancing their own defense against enemies. Sometimes, sequestered compounds may be involved in an insect's reproductive behavior (Opitz and Muller, 2009; Strauss et al., 2013).

Although sequestration demands a high degree of specialization, it is widespread amongst herbivores, appearing predominantly in butterflies and moths (Lepidoptera) as well as in beetles (Coleoptera). Moreover, sequestration frequently occurs in species of the order Heteroptera (bugs),

Hymenoptera (wasps, sawflies, bees and ants), Orthoptera (grasshoppers, locusts and crickets) and Sternorrhyncha (aphids, whiteflies and scale insects)(Opitz and Muller, 2009). The processes involved in sequestration are very complex and often compound-specific. However, the variety of compounds that can be sequestered is huge in comparison to the limited range of host plants available for sequestering species. Known sequestered compounds include various aromatic, nitrogen-containing substances such as alkaloids, cyanogenic glycosides, glucosinolates and other sulphur-containing metabolites as well as isoprenoids such as cardiac glycosides, cucurbitacins and iridoid glycosides (Opitz and Muller, 2009).

The viceroy butterfly (*Limenitis archippus*) is an example from the order lepidopteran that is able to sequester salicin, salicortin and tremulacin from its larval host plant, the coastal plain willow (*Salix coroliniana*, Salicaceae)(Prudic et al., 2007). A striking and well-studied example of an herbivore sequestering salicinoid compounds is the larva of the leaf beetle (*C. populi*), which, to deter predators, assimilates salicin from its Salicaceae host plants in order to generate salicylaldehyde (Pasteels et al., 1990; Pasteels et al., 1983). During the transport process – through the hemolymphs to the specialized defensive glands – salicin stays glucosylated and thus is kept inactive. The transformation ultimately happens within the reservoirs of these glands. In response to harassment or attack, larvae are able to eject the volatile salicylaldehyde from the reservoir (Michalski et al., 2008; Strauss et al., 2013).

Sequestering herbivores do not have to rely on the *de novo* production of defense compounds. Therefore, the ability of insects to sequester and use plant glucosides is an energy-saving strategy. However, this putative advantage demands a high level of host chemistry adaptation, which ultimately results in a dependent relationship between the insect and its host, and narrows the range of suitable host plants (Termonia et al., 2001).

1.5.3 Resistance by detoxification

Detoxification is the capability of an herbivore to transform foreign chemical substances (xenobiotics) into harmless compounds and ultimately store or remove them from the organism.

Depending on a chemical's structure, detoxification can involve up to three or even four steps. During phase I (functionalization), a functional group is introduced into the molecule. In phase II (conjugation), the new functional group is conjugated to a hydrophilic, endogenous building block, e.g. glucuronic acid, glutathione or sulfate; this building block increases water solubility, which supports the transport and ultimately the elimination (phase III) of the compound. Some authors propose an additional "phase 0", which refers to the active, transporter-mediated assimilation of xenobiotics right after the ingestion of the compound (Grant, 1991; Marquardt et al., 2013).

Enzymes involved in detoxification reactions are members of three main super-families: the cytochrome P450 monooxygenases (CYPs), the glutathione S-transferases (GSTs) and the carboxylesterases (COEs)(Després et al., 2007). Evidence has accumulated that the enzyme family of UDP-glycosyltransferases (UGTs) is also involved in insect resistance to plant chemicals (Ahmad and Hopkins, 1992; Mackenzie et al., 2005). The CYPs and COEs take part in phase I, while the GSTs as well as UGTs are involved in phase II detoxification reactions (Marquardt et al., 2013). It is assumed that amongst these enzyme families, the CYPs play a key role in most plant-insect interactions (Després et al., 2007; Heckel, 2014).

Although detoxification processes are well studied and understood in humans, our knowledge about detoxification in herbivores is very limited. In general, detoxification is connected with the induced overexpression of dedicated enzymes but is also limited to their activity, quantity or concentration. Furthermore, a modification in the enzymatic target of the toxic compound may decrease or even inhibit enzyme activity in insects. Hence, substrate availability and suitability also influence the success of detoxification. However, though endosymbionts may take over certain reaction steps, detoxification processes consume many of a plant's resources (Hansen and Moran, 2014; Shen and Dowd, 1991).

1.6 Scope of thesis

Numerous studies have shown that the properties that make a salicinoid compound both toxic and a feeding deterrent explain the deleterious effects an herbivore may experience after feeding on *Populus*

(and *Salix*) plants. Given that each representative of the Salicaceae possesses a variety of salicinoids, it is not surprising that members of this family have a powerful defense arsenal against unprepared enemies. Therefore, the various examples of herbivorous insects which are able to feed, grow, propagate and even compete on their Salicaceae host plants is striking. However, despite decades of research on salicinoids and their influence on plant-insect interactions, especially for Lepidoptera, our knowledge remains limited. Because these herbivores present such a potent danger for tree development, the research conducted during this thesis contributes importantly to investigations of the salicinoid phytochemicals and presents new knowledge that may help explain the influence of the compounds identified and isolated in the interaction of lepidopteran herbivores with plants. Furthermore, in a broader context, the present work supports the establishment of the *Populus* model organism as universal for forest ecosystems.

The isolation of salicortin was first described in 1964 by Thieme. He was not only able to obtain massive amounts of this compound within the bark (7.4 % d.w.) and the leaves (4 % d.w.) of the *Salix purpurea* (purple willow, Salicaceae), but he also described its occurrence in various other *Salix* and *Populus* species (Thieme, 1964). The presence of salicortin in nearly all Salicaceae investigated so far, along with the huge amounts of it found in the different parts of these trees, quickly revealed that salicortin is one of the Salicaceae's major secondary metabolites (Boeckler et al., 2011). Half a century later and despite the various studies conducted on salicortin, its absolute configuration was still unknown until now. Indeed, the chiral center at C-1 of the HCH function could theoretically lead to two isomers (*R* and *S*) that are discriminated by the orientation of the connected α-hydroxyl. Although not influencing physical parameters, the stereochemistry of a chiral compound such as salicortin influences its suitability as a substrate for enzymes. Therefore, the compound's stereochemistry can be said to influence its role in plant-insect interactions. The problem of elucidating the absolute configuration of salicortin and its derivatives, was successfully addressed by comparing chiroptical properties of salicortin (its derivatives tremulacin and HCH-salicortin) with those of (–)-idescarpin, a related compound with known stereochemistry.

The problem of how insects detoxify salicortin followed naturally. Salicortin is a representative for salicinoids from *Populus* and *Salix* species. Despite numerous investigations into the effects of salicinoids on herbivores their mode of actions as well as mechanisms for their sequestration in highly adapted insects are still obscure. Furthermore, little is known about insect detoxification strategies. Recently an approach addressing this topic for the classic generalist herbivore *L. dispar* (Lepidoptera) was published (Boeckler et al., 2016). So far, data about detoxification strategies from highly adapted lepidopteran herbivores have not been available. In order to approach this problem, we investigated fecal extracts of the poplar specialist herbivore *C. vinula* to identify putative down-stream products of salicortin transformation. To further investigate the salicortin metabolism *in vivo,* we produced [U-^{13}C]salicortin, using small poplar plants (*P. trichocarpa x deltoides Beaupré*) as bioreactors, by growing them in a specially designed automated growth enclosure with an artificial $^{13}CO_2$ atmosphere. We fed the poplar specialist *C. vinula* on *P. nigra* supplemented with [U-^{13}C]salicortin, and collected samples of feces and hemolymphs. To investigate the content of salicortin-related down-stream products in the samples, high resolution mass spectrometry (HRMS) and nuclear magnetic resonance (NMR) experiments were conducted. This approach led to the exciting insight into a novel counter-strategy against salicortin deployed by the poplar specialist *C. vinula*.

In the third part of the thesis, the most abundant phenolic compounds in the leaves of *I. polycarpa* were investigated. Previous phytochemical studies focused on the abundance of these compounds in the fruits and seeds of *I. polycarpa* (Baek et al., 2006; Chou et al., 1997; Dai et al., 2014; Guo et al., 2012). *Idesia* is so far the only plant known to contain Me-HCH, idesin and (–)-idescarpin, as well as their dimers (idesolide and (–)-idescarparide)(Kim et al., 2005; Kim et al., 2014; Moritake et al., 1987; Wang et al., 2013). The structural similarities between salicortin and (–)-idescarpin as well as salicin and idesin were striking. We hypothesized that (–)-idescarpin is the major secondary metabolite within *Idesia* and expected to find idesin derivatives decorated with different organic acids in the leaves of *I. polycarpa*. Since salicinoids are known defense compounds against leaf-chewing herbivores, with feeding-deterrent and toxic activity, it seemed likely we would find similar bioactivity for *Idesia*

phenolic compounds in the leaves. During the experimental phase, solid phase extraction (SPE) supported the isolation of the most abundant phenolics from *I. polycarpa* leaves, and their structure elucidation by means of HRMS and NMR techniques was performed. In order to test the ecological activity of the identified compounds in plant-insect interactions, fresh *Idesia* leaves were fed to known *Populus* generalist (*L. dispar*) and specialist (*C. vinula*) herbivores.

2. Overview of the Mansucripts

2.1 Mansucript I: *The Absolute Configuration of Salicortin, HCH-Salicortin and Tremulacin from* Populus trichocarpa × deltoides *Beaupré*

Felix Feistel[1*], Christian Paetz[1*], Sybille Lorenz[2] and Bernd Schneider[1]

1 Max Planck Institute for Chemical Ecology, Research Group Nuclear Magnetic Resonance and Biosynthesis, Hans-Knöll-Straße 8, Jena 07745, Germany
2 Max Planck Institute for Chemical Ecology, Research Group Mass Spectrometry and Proteomics, Hans-Knöll-Straße 8, Jena 07745, Germany

* These authors contributed equally to this work.

Published, *Molecules* March 2015, Vol. 20, No. 5, Pp 5566-5573

Abstract:

The absolute configuration of salicortin, HCH-salicortin and tremulacin, isolated from leaves of *Populus trichocarpa* × *deltoides* Beaupré, was determined by comparing spectroscopic data of these compounds with those of idescarpin, isolated from leaves of *Idesia polycarpa*. All compounds were characterized by nuclear magnetic resonance spectroscopy, high-resolution mass spectrometry, and circular dichroism spectroscopy. It was found that the hydroxy cyclohexenonoyl (HCH) moiety in all compounds is (*S*)-configured. In addition, it was shown that leaves of *Idesia polycarpa* contain high amounts of (–)-idescarpin (1.1 %, based on dry weight).

2.2 Manuscript II: *Acylated quinic acids are the main salicortin metabolites in the specialist herbivore* Cerura vinula

Felix Feistel[1*], Christian Paetz[1*], Riya C. Menezes[2], Daniel Veit[3], Bernd Schneider[1]

1 Max Planck Institute for Chemical Ecology, Research Group Nuclear Magnetic Resonance and Biosynthesis, Hans-Knöll-Straße 8, Jena 07745, Germany
2 Max Planck Institute for Chemical Ecology, Research Group Mass Spectrometry and Proteomics, Hans-Knöll-Straße 8, Jena 07745, Germany
3 Max Planck Institute for Chemical Ecology, Institute Workshop, Hans-Knöll-Straße 8, Jena 07745, Germany
4 Max Planck Institute for Chemical Ecology, Department of Biochemistry, Hans-Knöll-Straße 8, Jena 07745, Germany

[*] These authors contributed equally to this work.

Submitted, *Journal of Chemical Ecology* December 2017

Abstract:

Salicortin is a phenolic glucoside produced in Salicaceae as a chemical defense against herbivory. The specialist lepidopteran herbivorous larvae of *Cerura vinula* are able to overcome this defense. We examined the main frass constituents of *C. vinula* fed on *Populus nigra* leaves, and identified eleven quinic acid derivatives with benzoate and/or salicylate substitution. We asked whether the compounds are a result of salicortin breakdown and sought answers by carrying out feeding experiments with highly ^{13}C enriched salicortin. Using HRMS and NMR analyses, we were able to confirm that salicortin metabolism in *C. vinula* proceeds through deglucosylation and ester hydrolysis, after which saligenin is oxidatively transformed into salicylic acid and, eventually, conjugated to quinic acid.

2.3 Mansucript III: Idesia polycarpa *(Salicaceae) leaf constituents and their toxic effect on* Cerura vinula *and* Lymantria dispar *(Lepidoptera) larvae*

Felix Feistel[1*], Christian Paetz[1*], Sybille Lorenz[2], Franziska Beran[3], Grit Kunert[4] and Bernd Schneider[1]

1 Max Planck Institute for Chemical Ecology, Research Group Nuclear Magnetic Resonance and Biosynthesis, Hans-Knöll-Straße 8, Jena 07745, Germany
2 Max Planck Institute for Chemical Ecology, Research Group Mass Spectrometry and Proteomics, Hans-Knöll-Straße 8, Jena 07745, Germany
3 Max Planck Institute for Chemical Ecology, Research Group Sequestration and Detoxification in Insects, Hans-Knöll-Straße 8, Jena 07745, Germany
4 Max Planck Institute for Chemical Ecology, Department of Biochemistry, Hans-Knöll-Straße 8, Jena 07745, Germany

* These authors contributed equally to this work.

Published, *Phytochemistry* November 2017, Vol. 143, Pp 170-179

Abstract:

Phytochemical investigation of *Idesia polycarpa* (Salicaceae) resulted in the structure elucidation of nine previously undescribed phenolic natural products along with six known compounds. The compounds are structurally related to salicinoids that are known defense compounds from *Salix* and *Populus* species. The *I. polycarpa* diet was toxic, as shown in feeding experiments with larvae of *Lymantria dispar*, an herbivorous broadleaf tree generalist insect, and with larvae of *Cerura vinula*, a specialist adapted to poplar. The survival rate and mass gain of larvae was significantly lower when they fed on *I. polycarpa* leaves, compared to larvae fed on *Populus nigra* leaves. Potential reasons for the poor performance of both herbivores on *I. polycarpa* leaves are discussed.

3. Manuscripts

The Absolute Configuration of Salicortin, HCH-Salicortin and Tremulacin from *Populus trichocarpa* × *deltoides* Beaupré

Felix Feistel, Christian Paetz, Sybille Lorenz and Bernd Schneider

Molecules **2015**, Vol. 20, No. 5, Pp 5566-5573
doi:10.3390/molecules20045566

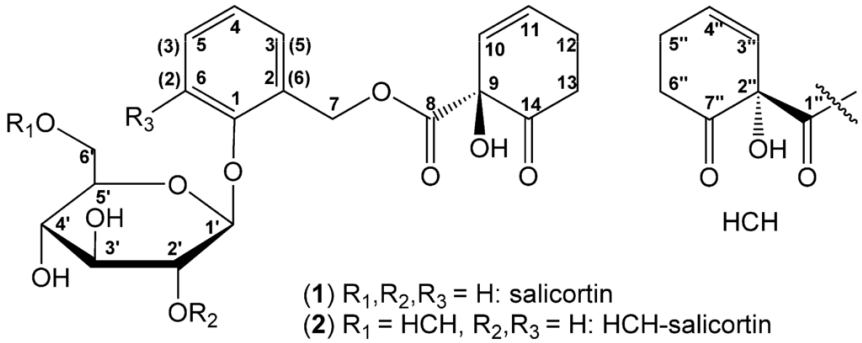

Molecules **2015**, *20*, 5566-5573; doi:10.3390/molecules20045566

OPEN ACCESS

molecules

ISSN 1420-3049

www.mdpi.com/journal/molecules

Article

The Absolute Configuration of Salicortin, HCH-Salicortin and Tremulacin from *Populus trichocarpa* × *deltoides* Beaupré

Felix Feistel †, Christian Paetz †, Sybille Lorenz and Bernd Schneider *

Max Planck Institute for Chemical Ecology, Hans-Knöll-Straße 8, Jena 07745, Germany;
E-Mails: ffeistel@ice.mpg.de (F.F.); cpaetz@ice.mpg.de (C.P.); lorenz@ice.mpg.de (S.L.)

† These authors contributed equally to this work.

* Author to whom correspondence should be addressed; E-Mail: schneider@ice.mpg.de;
Tel.: +49-364-157-1600; Fax: +49-364-157-1601.

Academic Editor: Derek J. McPhee

Received: 3 February 2015 / Accepted: 26 March 2015 / Published: 30 March 2015

Abstract: The absolute configuration of salicortin, HCH-salicortin and tremulacin, isolated from leaves of *Populus trichocarpa* × *deltoides* Beaupré, was determined by comparing spectroscopic data of these compounds with those of idescarpin, isolated from leaves of *Idesia polycarpa*. All compounds were characterized by nuclear magnetic resonance spectroscopy, high-resolution mass spectrometry, and circular dichroism spectroscopy. It was found that the hydroxy cyclohexenonoyl (HCH) moiety in all compounds is (*S*)-configured. In addition, it was shown that leaves of *Idesia polycarpa* contain high amounts of (−)-idescarpin (1.1%, based on dry weight).

Keywords: salicortin; HCH-salicortin; tremulacin; idescarpin; salicinoids; absolute configuration

1. Introduction

The salicinoids salicortin (**1**), HCH-salicortin (**2**) and tremulacin (**3**) (Figure 1) are phenolic secondary metabolites occurring in the Salicaceae family; they serve the plants as defense compounds with feeding deterrent and antifungal properties [1–5]. The mechanism underlying the biological activity is thought to be based on degradation, occurring either enzymatically or at pH > 7, and resulting in the production of saligenin, which is toxic to insects [5]. It has been shown that the hydroxy cyclohexenonoyl (HCH)

moiety is transformed into pyrocatechol, which subsequently interacts with proteins responsible for digestion by leaf-feeding organisms [6]. It has also been reported that salicinoids show anti-adipogenic activity [7–9], melanine biosynthesis inhibition [10], and nitric oxide production [11].

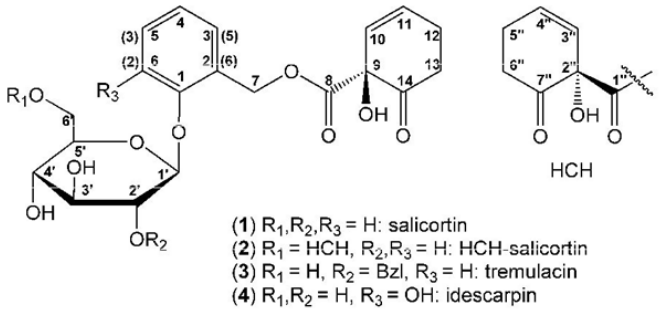

Figure 1. Structures of salicortin (**1**); HCH-salicortin (**2**); tremulacin (**3**) and idescarpin (**4**). Note the different numbering for idescarpin are in parentheses.

Questions remain, however, about salicortin (**1**), which is isolated and was described many years ago [12], its biosynthesis [13], and the absolute configuration of its structure. Recently, the absolute configuration of the structurally very similar salicinoid (−)-idescarpin (**4**) (Figure 1), isolated from fruits of *Idesia polycarpa* [14], was elucidated using single-crystal X-ray diffraction studies. Here, we report on the absolute configuration of salicortin (**1**), HCH-salicortin (**2**) and tremulacin (**3**) isolated from leaves of *Populus trichocarpa* × *deltoides* Beaupré by comparing spectroscopic data from these compounds with those of idescarpin (**4**).

2. Results and Discussion

Salicortin (**1**) was isolated from *Populus trichocarpa* × *deltoides* Beaupré leaves in 0.3% yield. HCH-salicortin (**2**) and tremulacin (**3**) were isolated in yields of 0.1% and 0.2%, respectively. Idescarpin (**4**) was isolated from leaves of *Idesia polycarpa* in a similarly high yield of 1.1% (all yields based on dry leaf weight). The methods described in the experimental section and in the supplementary information were used for separation. The structures of all compounds were confirmed by nuclear magnetic resonance (NMR) spectroscopy (Table 1 and supplementary information) and high-resolution mass spectrometry (HRMS) (see supplementary information). Recorded spectral data were consistent with the structures and in accordance with reported data [14–17]. The signals of neither ^{1}H- nor ^{13}C-NMR spectra show additional splitting or broadening, thus suggesting that all compounds are present as single diastereomers (Figures 2 and 3). The specific optical rotation of salicortin (**1**) was initially reported to be $[\alpha]_D^{20} = -164.2$ (c 1.38, H_2O) [12], but the absolute configuration has not yet been determined. The specific rotation of (−)-idescarpin (**4**) has been reported to be $[\alpha]_D^{25} = -156.6$ (c 1.0; tetrahydrofuran) [14]. For tremulacin (**3**), a specific rotation of $[\alpha]_D^{25} = -134.7$ (c 0.59; MeOH) has been reported [17]. No optical rotation data for **2** have been found in the literature. To determine the absolute configuration, the specific optical rotation and the circular dichroism (CD) spectra of all isolated compounds were measured and compared. The specific optical rotation of isolated salicortin (**1**) was

determined to be $[\alpha]_D^{22} = -118.6$ (c 0.65; H_2O) and $[\alpha]_D^{22} = -123.9$ (c 0.72, MeOH). For (−)-idescarpin (**4**), we determined a specific optical rotation of $[\alpha]_D^{22} = -57.3$ (c 0.73, MeOH). The negative values point to the same configuration at C-9 of **1** and **2**. Due to limited availability of the compounds, the specific optical rotation of compounds **2** and **3** was not determined. However, the CD spectra of all compounds show high similarities (Figure 4 and Supplementary Information). The following molar circular dichroism values Δε have been determined: Salicortin (**1**) Δε= −26.7 mdeg (λ_{max} = 221 nm, c = 1.66 mM); HCH-salicortin (**2**) Δε= −15.5 mdeg (λ_{max} = 213 nm, c = 1.19 mM); tremulacin (**3**) Δε = −9.2 mdeg (λ_{max} = 211 nm, c = 1.44 mM) and Δε = −10.5 mdeg (λ_{max} = 239 nm, c = 1.44 mM); idescarpin (**4**) Δε = −13.4 mdeg (λ_{max} = 224 nm, c = 1.61 mM). We conclude that the configuration at C-9 (and C-2" in HCH-salicortin) in all isolated compounds is identical and thus (*S*)-configured.

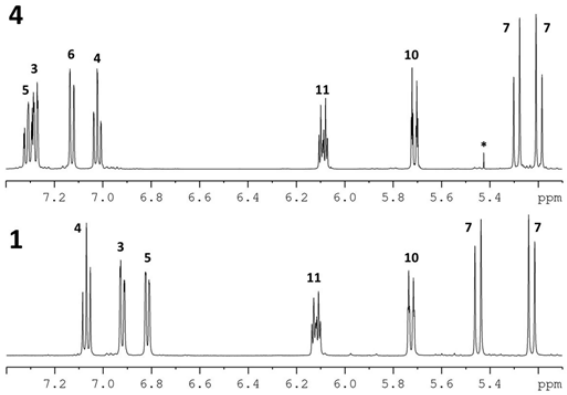

Figure 2. Partial ^{1}H-NMR spectra (500 MHz) of isolated salicortin (**1**) and idescarpin (**4**) in MeCN-d_3 with position numbering according to Figure 1. The signal marked with * represents an unidentified impurity.

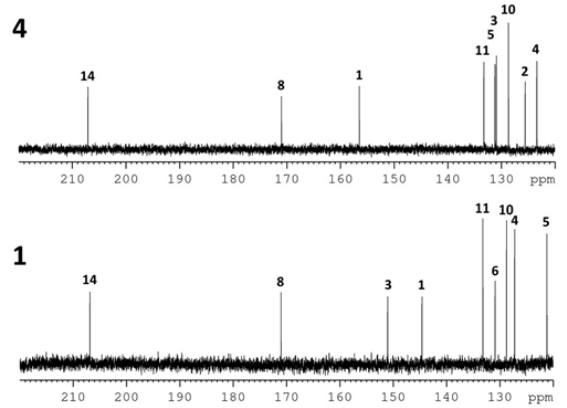

Figure 3. Partial ^{13}C-NMR spectra (125 MHz) of isolated salicortin (**1**) and idescarpin (**4**) in MeCN-d_3 with position numbering according to Figure 1.

Table 1. ^{1}H and ^{13}C-NMR data of salicinoids in MeCN-d_3. Salicortin (**1**) and idescarpin (**4**) and were measured at frequencies of 500 MHz for ^{1}H and 125 MHz for ^{13}C-NMR. HCH-salicortin (**3**) and tremulacin (**2**) were measured at 700 MHz and their ^{13}C-NMR data were obtained from Heteronuclear Single Quantum Coherence (HSQC) and Heteronuclear Multiple Bond Correlation (HMBC) spectra.

Pos.	Salicortin (1)		Tremulacin (2)		HCH-salicortin (3)		Idescarpin (4) [1]	
	δ_H, mult., *J* (Hz)	δ_C	δ_H, mult., *J* (Hz)	δ_C	δ_H, mult., *J* (Hz)	δ_C	δ_H, mult., *J* (Hz)	δ_C
1		156.3		155.8		156.3		144.4
2		125.4		125.6		126.0		150.9
3	7.30, *dd*, 7.5, 1.0	130.7	7.20, *d*, 7.6	130.0	7.35, *d*, 7.5	130.6	6.92, *dd*, 7.6, 1.2	118.3
4	7.05, *ddd*, 7.5, 7.5, 1.0	123.2	7.03, *dd*, 7.6, 7.6	123.6	7.11, *dd*, 7.5, 7.5	123.2	7.07, *dd*, 7.6, 7.6	127.0
5	7.33, *ddd*, 7.5, 7.5, 1.0	131.0	7.31, *dd*, 7.6, 7.6	130.7	7.41, *dd*, 7.5, 7.5	131.0	6.82, *dd*, 7.6, 1.2	121.0
6	7.15, *dd*, 7.5, 1.0	116.1	7.17, *d*, 7.6	116.2	7.13, *d*, 7.5	116.0		130.7
7a	5.30, *d*, 12.3	64.2	5.02, *d*, 12.5	63.5	5.30, *d*, 12.3	64.0	5.45, *d*, 12.6	64.5
7b	5.26, *d*, 12.3		4.78, *d*, 12.5		5.26, *d*, 12.3		5.23, *d*, 12.6	
8		170.8		170.4		170.3		170.9
9		78.9		78.7		78.7		79.0
10	5.74, *ddd*, 9.9, 1.8, 1.8	128.5	5.67, *d*, 9.8	128.4	5.69, *ddd*, 9.8, 1.6, 1.6	128.3	5.73, *ddd*, 9.9, 2.0, 2.0	128.6
11	6.11, *ddd*, 9.9, 3.4, 3.4	133.1	6.11, *ddd*, 9.8, 4.2, 4.2	132.9	6.09, *ddd*, 9.8, 3.7, 3.7	132.8	6.12, *ddd*, 9.9, 3.5, 3.5	133.0
12a	2.61, *m*/2.49, *m*	27.2	2.63, *m*/2.50, *m*	27.2	2.61, *m*/2.50, *m*	27.1	2.62, *m*/2.52, *m*	27.2
13a	2.85, *m*/2.52, *m*	36.2	2.83, *m*/2.50, *m*	36.0	2.83, *m*/2.52, *m*	36.0	2.90, *m*/2.54, *m*	36.2
14		206.9		206.8		206.7		206.7
1'	4.92, *d*, 7.5	101.6	5.25, *d*, 8.0	99.9	4.93, *d*, 7.8	101.5	4.57, *d*, 7.7	106.7
2'	3.42, *dd*, 9.0, 7.5	74.3	5.16, *d*, 8.0, 9.5	74.9	3.38, *dd*, 9.5, 7.8	74.0	3.45, *dd*, 8.8, 7.7	74.8
3'	3.46, *dd*, 9.0, 9.0	77.2	3.78, *m*	75.2	3.42, *dd*, 9.5, 9.5	76.9	3.39, *dd*, 8.8, 8.8	77.0
4'	3.39, *dd*, 9.0, 9.0	70.8	3.54, *m*	71.0	3.30, *dd*, 9.5, 9.5	70.6	3.34, *dd*, 8.8, 8.8	70.6
5'	3.42, *ddd*, 9.0, 5.4, 1.8	77.1	3.54, *m*	77.7	3.68, *ddd*, 9.5, 6.5, 2.0	74.7	3.29, *ddd*, 8.8, 5.2, 2.4	77.0
6'a	3.77, *dd*, 12.0, 1.8	62.2	3.84, *m*	62.1	4.53, *dd*, 12.0, 2.0	65.7	3.75, *dd*, 12.0, 2.4	62.1
6'b	3.61, *dd*, 12.0, 5.4		3.69, *m*		4.24, *dd*, 12.0, 6.5		3.62, *dd*, 12.0, 5.2	
1''				166.3		170.7		
2''				130.3		78.7		
3''			8.05, *d*, 7.6	130.3	5.74, *ddd*, 9.8, 1.7, 1.7	128.3		
4''			7.50, *dd*, 7.6, 7.6	129.4	6.12, *ddd*, 9.8, 3.5, 3.5	132.9		
5''			7.63, *dd*, 7.6, 7.6	134.2	2.61, *m*/2.50, *m*	27.1		
6''			7.50, *dd*, 7.6, 7.6	129.4	2.83, *m*/2.52, *m*	36.0		
7''			8.05, *d*, 7.6	130.3		207.1		

[1]: Please note different numbering of the aromatic ring (positions 2, 3, 5, and 6) in idescarpin (**4**) according to Figure 1 and Supplementary Figures S5.6.

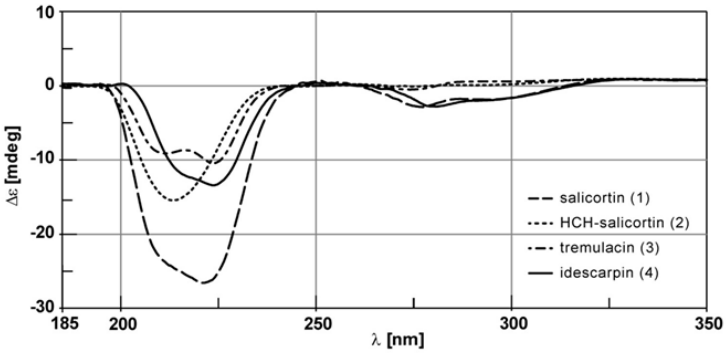

Figure 4. Superimposed CD spectra of isolated salicortin (**1**), HCH-salicortin (**2**), tremulacin (**3**) and idescarpin (**4**).

3. Experimental Section

3.1. General Information

Solvents used for extraction and chromatographic separation were purchased from Carl Roth GmbH, Karlsruhe, Germany and VWR International GmbH, Darmstadt, Germany, and used without further purification. Water used for HPLC was obtained from a Milli-Q Synthesis A10 purifier (Merck KGaA, Darmstadt, Germany). HR-X SPE cartridges (500 mg sorbent/6 mL volume) were purchased from Macherey-Nagel, Düren, Germany. Sephadex LH-20 and polyamide colums DPA-6S were purchased from Sigma-Aldrich GmbH, Schnelldorf, Germany. Separation on Sephadex LH-20 was performed in column chromatography mode using MeOH as a solvent. HPLC separations were carried out on an Agilent 1100 HPLC system, consisting of a degasser, binary pump, autosampler and DAD detector (Agilent Technologies GmbH, Böblingen, Germany). The column outlet was connected to an Advantec CHF122SB fraction collector (Jasco GmbH, Gross-Umstadt, Germany) triggered by a relay board from the Agilent 1100. An Isis RP-18e column (250 × 4.6 mm, 5 µm particle size) from Macherey-Nagel, Düren, Germany, was used for all separations. HPLC gradients are given in the supplementary information. Fractions were evaporated using a Genevac HT-4X vacuum centrifuge (Genevac Ltd., Ipswich, UK). HRMS data were measured via direct injection on a LTQ Orbitrap XL mass spectrometer in positive ionization mode (Fischer Scientific GmbH, Schwerte, Germany). NMR spectra were recorded on a Bruker Avance 500 spectrometer equipped with a cryoplatform and a 5 mm TCI cryoprobe and on a Bruker Avance III HD spectrometer, equipped with a cryoplatform and a 1.7 mm TCI micro-cryoprobe (Bruker Biospin GmbH, Rheinstetten, Germany). NMR tubes of 5 mm and 1.7 mm outer diameter, respectively, were used for measurements. All NMR spectra were recorded using MeCN-d_3 as solvent. Chemical shifts were referenced to the residual solvent peaks at δ_H 1.94 and δ_C 1.32. Data acquisition and processing were accomplished using TopSpin 2.1 and TopSpin 3.2, respectively. Standard pulse programs as implemented in TopSpin were used for data acquisition. Specific optical rotation was measured on a Jasco P-1030 polarimeter, CD spectra were recorded on a Jasco J-810 spectropolarimeter (Jasco GmbH, Gross-Umstadt, Germany). All compounds were measured in MeOH using a quartz cuvette of 1 mm width. Plants of *Populus trichocarpa* × *deltoides* Beaupré were raised in the greenhouse

facilities of the Max Planck Institute for Chemical Ecology in Jena, Germany. The *Idesia polycarpa* leaf specimen was taken from a tree growing in the Botanical Garden of the University of Leipzig, Germany.

*3.2. Isolation and Identification of Salicortin (**1**), HCH-Salicortin (**2**), Tremulacin (**3**) and Idescarpin (**4**)*

Because of the very complex leaf matrix of Salicaceae plants, a solid-phase extraction (SPE) separation course for the isolation of salicinoids was developed [18]. Generally, the plant material was harvested, snap-frozen in liquid nitrogen and subjected to lyophylization. Subsequently, after the exhaustive extraction of the ground material with 70% methanol in water, the extract was pre-purified by SPE followed by chromatography on Sephadex LH-20. From the resulting fractions, salicinoids were purified using HPLC (see supplementary information).

To determine metabolite concentration, salicortin (**1**), HCH-salicortin (**2**) and tremulacin (**3**) were isolated from 454 mg lyophylized *Populus trichocarpa* × *deltoides* Beaupré leaf material. Accordingly, the material was extracted (6 × 30 mL) with MeOH/H_2O (7:3 v/v), resulting in 201 mg crude extract after solvent evaporation. The remaining material was reconstituted with water and centrifuged to separate insoluble matter. The supernatant was subjected to pre-separation on HR-X SPE cartridges. After loading the cartridge, washing with H_2O (6 mL) and elution with MeOH, the eluate was passed through a DPA-6S polyamide SPE cartridge for the removal of procyanidins. The filtrate was evaporated to dryness by vacuum centrifugation. After reconstitution with MeOH, column separation on Sephadex LH-20 (160 mm × 15 mm) with MeOH as eluent was performed. The volumes of fractions taken were as follows: 1–20 mL, 2–10 mL, 3–10 mL, 4–10 mL, 5–15 mL, and 6–20 mL. Fractions 2 and 3 contained the desired compounds. Both fractions were pooled and evaporated to dryness, giving 68 mg pre-purified material. Aliquots were subjected to HPLC in order to isolate the salicinoids. To prevent sample from decomposing during the evaporation of the acidic HPLC solvent, each fractionated compound was immobilized on an HR-X SPE. Final evaporation of the MeOH eluate gave the pure compounds. The amount of salicortin isolated was 2.70 mg per gram lyophylized leaf material (0.3%). HCH-salicortin and tremulacin were obtained in yields of 0.1% and 0.2%, respectively.

To isolate idescarpin (**4**), 5.74 g of lyophylized *Idesia polycarpa* leaf material was exhaustively (6 × 150 mL) extracted using MeOH/H_2O (7:3 v/v), giving 1.6 g crude extract. This crude material was reconstituted with MeOH (70 mL), and the insoluble precipitate was removed by means of centrifugation. The combined supernatants were pooled and dried using a vacuum centrifuge. The dried extract was then reconstituted with water (70 mL), split into three equal portions and subjected to separation on HR-X SPE columns. After conditioning with MeOH and equilibration with H_2O, the water extract was loaded and columns were subsequently washed with H_2O (6 mL). Elution with MeOH and solvent evaporation by vacuum centrifugation gave 720 mg of pre-purified extract. A portion of 115 mg was then subjected to HPLC, resulting in 10 mg pure **4**. Accordingly, the leaf material used for the isolation contained about 1.1% of idescarpin (**4**), based on dry weight.

4. Conclusions

By comparing spectroscopic data of salicortin (**1**), HCH-salicortin (**2**) and tremulacin (**3**) with those of idescarpin (**4**), we conclude that the HCH moiety in all isolated salicinoids is (*S*)-configured at the stereogenic centers C-9 and C-2" (Figure 1). Moreover, one can assume that the HCH moiety in

salicinoids is generally (*S*)-configured, since other compounds bearing this structure element have never been shown to represent diastereomeric mixtures. It is also unlikely that these compounds are biosynthesized through routes other than those of the examined salicinoids. An identical assumption was made based on the results of chemoenzymatic studies; however, without a direct comparison with authentic samples [19]. It has been shown that leaves of *Idesia polycarpa* contain high amounts of (−)-idescarpin (**4**) and it is suggested that **4** serves as a defensive compound against herbivores and fungal infection.

Supplementary Materials

Supplementary materials can be accessed at: http://www.mdpi.com/1420-3049/20/04/5566/s1.

Acknowledgments

We are thankful to the Botanical Garden of the University of Leipzig for providing *Idesia polycarpa* leaf material and to Emily Wheeler for editorial assistance.

Author Contributions

F.F. developed and applied procedures for extraction and isolation (CC, HPLC) of the compounds, measured CD spectra, analyzed the data and contributed to the manuscript. C.P. measured the NMR, optical rotation, and CD spectra, and analyzed the data. S.L. measured the HRMS spectra and analyzed the data. C.P. and B.S. wrote the manuscript.

Conflicts of Interest

The authors declare no conflict of interest.

References

1. Massad, T.J.; Trumbore, S.E.; Ganbat, G.; Reichelt, M.; Unsicker, S.; Boeckler, A.; Gleixner, G.; Gershenzon, J.; Ruehlow, S. An optimal defense strategy for phenolic glycoside production in *Populus trichocarpa*—Isotope labeling demonstrates secondary metabolite production in growing leaves. *New Phytol.* **2014**, *203*, 607–619.
2. Haruta, M.; Pedersen, J.A.; Constabel, C.P. Polyphenol oxidase and herbivore defense in trembling aspen (*Populus tremuloides*): cDNA cloning, expression, and potential substrates. *Physiol. Plantarum.* **2001**, *112*, 552–558.
3. Julkunen-Tiitto, R.; Hakulinen, J.; Meier, B. The response of growth and secondary metabolism to *Melampsora* rusts in field cultivated willow (*Salix*) clones. *Acta Hortic.* **1994**, *381*, 679–682.
4. Boeckler, G.A.; Gershenzon, J.; Unsicker, S.B. Phenolic glycosides of the Salicaceae and their role as anti-herbivore defenses. *Phytochemistry* **2011**, *72*, 1497–1509.
5. Pentzold, S.; Zagrobelny, M.; Rook, F.; Bak, S. How insects overcome two-component plant chemical defence: Plant β-glucosidases as the main target for herbivore adaptation. *Biol. Rev.* **2014**, *89*, 531–551.

6. Clausen, T.P.; Reichardt, P.B.; Bryant, J.P.; Werner, R.A.; Post, K.; Frisby, K. Chemical model for short-term induction in quaking aspen (*Populus tremuloides*) foliage against herbivores. *J. Chem. Ecol.* **1989**, *15*, 2335–2346.
7. Lee, M.; Lee, S.H.; Kang, J.; Yang, H.; Jeong, E.J.; Kim, H.P.; Kim, Y.C.; Sung, S.H. Salicortin-derivatives from *Salix pseudo-lasiogyne* twigs inhibit adipogenesis in 3T3-L1 cells via modulation of C/EBPα and SREBP1c dependent pathway. *Molecules* **2013**, *18*, 10484–10496.
8. Lee, M.; Lee, H.H.; Lee, J.-K.; Ye, S.-K.; Kim, S.H.; Sung, S.H. Anti-adipogenic activity of compounds isolated from *Idesia polycarpa* on 3T3-L1 cells. *Bioorg. Med. Chem. Lett.* **2013**, *23*, 3170–3174.
9. Martineau, L.C.; Muhammad, A.; Saleem, A.; Herve, J.; Harris, C.S.; Arnason, J.T.; Haddad, P.S. Anti-adipogenic activities of *Alnus incana* and *Populus balsamifera* bark extracts, part II: Bioassay-guided identification of actives salicortin and oregonin. *Planta Med.* **2010**, *76*, 1519–1524.
10. Baek, S.; Kim, D.; Lee, C.; Kho, Y.; Lee, C. Idescarpin isolated from the fruits of *Idesia polycarpa* inhibits melanin biosynthesis. *J. Microbiol. Biotechnol.* **2006**, *16*, 667–672.
11. Kim, S.H.; Jang, Y.P.; Sung, S.H.; Kim, Y.C. Inhibitory activity of phenolic glycosides from the fruits of *Idesia polycarpa* on lipopolysaccharide-induced nitric oxide production in BV2 microglia. *Planta Med.* **2006**, *72*, 167–169.
12. Thieme, H. Isolierung eines neuen Phenolglucosids aus *Salix purpurea*. *Pharmazie* **1964**, *11*, 681.
13. Babst, B.A.; Harding, S.A.; Tsai, C.-J. Biosynthesis of phenolic glycosides from phenylpropanoid and benzenoid precursors in *Populus*. *J. Chem. Ecol.* **2010**, *36*, 286–297.
14. Kim, T.B.; Kim, H.W.; Lee, M.; Lee, H.H.; Kim, S.H.; Kang, S.K.; Sung, S.H. Isolation and structure elucidation of (–)-idescarparide, a new spiro compound from *Idesia polycarpa*. *Tetrahedron Lett.* **2014**, *55*, 5447–5449.
15. Rehill, B.; Clauss, A.; Wieczoek, L.; Whitham, T.; Lindroth, R. Foliar phenolic glycosides from *Populus fremontii*, *Populus angustifolia* and their hybrids. *Biochem. Syst. Ecol.* **2005**, *22*, 125–131.
16. Rasmussen, B.; Nkurunziza, A.-J.; Witt, M.; Oketch-Rabah, H.A.; Jaroszewski, J.W.; Stærk, D. Dovyalicin-type spermidine alkaloids from *Dovyalis* species. *J. Nat. Prod.* **2006**, *69*, 1300–1304.
17. Domisse, R.A.; van Hoof, L.; Vlietinck, A.J. Structural analysis of phenolic glycosides from Salicaceae by NMR spectroscopy. *Phytochemistry* **1986**, *25*, 1201–1204.
18. Maansson, M.; Phipps, R.K.; Gram, L.; Munro, M.H.G.; Larsen, T.O.; Nielsen, K.F. Ex-plorative solid-phase extraction (E-SPE) for accelerated microbial natural product discovery, dereplication, and purification. *J. Nat. Prod.* **2010**, *73*, 1126–1132.
19. Adams, D.R.; Aichinger, C.; Rinner, U.; Hudlicky, T. Chemoenzymatic synthesis of idesolide from benzoic acid. *Synlett* **2011**, *5*, 725–729.

Sample Availability: Samples of the compounds salicortin, HCH-salicortin, tremulacin and idescarpin are available from the authors.

Acylated quinic acids are the main salicortin metabolites in the specialist herbivore *Cerura vinula*

Felix Feistel, Christian Paetz, Riya C. Menezes,
Daniel Veit, Bernd Schneider

Submitted to *Journal of Chemical Ecology* December 2017

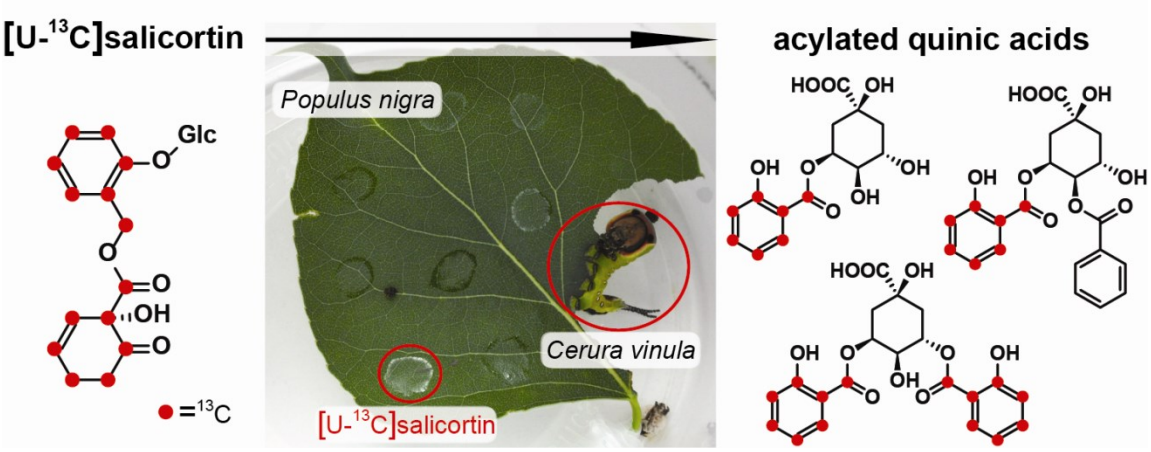

ACYLATED QUINIC ACIDS ARE THE MAIN SALICORTIN METABOLITES IN THE SPECIALIST HERBIVORE *Cerura Vinula*

FELIX FEISTEL, CHRISTIAN PAETZ, RIYA C. MENEZES, DANIEL VEIT, BERND SCHNEIDER*

Max Planck Institute for Chemical Ecology, Hans-Knöll-Straße 8, Beutenberg Campus, D-07745 Jena, Germany

Abstract - Salicortin is a phenolic glucoside produced in Salicaceae as a chemical defense against herbivory. The specialist lepidopteran herbivorous larvae of *Cerura vinula* are able to overcome this defense. We examined the main frass constituents of *C. vinula* fed on *Populus nigra leaves*, and identified eleven quinic acid derivatives with benzoate and/or salicylate substitution. We asked whether the compounds are a result of salicortin breakdown and sought answers by carrying out feeding experiments with highly ^{13}C-enriched salicortin. Using HRMS and NMR analyses, we were able to confirm that salicortin metabolism in *C. vinula* proceeds through deglucosylation and ester hydrolysis, after which saligenin is oxidatively transformed into salicylic acid and, eventually, conjugated to quinic acid.

Key Words - *Cerura vinula, Populus nigra, s*alicortin, down-stream metabolism, Salicaceae, stable isotope labeling

Acknowledgments - The authors thank the workshop and IT -teams of the Max Planck Institute for Chemical Ecology for constructive cooperation, the greenhouse team for rearing the *Populus beaupré* trees, Regina Seibt for establishing the *C. vinula* breeding at our institute and Emily Wheeler for polishing the language.

INTRODUCTION

The chemical defense of Salicaceae species is attributed to phenolic secondary metabolites. The total phenolic content in *Populus* species can reach concentrations of up to 30% of a plant's dry mass (Donaldson et al., 2006; Pentzold et al., 2014). Among the *Populus* phenolics, salicinoids – glycosides derived from salicyl alcohol (saligenin) – are the defensive chemicals of this species and of other members of the Salicaceae family (Lindroth, 1991; Palo, 1984). The structural diversity of salicinoids arises from their modular composition, which comprises a saligenin core unit, a glucose moiety and an organic acid. The most representative salicinoid in *Populus* is salicortin (**12**), as so far it has been found in all investigated species (Boeckler et al., 2011; Thieme, 1964). Numerous studies have investigated the effect of salicinoids on herbivorous insects, such as *Papilio glaucus* (Lindroth, 1991*)*, *Choristoneura conflictica* (Clausen et al., 1989), *Malacosoma disstria* and *Lymantria dispar* (Lindroth and Hemming, 1990) or *Operophtera brumata* (Boeckler et al., 2016; Ruuhola et al., 2001). Transcriptome analyses identified enzymes (e.g., cytochrome P450s) involved in the metabolic detoxification of these natural products and xenobiotics in herbivores (Giraudo et al., 2015; du Rand et al., 2015). Recently, a comprehensive study of the generalist herbivore *L. dispar* (Boeckler et al., 2016) provided the first detailed description of how a lepidopteran detoxifies salicinoid compounds. The digestive degradation of salicinoids in the insect gut (Haruta et al., 2001; Lindroth, 1988; Ruuhola et al., 2003) results in saligenin and an *o*-quinone (Clausen et al., 1989; Julkunen-Tiitto and Meier, 1992; Knuth et al., 2011). Both metabolites are known for their toxic and feeding-deterrent activities (Boeckler et al., 2011; Clausen et al., 1989; Ruuhola et al., 2001).

The larva of the lepidopteran *Cerura vinula* is native to Europe and Asia. In the temperate climate zone of Central Europe, imagines appear from April to August. Females lay eggs on the branches and leaves of their host plants. As the insects' nutritional spectrum is limited to plants of the Salicaceae family (*Salix* and *Populus* species), they are regarded as specialist herbivores (Ali and Agrawal, 2012; Hintze-Podufal, 1970).

The present work identifies salicinoid downstream products in the feces of the Salicaceae specialist herbivore *C. vinula*. Based on ^{13}C labeling experiments, we propose a salicinoid degradation pathway in the insect.

METHODS AND MATERIALS

General Information. NMR spectra for the structure elucidation of acylated quinic acids **1** to **11** were recorded on a Bruker Avance III HD 700 MHz spectrometer, equipped with a 1.7 mm TCI microcryoprobe (Bruker Biospin, Rheinstetten, Germany) using NMR tubes of 1.7 mm outer diameter. NMR spectra of fecal extracts from *C. vinula* larvae after [U-^{13}C]salicortin feeding experiments were obtained on a Bruker Avance III HD 500 MHz NMR spectrometer equipped with a 5 mm TCI cryoprobe (Bruker Biospin) using NMR tubes of 5 mm outer diameter. NMR spectra for the characterization of *in vivo*-generated [U-^{13}C]salicortin were recorded on a Bruker Avance III HD 400 MHz NMR spectrometer equipped with a 5 mm BBFO probe (Bruker Biospin) using NMR tubes of 5 mm outer diameter as well. All NMR spectra were recorded using MeOH-d_4 as a solvent. Chemical shifts were referenced to the residual solvent peaks at δ_H 3.31 and δ_C 49.15. Data acquisition and processing were accomplished using TopSpin 3.2. Standard pulse programs as implemented in TopSpin were used for data acquisition. The ultra-high-performance liquid chromatography–electrospray ionization–tandem mass spectrometry system (UHPLC–ESI–MS/MS) for structure elucidation and fecal compound analysis after [U-^{13}C]salicortin labeling consisted of an Ultimate 3000 series RSLC (Dionex, Sunnyvale, CA, USA) with an Acclaim C18 column (150 × 2.1 mm, 2.2 µm, Dionex, Sunnyvale, CA, USA) and a Q Exactive Plus - Orbitrap mass spectrometer (Thermo Fisher Scientific, Bremen, Germany) using heated-electrospray ionization (H-ESI). H-ESI source parameters were set to 4 kV for spray voltage and 35 V for transfer capillary voltage at a capillary temperature of 300 °C. The samples were measured in positive and negative ionization mode in the mass range of *m/z* 100 to 1000 using 70,000 *m/Δm* resolving power in the Orbitrap mass analyzer.

UHPLC-ESI-MS/MS for hemolymph analysis was performed with an Ultimate 3000 series RSLC (Dionex) and LTQ - Orbitrap XL mass spectrometer (Thermo Fisher Scientific) in which ionization was accomplished using electrospray ionization (ESI). ESI source parameters were set to 4 kV for spray voltage, 35 V for transfer capillary voltage at a capillary temperature 275 °C. The samples were measured in negative ionization mode in the mass range of m/z 100 to 1000 using 30,000 m/Δm resolving power in the Orbitrap mass analyzer. All UHPLC systems used an Acclaim C18 column (150 × 2.1 mm, 2.2 µm, Dionex) for chromatographic separation. All HRMS data were evaluated and interpreted using Xcalibur software (Thermo Fisher Scientific, Waltham, MA, USA). HPLC-ESI-MS was performed on an Agilent 1100 HPLC system, consisting of a degasser, quaternary solvent delivery pump G1311A, an autosampler G1313A (Agilent Technologies, Waldbronn, Germany), a photodiode array detector (detection 200-700 nm; J&M Analytik, Aalen, Germany) and an Esquire 3000 ion trap mass spectrometer (Bruker Daltonik, Bremen, Germany).

Acylated quinic acids **1-11** were separated on an Agilent 1100 HPLC system, consisting of a degasser, quaternary solvent delivery pump G1311A, an autosampler G1313A (Agilent Technologies) and a photodiode array detector (detection 200-700 nm; J&M Analytik). The column outlet was connected to a Bruker/Spark Holland Prospect 2 solid-phase extraction (SPE) system (Bruker Biospin) for post-column SPE trapping on HySphere resin GP cartridges. To reduce the eluotropic capacity of the HPLC solvent mixture, water was added with a flow rate of 2.5 mL min^{-1} using a make-up pump (Knauer, Berlin, Germany).

[U-^{13}C]salicortin was chromatographically purified on an Agilent 1100 HPLC system, consisting of a degasser G1322A, a binary pump G1312A, an autosampler G1313A and a photodiode array detector G1315B (Agilent Technologies). The column outlet was connected to an Advantec CHF122SB fraction collector (Jasco, Gross-Umstadt, Germany) triggered by a relay board from the Agilent 1100. All HPLC separations were carried out using an Isis RP-18e column (250 x 4.6 mm, 5 µm particle size) (Macherey-Nagel, Düren, Germany). Solvents were evaporated with a rotary evaporator Rotavapor R-114 (Büchi Labortechnik, Flawil, Switzerland) and a Genevac HT-4X vacuum centrifuge (Genevac, Ipswich, UK). Homogenization was carried out with a MINILYS cell disruptor (Bertin Technologies, Montigny-le-Bretonneux, France).

Solvents used for extraction and chromatographic separation were purchased from Carl Roth (Karlsruhe, Germany) and VWR International (Darmstadt, Germany), and used without further purification. Acetonitrile and water (hypergrade for LCMS) used for UHPLC-ESI-MS/MS were purchased from Merck (Darmstadt, Germany), and formic acid (eluent additive for LC-MS) was obtained from Sigma Aldrich (Steinheim, Germany). Water used for HPLC was obtained from a Milli-Q Synthesis A 10 purifier (Merck). $^{13}CO_2$ (isotopic purity 99 atom% ^{13}C, <3 atom% ^{18}O) and Phytacon™ vessels (H 140 mm, base diam. 86 mm) used as arenas for the larvae feeding experiments were purchased from Sigma-Aldrich (Taufkirchen, Germany). HR-X SPE cartridges (500 mg sorbent/6 ml volume), folded filters (90 mm) and paper filters (MN 615 ¼, 125 mm) were purchased from Macherey-Nagel. Syringe filters (0.45 µm, PA) were purchased from Carl Roth. (–)-Quinic acid was purchased from Thermo Fisher Kandel (Karlsruhe, Germany).

Plant Material and Insect Larvae. Plant samples of black poplar (*P. nigra*) were collected from trees growing in proximity to the Max Planck Institute for Chemical Ecology in Jena, Germany. *Populus trichocarpa x deltoides* Beaupré were grown in the greenhouse of the Max Planck Institute for Chemical Ecology. The light period was set from 6:30 to 20:30 (14 h), while temperatures were kept between 21 – 23 °C during the day and between 19 – 21 °C at night. The humidity was regulated between 50 to 60 %. Puss moth (*C. vinula*) larvae were hatched from eggs and reared on *P. nigra* leaves in the laboratory.

Extraction and Isolation of C. vinula *Feces.* Feces of *C. vinula* larvae fed on *P. nigra* leaves were collected and lyophilized, resulting in 73 g of dry material. Contaminated material (leaves, stalks and exuviae) was removed manually. Dried feces (20 g) were ground using a ceramic mortar and pestle, and extracted (5 x 200 ml, each 10 min) with MeOH. The extracts were filtered (paper filters and 0.45 µm PA syringe filters), pooled and evaporated under reduced pressure, resulting in 2.5 g dried crude extract. This dry matter (53.8 mg) was suspended in water (20 ml) using ultrasound and subjected to pre-separation on a HR-X SPE (PS/DVB) cartridge. After conditioning with MeOH (2 x 6 ml) and equilibration with water (3 x 6 ml), the cartridge was loaded with the extract suspension and washed with water (3 x 6 ml). After drying in vacuum, the cartridge was eluted with MeOH (3 x 6 ml). The eluate was then dried using a vacuum centrifuge, resulting in 24.7 mg pre-purified extract. For separation, an aliquot dissolved in MeOH (67.4 mg ml^{-1}) was subjected to HPLC-SPE.

A binary solvent system of 0.1% formic acid in water (solvent A) and 0.1% formic acid in MeOH (solvent B) was used for HPLC separation, starting with a 5 min isocratic flow of 100% solvent A and decreasing linearly for 90 min to 50% solvent A. Column temperature was set to 35 °C and the solvent flow rate was 0.8 mL min^{-1}. After each run, the column was washed with 100% MeOH for 5 min and equilibrated with 100% H_2O for 10 min. SPE cartridges loaded with metabolites were dried in a stream of N_2 gas before being eluted with MeOH. Eluted compounds were dried by vacuum centrifugation, yielding the following compounds (R_t retention time): **1** (R_t 32.69 min, 2.1 mg g^{-1} dry feces), **4** (R_t 36.69 min, 1.2 mg g^{-1}), **5** (R_t 39.71 min, 1.1 mg g^{-1}), **2** (R_t 41.00 min, 2.6 mg g^{-1}), **3** (R_t 52.59 min, 3.4 mg g^{-1}), **10** (R_t 61.70 min, 1.6 mg g^{-1}), **7** (R_t 64.14 min, 2.1 mg g^{-1}), **9** (R_t 65.52 min, 3.0 mg g^{-1}), **6** (R_t 68.34 min, 2.8 mg g^{-1}), **11** (R_t 70.18 min, 2.1 mg g^{-1}), **8** (R_t 72.73 min, 1.9 mg g^{-1}).

Structure elucidation was carried out using 1D (^1H NMR, selective TOCSY) and 2D NMR (^1H-^1H COSY, ^1H-^{13}C HSQC, ^1H-^{13}C HMBC) spectra recorded at 700 MHz and UHPLC-ESI-MS/MS measurements (Q Exactive Plus - Orbitrap MS) using a binary solvent system of H_2O (solvent A) and acetonitrile (solvent B), both of which contained 0.1% (v/v) formic acid with a flow rate of 300 µl min^{-1}. The linear gradient used started with 0% B and increased to 100% B within 15 min. Afterwards, the column was washed for 5 min with 100% B and then equilibrated at 0% B for 5 min.

In vivo *Generation and Isolation of ^{13}C-Labeled Salicortin.* Stable isotope labeling was achieved in a growth chamber resembling a setup described previously (Chen et al., 2011). The greenhouse light system (Philips SON-T Agro 400W) was used to provide constant light exposure from 6:30 to 22:00 (15.5 h). Temperature and relative humidity were kept between 20°C to 30°C and 50% to 80%, respectively. Six *P. trichocarpa x deltoides* Beaupré plants were pruned to a height of about 30 cm, leaving a few basal leaves. After being transferred to the growth chamber, plants were kept in darkness for the first two days. At the beginning of day three, the respired CO_2 (natural abundance isotope ratio) was removed from the chamber's atmosphere and 450 ppm $^{13}CO_2$ was injected into it. This $^{13}CO_2$ level was kept constant during the entire experimental time (26 days). At the end of each day's light period, $^{13}CO_2$ injection was stopped and respired CO_2 was continuously removed during the night. Details about the $^{13}CO_2$ labeling are provided in the supporting information (B.1 and B.2).

The $^{13}CO_2$-labeling experiment was stopped at day 28, and newly grown plant tissue (leaves with stalks) was collected and lyophilized yielding 13 g dry material. The material was manually crushed and filled equally into Falcon tubes (8 x 45 mL) containing steel beads (3 mm). Extraction was accomplished with MeOH (30 mL per tube) in a Skandex S-7 paint shaker (Fluid Management, Wheeling, IL, USA) for 2 x 4 min. Afterwards, the extracts were pooled, filtered, and the solvent was evaporated *in vacuo,* yielding 4.18 g (32 % dw) dry matter. The dry matter was suspended in 500 mL H_2O, divided into three parts and subjected to solid-phase extraction on HR-X SPE columns (each 1.5 g sorbent). After loading, columns were washed with H_2O (3 x 20 mL) and eluted with MeOH (20 mL). The combined methanolic fractions were dried *in vacuo,* yielding 2.26 g pre-purified extract (17.33 % dw). An aliquot solution (121 mg mL^{-1}) was subjected to HPLC separation.

[U-^{13}C]salicortin was separated using a binary solvent system consisting of 0.1% formic acid in H_2O (solvent A) and 0.1% formic acid in MeOH (solvent B). Column temperature was set to 35 °C and the solvent flow rate was 0.8 mL min^{-1}. The HPLC gradient that was used started with a 5 min isocratic flow of 100% solvent A and decreased linearly for 5 min to 85%, 25 min to 70% and finally 50 min to 50% solvent A. Afterwards, the column was washed for 10 min with 100% MeOH and equilibrated for 10 min with 100% H_2O. The salicortin UV signal peak (λ = 285 nm) appeared at R_t 42.6 min. Unlabeled salicortin (natural abundance ^{13}C) was isolated in the same manner from unlabeled *P. trichocarpa x deltoides* tissue.

Characterization of the salicortin isolated from the ^{13}C-labeled plant tissue and calculation of its ^{13}C-enrichment was done by means of ^{1}H, ^{13}C and ^{1}H-^{13}C HSQC NMR spectra (400 MHz) and HPLC-ESI-MS measurements using the chromatographic method as described above. The *in vivo*-generated salicortin showed uniform ^{13}C-labeling with 82% total ^{13}C-enrichment. Spectroscopic data of the [U-^{13}C]salicortin (82% ^{13}C) and detailed information about the calculation of the ^{13}C-enrichment are presented in the Supplementary data (SI B.2).

[U-^{13}C]Salicortin larval feeding. Freshly cut leaves of *P. nigra* (LPI 3-10) were used for feeding experiments. The leaf stalks were inserted into 2 mL Eppendorf micro reaction vessels. Lids of the vessels were removed for convenient handling prior to being filled with tap water. The opening of the vessels was sealed with Parafilm® fastening the leaf stalk to prevent the water in the vessel from spilling. An aqueous solution of [U-^{13}C]salicortin (2.5 mg mL^{-1}) was spotted evenly on the surface of five poplar leaves (10 x 20 µL droplets per leaf). Control leaves were spotted with water in an analogous fashion. Leaves were left under the fume hood for 3 h, allowing the droplets to dry completely. Subsequently, the [U-^{13}C]salicortin-coated leaves and the control leaves were transferred into arenas for feeding experiments. Each arena contained one leaf and one *C. vinula* larva (late 3rd to early 4th instars), which were placed onto the surface of each leaf. The larvae were kept in the arena until the leaves had been completely consumed. Feces were subsequently collected and lyophilized.

Freeze-dried feces were extracted with MeOH (3 x 1 ml) by homogenization in a Minilys cell disruptor (2 ml tubes, 60 sec and 4000 rpm), using 1.4 mm o.d. ZrO_2 beads. The supernatants of each sample were pooled and evaporated, while the residues were dried and subsequently extracted in the same way with H_2O (5 x 1 ml). The aqueous solutions were similarly pooled and dried. Afterwards, methanolic and aqueous extracts were subjected to NMR (500 MHz) and UHPLC-ESI-MS/MS (Q Exactive Plus – Orbitrap MS) analysis, using the chromatographic system described in Structure elucidation (2.3).

Collection of C. vinula *Hemolymphs.* The question of whether salicinoid metabolites are detectable in the hemolymph of *C. vinula* larvae was addressed as follows: six *C. vinula* larvae (3 × control, 3 × fed with [U-^{13}C]salicortin) were immobilized in 15 mL Falcon tubes and kept in the -20°C freezer for 15 min. A mid-abdominal proleg of an anesthetized larva was pierced with a scalpel, and the emerging hemolymph was transferred by means of a pipette into an ice-cooled 2 ml Eppendorf micro reaction vessel containing MeOH (1 mL). Subsequently, the mixture was centrifuged and the supernatant was evaporated by a stream of N_2 gas, yielding an average amount of 3.07 mg (SD ± 1.51 mg) residue per larva. The dried residues were dissolved in 1 mL MeOH and subjected to UHPLC-ESI-MS/MS (LTQ - Orbitrap XL MS) analysis, using a binary solvent system of H_2O (solvent A) and acetonitrile (solvent B), both of which contained 0.1% (v/v) formic acid with a flow rate of 300 µl min^{-1}. A linear gradient was used, starting with 5% B to 52% B within 20 min. Afterwards, the column was washed for 5 min with 100% B and then equilibrated at 5% B for another 5 min.

Spectroscopic data of the acylated quinic acids.

3-O-Salicyloyl quinic acid (1) - UV (MeOH/H_2O): λ_{max} = 203.5 nm, λ_{max} = 236.5 nm, λ_{max} = 303.9 nm; HRESIMS: *m/z* 311.0774 [M-H]$^-$ (calcd for $C_{14}H_{15}O_8$, 311.0772); ^{1}H and ^{13}C NMR data, see Table 1.

4-O-Salicyloyl quinic acid (2) - UV (MeOH/H_2O): λ_{max} = 203.5 nm, λ_{max} = 237.5 nm, λ_{max} = 303.9 nm; HRESIMS: *m/z* 311.0773 [M-H]$^-$ (calcd for $C_{14}H_{15}O_8$, 311.0772); ^{1}H and ^{13}C NMR data, see Table 1.

5-O-Salicyloyl quinic acid (3) - UV (MeOH/H_2O): λ_{max} = 203.5 nm, λ_{max} = 237.0 nm, λ_{max} = 305.9 nm; HRESIMS: *m/z* 311.0773 [M-H]$^-$ (calcd for $C_{14}H_{15}O_8$, 311.0772); ^{1}H and ^{13}C NMR data, see Table 1.

4-O-Benzoyl quinic acid (4)(Wan et al., 2016) - UV (MeOH/H_2O): λ_{max} = 279.4 nm; HRESIMS: *m/z* 295.0820 [M-H]$^-$ (calcd for $C_{14}H_{15}O_7$, 295.0823); ^{1}H and ^{13}C NMR data, see Table 1.

5-O-Benzoyl quinic acid (5) - UV (MeOH/H_2O): λ_{max} = 276.4 nm; HRESIMS: *m/z* 295.0819 [M-H]$^-$ (calcd for $C_{14}H_{15}O_7$, 295.0823); ^{1}H and ^{13}C NMR data, see Table 2.

3-O,4-O-Disalicyloyl quinic acid (6) - UV (MeOH/H_2O): λ_{max} = 204.5 nm, λ_{max} = 235.0 nm, λ_{max} = 305.4 nm; HRESIMS: *m/z* 431.0986 [M-H]$^-$ (calcd for $C_{21}H_{19}O_{10}$, 431.0984); ^{1}H and ^{13}C NMR data, see Table 2.

3-O,5-O-Disalicyloyl quinic acid (7) - UV (MeOH/H_2O): λ_{max} = 204.0 nm, λ_{max} = 236.0 nm, λ_{max} = 304.9 nm; HRESIMS: *m/z* 431.0985 [M-H]$^-$ (calcd for $C_{21}H_{19}O_{10}$, 431.0984); ^{1}H and ^{13}C NMR data, see Table 2.

4-O,5-O-Disalicyloyl quinic acid (8) - UV (MeOH/H_2O): λ_{max} = 208.0 nm, λ_{max} = 306.9 nm; HRESIMS: *m/z* 431.0987 [M-H]$^-$ (calcd for $C_{21}H_{19}O_{10}$, 431.0984); ^{1}H and ^{13}C NMR data, see Table 2.

3-O-Salicyloyl-4-O-benzoyl quinic acid ***(9)*** - UV (MeOH/H_2O): λ_{max} = 302.4 nm; HRESIMS: *m/z* 415.1038 [M-H]$^-$ (calcd for $C_{21}H_{19}O_9$, 415.1035); ^1H and ^{13}C NMR data, see Table 3.

3-O-Salicyloyl-5-O-benzoyl quinic acid ***(10)*** - UV (MeOH/H_2O): λ_{max} = 210.0 nm, λ_{max} = 309.9 nm; HRESIMS: *m/z* 415.1038 [M-H]$^-$ (calcd for $C_{21}H_{19}O_9$, 415.1035); ^1H and ^{13}C NMR data, see Table 3.

4-O-Salicyloyl-5-O-benzoyl quinic acid ***(11)*** - UV (MeOH/H_2O): λ_{max} = 217.5 nm, λ_{max} = 283.4 nm; HRESIMS: *m/z* 415.1038 [M-H]$^-$ (calcd for $C_{21}H_{19}O_9$, 415.1035); ^1H and ^{13}C NMR data, see Table 3.

RESULTS

Isolation and Structure Elucidation of Fecal Metabolites. Feces of *C. vinula* larvae fed on *P. nigra* leaves were collected and metabolites extracted as described in the Material and methods section. Eleven quinic acid derivatives representing almost 2.5% (23.9 mg/g) of the fecal dry mass were identified (Fig. 1). Among them, ten compounds (**1-3, 5-11**) were unknown and only compound **4** had been reported recently (Wan et al., 2016). NMR data of the isolated compounds are shown in Tables **1-3**. Spectra of all compounds, including salicortin (**12**) and quinic acid (**13**), are provided in the Supplementary data (SI A.1 to A.13).

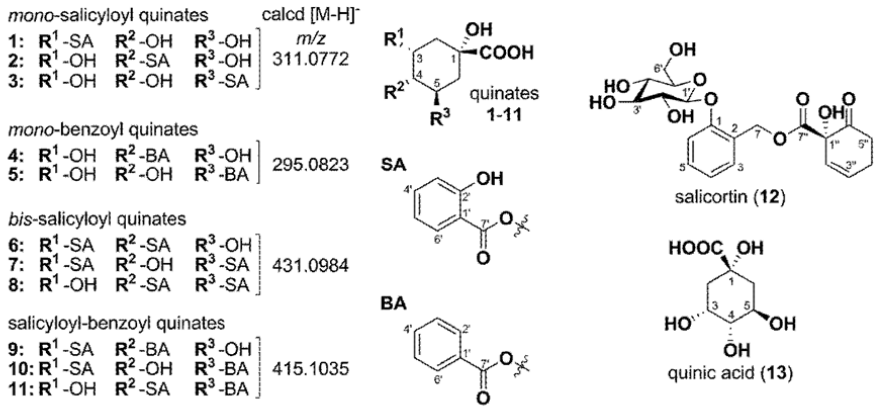

Fig. 1 Metabolites isolated from feces of *C. vinula* larvae fed on *P. nigra* leaves, and the structures of salicortin (**12**) and quinic acid. SA: salicyloyl; BA: benzoyl.

The HRESIMS data of compound **1** showed a molecular ion peak at *m/z* 311.0774 [M-H]$^-$ corresponding to a molecular formula of $C_{14}H_{16}O_8$ (calcd for $C_{14}H_{15}O_8$, *m/z* 311.0772). The ^1H NMR spectrum of compound **1** (Table 1) showed signals of eleven protons assignable to two different structural units. In the low-field region of the ^1H NMR spectra, we observed signals of an asymmetric four-spin system (ABCD) at δ_H 6.62 ($^3J_{HH}$ = 0.8/8.3 Hz; H-3'), δ_H

7.21 ($^3J_{HH}$ = 1.5/7.3/8.3 Hz; H-4'), δ_H 6.60 ($^3J_{HH}$ = 0.8/6.9/7.3 Hz; H-5') and δ_H 7.44 ($^3J_{HH}$ = 1.4/6.9 Hz; H-6'), characteristic of a 1,2-disubstituted aromatic ring. The corresponding ^{13}C chemical shifts were determined by an ^{1}H-^{13}C hetero-correlation single quantum coherence (HSQC) spectrum as δ_C 118.8 (C-3'), δ_C 135.5 (C-4'), δ_C 119.5 (C-5') and δ_C 132.5 (C-6'). Further evidence for a 1,2-disubstitution was provided by an ^{1}H-^{13}C hetero-nuclear multiple-bond correlation (HMBC) spectrum showing $^3J_{CH}$ correlations from H-4' and H-6' to a quaternary carbon atom at δ_C 159.9 (C-2') as well as from H-3' and H-5' to another quaternary carbon atom at δ_C 115.2 (C-1'). Because of its low-field ^{13}C chemical shift, C-2' was assigned as oxygenated. Furthermore, H-6' (δ_H 7.44) showed a long-range CH-correlation to a carboxyl functionality at δ_C 167.7 (C-7') tethered to C-1' (δ_C 115.2). Thus, the data suggest the presence of a salicyloyl moiety (SA). A double-doublet signal of a methine appeared at δ_H 5.70 ($^3J_{HH}$ = 3.1/3.4/3.1; H-3). The corresponding ^{13}C chemical shift was extracted from the ^{1}H-^{13}C HSQC spectrum at δ_C 72.8 (C-3), which is characteristic for a hydroxylated aliphatic carbon atom. Adjacent to H-3, another methine at δ_H 3.60 ($^3J_{HH}$ = 3.4/9.5 Hz; H-4), and a methylene group at δ_H 2.35 ($^3J_{HH}$ = 3.1/14.4 Hz; H-2a) and δ_H 2.11 ($^3J_{HH}$ = 3.1/14.4 Hz; H-2b) were determined from their $^3J_{HH}$ correlations by ^{1}H-^{1}H COSY. Furthermore, consecutive cross-peaks from H-4 to another methine at δ_H 4.06 ($^3J_{HH}$ = 4.6/9.5/12.0 Hz; H-5) and to a second methylene group at δ_H 2.10 ($^3J_{HH}$ = 12.0/12.5 Hz; H-6a) and δ_H 1.95 ($^3J_{HH}$ = 4.6/12.5 Hz; H-2b) were observed. The small $^3J_{HH}$ values (3.4 Hz) for H-3 and H-4 indicated equatorial configuration, whereas the large values (9.5 Hz) for H-4 and H-5 indicated axial configuration. The corresponding ^{13}C-chemical shifts were determined by ^{1}H-^{13}C HSQC as δ_C 36.8 (C-2), δ_C 75.6 (C-4), δ_C 68.0 (C-5) and δ_C 42.5 (C-6). As for C-3 (δ_C 72.8), large ^{13}C NMR chemical shift values indicated oxygenation for C-4 and C-5. The^{1}H-^{13}C HMBC spectrum revealed a $^3J_{CH}$ correlation of H-3 with an oxygenated quaternary carbon atom at δ_C 80.3 (C-1). Furthermore, both methylene groups (H-2ab and H-6ab) showed weak long-range CH correlations to C-1, as a result of which the entire aliphatic structure can be characterized as a cyclohexane ring system. Another HMBC correlation from H-6b to a quaternary carbon at δ_C 182.6 (C-7) tethered to C-1 revealed quinic acid. The characteristic low-field shift of H-3 indicated substitution in this position. This assumption was further supported by an ^{1}H-^{13}C HMBC correlation from H-3 to the carboxyl carbon C-7' (δ_C 167.7) of the salicyloyl moiety. Accordingly, the structure of compound **1** was assigned as 3-*O*-salicyloyl quinic acid.

Similar to **1**, the HRESIMS spectra of compounds **2** and **3** showed a molecular ion peak of *m/z* 311.0773 [M-H]$^-$, again corresponding to a molecular formula of $C_{14}H_{16}O_8$ (calcd for $C_{14}H_{15}O_8$, *m/z* 311.0772). The data from ^{1}H NMR, ^{1}H-^{1}H COSY, ^{1}H-^{13}C HSQC and the ^{1}H-^{13}C HMBC spectra resembled those of compound **1** (Table 1). Signals of the salicyloyl moiety and the quinic acid subunit were present, but the substitution patterns differed at C-3, C-4 and C-5 of the quinic acid moieties. Acylation of the hydroxyl groups in (–)-quinic acid (**13**) leads to low-field shifts of the signals of H-3, H-4 and H-5 (Pauli et al., 1998). However, the multiplicities and coupling constants remain unaffected. Thus, the shift of a characteristic multiplet to the low field indicates the substitution site (Fig. 2). The multiplets of H-4 (δ_H 5.02) in the ^{1}H NMR spectrum of compound **2** and H-5 (δ_H 5.55) in the spectrum of compound **3** – which in comparison with the corresponding signals of quinic acid (**13**) appeared at the low field – revealed esterification with salicyloyl units at the hydroxyl groups in positions 4 and 5, respectively.

The structures of **2** and **3** were further characterized by ^{1}H-^{13}C HMBC correlations of H-4 (**2**; δ_H 5.02) and H-5 (**3**; δ_H 5.55) with the carboxylic carbon atoms of their salicyloyl moieties at δ_C 170.8 (**2**; C-7') and 170.7 (**3**; C-7'), respectively. Accordingly, compound **2** was identified as 4-*O*-salicyloyl quinic acid and compound **3** was identified as 5-*O*-salicyloyl quinic acid.

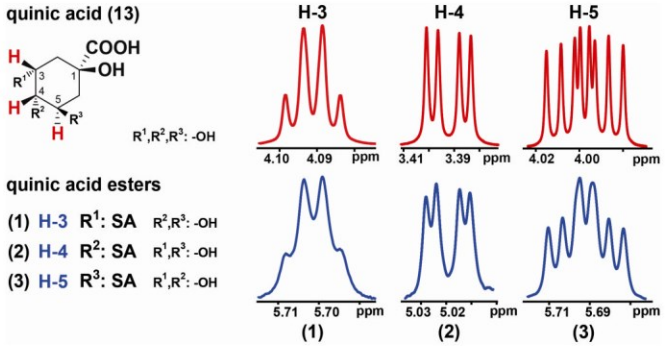

Fig. 2 ^{1}H NMR signals illustrating identical multiplicities and coupling constants of H-3, H-4 and H-5 of (–)-quinic acid (**13**) (red) compared to the corresponding ^{1}H NMR signals of acylated compounds **1-3** (blue), shifted to the low field. Full spectra are given in the Supplementary data.

The analytical data of compound **4** were in accordance with previously reported 4-*O*-benzoyl quinic acid (Wan et al., 2016).

The HRESIMS spectra of compound **5** showed a molecular ion peak of *m/z* 295.0819 [M-H]$^-$, corresponding to a molecular formula of $C_{14}H_{16}O_7$ (calcd for $C_{14}H_{15}O_7$, *m/z* 295.0823) and indicating an isomer of compound **4**. In accordance with this suggestion, the ^{1}H NMR, ^{1}H-^{1}H COSY, ^{1}H-^{13}C HSQC and the ^{1}H-^{13}C HMBC spectra of compound **5** (Table 2) showed very similar signals in comparison to compound **4**. Thus, both compounds are constitutional isomers consisting of a quinic acid moiety substituted with a benzoyl moiety. Accordingly, the ^{1}H NMR data of compound **5** showed signals assignable to a symmetrical five-spin system (AA'XX'Y) at δ_H 8.06 ($^{3}J_{HH}$ = 1.2/8.3 Hz, H-2'/6'), δ_H 7.47 ($^{3}J_{HH}$ = 7.4/8.3 Hz, H-3'/5') and δ_H 7.59 ($^{3}J_{HH}$ = 7.4/7.4 Hz, H-4'); these signals are characteristic of a mono-substituted aromatic ring. Corresponding ^{13}C chemicals shifts were extracted from the ^{1}H-^{13}C HSQC spectrum at δ_C 130.5 (C-2'/6'), δ_C 129.4 (C-3'/5') and δ_C 134.1 (C-4'). The aromatic ring structure was further determined by $^{3}J_{CH}$ correlations in the ^{1}H-^{13}C HMBC spectrum from H-3'/5' (δ_H 7.47) to a quaternary carbon atom at δ_C 131.6 (C-1'). Another long-range CH-correlation of H-2'/6' (δ_H 8.06) to a carboxyl carbon atom at δ_C 168.1 (C-7') tethered to the C-1' position of the aromatic ring was observed in the HMBC spectrum, confirming the benzoyl moiety. Substitution to the quinic acid moiety was determined by the characteristic low-field shift of the signal of H-5 (δ_H 5.52), indicating substitution at the hydroxyl group at position 5 (δ_C 73.3; δ_H 5.52). Accordingly, the structure of compound **5** was assigned as 5-*O*-benzoyl quinic acid.

The HRESIMS data of compound **6** showed a molecular ion peak of *m/z* 431.0986 [M-H]$^-$, corresponding to a molecular formula of $C_{21}H_{20}O_{10}$ (calcd for $C_{21}H_{19}O_{10}$, *m/z* 431.0984). The ^{1}H NMR, ^{1}H-^{1}H COSY, ^{1}H-^{13}C HSQC

and the ^{1}H-^{13}C HMBC spectra of compound **6** (Table 2) showed signals of a quinic acid as well as two salicyloyl moieties. The ^{1}H NMR spectra showed characteristic low-field shifts for H-3 (δ_H 5.95) and H-4 (δ_H 5.28), suggesting a bis-substituted quinate. Due to overlapping signals, selective TOCSY together with ^{1}H-^{1}H COSY and ^{1}H-^{13}C HSQC were employed to extract the chemical shifts of both salicyloyl moieties. Connectivities between quinate and salicyloyl moieties were established by ^{1}H-^{13}C long-range correlations of H-3 to δ_C 169.3 (C-7′) and of H-4 to δ_C 170.6 (C-7″), both characterized as carboxyl carbons of the respective salicyloyl units. Accordingly, the structure of compound **6** was assigned as 3-*O*,4-*O*-disalicyloyl quinic acid.

The HRESIMS spectra of compounds **7** and **8** showed molecular ion peaks of *m/z* 431.0985 $[M-H]^-$ and 431.0987 $[M-H]^-$, respectively. As in compound **6**, both values corresponded to a molecular formula of $C_{21}H_{20}O_{10}$ (calcd for $C_{21}H_{19}O_{10}$, *m/z* 431.0984). ^{1}H NMR, ^{1}H-^{1}H COSY, ^{1}H-^{13}C HSQC and the ^{1}H-^{13}C HMBC spectra showed almost the same signals (Table 2), indicating quinic acid esters with salicyloyl moieties as substituents. The structures were characterized by ^{1}H-^{13}C long-range correlations as well as the characteristic chemical shifts of ^{1}H NMR signals for H-3, H-4 and H-5. For compound **7**, we observed low-field shifts for H-3 (δ_H 5.708) and H-5 (δ_H 5.712), suggesting acylation at this positions. The assumption was proven by $^{3}J_{CH}$ correlations of H-3 to δ_C 169.8 (C-7′) and of H-5 to δ_C 170.3 (C-7″), indicating C-7′ and C-7″ as carboxyl carbons of two different salicyloyl moieties. Likewise, for compound **8**, we observed low-field shifts for H-4 at δ_H 5.42, which further showed a $^{3}J_{CH}$ correlation to δ_C 170.5 (C-7′). The ^{1}H NMR signal of H-5 appeared at δ_H 5.95 with a $^{3}J_{CH}$ correlation to δ_C 170.4 (C-7″). Accordingly, the structures of the compounds **7** and **8** were assigned as 3-*O*,5-*O*-disalicyloyl quinic acid and 4-*O*,5-*O*-disalicyloyl quinic acid, respectively.

The HRESIMS spectra of compound **9** showed a molecular ion peak of *m/z* 415.1038 $[M-H]^-$ corresponding to a molecular formula of $C_{21}H_{20}O_9$ (calcd for $C_{21}H_{19}O_9$, *m/z* 415.1035). The NMR data (Table 3) extracted from the ^{1}H NMR, ^{1}H-^{1}H COSY, ^{1}H-^{13}C HSQC and the ^{1}H-^{13}C HMBC spectra were very similar to those of compounds **1** and **6**. Accordingly, the presence of a salicyloyl quinate unit was suggested. Furthermore, signals of a benzoyl moiety as described for compound **4** were observed as a substituent of quinic acid. The ^{1}H NMR spectra showed characteristic low-field shifts for H-3 (δ_H 5.93) and H-4 (δ_H 5.22), suggesting substitution at those positions. Cross-signals observed in the ^{1}H-^{13}C HMBC between H-3 and the carboxylic carbon atom C-7′ (δ_C 169.5) of the salicyloyl moiety proved the substitution in position C-3 of the quinic acid via an ester bond. An additional $^{3}J_{CH}$ correlation of H-4 to the carboxylic carbon atom C-7″ (δ_C 167.2) of the benzoyl moiety revealed another esterification. Accordingly, the structure of compound **9** was assigned as 3-*O*-salicyloyl-4-*O*-benzoyl quinic acid.

Like the data for compound **9**, the HRESIMS data for compounds **10** and **11** showed a molecular ion peak of 415.1038 $[M-H]^-$ corresponding to a molecular formula of $C_{21}H_{20}O_9$ (calcd for $C_{21}H_{19}O_9$, *m/z* 415.1035). The NMR data for both compounds (Table 3) were very similar to those of **9**, suggesting acylated quinic acid derivatives with mixed salicyloyl and benzoyl substituents. The structures of compounds **10** and **11** were elucidated by characteristic ^{1}H NMR chemical shifts and ^{1}H-^{13}C long-range correlations as described for compounds **6**-**8**. For compound **10**, substitution with a salicyloyl group in position 3 (δ_C 74.4; δ_H 5.71) and with the benzoyl unit in position 5 (δ_C 72.9; δ_H 5.56) of the quinic acid was observed. For compound **11**, salicyloyl substitution was observed at position 4 (δ_C 77.6; δ_H 5.41), and benzoylation was found at position 5 (δ_C 69.8; δ_H 5.91) of the quinic acid moiety. Accordingly,

the structures were assigned as 3-*O*-salicyloyl-5-*O*-benzoyl quinic acid (**10**) and 4-*O*-salicyloyl-5-*O*-benzoyl quinic acid (**11**).

Qualitative Analysis of C. vinula *Hemolymphs.* Hemolymph samples of six larvae were analyzed by UHPLC-ESI-MS/MS. Mass spectra were scanned for the presence of the molecular ions of compounds **1-11** (*m/z* 311, 295, 431, 415 ± 0.5 $[M-H]^-$) as well as for the molecular ions of salicortin (**12**, *m/z* 424 ± 0.5 $[M-H]^-$) and salicin (*m/z* 285 ± 0.5 $[M-H]^-$). None of these compounds were detected. Data are provided in Supplementary data (SI D.1 and D.2).

Analysis of C. vinula *Feces after* ^{13}*C-Labeled Salicortin Feeding.* In order to investigate a possible precursor-product relationship of salicortin with the metabolites **1-11**, leaves of *P. nigra* were spotted with [U-^{13}C]salicortin (82% ^{13}C), as described in the Material and methods section (2.5), and subsequently fed to *C. vinula* larvae. The feces of larvae were extracted and analyzed by NMR and UHPLC-HRMS (see Supplementary data, C.2 and C.3). All larvae survived the feeding experiment without exhibiting negative effects arising from an elevated salicortin intake.

The ^{13}C NMR spectrum of the feces extract from the [U-^{13}C]salicortin feeding experiment showed signals characteristic for compounds **1-11**. Pronounced ^{13}C satellites appeared for signals of salicylates around δ_C 170, δ_C 165 and δ_C 135 – 130. No ^{13}C enrichment was found for glucosyl or quinate moieties (SI C.2-1 to C.2-5). Further structure elucidation was accomplished by 2D ^{1}H-^{13}C correlation spectroscopy. ^{1}H-^{13}C HSQC allowed for the identification of protons attached to the ^{13}C-enriched positions. The associated spin systems were assigned by selective TOCSY experiments to δ_H 7.93 (dd, $^3J_{HH}$ = 1.8/8.0 Hz)/δ_C 131.0, δ_H 7.98 (dd, $^3J_{HH}$ = 1.9/8.0 Hz)/δ_C 131.7 and δ_H 8.04 ($^3J_{HH}$ = 1.8/8.0 Hz)/δ_C 131.3, corresponding to salicylic acid moieties such as those observed for compounds **1-3** and **6-11**. The ^{1}H-^{13}C HMBC spectrum showed correlations of the salicylic acid moiety protons at δ_H 7.93 (δ_C 131.0; C-6), δ_H 7.98 (δ_C 131.6; C-6) and δ_H 8.04 (δ_C 131.3; C-6), with carbon atoms resonating at δ_C 136.7/136.5/136.2 (C-4), δ_C 162.1/162.8 (C-2) and δ_C 171.0/171.2/171.5 (C-7; COOH). ^{13}C-^{13}C Satellite signals for all those carbon signals indicated multiple ^{13}C enrichment of the salicyloyl moieties.

Interestingly, no ^{13}C-^{13}C satellites and thus no ^{13}C enrichment were observed for the benzoyl units. The low intensity of the ^{1}H-^{13}C HMBC correlations of the benzoyl protons at δ_H 8.09 (δ_C 130.5; C-2/6) and δ_H 8.13 (δ_C 130.6; C-2/6) with δ_C 134.0 (C-4) and δ_C 168.1 (C-7; COOH) (Fig. 3 and SI C.2-6 to C.2-17) confirmed that the benzoyl units remained unlabeled.

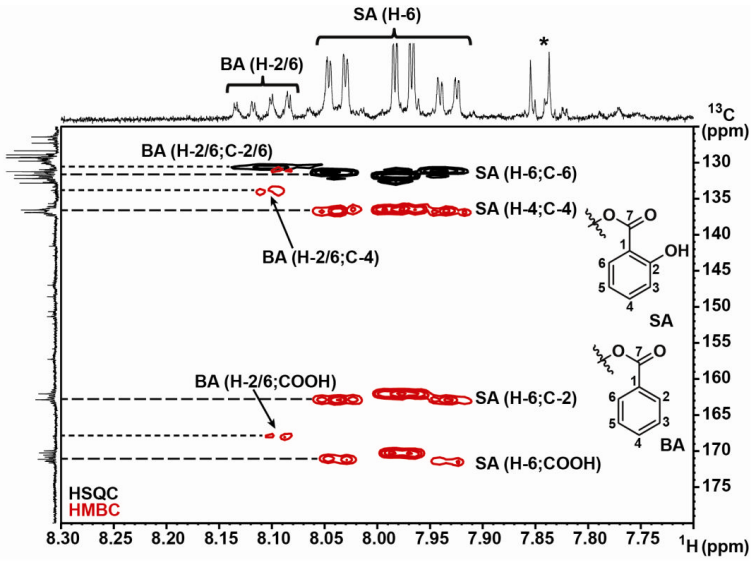

Fig. 3 Superimposed ^{1}H-^{13}C HSQC (black) and HMBC spectra (red) (500 MHz, MeOH-d_4) of *C. vinula* frass extract demonstrating ^{13}C enrichment of salicyloyl (SA) units but not of benzoyl (BA) units from [U-^{13}C]salicortin feeding. Top: Partial ^{1}H NMR spectrum showing signals of BA and SA. In the ^{13}C NMR spectrum (125 MHz) on the left, resonances of salicyloyl substituents show coupling patterns indicative of ^{13}C-enrichment. Cross-signals of * are not shown.

Furthermore, UHPLC-HRMS spectra of the frass extract of *C. vinula* larvae fed with [U-^{13}C]salicortin showed ^{13}C-isotopologue patterns from $[M-H+3]^-$ up to $[M-H+7]^-$ (Fig. 4; C.3-1 to C.3-23). Remarkably, only salicylate-containing quinate esters, mono-salicyloyl quinates **1-3**, di-salicyloyl quinates **6-8** and salicyloyl-benzoyl quinates **9-11**, were labeled, and benzoyl quinates **4** and **5** showed no ^{13}C enrichment. The incorporation of ^{13}C from [U-^{13}C]salicortin into the salicyloyl moiety of the acylated quinic acids **1-3** and **6-11** clearly indicated a substrate-product relationship. Accordingly, we concluded that the acylated quinic acids were downstream products of the salicortin metabolism in *C. vinula*.

Another seven (up to $[M-H+14]^-$) isotopologue peaks are present in the spectra of di-salicyloyl quinates **6-8**. The $[M-H+8]^-$ peak may be due to the presence of a natural abundance $^{13}C_1$ quinate or a $^{13}C_1$ salicyloyl substituent, in addition to the $^{13}C_7$-labeled first salicyloyl unit.

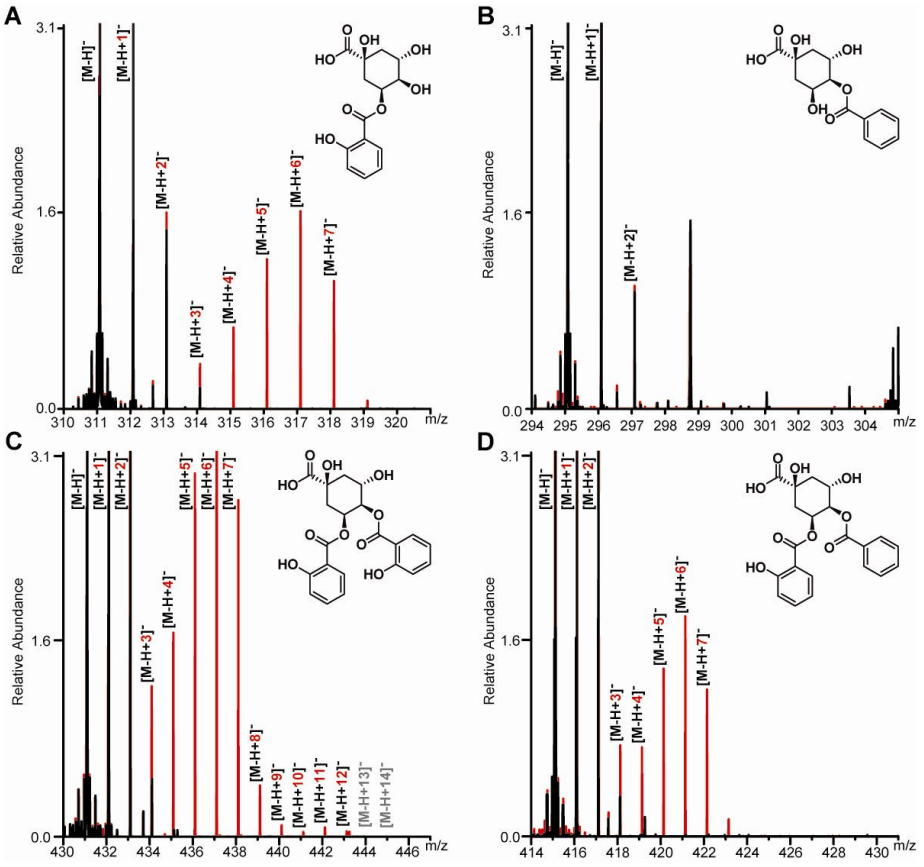

Fig. 4 Superimposed extracted ion HRMS spectra of the four acylated quinic acid groups – mono-salicyloyl quinates, mono-benzoyl quinates, di-salicyloyl quinates and salicyloyl-benzoyl quinates – isolated from the frass of *C. vinula* larva reared on [U-^{13}C]salicortin-coated *P. nigra* leaves (red) and unlabeled leaves (black). The groups are represented by compounds **1** (**A**), **4** (**B**), **6** (**C**) and **9** (**D**). The gray labeled isotopologue signals in panel **C** are very weak and thus not visible in this magnification.

DISCUSSION

The chemical defense of poplar is based on abundant phenolic glycosides, such as salicortin and tremulacin, which can make up to 4% of the leaf dry mass (Boeckler et al., 2011; Donaldson et al., 2006). It is widely accepted that the digestive activation of salicinoids leads to toxic products warding off non-adapted herbivores. For salicortin, it has been proposed that activation proceeds through deglucosylation by β-glucosidases (Clausen et al., 1990; Lindroth, 1988; Pentzold et al., 2014). The aglycon is hydrolyzed in the alkaline gut environment to saligenin and a 1-

hydroxy-6-oxocyclohex-2-en-1-oyl (HCH) fragment (Haruta et al., 2001; Julkunen-Tiitto and Meier, 1992). The latter is believed to be oxidized to pyrocatechol and finally to *o*-quinone (Appel, 1993; Barbehenn et al., 2010; Knuth et al., 2011; Ruuhola et al., 2003). *o*-Quinone has a high potential to bind to a variety of biomolecules, including amino acids and proteins (Haruta et al., 2001; Smith, 1985). Saligenin was proposed to serve as a disruptor of oxidative phosphorylation in mitochondria and thus to inhibit ATP synthesis in cell respiration (Terada, 1990). Generalist lepidopteran species, such as the gypsy moth (*L. dispar*), have developed another strategy of detoxification (Boeckler et al., 2016). These insects detoxify salicortin and tremulacin, the major salicinoids in *Populus nigra*, into typical phase II products (Grant, 1991), with salicin as the major metabolite (Boeckler et al., 2016).

The compounds **1-11** described in the present work are new quinic acid derivatives, isolated from the feces of *C. vinula*. The quinic acid moiety is substituted with either one or two salicylate units (**1-3**, **6-8**), benzoate units (**4**, **5**) or one of each units (**9-11**). Compound **4** is the only compound that has been previously reported, namely as a constituent of fruits of *Ficus hirta* (Wan, 2016). The results show that conjugation with quinic acid plays a decisive role in the transformation of salicinoids by *C. vinula*. Unlike in *L. dispar*, deglycosylation is an important feature of the metabolism of *C. vinula*, as glycosidic compounds or free sugars are absent in the frass extract. Generally, the salicinoid breakdown follows the reported route (Clausen et al., 1990; Lindroth, 1988; Pentzold et al., 2014). The structural diversity of the compounds – namely, the differential substitution of quinic acid with salicylate or benzoate – can be rationalized by acyl migration under basic conditions as present in the insect gut (Appel and Martin, 1990). An enzymatic and hence stereospecific conjugation with quinic acid may take place at first, but those products rapidly isomerize later on.

The question of whether the source of salicyloyl units in quinic acid derivatives **1-11** were indeed salicinoid glycosides was tackled by labeling experiments. *C. vinula* larvae were allowed to feed on leaves of *P. nigra* spotted with [U-^{13}C]salicortin (82%). Extracts of feces were analyzed by means of NMR and HRMS. The resulting data were screened for isotopic incorporation into **1-11**. The isotopologue pattern of both NMR and HRMS spectra indicated differences in the incorporation of labeled salicortin into mono-salicyloyl quinic acids (**1-3**), mono-benzoyl quinic acids (**4**, **5**), bis-salicyloyl quinic acids (**6-8**) and salicyloyl-benzoyl quinic acids (**9-11**). NMR data showed enrichment of ^{13}C only in the salicyloyl moiety of quinic acid derivatives (Fig. 3). ^{13}C enrichment was further supported by HRMS data (Fig. 4) which showed a specific isotopologue pattern spanning from $[M\text{-}H]^-$ to $[M\text{-}H+7]^-$ for **1-3**. The HRMS spectra of **4** and **5** did not show additional ^{13}C-isotopologue signals. Thus, neither quinic acid nor benzoyl moieties is thought to represent a downstream product of the [U-^{13}C]salicortin precursor. This suggestion was further reflected in the HRMS data of **6-11**. Whereas mixed salicyloyl-benzoyl substituted compounds show only isotopologue signals up to $[M\text{-}H+7]^-$, the bis-salicyloyl derivatives show signals up to $[M\text{-}H+14]^-$.

Accordingly, this finding is a clear evidence that saligenin is transformed into salicylic acid. We assume that structurally similar salicinoids are transformed in an analogous manner. No ^{13}C incorporation was detected in the quinic acid moieties of **1-11**. Therefore, quinic acids likely originate from chlorogenic acids (caffeoyl quinates),

which have already been described as leaf constituents of the Salicaceae (Júnior et al., 2016; Caseys et al., 2015; Glynn et al., 2004).

In our search for break-down products related to the HCH-moiety of salicortin, we did not find any further ^{13}C-labeled compound. Therefore, we speculate that there is a mechanism by which HCH degradation yields salicylic acid (Fig. 5). Under basic conditions, the HCH fragment could rearrange to an HCH-enolate followed by a spontaneous dehydration to form salicylic acid. The feasibility of such a transformation was observed in synthetic studies (Nagasawa et al., 2010). The origin of benzoyl substituents in **4**, **5**, **9**, **10** and **11** are likely common Salicaceae leaf constituents, such as chaenomeloidin, nigracin, populin, salireposid, tremulacin or tremuloidin (Boeckler et al., 2011).

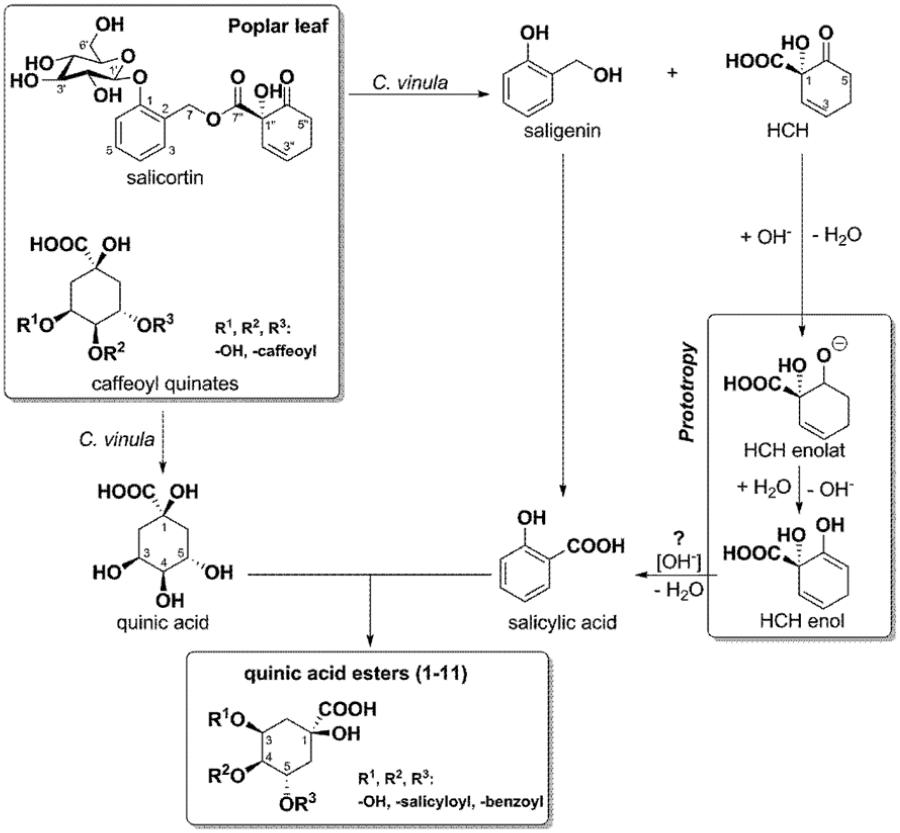

Fig. 5 Conversion of *Populus* leaf constituents to acylated quinic acid derivatives in the *C. vinula* larval gut.

REFERENCES

Ali JG, Agrawal AA (2012) Specialist versus generalist insect herbivores and plant defense. Trends Plant Sci. 17(5):293-302.

Appel HM, Martin MM (1990) Gut redox conditions in herbivorous lepidopteran larvae. J. Chem. Ecol. 16(12):3277-3290.

Appel HM (1993) Phenolics in ecological interactions: The importance of oxidation. J. Chem. Ecol. 19(7):1521-1552.

Barbehenn R, Dukatz C, Holt C, Reese A, Martiskainen O, Salminen J-P, Yip L, Tran L, Constabel CP (2010) Feeding on poplar leaves by caterpillars potentiates foliar peroxidase action in their guts and increases plant resistance. Oecologia 164(4):993-1004.

Boeckler GA, Gershenzon J, Unsicker SB (2011) Phenolic glycosides of the salicaceae and their role as anti-herbivore defenses. Phytochemistry 72(13):1497-1509.

Boeckler GA, Paetz C, Feibicke P, Gershenzon J, Unsicker SB (2016) Metabolism of poplar salicinoids by the generalist herbivore *Lymantria dispar* (Lepidoptera). Insect Biochem. Mol. Biol. 78:39-49.

Calixto Júnior JT, de Morais SM, Gomez CV, Molas CC, Rolon M, Boligon AA, Athayde ML, de Morais Oliveira CD, Tintino SR, Henrique Douglas MC (2016) Phenolic composition and antiparasitic activity of plants from the Brazilian Northeast "Cerrado". Saudi J. Biol. Sci. 23(3):434-440.

Caseys C, Stritt C, Glauser G, Blanchard T, Lexer C (2015) Effects of hybridization and evolutionary constraints on secondary metabolites: The genetic architecture of phenylpropanoids in European *Populus* species. Plos One 10(5):23.

Chen W-P, Yang X-Y, Harms GL, Gray WM, Hegeman AD, Cohen JD (2011) An automated growth enclosure for metabolic labeling of *Arabidopsis thaliana* with ^{13}C-carbon dioxide - an *in vivo* labeling system for proteomics and metabolomics research. Proteome Sci. 9(1): 9.

Clausen TP, Koller JW, Reichardt PB (1990) Aglycone fragmentation accompanies β-glucosidase catalyzed hydrolysis of salicortin, a naturally-occurring phenol glycoside. Tetrahedron Lett. 31(32):4537-4538.

Clausen TP, Reichardt PB, Bryant, JP, Werner RA, Post K, Frisby K (1989) Chemical model for short-term induction in quaking aspen (*Populus tremuloides*) foliage against herbivores. J. Chem. Ecol. 15(9):2335-2346.

du Rand EE, Smit S, Beukes M, Apostolides Z, Pirk CWW, Nicolson SW (2015) Detoxification mechanisms of honey bees (*Apis mellifera*) resulting in tolerance of dietary nicotine. Sci. Rep. 5:11779.

Donaldson JR, Stevens MT, Barnhill HR, Lindroth RL (2006) Age-related shifts in leaf chemistry of clonal aspen (*Populus tremuloides*). J. Chem. Ecol. 32(7):1415-1429.

Eisenreich W, Huber C, Kutzner E, Knispel N, Schramek N (2013) Isotopologue profiling – Toward a better understanding of metabolic pathways. In: Weckwerth W, Kahl G (ed.). The Handbook of Plant Metabolomics. Wiley-VCH Verlag GmbH & Co. KGaA. pp 25-56.

Feistel F, Paetz C, Lorenz S, Schneider B, (2015) The absolute configuration of salicortin, HCH-salicortin and tremulacin from *Populus trichocarpa x deltoides* Beaupré. Molecules 20(4):5566-5573.

Giraudo M, Hilliou F, Fricaux T, Audant P, Feyereisen R, Le Goff G (2015) Cytochrome P450s from the fall armyworm (*Spodoptera frugiperda*): responses to plant allelochemicals and pesticides. Insect Mol. Biol. 24(1):115-128.

Glynn C, Ronnberg-Wastljung AC, Julkunen-Tiitto R, Weih M (2004) Willow genotype, but not drought treatment, affects foliar phenolic concentrations and leaf-beetle resistance. Entomol. Exp. Appl. 113(1):1-14.

Grant DM (1991). Detoxification pathways in the liver. J. Inherited Metab. Dis. 14(4):421-430.

Haruta M, Pedersen JA, Constabel CP (2001) Polyphenol oxidase and herbivore defense in trembling aspen (*Populus tremuloides*): cDNA cloning, expression, and potential substrates. Physiol. Plant. 112(4):552-558.

Hintze-Podufal C (1970) Über die quantitativen Änderungen der Kotabgabe während der Larvalentwicklung von *Cerura vinula* L. (Lepidoptera). Oecologia 5(4):334-346.

Julkunen-Tiitto R, Meier B (1992) The enzymatic decomposition of salicin and its derivatives obtained from salicaceae species. J. Nat. Prod. 55(9):9.

Knuth S, Schübel H, Hellemann M, Jürgenliemk G (2011) Catechol, a bioactive degradation product of salicortin, reduces TNF-α induced ICAM-1 expression in human endothelial cells. Planta Med. 77(10):1024-1026.

Lindroth RL (1988) Hydrolysis of phenolic glycosides by midgut β-glucosidases in *Papilio glaucus* subspecies. Insect Biochem. 18(8):789-792.

Lindroth RL (1991) Biochemical ecology of *Aspen-Lepidoptera* interactions. J. Kans. Entomol. Soc. 64(4):372-380.

Lindroth RL, Hemming JDC (1990) Responses of the gypsy moth (Lepidoptera: Lymantriidae) to tremulacin, an aspen phenolic glycoside. Environ. Entomol. 19(4):842-847.

Nagasawa T, Shimada N, Torihata M, Kuwahara S (2010) Enantioselective total synthesis of idesolide via $NaHCO_3$-promoted dimerization. Tetrahedron 66(27-28):4965-4969.

Palo RT (1984) Distribution of birch (*Betula* spp.), willow (*Salix* spp.), and poplar (*Populus* spp.) secondary metabolites and their potential role as chemical defense against herbivores. J. Chem. Ecol. 10(3):499-520.

Pauli GF, Poetsch F, Nahrstedt A (1998) Structure assignment of natural quinic acid derivatives using proton nuclear magnetic resonance techniques. Phytochem. Anal. 9(4):177-185.

Pentzold S, Zagrobelny M, Rook F, Bak S (2014) How insects overcome two-component plant chemical defence: plant *β*-glucosidases as the main target for herbivore adaptation. Biol. Rev. Cambridge Philos. Soc. 89(3):531-551.

Ruuhola T, Julkunen-Tiitto R, Vainiotalo P (2003) *In vitro* degradation of willow salicylates. J. Chem. Ecol. 29(5):1083-1097.

Ruuhola T, Tikkanen O-P, Tahvanainen J (2001) Differences in host use efficiency of larvae of a generalist moth, *Operophtera brumata* on three chemically divergent *Salix* species. J. Chem. Ecol. 27(8):1595-1615.

Smith MT (1985) Quinones as mutagens, carcinogens, and anticancer agents: introduction and overview. J. Toxicol. Environ. Health 16(5):665-672.

Terada H (1990) Uncouplers of oxidative phosphorylation. Environ. Health Perspect. 87:213-218.

Thieme H (1964) Isolierung eines neuen Phenolglucosids aus *Salix purpurea* L. Pharmazie 19:725.

Wan C, Han J, Chen C, Yao L, Chen J, Yuan T (2016) Monosubstituted benzene derivatives from fruits of *Ficus hirta* and their antifungal activity against phytopathogen *Penicillium italicum*. J. Agric. Food Chem. 64(28):5621-5624.

Figure 1

Click here to download Figure Fig-1.tif

mono-salicyloyl quinates — calcd [M-H]⁻ *m/z*

1: R^1-SA R^2-OH R^3-OH
2: R^1-OH R^2-SA R^3-OH
3: R^1-OH R^2-OH R^3-SA

311.0772

mono-benzoyl quinates

4: R^1-OH R^2-BA R^3-OH
5: R^1-OH R^2-OH R^3-BA

295.0823

bis-salicyloyl quinates

6: R^1-SA R^2-SA R^3-OH
7: R^1-SA R^2-OH R^3-SA
8: R^1-OH R^2-SA R^3-SA

431.0984

salicyloyl-benzoyl quinates

9: R^1-SA R^2-BA R^3-OH
10: R^1-SA R^2-OH R^3-BA
11: R^1-OH R^2-SA R^3-BA

415.1035

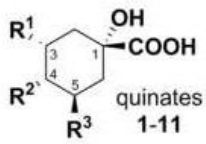

quinates **1-11**

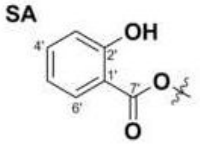

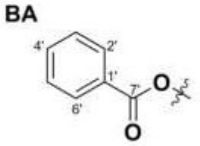

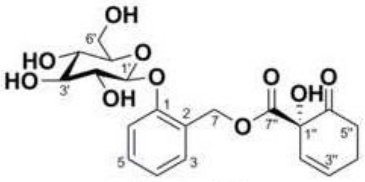

salicortin (**12**)

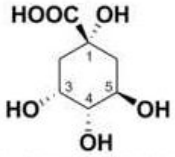

quinic acid (**13**)

Figure 2

Click here to download Figure Fig-2.tif

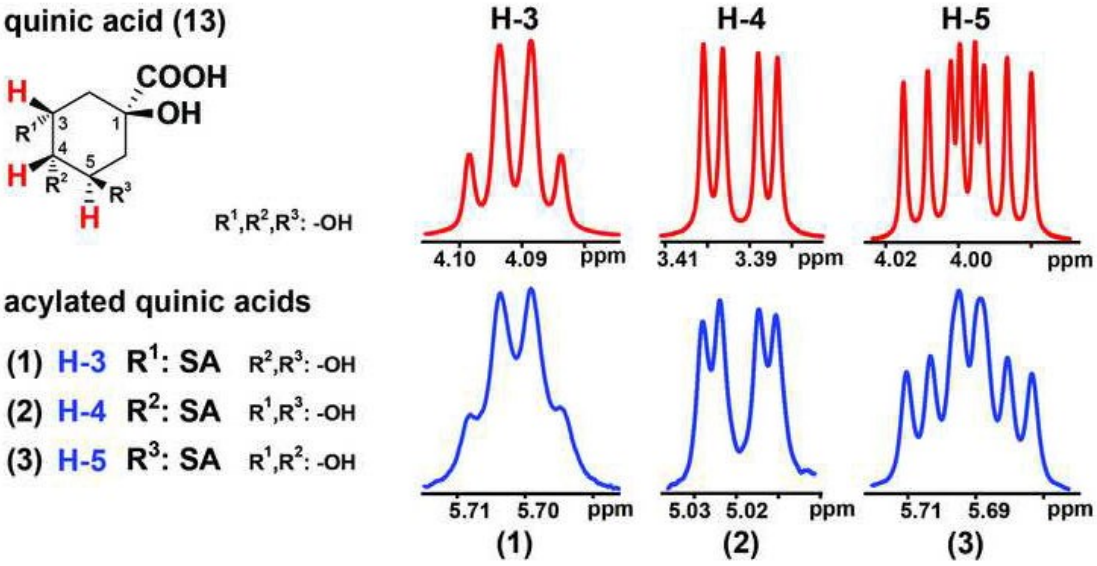

Figure 3

Click here to download Figure Fig-3.tif

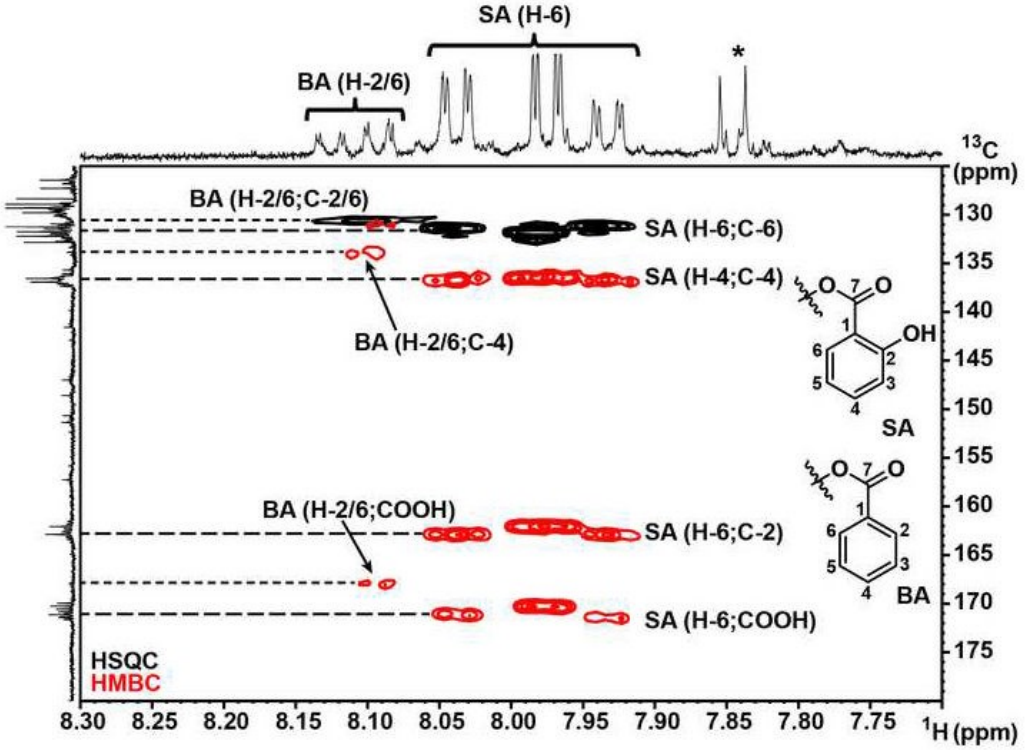

Figure 4

Click here to download Figure Fig-4.tif

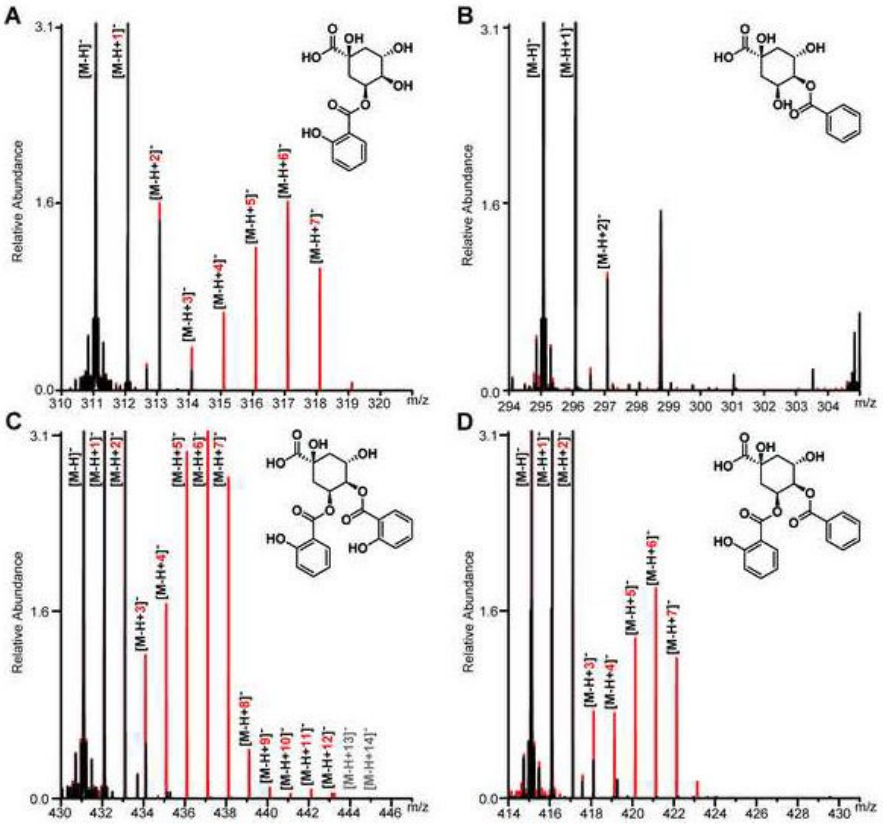

Figure 5

Click here to download Figure Fig-5.tif

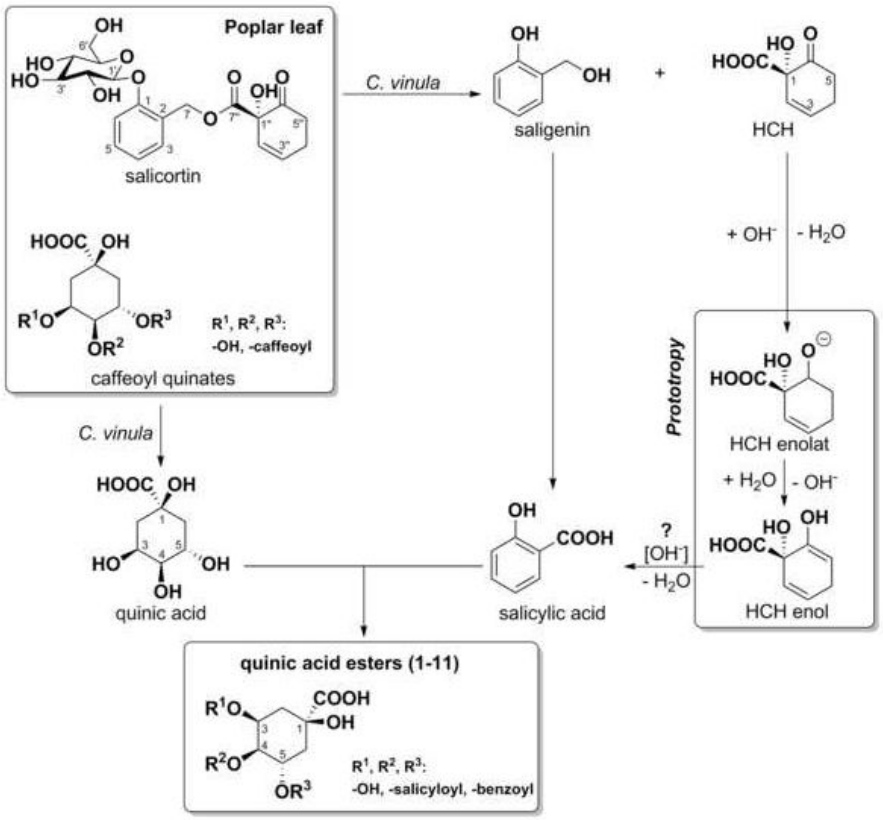

Table 1

Click here to download Table Table-1.docx

Table 1

^{1}H NMR (700 MHz) and ^{13}C NMR (175 MHz) data of compounds **1-4** in MeOH-d_4.

Position	1		2		3		4	
	δ_H mult. (*J* in Hz)	δ_C	δ_H mult. (*J* in Hz)	δ_C	δ_H mult. (*J* in Hz)	δ_C	δ_H mult. (*J* in Hz)	δ_C
1		80.3		76.4		76.2		76.5
2a	2.35 *dd* (3.1/14.4)	36.8	2.12 *dd* (2.8/14.5)	38.3	2.22 *dd* (2.3/14.1)	38.6	2.19 *dd* (2.6/13.6)	39.1
2b	2.11 *dd* (3.1/14.4)		2.07 *ddd* (2.6/3.8/14.5)		2.06 *dd* (4.4/14.1)		2.06 *dd* (2.7/13.6)	
3	5.70 *ddd* (3.1/3.4/3.1)	72.8	4.35 *ddd* (2.8/2.9/3.8)	69.5	4.19 *ddd* (2.3/3.2/4.4)	71.3	4.37 *ddd* (2.2/2.6/2.7)	68.7
4	3.60 *dd* (3.4/9.5)	75.6	5.02 *dd* (2.9/9.4)	80.0	3.83 *dd* (3.2/8.4)	72.9	5.02 *dd* (2.2/7.8)	79.1
5	4.06 *ddd* (4.6/9.5/12.0)	68.0	4.39 *ddd* (4.7/9.4/10.8)	65.6	5.55 *ddd* (3.6/8.4/9.6)	73.3	4.29 *ddd* (5.4/7.8/9.8)	66.3
6a	2.10 *dd* (12.0/12.5)	42.5	2.20 *ddd* (2.6/4.7/13.3)	42.0	2.28 *dd* (3.6/13.1)	38.6	2.15 *dd* (5.4/14.5)	39.1
6b	1.77 *dd* (4.6/12.5)		1.89 *dd* (10.8/13.3)		2.21 *dd* (9.6/13.1)		2.05 *dd* (9.8/14.5)	
7		182.6		181.8		177.5		179.8
1'		115.2		113.8		113.5		131.5
2'		159.9		162.6		162.7	8.13 *dd* (0.9/8.0)	130.6
3'	6.62 *dd* (0.8/8.3)	118.8	6.95 *d* (8.5)	118.0	6.94 *dd* (0.8/8.4)	118.0	7.49 *dd* (8.0/7.6)	129.2
4'	7.21 *ddd* (1.5/7.3/8.3)	135.5	7.49 *ddd* (1.6/7.4/8.5)	136.8	7.48 *ddd* (1.3/7.2/8.4)	136.6	7.61 *dd* (7.6/7.6)	134.0
5'	6.60 *ddd* (0.8/6.9/7.3)	119.5	6.93 *dd* (7.4/7.4)	120.0	6.91 *ddd* (0.8/7.2/8.0)	120.1	7.49 *dd* (8.0/7.6)	129.2
6'	7.44 *dd* (1.4/6.9)	132.5	8.05 *dd* (1.6/7.4)	131.6	7.88 *dd* (1.3/8.0)	131.1	8.13 *dd* (0.9/8.0)	130.6
7'		167.7		170.8		170.7		167.7

Table 2

Click here to download Table Table-2.docx

Table 2

^{1}H NMR (700 MHz) and ^{13}C NMR (175 MHz) data of compounds **5-8** in MeOH-d_4.

Position	5		6		7		8	
	δ_H mult. (*J* in Hz)	δ_C	δ_H mult. (*J* in Hz)	δ_C	δ_H mult. (*J* in Hz)	δ_C	δ_H mult. (*J* in Hz)	δ_C
1		77.3		75.0		79.9		77.3
2a	2.19 *dd* (3.9/13.8)	38.8	2.24 *dd* (2.8/15.1)	42.2	2.26 *dd* (3.2/14.8)	36.6	2.14 *m*	38.4
2b	1.98 *dd* (2.9/13.8)		2.48 *dd* (3.2/15.1)		2.41 *dd* (3.4/14.8)		2.38 *m*	
3	4.15 *ddd* (2.6/2.9/3.9)	72.9	5.95 *ddd* (2.8/3.2/3.4)	70.9	5.71 *ddd* (3.2/3.4/3.4)	74.2	4.49 *ddd* (2.9/3.2/3.6)	69.6
4	3.97 *dd* (2.6/9.4)	74.8	5.28 *dd* (3.4/9.2)	77.3	4.13 *dd* (3.4/8.9)	71.7	5.42 *dd* (2.9/9.4)	76.9
5	5.52 *ddd* (4.9/9.4/11.1)	73.3	4.48 *ddd* (6.6/9.2/10.9)	65.6	5.71 *ddd* (4.8/8.9/11.7)	73.3	5.95 *ddd* (6.7/8.3/9.4)	70.3
6a	2.19 *dd* (11.1/14.9)	40.1	2.13 *dd* (10.9/13.7)	42.2	2.30 *dd* (11.7/12.8)	39.9	2.37 *m*	39.4
6b	2.11 *dd* (4.9/14.9)		2.31 *dd* (6.6/13.7)		2.33 *dd* (4.8/12.8)		2.37 *m*	
7		176.2		177.5		182.3		178.8
1'		131.6		133.8		113.9		113.0
2'	8.06 *dd* (1.2/8.3)	130.5		161.9		162.1		162.1
3'	7.47 *dd* (7.4/8.3)	129.4	6.92 *d* (8.5)	118.5	6.94 *d* (8.5)	118.2	6.88 *d* (8.5)	118.1
4'	7.59 *dd* (7.4/7.4)	134.1	7.48 *ddd* (1.5/7.3/8.5)	136.7	7.47 *ddd* (1.2/6.9/8.5)	136.3	7.42 *ddd* (1.2/8.2/8.5)	137.1
5'	7.47 *dd* (7.4/8.3)	129.4	6.90 *dd* (7.3/7.9)	120.2	6.94 *dd* (6.9/8.0)	120.1	6.85 *dd* (8.0/8.2)	120.4
6'	8.06 *dd* (1.2/8.3)	130.5	7.91 *dd* (1.5/7.9)	131.8	8.04 *dd* (1.2/8.0)	132.2	7.88 *dd* (1.2/8.0)	131.1
7'		168.1		169.3		169.8		170.5
1''				113.4		113.9		113.0
2''				162.4		162.9		162.4
3''			6.93 *d* (8.5)	118.0	6.93 *d* (8.3)	118.1	6.87 *d* (8.5)	118.1
4''			7.44 *ddd* (1.5/7.1/8.5)	136.7	7.49 *ddd* (1.5/6.9/8.3)	136.7	7.43 *ddd* (1.3/7.8/8.5)	137.1
5''			6.74 *dd* (7.1/7.9)	120.0	6.93 *dd* (6.9/8.1)	120.1	6.83 *dd* (7.8/7.8)	120.4
6''			7.62 *dd* (1.5/7.9)	130.9	7.92 *dd* (1.5/8.1)	131.0	7.75 *dd* (1.3/7.8)	130.7
7''				170.6		170.3		170.4

Table 3

Click here to download Table Table-3.docx

Table 3

^{1}H NMR (700 MHz) and ^{13}C NMR (175 MHz) data of compounds **9-11** in MeOH-d_4.

Position	9		10		11	
	δ_H mult. (*J* in Hz)	δ_C	δ_H mult. (*J* in Hz)	δ_C	δ_H mult. (*J* in Hz)	δ_C
1		75.2		75.1		72.9
2a	2.22 *dd* (3.7/14.8)	37.2	2.26 *dd* (5.3/14.8)	36.6	2.11 *dd* (3.7/14.7)	38.7
2b	2.47 *dd* (3.2/14.8)		2.40 *dd* (4.6/14.8)		2.38 *dd* (3.6/14.7)	
3	5.93 *ddd* (3.2/3.3/3.7)	71.0	5.71 *ddd* (2.9/4.9/5.3)	74.4	4.47 *ddd* (3.1/3.6/3.7)	70.0
4	5.22 *dd* (3.3/9.2)	77.0	4.12 *dd* (2.9/8.3)	71.8	5.41 *dd* (3.1/9.5)	77.6
5	4.46 *ddd* (3.7/9.2/9.2)	65.8	5.56 *ddd* (5.6/8.3/10.0)	72.9	5.91 *ddd* (4.2/9.5/11.2)	69.8
6a	2.12 *dd* (9.2/14.4)	42.0	2.29 *dd* (10.0/13.5)	39.2	2.36 *m*	40.0
6b	2.30 *dd* (3.7/14.4)		2.29 *dd* (5.6/13.5)		2.36 *m*	
7		178.5		177.6		178.3
1'		113.8		114.1		113.2
2'		161.9		162.0		162.9
3'	6.92 *dd* (0.7/8.5)	118.3	6.93 *d* (8.2)	118.3	6.87 *dd* (0.5/8.7)	118.1
4'	7.48 *ddd* (1.1/7.5/8.5)	136.6	7.47 *dd* (7.4/8.2)	136.5	7.42 *ddd* (1.9/7.5/8.7)	136.8
5'	6.90 *ddd* (0.7/7.5/7.9)	120.1	6.94 *dd* (7.4/7.5)	120.0	6.83 *ddd* (0.5/7.5/7.9)	120.1
6'	7.88 *dd* (1.1/7.9)	131.8	8.04 *d* (7.5)	132.1	7.88 *dd* (1.9/7.9)	131.2
7'		169.5		169.7		170.9
1''		131.1		131.0		131.2
2''	7.91 *dd* (1.1/8.2)	130.4	8.06 *d* (8.5)	130.5	7.92 *dd* (1.0/8.1)	130.3
3''	7.39 *dd* (7.5/8.2)	129.2	7.49 *dd* (7.4/8.5)	129.2	7.40 *dd* (7.6/8.1)	129.3
4''	7.57 *dd* (7.5/7.5)	134.1	7.61 *dd* (7.4/7.4)	134.1	7.54 *dd* (7.6/7.6)	134.2
5''	7.39 *dd* (7.5/8.2)	129.2	7.49 *dd* (7.4/8.5)	129.2	7.40 *dd* (7.6/8.1)	129.3
6''	7.91 *dd* (1.1/8.2)	130.4	8.06 *d* (8.5)	130.5	7.92 *dd* (1.0/8.1)	130.3
7''		167.2		167.1		167.0

Idesia polycarpa (Salicaceae) leaf constituents and their toxic effect on *Cerura vinula* and *Lymantria dispar* (Lepidoptera) larvae

Felix Feistel, Christian Paetz, Sybille Lorenz, Franziska Beran,
Grit Kunert, Bernd Schneider

Phytochemistry **2017**, Vol. 143, Pp 170-179
doi: 10.1016/j.phytochem.2017.08.008

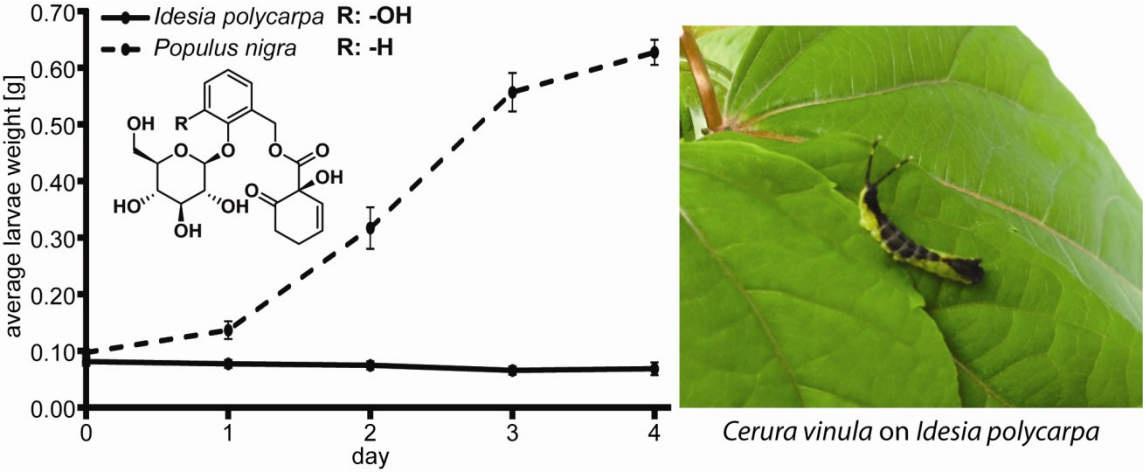

Phytochemistry 143 (2017) 170–179

Contents lists available at ScienceDirect

Phytochemistry

journal homepage: www.elsevier.com/locate/phytochem

Idesia polycarpa (Salicaceae) leaf constituents and their toxic effect on *Cerura vinula* and *Lymantria dispar* (Lepidoptera) larvae

Felix Feistel, Christian Paetz, Sybille Lorenz, Franziska Beran, Grit Kunert, Bernd Schneider*

Max Planck Institute for Chemical Ecology, Hans-Knöll-Straße 8, Beutenberg Campus, D-07745, Jena, Germany

ARTICLE INFO

Article history:
Received 8 June 2017
Received in revised form
1 August 2017
Accepted 7 August 2017

Keywords:
Cerura vinula
Idesia polycarpa
Lymantria dispar
Populus nigra
Salicaceae
Phenolic glycosides

ABSTRACT

Phytochemical investigation of *Idesia polycarpa* (Salicaceae) resulted in the structure elucidation of nine previously undescribed phenolic natural products along with six known compounds. The compounds are structurally related to salicinoids that are known defense compounds from *Salix* and *Populus* species. The *I. polycarpa* diet was toxic, as shown in feeding experiments with larvae of *Lymantria dispar*, an herbivorous broadleaf tree generalist insect, and with larvae of *Cerura vinula*, a specialist adapted to poplar. The survival rate and mass gain of larvae was significantly lower when they fed on *I. polycarpa* leaves, compared to larvae fed on *Populus nigra* leaves. Potential reasons for the poor performance of both herbivores on *I. polycarpa* leaves are discussed.

1. Introduction

Idesia polycarpa is a deciduous tree of the Salicaceae family and the only species of the monotypic genus *Idesia*. Originally native to East Asia, it is now a common ornamental tree worldwide. It forms edible orange berry-like fruits that remain on the tree after leaf senescence. The fruits have been phytochemically investigated, and a variety of compounds, including phenolic glycosides such as idesin, idescarpin (**15**), idesolide, salirepin and phenazine derivatives, were isolated (Chou et al., 1997; Kim et al., 2005; Moritake et al., 1987). Most previous studies focused on pharmaceutical applications. Extracts of *I. polycarpa* were reported to show antioxidant, anti-inflammatory and depigmenting effects (Baek et al., 2006; Ye et al., 2014), inhibition of platelet aggregation (Chou et al., 1997), apoptosis induction (Jung et al., 2010), nitric oxide production (Hwang et al., 2012) and anti-adipogenic activity (Hwang et al., 2012; Lee et al., 2013). The ecological function of compounds of *I. polycarpa*, however, has not yet been investigated. Except for the above-mentioned compounds from the fruit and some from the seed oil (Guo et al., 2012), natural products from other parts of this plant are unknown. Although extracts of *Idesia* seeds and leaves have been traditionally applied as insecticides in the Koreas, surprisingly, the underlying chemistry is still unknown (Kim, 1996; Kim et al., 2005). We isolated the major UV-active metabolites from leaf extracts and elucidated their chemical structures. Most of the compounds show a great similarity to phenolic defense compounds reported from other Salicaceae species, such as *Populus* and *Salix*. We also investigated anti-herbivory properties of *Idesia* leaves in feeding experiments with the larvae of the herbivorous generalist (*Lymantria dispar*) and the specialist (*Cerura vinula*) (both Lepidoptera) which is adapted to thrive on different Salicaceae species including *P. nigra* (Hintze-Podufal, 1970; Robinson et al., 2010).

2. Results and discussion

2.1. Isolation and structure elucidation

An extract of lyophilized leaves of *I. polycarpa* was prepared as described in Experimental. Subfractions of the extract were separated by high performance liquid chromatography coupled to solid phase extraction (HPLC-SPE). The separation resulted in isolation of 15 compounds with nine to-date-unknown natural products (**1**–**9**). Six compounds were formerly described as icaraside B2 (**10**), 4-(*E*)-

* Corresponding author.
E-mail address: schneider@ice.mpg.de (B. Schneider).

http://dx.doi.org/10.1016/j.phytochem.2017.08.008
0031-9422/

p-coumaroyl-glucopyranose (**11**), isograndidentatin (**12**), 1-*O*-(2-hydroxyphenyl)-4-*O*-(*E*)-*p*-coumaroyl-*β*-glucopyranose (**13**), idescarparide (**14**) and idescarpin (**15**) (Fig. 1). Spectroscopic data from the new compounds are shown in Tables 1 and 2 and in Experimental. Data from formerly described but insufficiently characterized compounds are provided in Experimental and Supplementary Data.

The molecular formula of compound **1** was determined to be $C_{17}H_{22}O_9$ by its molecular ion obtained in high resolution electrospray mass spectrometry (HRESIMS) at *m/z* 369.1185 $[M\text{-}H]^-$ (calcd for $C_{17}H_{21}O_9$, *m/z* 369.1191). The ^1H NMR data of compound **1** showed signals (Table 1) assignable to three different structural units with a total of 17 protons. The low-field range of the ^1H NMR spectrum showed a four-spin system (AA'XX') with signals at δ_H 6.84 (H-3″/5″) and δ_H 7.51 (H-2″/6″), both with a coupling constant $^3J_{HH} = 8.7$ Hz, a characteristic of a 1,4-disubstituted aromatic ring. The corresponding ^{13}C chemical shifts were determined by a cross-signal in the ^1H-^{13}C heterocorrelation single quantum coherence (HSQC) spectrum to be δ_C 116.7 (C-3″/5″) and δ_C 131.1 (C-2″/6″), respectively. The structure of the 1,4-disubstituted aromatic ring was corroborated by the ^1H-^{13}C heteronuclear multiple-bond correlation (HMBC) spectrum. The $^3J_{CH}$ correlation of H-2″/6″ with δ_C 161.3 determined C-4″ to be an oxygenated carbon atom. Another HMBC correlation from H-2″/6″ to a methine carbon atom at δ_C 147.1 (δ_H 7.70, $^3J_{HH} = 15.9$ Hz) marked the first position (C-7″) of a π-system tethered to C-1″ (δ_C 127.0) of the aromatic ring. A cross-signal in the ^1H-^1H correlation spectroscopy (^1H-^1H COSY) spectrum identified the second methine proton (H-8″) of the π-system at δ_H 6.40 ($^3J_{HH} = 15.9$ Hz, which is characteristic of an *E*-configuration). The ^{13}C chemical shift value of the corresponding carbon atom (δ_C 114.6, C-8″) was assigned by a ^1H-^{13}C HSQC correlation. Both methines showed long-range CH-correlations to a quaternary carbon atom at δ_C 168.4, which is assignable to C-9″ and, together with the signals of the aromatic ring and the double bond, indicated

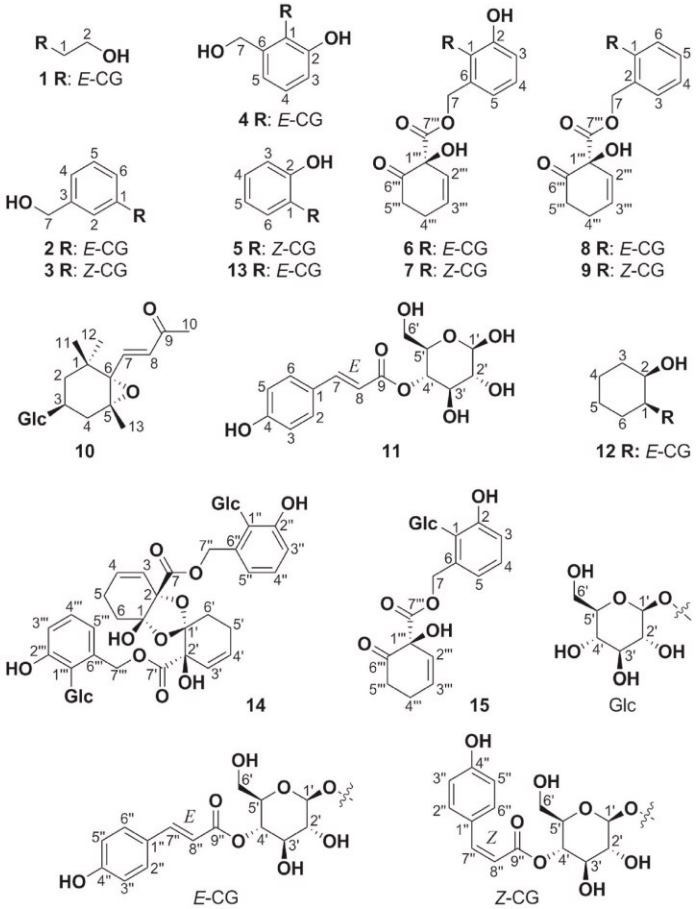

Fig. 1. Phenolic glycosides isolated from leaves of *I. polycarpa*. Compounds **1–9** are new natural products. The substituents are abbreviated as follows: *β*-glucose (Glc), 4-(*E*)-*p*-coumaroyl-*β*-glucopyranose (*E*-CG) and 4-(*Z*)-*p*-coumaroyl-*β*-glucopyranose (*Z*-CG).

Table 1
^{1}H NMR (700 MHz) and ^{13}C NMR data (175 MHz) of compounds **1**–**5** in MeOH-d_4.

Position	**1**		**2**		**3**		**4**		**5**	
	δ_H mult. (*J* in Hz)	δ_C	δ_H mult. (*J* in Hz)	δ_C	δ_H mult. (*J* in Hz)	δ_C	δ_H mult. (*J* in Hz)	δ_C	δ_H mult. (*J* in Hz)	δ_C
1a	3.69 *m*	72.3		159.2		159.0		144.3		146.3
1b	3.98 *m*									
2	3.73 *m*	62.2	7.13 *s*	116.1	7.12 *s*	116.2		150.6		147.7
3				144.5		144.2	6.85 *d* (8.0)	117.2	7.19 *dd* (1.3/8.0)	118.9
4			7.02 *m*	121.8	7.01 *d* (7.9)	121.8	7.03 *dd* (8.0/7.5)	126.7	6.78 *ddd* (1.5/7.6/8.0)	120.8
5			7.27 *dd* (7.8/7.8)	130.2	7.26 *dd* (7.9/8.0)	130.4	6.89 *d* (7.5)	121.0	6.92 *ddd* (1.3/7.6/8.0)	124.8
6			7.03 *m*	116.5	7.01 *d* (8.0)	116.5		136.5	6.84 *dd* (1.5/8.0)	117.0
7a			4.56 *s*	64.8	4.58 *s*	64.8	4.64 *d* (12.7)	60.4		
7b							4.81 *d* (12.7)			
1′	4.38 *d* (7.8)	104.3	4.99 *d* (7.8)	102.2	4.96 *d* (8.0)	102.3	4.68 *d* (8.0)	106.7	4.81 *d* (8.4)	104.1
2′	3.34 *dd* (9.0/7.8)	75.2	3.58 *dd* (7.8/9.3)	74.9	3.57 *dd* (8.0/9.2)	74.9	3.64 *dd* (8.0/9.4)	75.5	3.61 *dd* (8.4/9.4)	74.9
3′	3.65 *dd* (9.0/9.0)	75.4	3.75 *dd* (9.3/9.6)	75.6	3.70 *dd* (9.2/9.1)	76.2	3.72 *dd* (9.4/9.3)	75.6	3.70 *dd* (9.4/9.6)	75.1
4′	4.85 *m*	72.3	4.95 *dd* (9.6/9.9)	72.1	4.94 *dd* (9.1/10.0)	71.7	4.94 *dd* (9.3/9.7)	72.0	4.96 *d* (9.6/9.6)	71.6
5′	3.53 *m*	76.1	3.71 *ddd* (9.9/6.0/2.0)	76.1	3.70 *ddd* (2.0/6.5/10.0)	76.1	3.58 *ddd* (2.0/6.2/9.7)	76.5	3.62 *ddd* (2.0/5.8/9.6)	76.1
6′a	3.54 *dd* (5.6/12.6)	62.3	3.67 *dd* (12.6/6.0)	62.1	3.65 *dd* (6.5/12.3)	62.2	3.63 *dd* (2.0/12.2)	62.2	3.58 *dd* (5.8/12.1)	61.9
6′b	3.62 *dd* (2.0/12.6)		3.58 *dd* (12.6/2.0)		3.57 *dd* (2.0/12.3)		3.58 *dd* (6.2/12.2)		3.67 *dd* (2.0/12.1)	
1″		127.0		127.2		127.5		126.8		127.5
2″	7.51 *d* (8.7)	131.1	7.49 *d* (8.5)	131.1	7.70 *d* (8.6)	133.9	7.47 *d* (8.5)	131.0	7.70 *d* (8.6)	133.8
3″	6.84 *d* (8.7)	116.7	6.82 *d* (8.5)	116.7	6.76 *d* (8.6)	115.8	6.81 *d* (8.5)	116.6	6.76 *d* (8.6)	115.7
4″		161.3		161.6		160.0		161.2		160.0
5″	6.84 *d* (8.7)	116.7	6.82 *d* (8.5)	116.7	6.76 *d* (8.6)	115.8	6.81 *d* (8.5)	116.6	6.76 *d* (8.6)	115.7
6″	7.51 *d* (8.7)	131.1	7.49 *d* (8.5)	131.1	7.70 *d* (8.6)	133.9	7.47 *d* (8.5)	131.0	7.70 *d* (8.6)	133.8
7″	7.70 *d* (15.9)	147.1	7.69 *d* (15.9)	147.2	6.92 *d* (12.7)	145.9	7.67 *d* (16.0)	147.2	6.92 *d* (12.6)	146.0
8″	6.40 *d* (15.9)	114.6	6.39 *d* (15.9)	114.6	5.83 *d* (12.7)	115.9	6.36 *d* (16.0)	114.4	5.82 *d* (12.6)	115.8
9″		168.4		168.5		167.2		168.2		166.9

Table 2
^{1}H NMR (700 MHz) and ^{13}C NMR data (175 MHz) of compounds **6**–**9** in MeOH-d_4.

Position	**6**		**7**		**8**		**9**	
	δ_H mult. (*J* in Hz)	δ_C	δ_H mult. (*J* in Hz)	δ_C	δ_H mult. (*J* in Hz)	δ_C	δ_H mult. (*J* in Hz)	δ_C
1		144.5		144.7		156.8		156.8
2		151.0		150.9		126.0		126.0
3	6.90 *dd* (8.2/1.4)	118.2	6.90 *dd* (1.3/8.1)	118.3	7.31 *d* (7.2)	130.6	7.31 *m*	130.6
4	7.03 *dd* (7.8/8.2)	126.7	7.03 *dd* (8.1/7.9)	126.8	7.04 *dd* (7.2/8.0)	123.5	7.04 *m*	123.5
5	6.80 *dd* (7.8/1.4)	120.9	6.81 *dd* (1.3/7.9)	121.0	7.33 *dd* (8.0/8.6)	131.0	7.33 *m*	131.0
6		131.2		131.2	7.24 *d* (8.6)	116.6	7.22 *d* (8.5)	116.6
7a	5.54 *d* (12.6)	64.7	5.53 *d* (12.6)	64.7	5.28 *d* (12.6)	64.3	5.28 *d* (12.3)	64.3
7b	5.30 *d* (12.6)		5.29 *d* (12.6)		5.40 *d* (12.6)		5.39 *d* (12.3)	
1′	4.72 *d* (8.2)	107.0	4.68 *d* (7.9)	106.9	5.01 *d* (7.8)	102.3	4.99 *d* (7.8)	102.3
2′	3.62 *dd* (8.2/9.0)	75.4	3.61 *dd* (7.9/8.8)	75.4	3.61 *dd* (7.8/9.5)	74.9	3.60 *m*	75.0
3′	3.74 *dd* (9.0/9.5)	75.6	3.69 *dd* (9.7/8.8)	75.4	3.78 *dd* (9.5/10.2)	75.6	3.71 *m*	76.0
4′	4.98 *dd* (9.5/9.0)	71.8	4.96 *dd* (9.7/9.7)	71.4	4.95 *dd* (9.2/10.2)	72.0	4.93 *dd* (9.3/9.8)	71.7
5′	3.57 *ddd* (1.8/6.6/9.0)	76.4	3.50 *ddd* (2.5/6.3/9.7)	76.3	3.70 *m*	76.3	3.64 *m*	76.1
6′a	3.57 *dd* (6.6/12.3)	62.0	3.63 *dd* (2.5/11.8)	62.0	3.58 *m*	62.1	3.64 *m*	62.0
6′b	3.64 *dd* (1.8/12.3)		3.57 *dd* (6.3/11.8)		3.65 *m*		3.57 *m*	
1″		126.9		127.5		126.9		127.4
2″	7.47 *d* (8.6)	131.1	7.68 *d* (8.5)	133.9	7.49 *d* (8.9)	131.1	7.69 d (8.5)	133.8
3″	6.81 *d* (8.6)	116.9	6.77 *d* (8.5)	115.7	6.82 *d* (8.9)	116.8	6.78 d (8.5)	115.7
4″		161.3		160.0		161.3		160.0
5″	6.81 *d* (8.6)	116.9	6.77 *d* (8.5)	115.7	6.82 *d* (8.9)	116.8	6.78 d (8.5)	115.7
6″	7.47 *d* (8.6)	131.1	7.68 *d* (8.5)	133.9	7.49 *d* (8.9)	131.1	7.69 d (8.5)	133.8
7″	7.67 *d* (15.9)	147.2	6.92 *d* (12.6)	146.1	7.69 *d* (15.6)	147.3	6.93 d (12.9)	146.0
8″	6.37 *d* (15.9)	114.5	5.81 *d* (12.6)	114.6	6.39 *d* (15.6)	114.6	5.83 d (12.9)	115.8
9″		168.4		167.2		168.5		167.2
1‴		79.1		79.3		79.1		79.1
2‴	5.75 *ddd* (9.8/1.5/1.5)	129.2	5.74 *ddd* (2.2/2.2/9.7)	129.0	5.77 *ddd* (1.8/1.9/9.7)	129.1	5.77 *m*	129.1
3‴	6.16 *ddd* (9.8/3.6/3.6)	133.0	6.16 *ddd* (3.9/3.9/9.7)	133.3	6.17 *m*	133.2	6.17 *m*	133.2
4‴a	2.64 *m*	27.0	2.64 *m*	27.0	2.52 *m*	27.1	2.52 *m*	26.5
4‴b	2.52 *m*		2.52 *m*		2.65 *m*		2.71 *m*	
5‴a	2.93 *m*	36.9	2.56 *m*	36.8	2.89 *m*	36.8	2.89 *m*	36.8
5‴b	2.57 *m*		2.92 *m*		2.54 *m*		2.54 *m*	
6‴		207.2		206.6		207.4		207.4
7‴		171.5		171.4		171.5		171.5

the presence of an (*E*)-*p*-coumaroyl moiety. The doublet signal of the proton at the anomeric position of a *β*-glycopyranosyl unit appeared at δ_H 4.38 ($^{3}J_{HH}$ = 7.8 Hz; H-1′) in the ^{1}H NMR spectrum. The corresponding ^{13}C chemical shift of C-1′ at δ_C 104.3 was extracted from the ^{1}H-^{13}C HSQC spectrum. Due to overlapping signals, selective total correlation spectroscopy (SELTOCSY)

experiments together with correlation data from ^{1}H-^{13}C HSQC and ^{1}H-^{1}H COSY were employed to extract the chemical shifts and positions of all members of the glycopyranosyl spin system (see Supplementary Data). The large values of the $^{3}J_{HH}$ coupling constants (Table 1) indicated axial configuration throughout the glucosyl ring, thus assigning the sugar unit as glucopyranose with β-configuration at position 1'. Remarkable low-field shifts for the signals of H-4'/C-4' (δ_H 4.85/δ_C 72.3) indicated substitution in this position. This assumption was further supported by the correlation of H-4' to C-9'', which established an ester linkage of the (*E*)-*p*-coumaroyl unit to 4'-OH of the glucopyranosyl ring. A second SELTOCSY experiment was conducted to characterize a remaining AX_2A' spin system comprising two methylene units. Due to asymmetrical substitution, multiplet signals appeared at δ_H 3.69 and δ_H 3.98, with a corresponding ^{13}C chemical shift at δ_C 72.3 (C-1). An HMBC correlation showed this methylene group to be linked to position 1 of the β-glycosyl unit, C-1'. The multiplet signal of H-2/C-2 at δ_H 3.73/δ_C 62.2 indicated a hydroxylated terminus of the AX_2A' spin system. Accordingly, the structure of compound **1** was assigned as 1-*O*-(2-hydroxyethyl)-**4**-*O*-(*E*)-*p*-coumaroyl-β-glucopyranose.

The HRESIMS data of compound **2** showed a molecular ion peak of *m/z* 431.1336 [M-H]$^-$, which is consistent with a molecular formula of $C_{22}H_{24}O_9$ (calcd for $C_{22}H_{23}O_9$, *m/z* 431.1348). As for compound **1**, the ^{1}H NMR, ^{1}H-^{1}H COSY, ^{1}H-^{13}C HSQC and HMBC spectra showed signals of an (*E*)-*p*-coumaroyl unit connected to the 4'-OH position of a glycopyranosyl ring indicating a **4**-(*E*)-*p*-coumaroyl-β-glucopyranose moiety (*E*-CG) (Table 1). Furthermore, the low-field range of the ^{1}H NMR spectrum showed a singlet at δ_H 7.13 (H-2), overlapping signals at δ_H 7.03 (H-6) and δ_H 7.02 (H-**4**) as well as a doublet of doublets at δ_H 7.27 (H-5) with coupling constants of $^{3}J_{HH}$ = 7.8/7.8 Hz. The corresponding ^{13}C chemical shifts were determined by ^{1}H-^{13}C HSQC to be δ_C 121.8 (C-**4**), δ_C 130.2 (C-5), δ_C 116.5 (C-6) and δ_C 116.1 (C-2), respectively. Due to ^{1}H-^{1}H COSY correlations, the signals of H-**4**, H-5 and H-6 were assigned to a three-spin system (AMX) of an aromatic ring. The $^{3}J_{CH}$ correlations of H-2, H-**4** and H-6 in the ^{1}H-^{13}C HMBC spectrum corroborated the assignment of the corresponding carbon signals to a 1,3-disubstituted aromatic ring. The ring geometry was further characterized by long-range C-H correlations from H-5 to the signals of the quaternary carbon atoms at δ_C 159.2 (C-1) and δ_C 144.5 (C-3). HMBC correlations from H-**4** and H-2 to C-7 (δ_C 64.8/δ_H 4.56) established the connection to a terminal hydroxymethylene unit tethered to C-3 of the aromatic ring. The low-field shift of C-1 (δ_C 159.2) indicated oxygenation at this position. This assumption was further supported by HMBC correlations of H-6 and H-2 to C-1' (δ_C 102.2), establishing the linkage via the ester bond to the anomeric carbon atom of the β-glycopyranosyl unit. Accordingly, the structure of compound **2** was assigned as 1-*O*-(3-hydroxymethylphenyl)-**4**-*O*-(*E*)-*p*-coumaroyl-β-glucopyranose.

Compound **3** showed a molecular ion peak of *m/z* 431.1337 [M-H]$^-$ in HRESIMS. As for compound **2**, its mass was consistent with a molecular formula of $C_{22}H_{24}O_9$ (calcd for $C_{22}H_{23}O_9$, *m/z* 431.1348), suggesting isomeric structures for compounds **2** and **3**. Furthermore, a comparison of ^{1}H NMR, ^{1}H-^{1}H COSY, ^{1}H-^{13}C HSQC and ^{1}H-^{13}C HMBC signals with those of **2** (Table 1) revealed a close structural similarity between the two compounds. NMR spectra indicated the presence of compound **2** in sample **3** which might be the result of a spontaneous isomerization. The only difference observed for **3** was a high-field shift of the π-system resonances of the *p*-coumaroyl moiety. The ^{1}H NMR spectrum showed doublet signals at δ_H 6.92 (H-7'') and δ_H 5.83 (H-8''), both with a coupling constant $^{3}J_{HH}$ = 12.7 Hz characteristic of the *Z*-configuration of a C-C double bond. Accordingly, the structure of compound **3** was determined to be 1-*O*-(3-hydroxymethylphenyl)-**4**-*O*-(*Z*)-*p*-coumaroyl-β-glucopyranose.

The HRESIMS data of compound **4** showed a molecular ion peak of *m/z* 447.1287 [M-H]$^-$ consistent with a molecular formula of $C_{22}H_{24}O_{10}$ (calcd for $C_{22}H_{23}O_{10}$, *m/z* 447.1297). The NMR spectra showed the same signals for the *E*-CG unit as spectra of compounds **1** and **2** did. Furthermore, the ^{1}H NMR data (Table 1) showed signals for a three-spin system (AMX) in the low-field region at δ_H 6.85 ($^{3}J_{HH}$ = 8.0 Hz, H-3), δ_H 7.03 ($^{3}J_{HH}$ = 8.0/7.5 Hz, H-**4**) and δ_H 6.89 ($^{3}J_{HH}$ = 7.5 Hz, H-5). The corresponding ^{13}C chemical shifts were determined by ^{1}H-^{13}C HSQC to be δ_C 117.2 (C-3), δ_C 126.7 (C-**4**) and δ_C 121.0 (C-5). The observed chemical shifts together with the $^{3}J_{HH}$ values suggested the presence of a 1,2,3-trisubstituted aromatic ring. This assumption was corroborated by the ^{1}H-^{13}C HMBC spectrum, which showed $^{3}J_{CH}$ correlations of H-3, H-5 and H-**4** to a quaternary carbon atom at δ_C 144.3 (C-1). Additionally, H-**4** showed strong $^{3}J_{CH}$ correlation to two other quaternary carbon atoms at δ_C 150.6 (C-2) and δ_C 136.5 (C-6), respectively, confirming the geometry of the aromatic ring. An HMBC correlation between H-5 and C-7 (δ_C 60.4) established the connection of the hydroxymethylene group to C-6 of the aromatic ring. Because of their large ^{13}C chemical shift values, the quaternary carbon atoms C-1 and C-2 of the ring were determined to be oxygenated. Furthermore, the characteristic high-field shift of C-1 indicated substitution in this position. This assumption was supported by a $^{3}J_{CH}$ correlation between the proton at the anomeric center of the *E*-CG glucose unit at δ_H 4.68 (H-1') and C-1 in the ^{1}H-^{13}C HMBC spectrum. Accordingly, the structure of **4** was assigned as 1-*O*-(2-hydroxy-6-hydroxymethylphenyl)-**4**-*O*-(*E*)-*p*-coumaroyl-β-glucopyranose.

The HRESIMS data of compound **5** showed a molecular ion peak of *m/z* 417.1182 [M-H]$^-$ consistent with a molecular formula of $C_{21}H_{22}O_9$ (calcd for $C_{21}H_{21}O_9$, *m/z* 417.1191). The NMR spectra showed signals of the **4**-(*Z*)-*p*-coumaroyl-β-glucopyranose moiety (*Z*-CG) resembling those observed earlier for compound **3**. Furthermore, the ^{1}H NMR spectrum showed signals (Table 1) assignable to protons of a four-spin system (ABCD) in the low-field region at δ_H 7.19 ($^{3}J_{HH}$ = 8.0/1.3 Hz, H-3), δ_H 6.78 ($^{3}J_{HH}$ = 8.0/7.6/1.5 Hz, H-**4**), δ_H 6.92 ($^{3}J_{HH}$ = 7.6/8.0/1.3 Hz, H-5) and δ_H 6.84 ($^{3}J_{HH}$ = 8.0/1.5 Hz, H-6), characteristic of a 1,2-disubstituted aromatic ring. The corresponding ^{13}C chemical shifts were extracted from ^{1}H-^{13}C HSQC data to be δ_C 117.0 (C-6), δ_C 124.8 (C-5), δ_C 120.8 (C-**4**) and δ_C 118.9 (C-3). The structure was further characterized by ^{1}H-^{13}C HMBC data, showing $^{3}J_{CH}$ correlations of H-**4** with δ_C 146.3 (C-1) and H-5 with δ_C 147.7 (C-2). Because of their high ^{13}C chemical shift values, C-1 and C-2 were assumed to be oxygenated. Another HMBC correlation from the signal of H-1' (δ_H 4.81, $^{3}J_{HH}$ = 8.4) at the anomeric center to C-1 established the ester linkage of the aromatic ring to the β-glucopyranose of the *Z*-CG unit. Accordingly, the structure of compound **5** was assigned as 1-*O*-(2-hydroxyphenyl)-**4**-*O*-(*Z*)-*p*-coumaroyl-β-glucopyranose.

The HRESIMS data of compound **6** showed a molecular ion peak of *m/z* 585.1593 [M-H]$^-$ consistent with a molecular formula of $C_{29}H_{30}O_{13}$ (calcd for $C_{29}H_{29}O_{13}$, 585.1614). The NMR spectra showed signals similar to those observed for compound **4**. Additionally, the ^{1}H NMR spectrum (Table 2) showed two signals of a π-system at δ_H 5.75 ($^{3}J_{HH}$ = 9.8/1.5/1.5 Hz, H-2''') and δ_H 6.16 ($^{3}J_{HH}$ = 9.8/3.6/3.6 Hz, H-3'''). The π-system was attached to two consecutive methylene groups at δ_H 2.64/2.52 (H-4'''a/b) and δ_H 2.93/2.57 (H-5'''a/b), as revealed by ^{1}H-^{1}H COSY cross-signals between H-3''' and H-4'''. The corresponding ^{13}C chemical shifts were determined by ^{1}H-^{13}C HSQC to be δ_C 129.2 (C-2'''), δ_C 133.0 (C-3'''), δ_C 27.0 (C-4''') and δ_C 36.9 (C-5'''). The ^{1}H-^{13}C HMBC spectrum showed a $^{3}J_{CH}$ correlation of H-2''' with a quaternary carbon atom at δ_C 207.4 (C-6'''), which is characteristic of a keto functionality. Another HMBC correlation of H-3''' with a second quaternary carbon atom at δ_C 79.1 (C-1''') was observed, which was determined to

be oxygenated due to its ^{13}C chemical shift value. Further long-range CH-correlations suggested an aliphatic ring structure as corroborated by $^{3}J_{CH}$ correlations of H-5‴a/b to C-6‴ and H-5‴b to C-1‴. The geometry was also supported by $^{3}J_{CH}$ correlations of H-3‴/H-2‴ to C-4‴ and H-3‴ to C-5‴. An additional HMBC correlation of H-3‴ to a third quaternary carbon atom at δ_C 171.5 (C-7‴) indicated the linkage to a carboxyl functionality tethered to position C-1‴ of the aliphatic ring structure, which led to the characterization of the subunit as 1-hydroxy-cyclohex-2-en-6-onoyl moiety (HCH). Because another long-range CH-correlation from the methylene group of the aromatic ring at H-7a/b (δ_H 5.54/5.30; δ_C 64.7) to C-7‴ established the ester linkage of the HCH unit with the rest of the molecule, the structure was characterized as an idescarpin derivative (Fig. 1) with an additional *p*-coumaric acid linked to the 4′-OH of the *β*-glucopyranosyl moiety. Determination of the configuration at position C-1‴ in the HCH moiety was achieved by circular dichroism (CD) spectroscopy. The differential dichroic absorption of $\Delta\varepsilon = -6.9$ mdeg ($\lambda_{max} = 216$ nm, c = 0.75 mM, MeOH) of compound **6** was compared with the reported value of $\Delta\varepsilon = -13.4$ mdeg ($\lambda_{max} = 224$ nm, c = 1.61 mM) for (*S*)-idescarpin (Feistel et al., 2015; Kim et al., 2014). The negative $\Delta\varepsilon$ values reveal the same stereochemistry of **6** and idescarpin. Hence, we concluded that compound **6** had an (*S*)-configuration at the stereogenic position C-1‴. Accordingly, the structure of compound **6** was assigned as 4′-*O*-(*E*)-*p*-coumaroyl-idescarpin.

The HRESIMS data of compound **7** showed a molecular ion peak of *m/z* 585.1601 $[M-H]^-$. As for compound **6**, its mass was consistent with a molecular formula of $C_{29}H_{30}O_{13}$ (calcd for $C_{29}H_{29}O_{13}$, *m/z* 585.1614), suggesting isomeric structures for compounds **6** and **7**. Furthermore, a comparison of ^{1}H NMR, ^{1}H-^{1}H COSY, ^{1}H-^{13}C HSQC and ^{1}H-^{13}C HMBC data with those of compound **6** (Table 2) also suggested both compounds have very similar structures. Signals of compound **6** were also observed in the NMR spectra of compound **7**, which might be due to spontaneous isomerization. Compared to signals seen in the ^{1}H NMR spectrum of compound **6**, the proton signals of the *p*-coumaroyl π-system of compound **7** appeared at a higher field at δ_H 6.92 (H-7″) and δ_H 5.81 (H-8″). Both doublet signals showed a coupling constant of $^{3}J_{HH} = 12.6$ Hz, which indicates *Z*-configuration. CD spectroscopy resulted in $\Delta\varepsilon = -5.6$ mdeg ($\lambda_{max} = 218$ nm, c = 0.98 mM, MeOH), which is in accordance with the stereochemical description of compound **6** ((*S*)-configuration at position C-1‴). Accordingly, the structure of compound **7** was assigned as 4′-*O*-(*Z*)-*p*-coumaroyl-idescarpin.

Compounds **8** and **9** were obtained as a mixed fraction from HPLC-SPE-separation. UPLC-HRESIMS showed two molecular ions of *m/z* 569.1650 $[M-H]^-$ and *m/z* 569.1652 $[M-H]^-$, both corresponding to a molecular formula of $C_{29}H_{30}O_{12}$ (calcd for $C_{29}H_{29}O_{12}$, *m/z* 569.1664). The NMR data (Table 2) of compounds **8** and **9** showed close similarities with the data of compounds **6** and **7** described above. Matching signals for the presence of HCH rings as well as the *Z*-CG and *E*-CG moieties were found, indicating compounds **8** and **9** were a pair of *cis-trans* isomers. Comparative integration of the ^{1}H NMR signals of *E*-CG (**8**) (δ_H 6.39 with $^{3}J_{HH} = 15.6$, H-8″) and *Z*-CG (**9**) (δ_H 5.83 with $^{3}J_{HH} = 12.9$, H-8″) revealed a molar ratio of 2 to 1. Structure elucidation of compound **8** started from the NMR signals of its *E*-CG unit. The ^{1}H NMR signal of the proton (H-1′) at the anomeric position of a *β*-glucopyranosyl unit appeared at δ_H 5.01 ($^{3}J_{HH} = 7.8$ Hz). This signal showed a ^{1}H-^{13}C HMBC correlation to a quaternary carbon atom at δ_C 156.8. The chemical shift assigned the latter signal to the oxygenated C-1 of an aromatic system. The aromatic proton signals were assigned to a four-spin system (ABCD) consisting of δ_H 7.31 ($^{3}J_{HH} = 7.2$ Hz, H-3), δ_H 7.04 ($^{3}J_{HH} = 7.2/8.0$ Hz, H-4), δ_H 7.33 ($^{3}J_{HH} = 8.0/8.6$ Hz, H-5) and δ_H 7.24 ($^{3}J_{HH} = 8.6$ Hz, H-6). The corresponding ^{13}C chemical shifts were determined from ^{1}H-^{13}C HSQC correlations to be δ_C 130.6 (C-3), δ_C 123.5 (C-4), δ_C 131.0 (C-5) and δ_C 116.6 (C-6). The 1,2-disubstitution was determined from characteristic HMBC correlations of H-6 and H-4 with a quaternary carbon atom at δ_C 126.0 (C-2) and of H-3 and H-5 with C-1. The HMBC correlation between the protons H-7a/b at δ_H 5.28/5.40 ($^{3}J_{HH} = 12.6$) of the hydroxymethylene group to C-3 (δ_C 130.6) indicated that this substituent is attached to C-2 of the aromatic ring. Thus, the fragment was characterized as a salicylic alcohol moiety. Further $^{3}J_{CH}$ correlations between position H-7a/b and the carboxyl carbon atom C-7‴ (δ_C 171.5) revealed the linkage to the HCH moiety via an ester bond. Accordingly, the structure of compound **8** was assigned as 4′-*O*-(*E*)-*p*-coumaroyl-salicortin. Except for the signals of its CG unit, compound **9** showed very similar chemical shift values compared to **8** (Table 2). Although most signals were overlapping, the connectivities of the particular subsystems appeared to be identical. Accordingly, the structure of compound **9** was assigned as 4′-*O*-(*Z*)-*p*-coumaroyl-salicortin.

As for compounds **6** and **7**, the configuration at the stereogenic position C-1‴ in the HCH moieties of **8** and **9** was determined by CD spectroscopy. A differential dichroic absorption of $\Delta\varepsilon = -3.5$ mdeg ($\lambda_{max} = 219$ nm, c = 1.19 mM, MeOH) was found for the mixture and compared with the reported value of $\Delta\varepsilon = -26.7$ mdeg ($\lambda_{max} = 224$ nm, c = 1.61 mM) for salicortin (Fig. 1) (Feistel et al., 2015). Accordingly, (*S*)-configuration at position C-1‴ was concluded. Usually, determination of the configuration demands pure substances. However, here we determined $\Delta\varepsilon$ for a mixture of the isomeric compounds **8** and **9**; these differ only in the configuration of their double bond system, which does not interfere with the stereogenic position of interest. The very similar NMR spectra of these compounds highlight their close electronic similarity. However, in contrast to the reference compound salicortin, compounds **8** and **9** have stronger UV absorption due to the presence of additional chromophores, and these in turn influence the CD measurement. As a result, the determined $\Delta\varepsilon$ is still negative, but smaller compared to $\Delta\varepsilon$ of salicortin. Furthermore, the (*S*)-configuration of the main HCH-containing compounds idescarpaside (**14**) and idescarpin (**15**) was determined earlier by X-ray crystallography (Kim et al., 2014).

The HRESIMS of compound **12** showed a molecular ion peak of *m/z* 423.1651 $[M-H]^-$, which corresponds to a molecular formula of $C_{21}H_{28}O_9$ (calcd for $C_{21}H_{27}O_9$, *m/z* 423.1661). According to reported data (Si et al., 2009), the observed NMR signals suggest that this compound is an isograndidentatin isomer. The 1,2-cyclohexanediol ring of this structure features two stereogenic centers at positions C-1 and C-2. NMR data were inconsistent with (1*R*,2*S*)-*cis*-configuration (Si et al., 2009) and (1*S*,2*S*)-*trans*-configuration (Pichette et al., 2010). To the best of our knowledge (SciFinder® search, May 2017), no information about a possible (1*R*,2*R*)-*trans*-configured 1,2-cyclohexanediol has been reported. Therefore, compound **12** was hydrolyzed and the resulting aglycon was compared to authentic standards by chiral GC-MS measurements. The hydrolysis product was determined to be (1*R*,2*S*)-*cis*-1,2-cyclohexanediol. Accordingly, we identified **12** as isograndidentatin A.

The structures of compounds **1**–**15** from *I. polycarpa* resemble those of compounds reported from *Salix* (Thieme, 1964) and *Populus* species (Boeckler et al., 2011; Dommisse et al., 1986; Si et al., 2009). However, a typical *Idesia* feature is the presence of compounds with an additional hydroxyl group in the aromatic part of the parent salicinoids (**4**, **6**, **7** and **14**, **15**). Whereas *β*-glucopyranose substituents in compounds isolated from *Populus* are typically found on position C-2′ or C-6′, the corresponding *Idesia* compounds are acylated exclusively at position C-4′ (**1**–**9** and **11**–**13**).

Little is known about the ecological functions of *Idesia* constituents. Like *Populus* salicinoids, which are generally accepted as defense compounds with feeding-deterrent and anti-fungal

activity (Julkunen-Tiitto et al., 1994; Massad et al., 2014; Yang et al., 2013), the isolated compounds might also play a role in chemical defense. The HCH subunit, part of *Idesia* salicinoids (**6**–**9**, **14**, **15**), is believed to be oxidatively converted after hydrolysis, leading to *o*-quinones (Clausen et al., 1989; Haruta et al., 2001). The *o*-quinones may function as cross-linkers of dietary or digestive proteins in herbivores (Clausen et al., 1989; Haruta et al., 2001; Ruuhola et al., 2003). Furthermore, *p*-coumaroyl units in *Idesia* constituents may serve as substrates for an oxidative transformation, yielding further *o*-quinone derivatives (Chang, 2009), and these may increase feeding-deterrent activity.

2.2. Performance of lepidopteran larvae

2.2.1. Using C. vinula and L. dispar to determine anti-herbivory properties of leaf constituents

Feeding experiments were conducted to address the questions of whether and to what extent *Idesia* leaf constituents have anti-herbivory properties. Larvae of two insect species, *C. vinula*, a specialist herbivore whose life cycle is adapted to plants of the Salicaceae, and the generalist herbivore *L. dispar*, which has a broad range of host plants, were used in this study. Both species are able to thrive on nutrient sources containing salicinoids. The test insects were reared on *P. nigra* prior to the feeding assays and *P. nigra* diet served as a control in the experiments. To determine herbivore performance, 3rd-instar larvae of both species were placed in arenas equipped with leaves of *I. polycarpa*. The control group was supplied with *P. nigra* leaves. Performance of larvae was monitored as average mass for six days by daily balancing each individual. Due to mortality of some larvae, a statistical time frame from day 0 to day **4** was used. Furthermore, leaf consumption was determined as total consumed leaf area a_{total} as described in Experimental.

2.2.2. Performance of specialist herbivore C. vinula

The mass of *C. vinula* depended on the time (likelihood ratio = 24.378, $p < 0.001$) and the plant the larvae fed on (likelihood ratio = 42.285, $p < 0.001$). Whether *C. vinula* larvae gained mass over time, however, depended on the plant they fed on (interaction time: plant: likelihood ratio 172.041, $p < 0.001$). Only larvae fed on *P. nigra* gained mass (Fig. 2A). The average mass of *C. vinula* larvae fed on *I. polycarpa* leaves decreased from 81 mg on day 0 to 68 mg on day **4**, corresponding to an average mass loss of 2 mg per day. High mortality was observed, with 50% of individuals dead after four days. None of the larvae survived day 5 (Fig. 2B). All larvae changed their color from green to a dark yellowish shade. Additionally, fecal consistency changed from solid pellets to liquid excretions. Both symptoms might be interpreted as an effect of starvation caused by deterrent leaf ingredients. The control group fed on *P. nigra* leaves showed a strong increase of average mass from 97 mg (day 0) up to 697 mg (day 5), corresponding to a mass gain of 100 mg per day. The fold mass gain was dependent on the leaf area the larvae consumed during the experiment ($F = 689.086$ $p < 0.001$). When fed on *P. nigra* they gained significantly more mass compared to the *I. polycarpa* ($F = 48.620$ $p < 0.001$) diet. However, how much mass the caterpillars gained per ingested leaf area was different for the two plants ($F = 4.807$ $p = 0.049$). Caterpillars that fed on *P. nigra* gained mass but caterpillars fed on *I. polycarpa* slightly lost mass (Fig. 3A). These observations clearly show that *I. polycarpa* was highly toxic to *C. vinula* larvae.

2.2.3. Performance of generalist herbivore L. dispar

Larvae of L. *dispar* fed on *P. nigra* gained ca. 27 mg mass per day with an increase from 187 mg on day 0 to 301 mg on day 3. Larvae did not continue to grow after day 3. *L. dispar* fed on *I. polycarpa* grew slowly (187 mg on day 0 to 206 mg on day 5) (Fig. 2C). The mass of *L. dispar* also depended on the time (likelihood ratio = 23.374, $p < 0.001$). Compared to *C. vinula* (Fig. 2A), the change in mass over the experimental time was less prominent. Statistically, it did not change according to the plant the larvae fed on (likelihood ratio = 0.643, $p = 0.423$). However, whether *L. dispar* larvae gained mass over time did depend on the plant species they fed on (interaction time: plant: likelihood ratio 13.888, $p = 0.008$). Only when fed on *P. nigra* the larvae gained mass. By day 5 the majority (70%) of *L. dispar* larvae fed on *I. polycarpa* were deceased (Fig. 2D). The fold mass gain was only dependent on the amount the larvae fed during the experiment ($F = 18.107$ $p = 0.001$), but not on the plant species they fed on ($F = 0.196$ $p = 0.666$). How much mass the caterpillars gained per consumed leaf area was same for both plants ($F = 0.355$ $p = 0.563$) (Fig. 3B).

2.2.4. Survivorship of C. vinula and L. dispar

Both Lepidopteran species survived significantly better on *P. nigra* than on *I. polycarpa* ($z = -3.592$, $p < 0.001$). The survival rate of both species of larvae was the same ($z = -1.161$, $p = 0.2458$), and they reacted the same way to both plant species (interaction between plant and herbivore $z = 0.998$, $p = 0.318$) (Fig. 2).

3. Conclusions

In this work, 15 compounds from leaves of *I. polycarpa* were isolated and identified by means of spectroscopic methods. Compounds **1**–**9** are described for the first time as natural products. Compounds **1**–**13** had not previously been reported as constituents of *I. polycarpa*. These compounds are structurally related to salicinoids, which are known defense compounds from *Salix* and *Populus* species. Feeding experiments with larvae of the Salicaceae specialist herbivore *C. vinula* and the broadleaf tree generalist *L. dispar* showed differences in performance. Both insect species performed worse on *I. polycarpa* than on *P. nigra*. Although *C. vinula* larvae performed much better on *P. nigra* than the generalist *L. dispar*, total mortality on *I. polycarpa* was observed after five days. We observed a higher survivorship for *L. dispar* on *I. polycarpa* (30% in total) but with less leaf area consumed and less mass gain in comparison to larvae fed with *P. nigra*. In order to interpret the results, the adaption strategies of the insect larvae has to be taken into account. To compete effectively, specialists are extremely adapted to their ecosystems and hence much more dependent on the environmental conditions (Ali and Agrawal, 2012). As a result, a slight change in nutrition, for example, might have a notable impact on their fitness. The performance of generalists is more robust, as our observations indicate. It can be hypothesized that the differential toxicity is caused by different mechanisms of detoxification (Boeckler et al., 2016) or that plant defensive proteins such as protease inhibitors (Neiman et al., 2009) or polyphenol oxidases (Wang and Constabel, 2004) interfere with digestion by decreasing nutrient availability. Another reason for the mortality observed may be compounds unnoticed by UV/Vis detection. The combined effect of those compounds may interfere with digestion and eventually negatively affect nutrient acceptance; in our experiments, this may have resulted finally in the starvation of the tested lepidopteran larvae.

4. Experimental

4.1. General experimental procedures

Solvents used for extraction and chromatographic separation were purchased from Carl Roth GmbH, Karlsruhe, Germany, and VWR International GmbH, Darmstadt, Germany, and were used without further purification. The synthetic reference compounds

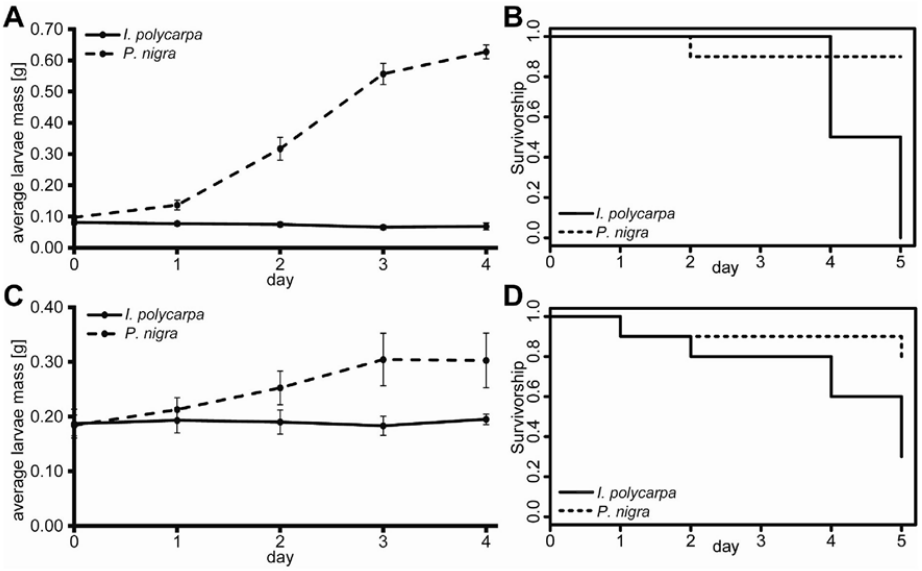

Fig. 2. Performance of lepidopteran larvae fed on *P. nigra* (dashed lines) and *I. polycarpa* (filled lines). Error bars represent standard errors. (**A**) Average mass of 3rd-instar larvae of *C. vinula*. (**B**) Kaplan-Meier graph illustrating the survivorship of *C. vinula*. (**C**) Average mass of 3rd-instar larvae of *L. dispar*. (**D**) Kaplan-Meier graph illustrating the survivorship of *L. dispar* larvae. (**A**) and (**C**) show the statistically analyzed time frame (day 0–4).

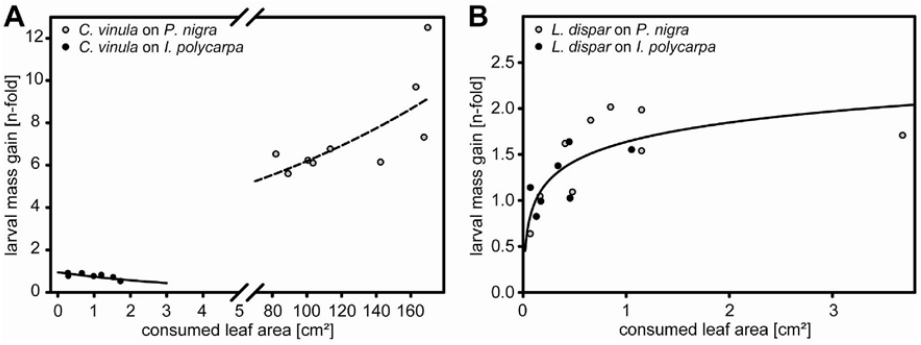

Fig. 3. Larval mass gain of *C. vinula* (**A**) and *L. dispar* (**B**) fed on *P. nigra* (black dots) and *I. polycarpa* (grey dots) including trend lines. Data were collected during 6 days for both experiments.

(1*R*,2*S*)-*cis*-cyclohexane diol, (1*S*,2*S*)-*trans*-cyclohexane diol and (1*R*,2*R*)-*trans*-1,2-cyclohexanediol were purchased from Sigma-Aldrich Chemie GmbH, Taufkirchen, Germany. Water used for HPLC was obtained from a Milli-Q Synthesis A 10 purifier (Merck KGaA, Darmstadt, Germany). Phytacon vessels (H 140 mm, base diam. 86 mm) used as arenas for the feeding experiments were purchased from Sigma-Aldrich. HR-X SPE cartridges (500 mg sorbent/6 ml volume) were purchased from Macherey-Nagel, Düren, Germany.

HPLC separations were carried out on an Agilent 1100 HPLC system, consisting of a degasser, quaternary solvent delivery pump G1311A, an autosampler G1313A (Agilent Technologies GmbH, Waldbronn, Germany) and a photodiode array detector (detection 200–700 nm; J&M Analytik AG, Aalen, Germany). An Isis RP-18e column (250 × 4.6 mm, 5 μm particle size) (Macherey-Nagel) was used for all separations. Column temperature was set to 30 °C, and the solvent flow rate was 0.8 ml min^{-1} using 0.1% formic acid in water and 0.1% formic acid in MeOH as a binary solvent system. An HPLC gradient starting with a 5 min isocratic flow of 30% MeOH and then linearly increasing for 90 min to 50% MeOH was used. After each run, the column was washed with 100% MeOH for 10 min and equilibrated with 30% MeOH for 10 min. The column outlet was connected to a Bruker/Spark Prospect 2 solid-phase extraction (SPE) system (Bruker Biospin GmbH, Rheinstetten, Germany),

equipped with HySphere GP resin cartridges. To reduce the eluotropic capacity of the HPLC solvent mixture, water with a flow rate of 2.5 ml min $^{-1}$ was added using a make-up pump (Knauer, Berlin, Germany). SPE cartridges loaded with metabolites were dried in a stream of nitrogen prior to elution with MeOH. Eluted compounds were dried using a Genevac HT-4X vacuum centrifuge (Genevac Ltd., Ipswich, UK).

The hydrolysis products of compound **12** as well as the isomeric cyclohexane diol references were analyzed using an Agilent 7890A gas chromatograph equipped with a chiral Cyclosil-B column (30 m × 0.25 mm ID with 0.25 μm film thickness, Agilent) coupled to a quadrupole mass spectrometer Agilent 5975C. The carrier gas was helium at a constant flow of 2 ml min $^{-1}$. One microliter of each sample was injected in splitless mode. The inlet temperature was set to 230 °C. The oven program started at 40 °C for 5 min, increased at 1 °C min $^{-1}$ to 90 °C, held for 10 min, then increased at 0.1 °C min $^{-1}$ to 95 °C, and finally at 30 °C min $^{-1}$ to 230 °C. MS conditions were electron impact mode (70 eV), and scan mode 33–250 amu.

ESI-HRMS data were measured in negative and positive mode at a mass resolution of $m/\Delta m$ 30.000 on a UHPLC system Ultimate 3000 series RSLC (Dionex) combined with LTQ Orbitrap XL mass spectrometer (Thermo Fisher Scientific, Bremen, Germany). Separation was done on an Acclaim C18 column (150 × 2.1 mm, 2.2 μm; Dionex, Sunnyvale, CA, USA) with a flow rate of 300 μL min $^{-1}$ using the following gradient conditions: MeCN in water, both containing 0.1% (v/v) formic acid: constant at 1% for 8 min, linearly increased to 85% within 7 min, kept constant at 85% for 4 min, finally returning to 1% for equilibration for 4 min.

NMR spectra (^{1}H NMR, 1D NOESY, ^{1}H-^{1}H COSY, SELTOCSY, HMBC, HSQC) were recorded on a Bruker Avance III HD 700 spectrometer, equipped with a cryoplatform and a 1.7 mm TCI microcryoprobe (Bruker Biospin GmbH, Rheinstetten, Germany). NMR tubes of 1.7 mm outer diameter were used for all measurements. All NMR spectra were recorded using MeOH-d_4 as a solvent. Chemical shifts were referenced to the residual solvent peaks at δ_H 3.31 and δ_C 49.15, respectively. Data acquisition and processing were accomplished using TopSpin 3.2. (Bruker Biospin). Standard pulse programs as implemented in TopSpin were used for data acquisition.

CD spectra were recorded on a Jasco J-810 CD spectropolarimeter (Jasco GmbH, Gross-Umstadt, Germany). Compounds were measured in MeOH using a quartz cuvette of 1 mm width. Spectra were recorded for 185–350 nm and were accumulated 10 times. Baseline correction was performed on the basis of a MeOH blank sample.

4.2. Plant material and insect larvae

I. polycarpa trees were purchased in 2015 from Baumschule Pflanzenvielfalt GmbH, Zetel, Germany, and maintained in the Max Planck Institute of Chemical Ecology (MPI-CE) Jena, Germany. Leaf samples of black poplar (*P. nigra*) were taken from trees growing in the area surrounding the Max Planck Institute of Chemical Ecology (MPI-CE) Jena, Germany. *C. vinula* (Lepidoptera) larvae were taken from a colony reared at the MPI-CE, hatched from eggs and maintained on *P. nigra* until they reached the 3rd instar. *L. dispar* (gypsy moth) (Lepidoptera) larvae (3rd instar), reared on a *P. nigra* leaf diet, were kindly provided by Dr. Sybille Unsicker, MPI-CE.

4.3. Extraction and isolation

The leaves of *I. polycarpa* were lyophilized, resulting in 4.8 g of dried material; this was ground in a ceramic mortar and extracted (7 × 60 ml, each 15 min) with MeCN. The combined extracts were filtered and evaporated using a rotary evaporator, resulting in 598 mg crude extract (8% of the dried leaf material). The extract was reconstituted with 30 ml water and centrifuged to separate insoluble matter. The supernatant was subjected to pre-separation on a HR-X SPE cartridge. After conditioning with MeOH (2 × 6 ml) and equilibration with water (3 × 6 ml), the cartridge was loaded and washed with water (3 × 6 ml). After air-drying, the cartridge was eluted with MeOH (3 × 6 ml) and the combined fractions were evaporated in a vacuum centrifuge, resulting in 259 mg methanolic crude extract. For separation, an aliquot of the crude extract was reconstituted with MeOH (78.6 mg ml $^{-1}$) and subjected to HPLC-SPE to yield the following compounds (R_t retention time): **1** (R_t 9.18 min, 0.10% of leaf d.w.), **10** (R_t 14.43 min, 0.09%), **15** (R_t 21.16 min, 1.10%), **2** (R_t 27.18 min, 0.13%), **3** (R_t 30.73 min, 0.11%), **11** (R_t 36.47 min, 0.08%), **4** (R_t 42.92 min, 0.10%), **12** (R_t 45.55 min, 0.10%), **13** (R_t 52.16 min, 0.20%), **5** (R_t 55.55 min, 0.11%), **14** (R_t 58.84 min, 0.16%), **8** & **9** (R_t 70.84 min, 0.19%), **6** (R_t 77.58 min, 0.09%), **7** (R_t 79.58 min, 0.08%).

4.4. Hydrolysis of isograndidentatin A (*12*)

In order to determine the absolute configuration of compound **12**, acidic hydrolysis was carried out. Compound **12** (125 μg; 0.3 μmol) was dissolved in 500 μL MeOH and added to a stirred solution of 4.5 ml MeOH:H_2O (1:1, v/v) containing 150 μL of conc. HCl. The mixture was refluxed for 8 h, and then dried in a stream of nitrogen gas. The residue was dissolved in CH_2Cl_2 and analyzed by gas chromatography – mass spectrometry (GC-MS) together with the reference standards (1*R*,2*S*)-*cis*-cyclohexane diol, (1*S*,2*S*)-*trans*-cyclohexane diol and (1*R*,2*R*)-*trans*-1,2-cyclohexanediol. Based on retention time and mass spectrum, the absolute configuration was determined.

4.5. Performance of C. vinula and L. dispar on I. polycarpa

For feeding experiments, 10 × 1 *I. polycarpa* leaves and, as a control, 10 × 1 *P. nigra* leaves with a leaf plastochron index (LPI) from 3 to 10, were placed in 20 separate arenas with their petioles immersed in a 25 ml glass beaker filled with cotton wetted with tap water. One *C. vinula* larva was placed on each leaf. Thus, ten feeding experiments per plant species were conducted in parallel. During the experiment, the mass of each larva was determined every day. Leaves were replaced when consumed or exchanged every second day. In order to detect consumption, leaves were scanned and printed in 1:1 scale on paper (80 g m $^{-2}$). After feeding, the consumed leaf area was reconstructed by comparison with the reference scans, cut out and weighed (m_{paper} *in mg*). The total consumed leaf area a_{total} was calculated according to Eqn. (1). The feeding experiment with *L. dispar* larvae was performed accordingly.

$$a_{total} = \frac{m_{paper}}{8}\text{cm}^2 \quad (1)$$

4.6. Statistical analysis

Because just a few larvae survived until day 5, larval masses were only analyzed until day 4 in order to have a sufficient number of replicates and because the two herbivore species generally differ in size, the change in their mass over time was analyzed separately. In order to test whether the caterpillars differed in their mass development depending on the plant they were feeding on, linear mixed effects models were applied (lme, nlme library (Pinheiro et al., 2016)) with plant and time as fixed factors and the larvae identity as a random intercept. In order to achieve normality of

residuals, data were log-transformed. For mass data from *C. vinula*, the varIdent variance structure (to allow data from each plant species to have a different variance) was applied to achieve variance homogeneity. P values were obtained by a stepwise removal of the explanatory variables and comparison of the more complex model with the simpler model with a likelihood ratio test (Zuur et al., 2009). The Cox proportional hazard model (coxph of the survival library (Therneau, 2015)) was used to investigate the survival of *C. vinula* and *L. dispar* on *P. nigra* and *I. polycarpa*. The model was simplified by removing non-significant factors. All analyses were done in R 3.3.1 (R Core Team, 2016).

In order to see to which extent larval mass was depending on the consumed leaf area *C. vinula* and *L. dispar* larvae were separately fed with either *P. nigra* or *I. polycarpa* leaves for 6 days. Data from non-feeding larvae were discarded from the analysis. For all other larvae it was considered how much they changed mass with respect to their start mass; the ratio of end mass and start mass gave an *n*-fold increase of mass for the respective larva. An analysis of covariance (ancova) with the consumed leaf area as continuous variable and the different food plants as categorical explanatory variable was undertaken. For the data analysis of *C. vinula* larvae mass gain data were log-transformed and for *L. dispar* larvae the consumed leaf area data were log-transformed to achieve homogeneity of variances and normality of the residuals.

4.7. Spectroscopic data of new compounds

4.7.1. 1-O-(2-Hydroxyethyl)-4-O-(E)-p-coumaroyl-β-glucopyranose (1)

UV (MeOH/H_2O): λ_{max} = 228, 313 nm; HRESIMS: *m/z* 369.1185 $[M-H]^-$ (calcd for $C_{17}H_{21}O_9$, 369.1191); ^1H and ^{13}C NMR, see Table 1.

4.7.2. 1-O-(3-Hydroxymethylphenyl)-4-O-(E)-p-coumaroyl-β-glucopyranose (2)

UV (MeOH/H_2O): λ_{max} = 210, 313 nm; HRESIMS: *m/z* 431.1336 $[M-H]^-$ (calcd for $C_{22}H_{23}O_9$, 431.1348); ^1H and ^{13}C NMR, see Table 1.

4.7.3. 1-O-(3-Hydroxymethylphenyl)-4-O-(Z)-p-coumaroyl-β-glucopyranose (3)

UV (MeOH/H_2O): λ_{max} = 209, 313 nm; HRESIMS: *m/z* 431.1337 $[M-H]^-$ (calcd for $C_{22}H_{23}O_9$, 431.1348); ^1H and ^{13}C NMR, see Table 1.

4.7.4. 1-O-(6-Hydroxy-2-hydroxymethylphenyl)-4-O-(E)-p-coumaroyl-β-glucopyranose (4)

UV (MeOH/H_2O): λ_{max} = 272, 316 nm; HRESIMS: *m/z* 447.1287 $[M-H]^-$ (calcd for $C_{22}H_{23}O_{10}$, 447.1297); ^1H and ^{13}C NMR, see Table 1.

4.7.5. 1-O-(2-Hydroxyphenyl)-4-O-(Z)-p-coumaroyl-β-glucopyranose (5)

UV (MeOH/H_2O): λ_{max} = 212, 281, 309 nm; HRESIMS: *m/z* 417.1182 $[M-H]^-$(calcd for $C_{21}H_{21}O_9$, 417.1191); ^1H and ^{13}C NMR, see Table 1.

4.7.6. 4′-O-(E)-p-Coumaroyl-idescarpin (6)

UV (MeOH/H_2O): λ_{max} = 216, 312 nm; CD: $\Delta\varepsilon$ = −6.9 mdeg (λ_{max} = 216 nm, c = 0.75 mM, MeOH); HRESIMS: *m/z* 585.1593 $[M-H]^-$ (calcd for $C_{29}H_{29}O_{13}$, 585.1614); ^1H and ^{13}C NMR, see Table 2.

4.7.7. 4′-O-(Z)-p-Coumaroyl-idescarpin (7)

UV (MeOH/H_2O): λ_{max} = 218, 310 nm; CD: $\Delta\varepsilon$ = −5.6 mdeg (λ_{max} = 218 nm, c = 0.98 mM, MeOH); HRESIMS: *m/z* 585.1601 $[M-H]^-$ (calcd for 585.1614, $C_{29}H_{29}O_{13}$); ^1H and ^{13}C NMR, see Table 2.

4.7.8. 4′-O-(E)-p-Coumaroyl-salicortin (8)

UV (MeOH/H_2O): λ_{max} = 210, 313 nm; CD: $\Delta\varepsilon$ = −3.5 mdeg (λ_{max} = 219 nm, c = 1.19 mM, MeOH); HRESIMS: *m/z* 569.1650 $[M-H]^-$ (calcd for 569.1664, $C_{29}H_{29}O_{12}$); ^1H and ^{13}C NMR, see Table 2.

4.7.9. 4′-O-(Z)-p-Coumaroyl-salicortin (9)

UV (MeOH/H_2O): λ_{max} = 210 nm, 313 nm; $\Delta\varepsilon$ = −3.5 mdeg (λ_{max} = 219 nm, c = 1.19 mM, MeOH); HRESIMS: *m/z* 569.1652 $[M-H]^-$ (calcd for 569.1664, $C_{29}H_{29}O_{12}$); ^1H and ^{13}C NMR, see Table 2.

4.8. Spectroscopic data of known compounds

Icaraside B2 (**10**): UV (MeOH/H_2O): λ_{max} = 230, 310 nm; HRESIMS: *m/z* 409.1831 $[M+Na]^+$ (calcd for $C_{19}H_{30}O_8Na$, 409.1833); ^1H and ^{13}C NMR, see S10.1 (Lee, 2012; Otsuka et al., 1995).

4-(*E*)-*p*-Coumaroyl-D-glucopyranose (**11**): UV (MeOH/H_2O): λ_{max} = 212, 313 nm; HRESIMS: *m/z* 349.0890 $[M+Na]^+$ (calcd for $C_{15}H_{18}O_8Na$), 349.0894; ^1H and ^{13}C NMR, see S10.9 (Birkofer et al., 1969; She et al., 2008).

Isograndidentatin A (**12**): UV (MeOH/H_2O): λ_{max} = 210, 222, 313 nm; HRESIMS: *m/z* 423.1651 $[M-H]^-$ (calcd for $C_{21}H_{27}O_9$, 423.1661); ^1H and ^{13}C NMR, see S11.12 (Si et al., 2009).

1-*O*-(2-Hydroxyphenyl)-4-*O*-(*E*)-p-coumaroyl-β-D-glucopyranose (**13**): UV (MeOH/H_2O): λ_{max} = 212, 313 nm; HRESIMS: *m/z* 417.1182 $[M-H]^-$ (calcd for $C_{21}H_{21}O_9$, 417.1191); ^1H and ^{13}C NMR, see S12.3 (Kumar et al., 2010).

Idescarpaside (**14**): UV (MeOH/H_2O): λ_{max} = 215, 275 nm; CD: $\Delta\varepsilon$ = −11.5 mdeg (λ_{max} = 215 nm, c = 0.55 mM, MeOH); HRESIMS: *m/z* 903.2532 $[M+Na]^+$ (calcd for $C_{40}H_{48}O_{22}Na$, 903.2529); ^1H and ^{13}C NMR, see S13.3 (Kim et al., 2014).

Idescarpin (**15**): UV (MeOH/H_2O): λ_{max} = 215, 277, 311 nm; CD: $\Delta\varepsilon$ = −11.5 mdeg (λ_{max} = 215 nm, c = 0.55 mM, MeOH); HRESIMS: *m/z* 463.1200 $[M+Na]^+$ (calcd for $C_{20}H_{24}O_{11}Na$, 463.1211); ^1H and ^{13}C NMR, see S14.1 (Feistel et al., 2015).

Acknowledgments

The authors thank Dr. Sybille Unsicker for providing *L. dispar* larvae, Regina Seibt for her support in rearing *C. vinula*, and Emily Wheeler for editorial assistance.

Appendix A. Supplementary data

Supplementary data related to this article can be found at http://dx.doi.org/10.1016/j.phytochem.2017.08.008.

References

Ali, J.G., Agrawal, A.A., 2012. Specialist versus generalist insect herbivores and plant defense. Trends Plant Sci. 17, 293–302.
Baek, S., Kim, D., Lee, C., Kho, Y., Lee, C., 2006. Idescarpin isolated from the fruits of *Idesia polycarpa* inhibits melanin biosynthesis. J. Microbiol. Biotechnol. 16, 667–672.
Birkofer, L., Kaiser, C., Hillges, B., Becker, F., 1969. NMR-spektroskopische Untersuchungen von Acyl-glykosen. Justus Liebigs Ann. Chem. 725, 196–202.
Boeckler, G.A., Gershenzon, J., Unsicker, S.B., 2011. Phenolic glycosides of the Salicaceae and their role as anti-herbivore defenses. Phytochemistry 72, 1497–1509.
Boeckler, G.A., Paetz, C., Feibicke, P., Gershenzon, J., Unsicker, S.B., 2016. Metabolism of poplar salicinoids by the generalist herbivore *Lymantria dispar* (Lepidoptera). Insect Biochem. Mol. Biol. 78, 39–49.
Chang, T.-S., 2009. An updated review of tyrosinase inhibitors. Int. J. Mol. Sci. 10, 2440–2475.
Chou, C.-J., Lin, L.-C., Tsai, W.-J., Hsu, S.-Y., Ho, L.-K., 1997. Phenyl-β-D-glucopyranoside derivatives from the fruits of *Idesia polycarpa*. J. Nat. Prod. 60, 375–377.
Clausen, T.P., Reichardt, P.B., Bryant, J.P., Werner, R.A., Post, K., Frisby, K., 1989. Chemical model for short-term induction in quaking aspen (*Populus tremuloides*) foliage against herbivores. J. Chem. Ecol. 15, 2335–2346.
Dommisse, R.A., Van Hoof, L., Vlietinck, A.J., 1986. Structural analysis of phenolic glucosides from Salicaceae by NMR spectroscopy. Phytochemistry 25, 1201–1204.
Feistel, F., Paetz, C., Lorenz, S., Schneider, B., 2015. The absolute configuration of

salicortin, HCH-salicortin and tremulacin from *Populus trichocarpa* x *deltoides* Beaupré. Molecules 20, 5566–5573.
Guo, H., Shen, Q.-W., Hu, Y.-C., 2012. Quality analysis of *Idesia polycarpa* maxim seed oil. Xiandai Shipin Keji 28, 345–347.
Haruta, M., Pedersen, J.A., Constabel, C.P., 2001. Polyphenol oxidase and herbivore defense in trembling aspen (*Populus tremuloides*): cDNA cloning, expression, and potential substrates. Physiol. Plant 112, 552–558.
Hintze-Podufal, C., 1970. Über die quantitativen Änderungen der Kotabgabe während der Larvalentwicklung vonCerura vinula L. (Lepidoptera). Oecologia 5, 334–346.
Hwang, J.-H., Moon, S.A., Lee, C.H., Byun, M.R., Kim, A.R., Sung, M.K., Park, H.-J., Hwang, E.S., Sung, S.H., Hong, J.-H., 2012. Idesolide inhibits the adipogenic differentiation of mesenchymal cells through the suppression of nitric oxide production. Eur. J. Pharmacol. 685, 218–223.
Julkunen-Tiitto, R., Hakulinen, J., Meier, B., 1994. The response of growth and secondary metabolism to *Melampsora* rusts in field cultivated willow (*Salix*) clones. Acta Hortic. 2, 679–682.
Jung, M.-H., Yoo, J.-M., Kang, Y.-J., Lee, H.W., Kim, S.H., Sung, S.H., Lee, Y.-J., Choi, I., Kim, T.-J., 2010. Idesolide, an isolate of *Idesia polycarpa*, inhibits apoptosis through induction of intracellular heat shock protein 70 in C_2C_{12} muscle cells. Biol. Pharm. Bull. 33, 1063–1066.
Kim, S.H., Sung, S.H., Choi, S.Y., Chung, Y.K., Kim, J., Kim, Y.C., 2005. Idesolide: A new spiro compound from *Idesia polycarpa*. Org. Lett. 7, 3275–3277.
Kim, T.B., Kim, H.W., Lee, M., Lee, H.H., Kim, S.H., Kang, S.K., Sung, S.H., 2014. Isolation and structure elucidation of (−)-idescarparide, a new spiro compound from *Idesia polycarpa*. Tetrahedron Lett. 55, 5447–5449.
Kim, T.W., 1996. The Woody Plants of Korea. Kyohak Press, Seoul, p. 126.
Kumar, M., Rawat, P., Khan, M.F., Tamarkar, A.K., Srivastava, A.K., Arya, K.R., Maurya, R., 2010. Phenolic glycosides from *Dodecadenia grandiflora* and their glucose-6-phosphatase inhibitory activity. Fitoterapia 81, 475–479.
Lee, M., Lee, H.H., Lee, J.-K., Ye, S.-K., Kim, S.H., Sung, S.H., 2013. Anti-adipogenic activity of compounds isolated from *Idesia polycarpa* on 3T3-L1 cells. Bioorg. Med. Chem. Lett. 23, 3170–3174.
Lee, S., 2012. A new megastigmane glucoside from the aerial parts of *Erythronium japonicum*. Nat. Prod. Sci. 18, 166–170.
Massad, T.J., Trumbore, S.E., Ganbat, G., Reichelt, M., Unsicker, S., Boeckler, A., Gleixner, G., Gershenzon, J., Ruehlow, S., 2014. An optimal defense strategy for phenolic glycoside production in *Populus trichocarpa* – isotope labeling demonstrates secondary metabolite production in growing leaves. New Phytol. 203, 607–619.
Moritake, M., Ueda, K., Mori, I., 1987. Two phenazine derivatives, polycartine A and B from *Idesia polycarpa* maxim (Flacourticaceae). Tetrahedron 28, 1425–1426.
Neiman, M., Olson, M.S., Tiffin, P., 2009. Selective histories of poplar protease inhibitors: elevated polymorphism, purifying selection, and positive selection driving divergence of recent duplicates. New Phytol. 183, 740–750.
Otsuka, H., Kamada, K., Yao, M., Yuasa, K., Kida, I., Takeda, Y., 1995. Alangionosides C-F, megastigmane glycosides from *Alangium premnifolium*. Phytochemistry 38, 1431–1435.
Pichette, A., Eftekhari, A., Georges, P., Lavoie, S., Mshvildadze, V., Legault, J., 2010. Cytotoxic phenolic compounds in leaf buds of *Populus tremuloides*. Can. J. Chem. 88, 104–110.
Pinheiro, J., Bates, D., DebRoy, S., Sarkar, D., R Core Team, 2016. nlme: Linear and Nonlinear Mixed Effects Models. R Package Version 3.1-128. http://CRAN.R-project.org/package=nlme.
R Core Team, 2016. R: a Language and Environment for Statistical Computing. R Foundation for Statistical Computing, Vienna, Austria. https://www.R-project.org/.
Robinson, G.S., Ackery, P.R., Kitching, I.J., Beccaloni, G.W., Hernández, L.M., 2010. HOSTS - a Database of the World's Lepidopteran Hostplants. Natural History Museum, London. http://www.nhm.ac.uk/hosts. (Accessed 13 June 2017).
Ruuhola, T., Julkunen-Tiitto, R., Vainiotalo, P., 2003. *In vitro* degradation of willow salicylates. J. Chem. Ecol. 29, 1083–1097.
She, G.-M., Wang, D., Zeng, S.-F., Yang, C.-R., Zhang, Y.-J., 2008. New phenylethanoid glycosides and sugar esters from Ku-Ding-Cha, a herbal tea produced from *Ligustrum purpurascens*. J. Food Sci. 73, C476–C481.
Si, C.-L., Kim, J.-K., Bae, Y.-S., Li, S.-M., 2009. Phenolic compounds in the leaves of *Populus ussuriensis* and their antioxidant activities. Planta Med. 75, 1165–1167.
Therneau, T., 2015. A Package for Survival Analysis in S. Version 2.38. http://CRAN.R-project.org/package=survival.
Thieme, H., 1964. The phenolic glycosides of the Salicaceae. II. Isolation and detection. Pharmazie 19, 471–475.
Wang, J., Constabel, C.P., 2004. Three polyphenol oxidases from hybrid poplar are differentially expressed during development and after wounding and elicitor treatment. Physiol. Plant. 122, 344–353.
Yang, H., Lee, S.H., Sung, S.H., Kim, J., Kim, Y.C., 2013. Neuroprotective compounds from *Salix pseudo-lasiogyne* twigs and their anti-amnesic effects on scopolamine-induced memory deficit in mice. Planta Med. 79, 78–82.
Ye, Y., Tang, X.-S., Chen, F., Tang, L., 2014. Optimization of phenolics extracted from *Idesia polycarpa* defatted fruit residue and its antioxidant and depigmenting activity *in vitro* and *in vivo*. J. Evidence-Based Complement. Altern. Med. 2014, 12.
Zuur, A.F., Ieno, E.N., Walker, N., Saveliev, A.A., Smith, G.M., 2009. Mixed Effects Models and Extensions in Ecology with R. Springer-Verlag, New York.

4. Discussion

4.1 The Absolute Configuration of Salicortin, HCH-Salicortin and Tremulacin from **Populus trichocarpa x deltoides *Beaupré***

*4.1.1 Configuration of salicortin and its HCH-bearing derivatives suggests a (*S*)-configuration in all salicinoids*

In 1964, salicortin was first isolated for the first time from the bark of *Salix purpurea* by Heinz Thieme and also found by him in other species from the genuses *Salix* and *Populus*. Considering flame point, optical rotation and reactivity due to exposure to selected chemicals (H_2SO_3, $Ba(OH)_2$, CH_3NaO, etc.), Thieme concluded that the isolated compound was a derivative of salicyloyl salicin with additional substituents at its sugar and salicyloyl moiety (Thieme, 1964). However, in 1970, this structure was revised by Pearl and Darling based on Thieme's data and on infrared spectroscopy (IR), mass spectrometry (MS) and NMR techniques (Pearl and Darling, 1970). However, the configuration of the α-hydroxyl functionality within the 1-hydroxy-6-oxocyclohex-2-en-1-oyl (HCH) moiety in salicortin and its derivatives remained unsolved.

In order to elucidate the absolute configuration of these molecules, we compared the chiroptical properties and X-ray single-crystal diffraction data of (–)-idescarpin (Kim et al., 2014) – a compound with known configuration and similar structure – with the data of salicortin. However, (–)-idescarpin had at that time been described only for *I. polycarpa* (Salicaceae, formerly Flacourtiaceae), and all investigations addressing the metabolic contents of this plant had exclusively focused on its orange berry-like fruits (Chou et al., 1997). Based on our knowledge of *Populus* trees and their salicinoids, we expected the occurrence of (–)-idescarpin not to be restricted to the fruits of *Idesia* but to be abundant in other plant parts such as the leaves. Furthermore, due to structural similarities, we expected salicortin (and its derivatives tremulacin and HCH-salicortin) to have the same configuration as (–)-idescarpin.

Indeed, we have been able to prove both hypotheses (manuscripts I and III)(Feistel et al., 2017; Feistel et al., 2015).

The ultimate elucidation of the (*S*)-configuration in salicortin, tremulacin and HCH-salicortin ends the previous half-century's uncertainty of these chemicals structures. Since salicinoids most likely share a biosynthetic pathway, this finding suggests that other HCH-bearing salicinoids, like 2'-cinnamoyl salicortin, 2'-*O*-acetyl salicortin and lasiandrin, have the same absolute configuration as salicortin (Fig. 10)(Boeckler et al., 2011). Obviously, it is mandatory to confirm the stereochemistry for each compound. To facilitate this process, we have been able to show that CD spectroscopy is a suitable tool for the stereochemical investigation of other HCH-bearing salicinoids, when a reference compound with known configuration is used. Alternative methods, such as X-ray crystallography and NMR spectroscopy, require larger amounts of sample and are more time-consuming. In NMR, besides long experimental times for certain techniques allowing the determination of intramolecular correlations (e.g. NOESY, ROESY), the analyte sometimes has to be modified with a chiral derivatization agent in order to obtain the conformational information (Wenzel, 2017). Single crystals are needed for X-ray structure analysis, and the generation of such a crystal with sufficient quality is a time- and compound-consuming task. For some analytes, it also appears impossible to initiate crystallization. Since some of the HCH-containing salicinoids are abundant only in minor amounts within the plant tissue and their chemical synthesis is still unfeasible, the usage of CD spectroscopy appears to be the most elegant and feasible method for stereochemical investigations. As a consequence, CD spectroscopy represents a simple and easy approach which will support and accelerate structural examinations of other HCH containing compounds in the future.

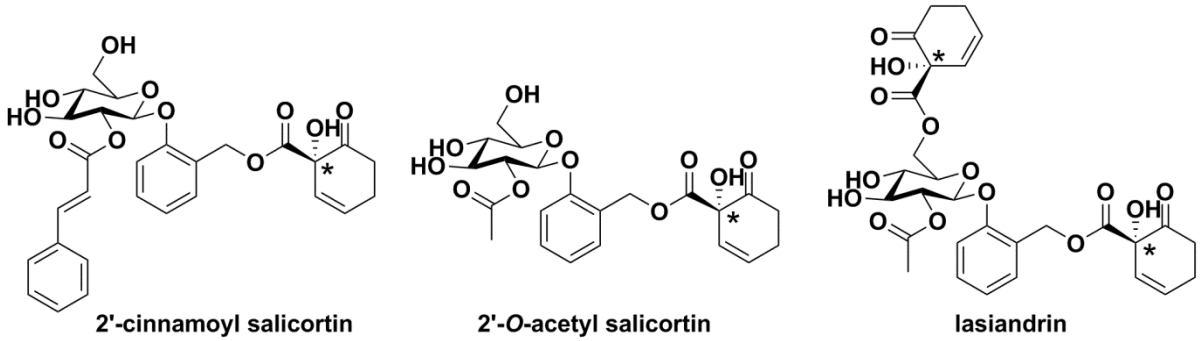

Figure 10 – Examples of other HCH-bearing compounds with hypothetical (*S*)-configuration at the (*)-marked positions.

4.1.2 I. polycarpa *leaves are a promising source for secondary metabolites*

The fact that *I. polycarpa* leaves contained (–)-idescarpin was not surprising, but the amount we isolated of this compound was astonishing. In the literature, it was reported that (–)-idescarpin accounts for only 0.5 % of the crude fruit extract mass (Kim et al., 2014), whereas we observed an eight-fold higher concentration of this compound in the crude extract of the *Idesia* leaves. This difference suggests that the leaves rather than the fruit should be used to isolate this particular compound. Since *Idesia* trees are dioecious plants, at most half of them are able to produce fruits. Additionally, fruit production occurs only in the presence of both male and female plants. The leaves, however, as photosynthesizing organs, are almost omnipresent at both sexes of these trees (except during winter). Accordingly, the leaf tissue is unarguably the preferable substrate for the isolation of (–)-idescarpin. Moreover, it is likely that in addition to the omnipresent (–)-idescarpin, other salicinoids with similar structural properties are also present in this tissue. This fact led us to investigate *Idesia* leaf metabolites further. Finally, we wanted to examine the ecological importance of these compounds and their potential impact on the performance of known *Populus* herbivores (see manuscript III).

4.2 Acylated quinic acids are the main salicortin metabolites in the specialist herbivore C. vinula

4.2.1 Quinic acid esters are a dominant substance group in the feces of C. vinula *larvae after they feed on* P. nigra

The analysis of fecal composition of the Salicaceae specialist *C. vinula* larvae reared on *P. nigra* revealed eleven acylated quinates. They were substituted with one or two salicyloyl, one benzoyl or both salicyloyl and benzoyl functionalities. One of the compounds was recently discovered in the fruit extracts of *Ficus hirta* (Wan et al., 2016), while the others have been unknown until now.

The literature offers various examples of quinic acid-related compounds in plants. However, these substances were never reported to occur in any kind of insect-derived sample (feces, exudates, hemolymphs, etc.). The most intensively studied quinate is chlorogenic acid, a compound with anti-bacterial, anti-mutagenic, anti-tumor and anti-viral properties, which occurs in many plants (Armesto et al., 2003). Various routes have been published that describe the synthesis of quinates that are closely related to those presented in manuscript III (Fig. 12A)(Armesto et al., 2003; Mercier et al., 1969). However, the pharmacological and ecological properties of these compounds have never been discussed or studied.

Like caffeoyl quinates, which can be isolated from coffee beans, acylated quinic acids are reportedly focused only on their function in plants (Corse et al., 1970). Additionally, a lot of structural isomers of galloyl-quinates have been isolated from the bark and acorns of different *Quercus* species (Fagaceae) and leaves of *Guiera senegalensis* (Combretaceae)(Fig. 12B)(Bouchet et al., 1996; Ishimaru et al., 1987; Nishimura et al., 1984). The extracts of *G. senegalensis* leaves are said to be used for the traditional treatment of colds, bronchitis and fever in West Africa, perhaps because of their anti-inflammatory, anti-oxidative and anti-microbial properties, which are typically observed for compounds containing phenolic moieties (Armesto et al., 2003; Bouchet et al., 1996; Shin et al., 2004). Additionally, anti-viral and neuroprotective effects have also been shown for some quinic acid

derivatives from the roots and stems of *Erycibe obtusifolia* (Convolvulaceae)(Fig. 12C) (Fan et al., 2015; Liu et al., 2014). However, the ecological effect of quinates remains to be studied.

The presence of the acylated quinates in the feces of the highly specialized *C. vinula* fed a diet rich in salicinoids suggests quinates are involved in the salicinoid transformation. The salicyloyl and benzoyl fragments may be derived from salicinoid metabolism (e.g. saligenin moiety). Furthermore, as often occurs for a phase II reaction, conjugation with quinic acid increases the hydrophilicity of salicylic or benzoic acid (Grant, 1991; Marquardt et al., 2013). Therefore, we assumed that the formation of the presented acylated quinic acids is part of a salicinoid adaptation strategy developed by the Salicaceae specialist *C. vinula* in order to use *P. nigra* as a food plant.

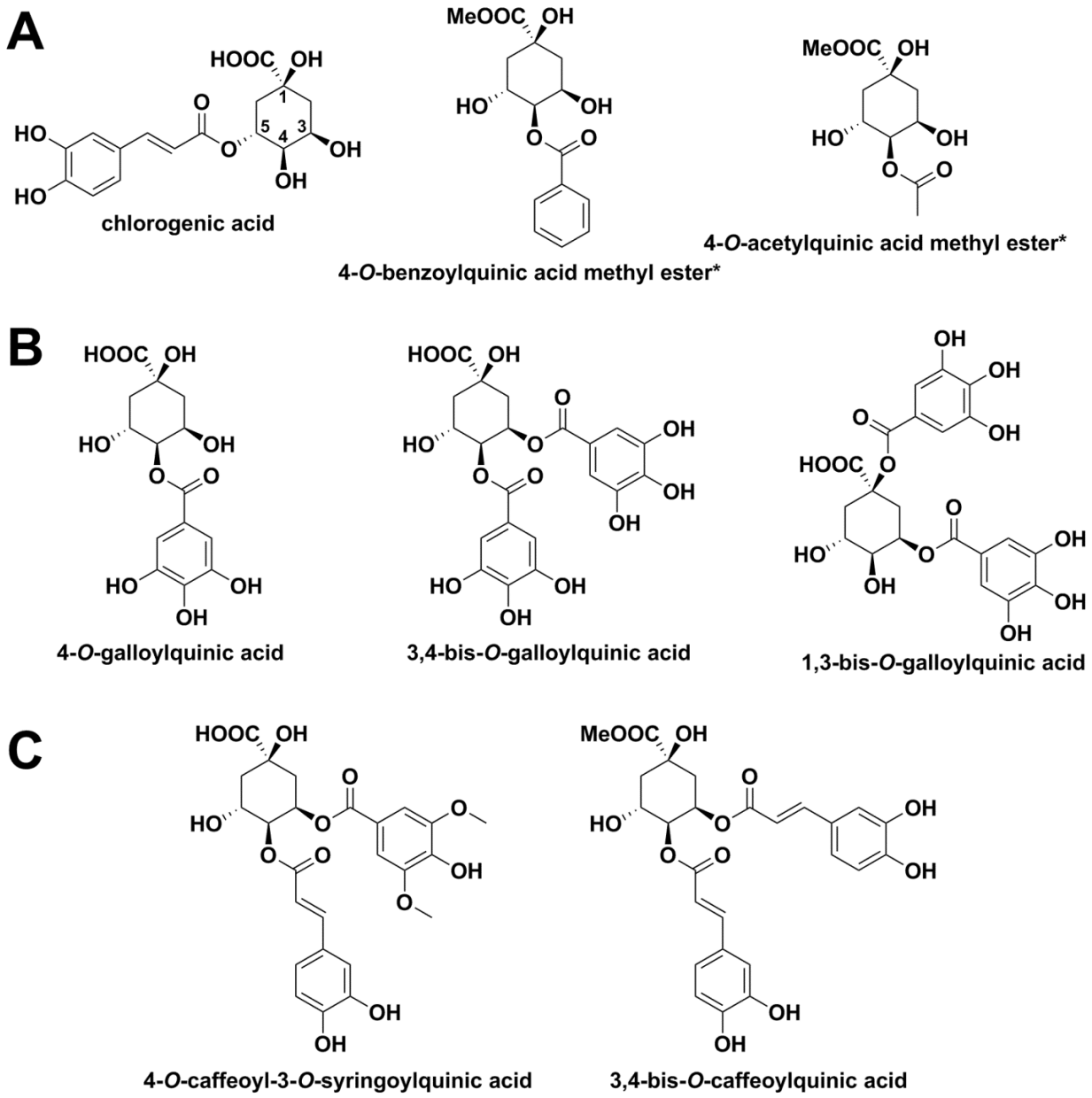

Figure 11 – Different acylated quinic acids from synthetic sources (*) or described as plant constituents.

4.2.2 ^{13}C Labeled precursors are useful to analyze metabolic transformations by NMR and MS techniques

Labeling experiments with stable isotope ^{13}C enable the analysis of metabolic pathways within organisms (Bacher et al., 1998; Cegelski and Schaefer, 2006; Schneider, 2007; Vederas, 1987). Due to

the distribution of the labeled compound and transformation within the living tissue, the ^{13}C label is eventually found in downstream products (Eisenreich and Bacher, 2000; Schaefer et al., 1980). In manuscript III, we used NMR and MS analysis to investigate ^{13}C incorporation into the fecal metabolites of the Salicaceae specialist *C. vinula*. In comparison to the mass spectra of the non-labeled compound, spectra of ^{13}C labeled compounds display additional peaks corresponding to the ^{13}C isotopologues (Eisenreich et al., 2013). The benefit of ^{13}C NMR spectroscopy is that we can determine not only whether a compound is labeled but also in which position the label occurs (Schneider, 2007). Furthermore, ^{13}C enrichment leads to an increase of the signals within the ^{13}C NMR spectra. Additionally, due to ^{13}C-^{13}C spin-spin coupling between adjacent ^{13}C atoms, satellite signals are observed. Both signal properties enable the identification of labeled compounds within mixtures (Gowda et al., 2012; Schneider, 2007; Vederas, 1987).

However, knowledge about the amount and position of ^{13}C isotope atoms in a potential precursor for feeding experiments with living organisms is essential for later data analysis (Eisenreich and Bacher, 2000). In the case of purchased ^{13}C labeled compounds, the information on the labeled position(s) is usually provided by the vendor. In our case, the ^{13}C labeled salicortin was generated *in vivo* because it was neither commercially available nor accessible by chemical synthesis (Cegelski and Schaefer, 2006; Nagasawa et al., 2010). After almost one month of stable isotope labeling with $^{13}CO_2$ in an automatic pulse-labeling assembly specially developed for this purpose (Fig. 13), salicortin was isolated and characterized by MS and NMR techniques, revealing a uniform labeling with a ^{13}C content of 82 % (Taubert et al., 2011). The high degree of incorporation and even distribution of the ^{13}C isotopes throughout the [U-^{13}C]salicortin molecule provided high sensitivity in NMR spectroscopy and MS after the feeding experiments and, hence, enabled a first insight into the salicinoid transformation by *C. vinula*.

Certainly, the number of studies using isotope incorporation seems endless and proves the value of ^{13}C labeling techniques on plant secondary metabolites (Calvin, 1956; Cegelski and Schaefer, 2006;

Hutchinson et al., 1976; Kurilich et al., 2003; Romisch-Margl et al., 2007; Schaefer et al., 1980). Surprisingly, labeling methods developed over more than half a century ago are still in use.

In our case, we developed a labeling assembly (Fig. 13) with a mini-computer connected to several sensor modules monitoring CO_2 and O_2 concentration, relative humidity, temperature, light, pressure and soil moisture. This setup allows the regulation of the CO_2 concentration, relative humidity and light supply (if requested). Furthermore, the mobility of the labeling assembly enables the free choice of experimental site (e.g. laboratory or green house) with the important advantage that the same temperature and light conditions can obtain everywhere. The computer platform allows the development of scripts to ensure both the complete automation of the labeling process and flexibility.

Figure 12 – Left: Automatic pulse labeling assembly for the cultivation of plants under controlled atmosphere with $^{13}CO_2$ as ^{13}C source. **Right:** Six young individuals of *P. trichocarpa x deltoides* Beaupré in the assembly during the labeling process.

4.2.3 Acylated quinic acids are salicortin transformation products of C. vinula *larvae*

The role of the quinates in the interaction between *C. vinula* larvae and poplar plants was studied by feeding experiments with [U-^{13}C]salicortin, as presented in manuscript III. NMR and MS analysis of larval feces obtained after the insects fed on a ^{13}C labeled diet confirmed the relationship of substrate to product between salicortin and the acylated quinic acids. Furthermore, ^{13}C incorporation was observed for the salicyloyl moiety but not for the quinic acid unit, indicating that at least one additional substrate is involved in the formation of the quinate compounds. Although, incorporation in the benzoyl moieties was not detected, it can be hypothesized that these acyl units originate from other salicinoid compounds carrying benzoyl- or cinnamoyl-derived substituents (Boeckler et al., 2011). We further hypothesized that chlorogenic acid or other caffeoyl quinates act as potential substrates for the quinic acid core fragment. These compounds have been described as constituents of Salicaceae species and, additionally, are known as plant defense compound due to their ability to yield toxic o-quinone and chlorogenoquinone in the presence of PPOs (Calixto Junior et al., 2016; Caseys et al., 2015; Glynn et al., 2004; Hammerschmidt, 2014; Patil and Dimond, 1967). However, both hypotheses have to be proven by future experiments.

The ^{13}C incorporation into the salicyloyl substituents gives clear evidence that saligenin is transformed into salicylic acid. Since we did not find other ^{13}C labeled compounds in the insect feces, we assume that HCH transformation also yields salicylic acid. A similar transformation has been observed under alkaline conditions during synthetic studies on Me-HCC (Nagasawa et al., 2010). Investigations of the pH value of the dissected insects (Fig. 14 B) revealed an acidic (pH value 4.4-5.0) foregut, a mild alkaline midgut (pH value 7.6-8.0) and a slightly acidic hindgut (pH value 6.5-6.6) in *C. vinula* larvae (unpublished results). The alkaline midgut milieu of *C. vinula* could cause HCH to spontaneously degrade to salicylic. Additionally, our observations of the pH gradient within the gut lumen of *C. vinula* are in consistence with studies of other lepidopteran herbivores, like the broadleaf tree generalist *L. dispar* (gypsy moth)(Appel and Martin, 1990).

In the case of *L. dispar*, a decrease in *β*-glucosidase activity was reported after elevated salicinoid ingestion, preventing the formation of toxic aglycons in the insect gut (Clausen et al., 1990; Lindroth and Hemming, 1990). Additionally, investigations into the activity of *L. dispar* larvae gut enzymes have indicated that esterases and glutathione transferases are involved in the detoxification of salicinoids (Hemming and Lindroth, 2000). However, a more recent study of *L. dispar* larvae reported that the salicortin degradation products saligenin and catechol (derived from HCH) were conjugated with glucose phosphates in order to deactivate their toxic properties and then to excrete them (Boeckler et al., 2016). A similar conjugation (phase II detoxification) by glycosylation (likely due to UDP-glycosyltransferases)(Després et al., 2007) has been reported for other lepidopterans such as *Manduca sexta* (Ahmad and Hopkins, 1992) and *Bombyx mori* (Luque et al., 2002). However, these examples refute the formation of phosphorylated conjugates as phase II detoxification products because phosphate is a limited resource for the insect and essential for its growth. Why phosphates should be used in the detoxification processes of *L. dispar* remains unknown (Boeckler et al., 2016; Elser et al., 2007; Visanuvimol and Bertram, 2011).

According to our data, reported in manuscript III, *C. vinula* has developed a transformation strategy that differs completely from that of other lepidopterans in order to promote the excretion of harmful salicinoids. Hence, we hypothesize the following degradation mechanism for salicortin (Fig.14 A):

During ingestion, the leaf material is mechanically ground by the insect's mouth parts. Sugar hydrolysis is induced in the mouth or inside the foregut region of the intestine by either plant-derived *β*-glucosidases and/or acidic pH value. Unfortunately, we cannot exclude the possibility that endogenous *β*-glucosidases contribute to this process (Pentzold et al., 2014). Afterwards, the ester bond of HCH-saligenin is cleaved, which results in the formation of saligenin and HCC. Even though it is possible that an esterase is involved in this process, we were able to show the rapid degradation of salicortin in aqueous solutions at pH values slightly above seven during *in vitro* experiments (unpublished results). Therefore, due to the alkaline environment in the larval middle gut, the spontaneous degradation of the aglycon appears possible. Spontaneous HCC transformation into

salicylic acid under the alkaline conditions in the midgut has been reported (Nagasawa et al., 2010). However, the transformation of saligenin to salicylic acid is a simple oxidative step. This reaction may be carried out by a cytochrome P450 monooxygenases (CYP), an enzyme class often associated with the insect gut membranes (Després et al., 2007; Heckel, 2014). The overexpression of CYPs related to the detoxification of plant chemicals has been reported for other lepidopteran species, such as the black swallowtail (*Papilio polyxenes*)(Petersen et al., 2001), the tobacco hawk moth (*M. sexta*)(Snyder et al., 1993) and the fall armyworm (*Spodoptera frugiperda*)(Giraudo et al., 2015). In these organisms, the induction of CYPs after toxin ingestion was associated with the midgut tissue of the representative larvae. Likewise, we expect that CYPs are involved in the saligenin oxidation that takes place in the midgut lumen of *C. vinula* larvae.

It is still unclear how and where the formation of the quinic acid conjugates takes place. However, since we were not able to find any trace of acylated quinic acids inside the insect hemolymph (manuscript III), it is likely that salicortin degradation occurs in the insect's gut.

Conjugation of salicylic acid with quinic acid could be described as a typical phase II reaction because of the increased water solubility of the resulting acylated quinic acids. According to this hypothesis, the hydrolysis of the ester bond and the oxidation, forming salicylic acid, are phase I reactions. They prevent the harmful species saligenin and HCH from initiating reactions that could cause serious damage to the organism. At the same time, these reactions enable the introduction of carboxyl functions and their conjugation with quinic acid, which ultimately supports compound excretion (phase III detoxification)(Grant, 1991; Marquardt et al., 2013).

In a nutshell, the results provided in manuscript III give a first glimpse into the salicortin transformation strategy of the Salicaceae specialist *C. vinula*. Due to the observed ^{13}C incorporation, there is no doubt about the product-substrate relationship to the acylated quinic acids. As a consequence, we were able to hypothesize the existence of a metabolic pathway which can easily be transferred to other salicinoids because salicortin possesses the majority of structural features

characterizing a salicinoid compound. To the best of our knowledge, that defense strategy against Salicaceae-derived salicinoids is unique to *C. vinula*.

Nevertheless, open questions remain to be answered in future studies. For example, feeding experiments with labeled chlorogenic acid and benzoyl-containing salicinoids may give information about the origin of the quinic acid and the benzoyl moieties within the acylated quinic acid compounds. Certainly, the toxicity of these compounds needs to be tested in order to confirm that they are less toxic to the insect than their salicinoid precursors. Indeed, as long as it is not proven that "detoxification" occurs, one should avoid this term.

C. vinula larvae are able to consume huge amounts of protoxic salicinoids, and it would be interesting to test if there is a lethal dose for these compound, as observed for the gypsy moth (*L. dispar*)(Lindroth and Hemming, 1990) and the forest tent caterpillar (*Malacosoma disstria*, Lepidoptera)(Lindroth and Bloomer, 1991). Furthermore, many insects have been shown to have a close association with symbiotic microorganisms. These bacteria may support herbivore defenses against plant-derived toxins. Accordingly, we cannot exclude the possibility that endosymbiotic organisms are involved in the supposed metabolism of salicinoids in *C. vinula* larvae (Baumann, 2005; Vogel et al., 2017). Analyzing the insect's gut transcriptome and its microbiome will provide valuable information about possible enzyme candidates and the endosymbionts that may be involved in the digestive mechanisms of *C. vinula* larvae (Vogel et al., 2017). Finally, in order to evaluate the ecologic relevance (and thus the potential for herbivorous pests) of the discussed hypothetical metabolism, it would be interesting to know if this pathway is indeed unique for *C. vinula*. If there are other species with this metabolic pathway, knowledge of their phylogenetic relationship might provide insights into the mechanism's evolutionary development.

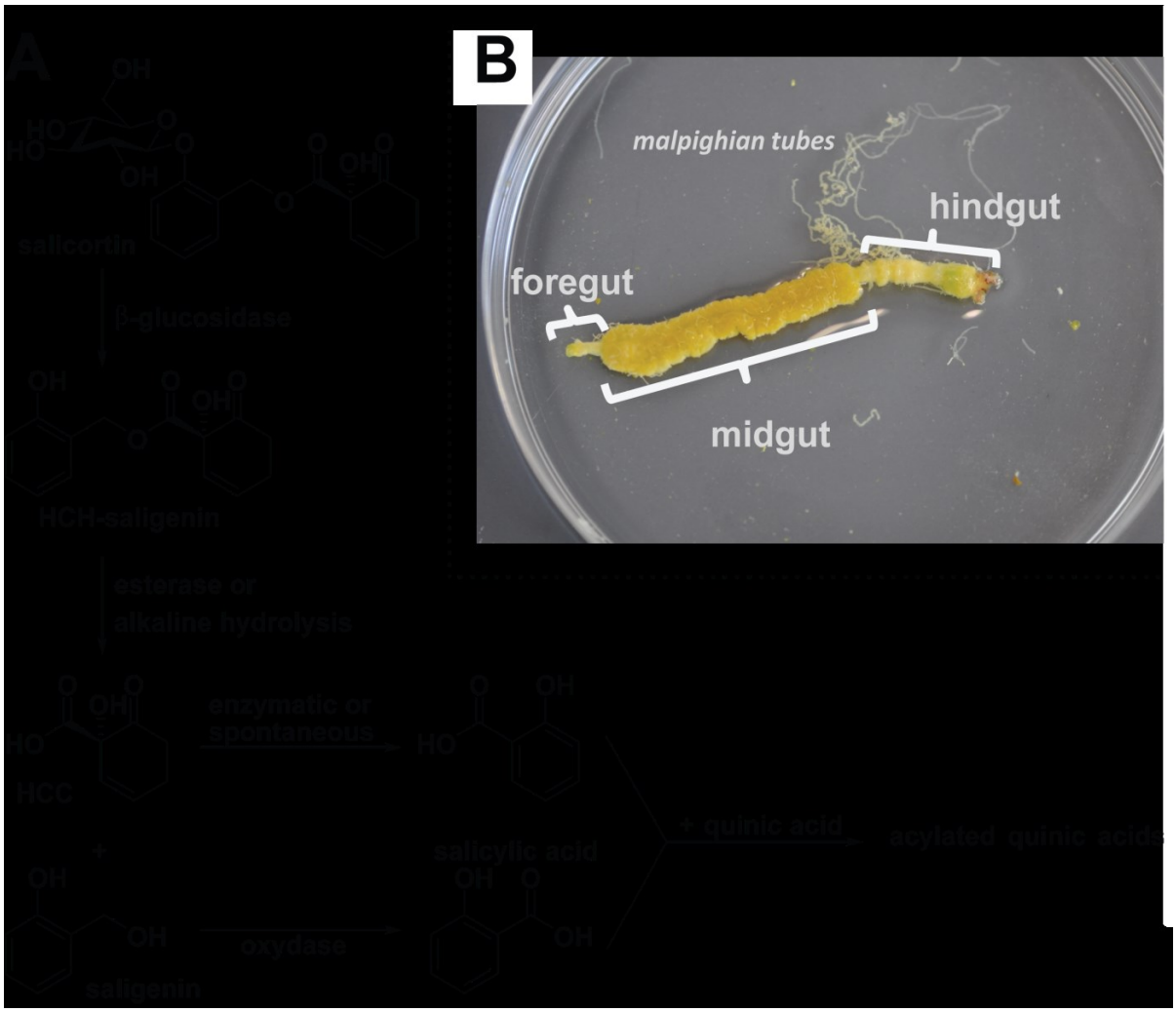

Figure 13 - A) Metabolic pathway of salicortin in *C. vinula* larvae. **B)** Photograph shows an empty gut from a late 5th-instar *C. vinula* larvae.

4.3 I. polycarpa *leaf constituents and their toxic effect on* C. vinula *and* L. dispar *larvae*

4.3.1 Idesia *phenolic glycosides resemble salicinoids with special structural features exclusively reported for* I. polycarpa

The structural similarities between (–)-idescarpin from *I. polycarpa* and salicortin from *Salix* and *Populus* genera were striking. From *Idesia* leaves, we identified an array of 15 natural products including nine new compounds. *Idesia* metabolites contain an additional hydroxyl group within the aromatic ring of the parent salicinoid structure; together, these form a 2,3-dihydroxy-benzyl alcohol core unit. This structural modification is unique in *Idesia* metabolites, that is, it is not found in the other natural products found in the Salicaceae. Another special feature observed for the majority of *Idesia* compounds is the acylation at position C-4' of the *β*-glucose moiety with a *p*-coumaroyl (either *cis* or *trans*) unit. This observation is surprising for two reasons: First, poplar salicinoids are substituted by a variety of organic acids at the *β*-glucopyranose instead of by *p*-coumaric acid alone, as observed for *Idesia* metabolites (see section 1.4.1). Second, *β*-glucopyranose substituents are typically found at position C-2' and/or C-6' in *Populus* and *Salix*; in contrast, the obtained *Idesia* salicinoids are substituted only at position C-4'. Other examples in which the substitution pattern differs from the pattern in most of the known salicinoids are found in extracts of the Korean king willow (*Salix glandulosa*, Salicaceae) and *Homalium cochinchinensis* (Salicaceae, formerly Flacourtiaceae), which contain 3'-*O*-acetyl salicortin, 3'-*O*-acetyl salicin and cochinchiside (Fig.11A) (Ishikawa et al., 2004; Kim et al., 2015). Furthermore, double substitution with benzoyl moieties at positions C-4' and C-6' were observed for salicinoids in *Homalium longifolium* (Salicaceae, formerly Flacourtiaceae) (Fig. 11C) (Shaari and Waterman, 1995). Salicinoids found in *Itoa orientalis* (Salicaceae, formerly Flacourtiaceae) bear only one substituent, a benzoyl moiety, which can be attached to any hydroxyl function of the *β*-glucopyranose (Fig. 11B) (Chai et al., 2008; Chai et al., 2007). We think this particular substitution

pattern might occur due to acyl-migration of the benzoyl moiety across the hydroxyls of the glucose ring structure (Fischer, 1920; Schmid and Voak, 1963). However, it remains unclear why the substitution of salicinoids of *Idesia* is limited to position C-4'.

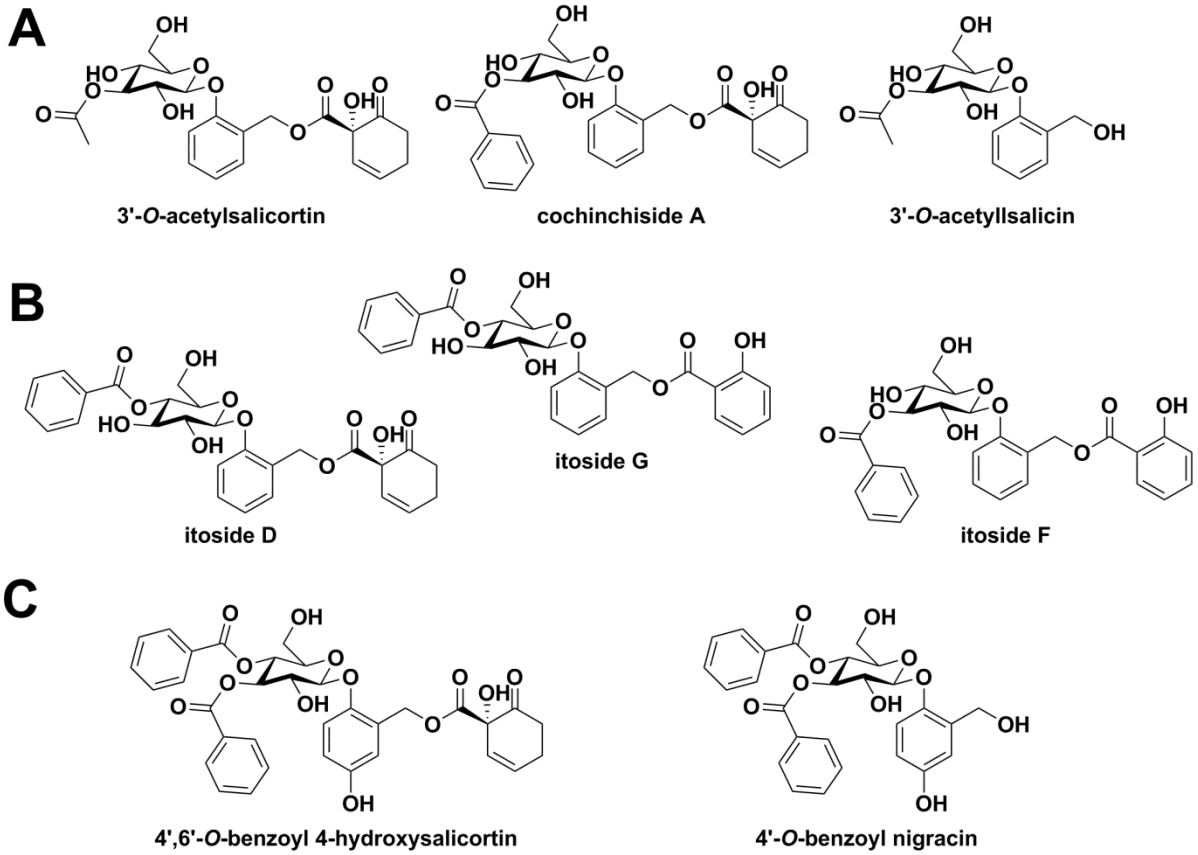

Figure 14 – Examples of structurally related substances with substitution patterns that differ from those of common *Populus* and *Salix* salicinoids, from (**A**) *Salix glandulosa* and *Homalium cochinchinensis,* (**B**) *Itoa orientalis* and (**C**) *Homalium longifolium*.

In our study, four of the isolated *Idesia* metabolites carried a HCH moiety. During the structure elucidation, we applied CD spectroscopy (in accordance with manuscript I) to determine their absolute configuration. It turned out that these compounds share the (*S*)-configuration in their HCH rings with salicortin, tremulacin, HCH-salicortin and (–)-idescarpin. This observation supports our hypothesis that all HCH-bearing salicinoids are (*S*)-configured at this particular position.

Unfortunately, little is known about the ecological importance and potential of the *Idesia* compounds. However, a few pharmacological effects of these substances have been reported. For example, extracts of *I. polycarpa* fruits that contain (–)-idescarpin and idesin showed anti-inflammatory effects, inhibited nitric oxide production (Kim et al., 2007) and exhibited anti-adipogenic activity (Lee et al., 2013). Additionally, in (–)-idescarpin, the inhibition of melanin biosynthesis as well as the presence of anti-oxidative properties have been observed (Baek et al., 2006; Ye et al., 2014).

Due to their structural similarity (e.g. the presence of HCH) and our knowledge of the salicinoids from *Populus* and *Salix,* it is likely that the compounds isolated from the *I. polycarpa* leaf tissue act as defense compounds, with feeding-deterrent and anti-fungal activity (Clausen et al., 1990; Julkunen-Tiitto et al., 1994; Massad et al., 2014). Since the *p*-coumaroyl moiety is a potential precursor for toxic *o*-quinone species, it can act as a cross-linker for dietary or digestive proteins in herbivores (Appel, 1993; Chang, 2009). Therefore, the presence of the *p*-coumaroyl substituents may contribute to the feeding-deterrent and toxic activity of the *Idesia* metabolites.

4.3.2 I. polycarpa *leaves show anti-herbivory activity against Salicaceae generalist and specialist herbivore larvae*

In order to test the effect of *I. polycarpa* leaf constituents on leaf-chewing herbivores, we carried out feeding experiments with the broadleaf tree generalist *L. dispar* and the Salicaceae specialist *C. vinula*. Both species are known to thrive on nutrient sources containing classic salicinoid compounds (see 1.4.1). To determine anti-herbivory properties, the performance of the caterpillar larvae was determined by monitoring larval weight, leaf consumption and mortality. The results of these experiments, presented in manuscript II, indicate that potent anti-herbivory activity results from the *Idesia* leaf diet. Both lepidopterans performed worse on *I. polycarpa* compared to the control groups feeding on *P. nigra*. Surprisingly, these effects appeared to be much more harmful to the specialist (all individuals died) than to the generalist (70 % of larvae died). As mentioned (section 1.5), a high level

of specialization is accompanied by an increased susceptibility to changing environmental conditions (Ali and Agrawal, 2012). As a consequence, it can be assumed that the adaptation of the Salicaceae specialist *C. vinula* is ineffective against the structurally modified compounds in the leaf tissue of *I. polycarpa*. In contrast, the generalist *L. dispar* was also affected by the new diet but appeared more robust. This robustness might be due to its less specialized adaptation, which allows it to exploit a broad range of host plants, including oak (Fagaceae), birch (Betulaceae) and maple (Sapindaceae), in addition to *Populus* and *Salix* (Salicaceae)(Barbosa and Greenblatt, 1979; Lindroth and Hemming, 1990).

Additionally, plant-derived defense proteins might support the anti-herbivory properties of *Idesia* (Baldwin and Preston, 1999). The best-studied defense proteins are protease inhibitors (PIs). They target the major proteolytic digestive enzymes of the herbivores and act as digestibility reducers (Neiman et al., 2009). Furthermore, plant-derived polyphenol oxidases (PPOs) decrease nutrient availability, because they catalyze the oxidation of phenolic secondary metabolites into quinones, on the one hand, and, on the other hand, covalently modify and cross-link dietary proteins during feeding (Felton et al., 1989; Wang and Constabel, 2004). For both systems – the PIs and the PPOs – induction due to herbivory has been demonstrated (Constabel et al., 1995, 1996; Koiwa et al., 1997). Future investigations of the expression levels of defensive proteins such as PIs or PPOs in *I. polycarpa* leaves could shed light on the enzymes' potential toxicity for the studied herbivores *L. dispar* and *C. vinula*.

Judging from what we know about other salicinoid-containing model plants (*Populus* and *Salix*), it is likely that the newly discovered *Idesia* compounds have value as plant defenses. To fully understand the defense mechanism of *Idesia,* we must investigate not only the impact of salicinoids but also the impact of digestive proteins on so-far unknown processes and factors.

5. Summary

Plants have developed a vast array of defenses against herbivores. For example, they produce und store compounds with feeding-deterrent and/or toxic activity as chemical defenses against herbivorous insects. However, attacking herbivores can be prone, adapted or immune to the defenses, with fatal consequences sometimes for the plant, sometimes for the herbivore. To investigate the mechanisms in plant-insect interactions, researchers in chemical ecology rely on model organisms. A so-far uncommon but uncommon model for forest ecosystems is *Populus*, a genus from the Salicaceae family.

In species of the Salicaceae family, including *Populus* and *Salix*, the chemical defense against herbivores is represented by phenolic glycosides. Along with less abundant compounds, like phenolic acids and flavonols, poplars deploy two types of phenolics: condensed tannins and salicinoids. Due to their ability to precipitate nutritional proteins, the tannins are assumed to act as an unspecific, broad-spectrum defense against a range of various herbivorous insects. Salicinoids are believed to play the major role against insect herbivory in *Populus*. These salicylated phenolic glycosides have been described as potent feeding-deterrent compounds with toxic properties that lead to decreased insect performance and increased mortality rates. This mode of action derives from the degradation of salicinoids into toxic saligenin and *o*-quinone species in the alkaline gut environment of the insect. Even after half a century of investigations into the role of these compounds in the plant-insect interactions of *Populus* species, their absolute configuration has been unknown until now. In theory, the HCH structural unit could lead to two enantiomers discriminated by the orientation of the α-hydroxyl group at C-1. The HCH moiety is present in the most abundant salicinoids occurring in *Populus* (e.g. salicortin and tremulacin). Additionally, in the salicinoid metabolism, the HCH unit is the precursor of the *o*-quinone moiety and thus a potent protoxic functionality, partially responsible for the observed defensive properties of HCH-bearing salicinoids.

In conclusion, in manuscript I, we investigated the stereochemistry of typical HCH-bearing salicinoids, i.e. salicortin, tremulacin and HCH-salicortin, by comparing them with (–)-idescarpin, a

structurally related compound from *I. polycarpa* (Salicaceae). Using CD spectroscopy we demonstrated that all measured salicinoids showed (*S*)-configuration at C-1 of the HCH moiety. Although knowledge about salicinoid biosynthesis is limited, it appears likely that all HCH fragments in salicinoids share the same biosynthetic route. Accordingly, our findings lead to the assumption that all HCH-bearing salicinoids are exclusively (*S*)-configured at the C-1 position within the HCH ring. This hypothesis was supported by the work on *I. polycarpa* leaf metabolites presented in manuscript III, where we observed four new salicinoids bearing HCH-moieties with (*S*)-configuration.

Although there are theories about salicinoid bioactivation, little is known about salicinoids' mode of action and impact on herbivores, or about insects' defenses against them. Numerous investigations about *in vitro* mechanisms of salicinoid degradation have been published. However, our knowledge about lepidopteran herbivores based on *in vivo* studies is limited. Our attempt to examine salicinoid degradation in the highly adopted lepidopteran herbivore *C. vinula* (a Salicaceae specialist) is presented in manuscript II. We focused on the transformation of salicortin, the most abundant salicinoid. By analyzing the feces after insects fed on *P. nigra* leaves, we discovered a group of eleven previously unknown compounds with a quinic acid core unit differently acylated by either salicylic, benzoic acid or a mixture of both. Due to their structural similarities with the salicinoids and their high abundance, these acylated quinates are assumed to be transformation products of salicinoid degradation. In order to prove this theory and because isotopic-labeled salicortin was not commercially or synthetically available, we generated the compound *in vivo* by growing small poplar trees in an ^{13}C labeling assembly specially developed for this purpose. By means of NMR spectroscopy and HRMS, a uniform ^{13}C incorporation of 82 % was determined for the salicortin isolated from the labeled plant tissue. The investigation of feces from *C. vinula* fed on *P. nigra* supplemented with the [U-^{13}C]salicortin (82 %) showed ^{13}C incorporation in the salicyloyl moiety of the acylated quinates. In accordance with these data, we concluded that during the degradation of salicortin, both saligenin and the HCH moiety are first transformed into salicylic acid, then connected to quinic acid and ultimately excreted by the larva. These observations are the first made *in vivo* for the salicinoid conversion in a specialist lepidopteran

herbivore. Furthermore, they provide the first evidence for a highly specialized metabolic conversion of Salicaceae salicinoids by *C. vinula*.

The (–)-idescarpin obtained from *I. polycarpa* shows striking similarities to the structure of salicortin. Unlike *Populus* salicinoids, which are known to occur in different plant parts such as bark and leaves, (–)-idescarpin has so far been isolated only from the fruits of *Idesia* trees. However, surprisingly, the leaves of *I. polycarpa* have never been screened for other salicinoid-like substances. In manuscript III, we described the first investigation of leaf metabolites from *I. polycarpa:* 15 natural products including nine new compounds. Additionally, 13 of them had never been described as constituents of *I. polycarpa*. Due to the structural similarities to the known salicinoids from *Populus* (e.g. salicortin), it appeared likely that the identified *Idesia* metabolites also acted as defense compounds. Therefore, the influence of *I. polycarpa* leaf diet on the performance of lepidopteran herbivores was tested in feeding experiments with the Salicaceae specialist *C. vinula* and the broadleaf generalist *L. dispar*. Our data showed an overall decreased performance of both insects fed on *Idesia* compared to the control group fed on *P. nigra*. Furthermore, we observed the specialist reacted drastically, experiencing total mortality after five days. In contrast, 30 % of the *L. dispar* larvae survived this time period but showed reduced mass gain and leaf consumption in comparison to the control group fed on *P. nigra*.

In summary, fast-growing poplar trees have huge economic and environmental potential, both as a source of lumber and for remediating and reforesting sites exposed to salt, heavy metals and organic contaminations. Accordingly, a full understanding of the environmental challenges faced by *P. nigra* will promote our perception of forest-ecosystems and hence enable us to more reliably predict future changes (such as, invading species) in broadleaf forest communities, and to develop strategies for dealing with them. Certainly, herbivore defense is one of the major environmental challenges plants face. Plant-insect interactions generally take place on a molecular level. In order to understand plant defense against insects and, inversely, the counter-strategies by which insects manage to survive on

their host plants, further investigations into and studies of the components of this particular chemical "language" are crucial.

The present thesis substantially contributes to the field of *Populus* research and the establishment of *Populus* as a model organism exploring secondary metabolites responsible for herbivore defense. It also provides methodological groundwork for the investigation of plant-insect interaction on *I. polycarpa* as an analogous system to plant-insect interaction on poplar. Additionally, it offers access to ^{13}C labeled salicinoids and builds a foundation for the detailed understanding of their transformation by adapted lepidopteran herbivores. Ultimately, the knowledge provided in this thesis will support upcoming studies on the ingenious counter-strategies of Salicaceae specialists.

6. Zusammenfassung

Zur Verteidigung gegen Herbivore haben Pflanzen ein breites Spektrum an Verteidigungsmechanismen entwickelt. Zum Beispiel produzieren und speichern sie Verbindungen mit abschreckenden und/ oder giftigen Eigenschaften. Die Effekte dieser chemischen Verteidigung sind unterschiedlich stark. Der angreifende Pflanzenfresser kann entweder anfällig, angepasst oder gänzlich immun sein. Im letzteren Fall hat dies mitunter fatale Konsequenzen für die Pflanze. Die Untersuchung derartiger Mechanismen, sogenannter Pflanze-Insekt-Interaktionen, erfolgt auf dem Gebiet der chemischen Ökologie mit Hilfe von Modellorganismen. Ein noch recht junges, aber sich stetig entwickelndes Modell für das Ökosystem Wald stellt der Genus *Populus* aus der Familie der Salicaceae dar.

Die chemische Verteidigung von Salicaceae-Spezies (einschließlich *Populus* und *Salix*) gegen pflanzenfressende Insekten besteht aus Phenylglykosiden. Neben einigen, vereinzelt auftretenden Verbindungen wie Phenolcarbonsäuren und Flavonolen setzen Pappeln vor allem folgende zwei Typen von Phenolen ein: Kondensierte Tannine und Salicinoide. Auf Grund ihrer Eigenschaft, Nahrungsproteine zu fällen, gelten Tannine als Breitbandverteidigung gegen verschiedene Arten von Herbivoren. Den Salicinoiden wird im Gegensatz dazu die Hauptrolle in der Verteidigung der Pflanze gegen herbivore Insekten zugesprochen. Diese salicylierten Phenolglykoside zeichnen sich durch potente fraßhemmende sowie toxische Eigenschaften aus, welche die Leistungsfähigkeit von Insekten reduzieren und deren Sterberaten erhöhen. Die Aktivität dieser Substanzen ergibt sich durch Zerfall in der basischen Darmumgebung der Insekten unter Bildung von Saligenin und *o*-Chinon.

Die Rolle der Salicinoide in den Pflanze-Insekt-Interaktionen von Pappeln wird seit etwa einem halben Jahrhundert erforscht. Die HCH-Einheit, der am häufigsten auftretenden Salicinoiden (z.B. Salicortin, Tremulacin), ist die Vorstufe für die oben genannten *o*-Chinone und stellt damit stellt damit eine potente protoxische Funktionalität der Salicinoide dar. Die absolute Konfiguration dieser strukturellen Einheit konnte jedoch erst in dieser Arbeit entschlüsselt werden. Die Untersuchung der

Stereochemie typischer HCH-enthaltender Salicinoide (Salicortin, Tremulacin und HCH-Salicortin) durch den Vergleich mit (–)-Idescarpin, einer strukturell verwandten Substanz aus *I. polycarpa* (Salicaceae), war Inhalt der Arbeit von Manuskript I. Anhand von CD-spektroskopischen Analysen konnten wir zeigen, dass die C-1-Position des HCH-Fragmentes aller gemessenen Salicinoide (*S*)-Konfiguration aufweist. Trotz des limitierten Wissens über die Salicinoidbiosynthese ist anzunehmen, dass alle in den Salicinoiden auftretenden HCH-Substituenten aus dem gleichen biosynthetischen Ursprung gebildet werden. Dementsprechend führen unsere Ergebnisse zu der Annahme, dass HCH-Substituenten in Salicinoiden ausschließlich (*S*)-Konfiguration aufweisen. Diese Vermutung wurde durch weitere Beobachtungen während der Arbeit an den Blattmetaboliten von *I. polycarpa* bekräftigt (Manuskript III). Hier gelang uns die Strukturaufklärung vier weitere Salicinoide mit (*S*)-Konfiguration.

Die Bioaktivierung der Salicinoide ist in zahlreichen Veröffentlichungen getestet und beschrieben worden. Über mögliche Verteidigungsmechanismen herbivorer Insekten gegen diese Verbindungen ist allerdings noch immer wenig bekannt. Trotz zahlreicher veröffentlichter Untersuchungen möglicher *in vitro*-Zerfallsmechanismen der Salicinoide ist unser Wissen über deren *in vivo*-Metabolisierung in Schmetterlingslarven nur sehr begrenzt. Manuskript II stellt die Salicinoidmetabolisierung durch Larven des Nachtschwärmers *C. vinula*, einem stark angepassten Salicaceae-Spezialisten in den Mittelpunkt. Hierzu wurde die Transformation des am häufigsten auftretenden Salicinoids, des Salicortins, stellvertretend für die anderen Verbindungen dieser Substanzgruppe untersucht. Analysen der Larvenfäkalien nach dem Konsum von *P. nigra*-Blättern ergaben elf unbekannte Chinasäureester, welche unterschiedliche Acylierungen durch Salizylsäure, Benzoesäure oder einer Kombination aus beiden aufwiesen. Auf Grund der strukturellen Ähnlichkeit zu den Salicinoiden sowie ihrer großen Menge im Kotmaterial wurden diese acylierten Chinasäureester als Transformationsprodukte des Salicinoidmetabolismus von *C. vinula*-Larven vorgeschlagen. Die Überprüfung dieser Hypothese erfolgte durch die Verwendung von ^{13}C-markiertem Salicortin in einem Raupenfütterungsexperiment. Da isotopenmarkiertes Salicortin weder synthetisch noch käuflich zugänglich war, erfolgte dessen

Herstellung *in vivo*. Zu diesem Zweck wurden junge Pappelbäume in einem von uns speziell für derartige ^{13}C-Markierungsversuche entwickelten Aufbau unter $^{13}CO_2$-Atmosphäre kultiviert. Mit Hilfe von NMR-Spektroskopie sowie HRMS konnte ein gleichmäßiger ^{13}C-Einbau mit einer Anreicherung von 82 % für das aus dem markierten Pflanzenmaterial isolierte Salicortin bestimmt werden. Die anschließende Untersuchung des *C. vinula* Kotes nach dem Konsum von, mit [U-^{13}C]Salicortin (82 %) bestrichenen, *P. nigra*-Blättern zeigte einen Einbau von ^{13}C in die Salizylsäure-Einheiten der acylierten Chinasäureverbindungen. Diese Ergebnisse implizieren, dass während des Salicortinabbaus im Darm des Insektes sowohl das Saligenin als auch das HCH-Fragment zur Salizylsäure transformiert, anschließend an die Chinasäurespezies gebunden und schließlich über den Kot ausgeschieden werden. Diese Daten geben folglich erste Hinweise über den hoch spezialisierten metabolischen Abbau von Salicortin durch *C. vinula* und stellen zudem die ersten *in vivo*-Beobachtungen für die Umwandlung von Salicaceae-Salicinoiden durch auf Pappel spezialisierte Schmetterlingslarven dar

Die strukturelle Ähnlichkeit zwischen (–)-Idescarpin aus *I. polycarpa* und Salicortin erschien verblüffend. Aber anders als die Salicinoide aus *Populus*, welche sich in unterschiedlichen Pflanzenteilen wie Rinde und Blätter befinden, wurde (–)-Idescarpin bisher ausschließlich aus den Früchten des *Idesia*-Baumes isoliert. In Manuskript III beschreiben wir die erste Untersuchung der Blattmetabolite von *I. polycarpa*. Von den 15 gefundenen Naturstoffen wurden 13 bis dato niemals als chemische Bestandteile von *Idesia* beobachtet und neun waren unbekannt. Aufgrund der strukturellen Ähnlichkeiten zu den aus *Populus* bekannten Salicinoiden erschien es wahrscheinlich, dass die aus *Idesia* neuen Metabolite aus *Idesia* ebenfalls zur chemischen Verteidigung gegen Herbivore dienen. Aus diesem Grund wurde in Fütterungsversuchen der Einfluss einer Ernährung aus *I. polycarpa*-Blättern auf die Leistungsfähigkeit des Salicaceae-Spezialisten *C. vinula* und des Laubbaum-Generalisten *L. dispar* getestet. Unsere Ergebnisse zeigten eine generelle Abnahme der Leistungsfähigkeit beider Spezies im Vergleich zu deren Kontrollgruppen mit Pappeldiät. Die Spezialisten zeigten eine drastische Reaktion auf die *Idesia*–Ernährung, welche durch den Tod aller Individuen der Versuchsreihe nach fünf Tagen gekennzeichnet war. Vom Generalist *L. dispar* hingegen

überlebten in diesem Zeitraum 30 % der Individuen. Diese wiesen allerdings einen gehemmten Fraßverhalten sowie reduzierte Gewichtszunahme im Vergleich zur Kontrollgruppe auf.

Pappeln besitzen ein großes ökonomisches sowie ökologisches Potenzial. Das zeigt sich in ihrer Anwendung zur Holzgewinnung in der Forstwirtschaft sowie bei der Sanierung und Wiederbewaldung von kontaminierten und nährstoffarmen Böden. Um diese Ressourcen zu nutzen, ist ein umfassendes Verständnis der Umweltinteraktionen und daraus resultierender Herausforderungen notwendig. Darüber hinaus hilft uns das gewonnene Wissen, Waldökosysteme besser zu verstehen. Es ermöglicht vertrauenswürdigere Interpretationen sowie präzisere Vorhersagen bezüglich systematischer Veränderungen von Waldökosystemen, wie sie sich zum Beispiel durch den Einfall invasiver Spezies ergeben. Unter den Umweltherausforderungen, denen Pflanzen ausgesetzt sind, stellt die Verteidigung gegen Herbivore eines der Hauptprobleme dar. Diese Art der Interaktion zwischen Pflanzen und Insekten findet für gewöhnlich auf molekularer Ebene statt. Um die Verteidigung der Pflanzen gegen Insekten sowie deren Konterstrategien, zu verstehen, sind noch viele Untersuchungen und Studien dieser spezifischen chemischen Sprache notwendig. Durch die strukturellen Untersuchungen der, für die Verteidigung von *Populus* gegen Herbivore verantwortlichen, Sekundärmetaboliten trägt die vorliegende Arbeit substanziell zum tieferen Verständnis der Gattung und deren Etablierung als Modellorganismus bei. Darüber hinaus liefert sie das methodische Grundgerüst für die zukünftige Erforschung der Pflanzen-Insekt-Interaktionen bei *I. polycarpa* als analoges Vergleichssystem zu *Populus*. Diese Arbeit ermöglicht zusätzlich einen Zugang zu ^{13}C-markierten Salicinoiden und legt die Grundlage für ein detailliertes Verständnis ihrer Transformation durch hochgradig angepasste, pflanzenfressende Schmetterlingslarven. Die Erkenntnisse, erworben durch diese Arbeit, werden schließlich zukünftige Studien über die erfindungsreichen Konter-Strategien von Salicaceae-Spezialisten unterstützen und damit unser Verständnis dieser Thematik weiter fördern.

References of General Introduction and Discussion

Adhikari, K. B., Tanwir, F., Gregersen, P. L., Steffensen, S. K., Jensen, B. M., Poulsen, L. K., Nielsen, C. H., Høyer, S., Borre, M., Fomsgaard, I. S., **2015**. Benzoxazinoids: Cereal phytochemicals with putative therapeutic and health-protecting properties. Molecular Nutrition & Food Research 59, 1324-1338.

Ahmad, S. A., Hopkins, T. L., **1992**. Phenol β-glucosyltransferase and β-glucosidase activities in the tobacco hornworm larva *manduca-sexta* (L.) - properties and tissue localization. Archives of Insect Biochemistry and Physiology 21, 207-224.

Aitchison, E. W., Kelley, S. L., Alvarez, P. J. J., Schnoor, J. L., **2000**. Phytoremediation of 1,4-dioxane by hybrid poplar trees. Water Environment Research 72, 313-321.

Alfred, J., Baldwin, I. T., **2015**. New opportunities at the wild frontier. eLife 4, e06956.

Ali, J. G., Agrawal, A. A., **2012**. Specialist versus generalist insect herbivores and plant defense. Trends in Plant Science 17, 293-302.

Anderson, A. B., Riffer, R., Wong, A., **1969**. Monoterpenes, fatty and resin acids of *Pinus contorta* and *Pinus attenuata*. Phytochemistry 8, 2401-2403.

Appel, H. M., **1993**. Phenolics in ecological interactions: The importance of oxidation. Journal of Chemical Ecology 19, 1521-1552.

Appel, H. M., Martin, M. M., **1990**. Gut redox conditions in herbivorous lepidopteran larvae. Journal of Chemical Ecology 16, 3277-3290.

Armesto, N., Ferrero, M., Fernandez, S., Gotor, V., **2003**. Novel enzymatic synthesis of 4-O-cinnamoyl quinic and shikimic acid derivatives. The Journal of Organic Chemistry 68, 5784-5787.

Babst, B. A., Harding, S. A., Tsai, C.-J., **2010**. Biosynthesis of phenolic glycosides from phenylpropanoid and benzenoid precursors in *Populus*. Journal of Chemical Ecology 36, 286-297.

Bacher, A., Rieder, C., Eichinger, D., Arigoni, D., Fuchs, G., Eisenreich, W., **1998**. Elucidation of novel biosynthetic pathways and metabolite flux patterns by retrobiosynthetic NMR analysis. FEMS Microbiology Reviews 22, 567-598.

Baek, S., Kim, D., Lee, C., Kho, Y., Lee, C., **2006**. Idescarpin isolated from the fruits of *Idesia polycarpa* inhibits melanin biosynthesis. Journal of Microbiology and Biotechnology 16, 667-672.

Baldwin, I. T., Preston, C. A., **1999**. The eco-physiological complexity of plant responses to insect herbivores. Planta 208, 137-145.

Ballach, H. J., **1997**. Suitability and use of poplars as bioindicators - a new concept. Environmental Science and Pollution Research 4, 37-45.

Barbehenn, R., Dukatz, C., Holt, C., Reese, A., Martiskainen, O., Salminen, J. P., Yip, L., Tran, L., Constabel, C. P., **2010**. Feeding on poplar leaves by caterpillars potentiates foliar peroxidase action in their guts and increases plant resistance. Oecologia 164, 993-1004.

Barbehenn, R. V., Jaros, A., Lee, G., Mozola, C., Weir, Q., Salminen, J. P., **2009**. Tree resistance to *Lymantria dispar* caterpillars: Importance and limitations of foliar tannin composition. Oecologia 159, 777-788.

Barbosa, P., Greenblatt, J., **1979**. Suitability, digestibility and assimilation of various host plants of the gypsy moth *Lymantria dispar* L. Oecologia 43, 111-119.

Baumann, P., **2005**. Biology bacteriocyte-associated endosymbionts of plant sap-sucking insects. Annual Review of Microbiology 59, 155-189.

Baycu, G., Tolunay, D., Ozden, H., Gunebakan, S., **2006**. Ecophysiological and seasonal variations in Cd, Pb, Zn, and Ni concentrations in the leaves of urban deciduous trees in Istanbul. Environmental Pollution 143, 545-554.

Becerra, J. X., **2003**. Synchronous coadaptation in an ancient case of herbivory. Proceedings of the National Academy of Sciences, USA 100, 12804-12807.

Bennett, R. N., Wallsgrove, R. M., **1994**. Secondary metabolites in plant defense-mechanisms. New Phytologist 127, 617-633.

Benyó, D., Horváth, E., Németh, E., Leviczky, T., Takács, K., Lehotai, N., Feigl, G., Kolbert, Z., Ördög, A., Gallé, R., Csiszár, J., Szabados, L., Erdei, L., Gallé, Á., **2016**. Physiological and molecular responses to heavy metal stresses suggest different detoxification mechanism of *Populus deltoides* and *P. x canadensis*. Journal of Plant Physiology 201, 62-70.

Bissonnette, L., St-Arnaud, M., Labrecque, M., **2010**. Phytoextraction of heavy metals by two Salicaceae clones in symbiosis with arbuscular mycorrhizal fungi during the second year of a field trial. Plant and Soil 332, 55-67.

Blom, D., Fabbri, C., Eberl, L., Weisskopf, L., **2011**. Volatile-mediated killing of *Arabidopsis thaliana* by bacteria is mainly due to hydrogen cyanide. Applied and Environmental Microbiology 77, 1000-1008.

Blount, Z. D., **2015**. The unexhausted potential of *E. coli*. eLife 4, e05826.

Boeckler, G. A., Gershenzon, J., Unsicker, S. B., **2011**. Phenolic glycosides of the Salicaceae and their role as anti-herbivore defenses. Phytochemistry 72, 1497-1509.

Boeckler, G. A., Paetz, C., Feibicke, P., Gershenzon, J., Unsicker, S. B., **2016**. Metabolism of poplar salicinoids by the generalist herbivore *Lymantria dispar* (Lepidoptera). Insect Biochemistry and Molecular Biology 78, 39-49.

Bouchet, N., Levesque, J., Blond, A., Bodo, B., Pousset, J. L., **1996**. 1,3-Di-O-galloylquinic acid from *Guiera senegalensis*. Phytochemistry 42, 189-190.

Bowers, M. D., **1991**. Iridoid glycosides. In: Rosenthal, G. B., M. (Ed.), Herbivores: Their interactions with secondary plant metabolites, vol. 1. Academic Press, San Diego, pp. 251-295.

Bowers, M. D., Farley, S., **1990**. The behaviour of grey jays, *Perisoreus canadensis*, towards palatable and unpalatable Lepidoptera. Animal Behaviour 39, 699-705.

Bradshaw, H. D., Ceulemans, R., Davis, J., Stettler, R., **2000**. Emerging model systems in plant biology: Poplar (*Populus*) as a model forest tree. Journal of Plant Growth Regulation 19, 306-313.

Bradshaw, H. D., Stettler, R. F., **1993**. Molecular genetics of growth and development in *Populus*. I. Triploidy in hybrid poplars. Theoretical and Applied Genetics 86, 301-307.

Bulduk, I., Gezer, B., Cengiz, M., **2015**. Optimization of ultrasound-assisted extraction of morphine from capsules of *Papaver somniferum* by response surface methodology. International Journal of Analytical Chemistry 2015, 8.

Burken, J. G., Schnoor, J. L., **1997**. Uptake and metabolism of atrazine by poplar trees. Environmental Science & Technology 31, 1399-1406.

Calixto Junior, J. T., de Morais, S. M., Gomez, C. V., Molas, C. C., Rolon, M., Boligon, A. A., Athayde, M. L., de Morais Oliveira, C. D., Tintino, S. R., Henrique Douglas, M. C., 2016. Phenolic composition and antiparasitic activity of plants from the Brazilian Northeast "Cerrado". Saudi Journal of Biological Sciences 23, 434-440.

Calvin, M., **1956**. The photosynthetic carbon cycle. Journal of the Chemical Society.

Caseys, C., Stritt, C., Glauser, G., Blanchard, T., Lexer, C., **2015**. Effects of hybridization and evolutionary constraints on secondary metabolites: The genetic architecture of phenylpropanoids in european *Populus* species. Plos One 10, 23.

Casida, J. E., Quistad, G. B., **1998**. Golden age of insecticide research: past, present, or future? Annual Review of Entomology 43, 1-16.

Cegelski, L., Schaefer, J., **2006**. NMR determination of photorespiration in intact leaves using *in vivo* $^{13}CO_2$ labeling. Journal of Magnetic Resonance 178, 1-10.

Chai, X. Y., Song, Y. L., Xu, Z. R., Shi, H. M., Bai, C. C., Bi, D., Wen, J., Li, F. F., Tu, P. F., **2008**. Itosides J-N from *Itoa orientalis* and structure - anti-COX-2 activity relationship of phenolic glycosides. Journal of Natural Products 71, 814-819.

Chai, X. Y., Xu, Z. R., Ren, H. Y., Shi, H. M., Lu, Y. N., Li, F. F., Tu, P. F., **2007**. Itosides A – I, new phenolic glycosides from *Itoa orientalis*. Helvetica Chimica Acta 90, 2176-2185.

Chang, T. S., **2009**. An updated review of tyrosinase inhibitors. International Journal of Molecular Sciences 10, 2440-2475.

Chase, M. W., Sue, Z., Lledo, M. D., Wurdack, K. J., Swensen, S. M., Fay, M. F., **2002**. When in doubt, put it in Flacourtiaceae: a molecular phylogenetic analysis based on plastid rbcl DNA sequences. Kew Bulletin 57, 141-181.

Chedgy, R. J., Kollner, T. G., Constabel, C. P., **2015**. Functional characterization of two acyltransferases from *Populus trichocarpa* capable of synthesizing benzyl benzoate and salicyl benzoate, potential intermediates in salicinoid phenolic glycoside biosynthesis. Phytochemistry 113, 149-159.

Chou, C.-J., Lin, L.-C., Tsai, W.-J., Hsu, S.-Y., Ho, L.-K., **1997**. Phenyl-*β*–D-glucopyranoside derivatives from the fruits of *Idesia polycarpa*. Journal of Natural Products 60, 375-377.

Clausen, T. P., Koller, J. W., Reichardt, P. B., **1990**. Aglycone fragmentation accompanies *β*-glucosidase catalyzed hydrolysis of salicortin, a naturally-occurring phenol glycoside. Tetrahedron Letters 31, 4537-4538.

Clausen, T. P., Reichardt, P. B., Bryant, J. P., Werner, R. A., Post, K., Frisby, K., **1989**. Chemical model for short-term induction in quaking aspen (*Populus tremuloides*) foliage against herbivores. Journal of Chemical Ecology 15, 2335-2346.

Constabel, C. P., Bergey, D. R., Ryan, C. A., **1995**. Systemin activates synthesis of wound-inducible tomato leaf polyphenol oxidase via the octadecanoid defense signaling pathway. Proceedings of the National Academy of Sciences, USA 92, 407-411.

Constabel, C. P., Bergey, D. R., Ryan, C. A., **1996**. Polyphenol oxidase as a component of the inducible defense response in tomato against herbivores. In: Romeo, J. T., Saunders, J. A., Barbosa, P. (Eds.), Phytochemical Diversity and Redundancy in Ecological Interactions. Springer US, Boston, MA, pp. 231-252.

Corse, J., Layton, L. L., Patterson, D. C., **1970**. Isolation of chlorogenic acids from roasted coffee. Journal of the Science of Food and Agriculture 21, 164-168.

Croteau, R., Kutchan, T. M., Lewis, N. G., **2000**. Natural products (secondary metabolites). In: Buchanan, B., Gruissem, W., Jones, R. (Eds.), Biochemistry and Molecular Biology of Plants. American Society of Plant Physiologists, pp. 1250-1318.

Dai, L., Wang, Y., Liu, Z., Li, F., Wang, H., **2014**. Fruit quality of 12 provenances of *Idesia polycarpa* in China. Food, Agriculture and Environment (JFAE) 12, 802-807.

Davini, E., Iavarone, C., Trogolo, C., Aureli, P., Pasolini, B., **1986**. The quantitative isolation and antimicrobial activity of the aglycone of aucubin. Phytochemistry 25, 2420-2422.

de Kraker, J.-W., Franssen, M. C. R., Dalm, M. C. F., de Groot, A., Bouwmeester, H. J., **2001**. Biosynthesis of germacrene a carboxylic acid in chicory roots. Demonstration of a cytochrome P450 (+)-germacrene a hydroxylase and $nadp^+$-dependent sesquiterpenoid dehydrogenase(s) involved in sesquiterpene lactone biosynthesis. Plant Physiology 125, 1930-1940.

Dekant, W., **2009**. The role of biotransformation and bioactivation in toxicity. In: Luch, A. (Ed.), Molecular, Clinical and Environmental Toxicology, vol. 1. Birkhäuser Verlag AG, Basel, pp. 57-86.

Després, L., David, J. P., Gallet, C., **2007**. The evolutionary ecology of insect resistance to plant chemicals. Trends in Ecology & Evolution 22, 298-307.

Desroches, P., El Shazly, E., Mandon, N., Duc, G., Huignard, J., **1995**. Development of *Callosobruchus chinensis* (L.) and *C. maculatus* (F.) (Coleoptera: Bruchidae) in seeds of *Vicia faba* L. differing in their tannin, vicine and convicine contents. Journal of Stored Products Research 31, 83-89.

Desroches, P., Mandon, N., Baehr, J. C., Huignard, J., **1997**. Mediation of host-plant use by a glucoside in *Callosobruchus maculatus* F. (Coleoptera: Bruchidae). Journal of Insect Physiology 43, 439-446.

Dickmann, D. I., Kuzovkina, J., **2014**. *Po*plars and willows of the world, with emphasis on silviculturally important species. In: Isebrands, J. G., Richardson, J. (Eds.), Poplars and Willows Trees for Society and the Environment. published jointly by CAB International and Food and Agriculture Organization of the United Nations (FAO), Viale delle Terme di Caracalla, 00153 Rome, Italy, pp. 8-91.

Dixon, D. P., Sellars, J. D., Kenwright, A. M., Steel, P. G., **2012**. The maize benzoxazinone DIMBOA reacts with glutathione and other thiols to form spirocyclic adducts. Phytochemistry 77, 171-178.

Dobler, S., Petschenka, G., Pankoke, H., **2011**. Coping with toxic plant compounds - the insect's perspective on iridoid glycosides and cardenolides. Phytochemistry 72, 1593-1604.

Donaldson, J. R., Stevens, M. T., Barnhill, H. R., Lindroth, R. L., **2006**. Age-related shifts in leaf chemistry of clonal aspen (*Populus tremuloides*). Journal of Chemical Ecology 32, 1415-1429.

Drake, D., Lam, J., **1974**. Polyacetylenes of *Artemisia vulgaris*. Phytochemistry 13, 455-457.

Dussourd, D. E., **2003**. Chemical stimulants of leaf-trenching by cabbage loopers: natural products, neurotransmitters, insecticides, and drugs. Journal of Chemical Ecology 29, 2023-2047.

Eckenwalder, J. E., **1996**. Systematics and evolution of *Populus*. In: Stettler, R. F., Bradshawm, H. D., Jr., Heilman, P. E., Hinckley, T. M. (Eds.), Biology of Populus and its implications for managament and conservation. NRC Research Press, Ottawa, Ontario, Canada, pp. 7-32.

Eisenreich, W., Bacher, A., **2000**. Elucidation of biosynthetic pathways by retrodictive/predictive comparison of isotopomer patterns determined by NMR spectroscopy. In: Setlow, J. K. (Ed.), Genetic Engineering: Principles and Methods. Springer US, Boston, MA, pp. 121-153.

Eisenreich, W., Huber, C., Kutzner, E., Knispel, N., Schramek, N., **2013**. Isotopologue profiling – toward a better understanding of metabolic pathways. In: Weckwerth, W., Kahl, G. (Ed.), The Handbook of Plant Metabolomics. Wiley-VCH Verlag GmbH & Co. KGaA, pp. 25-56.

Eisner, T., **2003**. Chemical ecology: Can it survive without natural products chemistry? Proceedings of the National Academy of Sciences, USA 100, 14517-14518.

Eisner, T., Meinwald, J., **1995**. Chemical ecology. Proceedings of the National Academy of Sciences, USA 92, 1.

Elser, J. J., Bracken, M. E., Cleland, E. E., Gruner, D. S., Harpole, W. S., Hillebrand, H., Ngai, J. T., Seabloom, E. W., Shurin, J. B., Smith, J. E., **2007**. Global analysis of nitrogen and phosphorus limitation of primary producers in freshwater, marine and terrestrial ecosystems. Ecology Letters 10, 1135-1142.

Escobar, C. A., Sicker, D., Niemeyer, H. M., **1999**. Evaluation of DIMBOA analogs as antifeedants and antibiotics towards the aphid *Sitobion avenae* in artificial diets. Journal of Chemical Ecology 25, 1543-1554.

Fan, L., Wang, Y., Liang, N., Huang, X. J., Fan, C. L., Wu, Z. L., He, Z. D., Li, Y. L., Ye, W. C., **2015**. Quinic acid derivatives and coumarin glycoside from the roots and stems of *Erycibe obtusifolia*. Phytochemistry Letters 14, 185-189.

Feistel, F., Paetz, C., Lorenz, S., Beran, F., Kunert, G., Schneider, B., **2017**. *Idesia polycarpa* (Salicaceae) leaf constituents and their toxic effect on *Cerura vinula* and *Lymantria dispar* (Lepidoptera) larvae. Phytochemistry 143, 170-179.

Feistel, F., Paetz, C., Lorenz, S., Schneider, B., **2015**. The absolute configuration of salicortin, HCH-salicortin and tremulacin from *Populus trichocarpa x deltoides* Beaupré. Molecules 20, 5566-5573.

Felton, G. W., Donato, K., Del Vecchio, R. J., Duffey, S. S., **1989**. Activation of plant foliar oxidases by insect feeding reduces nutritive quality of foliage for noctuid herbivores. Journal of Chemical Ecology 15, 2667-2694.

Fields, S., Johnston, M., **2005**. Cell biology. Whither model organism research? Science 307, 1885-1886.

Fischer, E., **1920**. Wanderung von Acyl bei den Glyceriden. Berichte der Deutschen Chemischen Gesellschaft (A and B Series) 53, 1621-1633.

Fitzgerald, T. D., **2008**. Larvae of the fall webworm, *Hyphantria cunea*, inhibit cyanogenesis in *Prunus serotina*. The Journal of Experimental Biology 211, 671-677.

Food and Agricultural Organization of the United Nations, **2003**. State of the world's forests. FAO, Rome.

Fox, C. W., Stillwell, R. C., Amarillo-S., A. R., Czesak, M. E., Messina, F. J., **2004**. Genetic architecture of population differences in oviposition behaviour of the seed beetle *Callosobruchus maculatus*. Journal of Evolutionary Biology 17, 1141-1151.

Friedman, M., **1996**. Food browning and its prevention: An overview. Journal of Agricultural and Food Chemistry 44, 631-653.

Giraudo, M., Hilliou, F., Fricaux, T., Audant, P., Feyereisen, R., Le Goff, G., **2015**. Cytochrome P450s from the fall armyworm (*Spodoptera frugiperda*): responses to plant allelochemicals and pesticides. Insect Molecular Biology 24, 115-128.

Glauser, G., Marti, G., Villard, N., Doyen, G. A., Wolfender, J. L., Turlings, T. C., Erb, M., **2011**. Induction and detoxification of maize 1,4-benzoxazin-3-ones by insect herbivores. Plant Journal 68, 901-911.

Glynn, C., Ronnberg-Wastljung, A. C., Julkunen-Tiitto, R., Weih, M., **2004**. Willow genotype, but not drought treatment, affects foliar phenolic concentrations and leaf-beetle resistance. Entomologia Experimentalis et Applicata 113, 1-14.

Goldstein, B., King, N., **2016**. The future of cell biology: Emerging model organisms. Trends in Cell Biology 26, 818-824.

Gowda, G. A. N., Shanaiah, N., Raftery, D., **2012**. Isotope enhanced approaches in metabolomics. Advances in Experimental Medicine and Biology 992, 147-164.

Grant, D. M., **1991**. Detoxification pathways in the liver. Journal of Inherited Metabolic Disease 14, 421-430.

Guo, H., Shen, Q.-W., Hu, Y.-C., **2012**. Quality analysis of *Idesia polycarpa* Maxim seed oil. Xiandai Shipin Keji 28, 345-347.

Hamilton, A. J., Basset, Y., Benke, K. K., Grimbacher, P. S., Miller, S. E., Novotny, V., Samuelson, G. A., Stork, N. E., Weiblen, G. D., Yen, J. D., **2010**. Quantifying uncertainty in estimation of tropical arthropod species richness. The American Naturalist 176, 90-95.

Hammerschmidt, R., **2014**. Chlorogenic acid: A versatile defense compound. Physiological and Molecular Plant Pathology 88, iii-iv.

Hansen, A. K., Moran, N. A., **2014**. The impact of microbial symbionts on host plant utilization by herbivorous insects. Molecular Ecology 23, 1473-1496.

Hartmann, T., **2007**. From waste products to ecochemicals: Fifty years research of plant secondary metabolism. Phytochemistry 68, 2831-2846.

Hartmann, T., **2008**. The lost origin of chemical ecology in the late 19th century. Proceedings of the National Academy of Sciences, USA 105, 4541-4546.

Haruta, M., Pedersen, J. A., Constabel, C. P., **2001**. Polyphenol oxidase and herbivore defense in trembling aspen (*Populus tremuloides*): cDNA cloning, expression, and potential substrates. Physiologia Plantarum 112, 552-558.

Heckel, D. G., **2014**. Insect detoxification and sequestration strategies. Annual Plant Reviews 47, 77-114.

Helmus, M. R., Dussourd, D. E., **2005**. Glues or poisons: which triggers vein cutting by monarch caterpillars? Chemoecology 15, 45-49.

Hemming, J. D., Lindroth, R. L., **1995**. Intraspecific variation in aspen phytochemistry: Effects on performance of gypsy moths and forest tent caterpillars. Oecologia 103, 79-88.

Hemming, J. D. C., Lindroth, R. L., **2000**. Effects of phenolic glycosides and protein on gypsy moth (Lepidoptera: Lymantriidae) and forest tent caterpillar (Lepidoptera: Lasiocampidae) performance and detoxication activities. Environmental Entomology 29, 1108-1115.

Howe, G. A., Jander, G., **2008**. Plant immunity to insect herbivores. Annual Review of Plant Biology 59, 41-66.

Hutchinson, C. R., Stephen, M. T., Hsia, S., Carver, R. A., **1976**. Biosynthetic studies with $^{13}CO_2$ of secondary plant metabolites. *Nicotiana* alkaloids. 1. Initial experiments. Journal of the American Chemical Society 98, 6006-6011.

Isebrands, J. G., Richardson, J., **2014**. Introduction. In: Isebrands, J. G., Richardson, J. (Eds.), Poplars and Willows - Trees for Society and the Environment. published jointly by CAB International and Food and Agriculture Organization of the United Nations (FAO).
Viale delle Terme di Caracalla, 00153 Rome, Italy, pp. 1-7.

Ishikawa, T., Nishigaya, K., Takami, K., Uchikoshi, H., Chen, I. S., Tsai, I. L., **2004**. Isolation of salicin derivatives from *Homalium cochinchinensis* and their antiviral activities. Journal of Natural Products 67, 659-663.

Ishimaru, K., Nonaka, G., Nishioka, I., **1987**. Gallic acid esters of proto-quercitol, quinic acid and (−)-shikimic acid from *Quercus mongolica* and *Q. myrsinaefolia*. Phytochemistry 26, 1501-1504.

Iwashina, T., **2000**. The structure and distribution of the flavonoids in plants. Journal of Plant Research 113, 287-299.

Jeschke, V., Gershenzon, J., Vassao, D. G., **2016**. A mode of action of glucosinolate-derived isothiocyanates: Detoxification depletes glutathione and cysteine levels with ramifications on protein metabolism in *Spodoptera littoralis*. Insect Biochemistry and Molecular Biology 71, 37-48.

Joslyn, M. A., Ponting, J. D., **1951**. Enzyme-catalyzed oxidative browning of fruit products. In: Mrak, E. M., Stewart, G. F. (Eds.), Advances in Food Research, vol. 3. Academic Press, pp. 1-44.

Julkunen-Tiito, R., Virjamo, V., **2016**. Biosynthesis and roles of Salicaceae salicylates. In: Arimura, G.-i., Maffei, M. (Eds.), Plan Specialized Metabolism: Genomics, Biochemistry and Biological Functions. CRC Press, Tayler and Francis Group, 6000 Broken Sound Parkway NW, Suite 300, Boca Raton, FL 33487-2742, pp. 65-83.

Julkunen-Tiitto, R., Hakulinen, J., Meier, B., **1994**. The response of growth and secondary metabolism to *Melampsora* rusts in field cultivated willow (*Salix*) clones. Acta Horticulturae 2, 679-682.

Julkunen-Tiitto, R., Meier, B., **1992**. The enzymatic decomposition of salicin and its derivatives obtained from Salicaceae species. Journal of Natural Products 55, 9.

Kaandorp, N., **2011**. MonumentalTrees.com. https://www.monumentaltrees.com/db/04/600/04826.jpg (accessed 20. September 2017).

Kim, C. S., Subedi, L., Park, K. J., Kim, S. Y., Choi, S. U., Kim, K. H., Lee, K. R., **2015**. Salicin derivatives from *Salix glandulosa* and their biological activities. Fitoterapia 106, 147-152.

Kim, D. H., Kim, B. R., Kim, J. Y., Jeong, Y. C., **2000**. Mechanism of covalent adduct formation of aucubin to proteins. Toxicology Letters 114, 181-188.

Kim, S. H., Jang, Y. P., Sung, S. H., Kim, Y. C., **2007**. Inhibitory activity of phenolic glycosides from the fruits of *Idesia polycarpa* on lipopolysaccharide-induced nitric oxide production in BV2 microglia. Planta Medica 73, 167-169.

Kim, S. H., Sung, S. H., Choi, S. Y., Chung, Y. K., Kim, J., Kim, Y. C., **2005**. Idesolide: A New Spiro Compound from *Idesia polycarpa*. Organic Letters 7, 3275-3277.

Kim, T. B., Kim, H. W., Lee, M., Lee, H. H., Kim, S. H., Kang, S. K., Sung, S. H., **2014**. Isolation and structure elucidation of (−)-idescarparide, a new spiro compound from *Idesia polycarpa*. Tetrahedron Letters 55, 5447-5449.

Koiwa, H., Bressan, R. A., Hasegawa, P. M., **1997**. Regulation of protease inhibitors and plant defense. Trends in Plant Science 2, 379-384.

Kolehmainen, J., Julkunen-Tiitto, R., Roininen, H., Tahvanainen, J., **1995**. Phenolic glucosides as feeding cues for willow-feeding leaf beetles. Entomologia Experimentalis et Applicata 74, 235-243.

Krämer, U., **2015**. Planting molecular functions in an ecological context with *Arabidopsis thaliana*. eLife 4, e06100.

Kurilich, A. C., Britz, S. J., Clevidence, B. A., Novotny, J. A., **2003**. Isotopic labeling and LC-APCI-MS quantification for investigating absorption of carotenoids and phylloquinone from kale (*Brassica oleracea*). Journal of Agricultural and Food Chemistry 51, 4877-4883.

Lee, M., Lee, H. H., Lee, J.-K., Ye, S.-K., Kim, S. H., Sung, S. H., **2013**. Anti-adipogenic activity of compounds isolated from *Idesia polycarpa* on 3T3-L1 cells. Bioorganic & Medicinal Chemistry Letters 23, 3170-3174.

Li, X., Baudry, J., Berenbaum, M. R., Schuler, M. A., **2004**. Structural and functional divergence of insect CYP6B proteins: From specialist to generalist cytochrome P450. Proceedings of the National Academy of Sciences, USA 101, 2939-2944.

Lindroth, R. L., **1988**. Hydrolysis of phenolic glycosides by midgut *β*-glucosidases in *Papilio glaucus* subspecies. Insect Biochemistry 18, 789-792.

Lindroth, R. L., **1991**. Biochemical ecology of aspen-lepidoptera interactions. Journal of the Kansas Entomological Society 64, 372-380.

Lindroth, R. L., Bloomer, M. S., **1991**. Biochemical ecology of the forest tent caterpillar: responses to dietary protein and phenolic glycosides. Oecologia 86, 408-413.

Lindroth, R. L., Hemming, J. D. C., **1990**. Responses of the gypsy moth (Lepidoptera: Lymantriidae) to tremulacin, an aspen phenolic glycoside. Environmental Entomology 19, 842-847.

Lindroth, R. L., Scriber, J. M., Hsia, M. T. S., **1988**. Effects of the quaking aspen compounds catechol, salicin and isoniazid on two subspecies of tiger swallowtails. The American Midland Naturalist 119, 1-6.

Liti, G., **2015**. The fascinating and secret wild life of the budding yeast *S. cerevisiae*. eLife 4, e05835.

Liu, Z., Feng, Z., Yang, Y., Jiang, J., Zhang, P., **2014**. Acyl quinic acid derivatives from the stems of *Erycibe obtusifolia*. Fitoterapia 99, 109-116.

Luque, T., Okano, K., O'Reilly, D. R., **2002**. Characterization of a novel silkworm (*Bombyx mori*) phenol UDP-glucosyltransferase. European Journal of Biochemistry 269, 819-825.

Mackenzie, P. I., Bock, K. W., Burchell, B., Guillemette, C., Ikushiro, S., Iyanagi, T., Miners, J. O., Owens, I. S., Nebert, D. W., **2005**. Nomenclature update for the mammalian UDP glycosyltransferase (UGT) gene superfamily. Pharmacogenet Genomics 15, 677-685.

Markow, T. A., **2015**. The secret lives of *Drosophila* flies. eLife 4, e06793.

Marmiroli, M., Pietrini, F., Maestri, E., Zacchini, M., Marmiroli, N., Massacci, A., **2011**. Growth, physiological and molecular traits in Salicaceae trees investigated for phytoremediation of heavy metals and organics. Tree Physiology 31, 1319-1334.

Marquardt, Schäfer, Barth, **2013**. Klassifizierung fremdstoffmetabolisierender Enzyme. Toxikologie, vol. 3. Wissenschaftliche Verlagsgesellschaft Stuttgart (WVG), Stuttgart, pp. 90-92.

Massad, T. J., Trumbore, S. E., Ganbat, G., Reichelt, M., Unsicker, S., Boeckler, A., Gleixner, G., Gershenzon, J., Ruehlow, S., **2014**. An optimal defense strategy for phenolic glycoside production in *Populus trichocarpa* – isotope labeling demonstrates secondary metabolite production in growing leaves. New Phytologist 203, 607-619.

Matsuki, M., MacLean, S. F., Jr., **1994**. Effects of different leaf traits on growth rates of insect herbivores on willows. Oecologia 100, 141-152.

Meinwald, J., Eisner, T., **2008**. Chemical ecology in retrospect and prospect. Proceedings of the National Academy of Sciences, USA 105, 4539-4540.

Mercier, D., Cléophax, J., Hildesheim, J., Sépulchre, A. M., Géro, S. D., **1969**. Selective reactivity of the hydroxyls of methyl quinate towards acylating agents. Tetrahedron Letters 10, 2497-2500.

Michalski, C., Mohagheghi, H., Nimtz, M., Pasteels, J., Ober, D., **2008**. Salicyl alcohol oxidase of the chemical defense secretion of two chrysomelid leaf beetles. Molecular and functional characterization of two new members of the glucose-methanol-choline oxidoreductase gene family. The Journal of Biological Chemistry 283, 19219-19228.

Moller, B. L., **2010**. Functional diversifications of cyanogenic glucosides. Current Opinion in Plant Biology 13, 338-347.

Mora, C., Tittensor, D. P., Adl, S., Simpson, A. G., Worm, B., **2011**. How many species are there on Earth and in the ocean? PLoS Biology 9, e1001127.

Moritake, M., Ueda, K., Mori, I., **1987**. Two phenazine derivatives, polycartine A and B from *Idesia polycarpa* Maxim (Flacourticaceae). Tetrahedron 28, 1425-1426.

Musser, R. O., Hum-Musser, S. M., Eichenseer, H., Peiffer, M., Ervin, G., Murphy, J. B., Felton, G. W., **2002**. Herbivory: caterpillar saliva beats plant defences. Nature 416, 599-600.

Nagasawa, T., Shimada, N., Torihata, M., Kuwahara, S., **2010**. Enantioselective total synthesis of idesolide via $NaHCO_3$-promoted dimerization. Tetrahedron 66, 4965-4969.

Nealis, V. G., Nault, J. R., **2005**. Seasonal changes in foliar terpenes indicate suitability of Douglas-fir buds for western spruce budworm. Journal of Chemical Ecology 31, 683-696.

Neiman, M., Olson, M. S., Tiffin, P., **2009**. Selective histories of poplar protease inhibitors: elevated polymorphism, purifying selection, and positive selection driving divergence of recent duplicates. New Phytologist 183, 740-750.

Nishimura, H., Nonaka, G., Nishioka, I., **1984**. Seven quinic acid gallates from *Quercus stenophylla*. Phytochemistry 23, 2621-2623.

Nyman, T., Julkunen-Tiitto, R., **2000**. Manipulation of the phenolic chemistry of willows by gall-inducing sawflies. Proceedings of the National Academy of Sciences, USA 97, 13184-13187.

Opitz, S. E. W., Muller, C., **2009**. Plant chemistry and insect sequestration. Chemoecology 19, 117-154.

Palo, R. T., **1984**. Distribution of birch (*Betula* spp.), willow (*Salix* spp.), and poplar (*Populus* spp.) secondary metabolites and their potential role as chemical defense against herbivores. Journal of Chemical Ecology 10, 499-520.

Pankoke, H., Bowers, M. D., Dobler, S., **2012**. The interplay between toxin-releasing *β*-glucosidase and plant iridoid glycosides impairs larval development in a generalist caterpillar, *Grammia incorrupta* (Arctiidae). Insect Biochemistry and Molecular Biology 42, 426-434.

Pasteels, J. M., Duffey, S., Rowell-Rahier, M., **1990**. Toxins in Chrysomelid beetles - Possible evolutionary sequence from *de novo* synthesis to derivation from food-plant chemicals. Journal of Chemical Ecology 16, 211-222.

Pasteels, J. M., Rowell-Rahier, M., Braekman, J. C., Dupont, A., **1983**. Salicin from host plant as precursor of salicylaldehyde in defensive secretion of Chrysomeline larvae. Physiological Entomology 8, 307-314.

Patil, S. S., Dimond, A. E., **1967**. Inhibition of *Verticillium* polygalacturonase by oxidation products of polyphenols. Phytopathology 57, 492-496.

Pearl, I. A., Darling, S. F., **1970**. The structures of salicortin and tremulacin. Tetrahedron Letters 11, 3827-3830.

Pentzold, S., Zagrobelny, M., Rook, F., Bak, S., **2014**. How insects overcome two-component plant chemical defence: Plant *β*-glucosidases as the main target for herbivore adaptation. Biological Reviews 89, 531-551.

Petersen, R. A., Zangerl, A. R., Berenbaum, M. R., Schuler, M. A., **2001**. Expression of CYP6B1 and CYP6B3 cytochrome P450 monooxygenases and furanocoumarin metabolism in different tissues of *Papilio polyxenes* (Lepidoptera: Papilionidae). Insect Biochemistry and Molecular Biology 31, 679-690.

Pichersky, E., Gang, D. R., **2000**. Genetics and biochemistry of secondary metabolites in plants: An evolutionary perspective. Trends in Plant Science 5, 439-445.

Pourcel, L., Routaboul, J. M., Cheynier, V., Lepiniec, L., Debeaujon, I., **2007**. Flavonoid oxidation in plants: From biochemical properties to physiological functions. Trends in Plant Science 12, 29-36.

Prudic, K. L., Khera, S., Solyom, A., Timmermann, B. N., **2007**. Isolation, identification, and quantification of potential defensive compounds in the viceroy butterfly and its larval host-plant, *Carolina willow*. Journal of Chemical Ecology 33, 1149-1159.

Rank, N. E., Kopf, A., Julkunen-Tiitto, R., Tahvanainen, J., **1998**. Host preference and larval performance of the salicylate-using leaf beetle *Phratora vitellinae*. Ecology 79, 618-631.

Razon, L. F., Bacani, F. T., Evangelista, R. L., Knothe, G., **2013**. Fatty acid profile of kenaf seed oil. Journal of the American Oil Chemists' Society 90, 835-840.

Richardson, A. M., Chen, C. H., Snider, B. B., **2007**. Synthesis of methyl 1-hydroxy-6-oxo-2-cyclohexenecarboxylate, a component of salicortin and tremulacin, and the monomer of idesolide. The Journal of Organic Chemistry 72, 8099-8102.

Roininen, H., Price, P. W., Julkunen-Tiitto, R., Tahvanainen, J., Ikonen, A., **1999**. Oviposition stimulant for a gall-inducing sawfly, *Euura lasiolepis*, on willow is a phenolic glucoside. Journal of Chemical Ecology 25, 943-953.

Romisch-Margl, W., Schramek, N., Radykewicz, T., Ettenhuber, C., Eylert, E., Huber, C., Romisch-Margl, L., Schwarz, C., Dobner, M., Demmel, N., Winzenhorlein, B., Bacher, A., Eisenreich, W., **2007**. $^{13}CO_2$ as a universal metabolic tracer in isotopologue perturbation experiments. Phytochemistry 68, 2273-2289.

Ruuhola, T., Julkunen-Tiitto, R., **2003**. Trade-off between synthesis of salicylates and growth of micropropagated *Salix pentandra*. Journal of Chemical Ecology 29, 1565-1588.

Ruuhola, T., Julkunen-Tiitto, R., Vainiotalo, P., **2003**. In vitro degradation of willow salicylates. Journal of Chemical Ecology 29, 1083-1097.

Ruuhola, T., Tikkanen, O.-P., Tahvanainen, J., **2001**. Differences in host use efficiency of larvae of a generalist moth, *Operophtera Brumata* on three chemically divergent *Salix* species. Journal of Chemical Ecology 27, 1595-1615.

Sasai, H., Ishida, M., Murakami, K., Tadokoro, N., Ishihara, A., Nishida, R., Mori, N., **2009**. Species-specific glucosylation of DIMBOA in larvae of the rice armyworm. Bioscience, Biotechnology, and Biochemistry 73, 1333-1338.

Schaefer, J., Kier, L. D., Stejskal, E. O., **1980**. Characterization of photorespiration in intact leaves using ^{13}carbon dioxide labeling. Plant Physiology 65, 254-259.

Schmid, O., Voak, D., **1963**. Über Acylwanderung und Acylabspaltung an den beiden isomeren Monocarbaminsäureestern des 3-Guajacylglycerinäthers und ihren O-Acetylverbindungen. Monatshefte für Chemie und verwandte Teile anderer Wissenschaften 94, 339-358.

Schneider, B., **2007**. Nuclear magnetic resonance spectroscopy in biosynthetic studies. Progress in Nuclear Magnetic Resonance Spectroscopy 51, 155-198.

Shaari, K., Waterman, P. G., **1995**. Glucosides of 2,5-dihydroxybenzyl alcohol from *Homalium longifolium*. Phytochemistry 39, 1415-1421.

Shen, S. K., Dowd, P. F., **1991**. Detoxification spectrum of the cigarette beetle symbiont *Symbiotaphrina kochii* in culture. Entomologia Experimentalis et Applicata 60, 51-59.

Shin, K.-M., Kim, I.-T., Park, Y.-M., Ha, J., Choi, J.-W., Park, H.-J., Lee, Y. S., Lee, K.-T., **2004**. Anti-inflammatory effect of caffeic acid methyl ester and its mode of action through the inhibition of prostaglandin E2, nitric oxide and tumor necrosis factor-α production. Biochemical Pharmacology 68, 2327-2336.

Si, C.-L., Xu, J., Kim, J.-K., Bae, Y.-S., Liu, P.-T., Liu, Z., **2011**. Antioxidant properties and structural analysis of phenolic glucosides from bark of *Populus ussuriensis* Kom. Wood Science and Technology 45, 5-13.

Si, C. L., Kim, J. K., Bae, Y. S., Li, S. M., **2009**. Phenolic compounds in the leaves of *Populus ussuriensis* and their antioxidant activities. Planta Medica 75, 1165-1167.

Smith, M. T., **1985**. Quinones as mutagens, carcinogens, and anticancer agents: Introduction and overview. Journal of Toxicology and Environmental Health 16, 665-672.

Snyder, M. J., Hsu, E. L., Feyereisen, R., **1993**. Induction of cytochrome P-450 activities by nicotine in the tobacco hornworm, *Manduca sexta*. Journal of Chemical Ecology 19, 2903-2916.

Strauss, A. S., Peters, S., Boland, W., Burse, A., **2013**. ABC transporter functions as a pacemaker for sequestration of plant glucosides in leaf beetles. eLife 2, e01096.

Taubert, M., Jehmlich, N., Vogt, C., Richnow, H. H., Schmidt, F., von Bergen, M., Seifert, J., **2011**. Time resolved protein-based stable isotope probing (Protein-SIP) analysis allows quantification of induced proteins in substrate shift experiments. Proteomics 11, 2265-2274.

Terada, H., **1990**. Uncouplers of oxidative phosphorylation. Environmental Health Perspectives 87, 213-218.

Termonia, A., Hsiao, T. H., Pasteels, J. M., Milinkovitch, M. C., **2001**. Feeding specialization and host-derived chemical defense in Chrysomeline leaf beetles did not lead to an evolutionary dead end. Proceedings of the National Academy of Sciences, USA 98, 3909-3914.

The Angiosperm Phylogeny Group, **2003**. An update of the Angiosperm Phylogeny Group classification for the orders and families of flowering plants: APG II. Botanical Journal of the Linnean Society 141, 399-436.

Thieme, H., **1964**. Isolierung eines neuen Phenolglucosids aus *Salix purpurea* L. Pharmazie 19, 725.

Thompson, P. L., Polebitski, A. S., **2010**. Effect of mycorrhizal fungi on the phytoremediation of hexahydro-1,3,5-trinitro-1,3,5-triazine (RDX). Environmental Science & Technology 44, 1112-1115.

Thompson, P. L., Ramer, L. A., Schnoor, J. L., **1998**. Uptake and transformation of TNT by hybrid poplar trees. Environmental Science & Technology 32, 975-980.

Tuskan, G. A., Difazio, S., Jansson, S., Bohlmann, J., Grigoriev, I., Hellsten, U., Putnam, N., Ralph, S., Rombauts, S., Salamov, A., Schein, J., Sterck, L., Aerts, A., Bhalerao, R. R., Bhalerao, R. P., Blaudez, D., Boerjan, W., Brun, A., Brunner, A., Busov, V., Campbell, M., Carlson, J., Chalot, M., Chapman, J., Chen, G. L., Cooper, D., Coutinho, P. M., Couturier, J., Covert, S., Cronk, Q., Cunningham, R., Davis, J., Degroeve, S., Dejardin, A., Depamphilis, C., Detter, J., Dirks, B., Dubchak, I., Duplessis, S., Ehlting, J., Ellis, B., Gendler, K., Goodstein, D., Gribskov, M., Grimwood, J., Groover, A., Gunter, L., Hamberger, B., Heinze, B., Helariutta, Y., Henrissat, B., Holligan, D., Holt, R., Huang, W., Islam-Faridi, N., Jones, S., Jones-Rhoades, M., Jorgensen, R., Joshi, C., Kangasjarvi, J., Karlsson, J., Kelleher, C., Kirkpatrick, R., Kirst, M., Kohler, A., Kalluri, U., Larimer, F., Leebens-Mack, J., Leple, J. C., Locascio, P., Lou, Y., Lucas, S., Martin, F., Montanini, B., Napoli, C., Nelson, D. R., Nelson, C., Nieminen, K., Nilsson, O., Pereda, V., Peter, G., Philippe, R., Pilate, G., Poliakov, A., Razumovskaya, J., Richardson, P., Rinaldi, C., Ritland, K., Rouze, P., Ryaboy, D., Schmutz, J., Schrader, J., Segerman, B., Shin, H., Siddiqui, A., Sterky, F., Terry, A., Tsai, C. J., Uberbacher, E., Unneberg, P., Vahala, J., Wall, K., Wessler, S., Yang, G., Yin, T., Douglas, C., Marra, M., Sandberg, G., Van de Peer, Y., Rokhsar, D., **2006**. The genome of black cottonwood, *Populus trichocarpa* (Torr. & Gray). Science 313, 1596-1604.

van der Vijver, L. M., **1972**. Distribution of plumbagin in the Plumbaginaceae. Phytochemistry 11, 3247-3248.

Vederas, J. C., **1987**. The use of stable isotopes in biosynthetic-studies. Natural Product Reports 4, 277-337.

Vetter, J., **2000**. Plant cyanogenic glycosides. Toxicon 38, 11-36.

Visanuvimol, L., Bertram, S. M., **2011**. How dietary phosphorus availability during development influences condition and life history traits of the cricket, *Acheta domesticus*. Journal of Insect Science 11, 63.

Vogel, H., Shukla, S. P., Engl, T., Weiss, B., Fischer, R., Steiger, S., Heckel, D. G., Kaltenpoth, M., Vilcinskas, A., **2017**. The digestive and defensive basis of carcass utilization by the burying beetle and its microbiota. Nat Commun 8, 15186.

Vogt, T., **2010**. Phenylpropanoid biosynthesis. Molecular Plant 3, 2-20.

Wan, C., Han, J., Chen, C. H., Yao, L., Chen, J., Yuan, T., **2016**. Monosubstituted benzene derivatives from fruits of *Ficus hirta* and their antifungal activity against phytopathogen *Penicillium italicum*. Journal of Agricultural and Food Chemistry 64, 5621-5624.

Wang, J., Constabel, C. P., **2004**. Three polyphenol oxidases from hybrid poplar are differentially expressed during development and after wounding and elicitor treatment. Physiologia Plantarum 122, 344-353.

Wang, Q. Y., Li, X., Du, K. F., Yao, S., Song, H., **2013**. Conjugated linoleic acid production by alkali isomerization of linoleic acid from *Idesia Polycarpa* Maxim. *var. vestita* Diels oil. Asian Journal of Chemistry 25, 3744-3748.

Wang, X., Dossett, M. P., Gordon, M. P., Strand, S. E., **2004**. Fate of carbon tetrachloride during phytoremediation with poplar under controlled field conditions. Environmental Science & Technology 38, 5744-5749.

Weisgerber, H., **1999**. *Populus nigra* Linné, 1753. Enzyklopädie der Holzgewächse 16. Wiley-VCH, Weinheim, Germany.

Wenzel, T. J., **2017**. Strategies for using NMR spectroscopy to determine absolute configuration. Tetrahedron: Asymmetry 28, 1212-1219.

Whitney, N. J., Mortimore, C. G., **1959**. Isolation of the antifungal substance, 6-methoxybenzoxazolinone, from field corn (*Zea mays* L.) in Canada. Nature 184, 1320-1320.

Wittstock, U., Kliebenstein, D. J., Lambrix, V., Reichelt, M., Gershenzon, J., **2003**. Glucosinolate hydrolysis and its impact on generalist and specialist insect herbivores. In: Romeo, J. T. (Ed.), Recent Advances in Phytochemistry, vol. 37. Elsevier, pp. 101-125.

Wolansky, M. J., Harrill, J. A., **2008**. Neurobehavioral toxicology of pyrethroid insecticides in adult animals: A critical review. Neurotoxicology and Teratology 30, 55-78.

Woo, C. S., Shin, S. Y., Ko, S. H., Kwon, M. J., Seo, H. J., **2010**. Perfume compositions for reproducing fragrance of *Dictamnus dasycarpus*. AMOREPACIFIC Corp., S. Korea

Yamakoshi, H., Shibuya, M., Tomizawa, M., Osada, Y., Kanoh, N., Iwabuchi, Y., **2010**. Total synthesis and determination of the absolute configuration of (-)-idesolide. Organic Letters 12, 980-983.

Ye, Y., Tang, X.-S., Chen, F., Tang, L., **2014**. Optimization of phenolics extracted from *Idesia polycarpa* defatted fruit residue and its antioxidant and depigmenting activity *in vitro* and *in vivo*. Evidence-Based Complementary and Alternative Medicine 2014, 12.

Zagrobelny, M., Bak, S., Moller, B. L., **2008**. Cyanogenesis in plants and arthropods. Phytochemistry 69, 1457-1468.

Zagrobelny, M., Bak, S., Rasmussen, A. V., Jorgensen, B., Naumann, C. M., Lindberg Moller, B., **2004**. Cyanogenic glucosides and plant-insect interactions. Phytochemistry 65, 293-306.

Zenk, M. H., **1967**. Pathways of salicyl alcohol and salicin formation in *Salix purpurea* L. Phytochemistry 6, 245-&.

Supplementary information I – SI of the manuscripts

SI Manuscript I

Supplementary Information

Table S1.1. HPLC method- salicinoids from *Populus trichocarpa* × *deltoides* Beaupré.

HPLC Method for Isolation of Salicinoids (1–3) (Sample Concentration 3 mg/mL)			
Column Temp.	**35 °C**	**Injection Volume**	**40 µL**
Flow Rate	**0.8 mL/min**	***Isis Nucleodur 250 mm × 4.6 mm; 5 µm; MN***	
Time	**Solvent A**		**Solvent B**
t [min]	**H_2O (0.1% FA) in %**		**MeOH (0.1% FA) in %**
0	100		0
5	100		0
10	85		15
35	70		30
85	50		50
90	0		100
100	0		100
110	100		0
115	100		0

Retention times: salicortin (**1**): 42.6 min; HCH-salicortin (**2**): 63.6 min; tremulacin (**3**): 87.8 min.

Table S1.2. HPLC method- salicinoids from *Idesia polycarpa.*

HPLC Method for Isolation of Idescarpin (4) (Sample Concentration 115 mg/mL)			
Column Temp.	**40 °C**	**Injection Volume**	**5 µL**
Flow Rate	**0.8 mL/min**	***Isis Nucleodur 250 mm × 4.6 mm; 5 µm; MN***	
Time	**Solvent A**		**Solvent B**
t [min]	**H_2O (0.1% FA) in %**		**MeOH (0.1% FA) in %**
0	67.5		32.5
1	67.5		32.5
21	32		68
25	0		100
30	0		100
35	67.5		32.5
40	67.5		32.5

Retention times: idescarpin (**4**): 21.7 min.

Table S1.3. Specific optical rotation of salicortin (**1**) and idescarpin (**4**).

Measurement	Salicortin (1)		Idescarpin (4)
	$[\alpha]_D^{22}$ (c 0.72; MeOH)	$[\alpha]_D^{22}$ (c 0.65; H_2O)	$[\alpha]_D^{22}$ (c 0.73; MeOH)
1	−123.91°	−119.06°	−57.12°
2	−123.67°	−118.84°	−56.97°
3	−124.06°	−118.55°	−57.59°
4	−124.06°	−118.83°	−57.44°
5	−124.10°	−118.87°	−57.66°
6	−123.53°	−118.22°	−56.90°
7	−124.18°	−118.43°	−57.48°
8	−123.95°	−118.98°	−57.40°
9	−123.87°	−118.42°	−57.60°
10	−123.62°	−118.06°	−57.27°
mean $[\alpha]_D$	−123.89°	−118.63°	−57.34°
stdev.	±0.22°	±0.34°	±0.27°

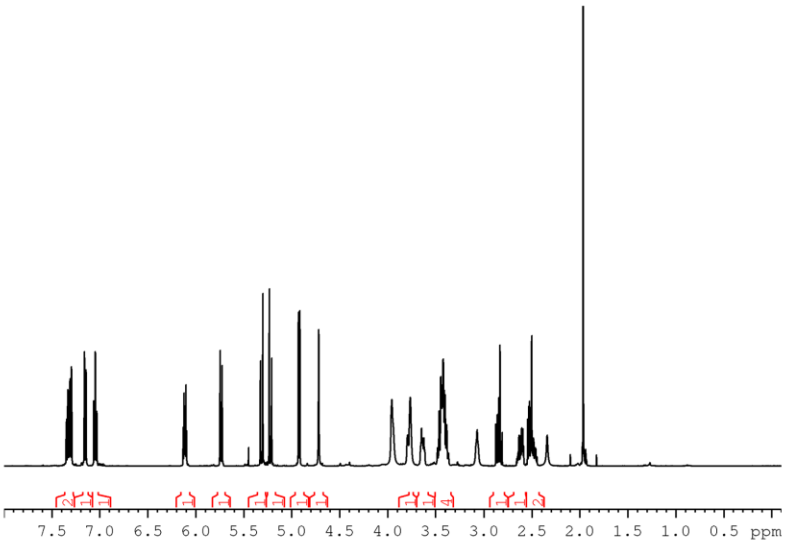

Figure S2.1. Salicortin (**1**), ^{1}H-NMR spectrum (500 MHz, MeCN-d_3).

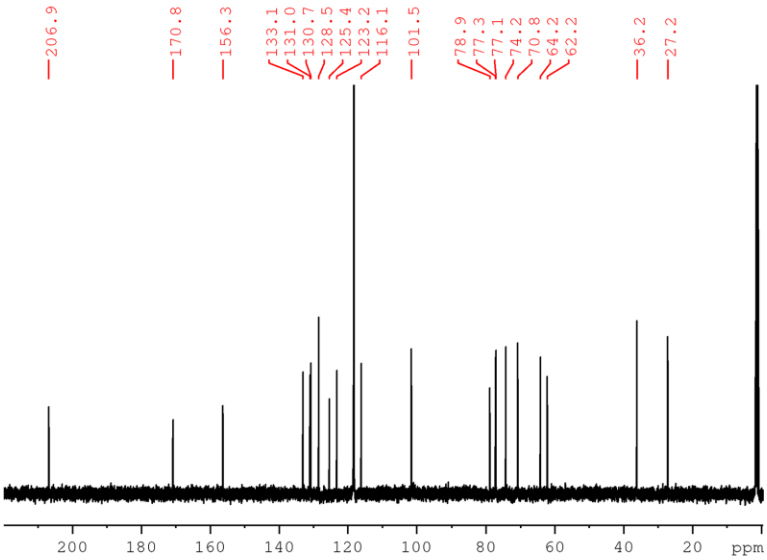

Figure S2.2. Salicortin (**1**), ^{13}C-NMR spectrum (125 MHz, MeCN-d_3).

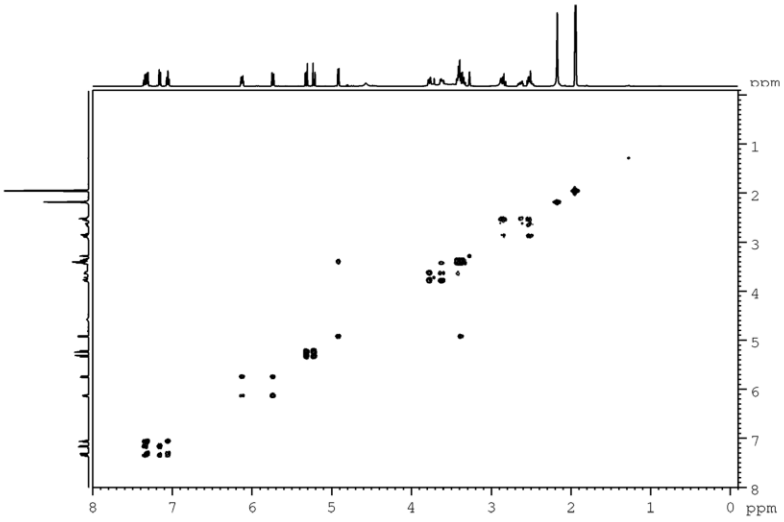

Figure S2.3. Salicortin (**1**), ^{1}H-^{1}H COSY spectrum (500 MHz, MeCN-d_3).

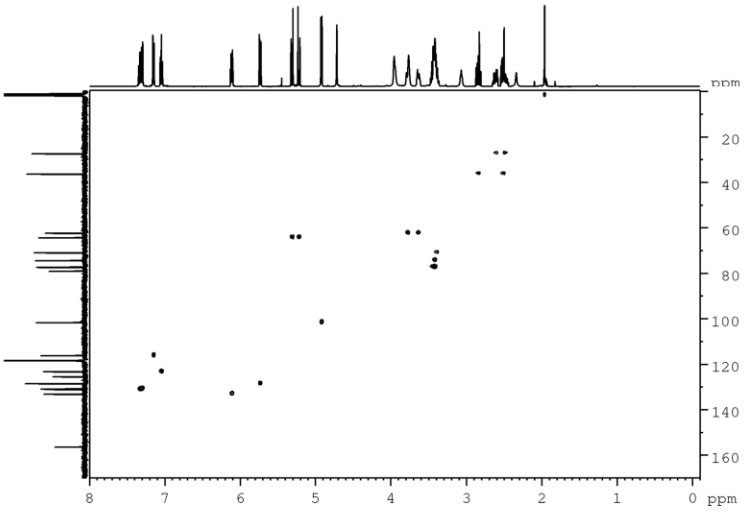

Figure S2.4. Salicortin (**1**), ^{1}H-^{13}C HSQC spectrum (500 MHz, MeCN-d_3).

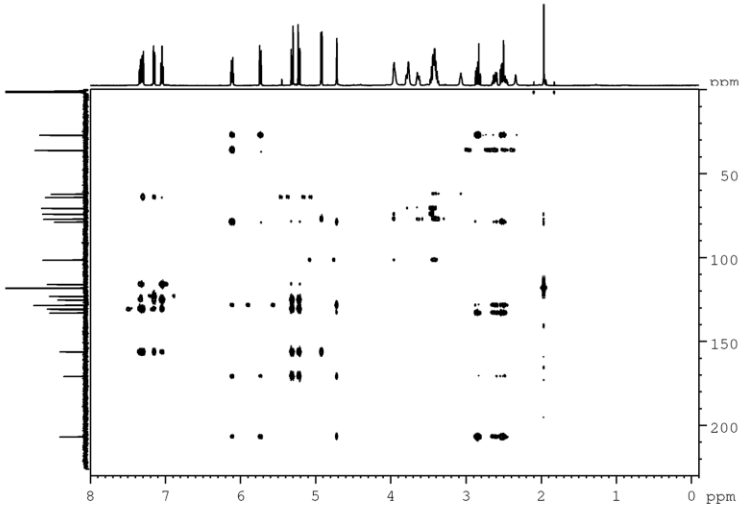

Figure S2.5. Salicortin (**1**), ^{1}H-^{13}C HMBC spectrum (500 MHz, MeCN-d_3).

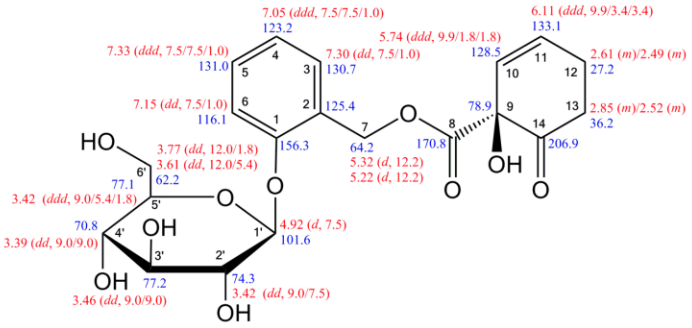

Figure S2.6. Salicortin (**1**), structure with chemical shifts (MeCN-d_3), multiplicities and coupling constants (J in Hz). Red: ^{1}H-NMR (500 MHz); blue: ^{13}C-NMR (125 MHz).

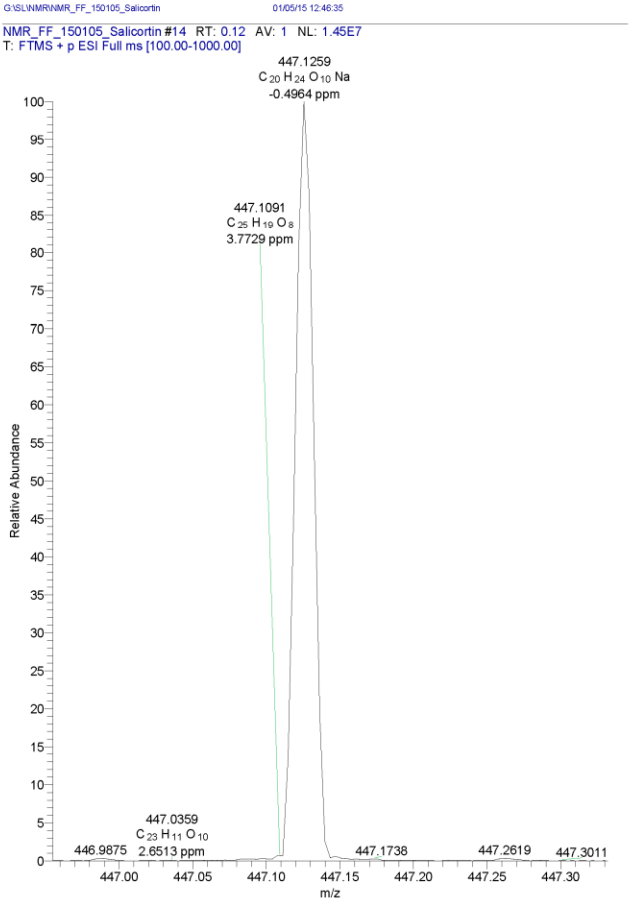

Figure S2.7. Salicortin (**1**), result of the HRMS measurement.

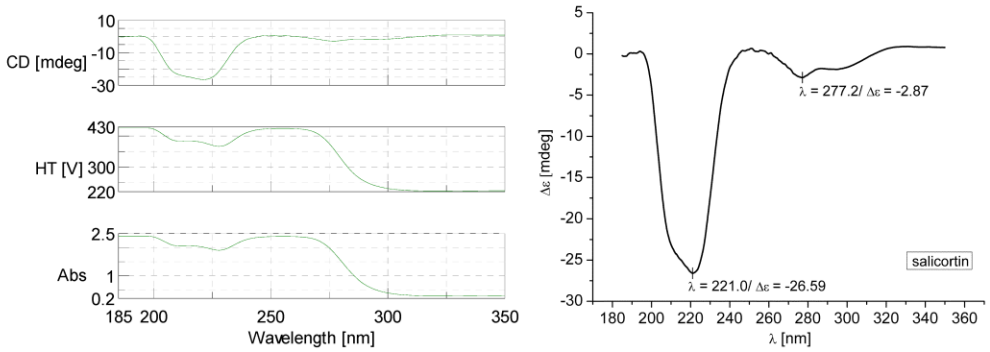

(**a**) (**b**)

Figure S2.8. Salicortin (**1**), (**a**) results of the CD measurement (concentration 0.70 mg/mL (1.66 mM in MeOH), cuvette width 1 mm). (**b**) Molar circular dichroism Δε at maximum wavelengths.

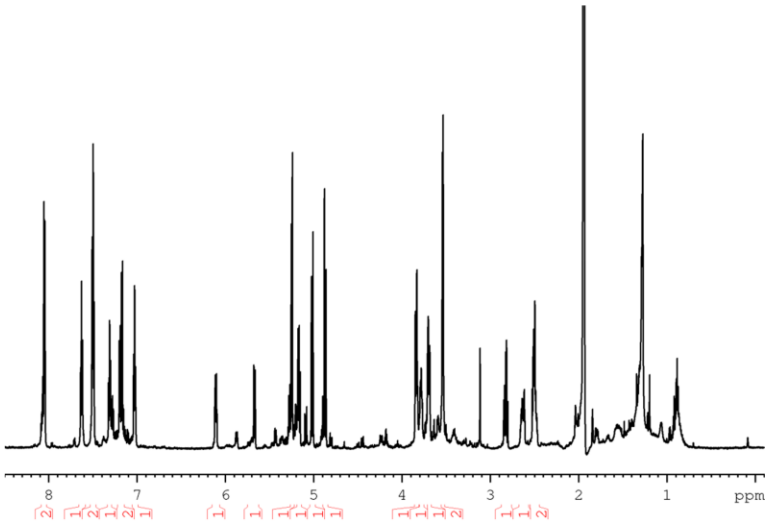

Figure S3.1. Tremulacin (**2**), ^{1}H-NMR spectrum (700 MHz, MeCN-d_3).

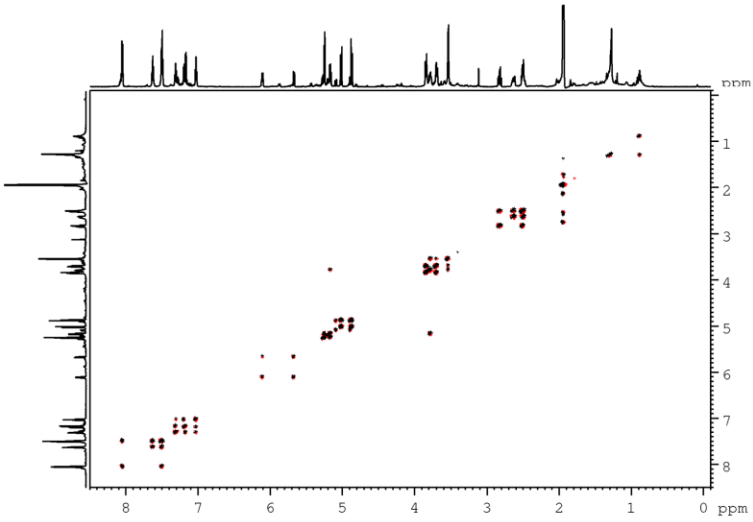

Figure S3.2. Tremulacin (**2**), ^{1}H-^{1}H COSY spectrum (700 MHz, MeCN-d_3).

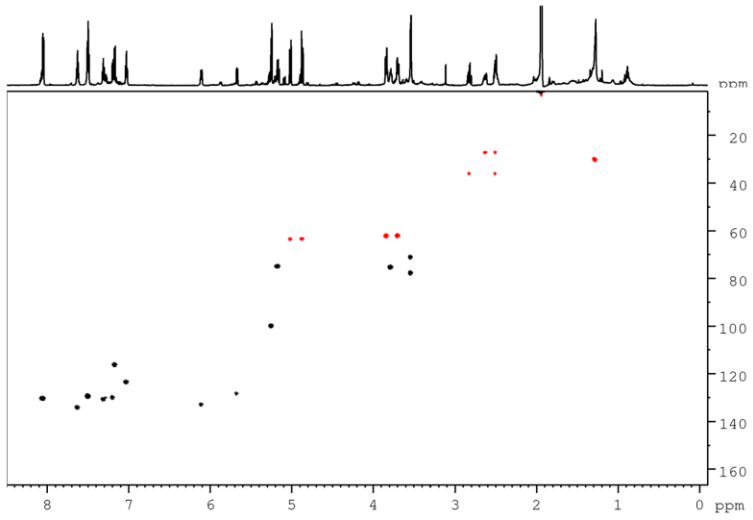

Figure S3.3. Tremulacin (**2**), ^{1}H-^{13}C HSQC spectrum (700 MHz, MeCN-d_3).

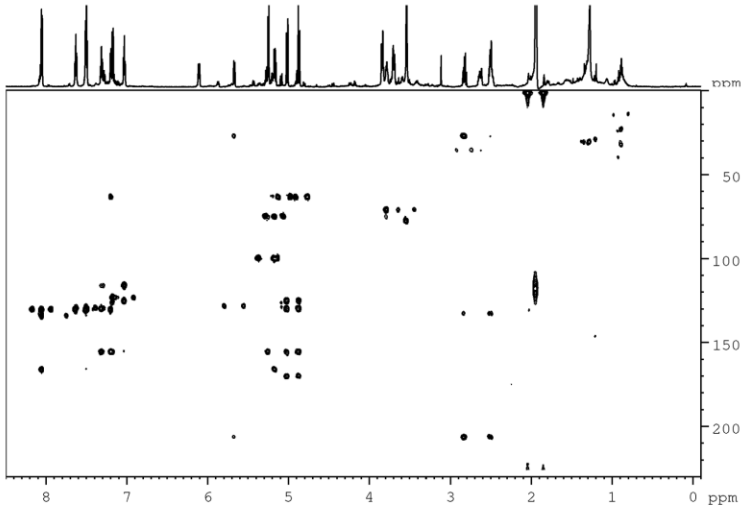

Figure S3.4. Tremulacin (**2**), ^{1}H-^{13}C HMBC spectrum (700 MHz, MeCN-d_3).

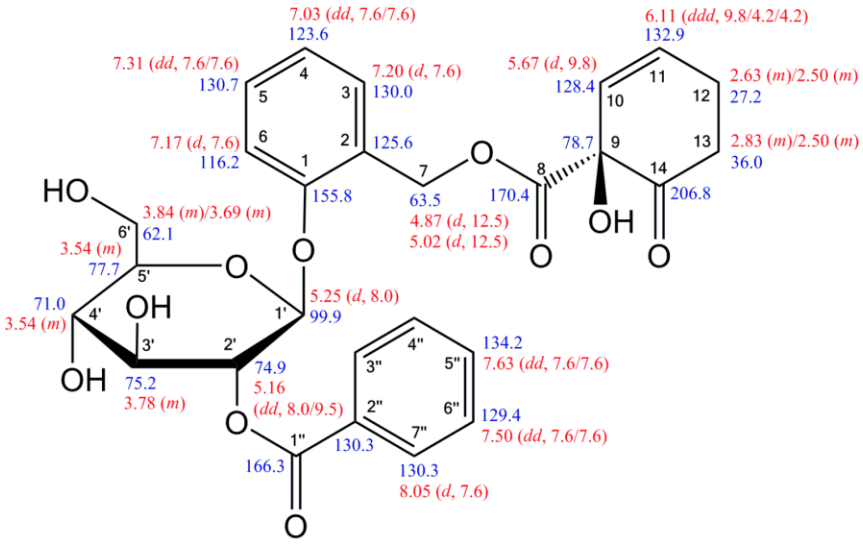

Figure S3.5. Tremulacin (**2**), structure with chemical shifts (MeCN-d_3), multiplicities and coupling constants (J in Hz). Red: ^{1}H-NMR (700 MHz); blue: ^{13}C-NMR (175 MHz).

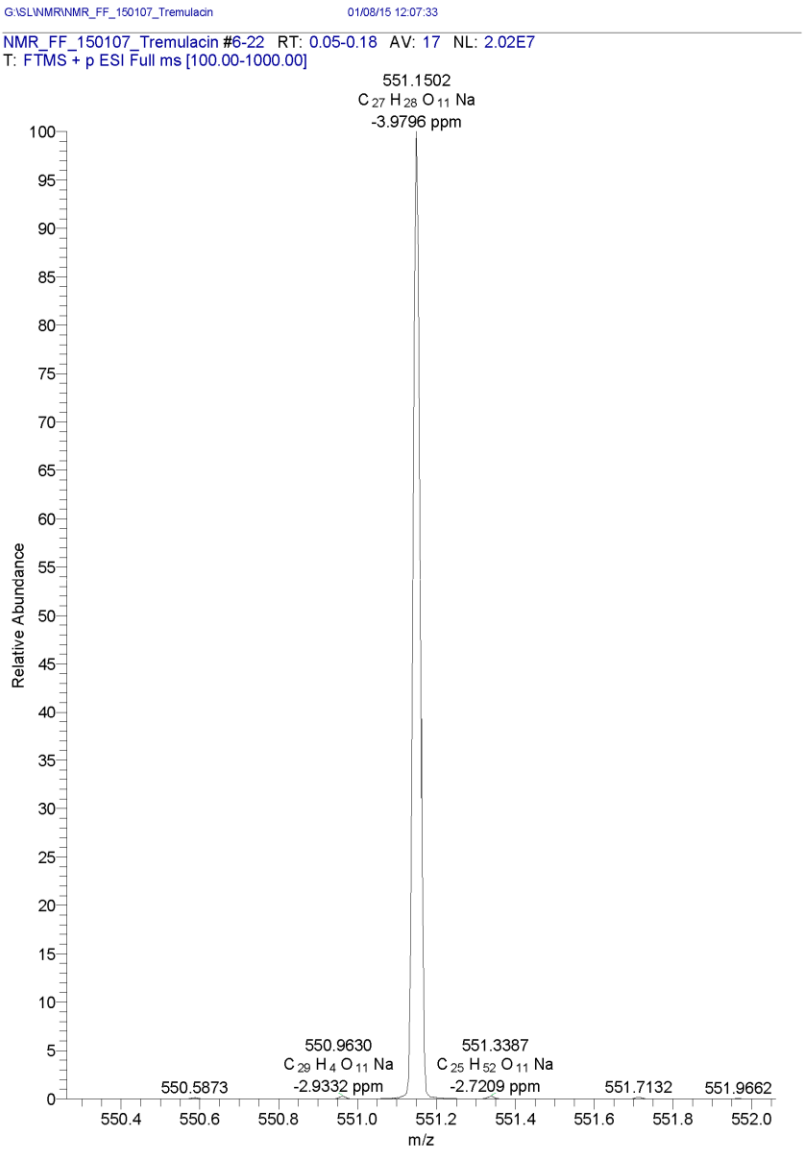

Figure S3.6. Tremulacin (**2**), result of the HRMS measurement.

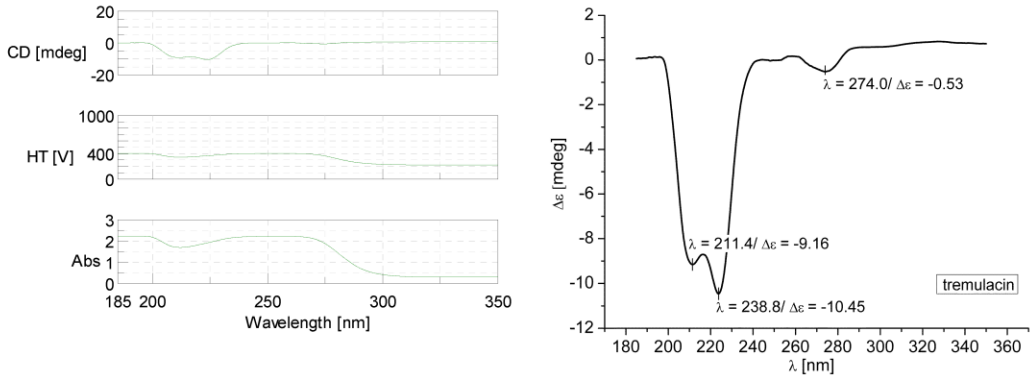

(**a**) (**b**)

Figure S3.7. Tremulacin (**2**), (**a**) results of the CD measurement (concentration 0.76 mg/mL (1.44 mM in MeOH), cuvette width 1 mm). (**b**) Molar circular dichroism Δε at maximum wavelengths.

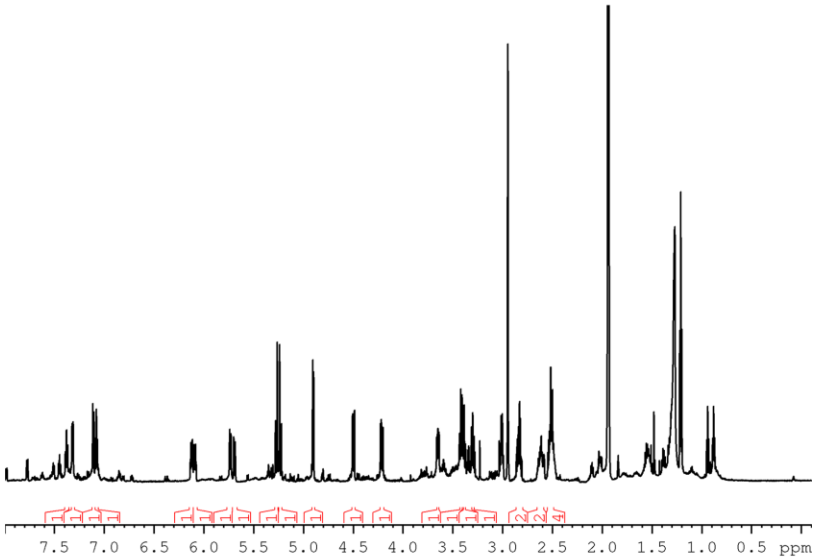

Figure S4.1. HCH-Salicortin (**3**), ^{1}H-NMR spectrum (700 MHz, MeCN-d_3).

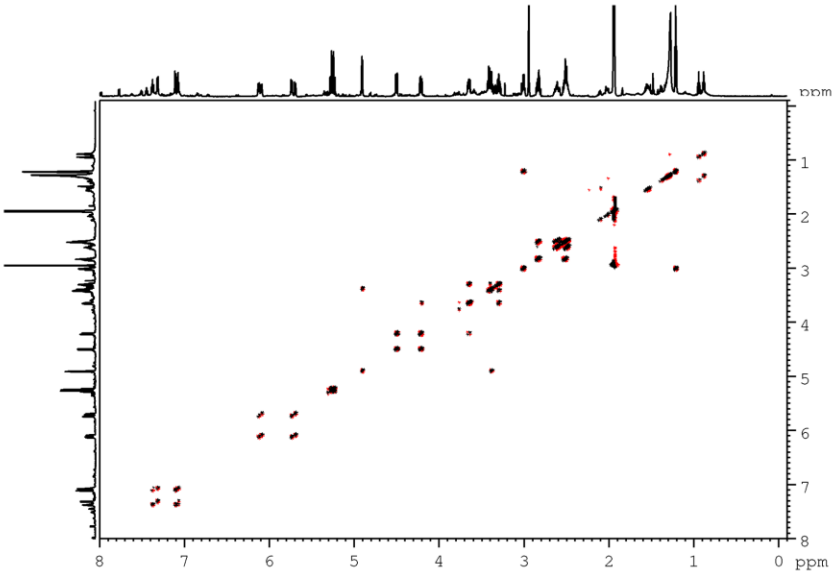

Figure S4.2. HCH-Salicortin (**3**), ^{1}H-^{1}H COSY spectrum (700 MHz, MeCN-d_3).

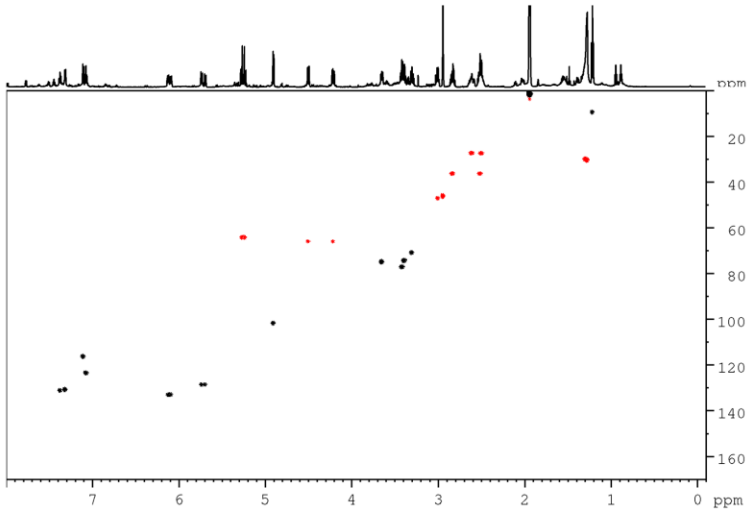

Figure S4.3. HCH-Salicortin (**3**), ^{1}H-^{13}C HSQC spectrum (700 MHz, MeCN-d_3).

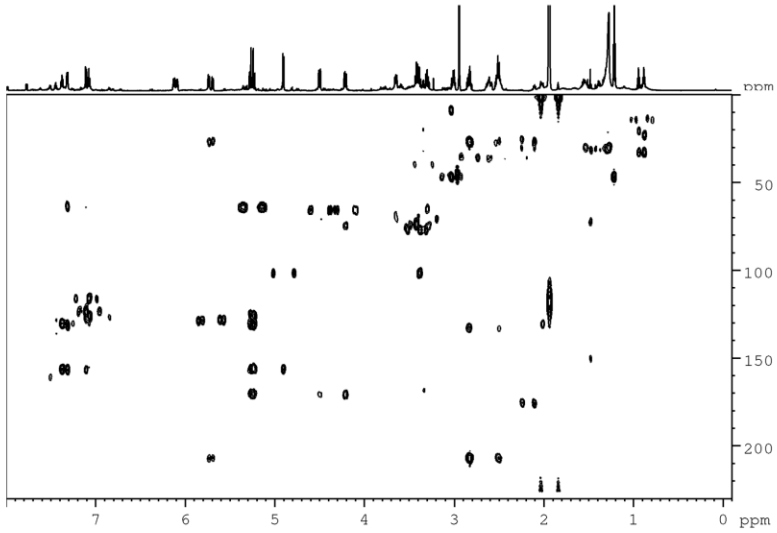

Figure S4.4. HCH-Salicortin (**3**), ^{1}H-^{13}C HMBC spectrum (700 MHz, MeCN-d_3).

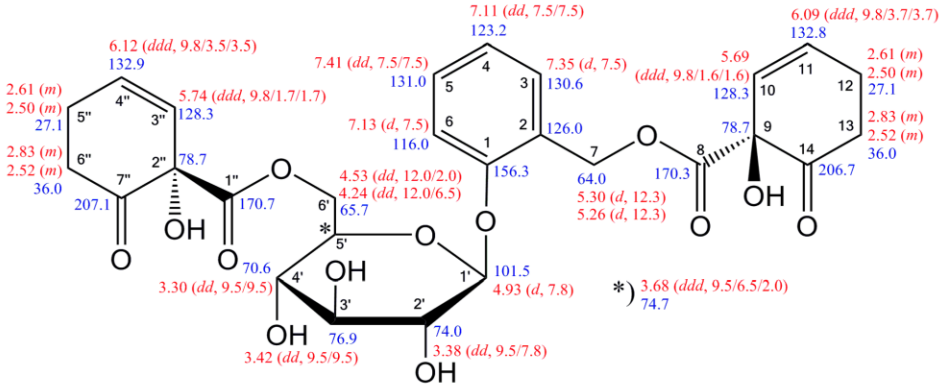

Figure S4.5. HCH-Salicortin (**3**), structure with chemical shifts (MeCN-d_3) multiplicities and coupling constants (J in Hz). Red: ^{1}H-NMR (700 MHz); blue: ^{13}C-NMR (175 MHz).

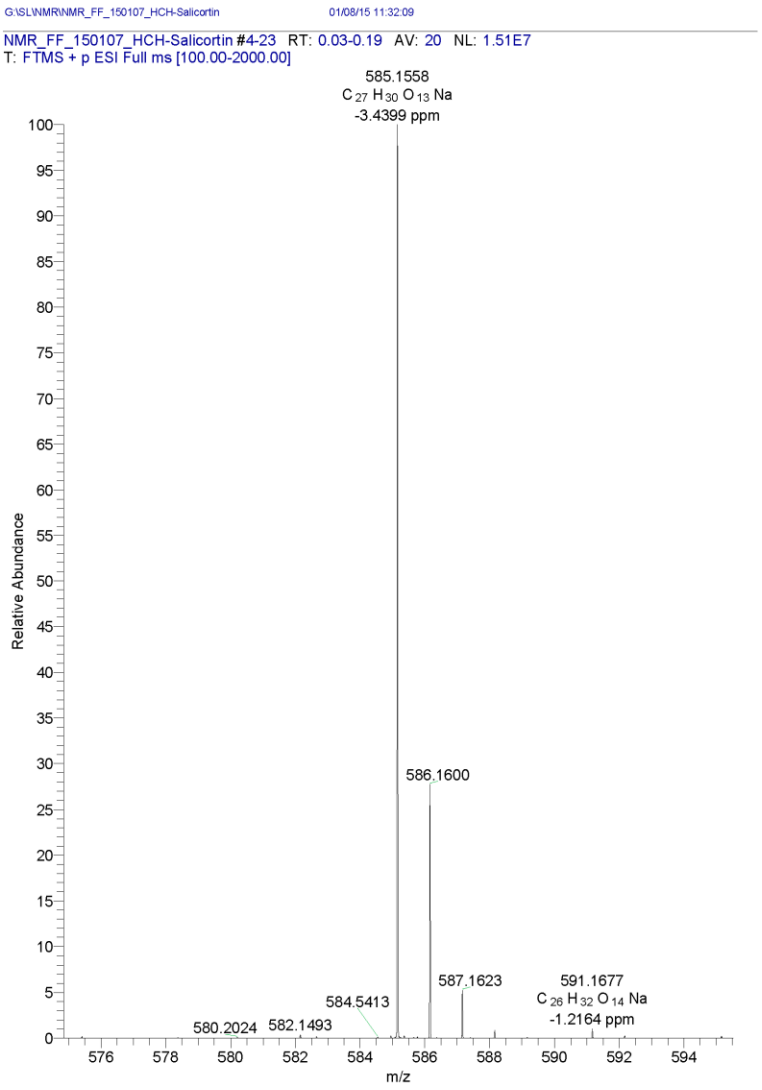

Figure S4.6. HCH-Salicortin (**3**), result of the HRMS measurement.

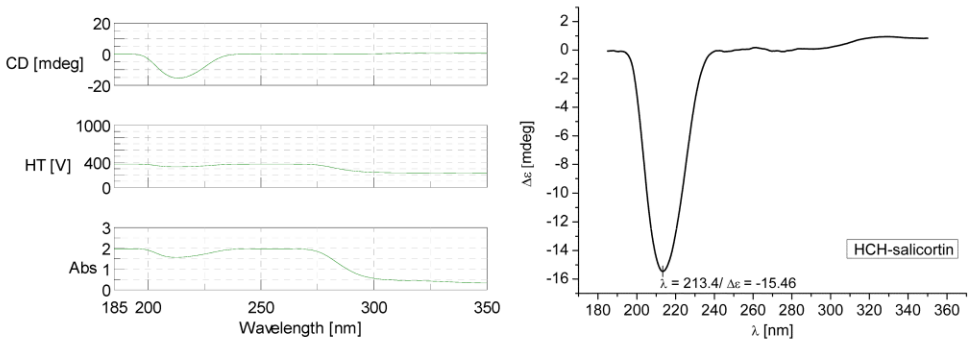

(**a**) (**b**)

Figure S4.7. HCH-Salicortin (**3**), (**a**) results of the CD measurement (concentration 0.67 mg/mL (1.19 mM in MeOH), cuvette width 1 mm). (**b**) Molar circular dichroism Δε at maximum wavelength.

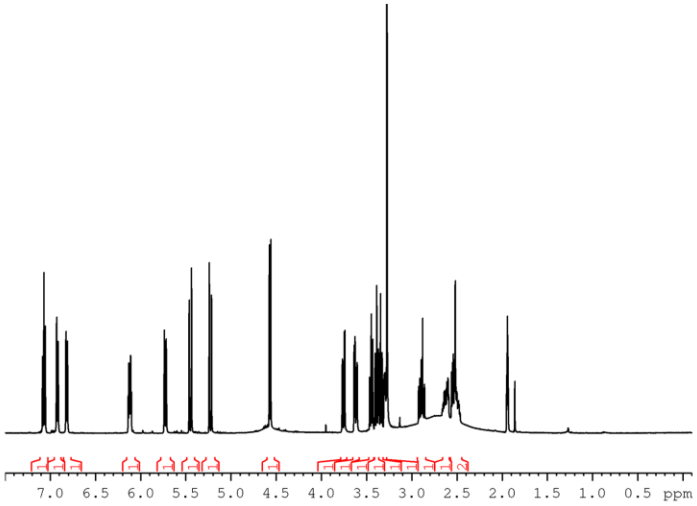

Figure S5.1. Idescarpin (**4**), ^{1}H-NMR spectrum (500 MHz, MeCN-d_3).

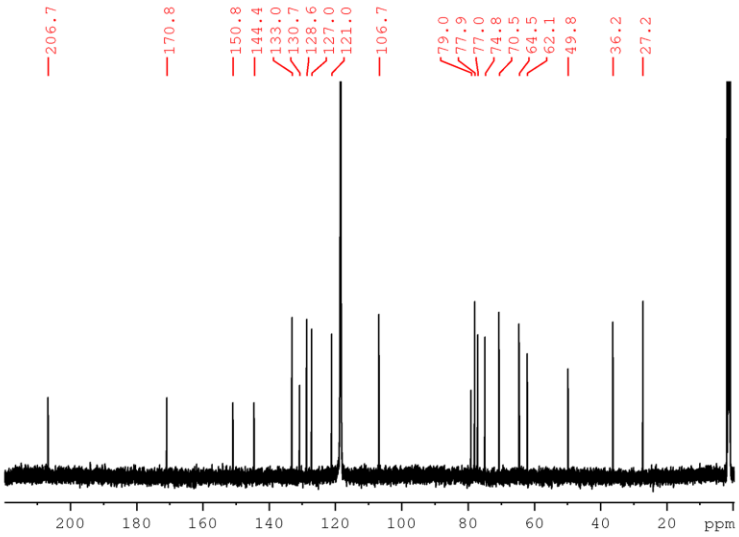

Figure S5.2. Idescarpin (**4**), ^{13}C-NMR spectrum (125 MHz, MeCN-d_3).

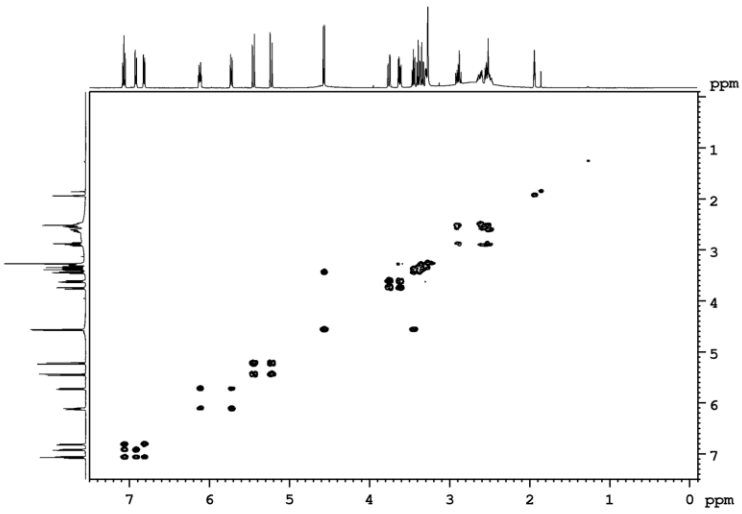

Figure S5.3. Idescarpin (**4**), ^{1}H-^{1}H COSY spectrum (500 MHz, MeCN-d_3).

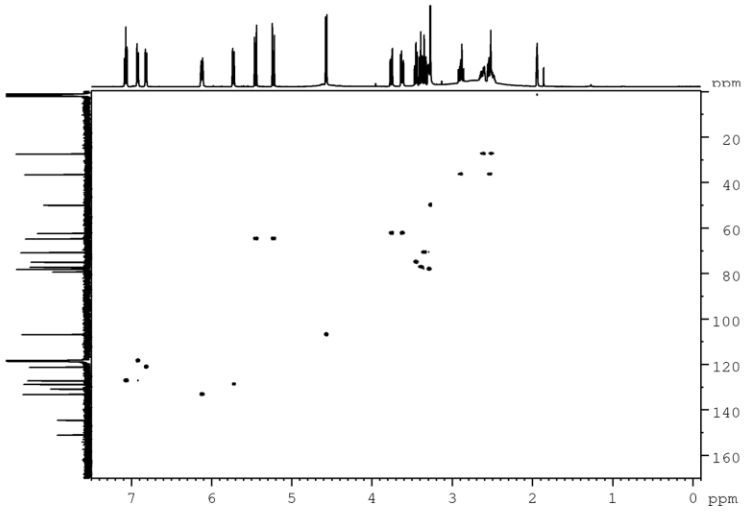

Figure S5.4. Idescarpin (**4**), ^{1}H-^{13}C HSQC spectrum (500 MHz, MeCN-d_3).

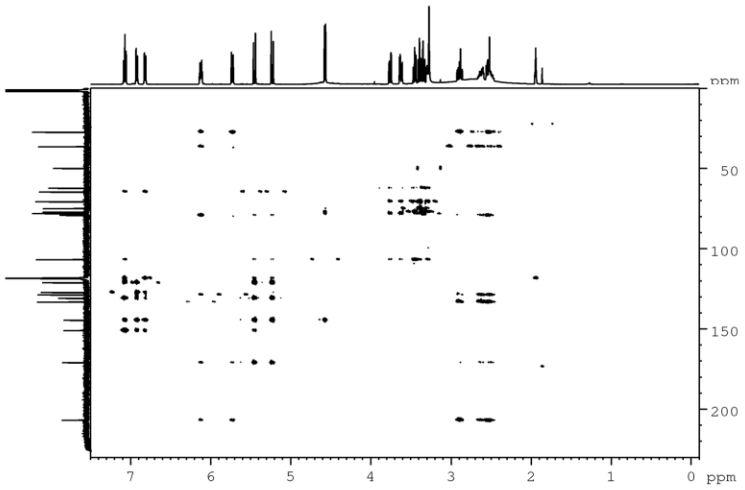

Figure S5.5. Idescarpin (**4**), ^{1}H-^{13}C HMBC spectrum (500 MHz, MeCN-d_3).

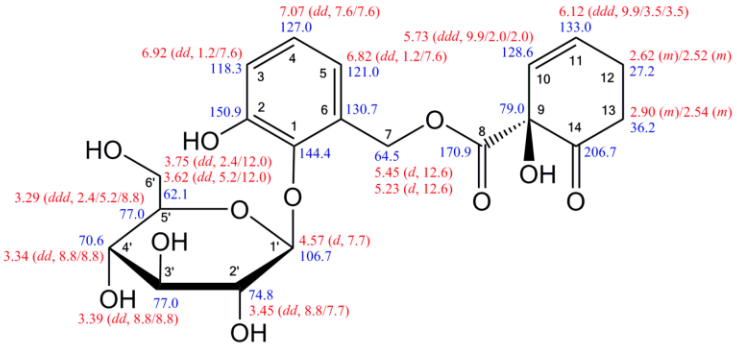

Figure S5.6. Idescarpin (**4**), structure with chemical shifts (MeCN-d_3), multiplicities and coupling constants (J in Hz). Red: ^{1}H-NMR (500 MHz); blue: ^{13}C-NMR (125 MHz).

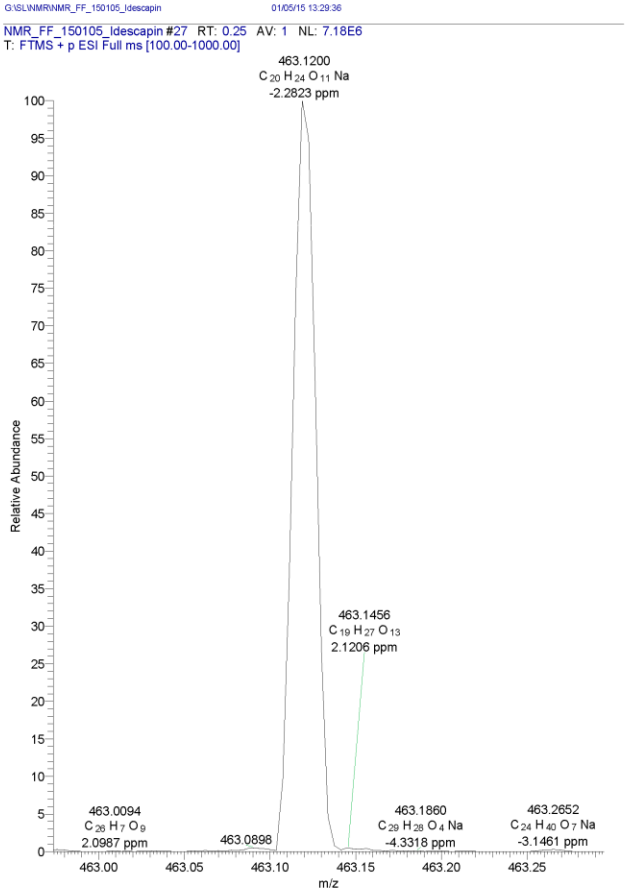

Figure S5.7. Idescarpin (**4**), result of the HRMS measurement.

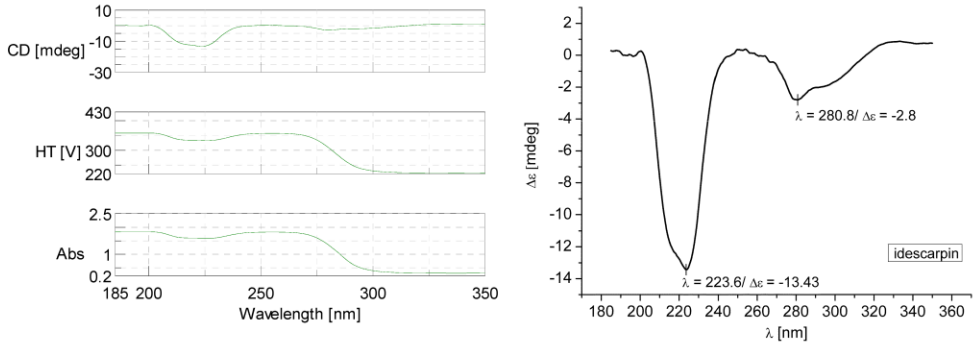

(**a**) (**b**)

Figure S5.8. Idescarpin (**4**), (**a**) results of the CD measurement (concentration 0.71 mg/mL (1.61 mM in MeOH), cuvette width 1 mm). (**b**) Molar circular dichroism Δε at maximum wavelengths.

Supplementary data

Acylated quinic acids are the main salicortin metabolites in the specialist herbivore *Cerura vinula*

Felix Feistel, Christian Paetz, Riya C. Menezes, Daniel Veit, Bernd Schneider
Max Planck Institute for Chemical Ecology, Hans-Knöll-Straße 8, 07745 Jena, Germany

Table of Contents

List of Tables

List of Figures

A)Spectroscopic data for structure elucidation

A.1) 3-*O*-salicyloyl quinic acid (1):

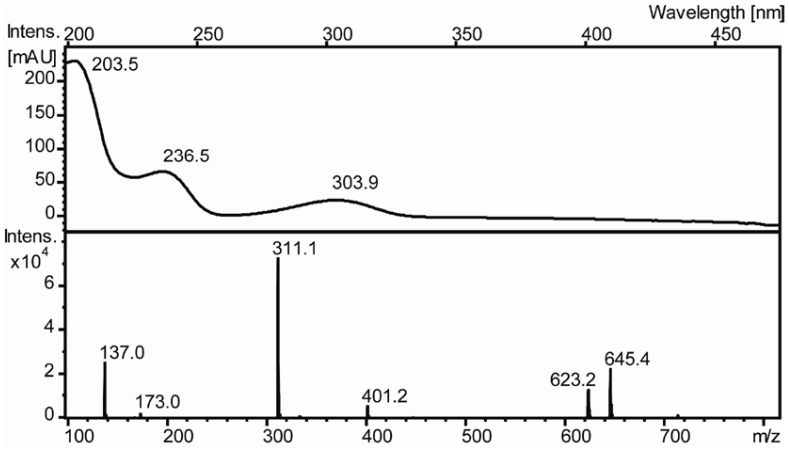

Figure A.1-1 Compound **1**, UV spectrum obtained from HPLC-DAD (top) and mass spectrum (*m/z* 311.1 $[M-H]^-$, bottom).

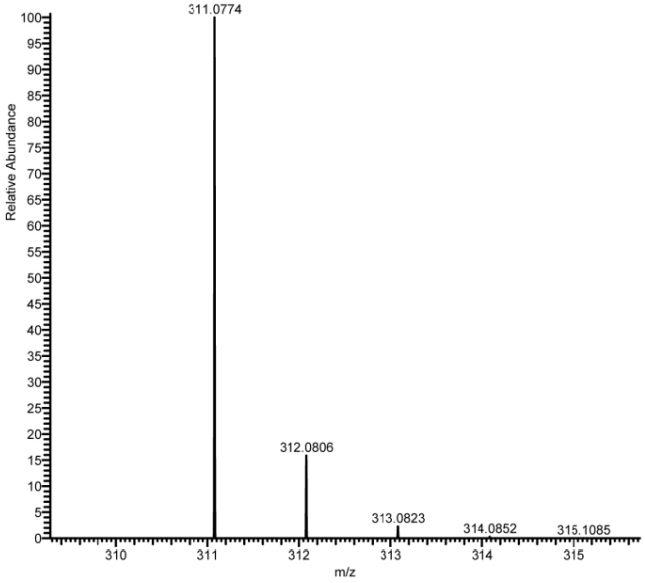

Figure A.1-2 Compound **1**, HRESIMS spectrum, *m/z* 311.0774 $[M-H]^-$.

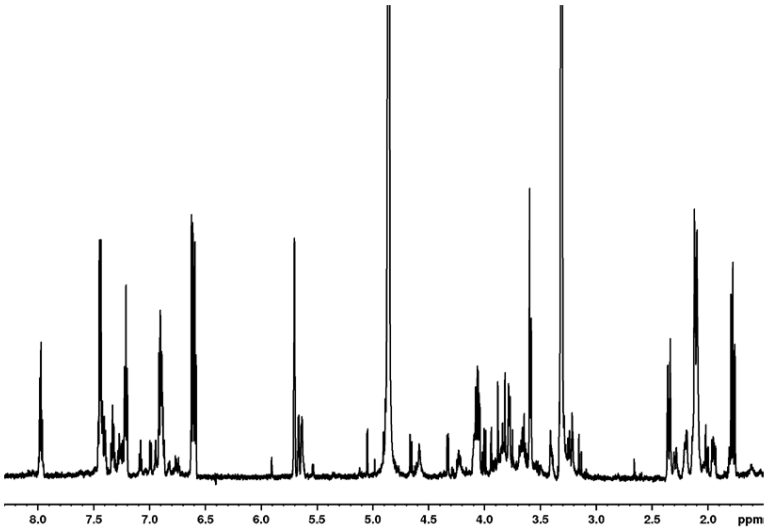

Figure A.1-3 Compound **1**, ^{1}H NMR spectrum (700 MHz, MeOH-d_4).

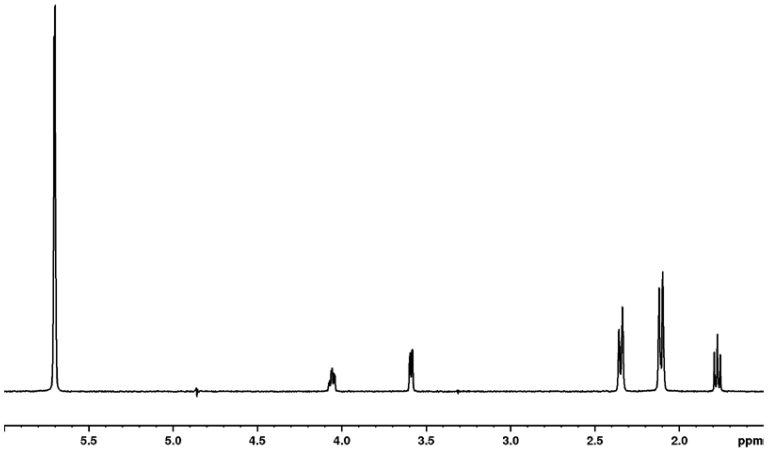

Figure A.1-4 Compound **1**, selective 1D TOCSY spectrum (700 MHz, MeOH-d_4, o1p = 5.70 ppm).

L

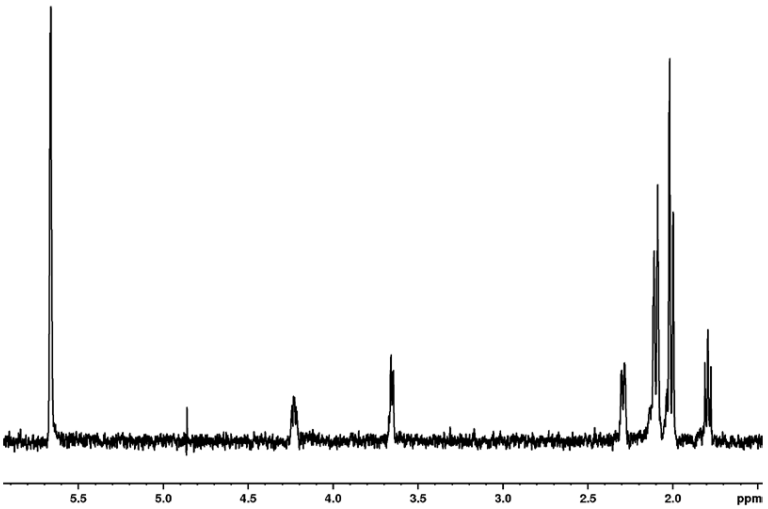

Figure A.1-5 Compound **1**, selective 1D TOCSY spectrum (700 MHz, MeOH-d_4, o1p = 5.66 ppm).

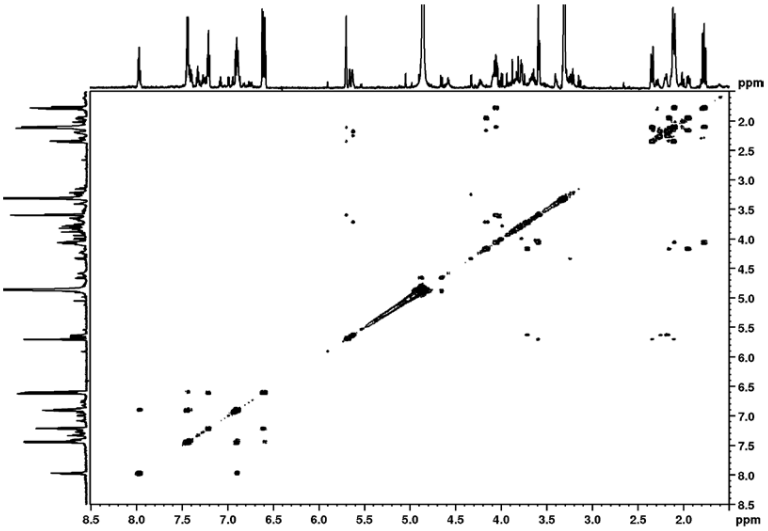

Figure A.1-6 Compound **1**, ^{1}H-^{1}H COSY spectrum (700 MHz, MeOH-d_4).

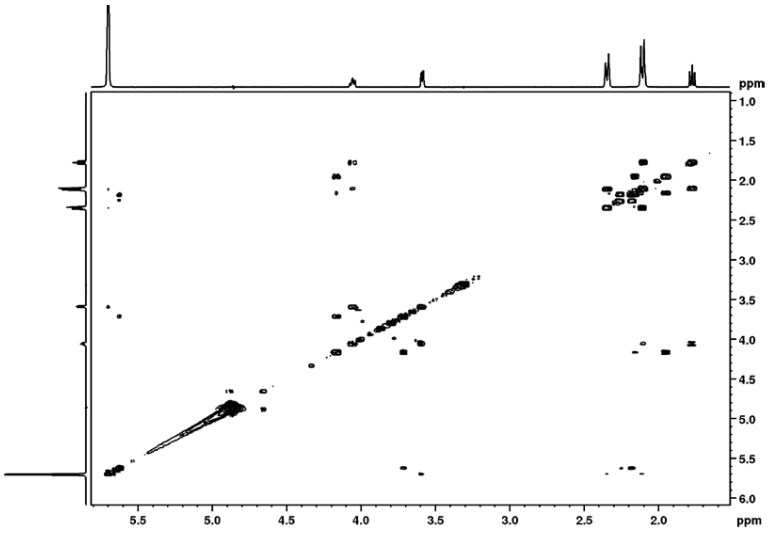

Figure A.1-7 Compound **1**, ^{1}H-^{1}H COSY spectrum (700 MHz, MeOH-d_4) with selective 1D TOCSY projections (**Fig. A.1-5**).

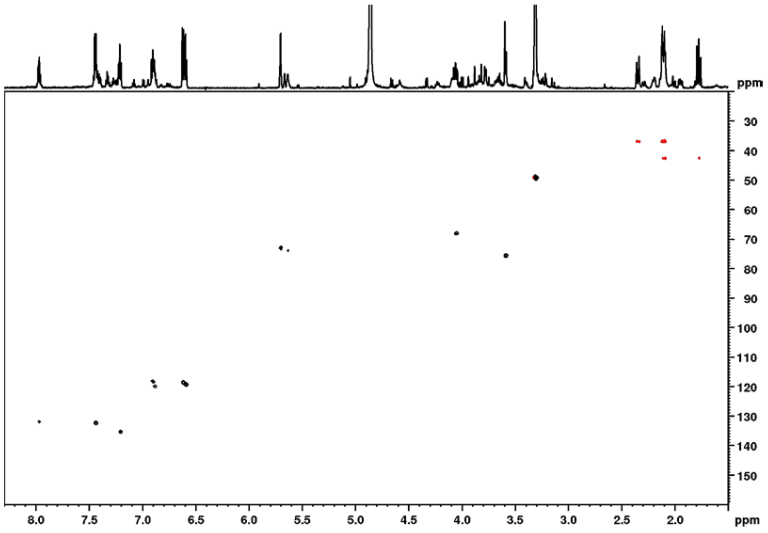

Figure A.1-8 Compound **1**, ^{1}H-^{13}C HSQC spectrum (700 MHz, MeOH-d_4).

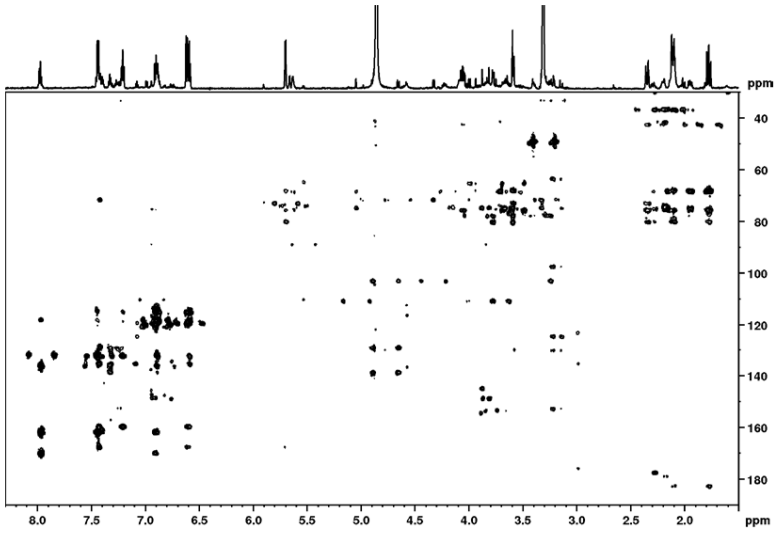

Figure A.1-9 Compound **1**, ^{1}H-^{13}C HMBC spectrum (700 MHz, MeOH-d_4).

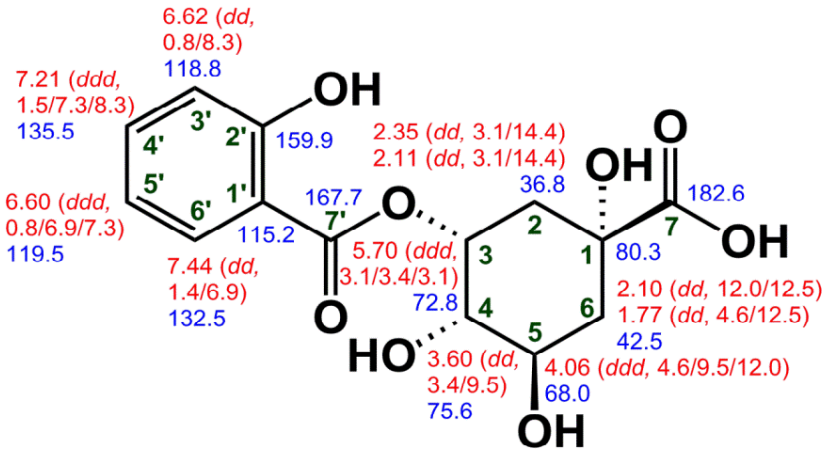

Figure A.1-10 Compound **1**, chemical structure with chemical shifts (MeOH-d_4).

A.2) 4-*O*-Salicyloyl quinic acid (2):

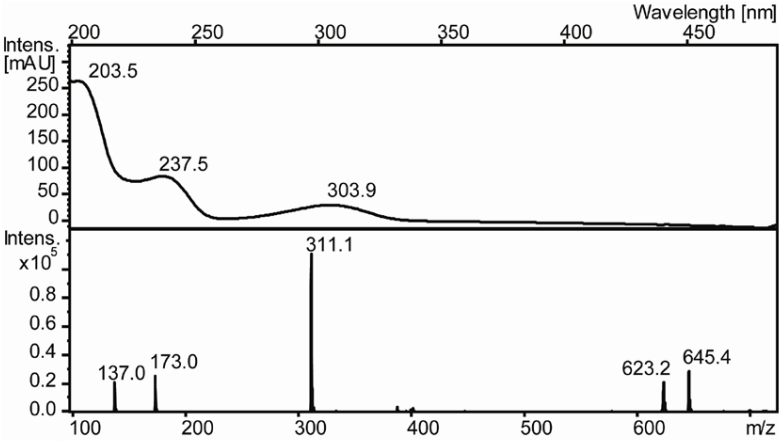

Figure A.2-1 Compound 2, UV spectrum obtained from HPLC-DAD (top) and mass spectrum (*m/z* 311.1 $[M-H]^-$, bottom).

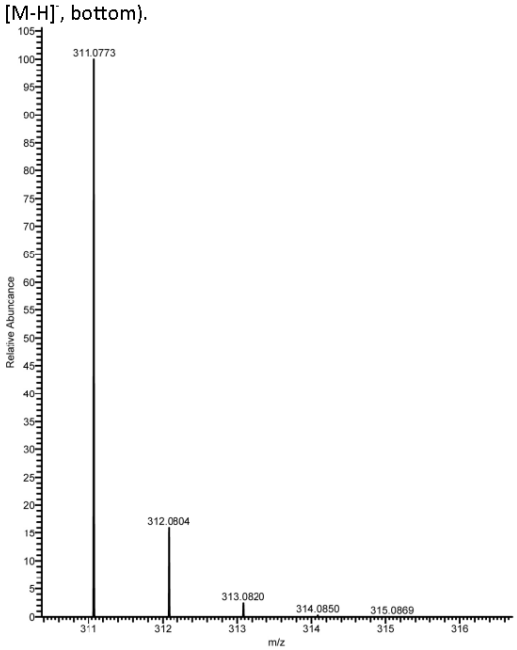

Figure A.2-2 Compound 2, HRESIMS spectrum, *m/z* 311.0773 $[M-H]^-$.

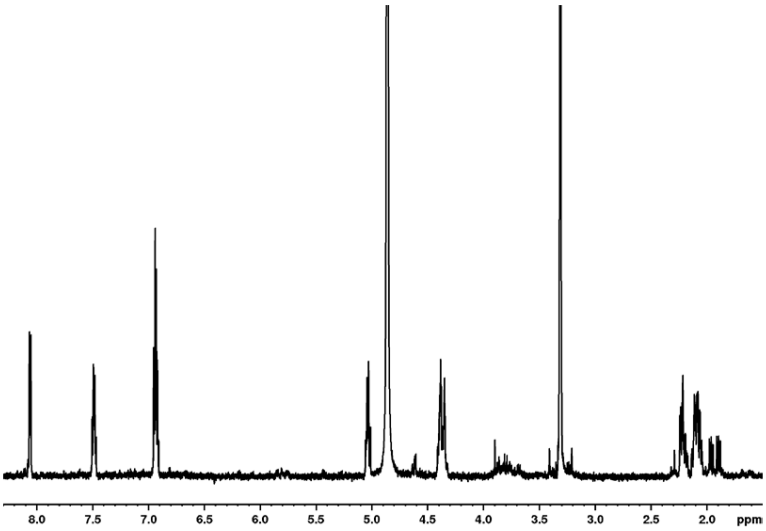

Figure A.2-3 Compound **2**, ^{1}H NMR spectrum (700 MHz, MeOH-d_4)

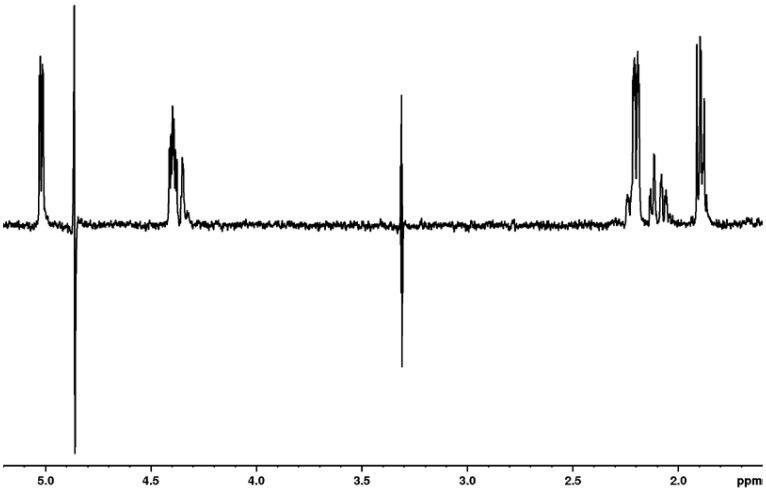

Figure A.2-4 Compound **2**, selective 1D TOCSY spectrum (700 MHz, MeOH-d_4, o1p = 1.89 ppm).

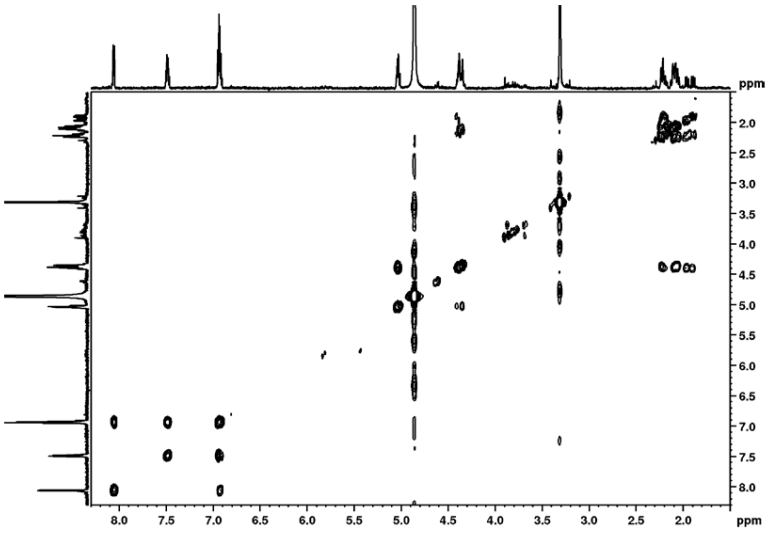

Figure A.2-5 Compound **2**, ^{1}H-^{1}H COSY spectrum (700 MHz, MeOH-d_4).

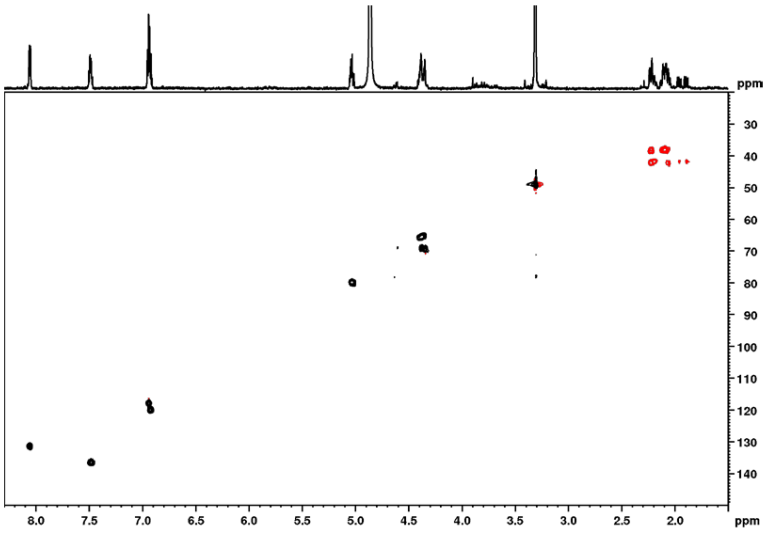

Figure A.2-6 Compound **2**, ^{1}H-^{13}C HSQC spectrum (700 MHz, MeOH-d_4).

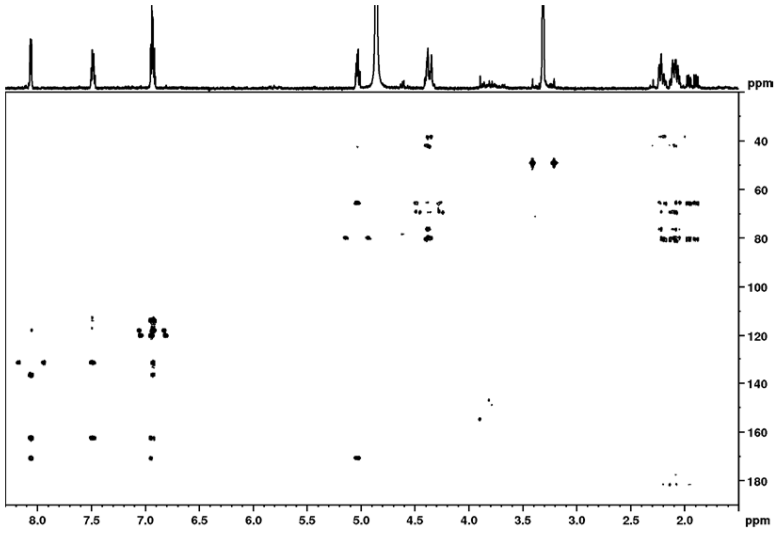

Figure A.2-7 Compound 2, ^{1}H-^{13}C HMBC spectrum (700 MHz, MeOH-d_4).

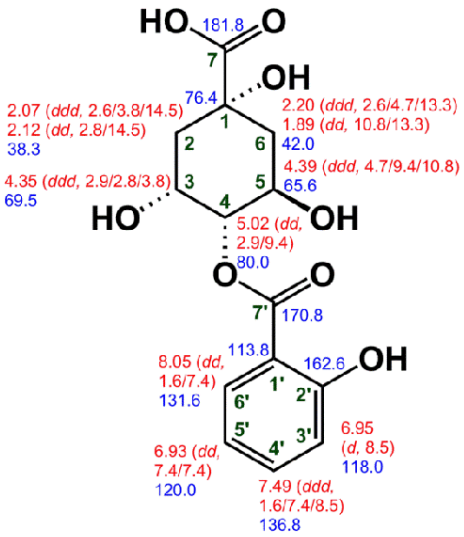

Figure A.2-8 Compound 2, chemical structure with chemical shifts (MeOH-d_4).

A.3) 5-*O*-Salicyloyl quinic acid (3):

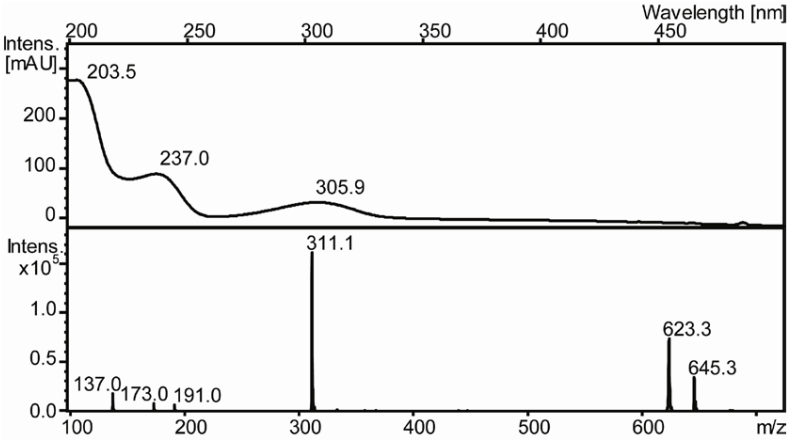

Figure A.3-1 Compound **3**, UV spectrum obtained from HPLC-DAD (top) and mass spectrum (*m/z* 311.1 $[M-H]^-$, bottom).

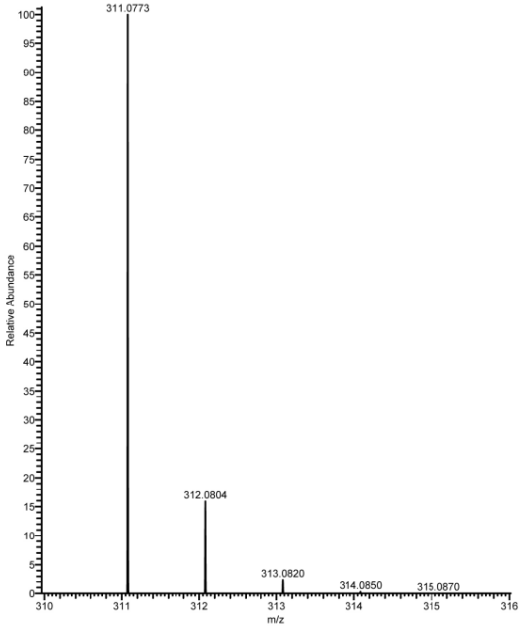

Figure A.3-2 Compound **3**, HRESIMS spectrum, *m/z* 311.0773 $[M-H]^-$.

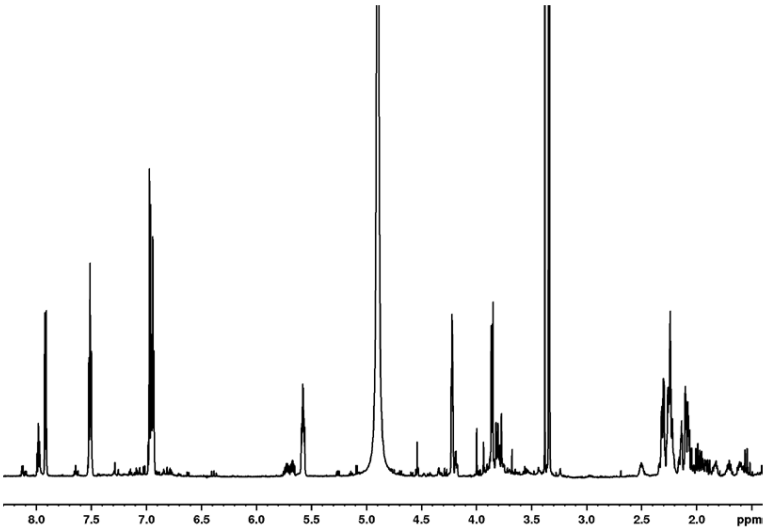

Figure A.3-3 Compound **3**, ^{1}H NMR spectrum (700 MHz, MeOH-d_4).

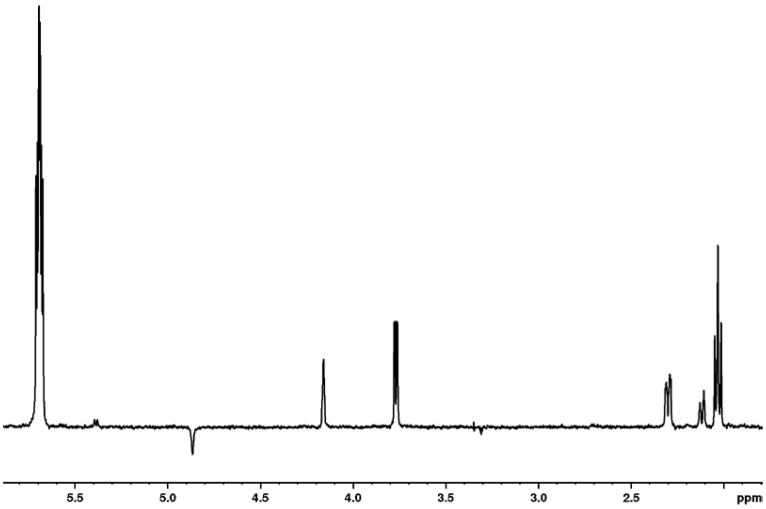

Figure A.3-4 Compound **3**, selective 1D TOCSY spectrum (700 MHz, MeOH-d_4, o1p = 5.55 ppm).

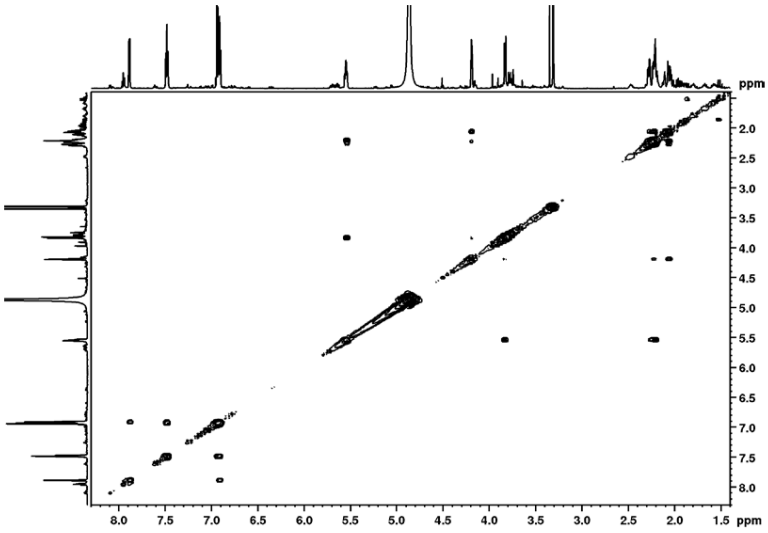

Figure A.3-5 Compound **3**, ^{1}H-^{1}H COSY spectrum (700 MHz, MeOH-d_4).

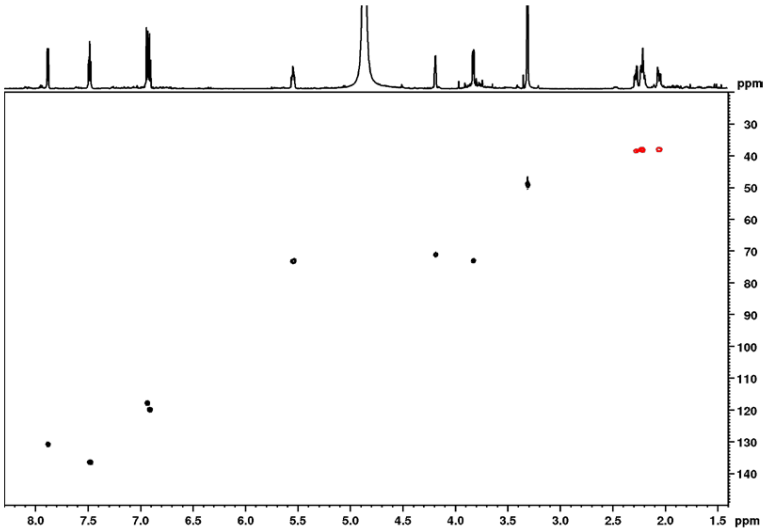

Figure A.3-6 Compound **3**, ^{1}H-^{13}C HSQC spectrum (700 MHz, MeOH-d_4).

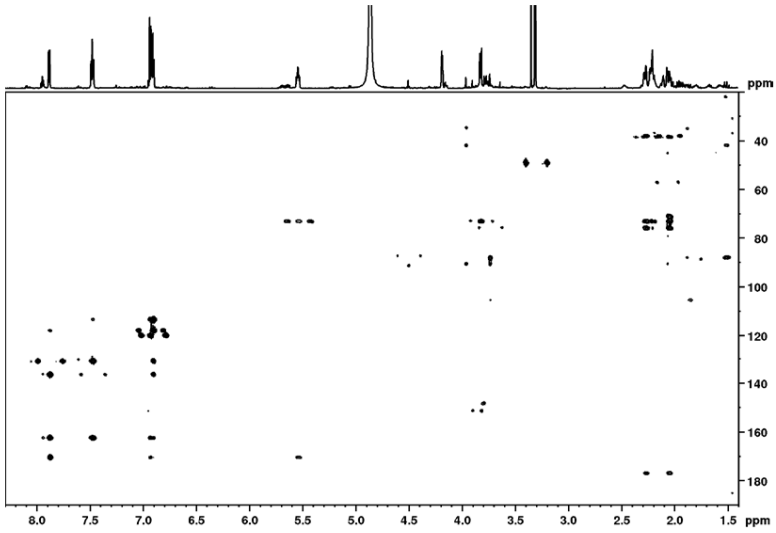

Figure A.3-7 Compound 3, ^{1}H-^{13}C HMBC spectrum (700 MHz, MeOH-d_4).

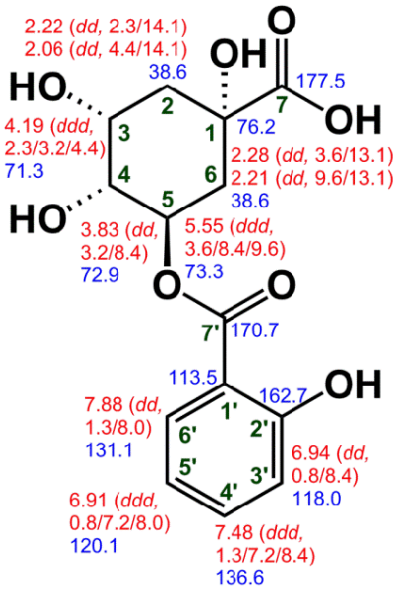

Figure A.3-8 Compound 3, chemical structure with chemical shifts (MeOH-d_4).

A.4) 4-*O*-Benzoyl quinic acid (4):

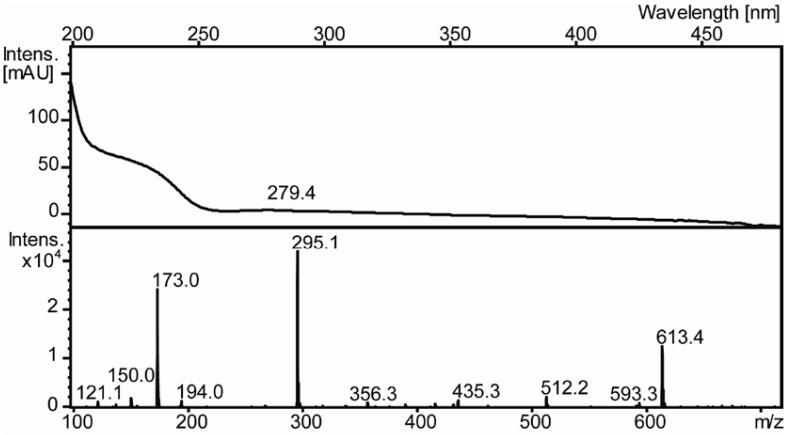

Figure A.4-1 Compound **4**, UV spectrum obtained from HPLC-DAD (top) and mass spectrum (*m/z* 295.1 $[M-H]^-$, bottom).

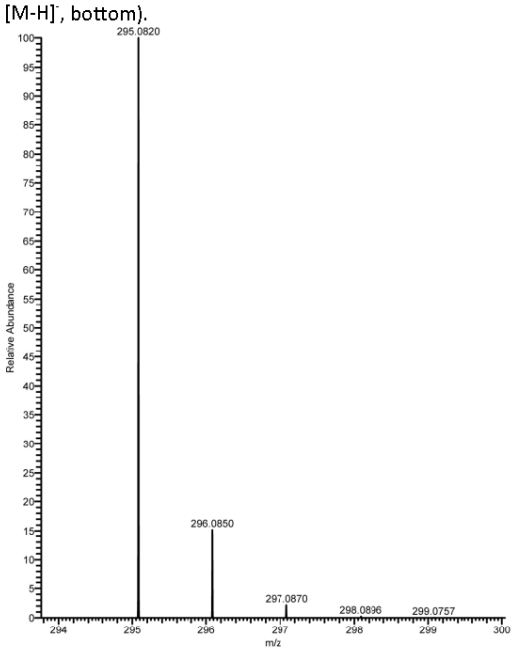

Figure A.4-2 Compound **4**, HRESIMS spectrum, *m/z* 295.0820 $[M-H]^-$.

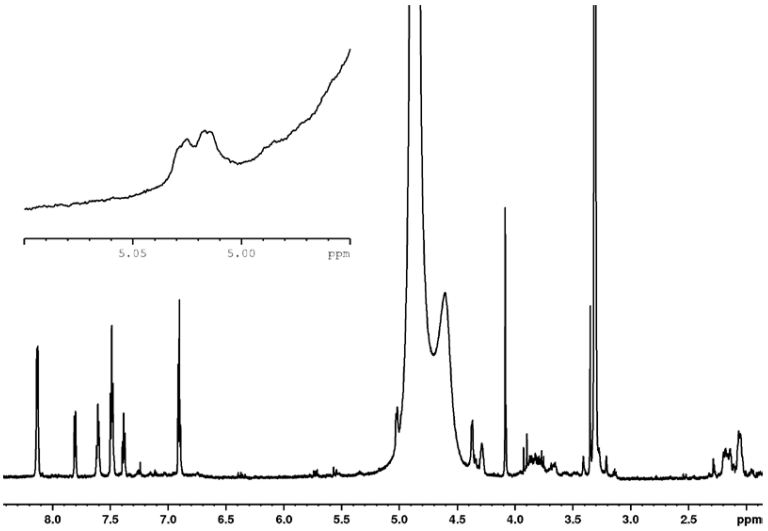

Figure A.4-3 Compound **4**, ^{1}H NMR spectrum (700 MHz, MeOH-d_4); insert: magnified signal of H-4 (δ_H 5.02).

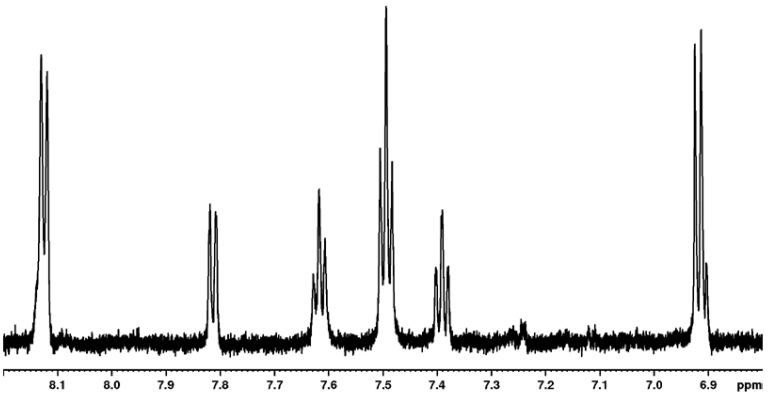

Figure A.4-4 Compound **4**, ^{1}H NMR spectrum (700 MHz, MeOH-d_4); 6.8 to 8.2 ppm.

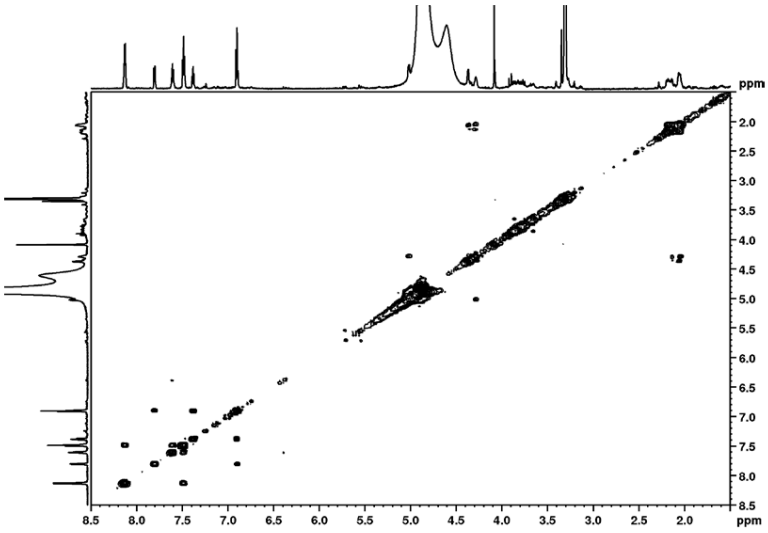

Figure A.4-5 Compound **4**, ^{1}H-^{1}H COSY spectrum (700 MHz, MeOH-d_4).

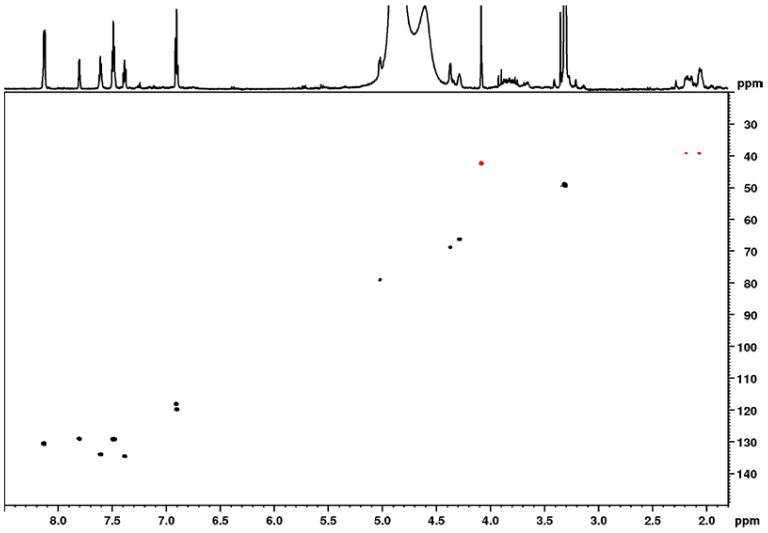

Figure A.4-6 Compound **4**, ^{1}H-^{13}C HSQC spectrum (700 MHz, MeOH-d_4).

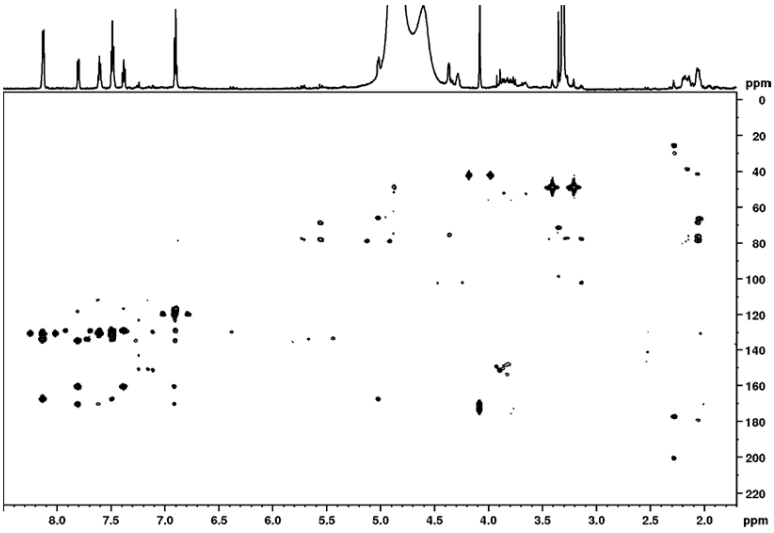

Figure A.4-7 Compound **4**, ^{1}H-^{13}C HMBC spectrum (700 MHz, MeOH-d_4).

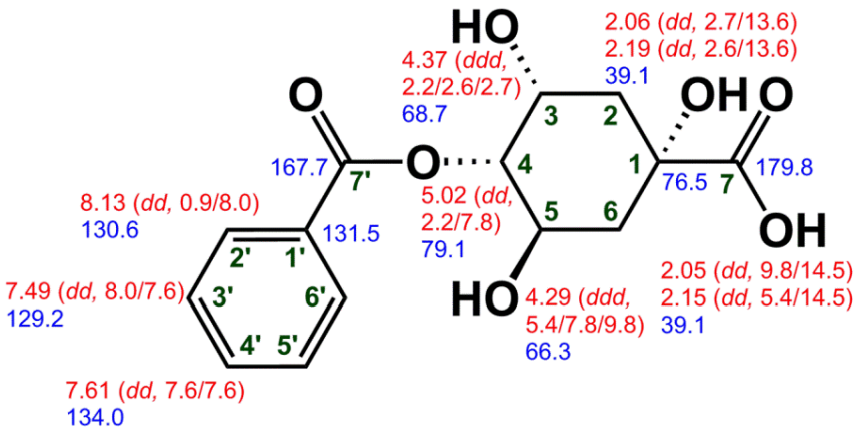

Figure A.4-8 Compound **4**, chemical structure with chemical shifts (MeOH-d_4).

A.5) 5-*O*-Benzoyl quinic acid (5):

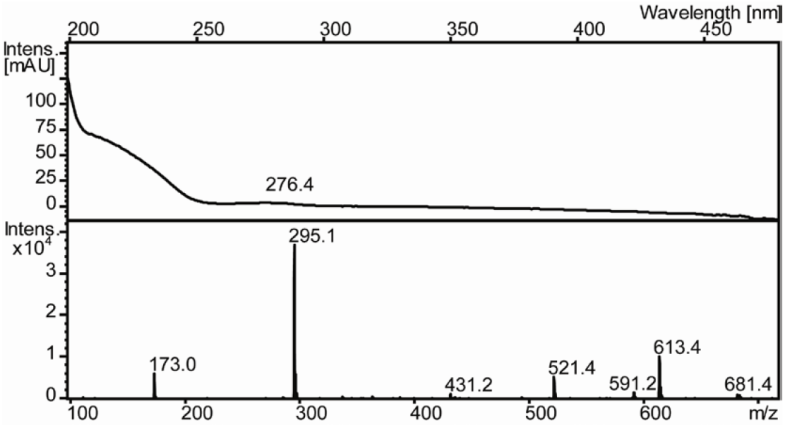

Figure A.5-1 Compound **5**, UV spectrum obtained from HPLC-DAD (top) and mass spectrum (*m/z* 295.1 $[M-H]^-$, bottom).

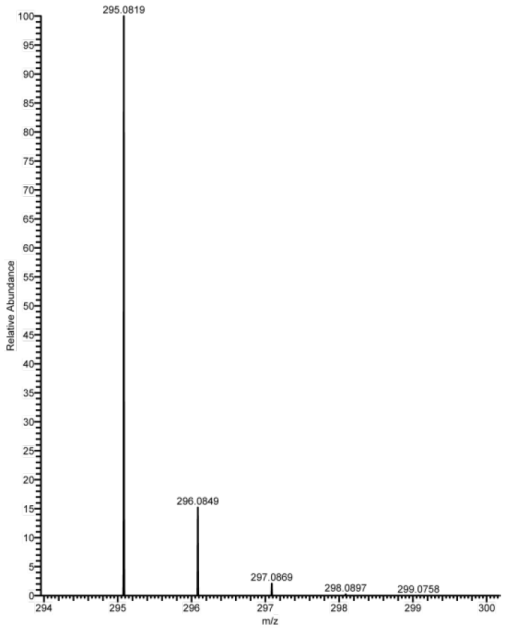

Figure A.5-2 Compound **5**, HRESIMS spectrum, *m/z* 295.0819 $[M-H]^-$.

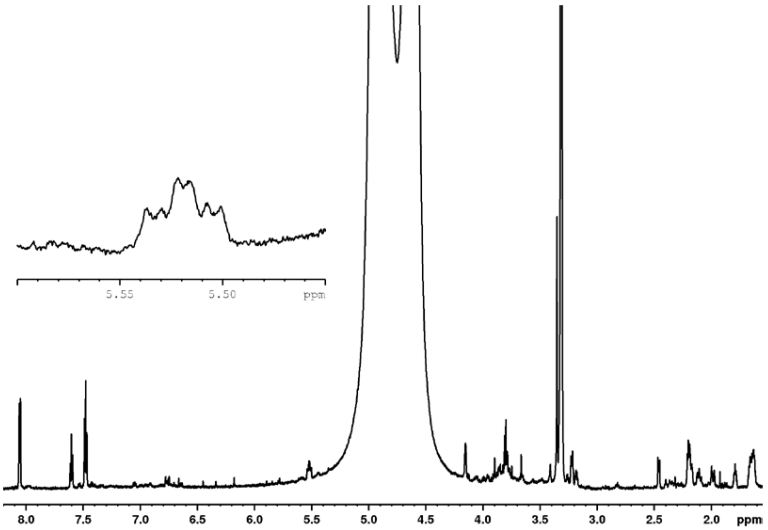

Figure A.5-3 Compound **5**, ^{1}H NMR spectrum (700 MHz, MeOH-d_4); Insert: magnified signal of H-5 (δ_H 5.52).

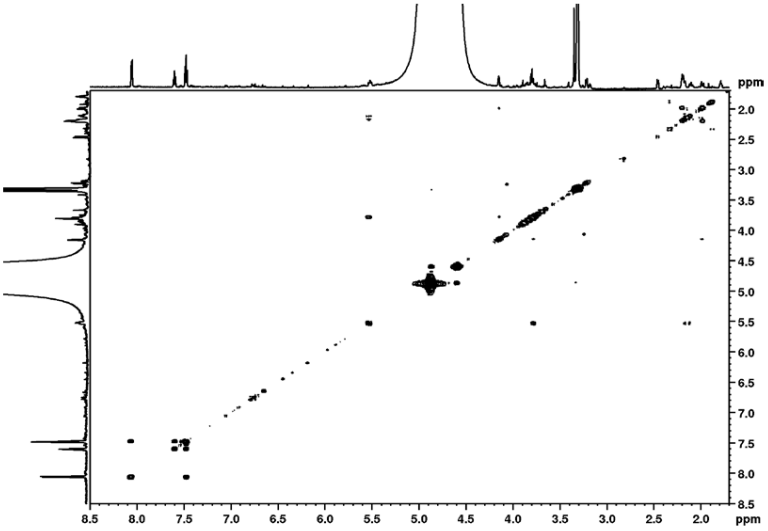

Figure A.5-4 Compound **5**, ^{1}H-^{1}H COSY spectrum (700 MHz, MeOH-d_4).

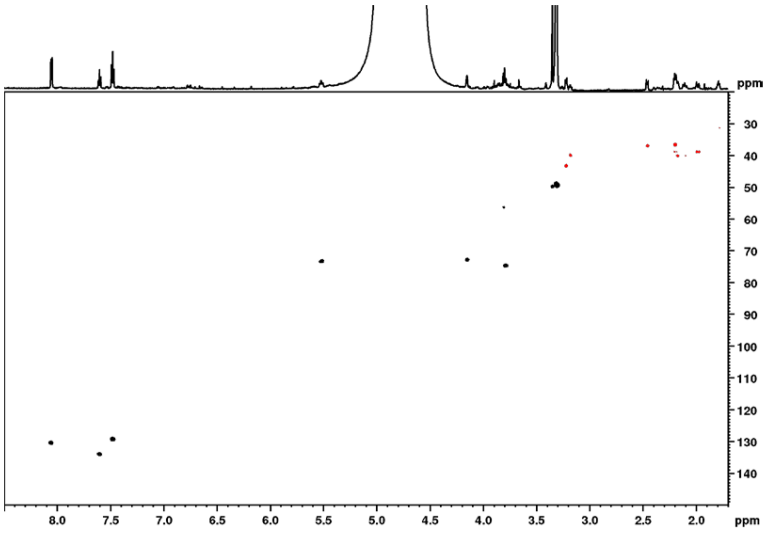

Figure A.5-5 Compound **5**, ^{1}H-^{13}C HSQC spectrum (700 MHz, MeOH-d_4).

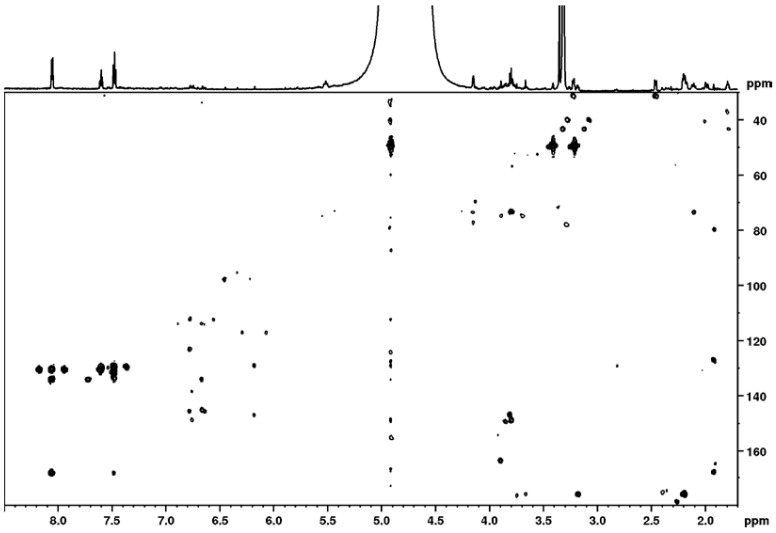

Figure A.5-6 Compound **5**, ^{1}H-^{13}C HMBC spectrum (700 MHz, MeOH-d_4).

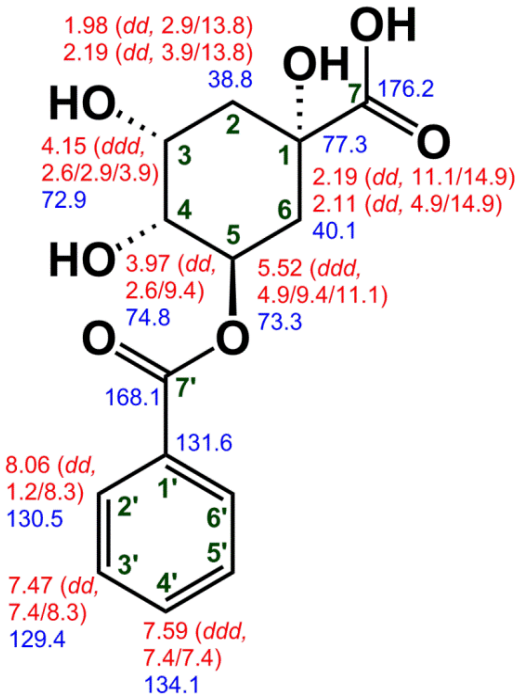

Figure A.5-7 Compound **5**, chemical structure with chemical shifts (MeOH-d_4).

A.6) 3-*O*,4-*O*-Disalicyloyl quinic acid (6):

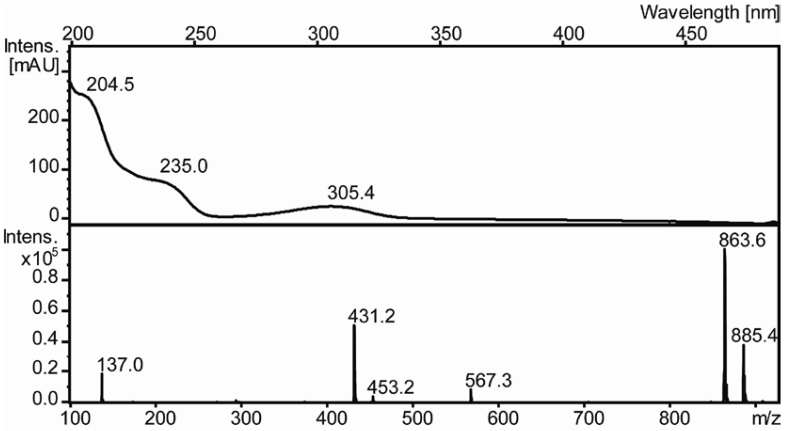

Figure A.6-1 Compound **6**, UV spectrum obtained from HPLC-DAD (top) and mass spectrum (*m/z* 431.2 $[M-H]^-$, bottom).

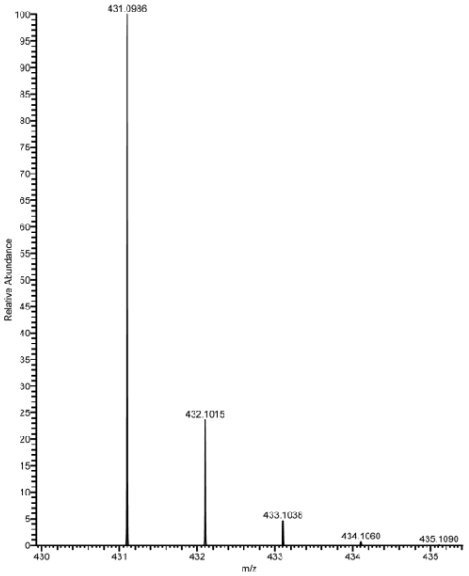

Figure A.6-2 Compound **6**, HRESIMS spectrum, *m/z* 431.0986 $[M-H]^-$.

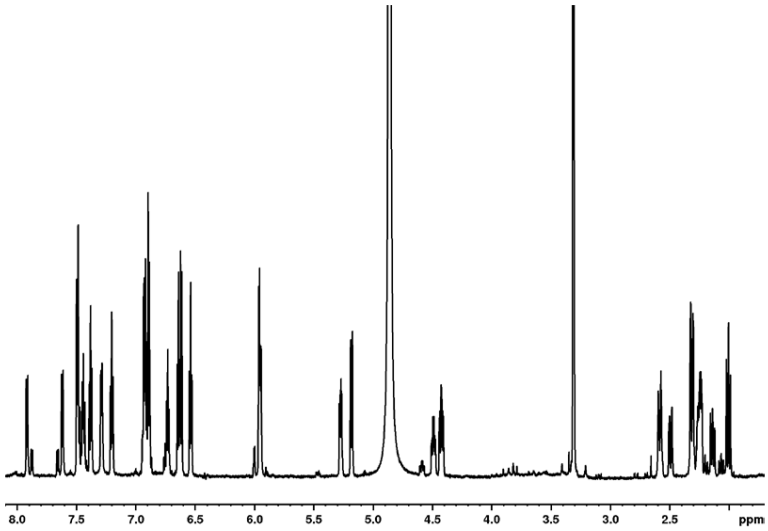

Figure A.6-3 Compound **6**, ^{1}H NMR spectrum (700 MHz, MeOH-d_4).

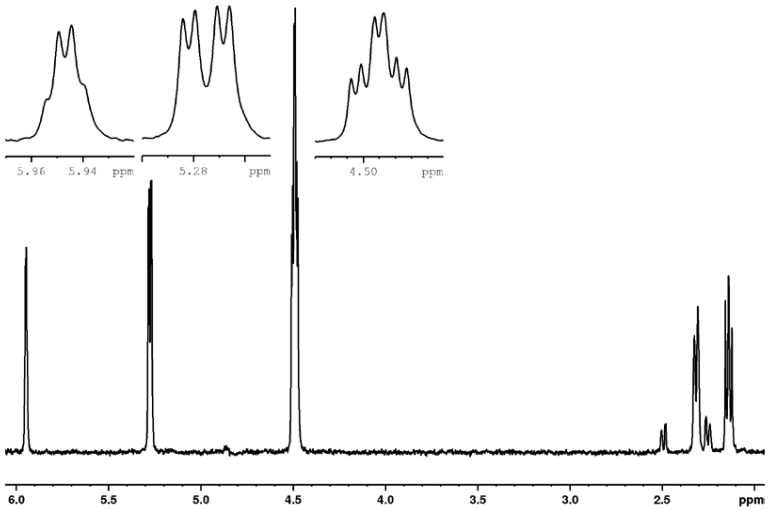

Figure A.6-4 Compound **6**, selective 1D TOCSY spectrum (700 MHz, MeOH-d_4, o1p = 4.48 ppm); Inserts: magnified signals of H-3 (δ_H 5.95), H-4 (δ_H 5.28) and H-5 (δ_H 4.48).

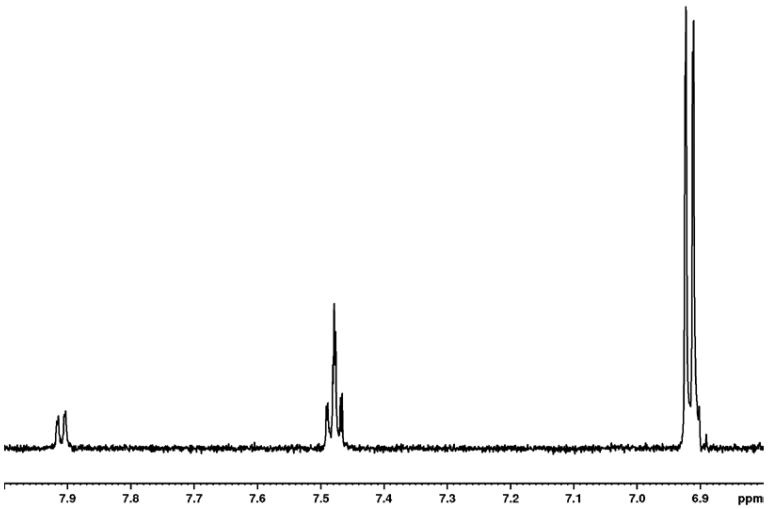

Figure A.6-5 Compound **6**, selective 1D TOCSY spectrum (700 MHz, MeOH-d_4, o1p = 7.91 ppm); signals displayed for H-6' (δ_H 7.91), H-4' (δ_H 6.92), H-3' (δ_H 7.48) and H-5' (δ_H 6.90).

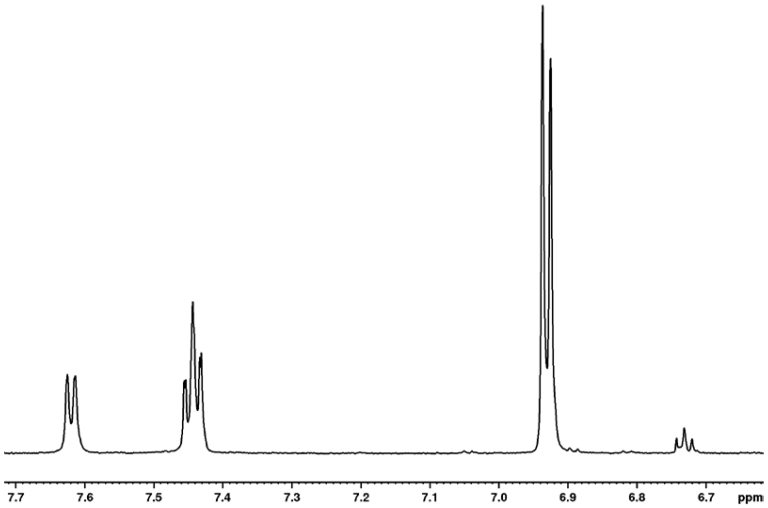

Figure A.6-6 Compound **6**, selective 1D TOCSY spectrum (700 MHz, MeOH-d_4, o1p = 7.62 ppm); signals displayed for H-6'' (δ_H 7.62), H-4'' (δ_H 7.44), H-3'' (δ_H 6.93) and H-5'' (δ_H 6.74).

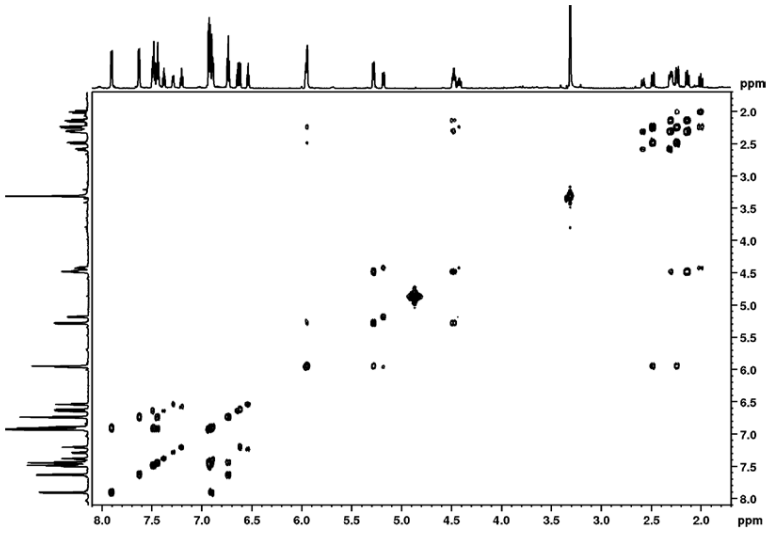

Figure A.6-7 Compound **6**, ^{1}H-^{1}H COSY spectrum (700 MHz, MeOH-d_4).

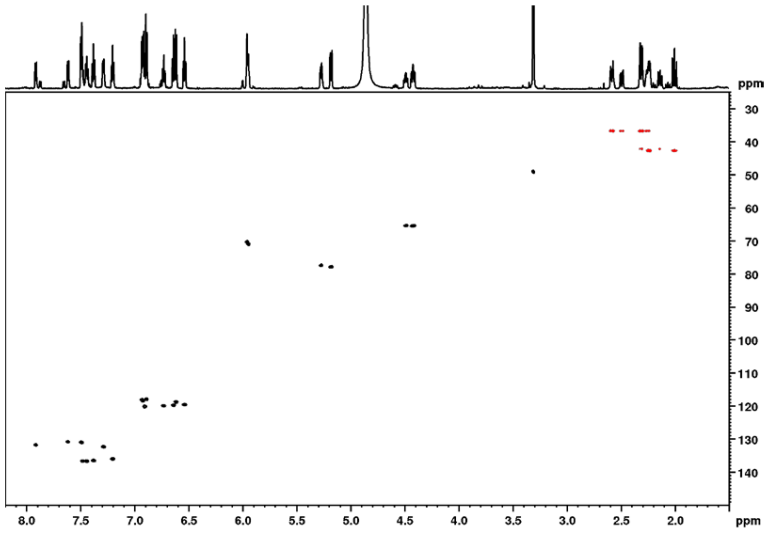

Figure A.6-8 Compound **6**, ^{1}H-^{13}C HSQC spectrum (700 MHz, MeOH-d_4).

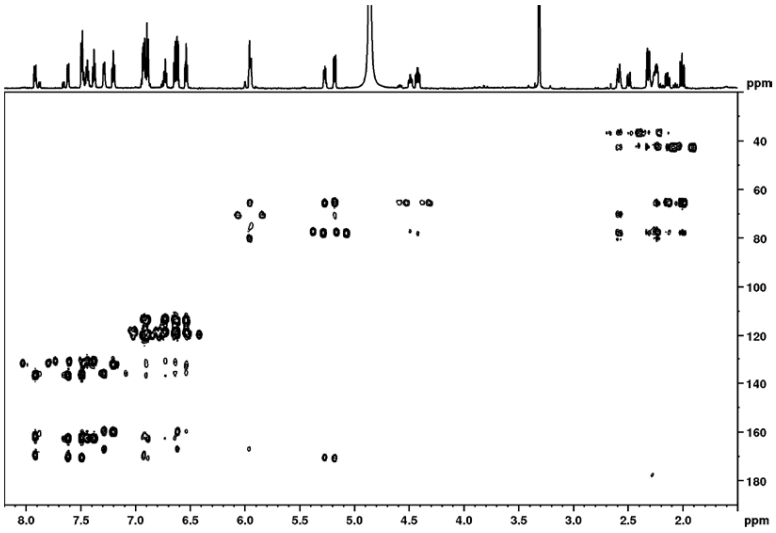

Figure A.6-9 Compound **6**, ^{1}H-^{13}C HMBC spectrum (700 MHz, MeOH-d_4).

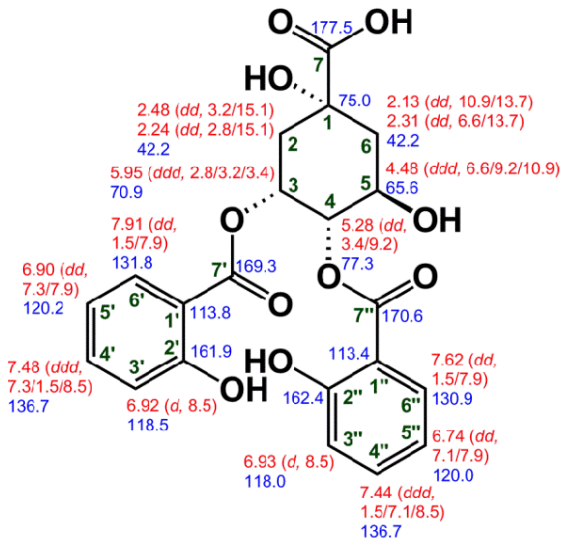

Figure A.6-10 Compound **6**, chemical structure with chemical shifts (MeOH-d_4).

A.7) 3-*O*,5-*O*-Disalicyloyl quinic acid (7):

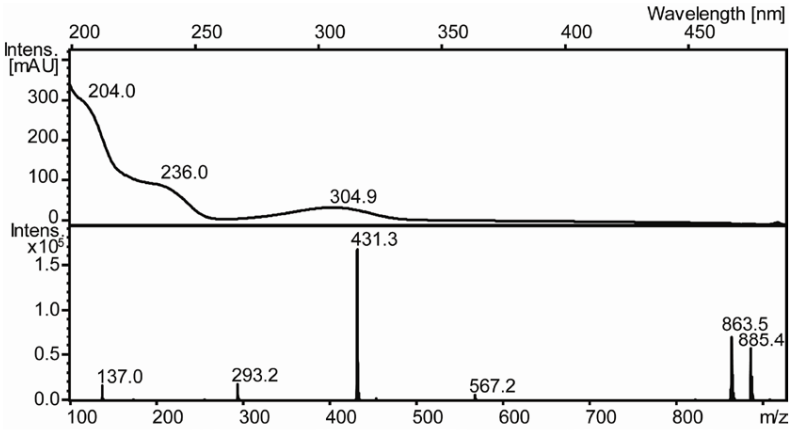

Figure A.7-1 Compound **7**, UV spectrum from HPLC-DAD (top) and mass spectrum (m/z 431.3 $[M-H]^-$, bottom).

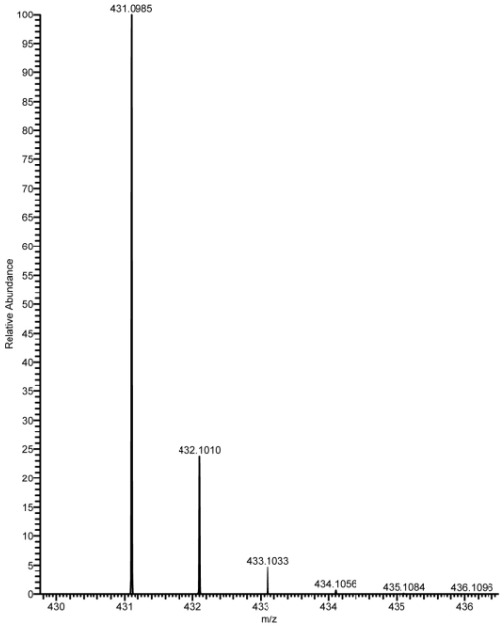

Figure A.7-2 Compound **7**, HRESIMS spectrum, *m/z* 431.0985 $[M-H]^-$.

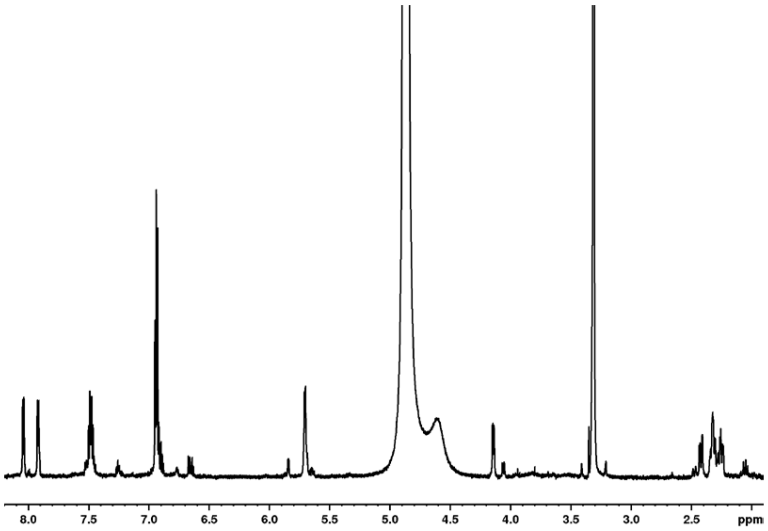

Figure A.7-3 Compound **7**, ^{1}H NMR spectrum (700 MHz, MeOH-d_4).

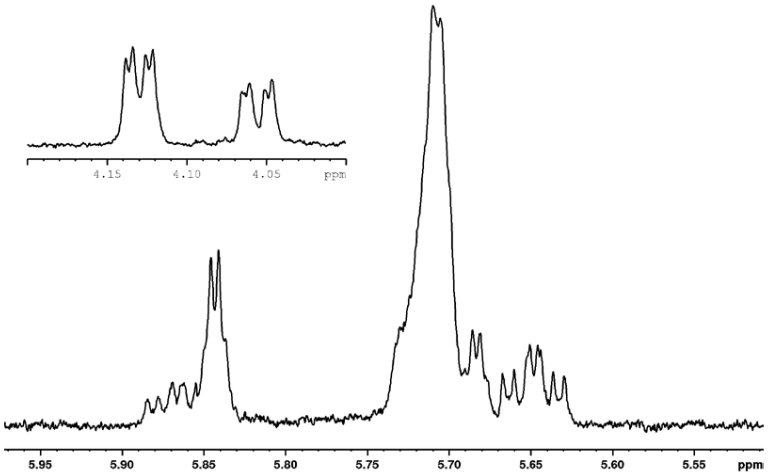

Figure A.7-4 Compound **7**, ^{1}H NMR spectrum (700 MHz, MeOH-d_4); region from 5.55 to 5.95 ppm, signal H-3 and H-5 are overlapping (δ_H 5.71); insert: magnified signal of H-4 (δ_H 4.13).

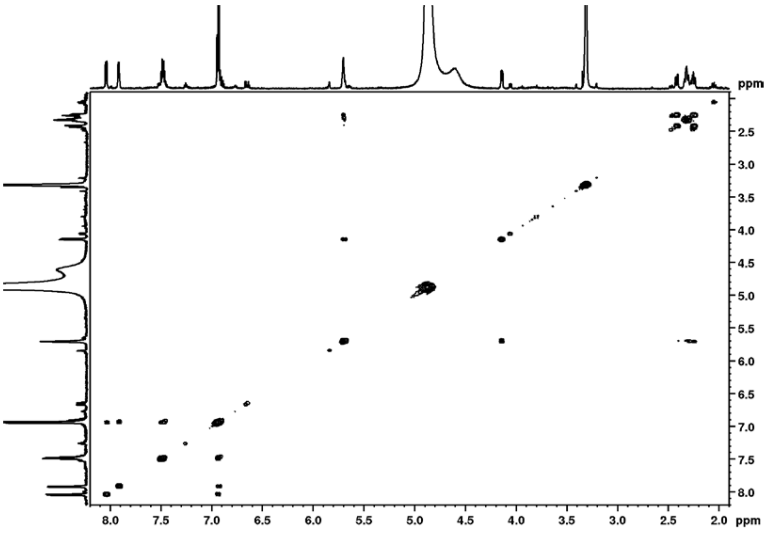

Figure A.7-5 Compound **7**, ^{1}H-^{1}H COSY spectrum (700 MHz, MeOH-d_4).

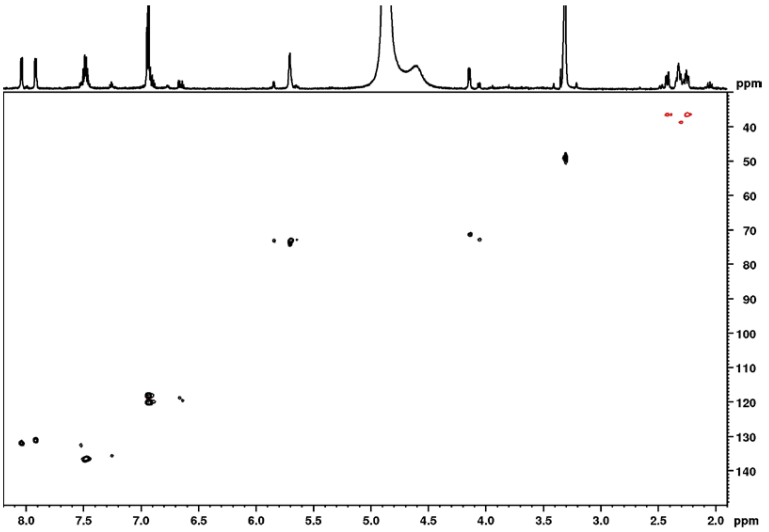

Figure A.7-6 Compound **7**, ^{1}H-^{13}C HSQC spectrum (700 MHz, MeOH-d_4).

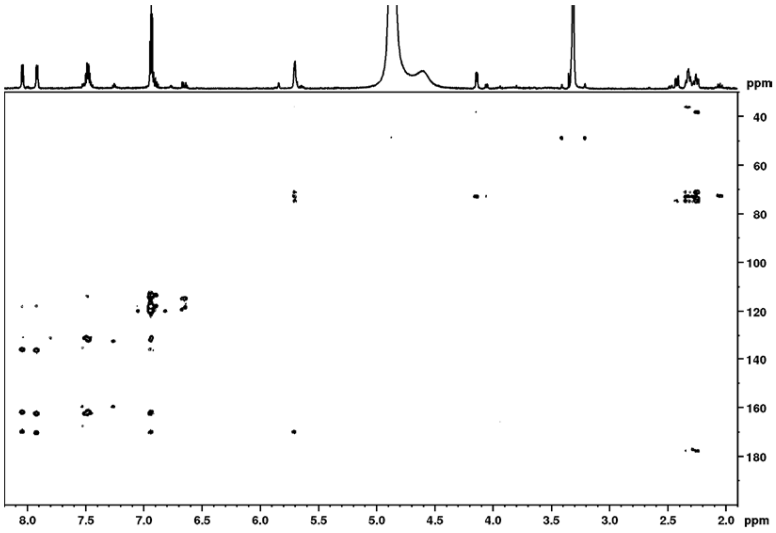

Figure A.7-7 Compound **7**, ^{1}H-^{13}C HMBC spectrum (700 MHz, MeOH-d_4).

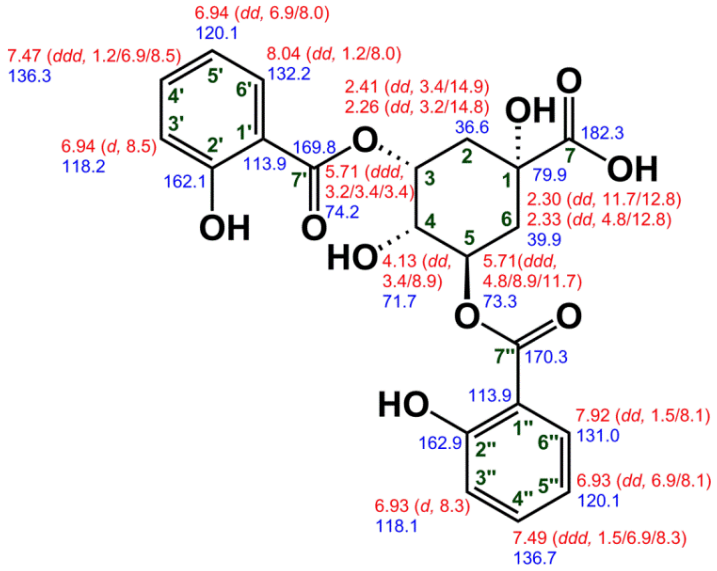

Figure A.7-8 Compound **7**, chemical structure with chemical shifts (MeOH-d_4).

A.8) 4-*O*,5-*O*-Disalicyloyl quinic acid (8):

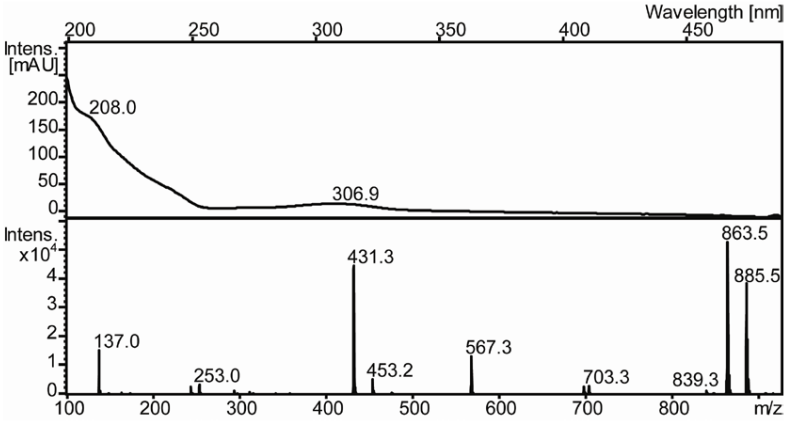

Figure A.8-1 Compound **8**, UV spectrum obtained from HPLC-DAD (top) and mass spectrum (*m/z* 431.3 $[M-H]^-$, bottom).

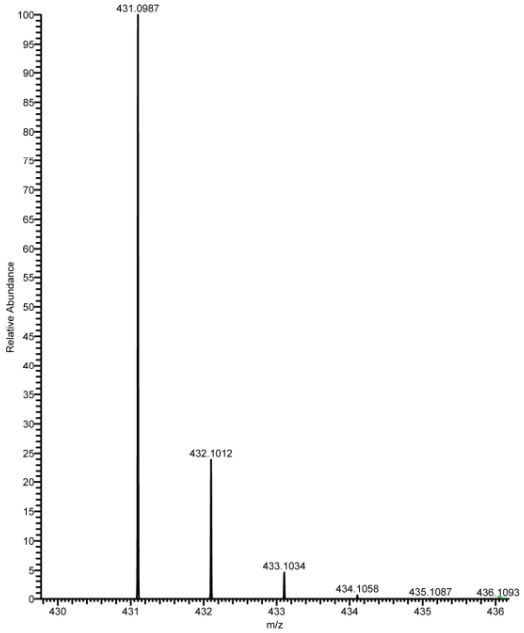

Figure A.8-2 Compound **8**, HRESIMS spectrum, *m/z* 431.0987 $[M-H]^-$.

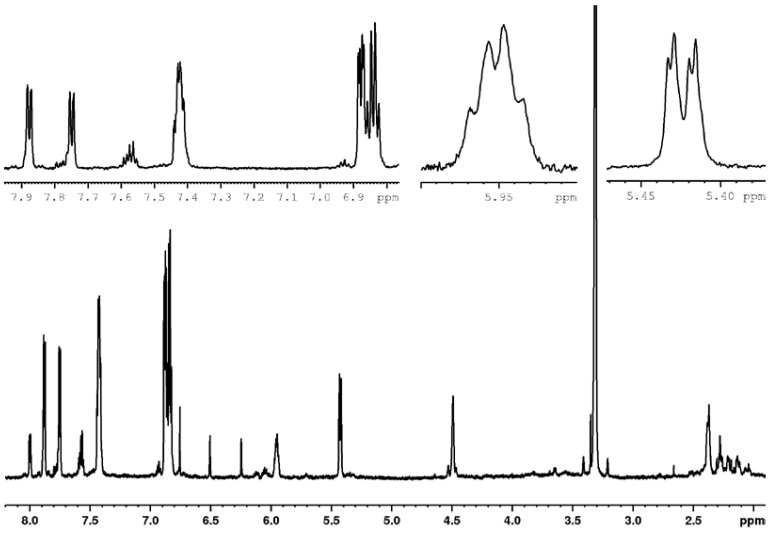

Figure A.8-3 Compound **8**, 1D NOESY spectrum (700 MHz, MeOH-d_4, o1p = 4.92 ppm), region 7.9 to 6.8 ppm; inserts: magnified signals of H-5 (δ_H 5.95) and H-4 (δ_H 5.42).

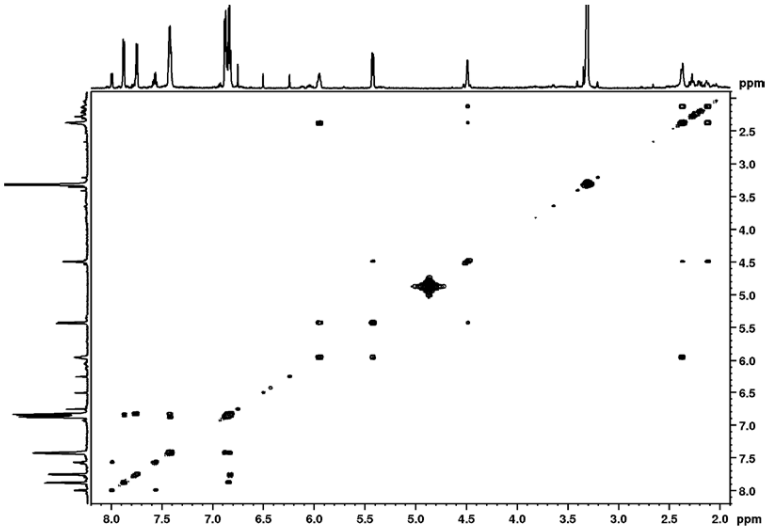

Figure A.8-4 Compound **8**, ^{1}H-^{1}H COSY spectrum (700 MHz, MeOH-d_4).

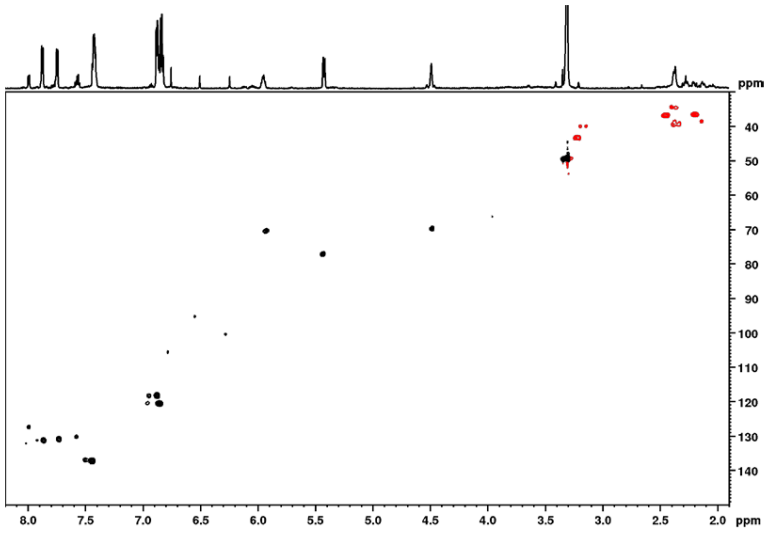

Figure A.8-5 Compound **8**, ^{1}H-^{13}C HSQC spectrum (700 MHz, MeOH-d_4).

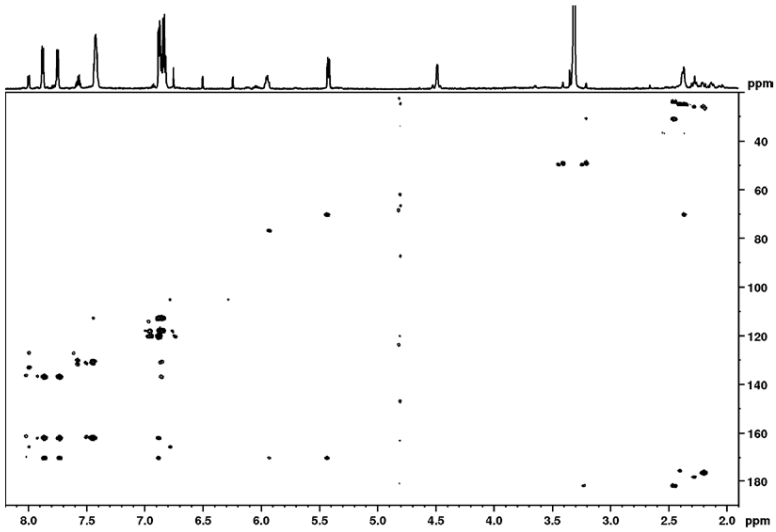

Figure A.8-6 Compound **8**, ^{1}H-^{13}C HMBC spectrum (700 MHz, MeOH-d_4).

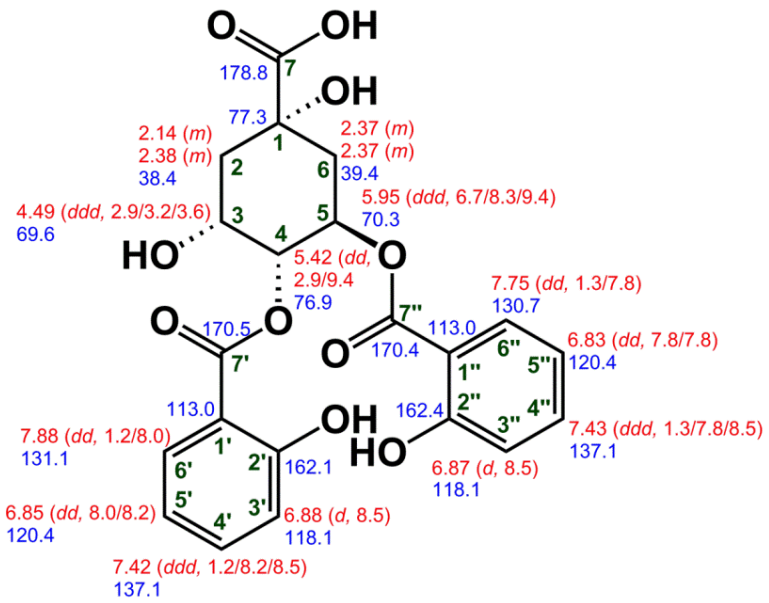

Figure A.8-7 Compound **8**, chemical structure with chemical shifts (MeOH-d_4).

A.9) 3-*O*-Salicyloyl-4-*O*-benzoyl quinic acid (9):

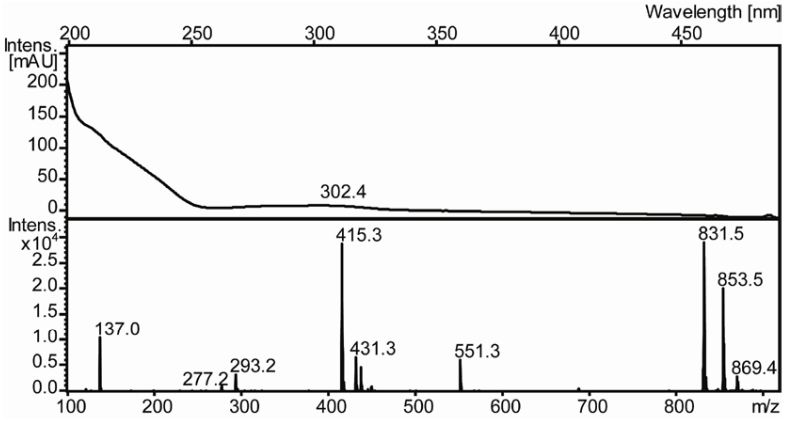

Figure A.9-1 Compound **9**, UV spectrum obtained from HPLC-DAD (top) and mass spectrum (m/z 415.3 $[M-H]^-$, bottom).

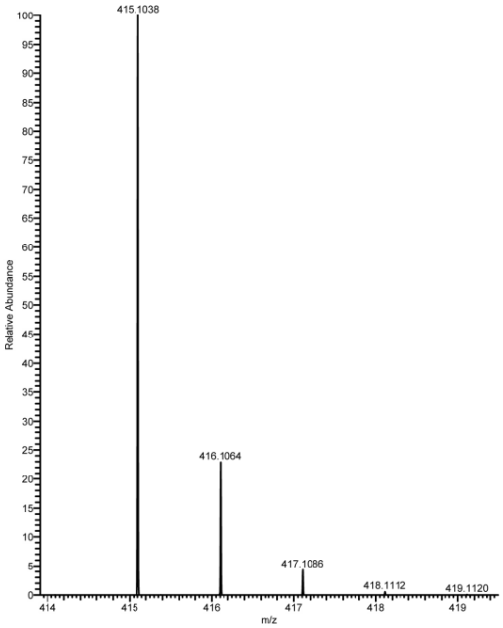

Figure A.9-2 Compound **9**, HRESIMS spectrum, *m/z* 415.1038 $[M-H]^-$.

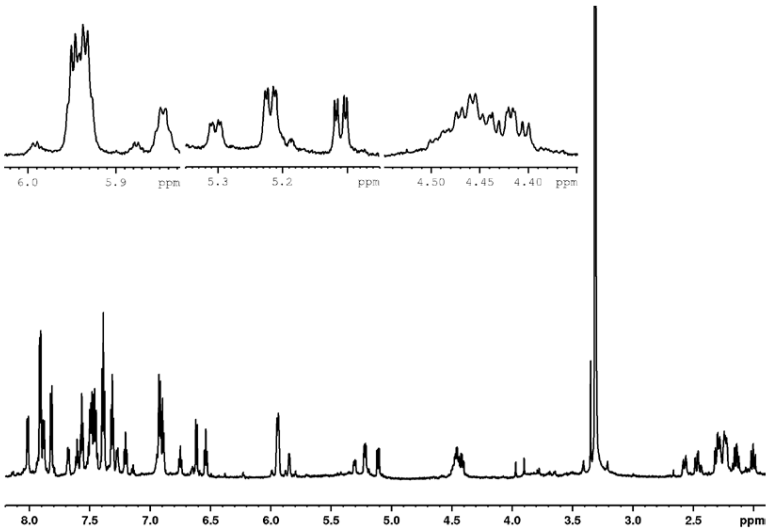

Figure A.9-3 Compound **9**, 1D NOESY spectrum (700 MHz, MeOH-d_4, o1P = 4.92 ppm); inserts: magnified signals of H-3 (δ_H 5.93), H-4 (δ_H 5.22) and H-5 (δ_H 4.46).

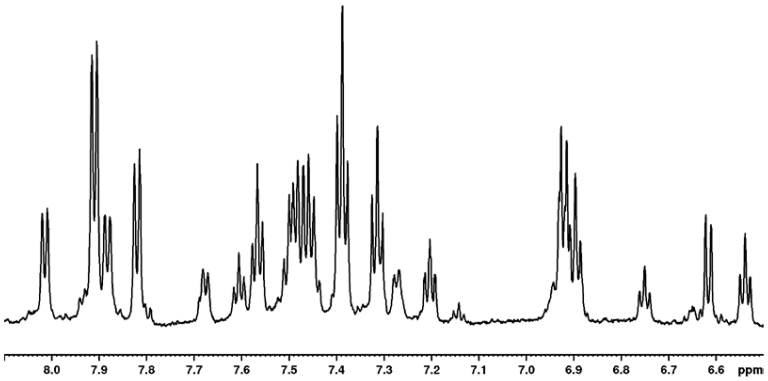

Figure A.9-4 Compound **9**, 1D NOESY spectrum (700 MHz, MeOH-d_4, o1p = 4.92 ppm); region 8.1 to 6.5 ppm.

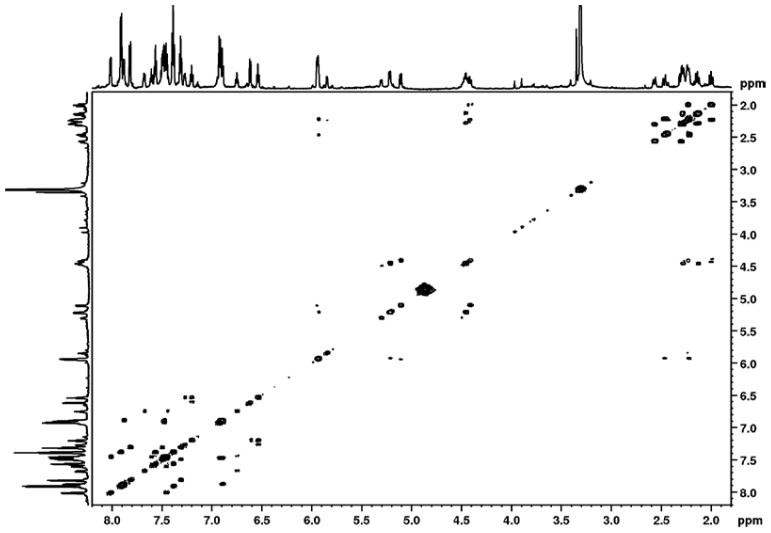

Figure A.9-5 Compound **9**, ^{1}H-^{1}H COSY spectrum (700 MHz, MeOH-d_4).

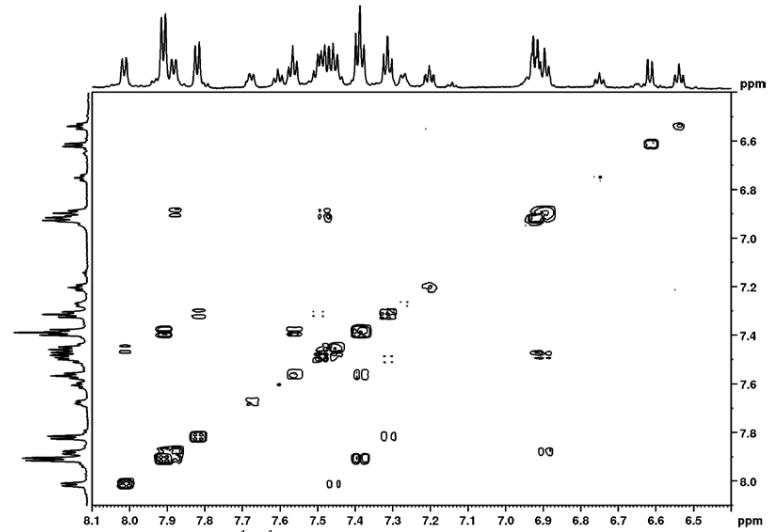

Figure A.9-6 Compound **9**, ^{1}H-^{1}H COSY spectrum (700 MHz, MeOH-d_4); region 8.1 to 6.5 ppm.

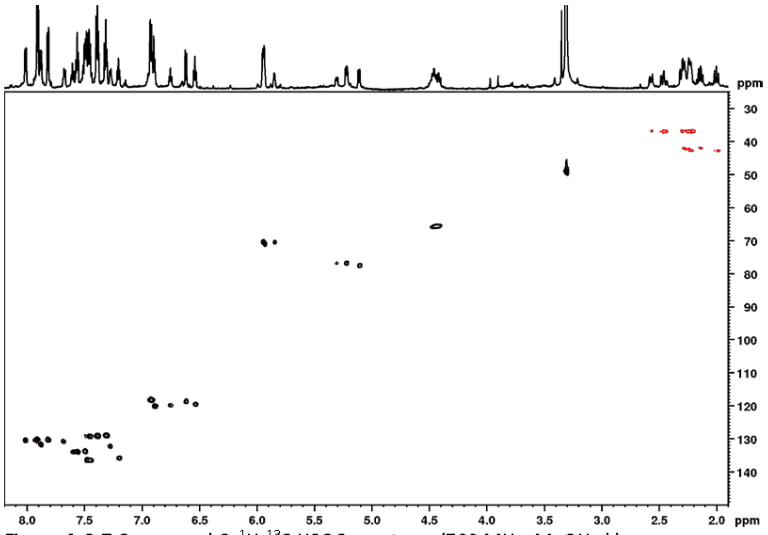

Figure A.9-7 Compound **9**, ^{1}H-^{13}C HSQC spectrum (700 MHz, MeOH-d_4).

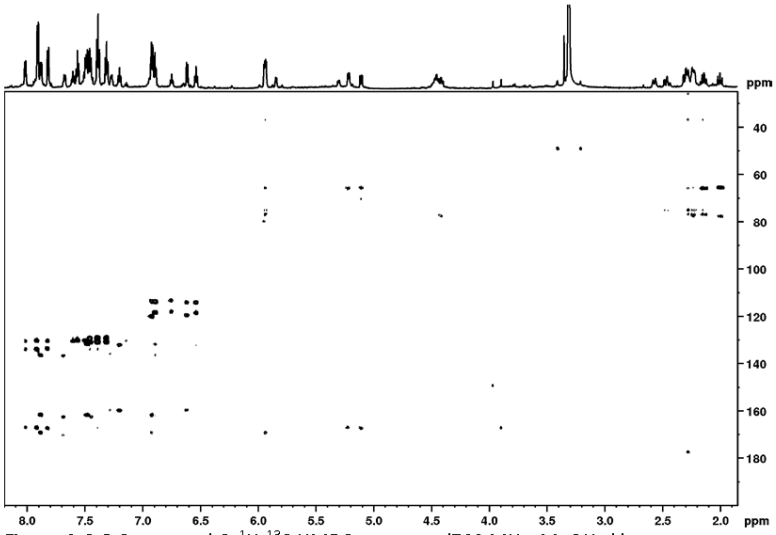

Figure A.9-8 Compound **9**, ^{1}H-^{13}C HMBC spectrum (700 MHz, MeOH-d_4).

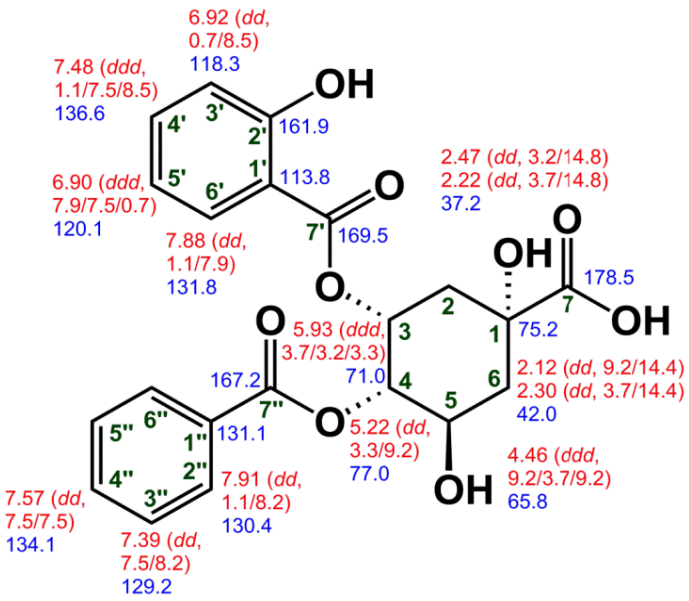

Figure A.9-9 Compound **9**, structure with chemical shifts (MeOH-d_4).

A.10) 3-*O*-Salicyloyl-5-*O*-benzoyl quinic acid (10):

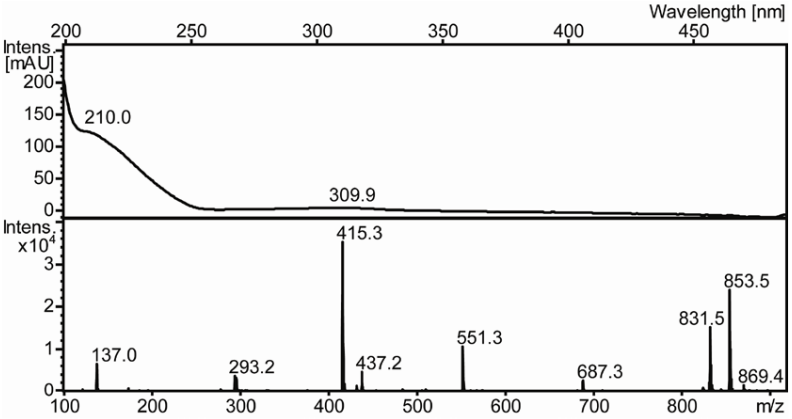

Figure A.10-1 Compound **10**, UV spectrum obtained from HPLC-DAD (top) and mass spectrum (*m/z* 415.3 $[M-H]^-$, bottom).

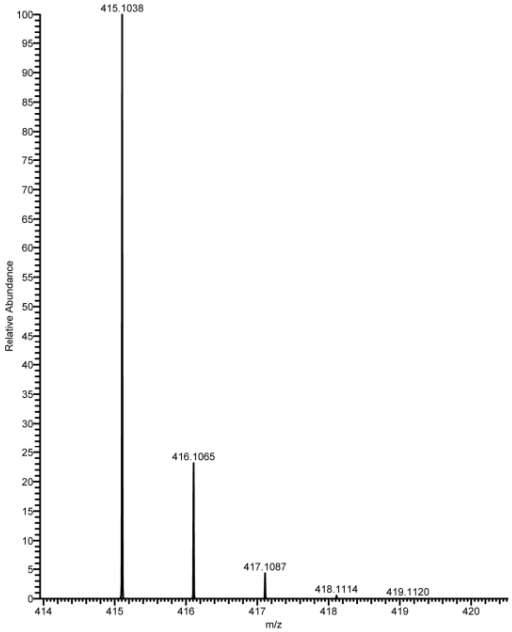

Figure A.10-2 Compound **10**, HRESIMS spectrum, *m/z* 415.1038 $[M-H]^-$.

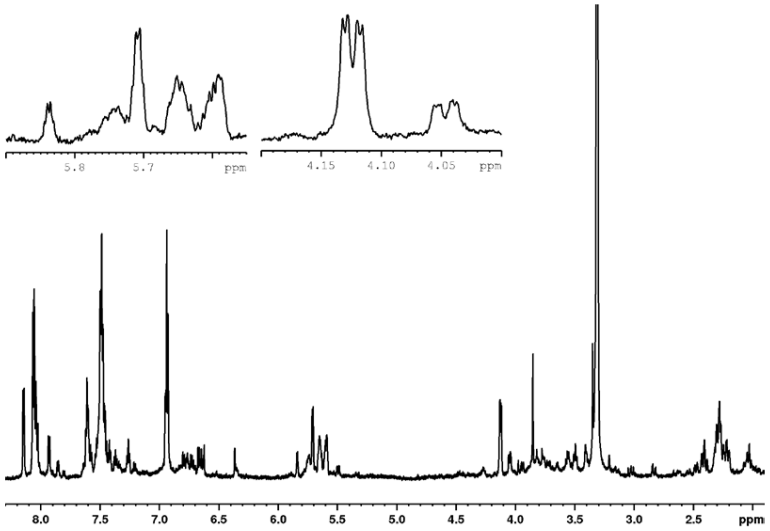

Figure A.10-3 Compound **10**, 1D NOESY spectrum (700 MHz, MeOH-d_4, o1P = 4.92 ppm); inserts: magnified signals of H-3 (δ_H 5.71), H-5 (δ_H 5.56) and H-3 (δ_H 4.12).

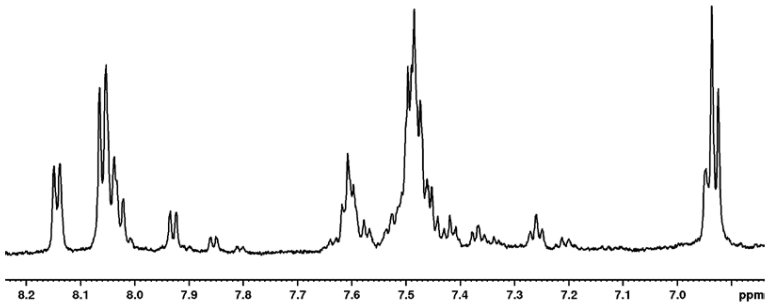

Figure A.10-4 Compound **10**, 1D NOESY spectrum (700 MHz, MeOH-d_4, o1P = 4.92 ppm); region 8.2 to 6.8 ppm.

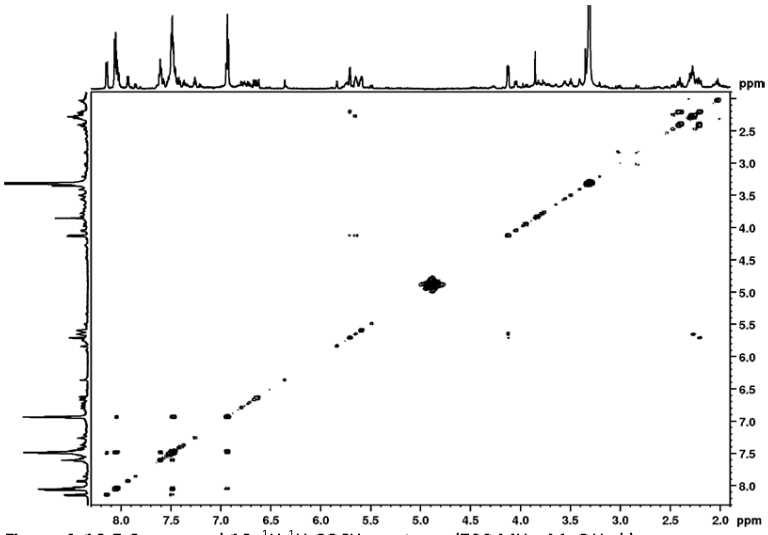

Figure A.10-5 Compound **10**, ^{1}H-^{1}H COSY spectrum (700 MHz, MeOH-d_4).

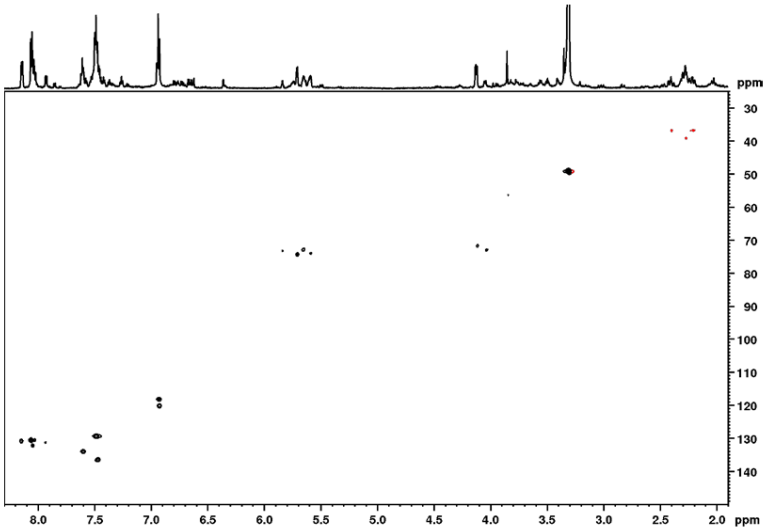

Figure A.10-6 Compound **10**, ^{1}H-^{13}C HSQC spectrum (700 MHz, MeOH-d_4).

XC

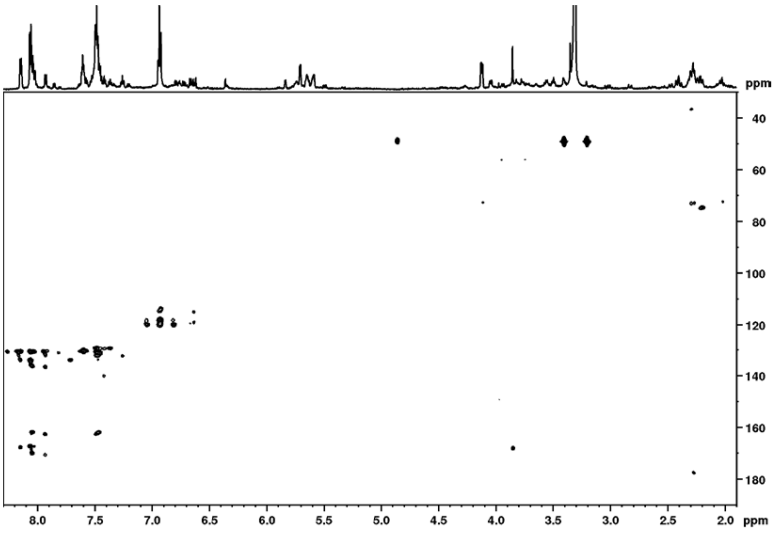

Figure A.10-7 Compound **10**, ^{1}H-^{13}C HMBC spectrum (700 MHz, MeOH-d_4).

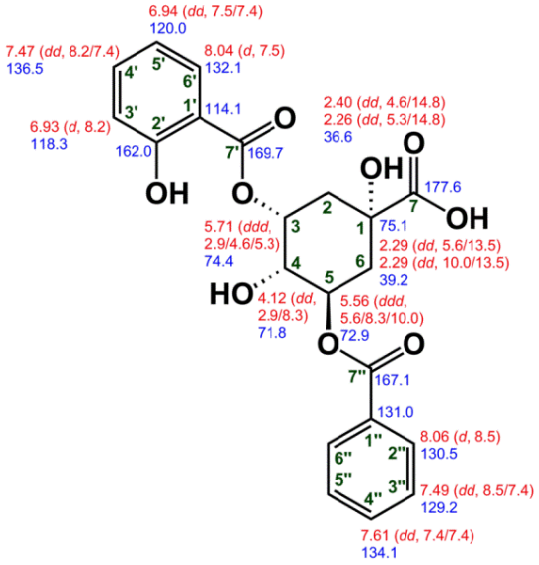

Figure A.10-8 Compound **10**, structure with chemical shifts (MeOH-d_4).

A.11) 4-*O*-Salicyloyl-5-*O*-benzoyl quinic acid (11):

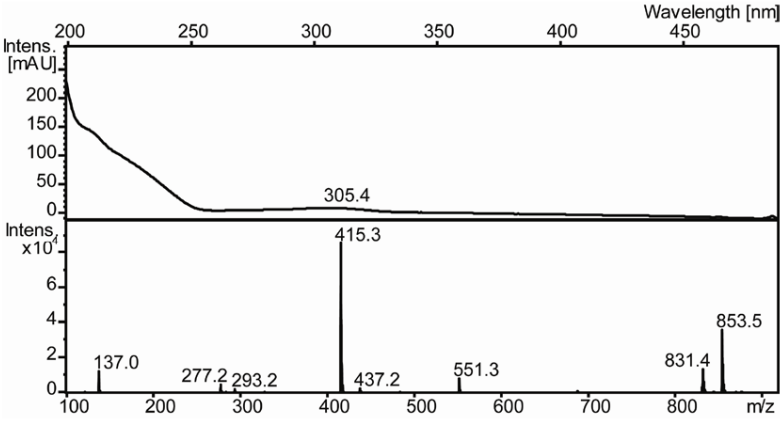

Figure A.11-1 Compound **11**, UV-spectra from HPLC-DAD (top) and mass spectrum (*m/z* 415.3 $[M-H]^-$, bottom).

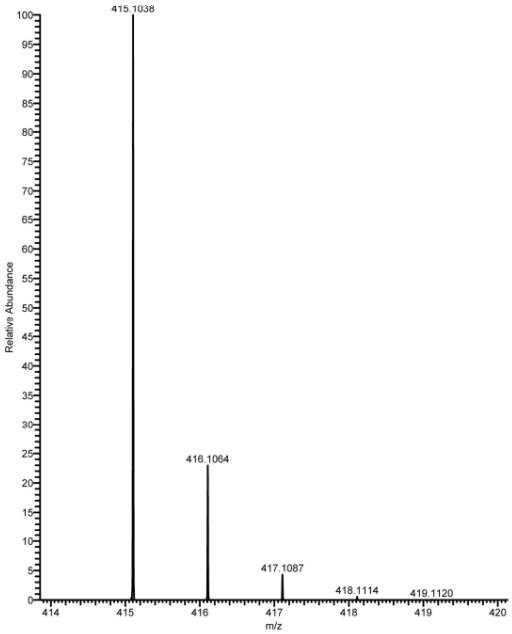

Figure A.11-2 Compound **11**, HRESIMS spectrum, *m/z* 415.1038 $[M-H]^-$.

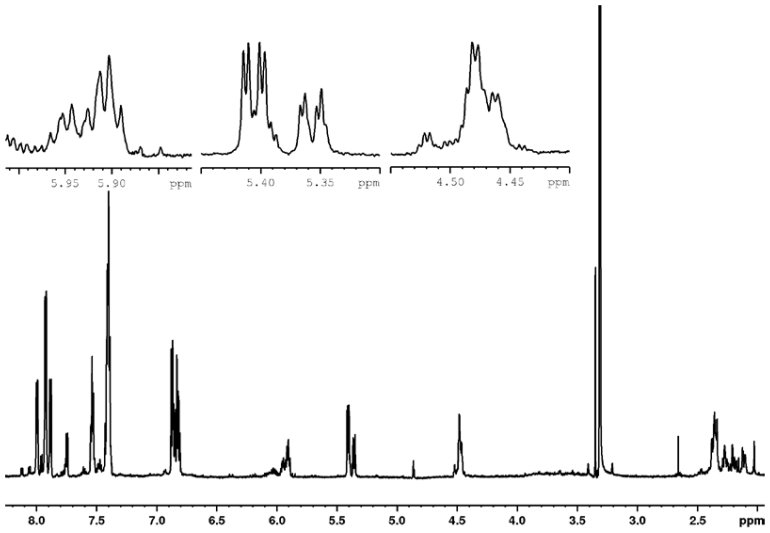

Figure A.11-3 Compound **11**, 1D NOESY spectrum (700 MHz, MeOH-d_4, o1P = 4.92 ppm); signal H-5 (δ_H 5.91), H-4 (δ_H 5.41) and H-3 (δ_H 4.47) are magnified.

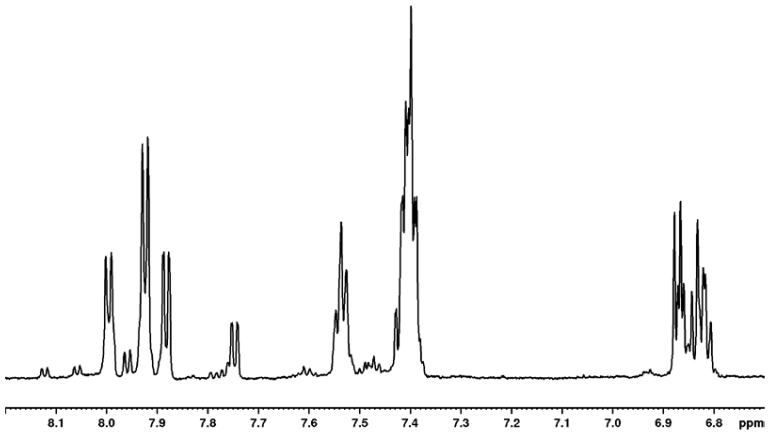

Figure A.11-4 Compound **11**, 1D NOESY spectrum (700 MHz, MeOH-d_4, o1P = 4.92 ppm); region 8.2 to 6.7 ppm.

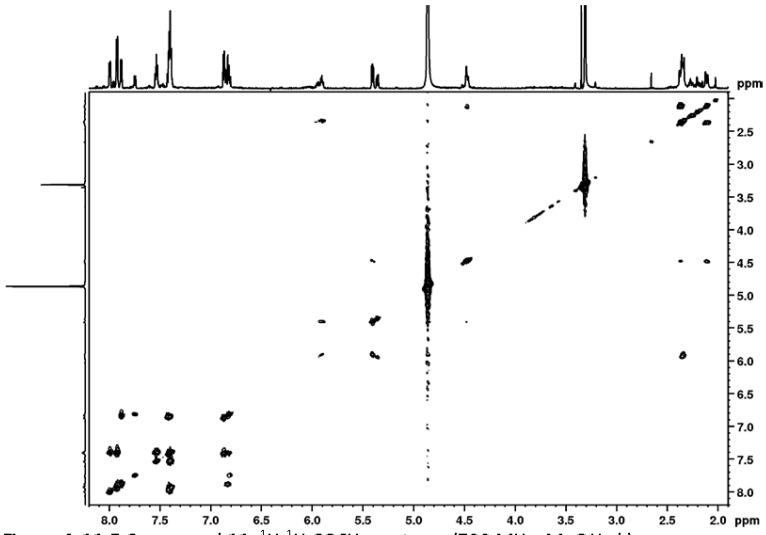

Figure A.11-5 Compound **11**, ^{1}H-^{1}H COSY spectrum (700 MHz, MeOH-d_4).

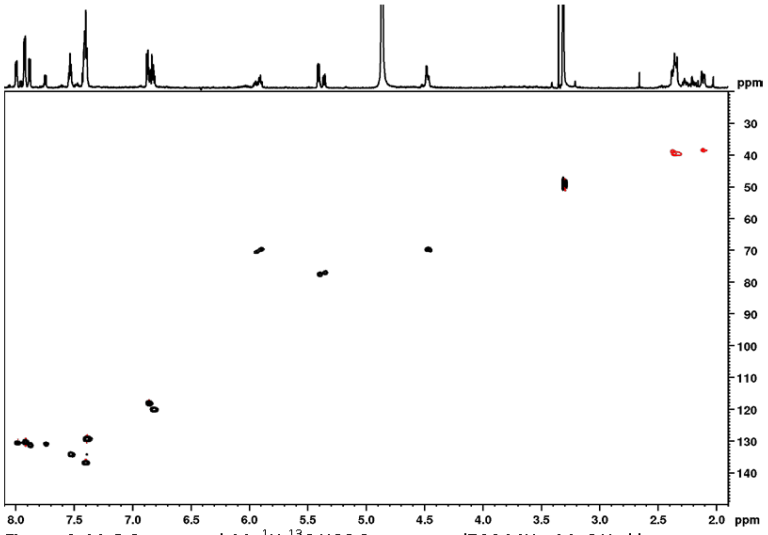

Figure A.11-6 Compound **11**, ^{1}H-^{13}C HSQC spectrum (700 MHz, MeOH-d_4).

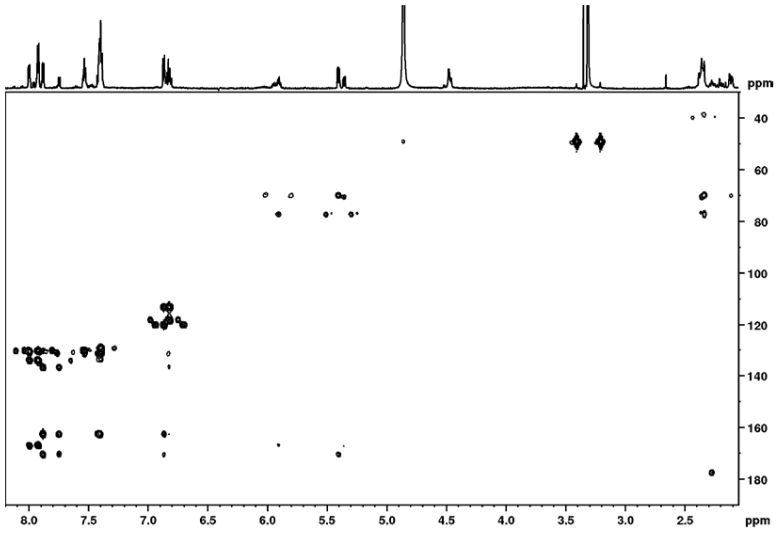

Figure A.11-7 Compound **11**, ^{1}H-^{13}C HMBC spectrum (700 MHz, MeOH-d_4).

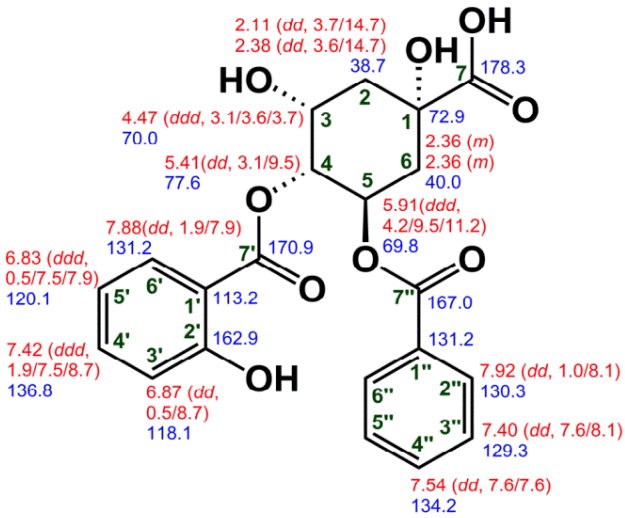

Figure A.11-8 Compound **11**, chemical structure with chemical shifts (MeOH-d_4).

A.12) Salicortin (12):

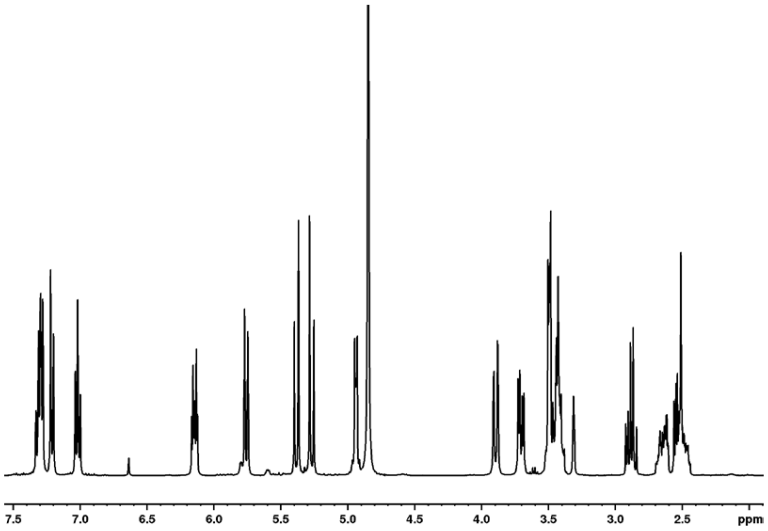

Figure A.12-1 Salicortin (**12**), ^{1}H NMR spectrum (400 MHz, MeOD-d_4).

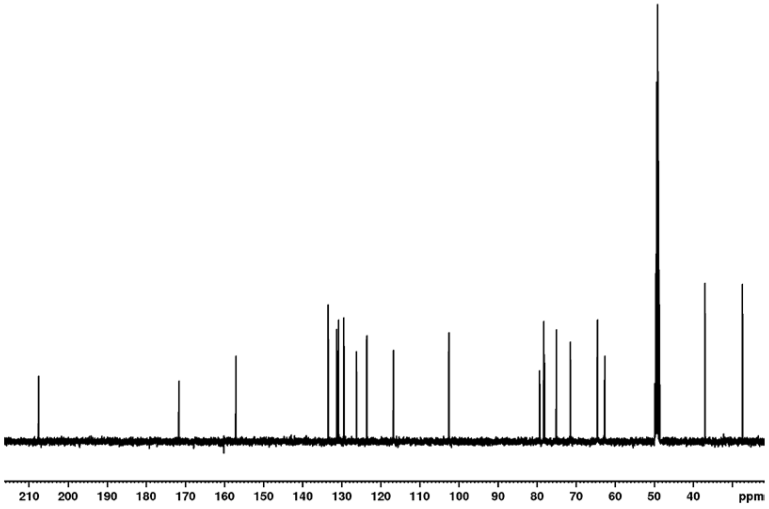

Figure A.12-2 Salicortin (**12**), ^{13}C NMR spectrum (100 MHz, MeOD-d_4).

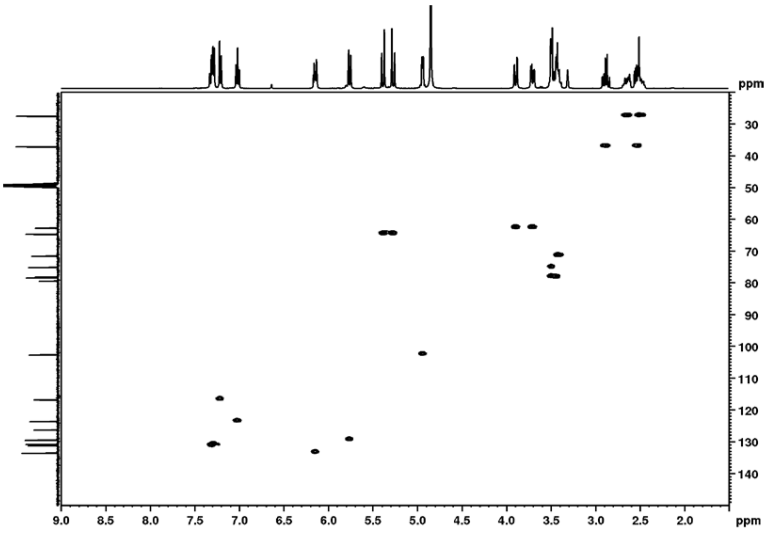

Figure A.12-3 Salicortin (**12**), ^{1}H-^{13}C HSQC spectrum (400 MHz, MeOD-d_4).

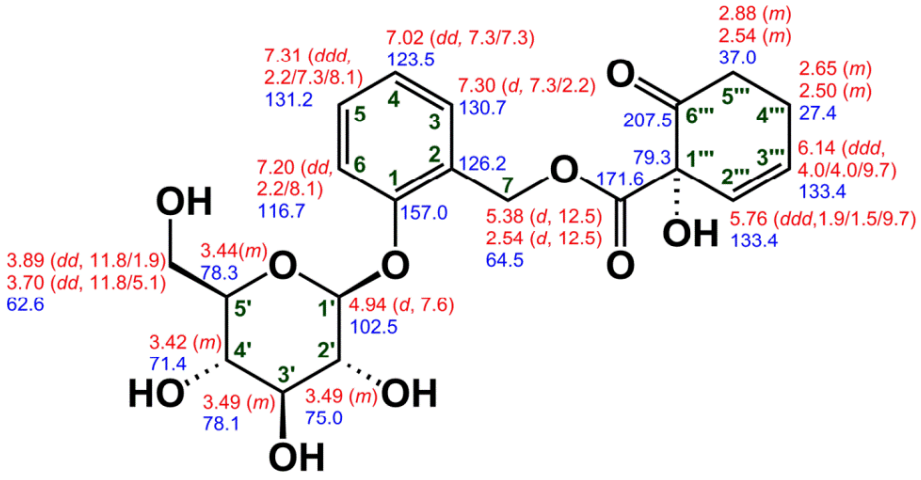

Figure A.12-4 Salicortin (**12**), chemical structure with chemical shifts (MeOH-d_4).

A.13) Quinic acid (13):

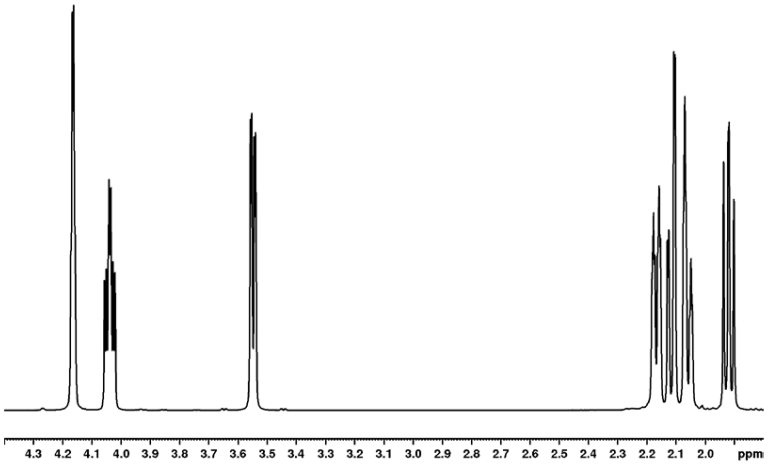

Figure A.13-1 Quinic acid (**13**), ^{1}H NMR spectrum (700 MHz, D_2O).

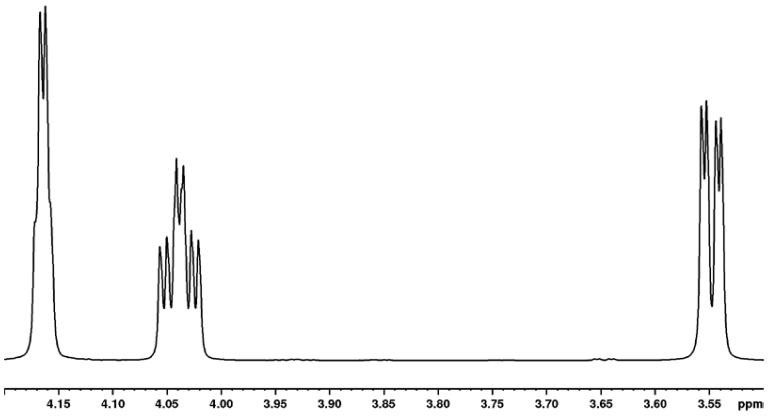

Figure A.13-2 Quinic acid (**13**), Partial ^{1}H NMR spectrum (700 MHz, D_2O); region 3.5 to 4.2 ppm.

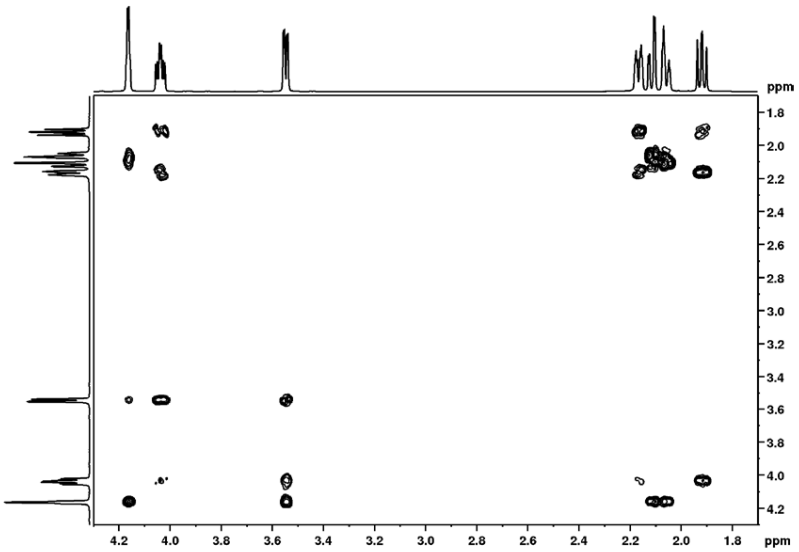

Figure A.13-3 Quinic acid (**13**), ^{1}H-^{1}H COSY spectrum (700 MHz, D_2O).

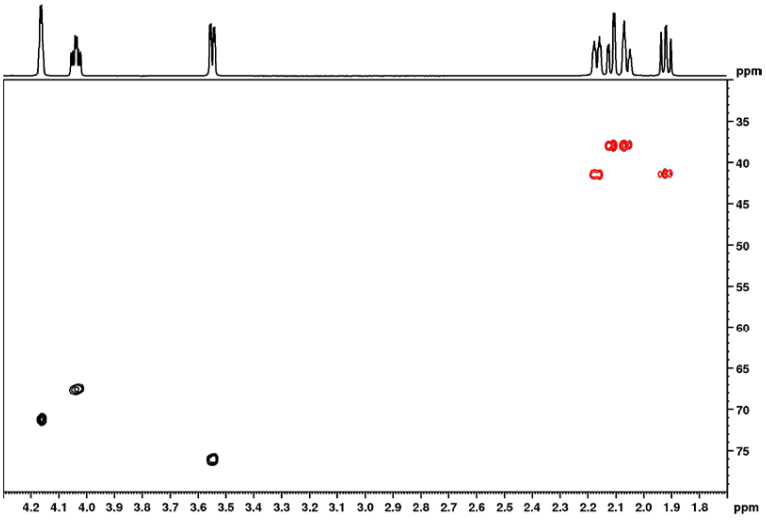

Figure A.13-4 Quinic acid (**13**), ^{1}H-^{13}C HSQC spectrum (700 MHz, D_2O).

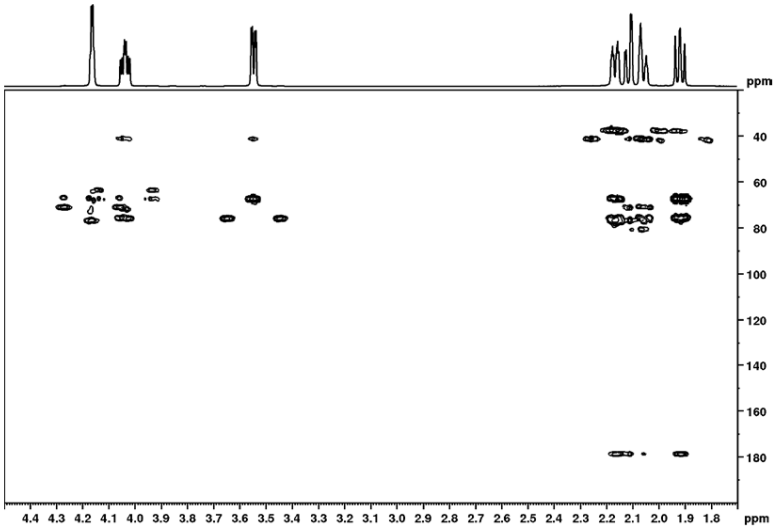

Figure A.13-5 Quinic acid (**13**), ^{1}H-^{13}C HMBC spectrum (700 MHz, D_2O).

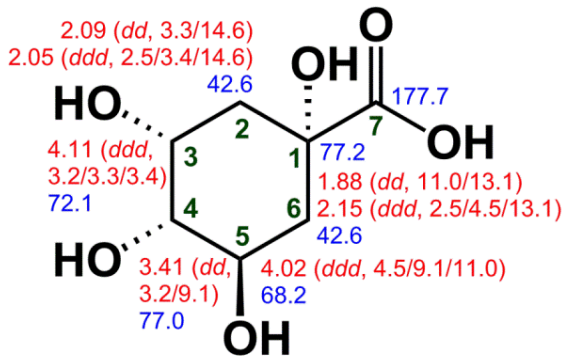

Figure A.13-6 Quinic acid (**13**), chemical structure with chemical shifts (D_2O).

C

B) *In vivo* ^{13}C-labeling of salicortin (12)

B.1) Growth enclosure – Labeling process

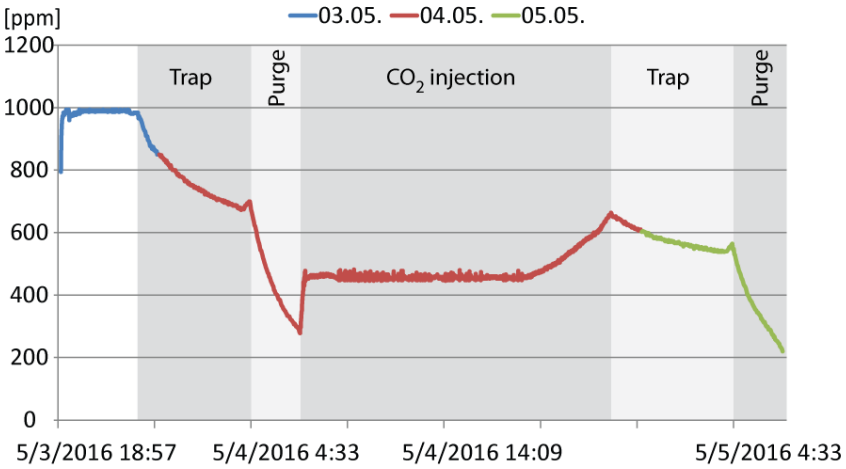

Figure B.1-1 CO_2-curve [in ppm] of the 1st (blue), 2nd (red) and 3rd (green) experimental day.

- The highlighted areas represent different daily modes of action of the labeling setup:
  Purge (4:30-7:00) – strong CO_2 scrubbing with soda lime
  Trap (22:30-4:15) – weak CO_2 scrubbing and trapping with saturated $Ba(OH)_2$ solution
  CO_2 injection (7:00-22:00) –automatized pulse-labeling with $^{13}CO_2$ gas from lecture bottle
- The CO_2 level was set to 450 ppm. The CO_2-IR sensor probe did not discriminate between $^{12}CO_2$ and $^{13}CO_2$. Therefore the CO_2-value was corrected by use of the isotope ratio factor for $^{13}CO_2$:$^{12}CO_2$:

  Gas bottle with a $^{13}CO_2$ conc. of 380 ppm and constant volume flow gave a mean signal of 57.09 ppm, yielding an isotope factor of 6.7:1 {$^{12}CO_2$:$^{13}CO_2$}.
- $^{13}CO_2$ bottles were empty at day 12 and 19 and therefore exchanged for full bottles (see Fig. B.1-2).
- During the night between day 21 and 22, leaf samples were taken in order to distinguish the ^{13}C-enrichment (see B.2).
- Last bottle was emptied at early evening of day 25. Afterwards plants were kept in the chamber for further 3 days in order to consume the remaining $^{13}CO_2$.

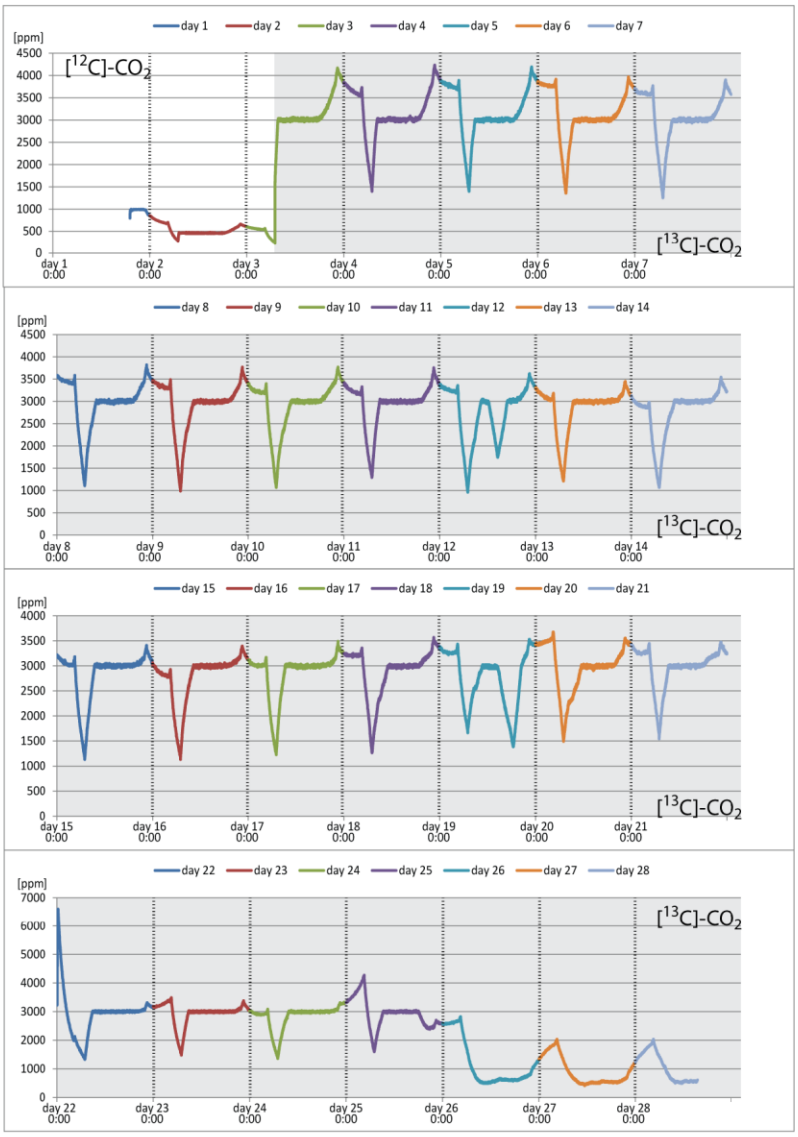

Figure B.1-2 Overall CO_2-curve [in ppm] of the $^{13}CO_2$ labeling experiment.

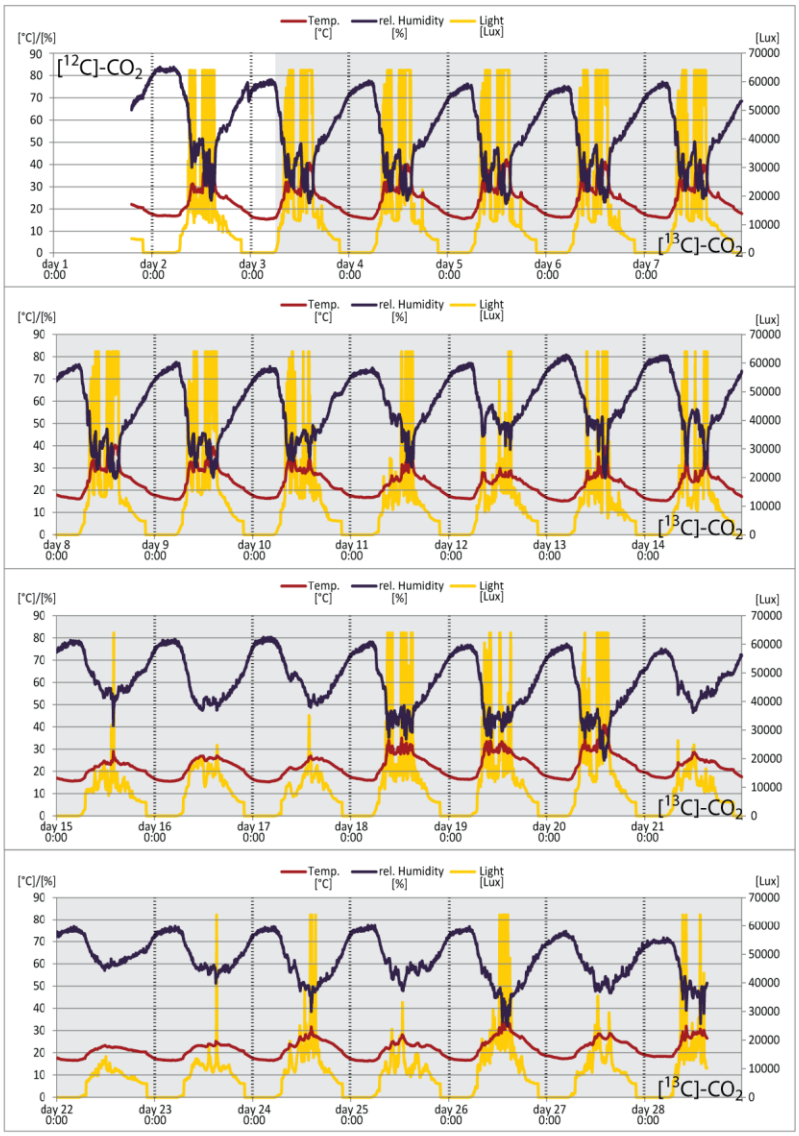

Figure B.1-3 Overall temperature [°C], rel. humidity [%] and light-curve [Lux] of the $^{13}CO_2$ feeding experiment.

Figure B.1-4 Pictures of the automated growth enclosure for stable isotope $^{13}CO_2$ labeling experiments.

Left – Enclosure located in the greenhouse of the MPI-CE during $^{13}CO_2$ labeling of *P. beaupré*.
Right – The chamber is equipped with six specimen of *P. beaupré* during the labeling experiment.

B.2) Characterization of in vivo generated [U-^{13}C]salicortin

In order to investigate the ^{13}C enrichment, leaf samples of old (source) and young, newly grown (sink) leaf tissue were collected during the night between days 21 and 22, lyophilized and balanced, yielding 42.58 mg (source) and 45.02 mg (sink) dried material. Afterwards, the samples were transferred into homogenizer vials (2 mL) with ZrO_2 beats (1.4 mm, 700 mg), homogenized 3 times (60 sec; 5000 rpm; 15 sec breaks) with 70% MeOH (1 mL) and subsequently centrifuged (10 min, 13200 rcf). The supernatant was collected and transferred to LC-MS (10 µL injection) and NMR.

HPLC-ESI-MS was performed on an Agilent 1100 HPLC system, consisting of a degasser, quaternary solvent delivery pump G1311A, an autosampler G1313A (Agilent Technologies, Waldbronn, Germany), a photodiode array detector (detection 200-700 nm; J&M Analytik, Aalen, Germany) and an Esquire 3000 ion trap mass spectrometer (Bruker Daltonik, Bremen, Germany). An Isis RP-18e column (250 x 4.6 mm, 5 µm particle size) (Macherey-Nagel, Düren, Germany) was used for separation. Column temperature was set to 35 °C, and the solvent flow rate was 0.8 mL min^{-1} using 0.1% formic acid in water and 0.1% formic acid in MeOH as binary solvent system. An HPLC gradient was used starting with a 5 min isocratic flow of 100% H_2O, and then decreasing linearly for 5 min to 85%, 25 min to 70% and finally 50 min to

50% H_2O. Afterwards, the column was washed for 10 min with 100% MeOH and equilibrated for 10 min with 100% H_2O.

NMR spectra were recorded on a Bruker Avance III HD 400 MHz spectrometer equipped with a 5 mm BBFO probe (Bruker Biospin, Rheinstetten, Germany). NMR tubes of 5 mm outer diameter were used for measurements.

Identification and characterization was done by means of ^{1}H, ^{13}C and ^{1}H-^{13}C NMR (Fig. B.2-6 to B.2-8) and ESI-MS in comparison to spectra of an unlabeled reference (B.2-1 to B.2-5). The ^{1}H-^{13}C HSQC was in accordance with the spectrum of the reference, confirming its identity as salicortin (**12**, spectra see A.12). Furthermore, as a result of spin-spin coupling between adjacent ^{13}C atoms, the ^{13}C NMR spectrum showed multiplet signal structures for every carbon resonance in the molecule (Schneider, 2007; Schneider et al., 2003) (Fig. B.2-9). These characteristic multiplets indicated uniform ^{13}C-incorporation into the molecule. That observation was confirmed by the ^{1}H NMR spectra, which also showed numerous satellites for all signals resulting from ^{1}H-^{13}C spin-spin couplings.

The mass spectra obtained from extracts of young leaf tissues displayed peaks corresponding to the salicortin isotopologues of *m/z* 423 to 444 (Table B.2-1). An average ^{13}C enrichment of 82% (R^2 = 0.994) was calculated based on the comparison of theoretical and experimental MS data, according to a method previously described (Taubert et al., 2011). Accordingly, the isotopologue patterns of characteristic salicortin fragments, generated by in-source fragmentation, were extracted from the mass spectra (Table B.2-2) and used to determine the ^{13}C enrichment of the different parts of the molecule. The calculation yielded an average ^{13}C enrichment of 82% for the glucose (*m/z* 161 $[M\text{-}262\text{-}H]^-$; R^2 = 0.987) as well as the 1-hydroxy-6-oxocyclohex-2-en-1-oyl (HCH) fragment (*m/z* 111 $[M\text{-}312\text{-}H]^-$; R^2 = 0.952) and 81% for the salicin fragment (*m/z* 285 $[M\text{-}138\text{-}H]^-$; R^2 = 0.947).

The salicortin mass spectrum from the extract of old leaves, however, also showed an isotopologue pattern which reached from *m/z* 423 to 443. Unlike the molecular ion peaks in the spectra of young plant tissue, the molecular ion peak *m/z* 423 $[M\text{-}H]^-$ is the by far most intense signal in the mass spectrum of old leaves (Table B.2-1). Furthermore, the signal intensity of the ^{13}C-enriched isotopologues appeared to be notably weak, which assumed that only a minor amount of $^{13}CO_2$ had been incorporated. The calculation of ^{13}C-enrichment yielded 1.1% (R^2 = 0.989), confirming that assumption.

References:

Schneider, B., 2007. Nuclear magnetic resonance spectroscopy in biosynthetic studies. Prog. Nucl. Magn. Reson. Spectrosc. 51, 155-198.

Schneider, B., Gershenzon, J., Graser, G., Hölscher, D., Schmitt, B., 2003. One-dimensional ^{13}C NMR and HPLC-^{1}H NMR techniques for observing carbon-13 and deuterium labelling in biosynthetic studies. Phytochem. Rev. 2, 31-43.

Taubert, M., Jehmlich, N., Vogt, C., Richnow, H.H., Schmidt, F., von Bergen, M., Seifert, J., 2011. Time resolved protein-based stable isotope probing (Protein-SIP) analysis allows quantification of induced proteins in substrate shift experiments. Proteomics 11, 2265-2274.

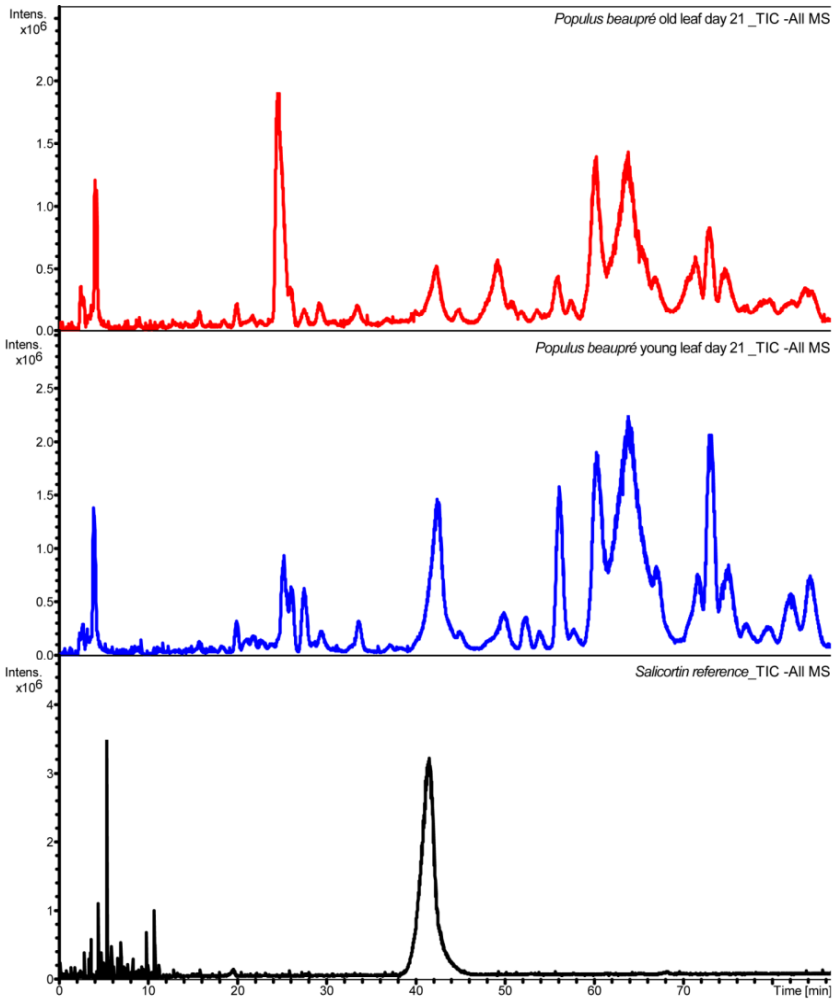

Figure B.2-1 Stacked TIC spectra of young (blue) and old (red) leaf sample extracts of *P. beaupré* in comparison with a salicortin (**12**) reference (black).

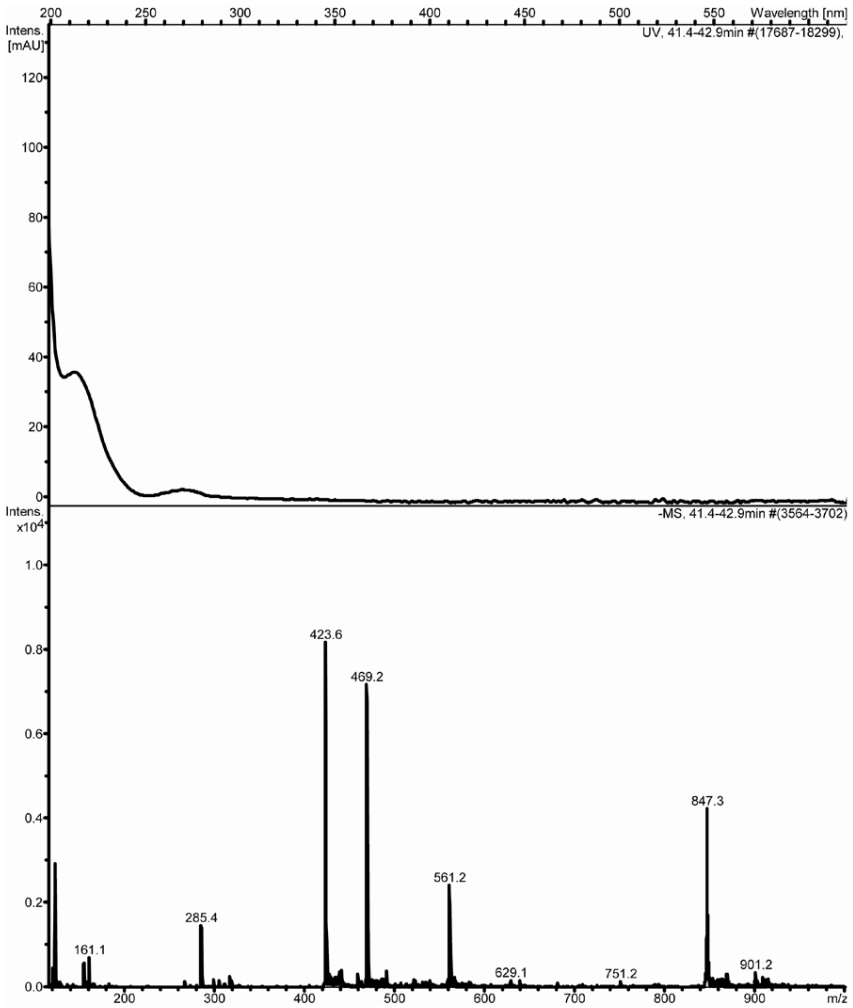

Figure B.2-2 UV spectrum (top) and ESI ion trap mass spectrum (bottom) of salicortin (**12**) (*m/z* 423.6 $[M-H]^-$, $^{12}C_{20}H_{23}O_{10}$) in the old leaf sample.

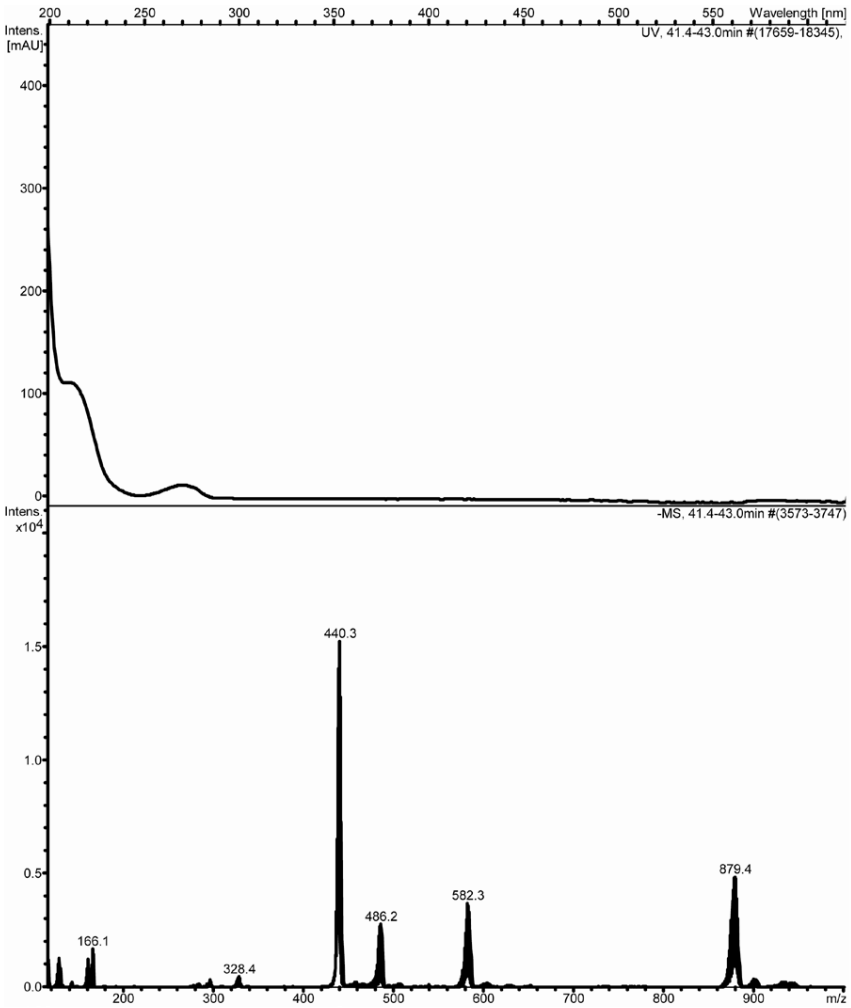

Figure B.2-3 UV spectrum (top) and ESI ion trap mass spectrum (bottom) of salicortin (**12**) (*m/z* 440.3 $[M-H]^-$, $^{13}C_{17}{}^{12}C_3H_{23}O_{10}$) in the young leaf sample.

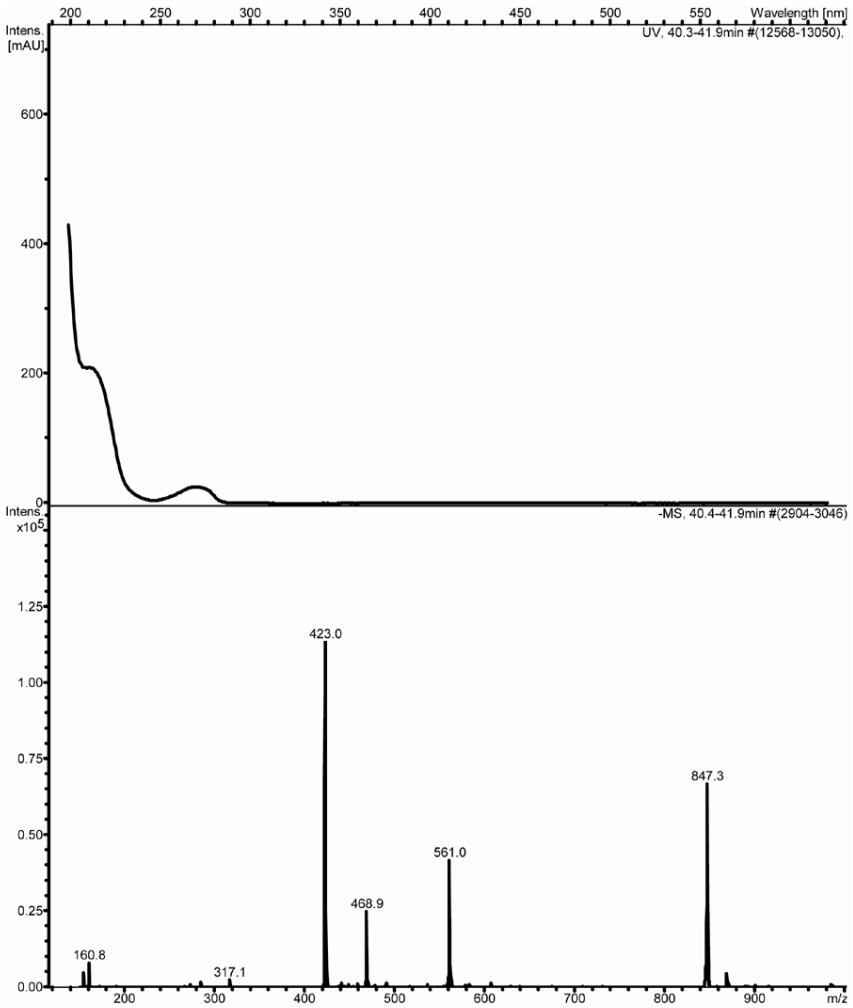

Figure B.2-4 UV spectrum (top) and ESI ion trap mass spectrum (bottom) of the salicortin (**12**) reference (*m/z* 423.6 $[M-H]^-$, $^{12}C_{20}H_{23}O_{10}$).

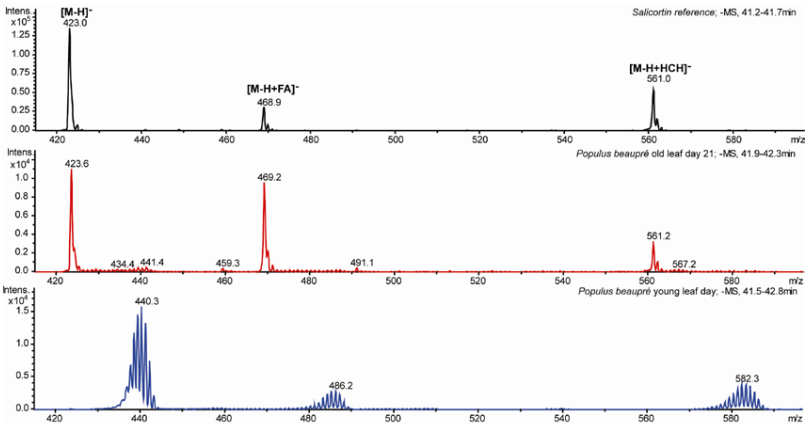

Figure B.2-5 Stacked mass spectra of salicortin (**12**) from young (blue) and old (red) leaf sample extract in comparison with a salicortin (**12**) reference (black). The mass range from *m/z* 420 to 600 is displayed.

Table B.2-1 Extracted MS data which were used for the calculation of the ^{13}C-enrichment of the salicortin isotopologues (*m/z*) together with their signal intensity and their signal-to-noise ratio (S/N). Only signals of S/N > 2 were extracted. *Italic* values were artificially added for the calculation.

C-isotope		Salicortin in old leaves				Salicortin in young leaves		
^{12}C	^{13}C	*m/z*	intensity	S/N		*m/z*	intensity	S/N
20	0	423.6	10223	468.9		*423.0*	*0*	-
19	1	424.4	2321	106.5		*424.0*	*0*	-
18	2	425.4	611	28.0		*425.0*	*0*	-
17	3	426.3	191	8.8		*426.0*	*0*	-
16	4	427.3	227	10.4		*427.0*	*0*	-
15	5	428.4	237	10.9		*428.0*	*0*	-
14	6	429.4	243	11.2		*429.0*	*0*	-
13	7	430.4	202	9.3		430.6	109	2.1
12	8	431.4	137	6.3		431.7	139	2.7
11	9	432.4	152	7.0		432.5	194	3.7
10	10	433.4	208	9.5		433.7	335	6.4
9	11	434.4	270	12.4		435.0	654	12.5
8	12	435.4	233	10.7		435.9	1420	27.2
7	13	436.4	259	11.9		436.9	3370	64.5
6	14	437.4	244	11.2		437.8	6567	125.7
5	15	438.4	341	15.7		438.6	11446	219.0
4	16	439.4	433	19.8		439.4	14074	269.3
3	17	440.4	381	17.5		440.3	15363	294.0
2	18	441.4	447	20.5		441.3	12920	247.2
1	19	442.4	196	9.0		442.3	7304	139.8
0	20	443.4	106	4.9		443.3	2079	39.8

CX

Table B.2-2 Isotopologue patterns (*m/z*) observed for the fragment ions of labeled salicortin (**12**). MS data were used to calculate the ^{13}C-enrichment. Only signals of S/N > 1 were extracted from the mass spectra. *Italic* values were artificially added for the calculation. Values marked with (*) resulted from overlapping signals and were assumed as zero for calculation.

	HCH fragment ion			glucose fragment ion			salicin fragment ion		
	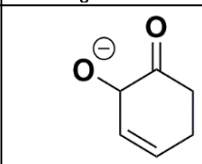 Chemical Formula: $C_6H_7O_2^-$ Exact Mass: 111.05			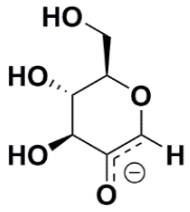 Chemical Formula: $C_6H_9O_5^-$ Exact Mass: 161.05			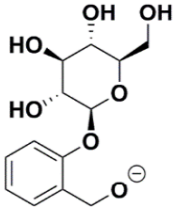 Chemical Formula: $C_{13}H_{17}O_7^-$ Exact Mass: 285.10		
	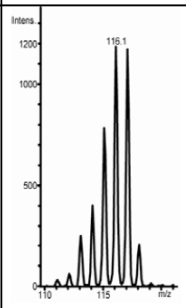			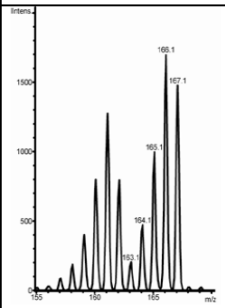			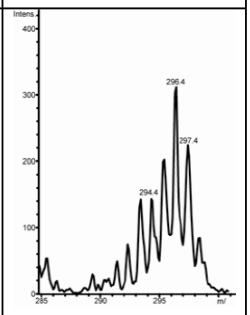		
^{13}C	*m/z*	intensity	S/N	*m/z*	intensity	S/N	*m/z*	intensity	S/N
0	111	*0*	-	161.1	(1274)*	(24.7)*	285	*0*	-
1	112.1	63	1.2	162.1	(797)*	(15.5)*	286	*0*	-
2	113.1	254	4.9	163.1	206	4.0	287	*0*	-
3	114.1	404	7.8	164.1	473	9.2	288	*0*	-
4	115.1	785	15.2	165.1	1000	19.4	289	*0*	-
5	116.1	1184	23.0	166.1	1701	33.0	290	*0*	-
6	117.1	1175	22.8	167.1	1479	28.7	291	*0*	-
7							292.3	75	1.5
8							293.4	143	2.8
9							294.4	144	2.8
10							295.4	202	3.9
11							296.4	313	6.1
12							297.4	224	4.3
13							298.3	85	1.7

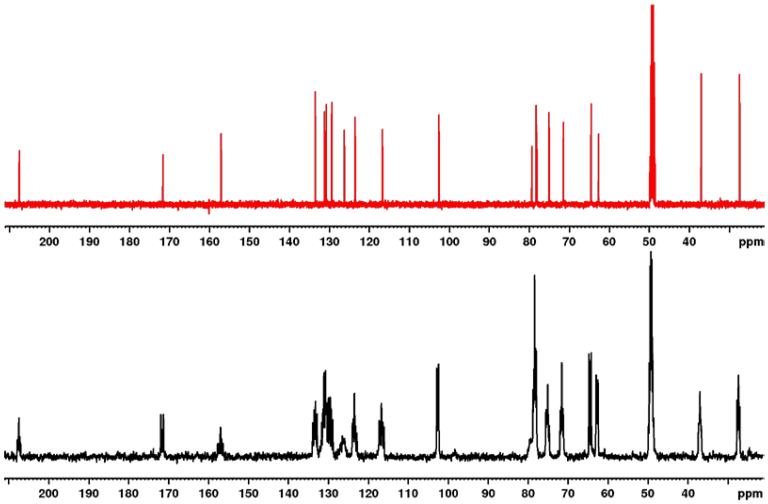

Figure B.2-6 ^{13}C NMR spectra (100 MHz, MeOH-d_4) of salicortin (**12**) isolated from young leaf tissue of the ^{13}C- enriched *P. beaupré* plants (black) and the reference (red).

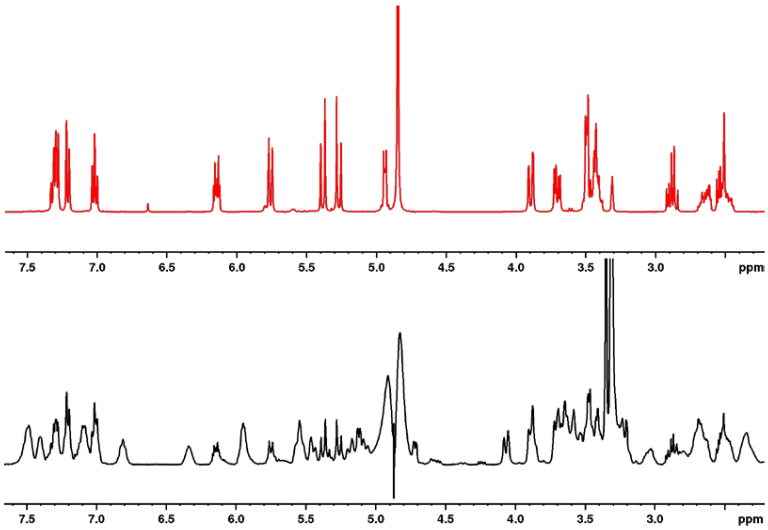

Figure B.2-7 ^{1}H NMR spectra (400 MHz, MeOH-d_4) of salicortin (**12**) isolated from young leaf tissue of the ^{13}C- enriched *P. beaupré* plants (black; with water suppression o1p = 4.887 ppm) and the reference (red).

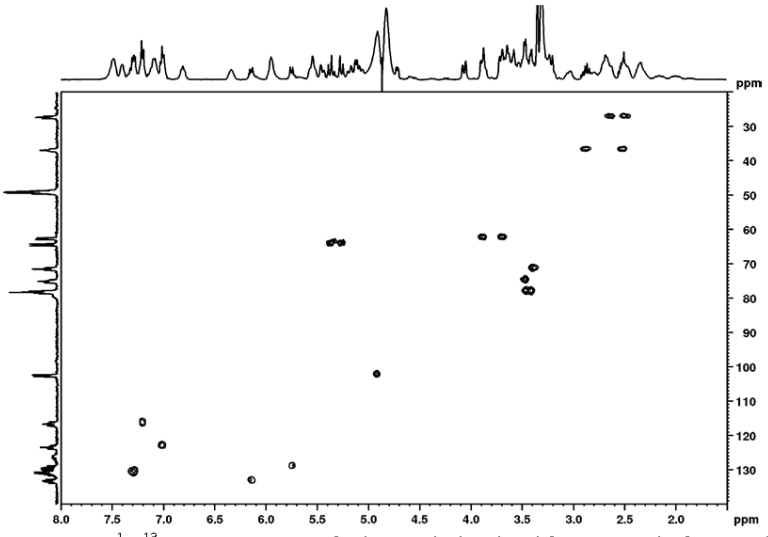

Figure B.2-8 ^{1}H-^{13}C HSQC spectrum of salicortin (**12**) isolated from young leaf tissue of the ^{13}C-enriched *P. beaupré* plants.

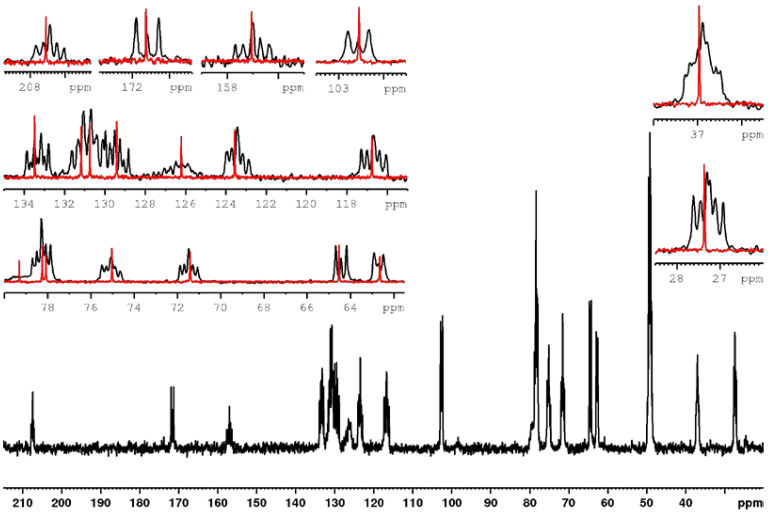

Figure B.2-9 ^{13}C NMR spectrum (100 MHz, MeOH-d_4) of salicortin (**12**) isolated from young leaf tissue of the ^{13}C-enriched *Populus beaupré* plants (black). The inserts show multiplets, which result from ^{13}C-^{13}C spin-spin coupling (black), in comparison to the singlet signals of the unlabeled reference (red).

C) [U-^{13}C]Salicortin *C. vinula* larvae feeding

C.1) Experimental setup

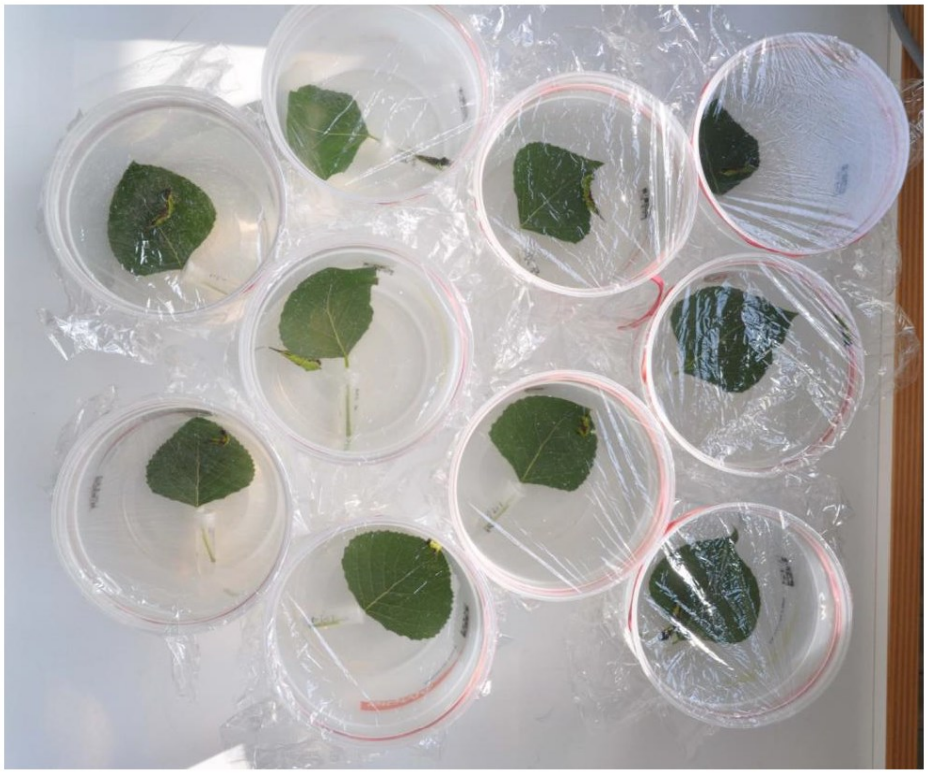

Figure C.1-1 Arena setups including coated leaves and *C. vinula* larvae

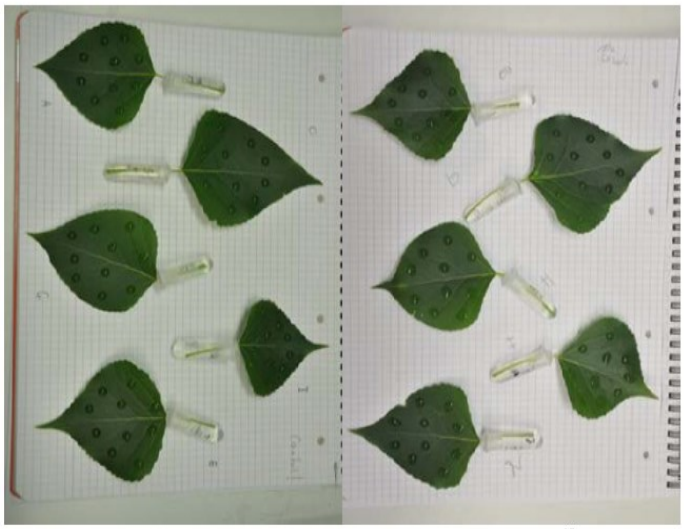

Figure C.1-2 Leaves of *P. beaupré* coated with H_2O (left) and [U-^{13}C]salicortin solution (right).

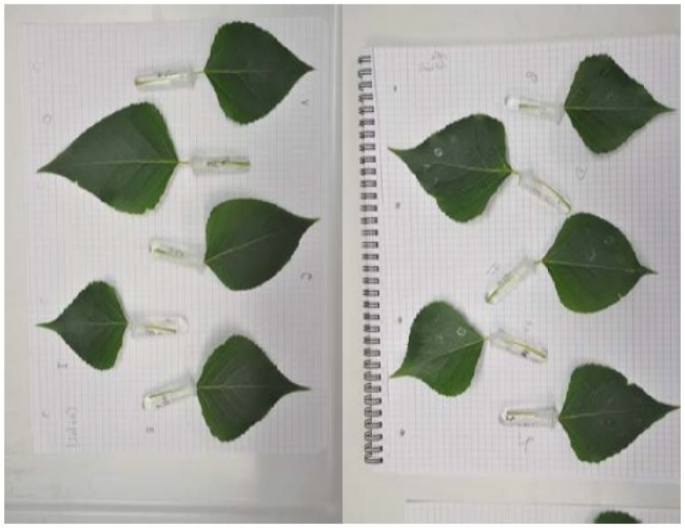

Figure C.1-3 Leaves of *P. beaupré* coated with H_2O (left) and [U-^{13}C]salicortin solution (right) after drying.

C.2) NMR spectra

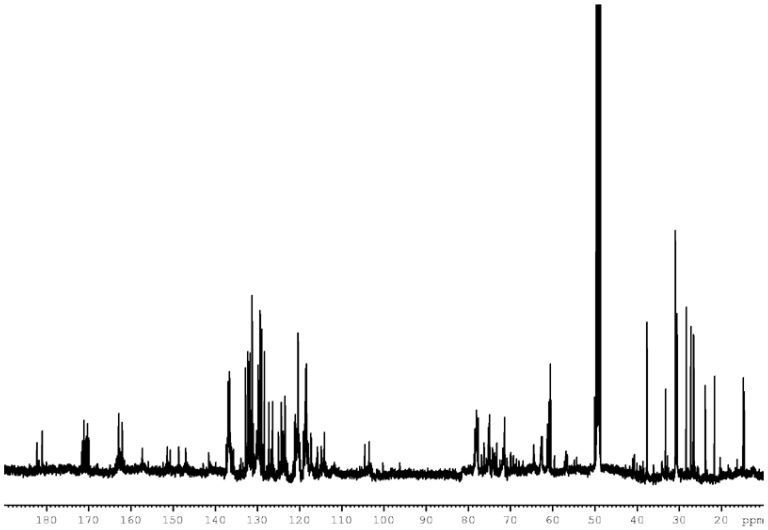

Figure C.2-1 ^{13}C NMR spectrum (125 MHz; MeOH-d_4; 20k scans) of feces from *C. vinula* which fed on *P. nigra* diet supplemented with [U-^{13}C]salicortin.

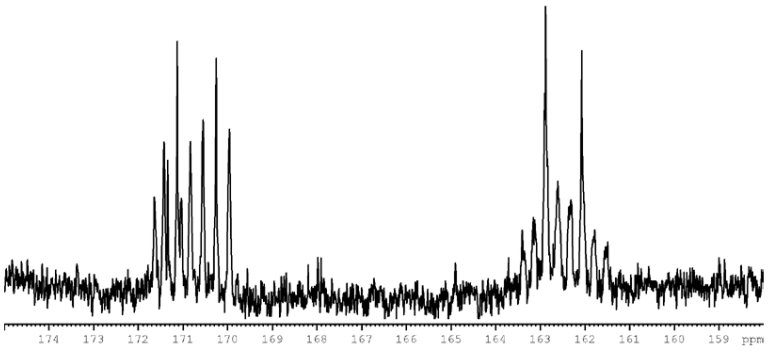

Figure C.2-2 Partial ^{13}C NMR spectrum (125 MHz; MeOH-d_4; 20k scans; 155-175 ppm) of feces from *C. vinula* which fed on *P. nigra* diet supplemented with [U-^{13}C]salicortin.

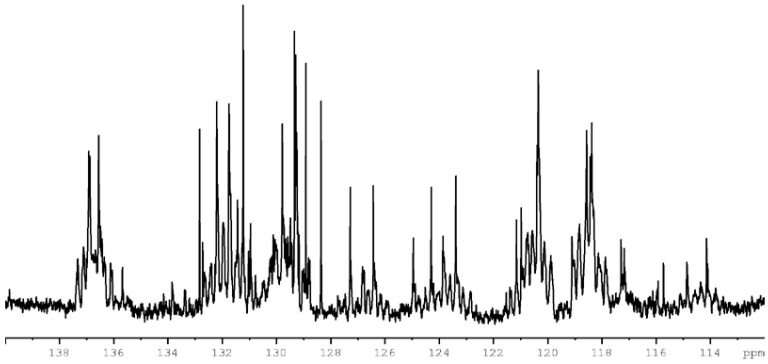

Figure C.2-3 Partial ^{13}C NMR spectrum (125 MHz; MeOH-d_4; 20k scans; 110-140 ppm) of feces from *C. vinula* which fed on *P. nigra* diet supplemented with [U-^{13}C]salicortin.

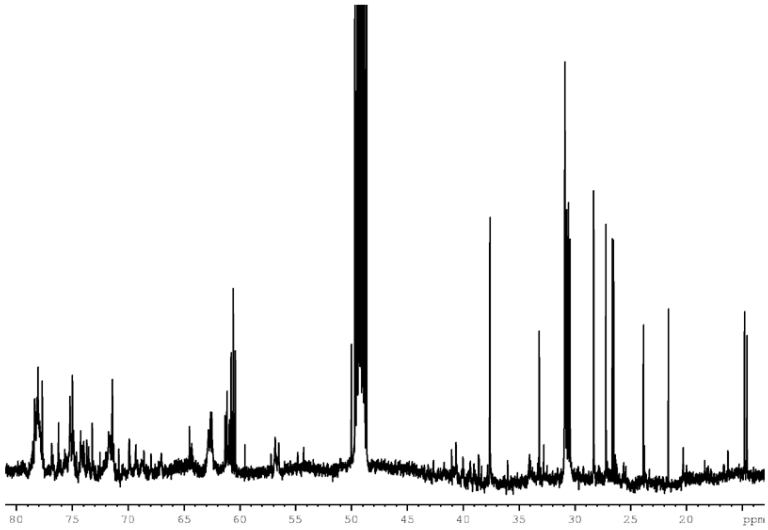

Figure C.2-4 Partial ^{13}C NMR spectrum (125 MHz; MeOH-d_4; 20k scans; 1-80 ppm) of feces from *C. vinula* which fed on *P. nigra* diet supplemented with [U-^{13}C]salicortin.

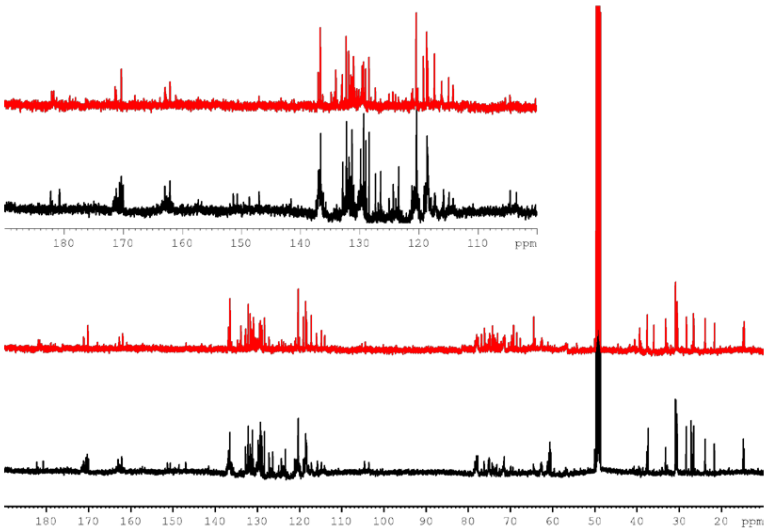

Figure C.2-5 ^{13}C NMR spectra (125 MHz; MeOH-d_4; 6k scans; 10-190 ppm) of feces from *C. vinula* which fed on *P. nigra* diet supplemented with [U-^{13}C]salicortin (black) and the control leaves (red). The insert shows the partial spectra between 100 and 190 ppm.

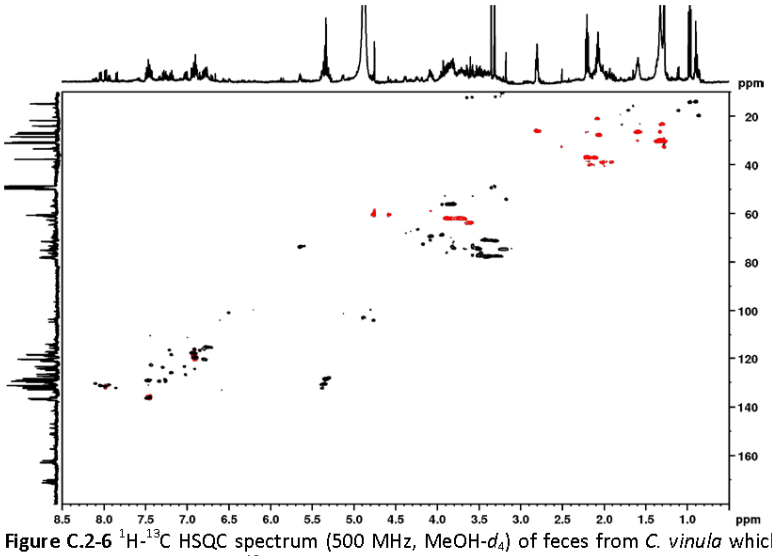

Figure C.2-6 ^{1}H-^{13}C HSQC spectrum (500 MHz, MeOH-d_4) of feces from *C. vinula* which fed on *P. nigra* diet supplemented with [U-^{13}C]salicortin.

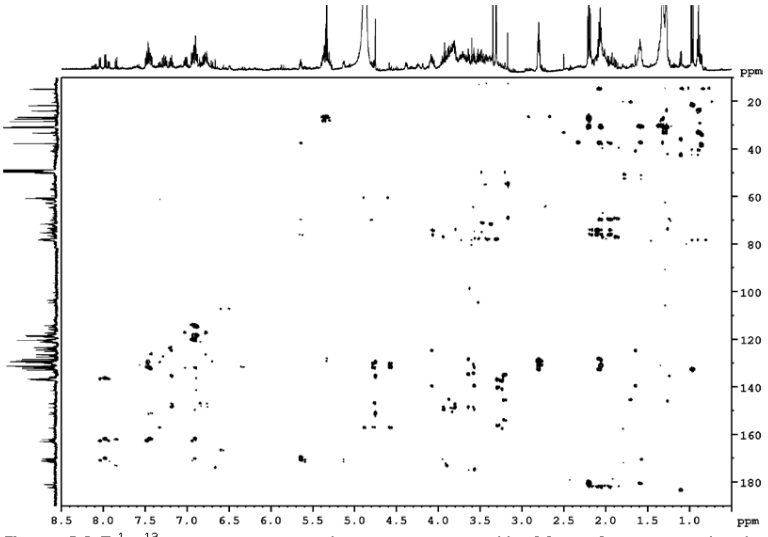

Figure C.2-7 ^{1}H-^{13}C HMBC spectrum (500 MHz, MeOH-d_4) of feces from *C. vinula* which fed on *P. nigra* diet supplemented with [U-^{13}C]salicortin.

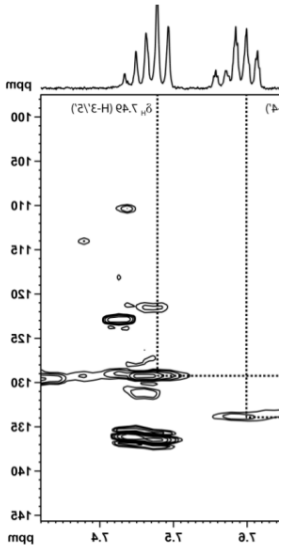

Figure C.2-8 ^{1}H-^{13}C HSQC spectrum (500 MHz, MeOH-d_4) with selective 1D TOCSY spectrum (top) (500 MHz, MeOH-d_4; o1p= 8.13 ppm with 16 Hz) and ^{13}C NMR spectrum (left) (125 MHz).

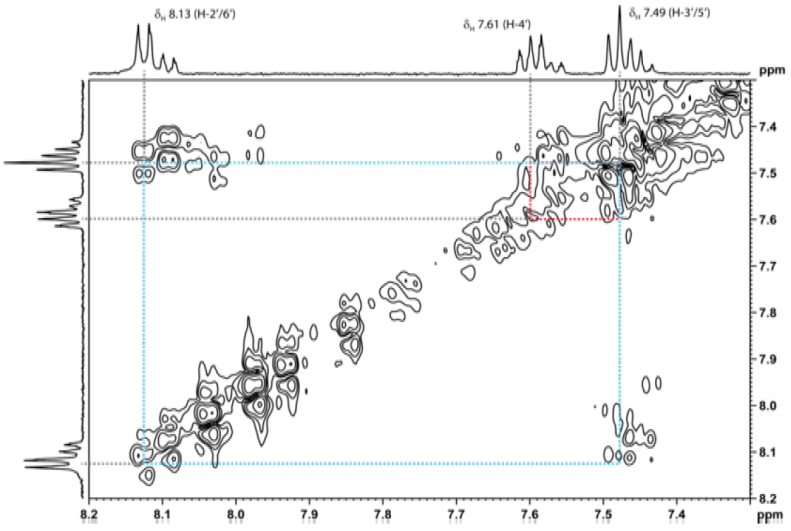

Figure C.2-9 ^{1}H-^{1}H COSY (500 MHz, MeOH-d_4) with selective 1D TOCSY spectrum (top and left) (500 MHz, MeOH-d_4; o1p= 8.13 ppm with 16 Hz).

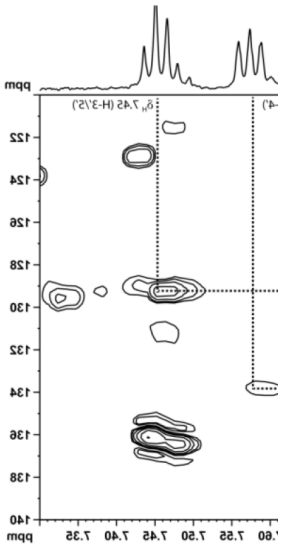

Figure C.2-10 ^{1}H-^{13}C HSQC spectrum (500 MHz, MeOH-d_4) with selective 1D TOCSY spectrum (top) (500 MHz, MeOH-d_4; o1p= 8.09 ppm with 16 Hz) and ^{13}C NMR spectrum (left) (125 MHz).

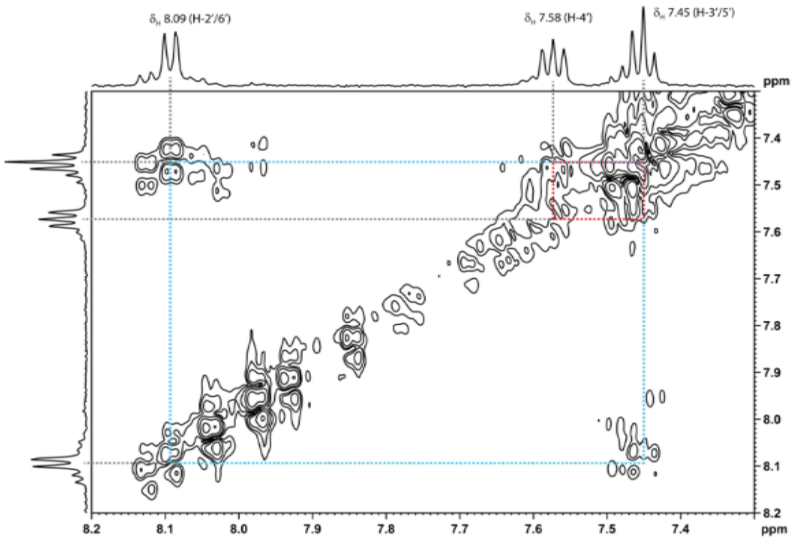

Figure C.2-11 ^{1}H-^{1}H COSY spectrum (500 MHz, MeOH-d_4) with selective 1D TOCSY spectrum (top and left) (500 MHz, MeOH-d_4; o1p= 8.09 ppm with 16 Hz).

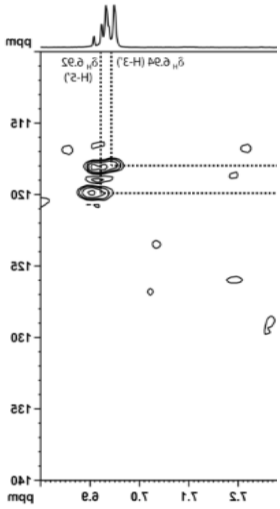

Figure C.2-12 ^{1}H-^{13}C HSQC spectrum (500 MHz, MeOH-d_4) with selective 1D TOCSY spectrum (top) (500 MHz, MeOH-d_4; o1p= 8.04 ppm with 16 Hz) and ^{13}C NMR spectrum (left) (125 MHz).

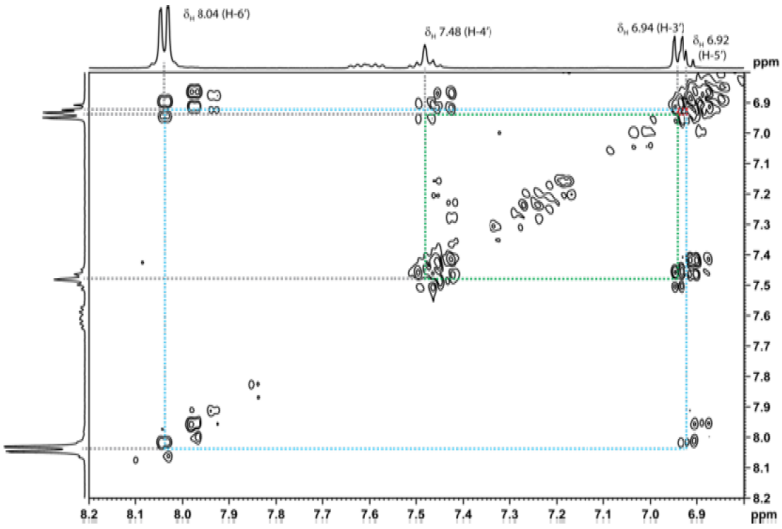

Figure C.2-13 ^{1}H-^{1}H COSY spectrum (500 MHz, MeOH-d_4) with selective 1D TOCSY spectrum (top and left) (500 MHz, MeOH-d_4; o1p= 8.04 ppm with 16 Hz).

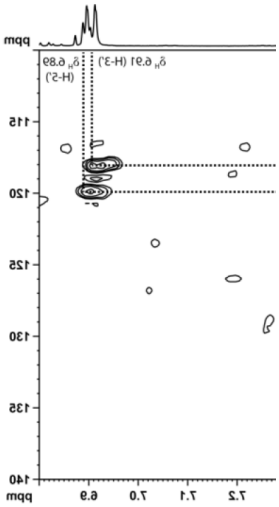

Figure C.2-14 ^{1}H-^{13}C HSQC spectrum (500 MHz, MeOH-d_4) with selective 1D TOCSY spectrum (top) (500 MHz, MeOH-d_4; o1p= 7.98 ppm with 16 Hz) and ^{13}C NMR spectrum (left) (125 MHz).

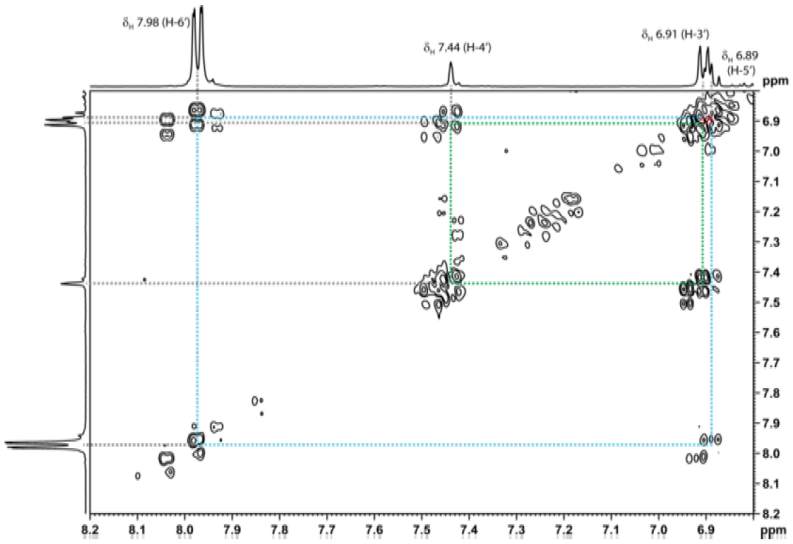

Figure C.2-15 ^{1}H-^{1}H COSY spectrum (500 MHz, MeOH-d_4) with selective 1D TOCSY spectrum (top and left) (500 MHz, MeOH-d_4; o1p= 7.98 ppm with 16 Hz).

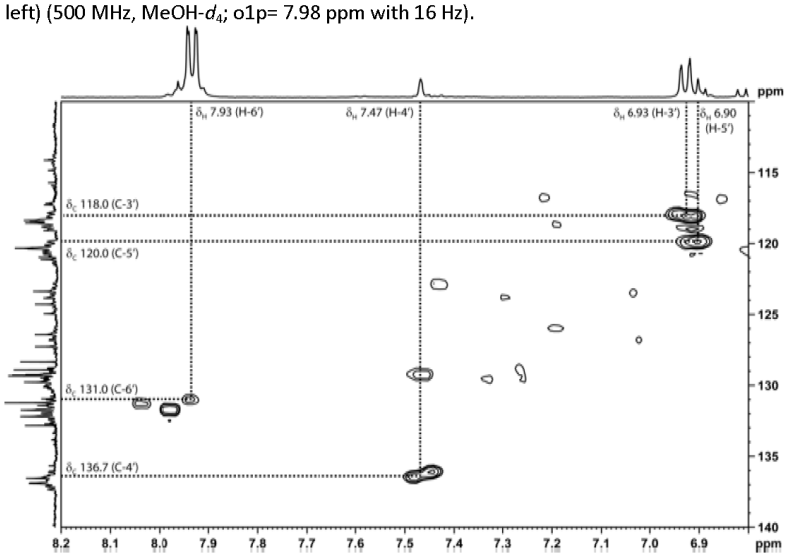

Figure C.2-16 ^{1}H-^{13}C HSQC spectrum (500 MHz, MeOH-d_4) with selective 1D TOCSY spectrum (top) (500 MHz, MeOH-d_4; o1p= 7.93 ppm with 16 Hz) and ^{13}C NMR spectrum (left) (125 MHz).

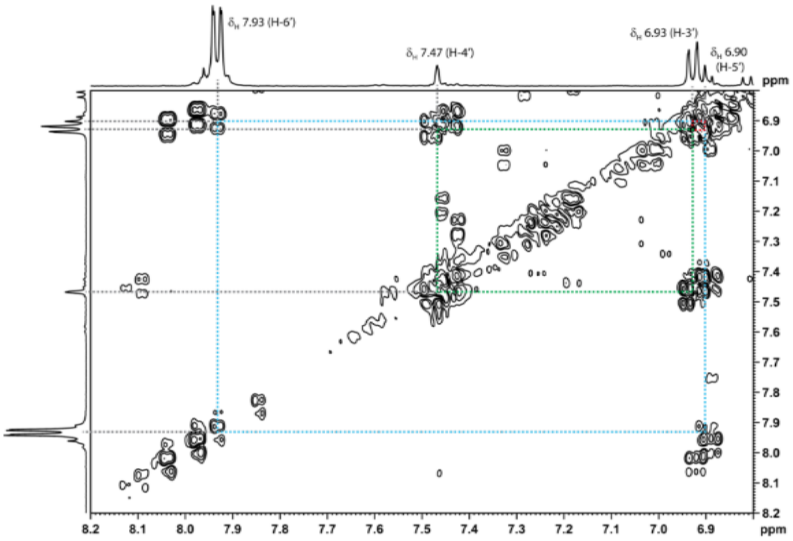

Figure C.2-17 ^{1}**H-**^{1}**H COSY spectrum (500 MHz, MeOD-**d_4**) with selective 1D TOCSY spectrum (top and left) (500 MHz, MeOH-**d_4**; o1p= 7.93 ppm with 16 Hz).**

C.3) HRESIMS spectra

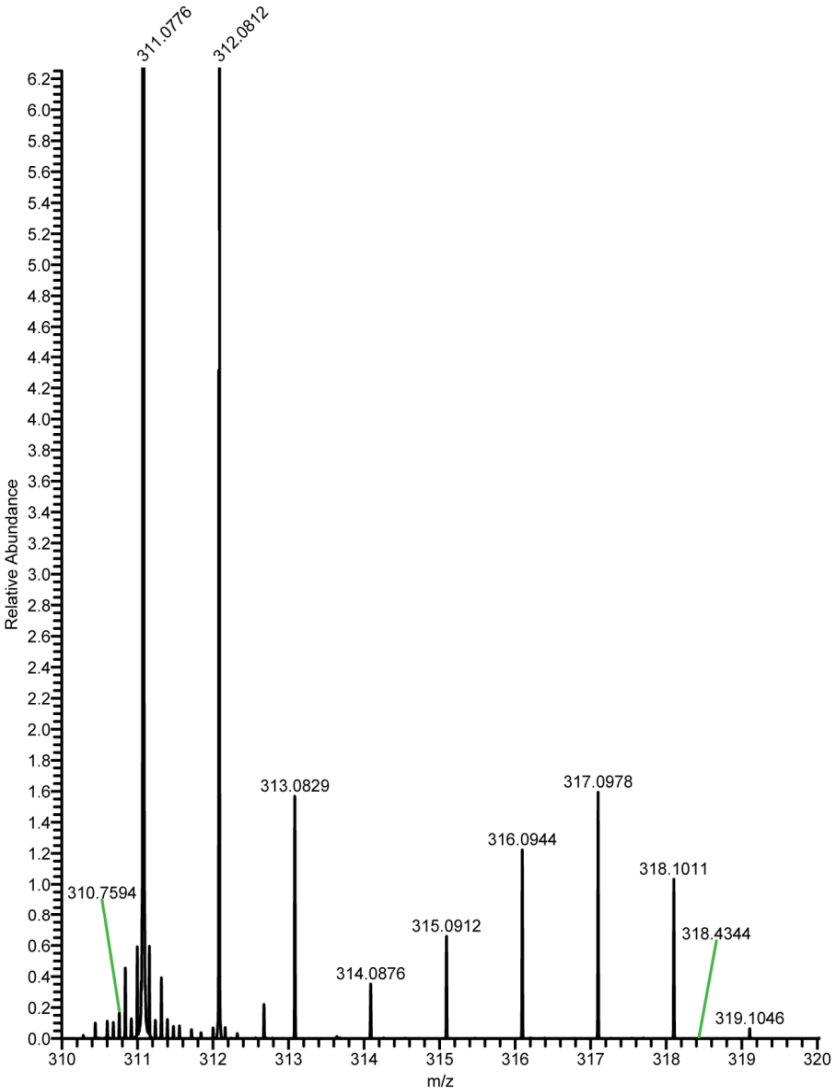

Figure C.3-1 Compound **1**; HRESIMS spectrum (*m/z* 311.0776 [M-H]⁻) of *C. vinula* feces after consumption of leaves labeled with [U-^{13}C]salicortin.

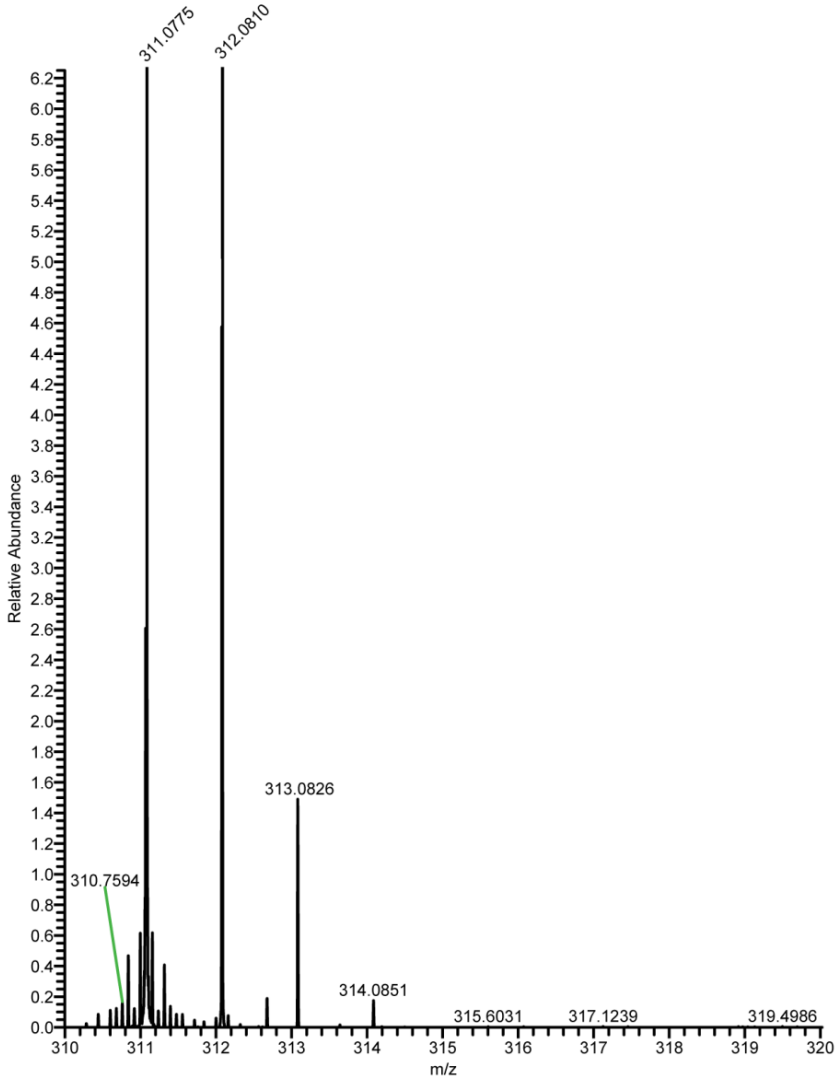

Figure C.3-2 Compound **1**; HRESIMS spectrum (*m/z* 311.0775 [M-H]$^-$) of *C. vinula* feces after consumption of control tissue.

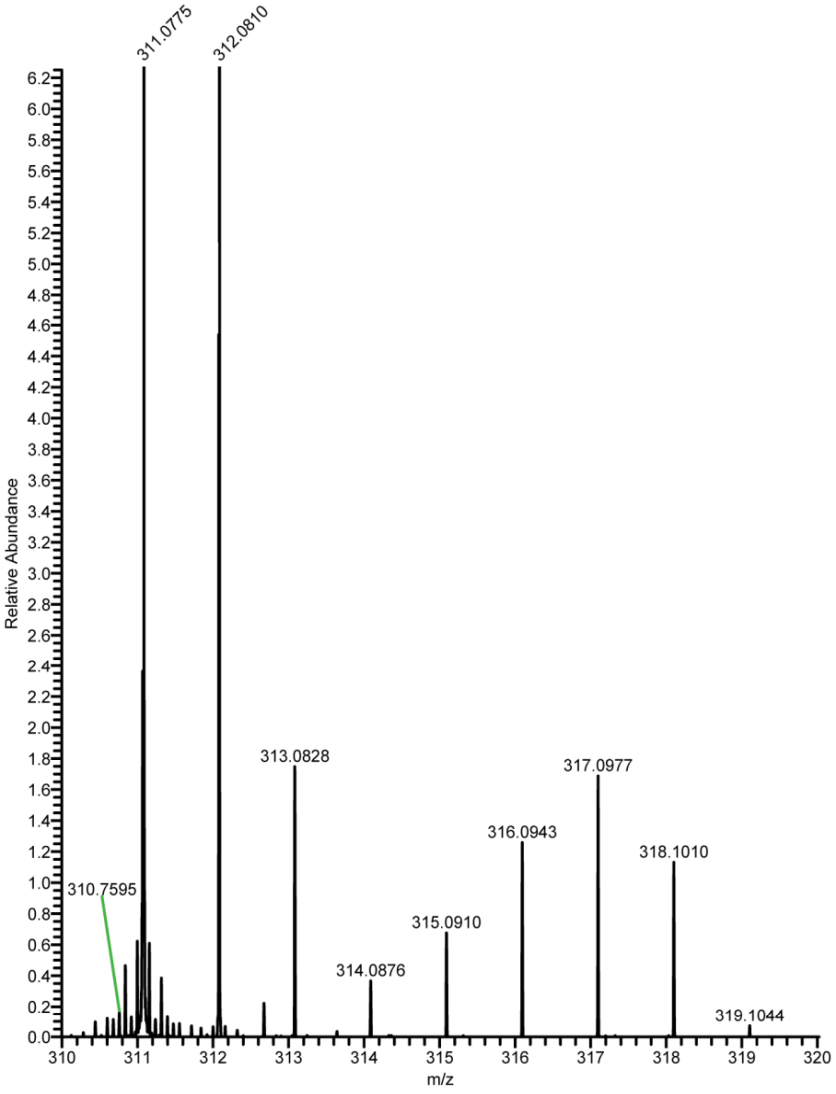

Figure C.3-3 Compound **2**; HRESIMS spectrum {*m/z* 311.0775 $[M-H]^-$} of *C. vinula* feces after consumption of leaves labeled with [U-^{13}C]salicortin.

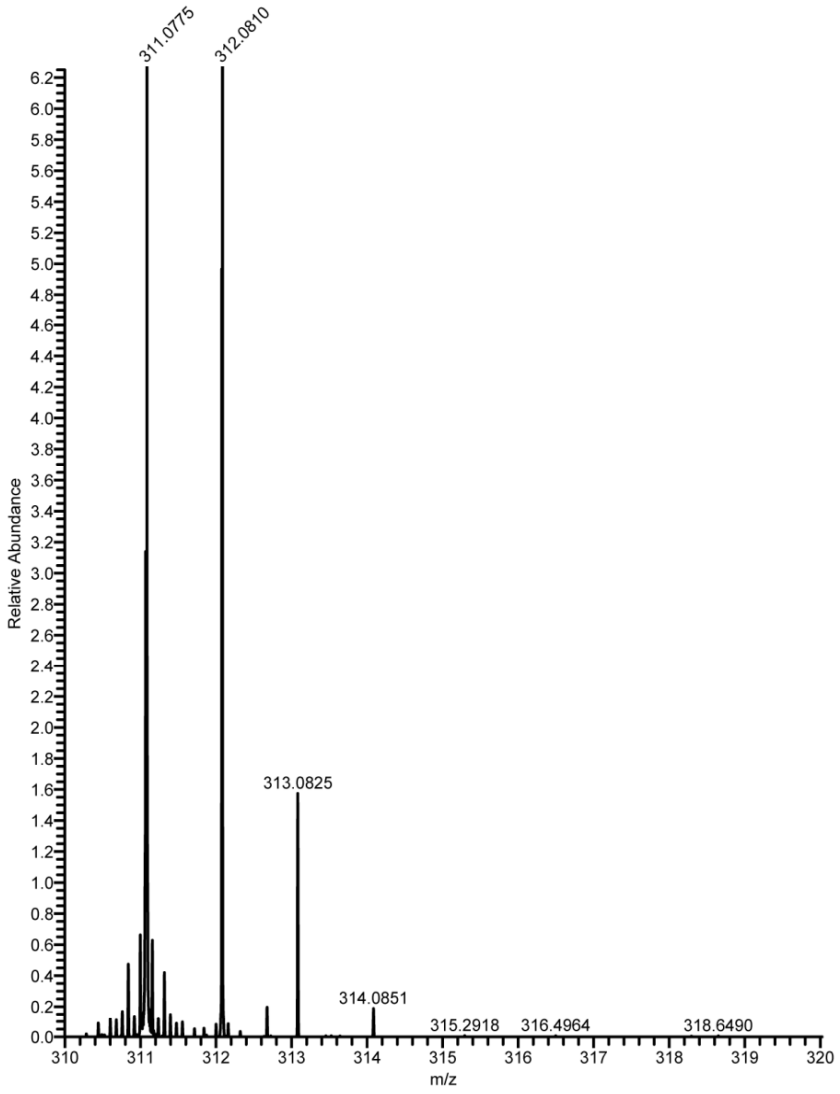

Figure C.3-4 Compound **2**; HRESIMS spectrum (*m/z* 311.0775 $[M-H]^-$) of *C. vinula* feces after consumption of control tissue.

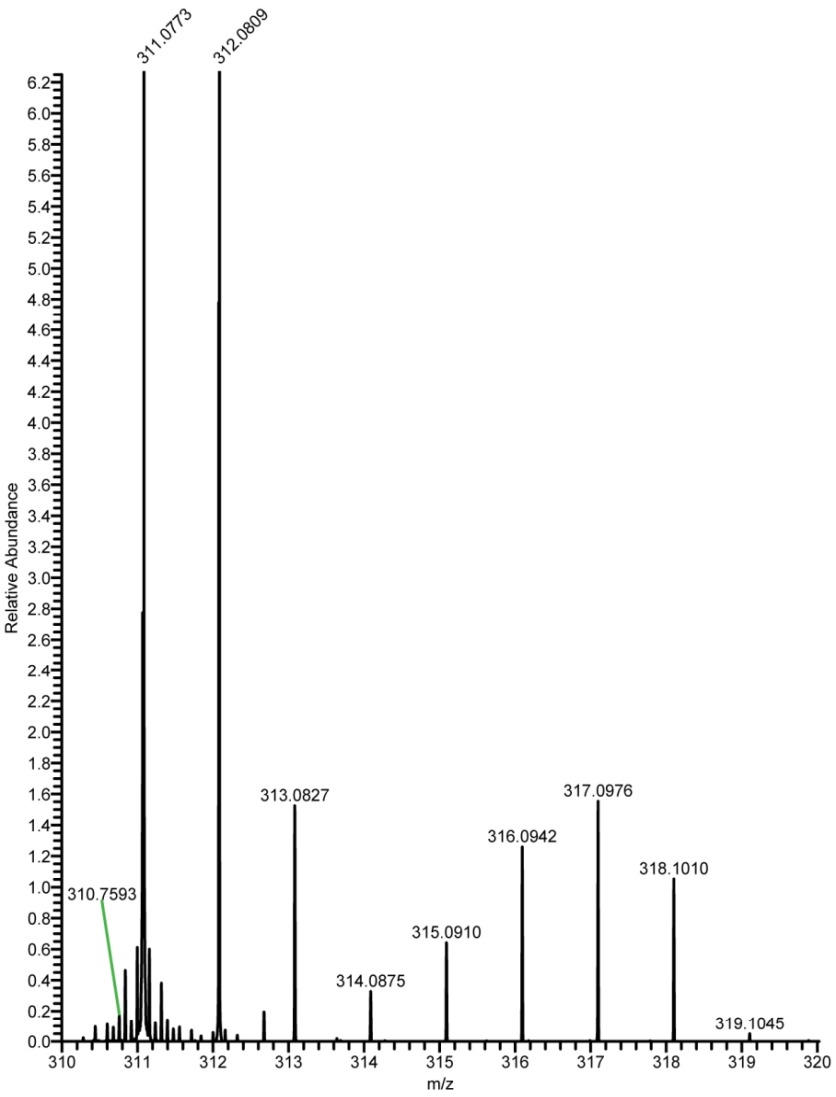

Figure C.3-5 Compound **3**; HRESIMS spectrum {*m/z* 311.0773 $[M-H]^-$} of *C. vinula* feces after consumption of leaves labeled with [U-^{13}C]salicortin.

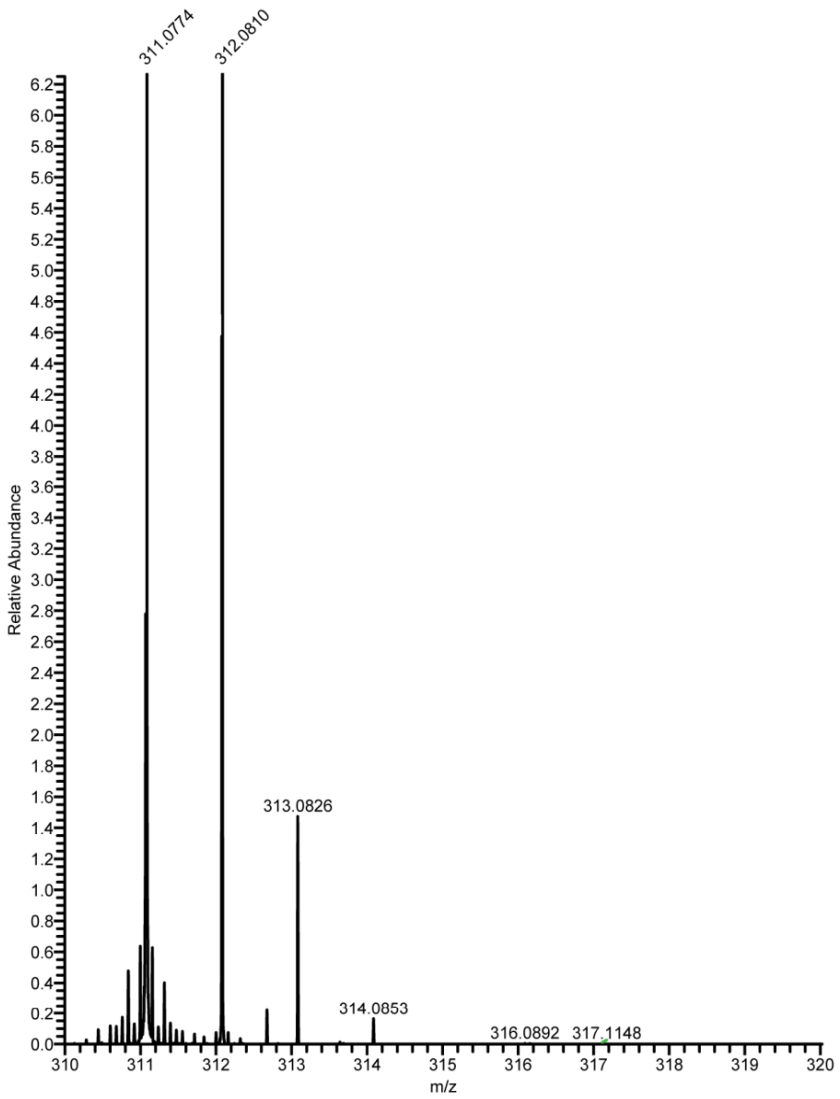

Figure C.3-6 Compound **3**; HRESIMS spectrum (*m/z* 311.0774 [M-H]$^-$) of *C. vinula* feces after consumption of control tissue.

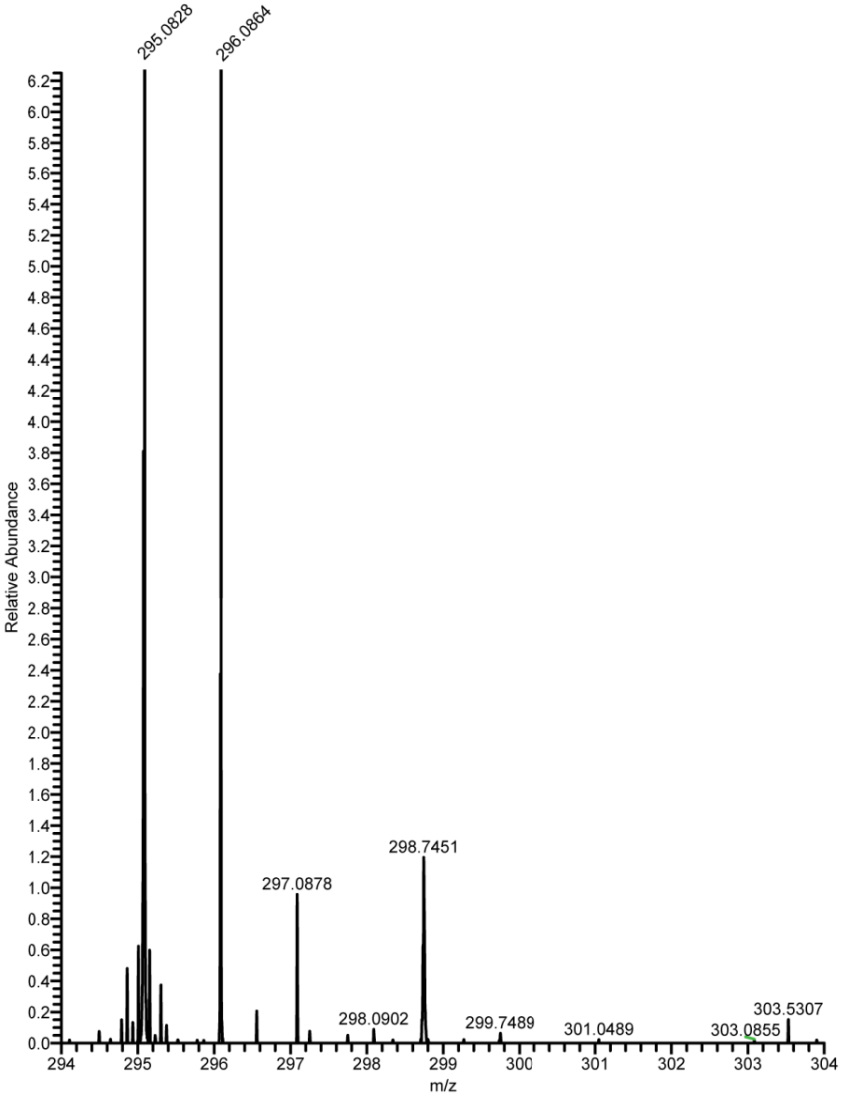

Figure C.3-7 Compound 4; HRESIMS spectrum (*m/z* 295.0828 [M-H]$^-$) of *C. vinula* feces after consumption of leaves labeled with [U-^{13}C]salicortin.

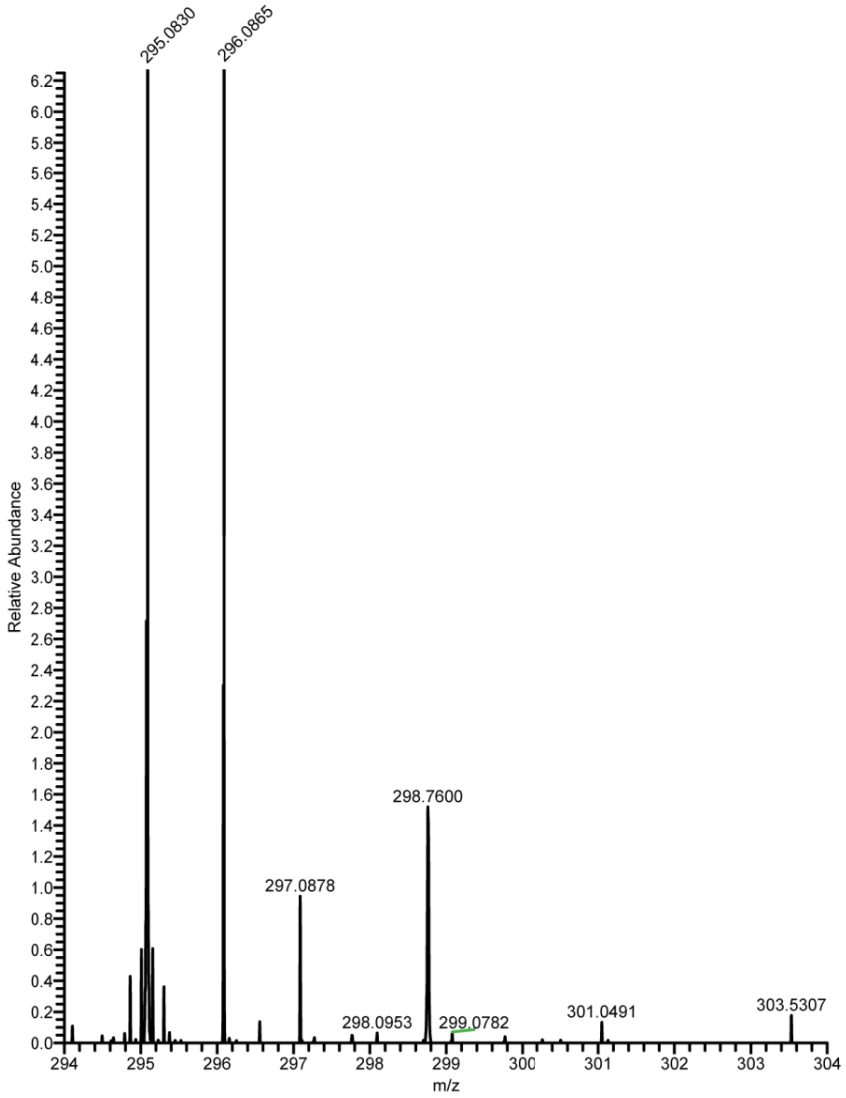

Figure C.3-8 Compound 4; HRESIMS spectrum (*m/z* 295.0830 [M-H]$^-$) of *C. vinula* feces after consumption of control tissue.

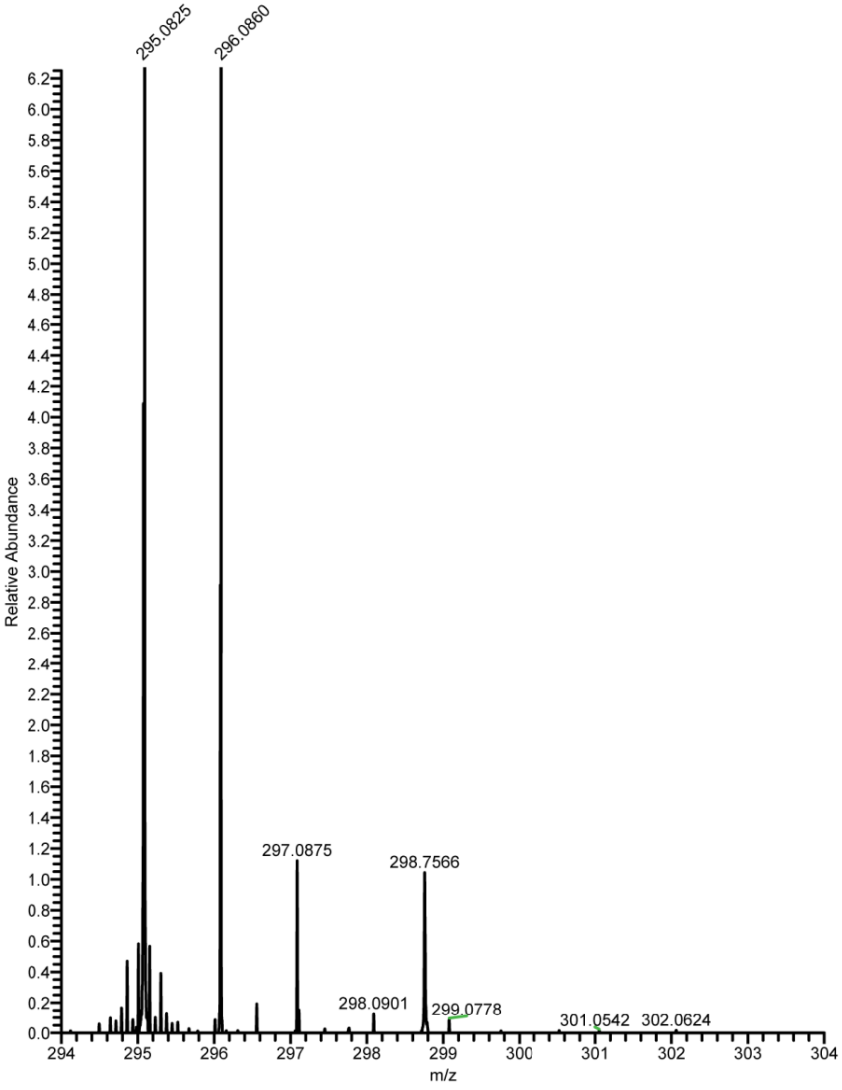

Figure C.3-9 Compound **5**; HRESIMS spectrum (*m/z* 295.0825 [M-H]$^-$) of *C. vinula* feces after consumption of leaves labeled with [U-^{13}C]salicortin.

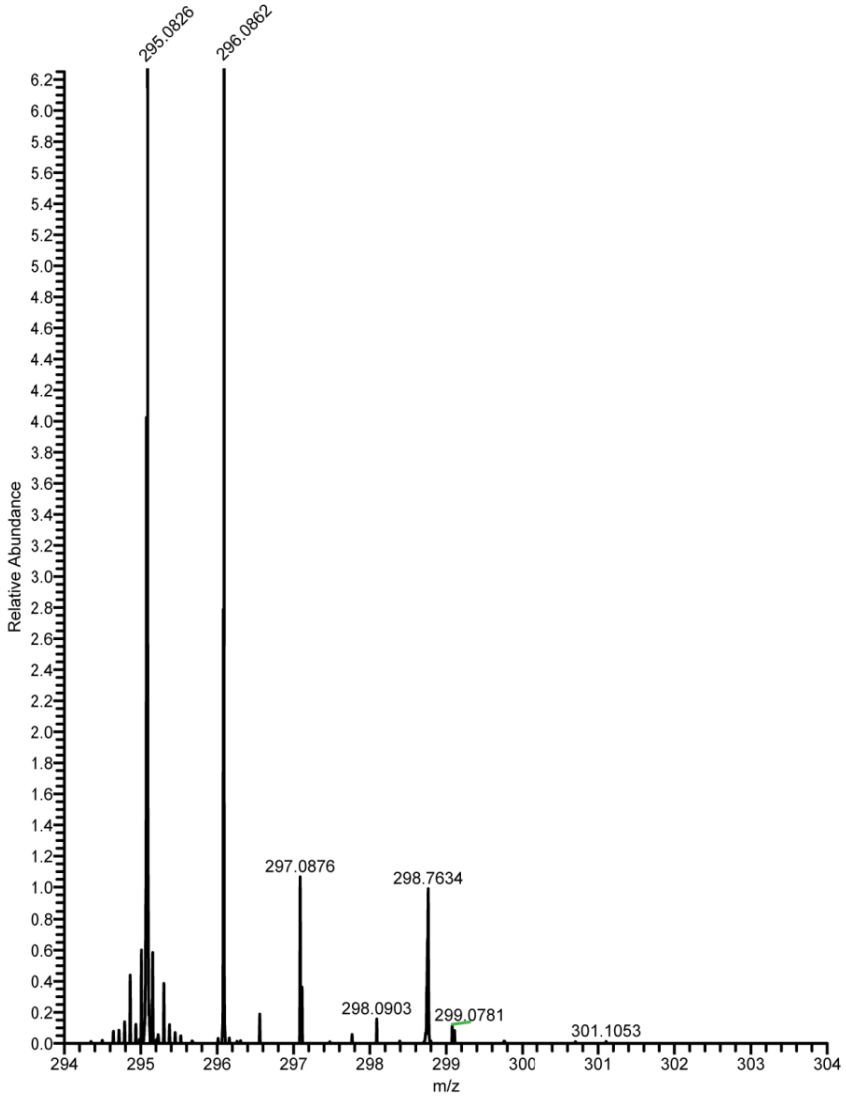

Figure C.3-10 Compound **5**; HRESIMS spectrum {*m/z* 295.0826 [M-H]$^-$} of *C. vinula* feces after consumption of control tissue.

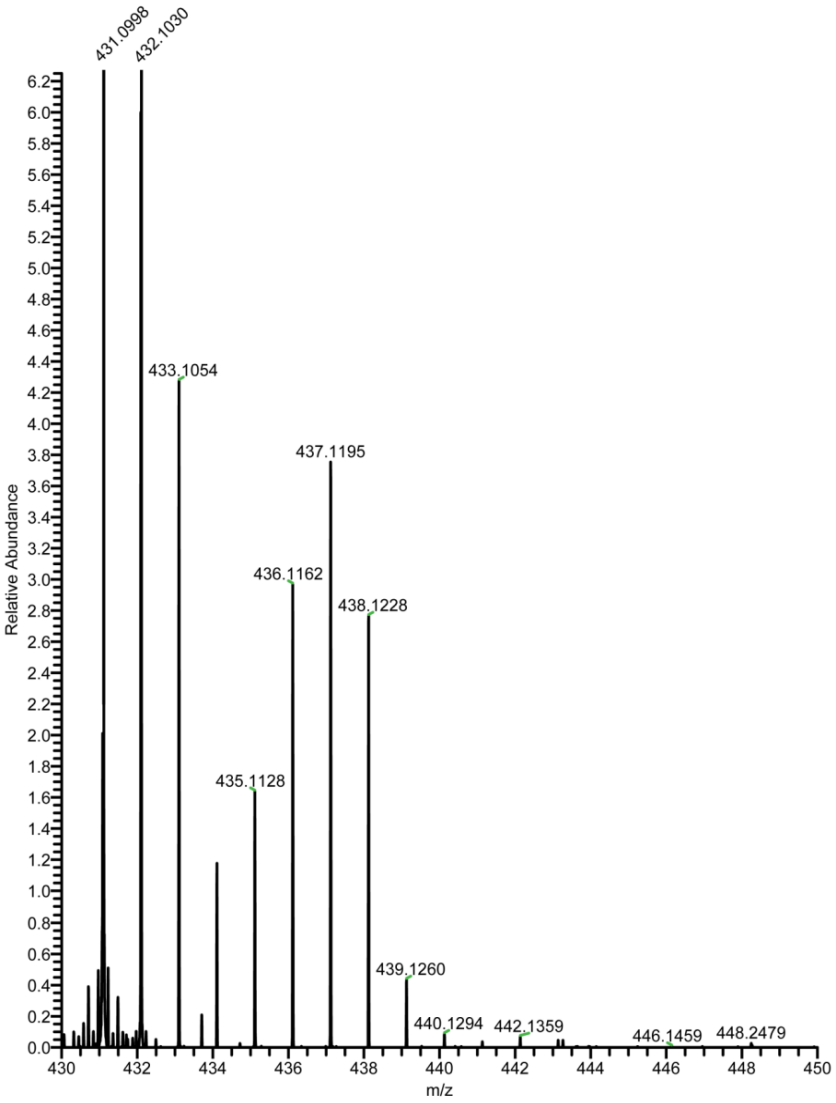

Figure C.3-11 Compound **6**; HRESIMS spectrum (*m/z* 431.0998 [M-H]$^-$) of *C. vinula* feces after consumption of leaves labeled with [U-^{13}C]salicortin.

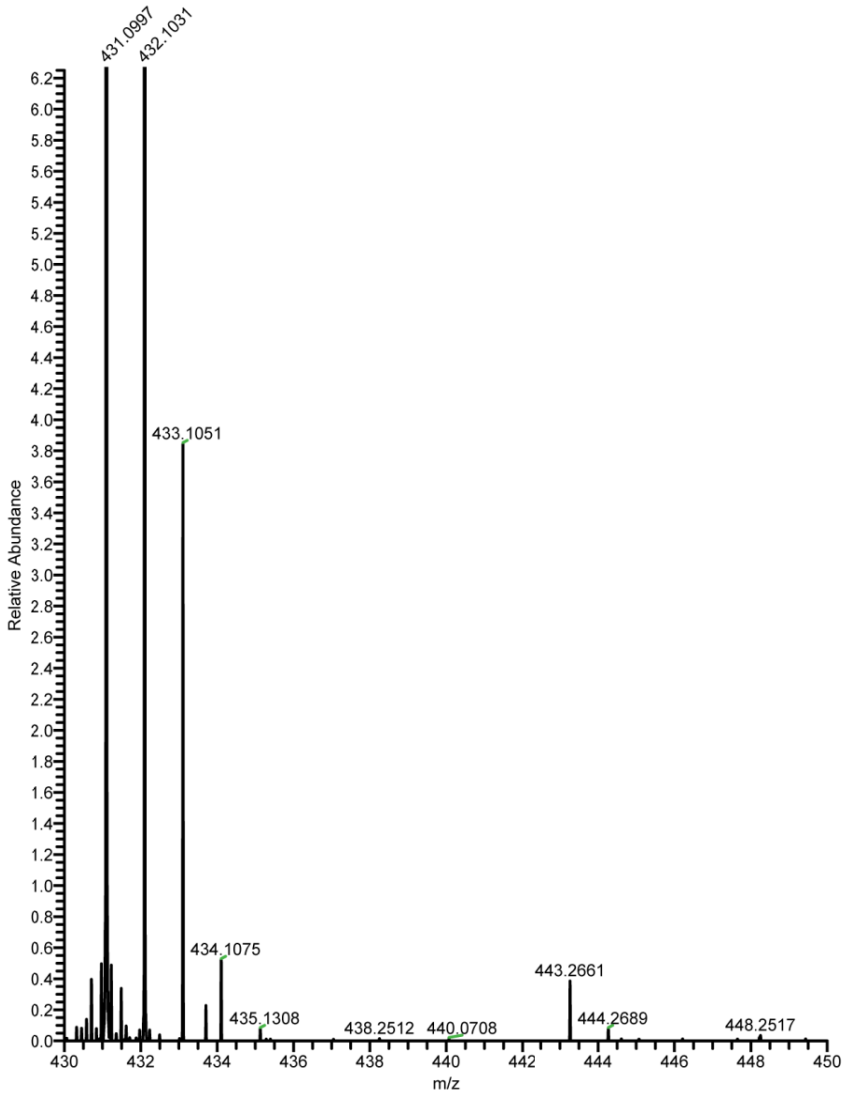

Figure C.3-12 Compound **6**; HRESIMS spectrum (*m/z* 431.0997 [M-H]$^-$) of *C. vinula* feces after consumption of control tissue.

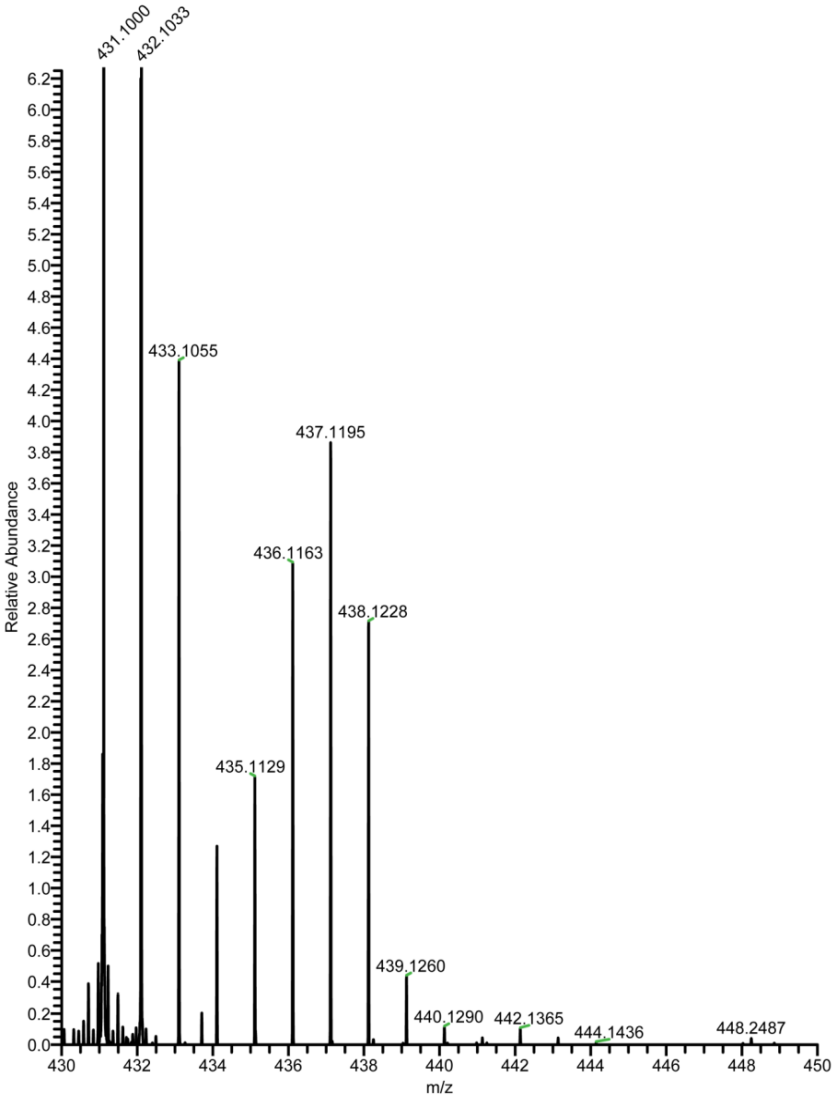

Figure C.3-13 Compound **7**; HRESIMS spectrum (*m/z* 431.1000 [M-H]$^-$) of *C. vinula* feces after consumption of leaves labeled with [U-^{13}C]salicortin.

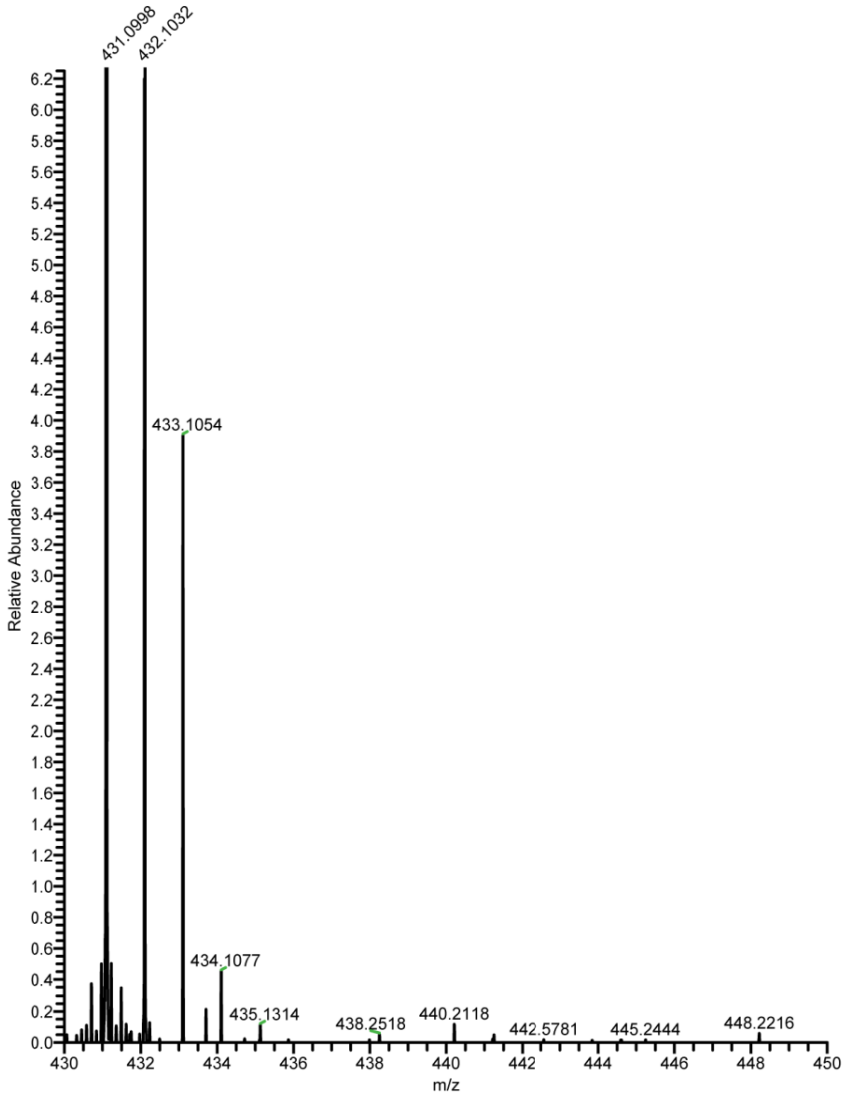

Figure C.3-14 Compound **7**; HRESIMS spectrum (*m/z* 431.0998 [M-H]$^-$) of *C. vinula* feces after consumption of control tissue.

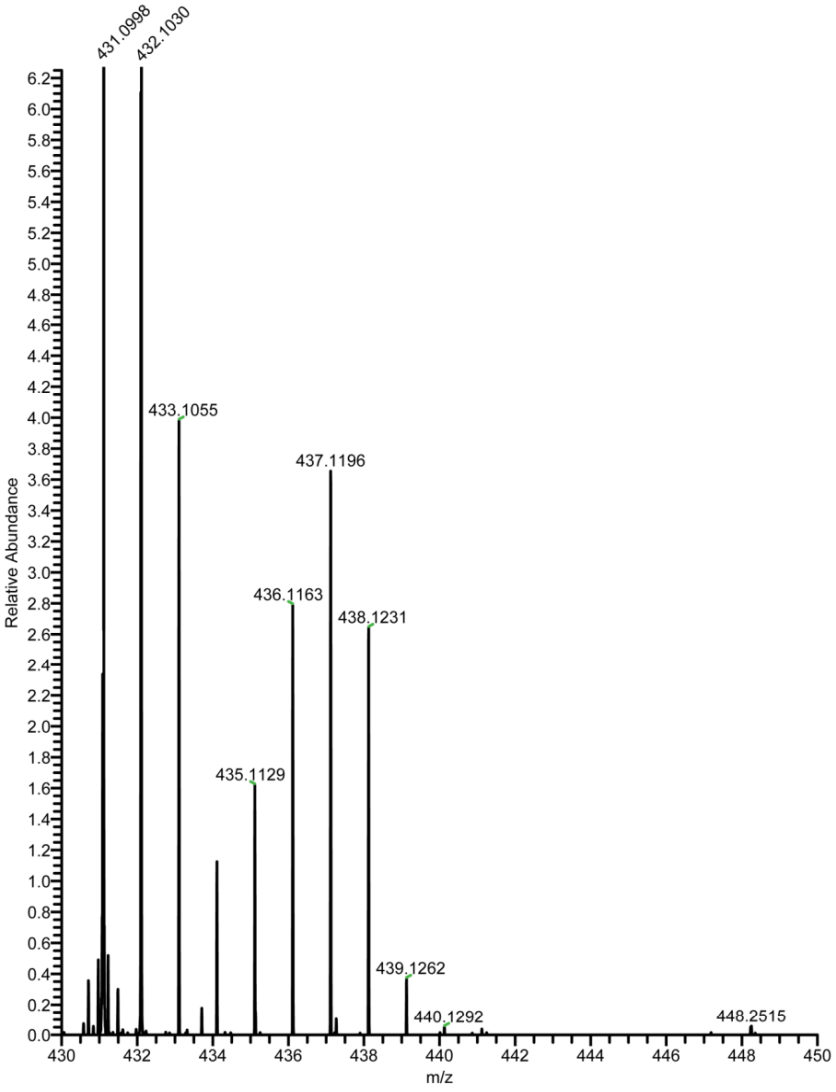

Figure C.3-15 Compound **8**; HRESIMS spectrum (*m/z* 431.0998 [M-H]$^-$) of *C. vinula* feces after consumption of leaves labeled with [U-^{13}C]salicortin.

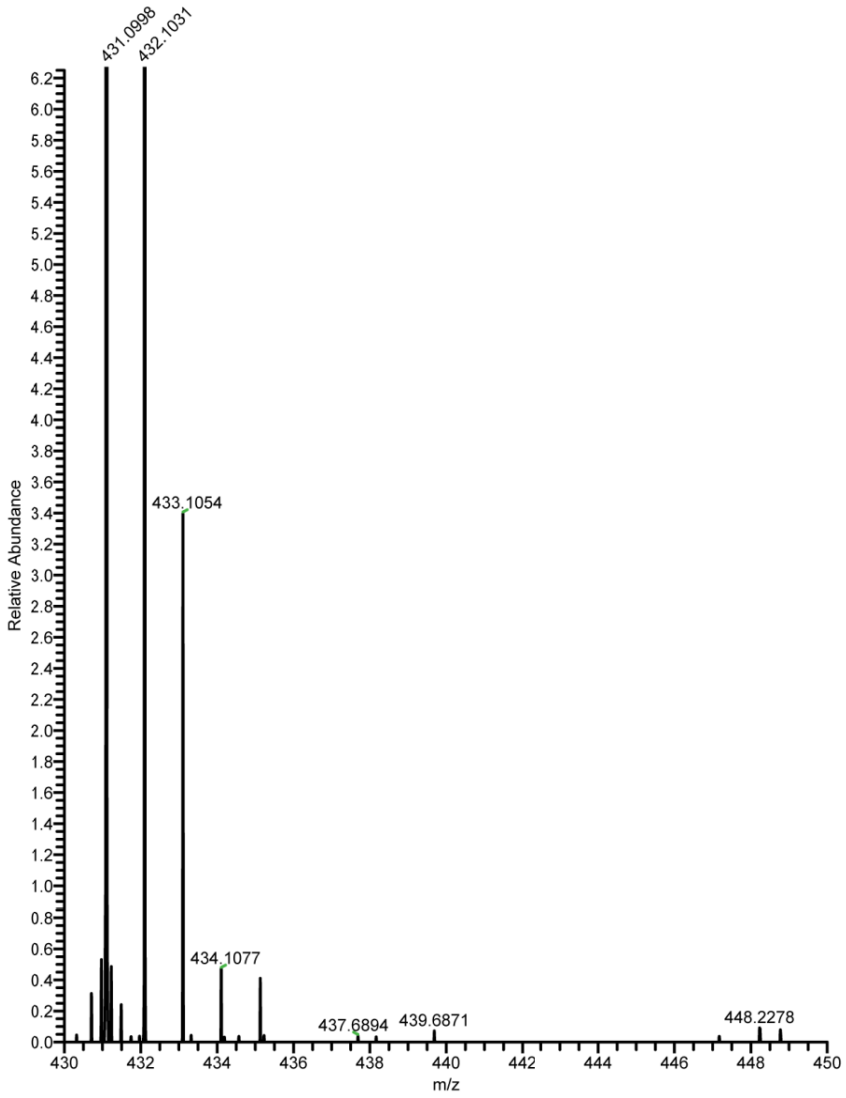

Figure C.3-16 Compound **8**; HRESIMS spectrum (*m/z* 431.0998 [M-H]$^-$) of *C. vinula* feces after consumption of control tissue.

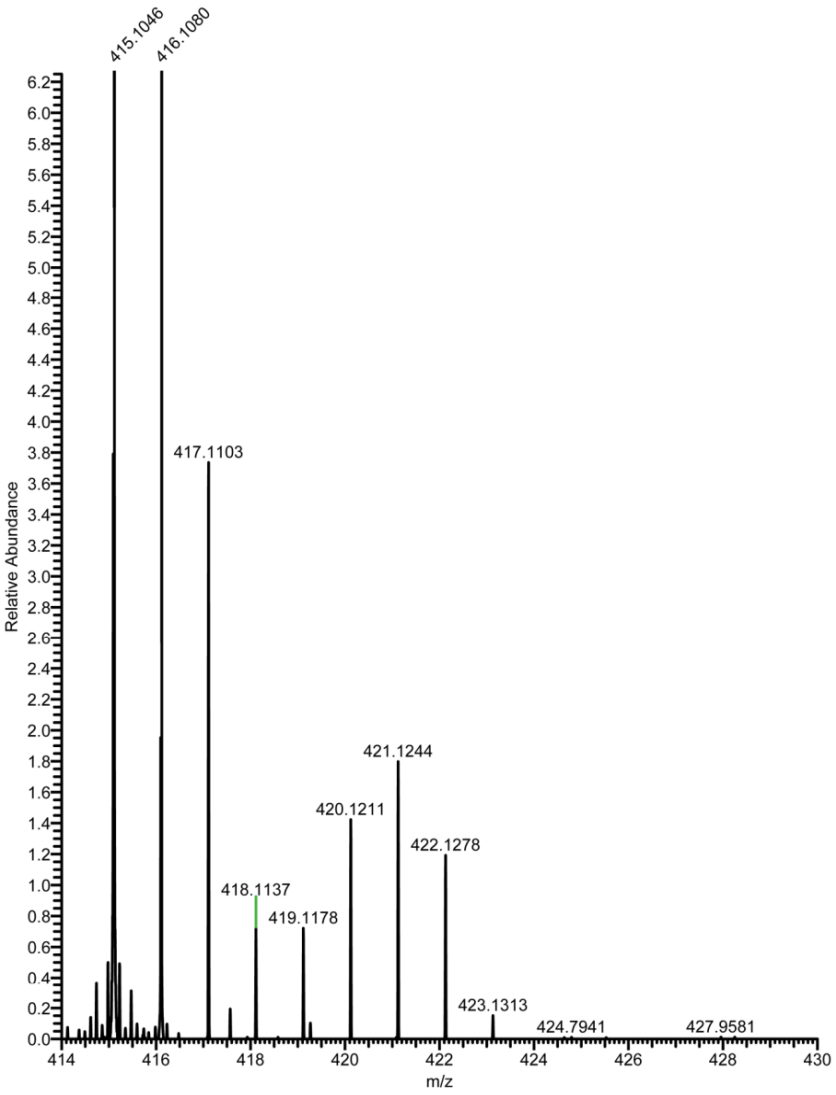

Figure C.3-17 Compound **9**; HRESIMS spectrum (*m/z* 415.1046 [M-H]$^-$) of *C. vinula* feces after consumption of leaves labeled with [U-^{13}C]salicortin.

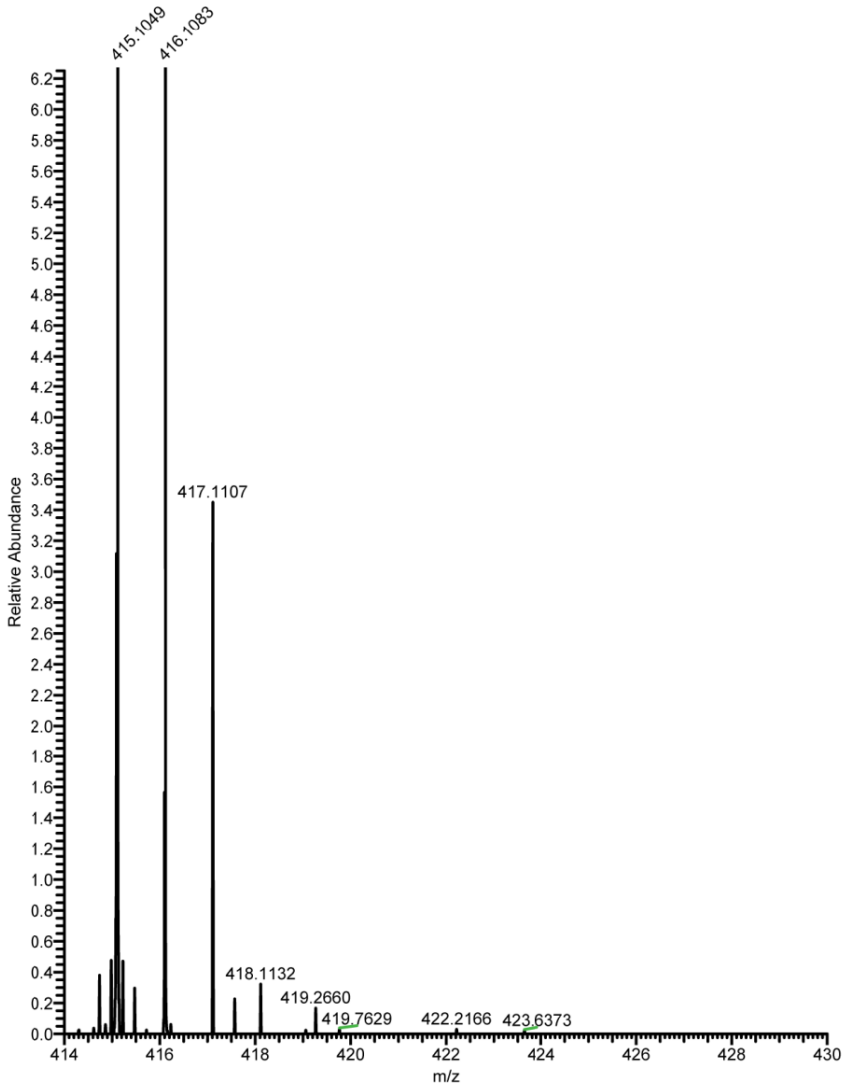

Figure C.3-18 Compound **9**; HRESIMS spectrum (*m/z* 415.1049 [M-H]$^-$) of *C. vinula* feces after consumption of control tissue.

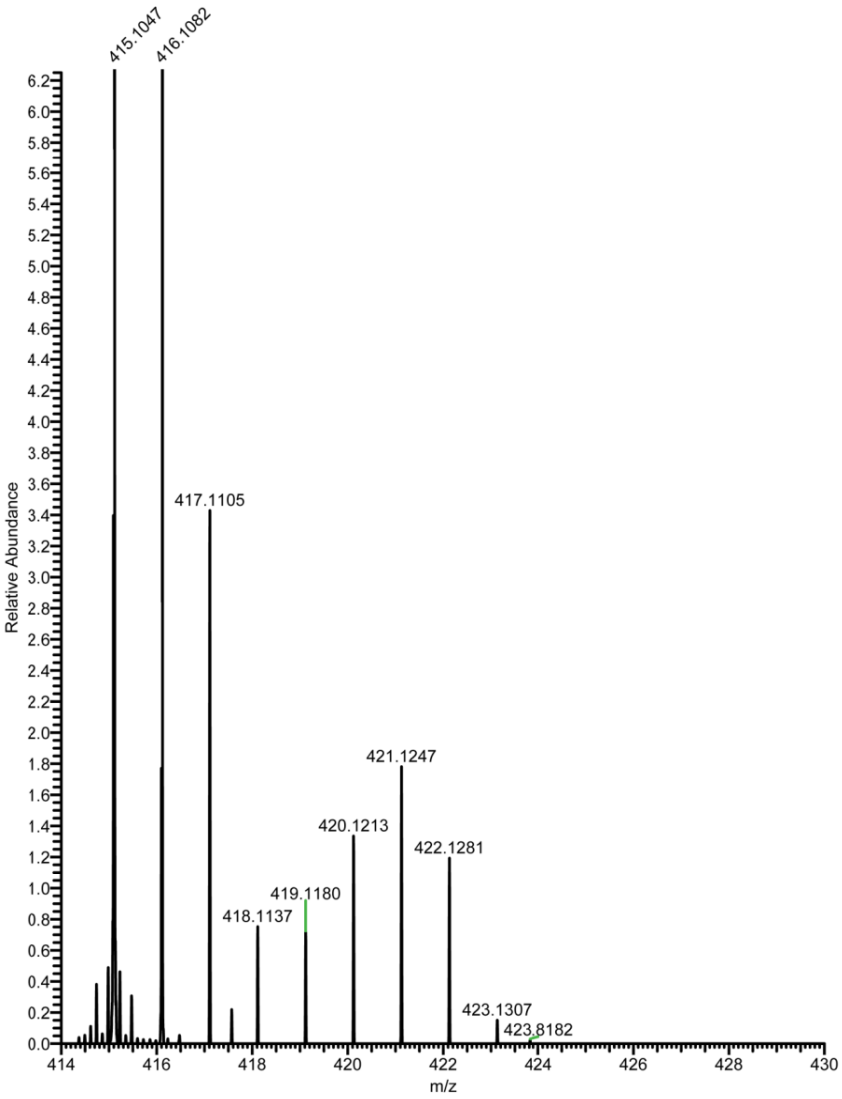

Figure C.3-19 Compound **10**; HRESIMS spectrum (*m/z* 415.1047 [M-H]$^-$) of *C. vinula* feces after consumption of leaves labeled with [U-^{13}C]salicortin.

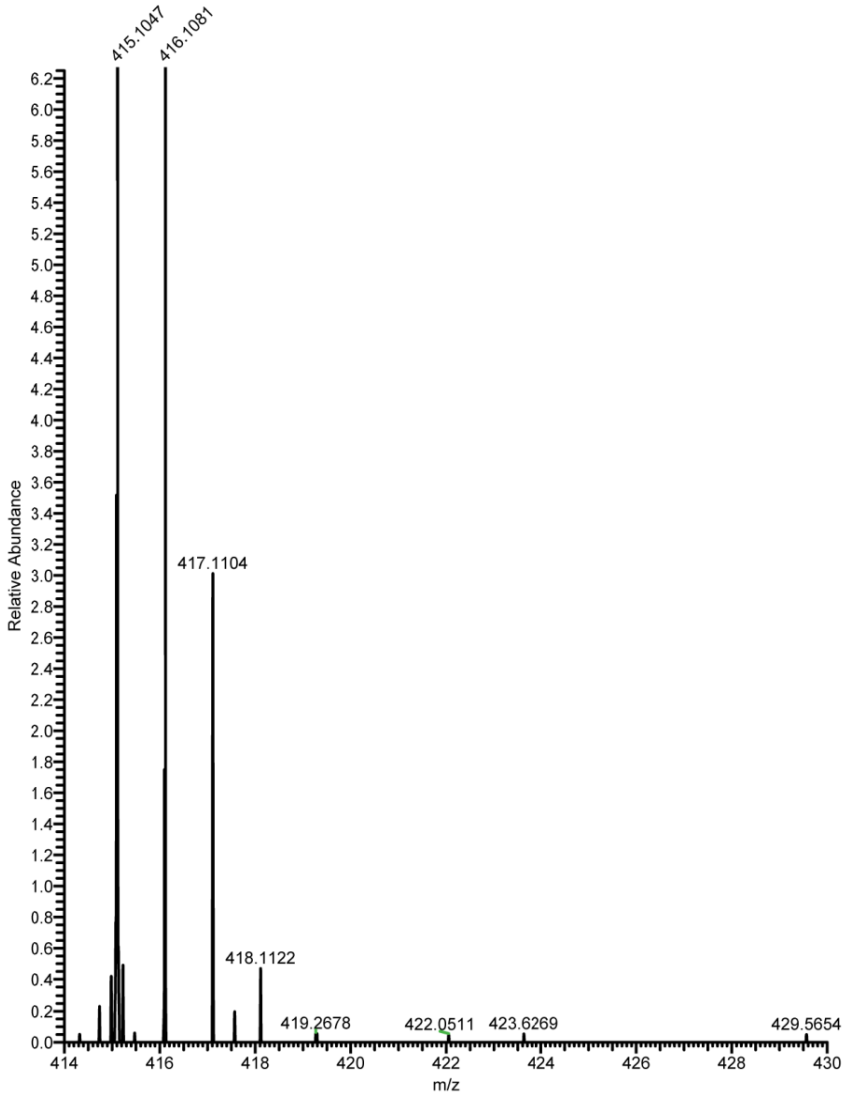

Figure C.3-20 Compound **10**; HRESIMS spectrum (*m/z* 415.1047 [M-H]$^-$) of *C. vinula* feces after consumption of control tissue.

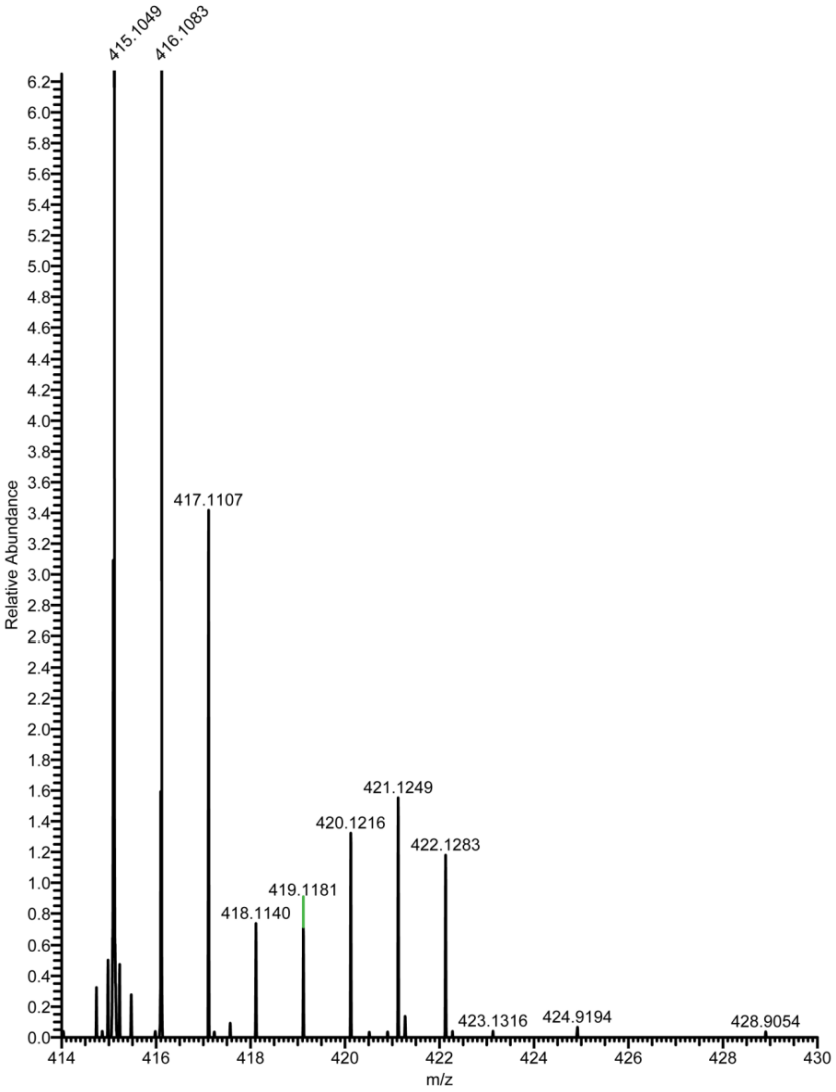

Figure C.3-21 Compound **11**; HRESIMS spectrum (*m/z* 415.1049 [M-H]$^-$) of *C. vinula* feces after consumption of leaves labeled with [U-^{13}C]salicortin.

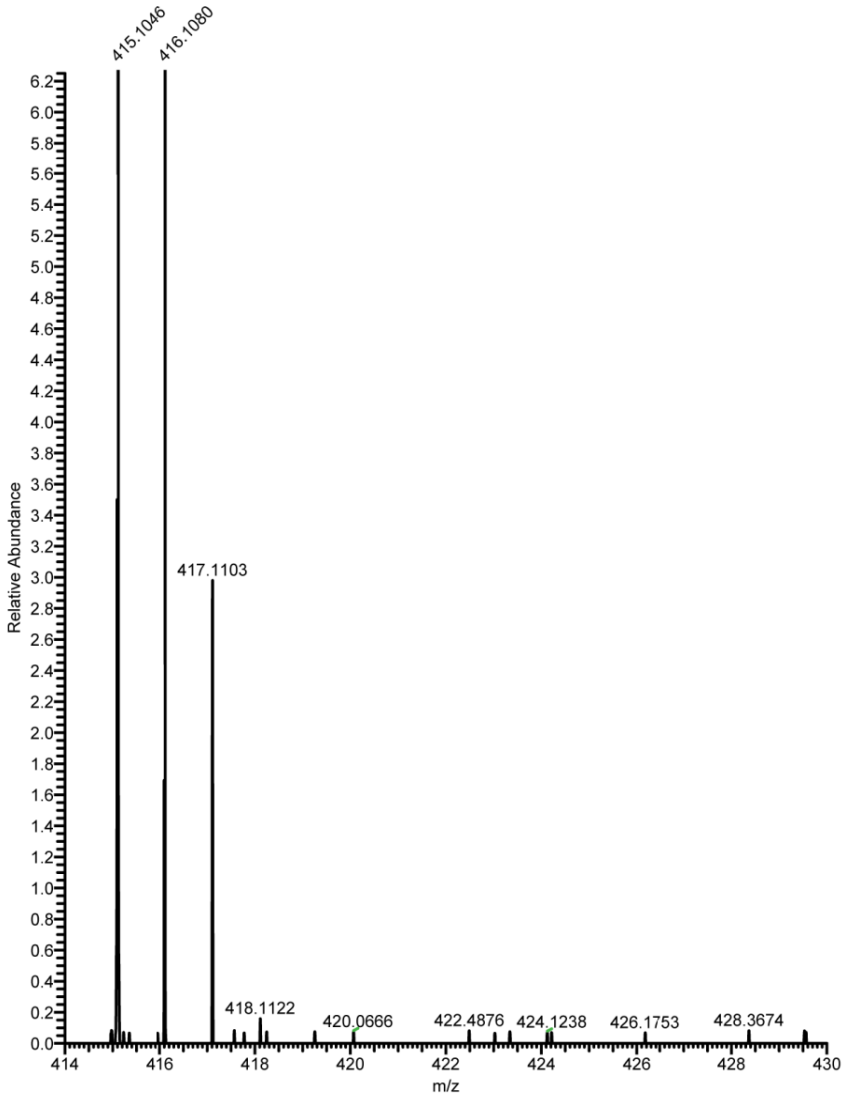

Figure C.3-22 Compound **11**; HRESIMS spectrum (*m/z* 415.1046 [M-H]$^-$) of *C. vinula* feces after consumption of control tissue.

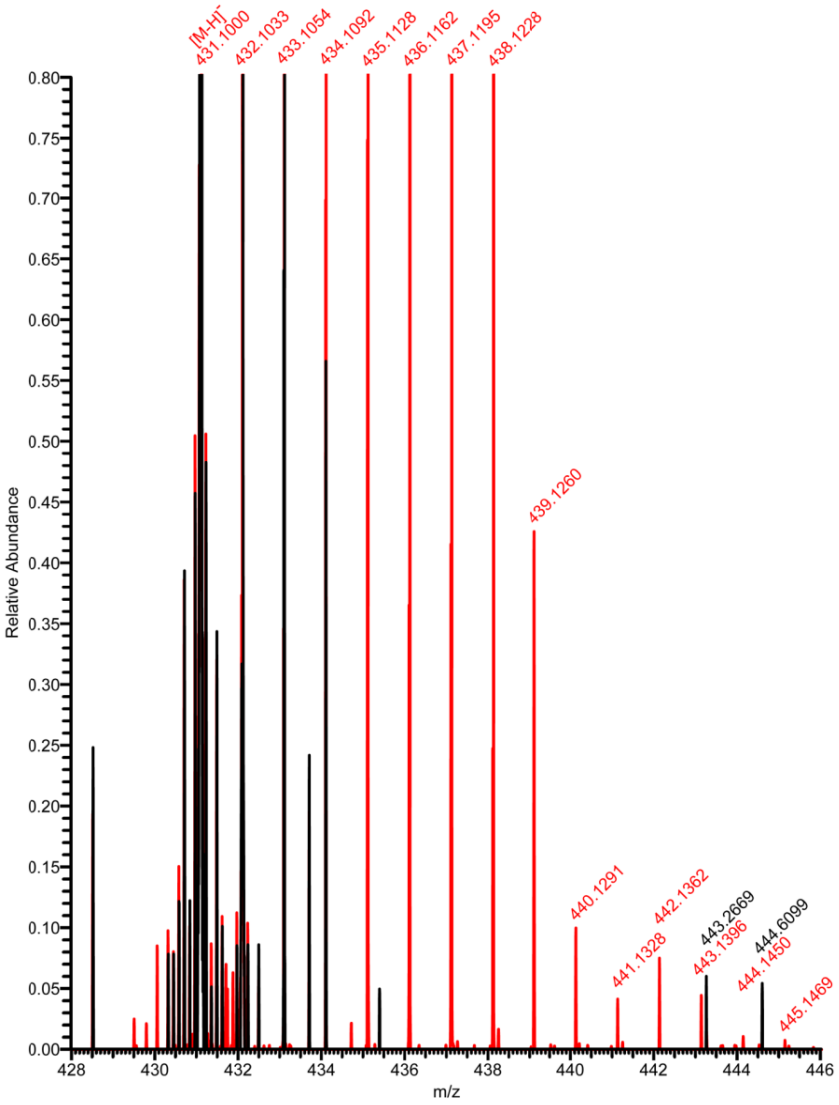

Figure C.3-23 Strongly amplified, superimposed HRESIMS spectrum of compound **7** (*m/z* 431) from *C. vinula* feces after consumption of control tissue (black) and leaves labeled with [U-^{13}C]salicortin (red). The spectrum is strongly amplified to show occurrence of isotopologues up to $[M-H+14]^-$.

D)Qualitative analysis of *C. vinula* hemolymphs:

D.1) HRESIMS of six caterpillars testes (I to VI)

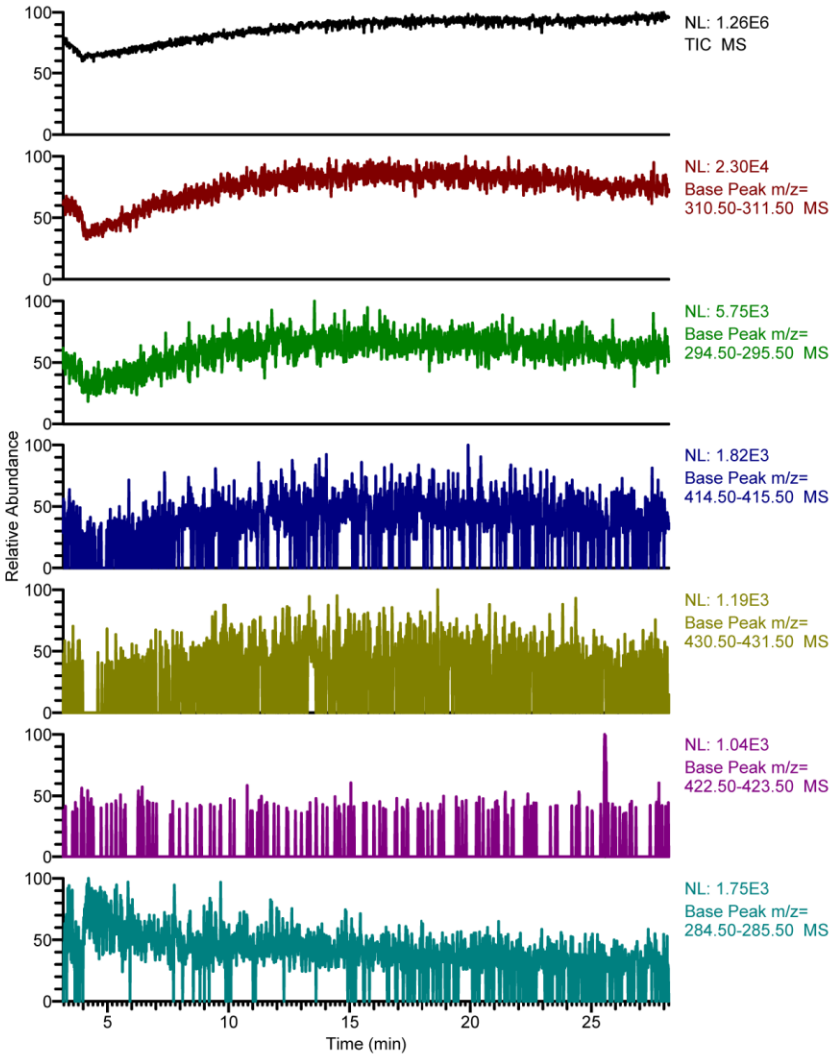

Figure D.1-1 HRESIMS; TIC and base peak chromatograms of hemolymphs from *C. vinula* larva I.

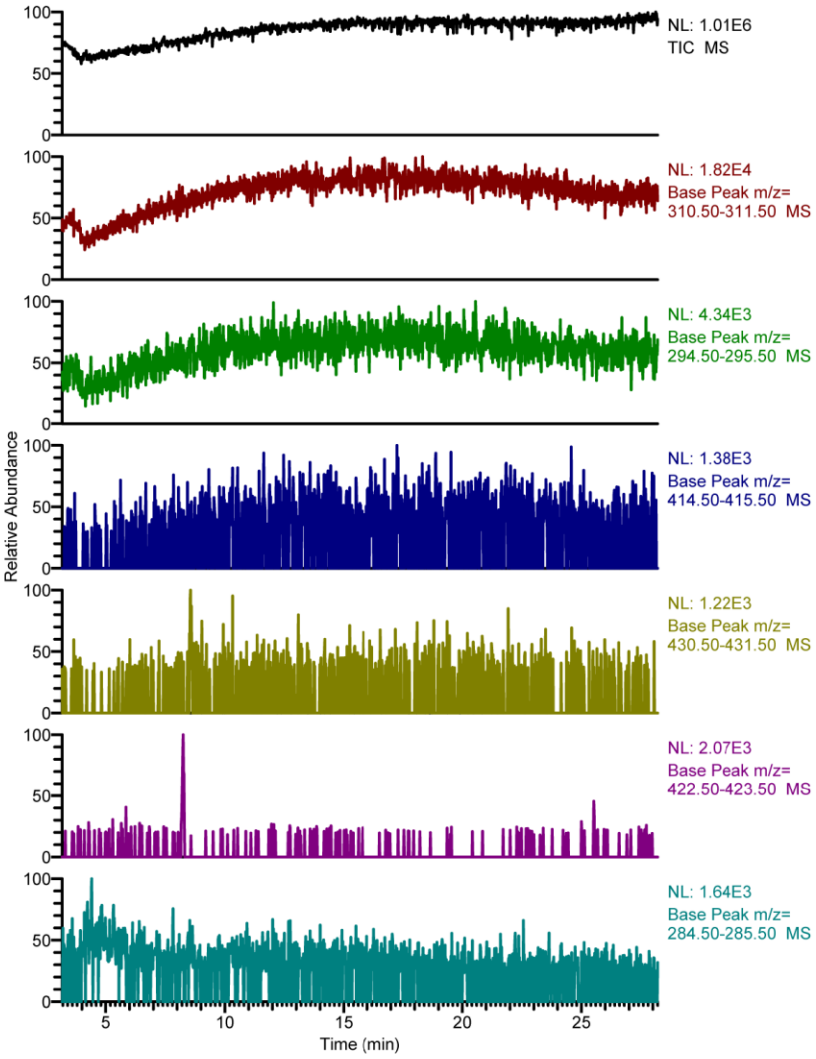

Figure D.1-2 HRESIMS; TIC and base peak chromatograms of hemolymphs from *C. vinula* larva II.

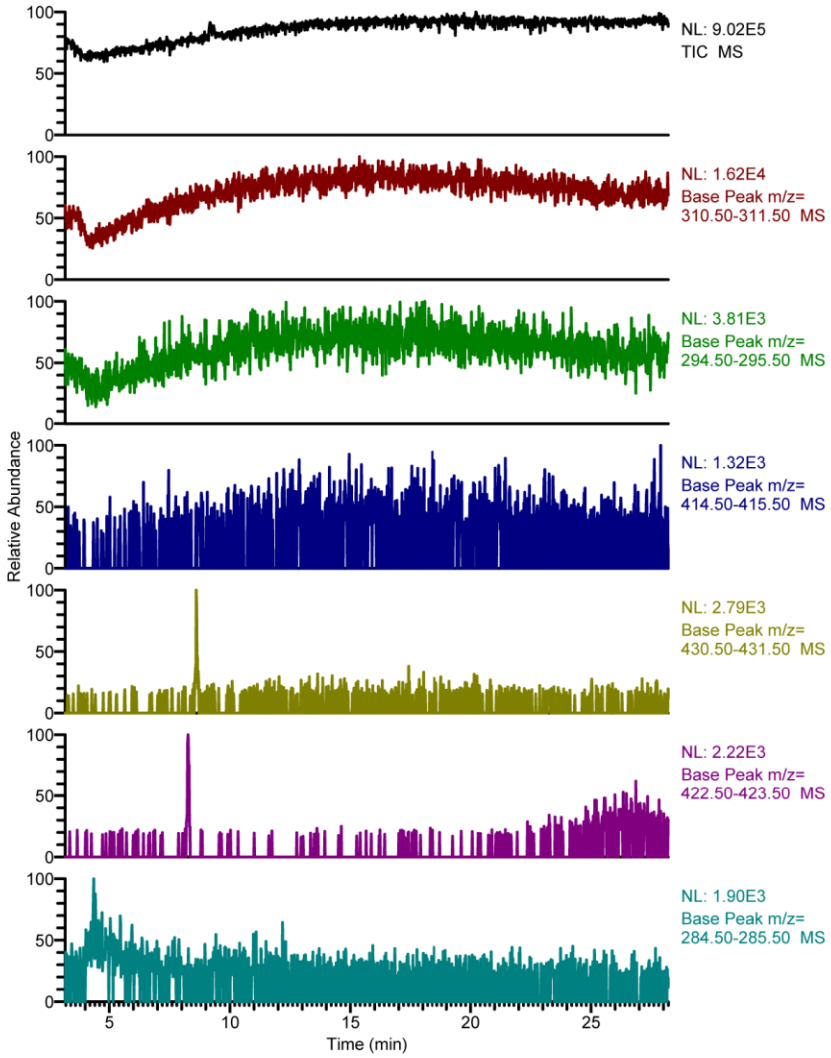

Figure D.1-3 HRESIM; TIC and base peak chromatograms of hemolymphs from *C. vinula* larva III.

CL

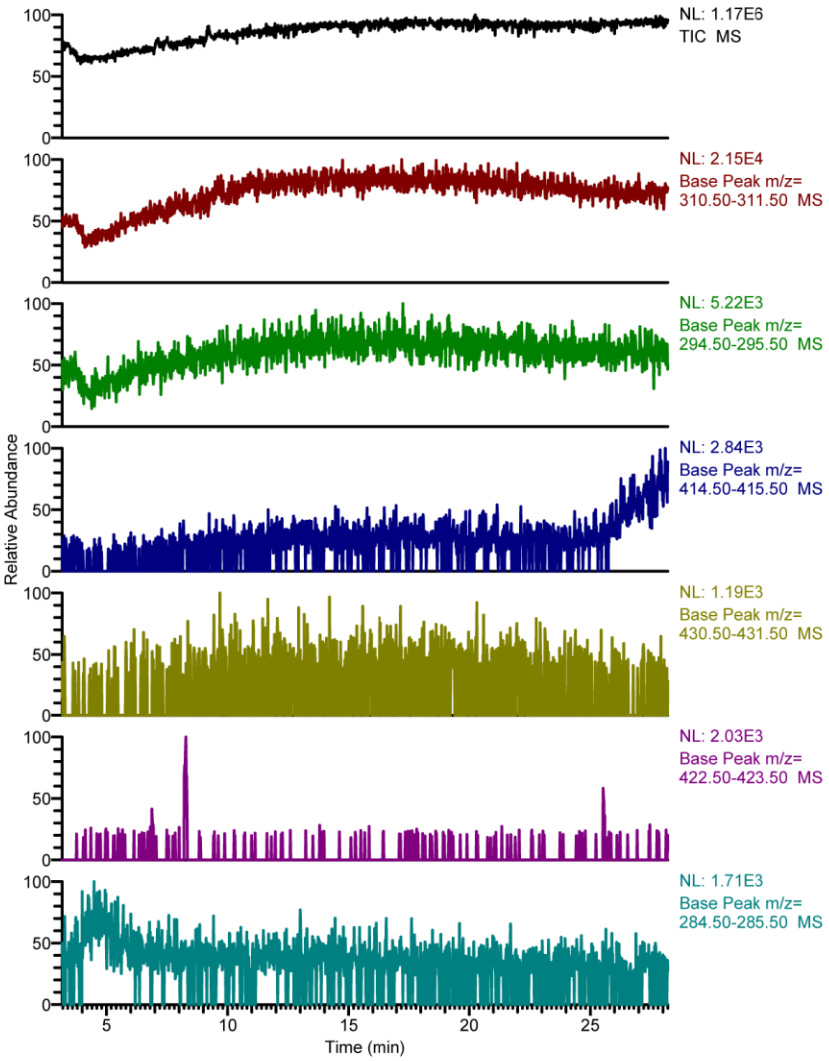

Figure D.1-4 HRESIMS; TIC and base peak chromatograms of hemolymphs from *C. vinula* larva IV.

CLI

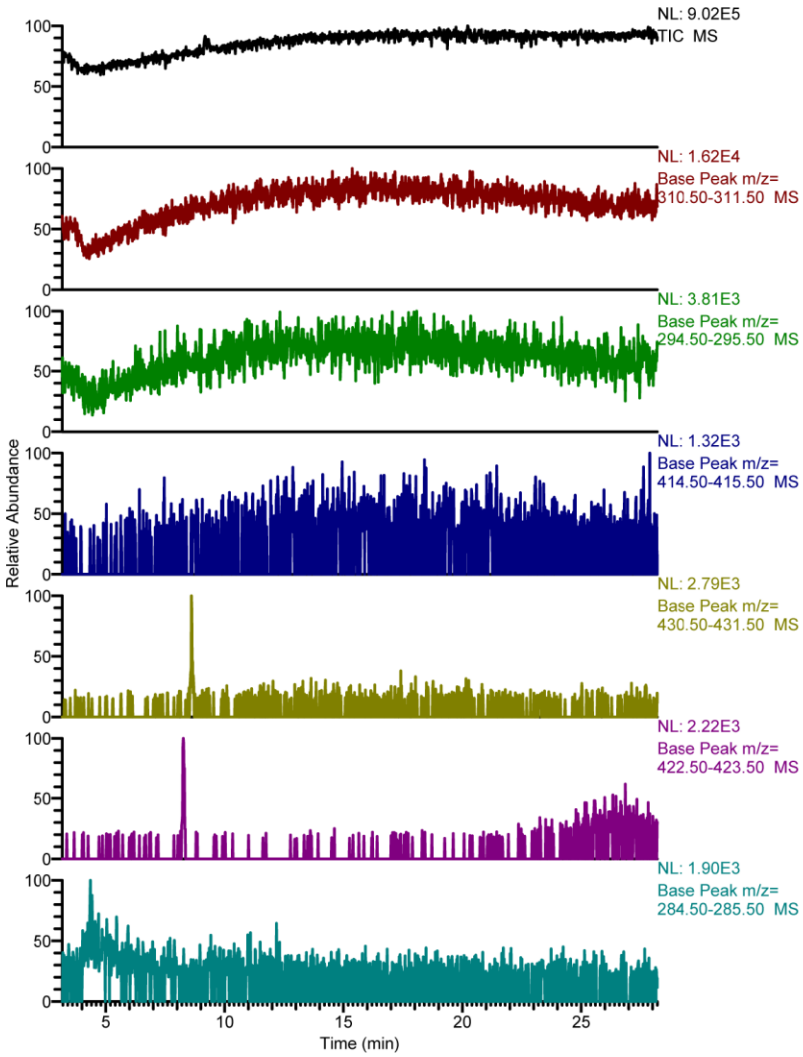

Figure D.1-5 HRESIMS; TIC and base peak chromatograms of hemolymphs from *C. vinula* larva V.

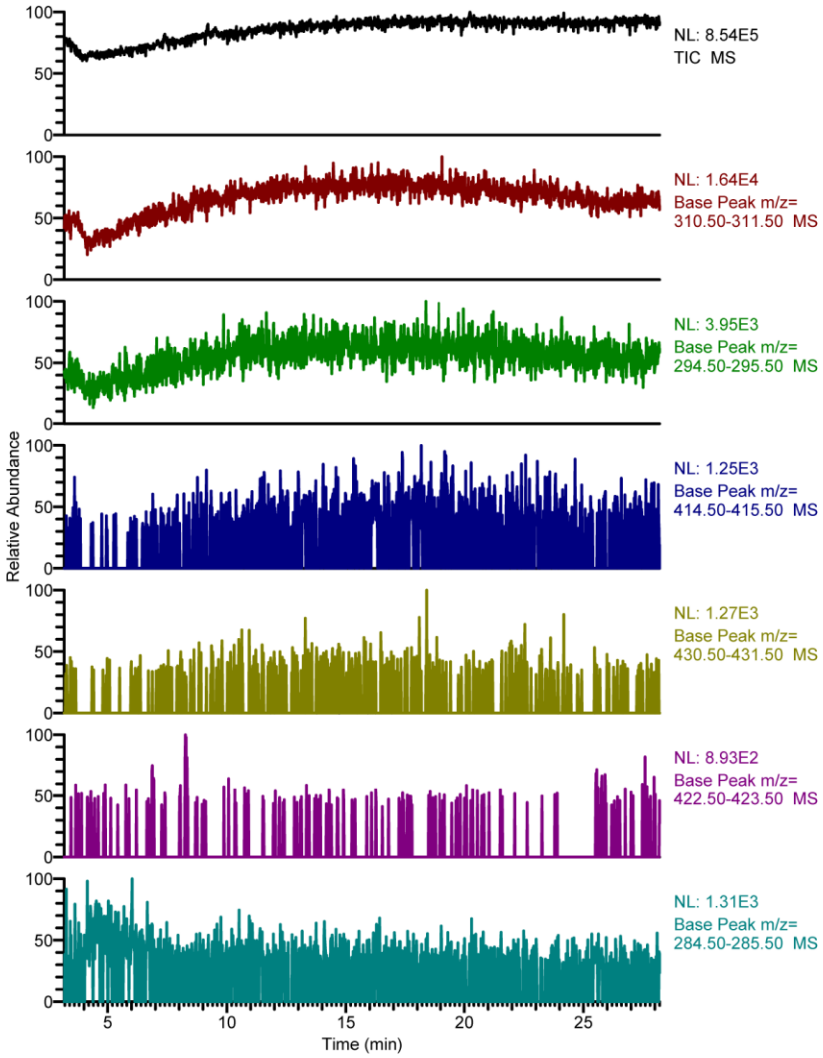

Figure D.1-6 HRESIMS; TIC and base peak chromatograms of hemolymphs from *C. vinula* larva VI.

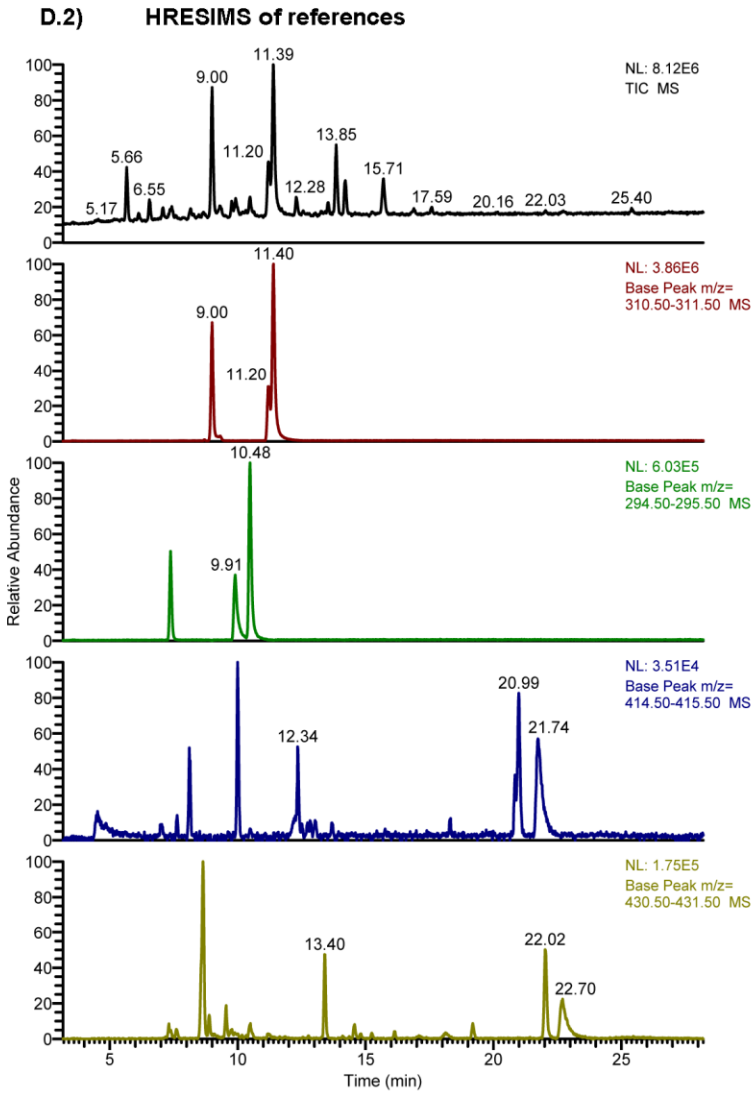

Figure D.2-1 HRESIMS; TIC and base peak chromatograms of *C. vinula* feces. The peaks of quinic acid esters are labeled with retention times. R_t (compound): 9.00 (**1**), 9.91 (**4**), 10.48 (**5**), 11.20 (**2**), 11.40 (**3**), 12.34 (**10**), 13.40 (**7**), 20.99 (**9**), 21.74 (**11**), 22.02 (**6**), 22.70 (**8**).

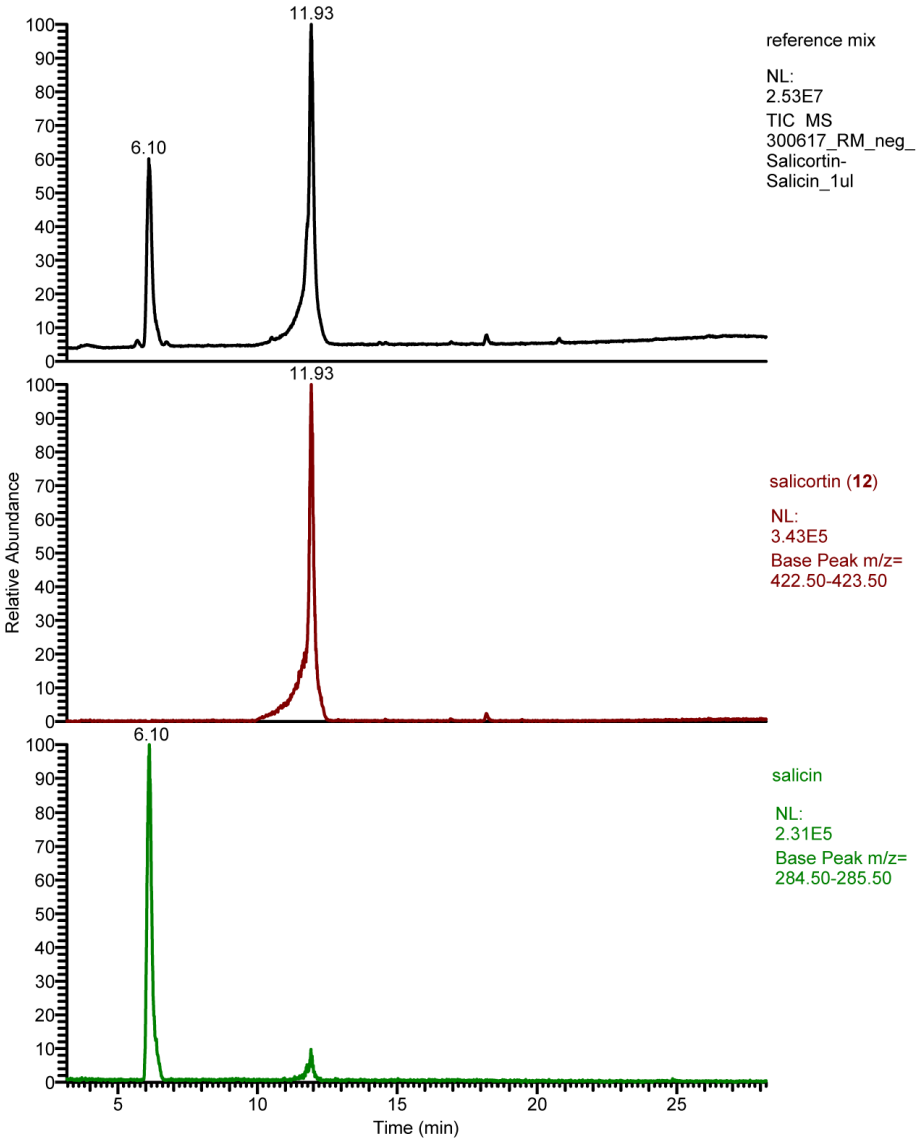

Figure D.2-2 HRESIMS; TIC and base peak chromatograms from a reference mix of salicortin (**12**) (red; 11.93 min) and salicin (green; 6.10 min).

Supplementary data

Idesia polycarpa (Salicaceae) leaf constituents and their toxic effect on *Cerura vinula* and *Lymantria dispar* (Lepidoptera) larvae

Felix Feistel, Christian Paetz, Sybille Lorenz, Franziska Beran, Grit Kunert, Bernd Schneider

Max Planck Institute for Chemical Ecology, Hans-Knöll-Straße 8, 07745 Jena, Germany

1. **Supplementary data of 1-*O*-(2-hydroxyethyl)-4-*O*-(*E*)-*p*-coumaroyl-β-glucopyranose (1):**

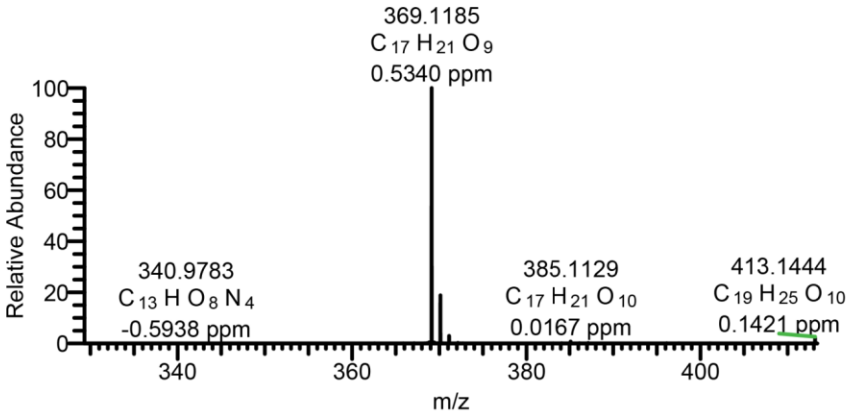

HRMS (-p ESI)
369.1185 $[M-H]^-$ (100.00)
370.1216 $[M-H]^-$ (18.83)
371.1234 $[M-H]^-$ (2.75)

Figure S1.1 Compound **1,** HRESI-MS data

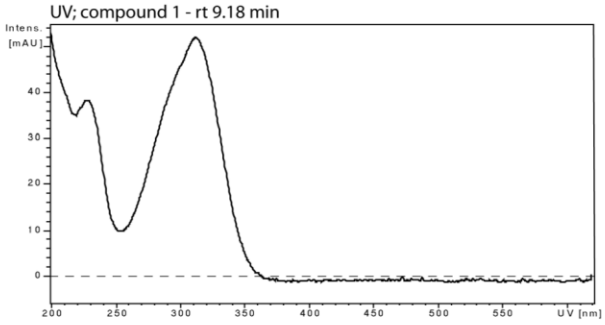

Figure S1.2 Compound **1**, UV-Vis spectrum

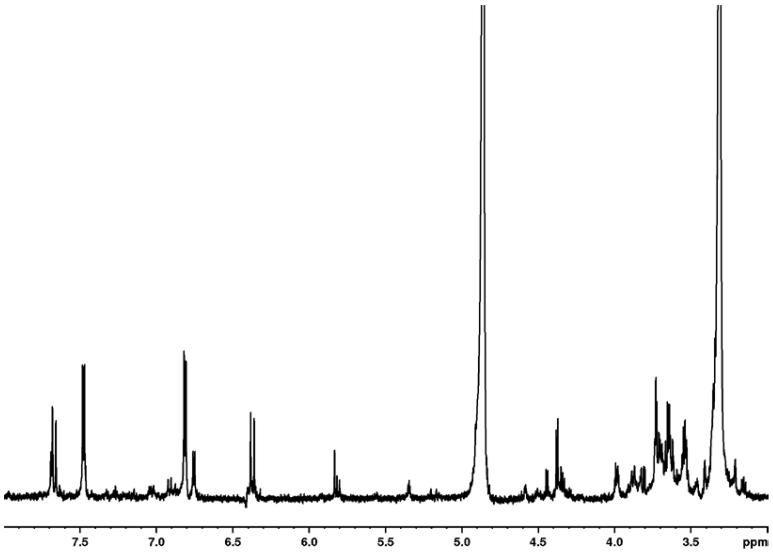

Figure S1.3 Compound **1**, ^{1}H-NMR spectrum (700 MHz, MeOH-d_4)

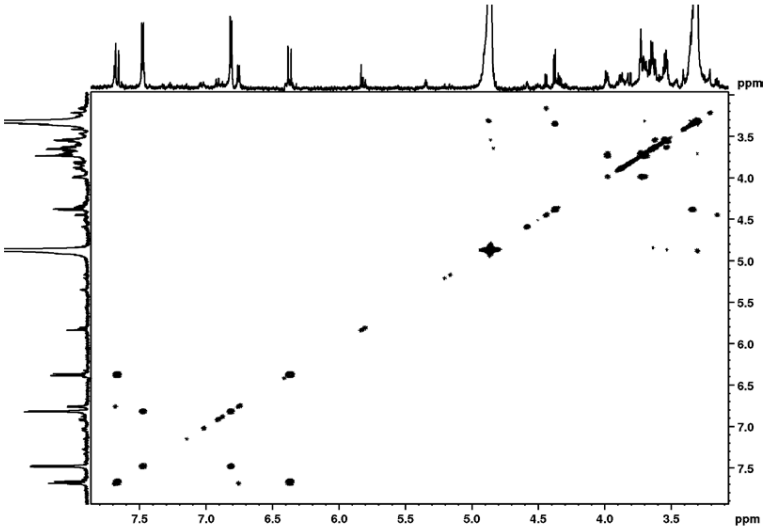

Figure S1.4 Compound **1**, ^{1}H-^{1}H COSY spectrum (700 MHz, MeOH-d_4)

CLX

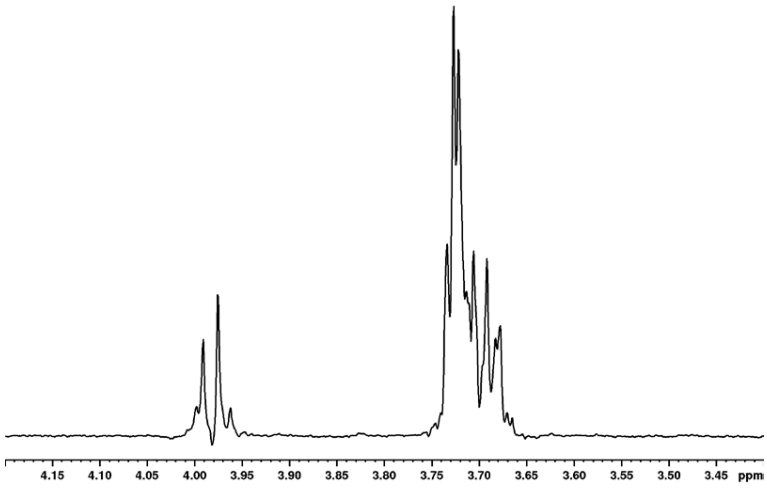

Figure S1.5 Compound **1**, selective 1D TOCSY spectrum (700 MHz, MeOH-d_4, o1p = 3.98 ppm)

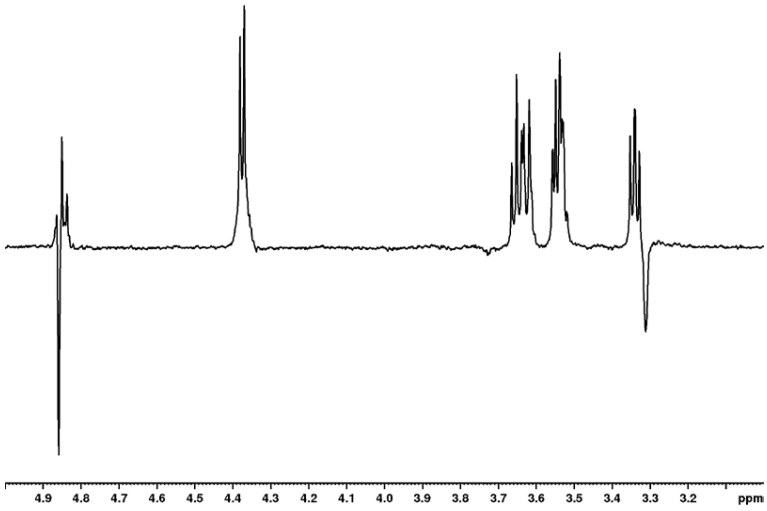

Figure S1.6 Compound **1**, selective 1D TOCSY spectrum (700 MHz, MeOH-d_4, o1p = 4.38 ppm)

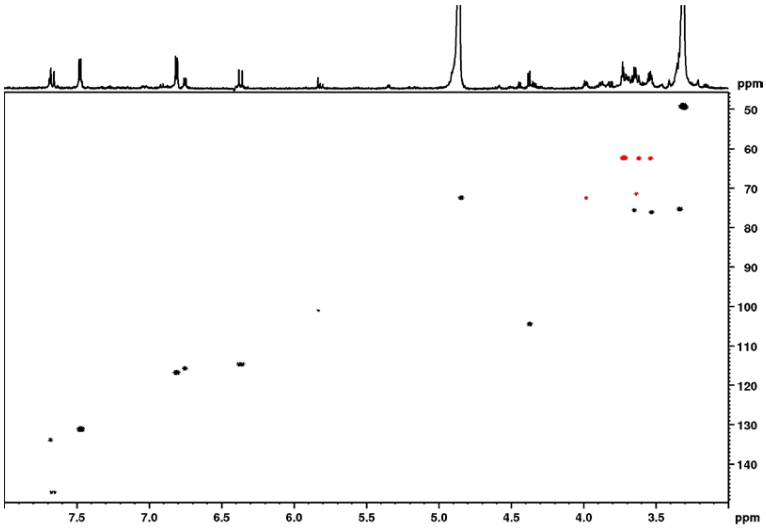

Figure S1.7 Compound **1**, ^{1}H-^{13}C HSQC spectrum (700 MHz, MeOH-d_4)

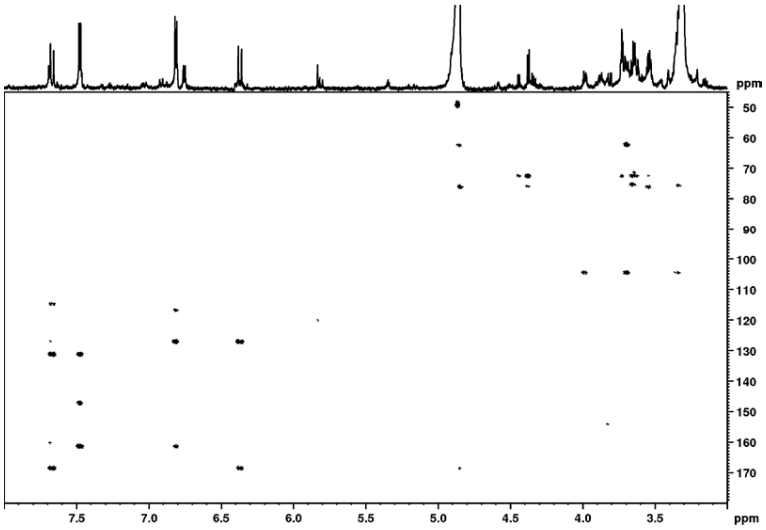

Figure S1.8 Compound **1**, ^{1}H-^{13}C HMBC spectrum (700 MHz, MeOH-d_4)

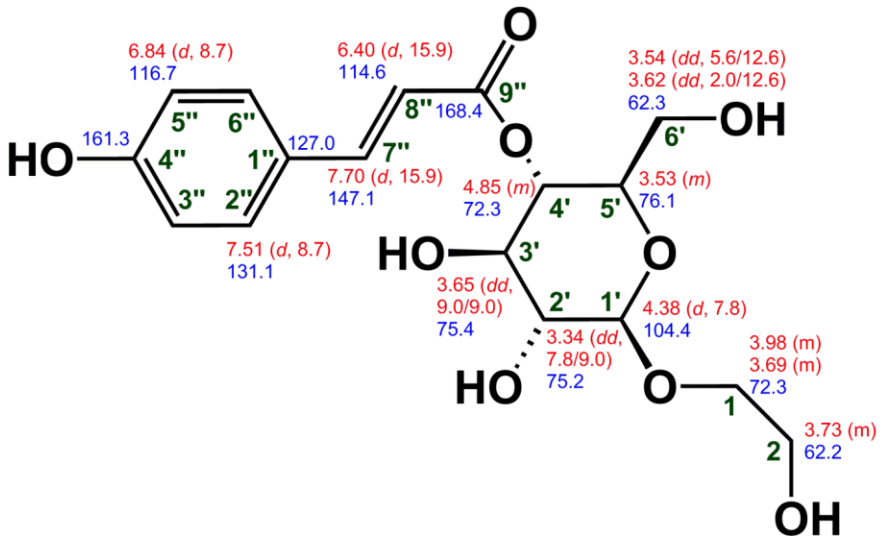

Figure S1.9 Compound **1**, structure with chemical shifts

2. **Supplementary data of 1-*O*-(3-hydroxymethylphenyl)-4-*O*-(*E*)-*p*-coumaroyl-*β*-glucopyranose (2):**

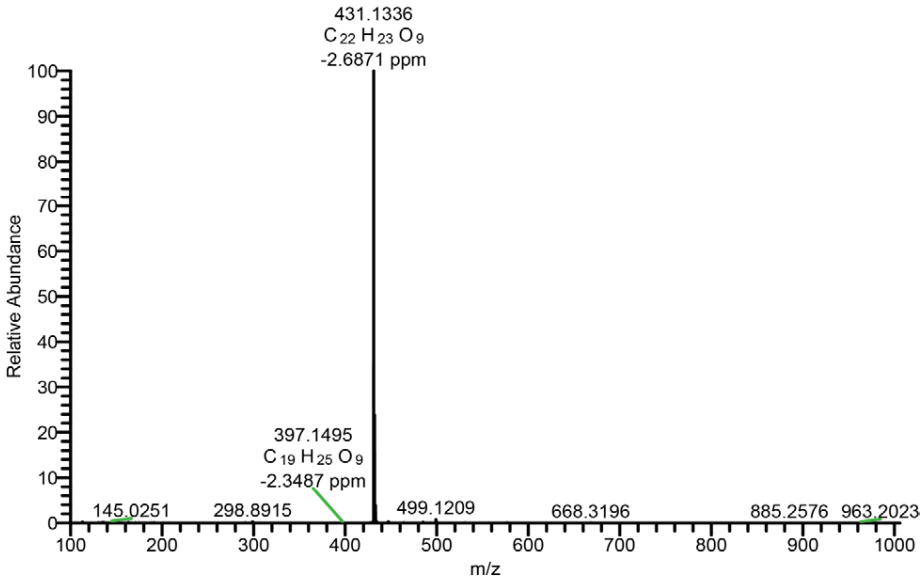

HRMS (-p ESI)
431.1336 $[M-H]^-$ (100)
432.1366 $[M-H]^-$ (24.07)
433.1388 $[M-H]^-$ (3.82)

Figure S2.1 Compound **2,** HRESI-MS data

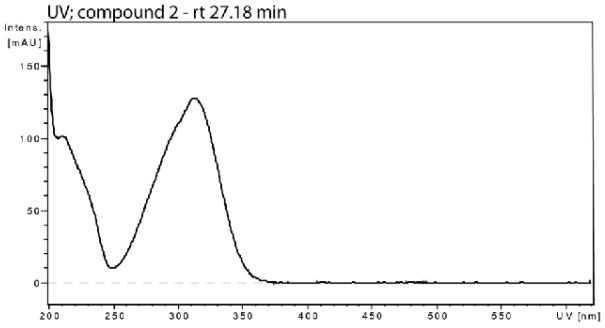

Figure S2.2 Compound **2**, UV-Vis spectrum

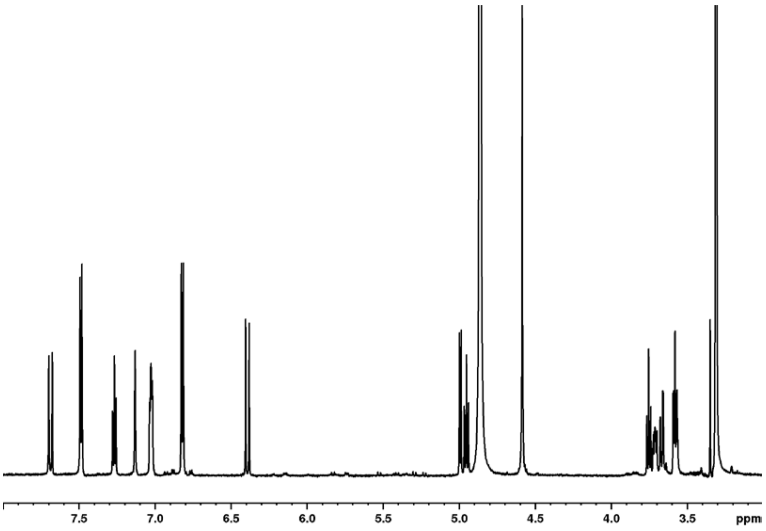

Figure S2.3 Compound **2**, ^{1}H-NMR spectrum (700 MHz, MeOH-d_4)

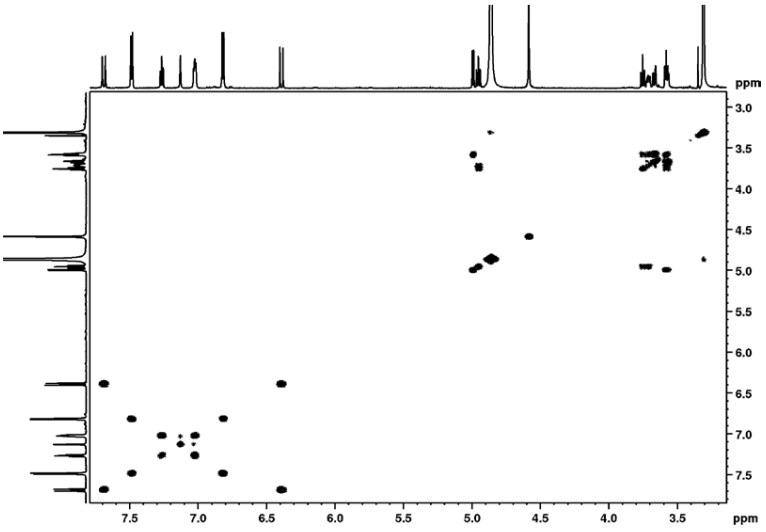

Figure S2.4 Compound **2**, ^{1}H-^{1}H COSY spectrum (700 MHz, MeOH-d_4)

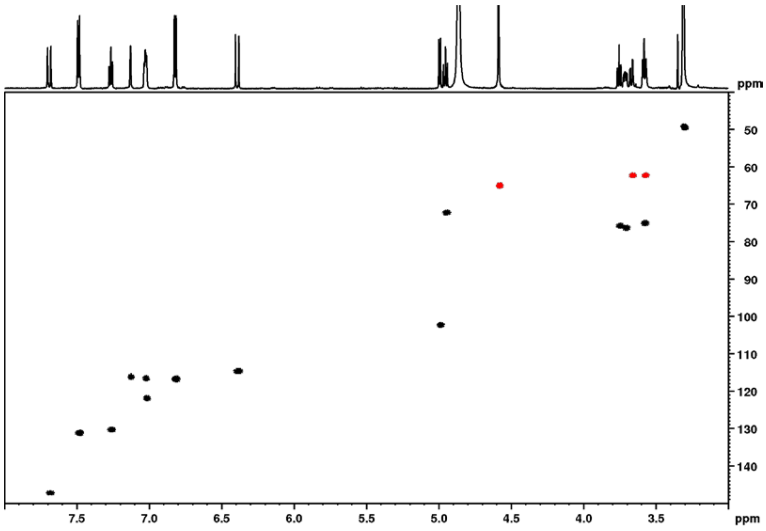

Figure S2.5 Compound **2**, ^{1}H-^{13}C HSQC spectrum (700 MHz, MeOH-d_4)

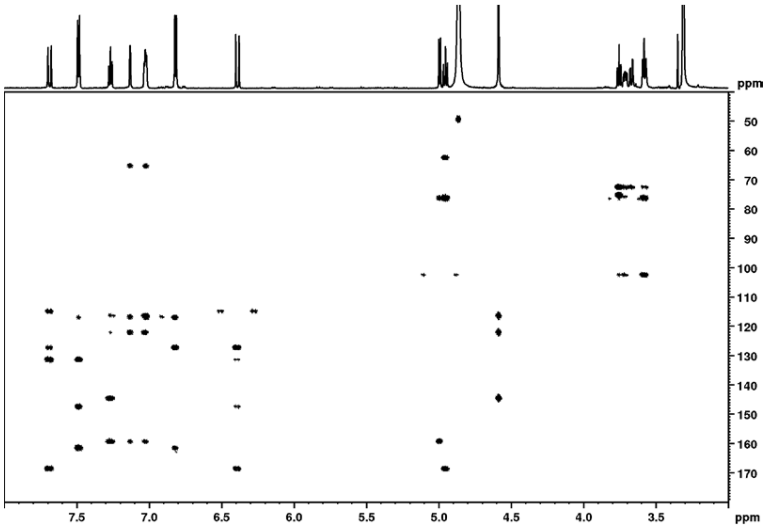

Figure S2.6 Compound **2**, ^{1}H-^{13}C HMBC spectrum (700 MHz, MeOH-d_4)

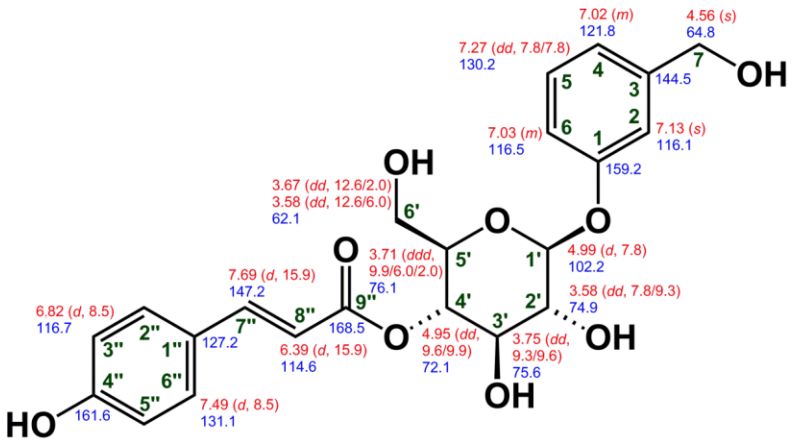

Figure S2.7 Compound **2**, structure with chemical shifts

3. **Supplementary data of 1-*O*-(3-hydroxymethylphenyl)-4-*O*-(*Z*)-*p*-coumaroyl-*β*-glucopyranose (3):**

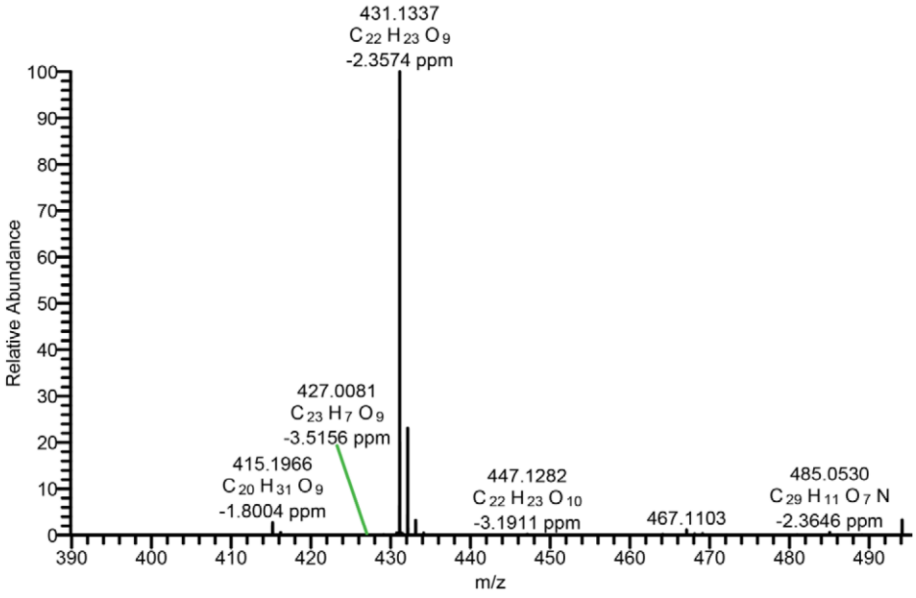

HRMS (-p ESI)
431.1337 $[M-H]^-$ (100)
432.1371 $[M-H]^-$ (23.66)
433.1394 $[M-H]^-$ (3.27)

Figure S3.1 Compound **3,** HRESI-MS data

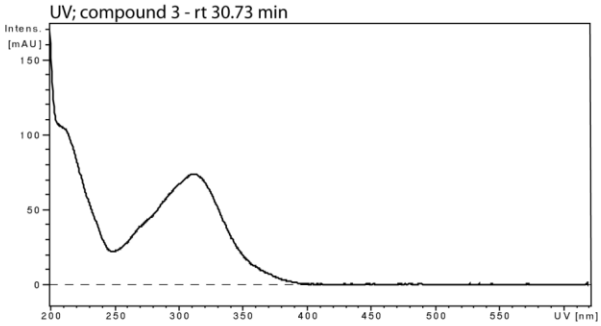

Figure S3.2 Compound **3**, UV-Vis spectrum

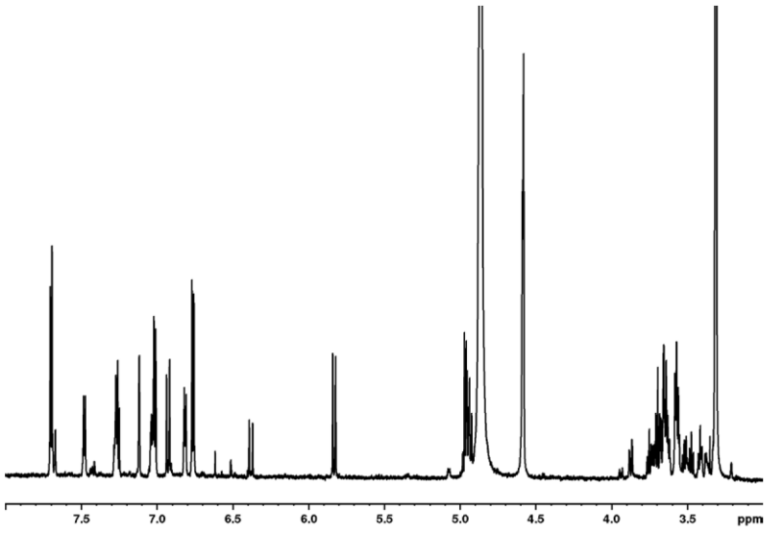

Figure S3.3 Compound **3**, ^{1}H-NMR spectrum (700 MHz, MeOH-d_4)

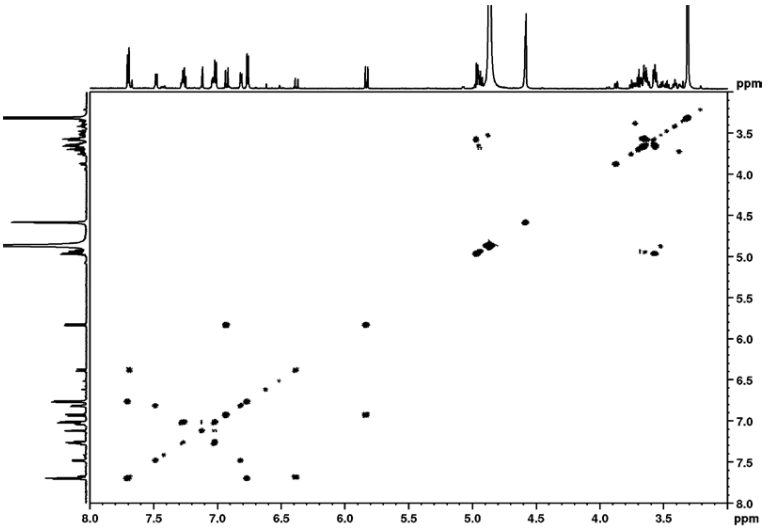

Figure S3.4 Compound **3**, ^{1}H-^{1}H COSY spectrum (700 MHz, MeOH-d_4)

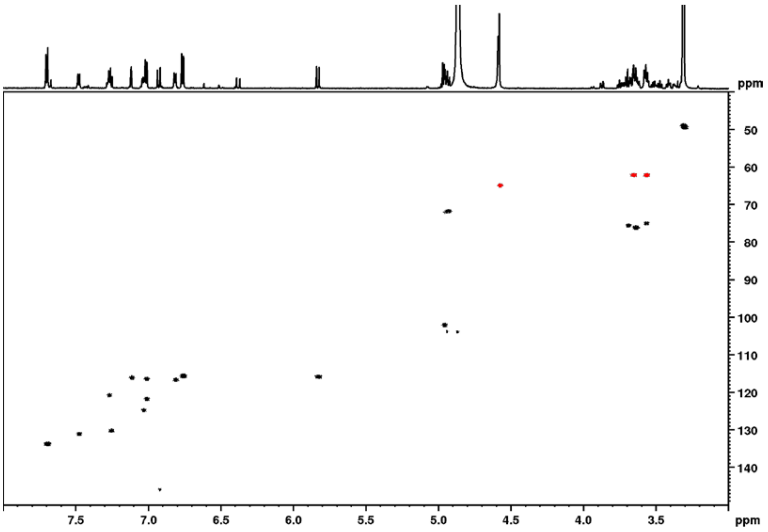

Figure S3.5 Compound **3**, ^{1}H-^{13}C HSQC spectrum (700 MHz, MeOH-d_4)

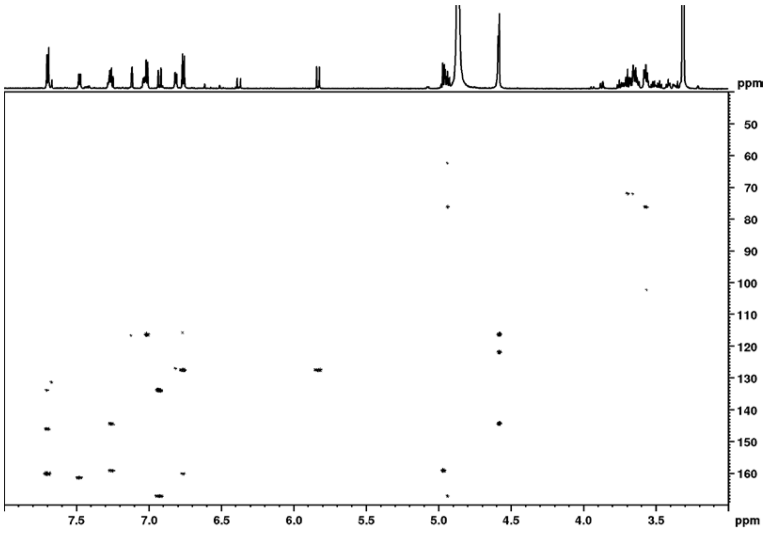

Figure S3.6 Compound 3, ^{1}H-^{13}C HMBC spectrum (700 MHz, MeOH-d_4)

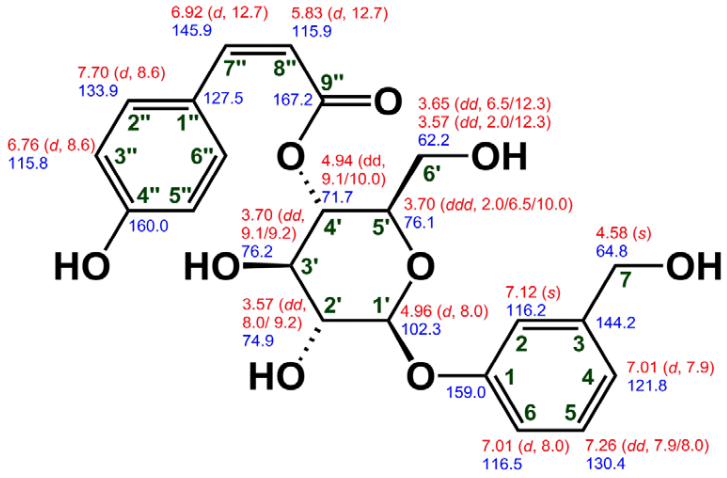

Figure S3.7 Compound 3, structure with chemical shifts

4. **Supplementary data of 1-*O*-(6-hydroxy-2-hydroxymethylphenyl)-4-*O*-(*E*)-*p*-coumaroyl-*β*-glucopyranose (4):**

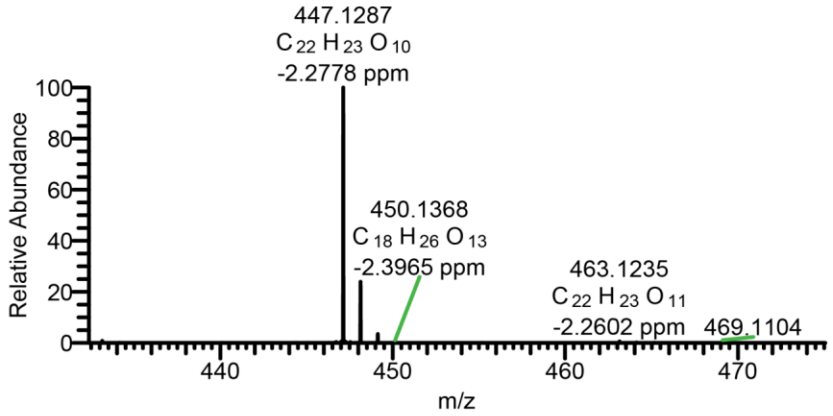

HRMS (-p ESI)
447.1287 $[M-H]^-$ (100)
448.1320 $[M-H]^-$ (23.20)
449.1342 $[M-H]^-$ (3.40)

Figure S4.1 Compound **4**, HRESI-MS data

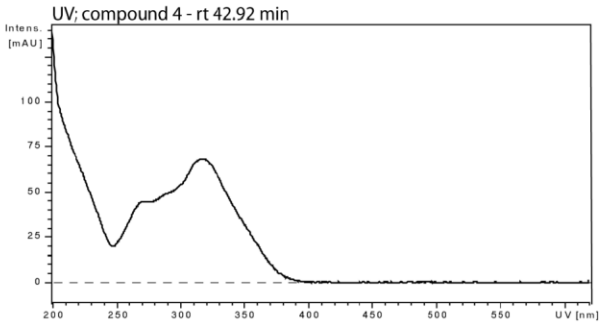

Figure S4.2 Compound **4**, UV-Vis spectrum

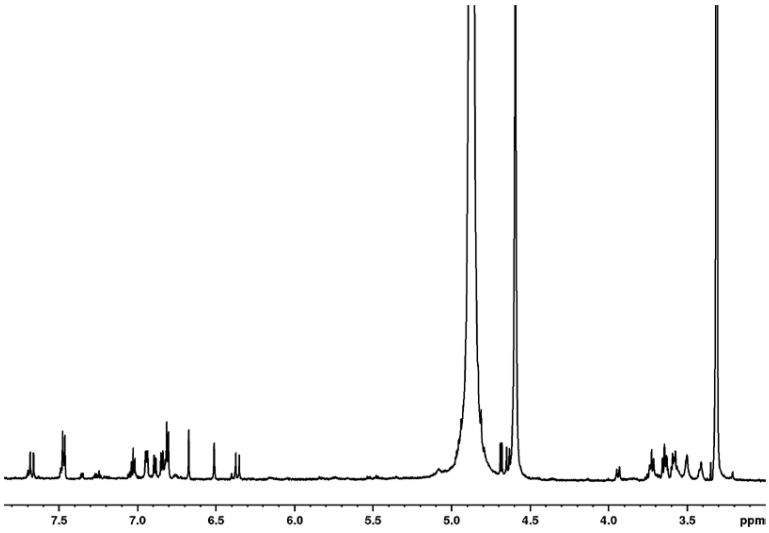

Figure S4.3 Compound **4**, ^{1}H-NMR spectrum (700 MHz, MeOH-d_4)

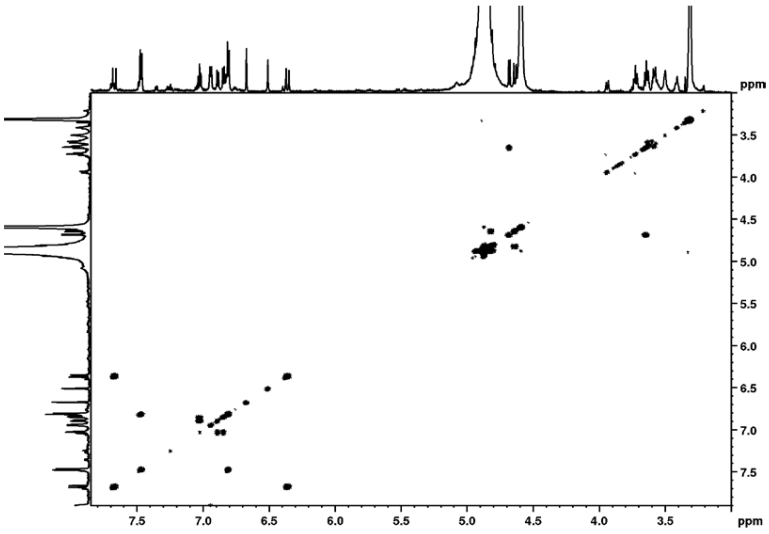

Figure S4.4 Compound **4**, ^{1}H-^{1}H COSY spectrum (700 MHz, MeOH-d_4)

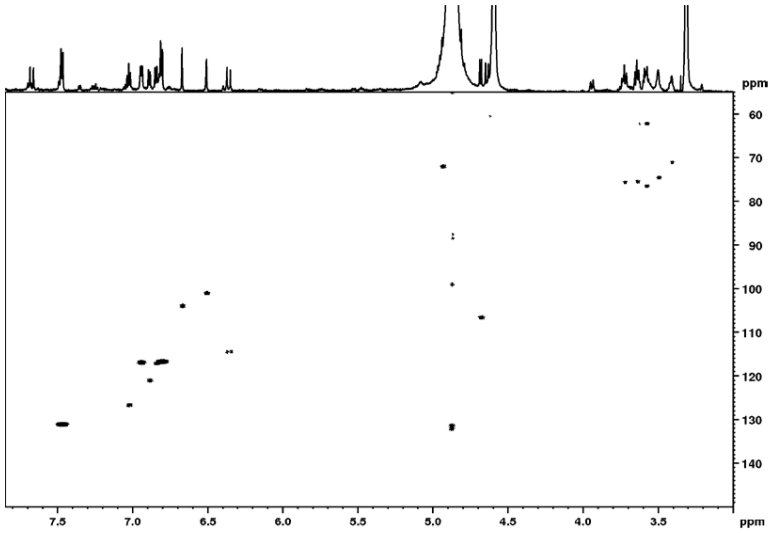

Figure S4.5 Compound **4**, ^{1}H-^{13}C HSQC spectrum (700 MHz, MeOH-d_4)

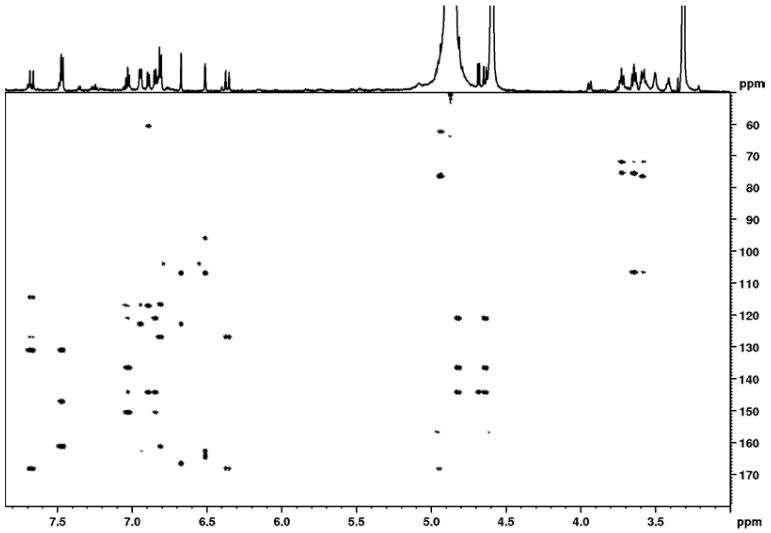

Figure S4.6 Compound **4**, ^{1}H-^{13}C HMBC spectrum (700 MHz, MeOH-d_4)

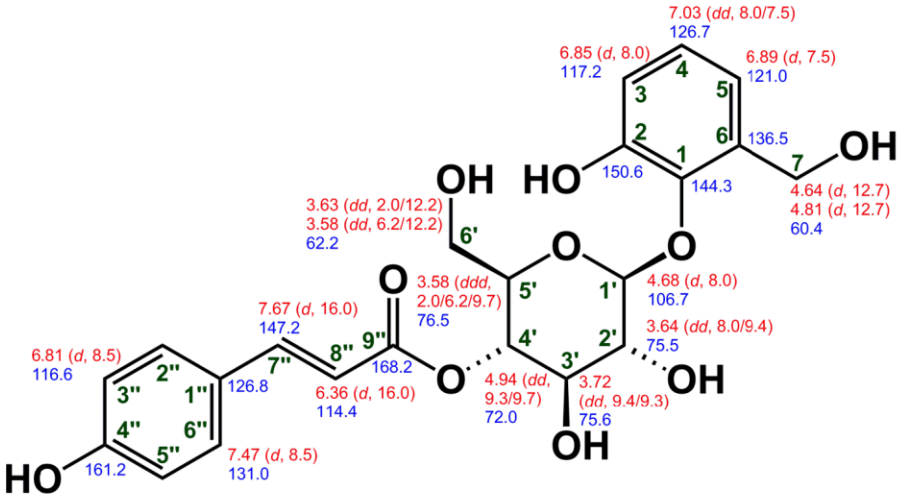

Figure S4.7 Compound **4**, structure with chemical shifts

5. **Supplementary data of 1-*O*-(2-hydroxyphenyl)-4-*O*-(*Z*)-*p*-coumaroyl-*β*-glucopyranose (5):**

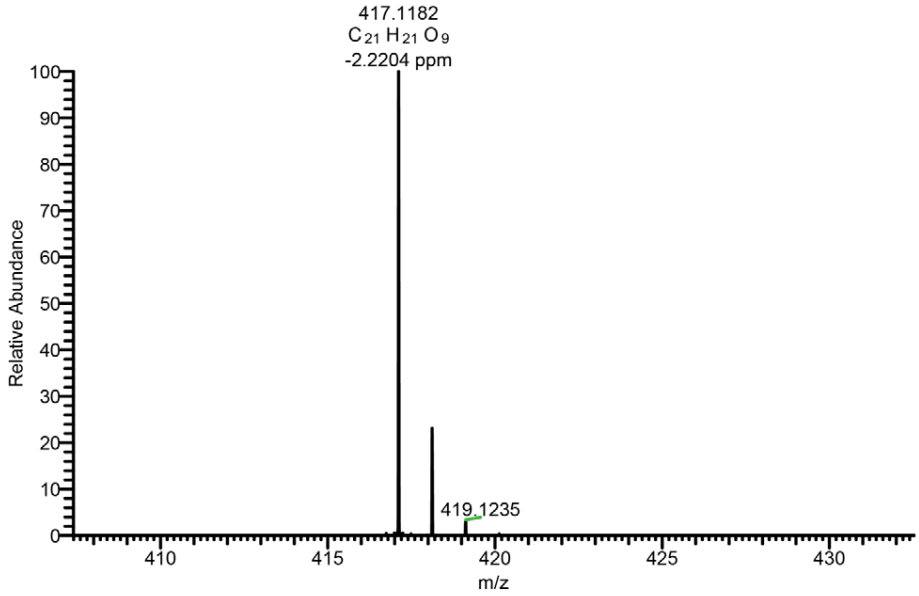

HRMS (-p ESI)
417.1182 $[M-H]^-$ (100)
418.1214 $[M-H]^-$ (23.03)
419.1235 $[M-H]^-$ (3.15)

Figure S5.1 Compound **5**, HRESI-MS data

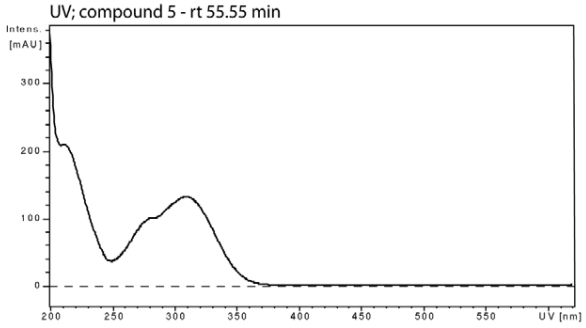

Figure S5.2 Compound **5**, UV-Vis spectrum

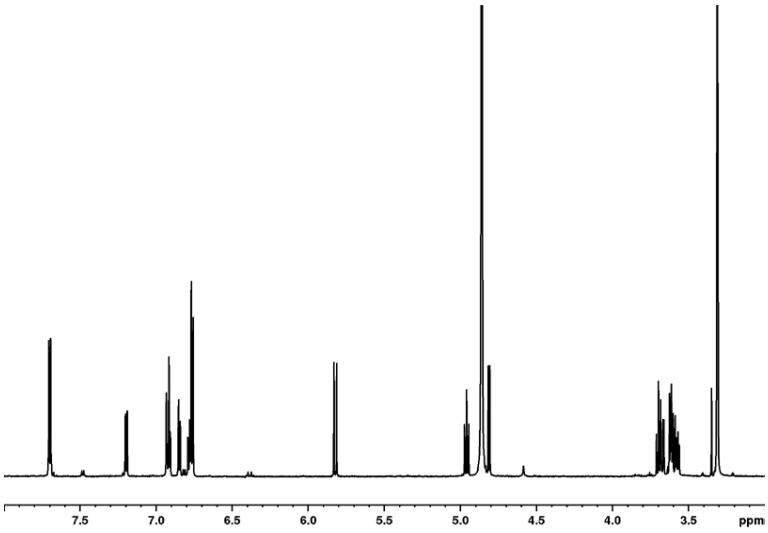

Figure S5.3 Compound **5**, ^{1}H-NMR spectrum (700 MHz, MeOH-d_4)

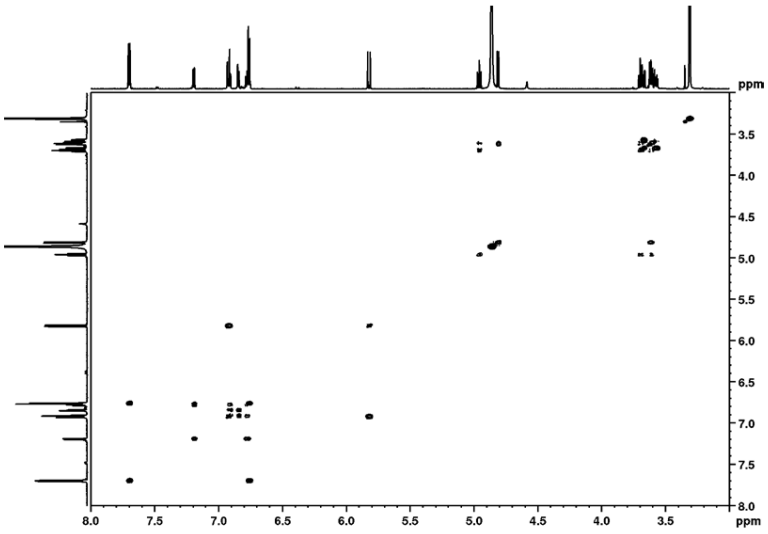

Figure S5.4 Compound **5**, ^{1}H-^{1}H COSY spectrum (700 MHz, MeOH-d_4)

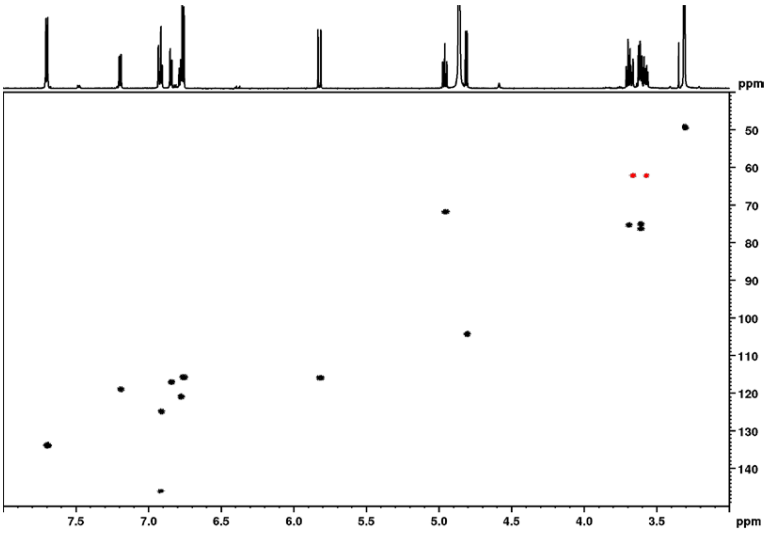

Figure S5.5 Compound **5**, ^{1}H-^{13}C HSQC spectrum (700 MHz, MeOH-d_4)

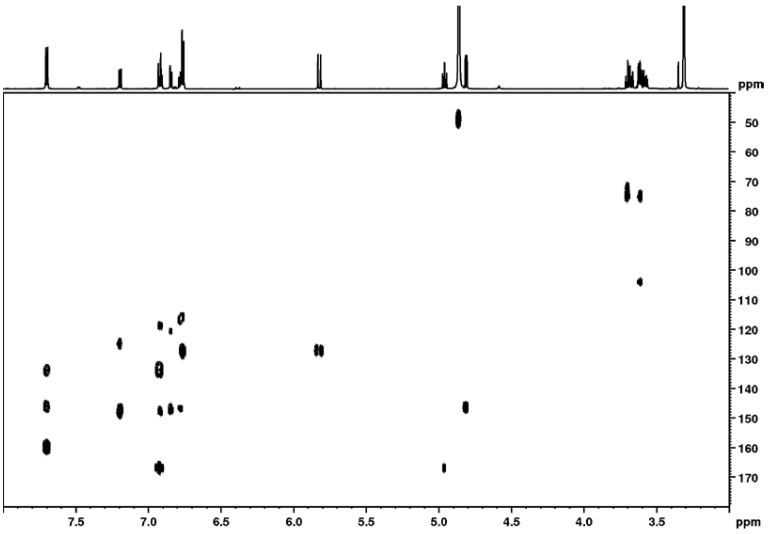

Figure S5.6 Compound **5**, ^{1}H-^{13}C HMBC spectrum (700 MHz, MeOH-d_4)

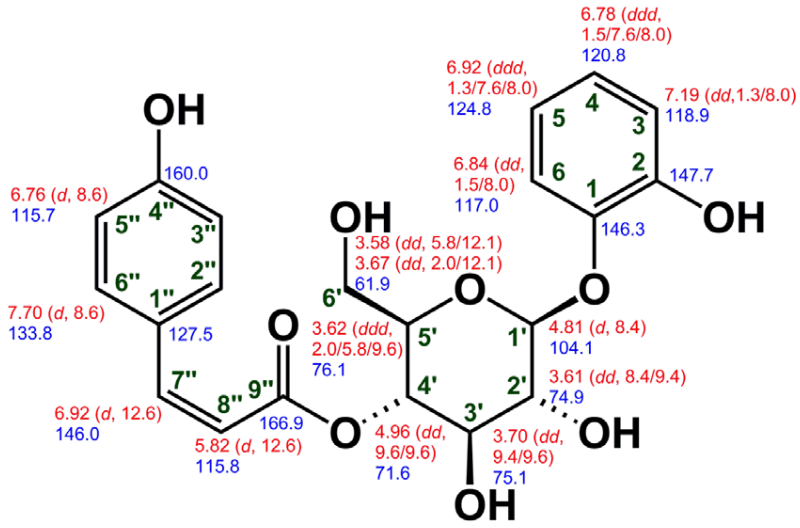

Figure S5.7 Compound **5**, structure with chemical shifts

6. Supplementary data of 4'-*O*-(*E*)-*p*-coumaroyl-idescarpin (6):

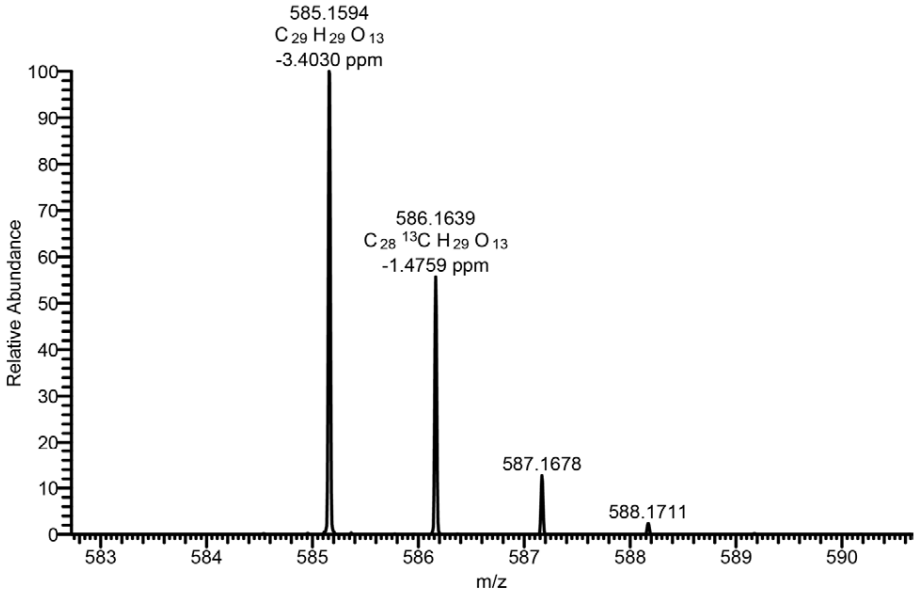

HRMS (-p ESI)
585.1593 $[M-H]^-$ (100)
586.1638 $[M-H]^-$ (54.56)
587.1678 $[M-H]^-$ (12.47)
588.1711 $[M-H]^-$ (2.35)

Figure S6.1 Compound **6**, HRESI-MS data

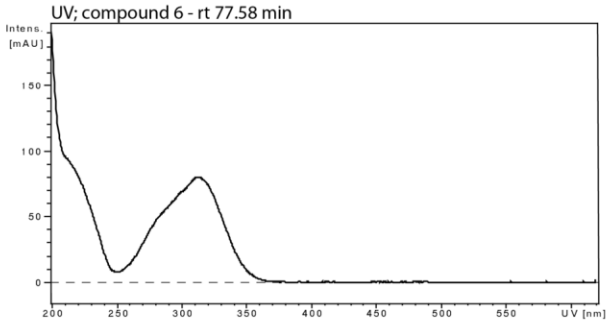

Figure S6.2 Compound **6**, UV-Vis data

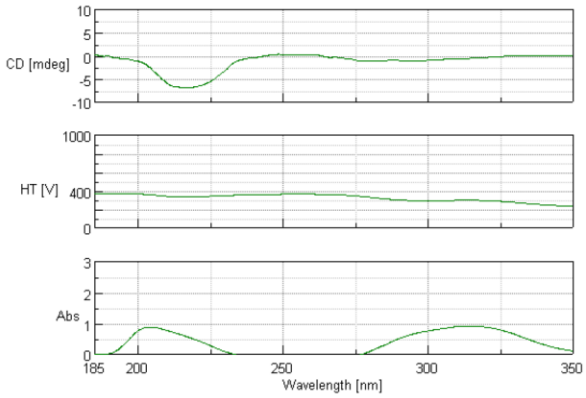

Figure S6.3 Compound **6**, CD data

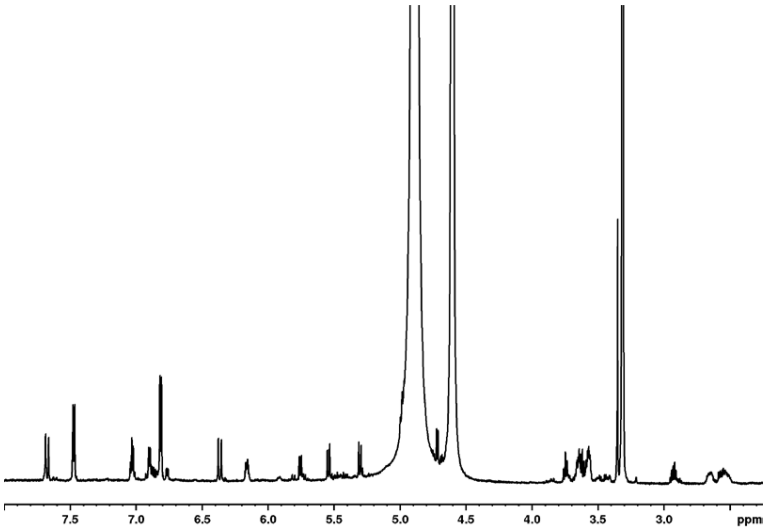

Figure S6.4 Compound **6**, ^{1}H-NMR spectrum (700 MHz, MeOH-d_4)

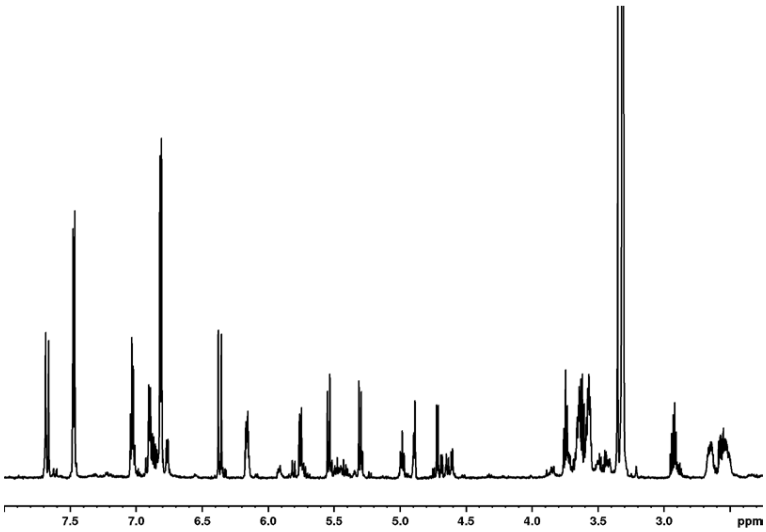

Figure S6.5 Compound **6**, 1D NOESY NMR spectrum (700 MHz, MeOH-d_4, o1p = 4.89 ppm)

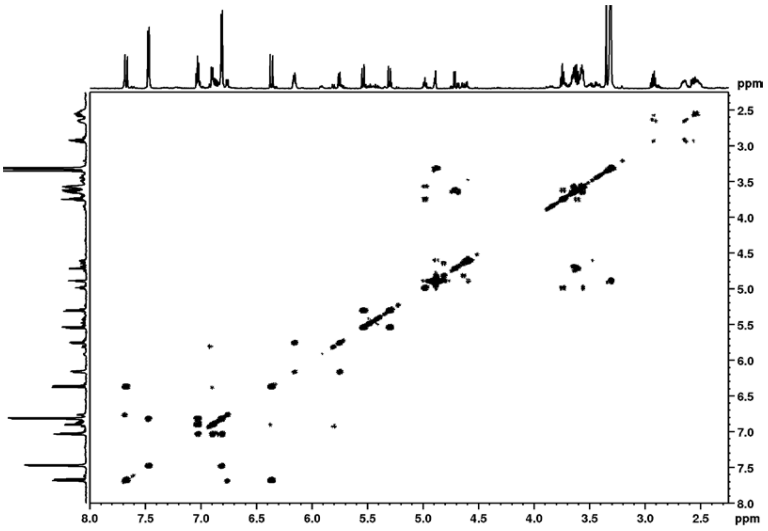

Figure S6.6 Compound **6**, ^{1}H-^{1}H COSY spectrum (700 MHz, MeOH-d_4)

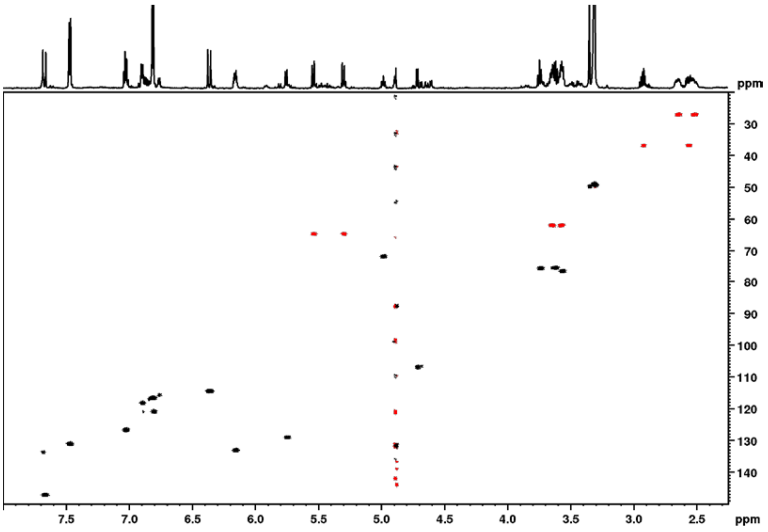

Figure S6.7 Compound **6**, ^{1}H-^{13}C HSQC spectrum (700 MHz, MeOH-d_4)

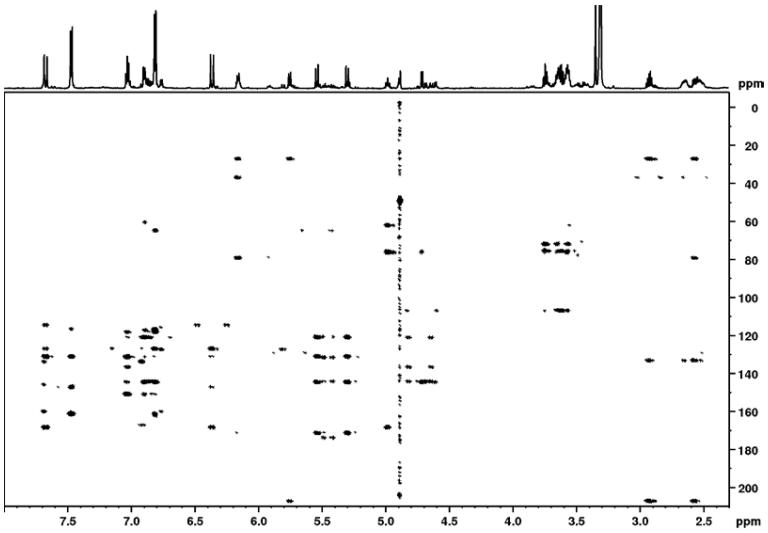

Figure S6.8 Compound **6**, ^{1}H-^{13}C HMBC spectrum (700 MHz, MeOH-d_4)

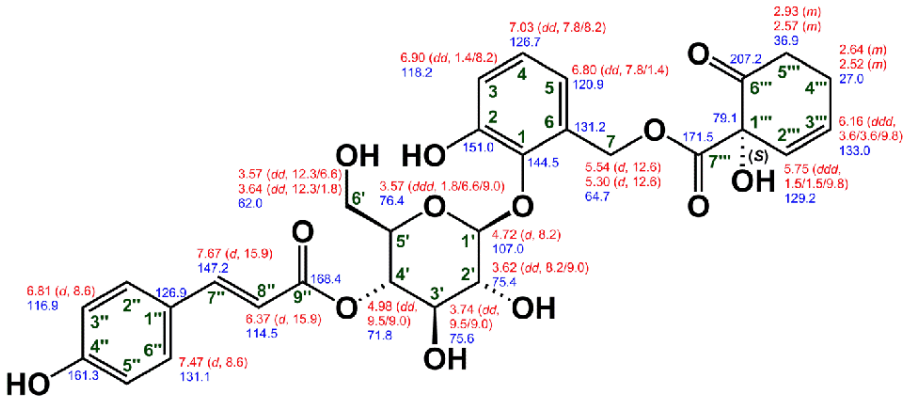

Figure S6.9 Compound **6**, structure with chemical shifts

7. Supplementary data of 4'-*O*-(*Z*)-*p*-coumaroyl-idescarpin (7):

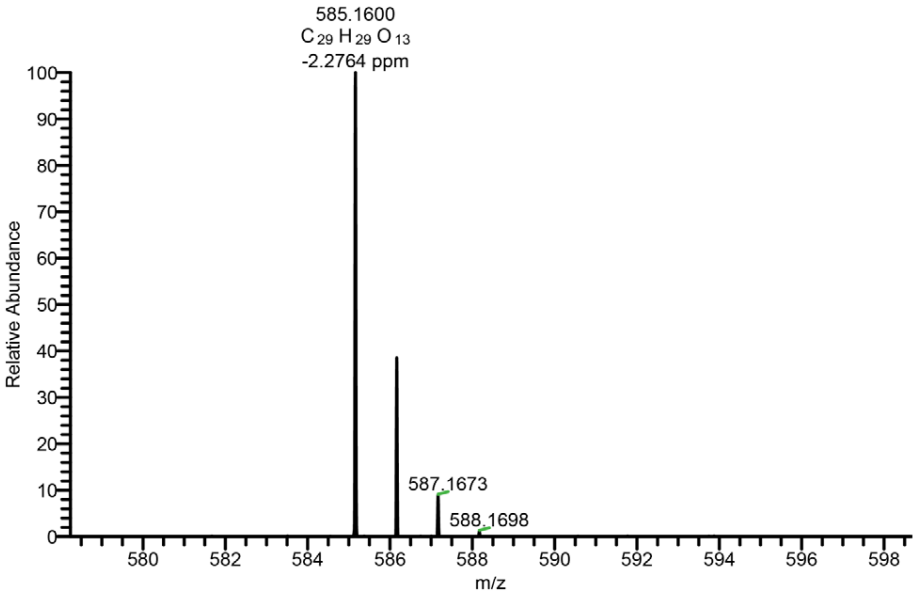

HRMS (-p ESI)
585.1601 $[M-H]^-$ (100)
586.1641 $[M-H]^-$ (37.32)
587.1674 $[M-H]^-$ (8.25)
588.1701 $[M-H]^-$ (1.08)

Figure S7.1 Compound **7**, HRESI-MS data

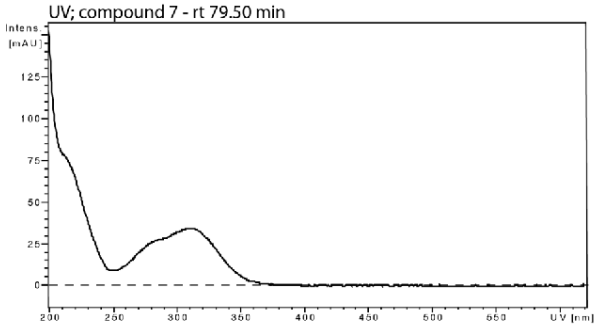

Figure S7.2 Compound **7**, UV-Vis data

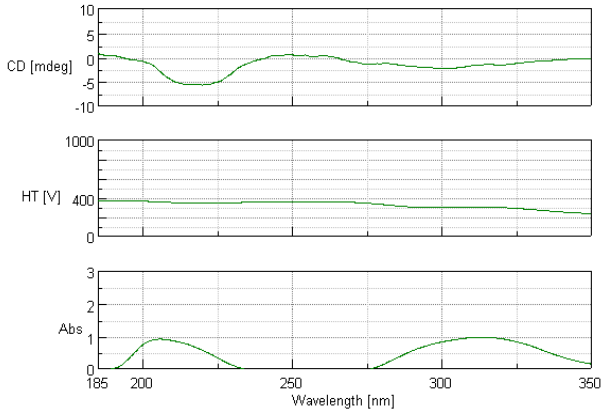

Figure S7.3 Compound **7,** CD data

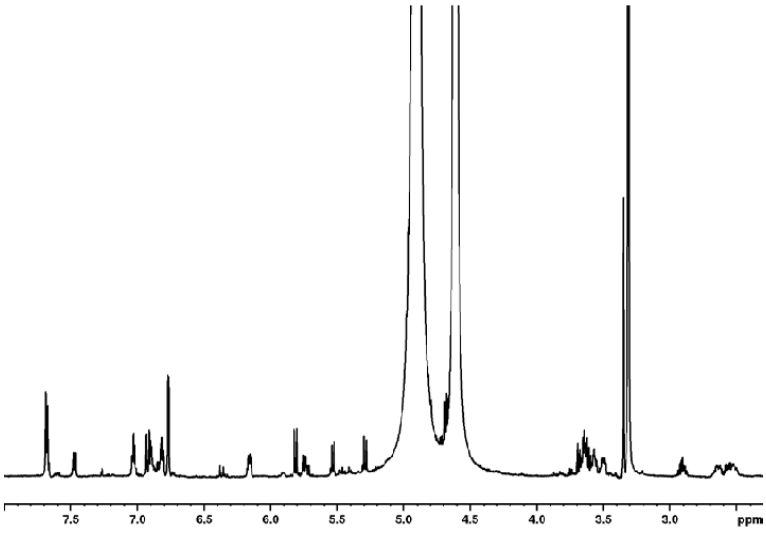

Figure S7.4 Compound **7**, ^{1}H-NMR spectrum (700 MHz, MeOH-d_4)

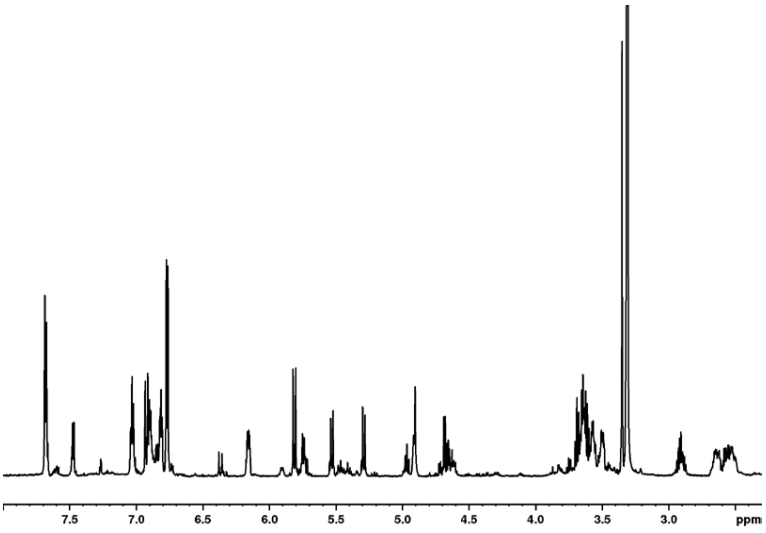

Figure S7.5 Compound **7**, 1D NOESY NMR spectrum (700 MHz, MeOH-d_4, o1p = 4.89 ppm)

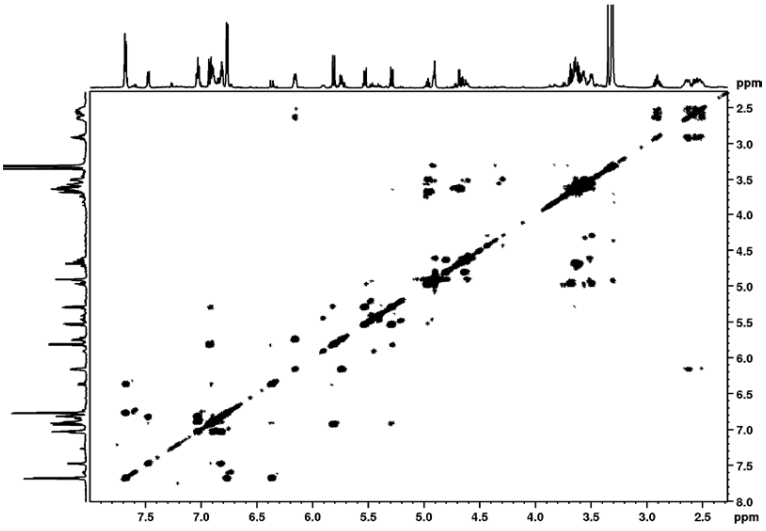

Figure S7.6 Compound **7**, ^{1}H-^{1}H COSY spectrum (700 MHz, MeOH-d_4)

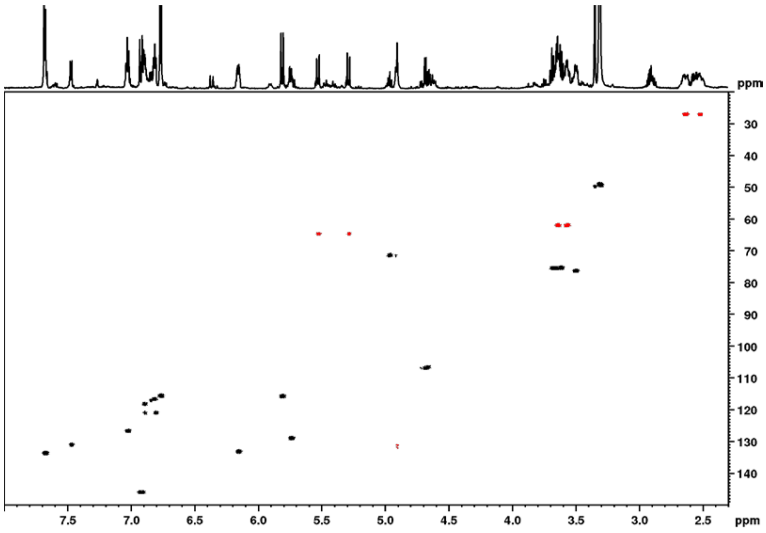

Figure S7.7 Compound **7**, ^{1}H-^{13}C HSQC spectrum (700 MHz, MeOH-d_4)

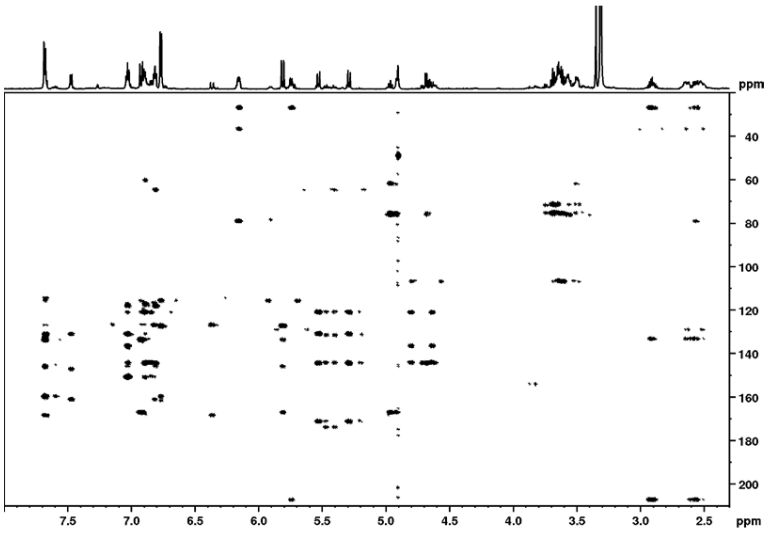

Figure S7.8 Compound **7**, ^{1}H-^{13}C HMBC spectrum (700 MHz, MeOH-d_4)

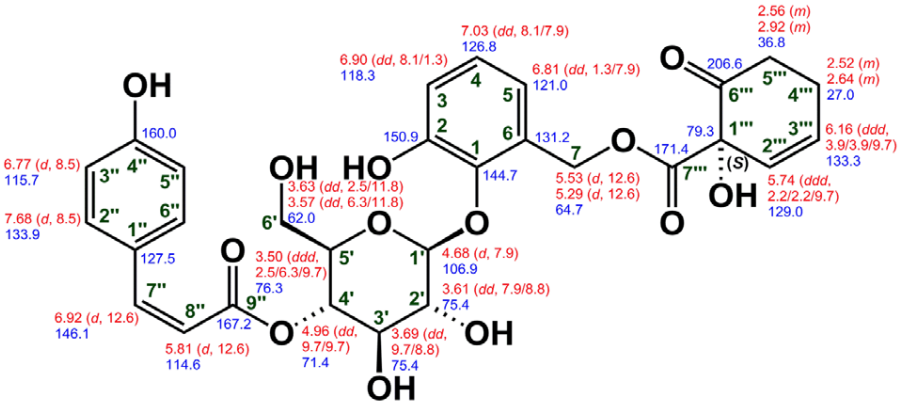

Figure S7.9 Compound **7**, structure with chemical shifts

8. **Supplementary data of 4'-*O*-(*E*)-*p*-coumaroyl-salicortin (8) & 4'-*O*-(*Z*)-*p*-coumaroyl-salicortin (9):**

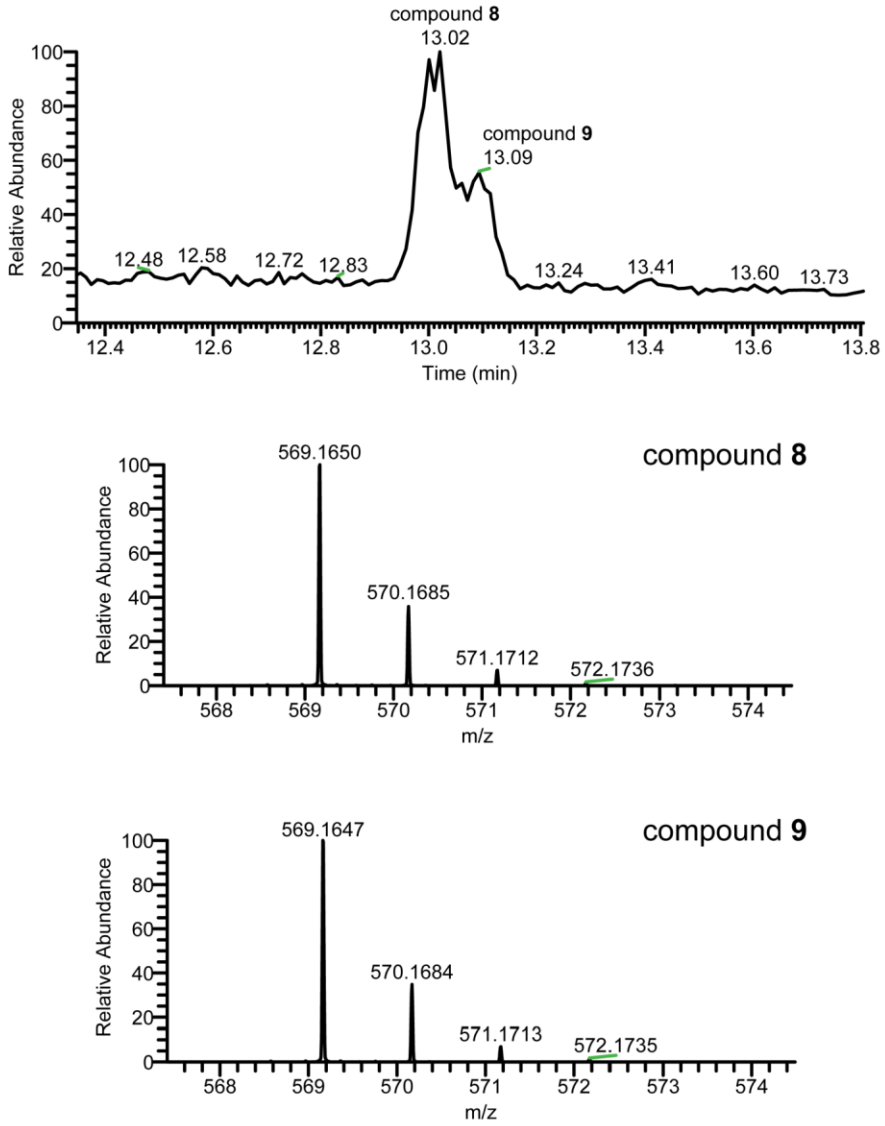

Figure S8.1 UPLC-HRESI MS total ion chromatogram (top) and MS-spectra of compound **8** and compound **9** (middle and bottom)

HRMS (-p ESI)
569.1650 $[M-H]^-$ (100)
570.1685 $[M-H]^-$ (34.81)
571.1712 $[M-H]^-$ (7.01)
572.1736 $[M-H]^-$ (0.95)

Figure S8.2 Compound **8**, extracted HRESI-MS data

HRMS (-p ESI)
569.1652 $[M-H]^-$ (100)
570.1691 $[M-H]^-$ (34.73)
571.1713 $[M-H]^-$ (6.28)
572.1729 $[M-H]^-$ (0.79)

Figure S8.3 Compound **9**, extracted HRESI-MS data

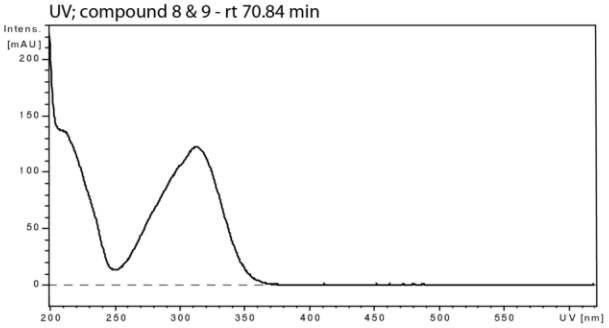

Figure S8.4 Compound **8** & **9**, UV-Vis data

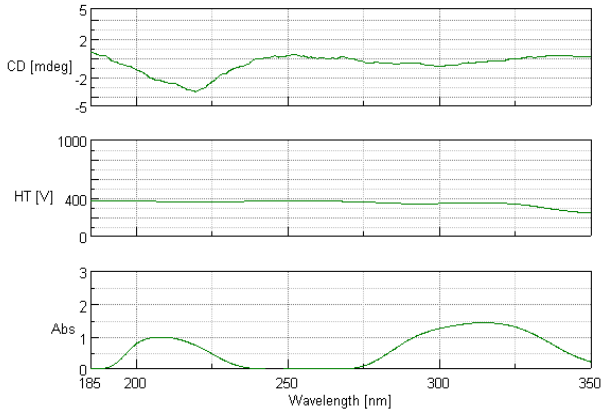

Figure S8.5 Compound **8** & **9**, CD data

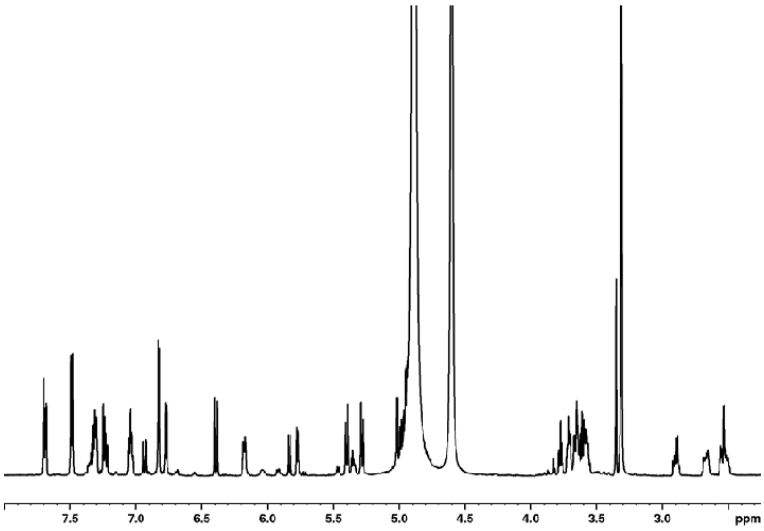

Figure S8.6 Compound **8** & **9**, ^{1}H-NMR spectrum (700 MHz, MeOH-d_4)

CXC

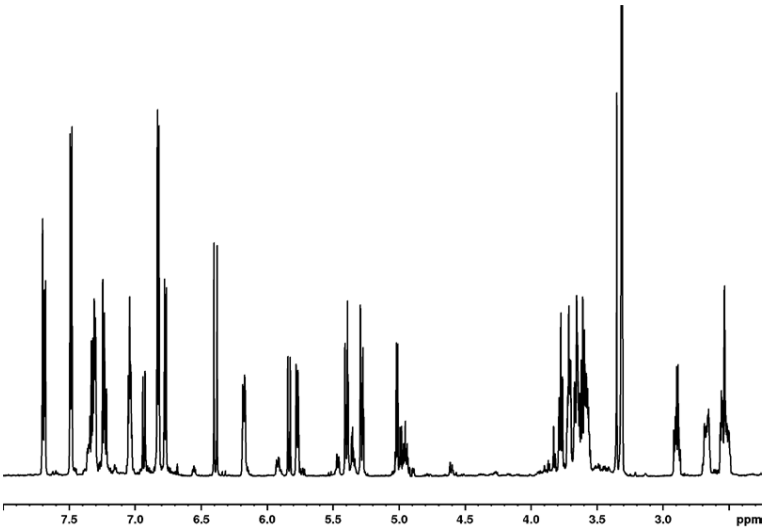

Figure S8.7 Compound **8** & **9**, 1D NOESY NMR spectrum (700 MHz, MeOH-d_4, o1p = 4.89 ppm)

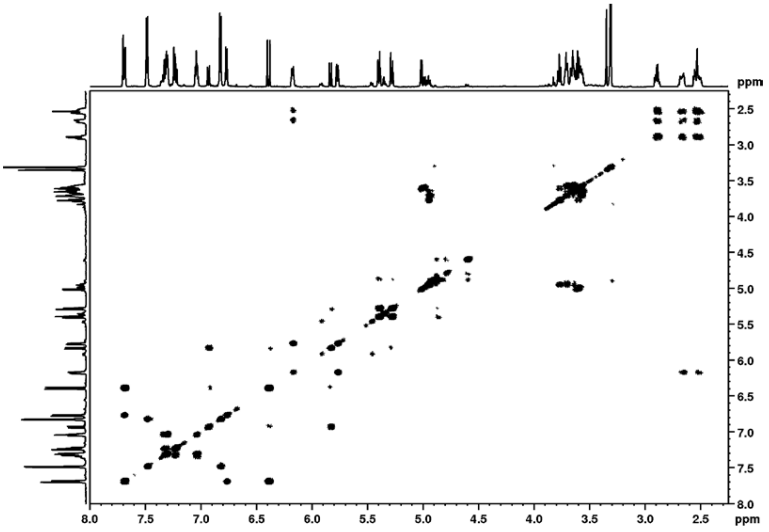

Figure S8.8 Compound **8** & **9**, ^{1}H-^{1}H COSY spectrum (700 MHz, MeOH-d_4)

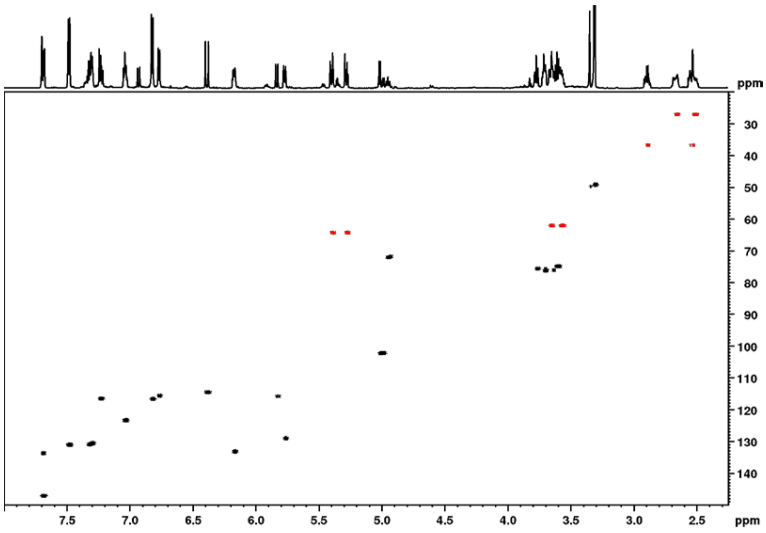

Figure S8.9 Compound **8** & **9**, ^{1}H-^{13}C HSQC spectrum (700 MHz, MeOH-d_4)

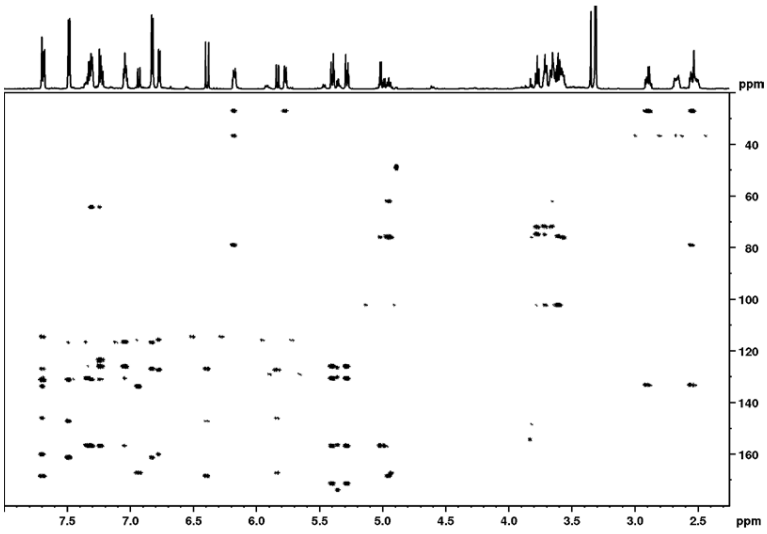

Figure S8.10 Compound **8** & **9**, ^{1}H-^{13}C HMBC spectrum (700 MHz, MeOH-d_4)

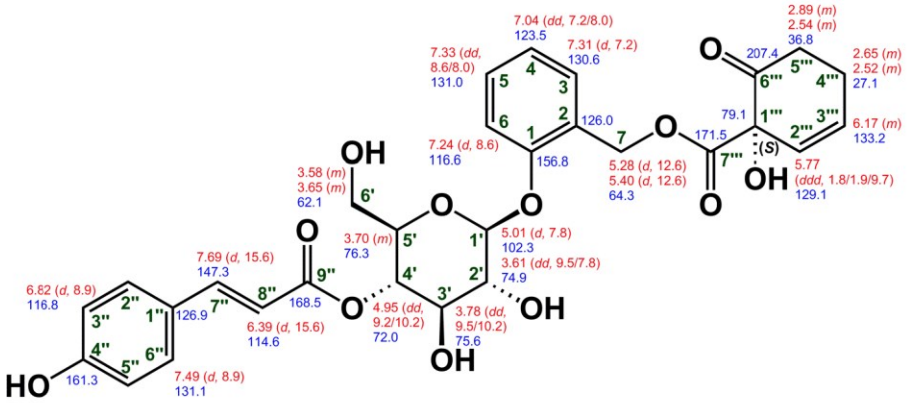

Figure S8.11 Compound **8**, structure with chemical shifts

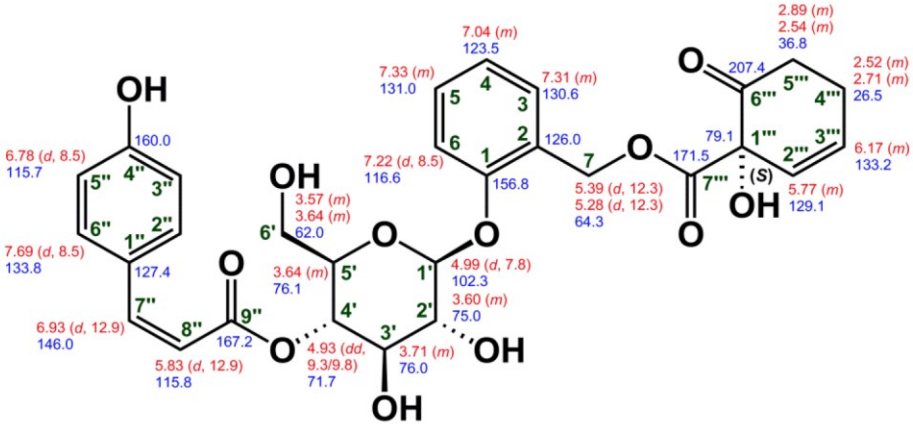

Figure S8.12 Compound **9**, structure with chemical shifts

9. Supplementary data of icaraside B2 (10):

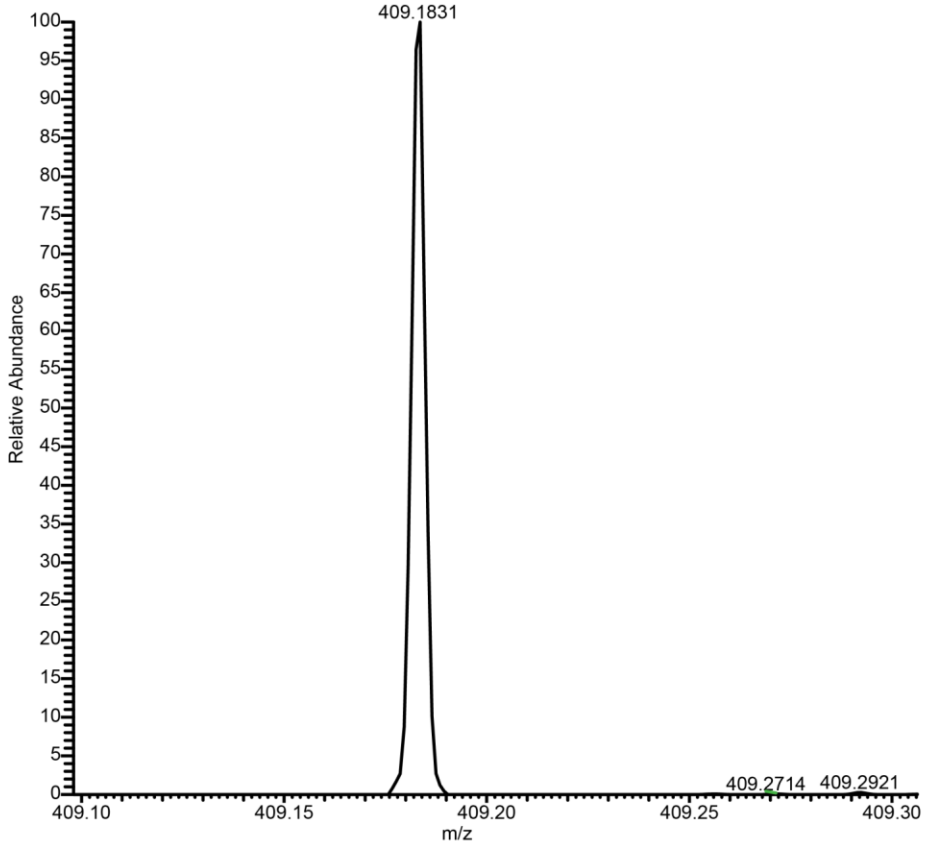

HRMS (+p ESI)
409.1831 $[M+Na]^+$ (100)
410.1866 $[M+Na]^+$ (21.44)
411.1886 $[M+Na]^+$ (2.26)

Figure S9.1 Icaraside B2 (**10**), HRESI-MS data

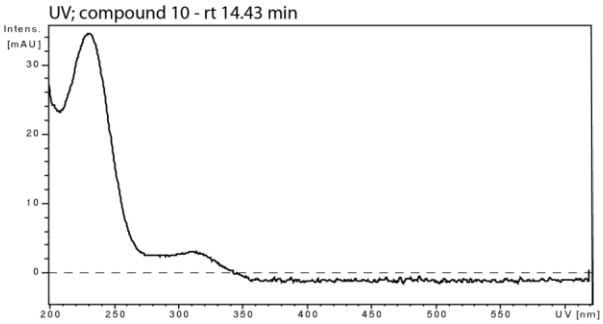

Figure S9.2 Icaraside B2 (**10**), UV-Vis data

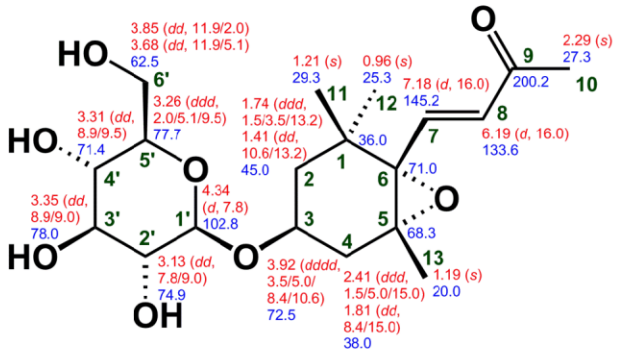

Figure S9.3 Icaraside B2 (**10**), structure with chemical shifts

Analytical data in accordance with:

Lee, S., 2012. A new megastigmane glucoside from the aerial parts of *Erythronium japonicum*. Nat. Prod. Sci. 18, 166-170.

Otsuka, H., Kamada, K., Yao, M., Yuasa, K., Kida, I., Takeda, Y., 1995. Alangionosides C-F, megastigmane glycosides from *Alangium premnifolium*. Phytochemistry 38, 1431-1435.

10. Supplementary data of 4-(*E*)-*p*-coumaroyl-D-glucopyranose (11):

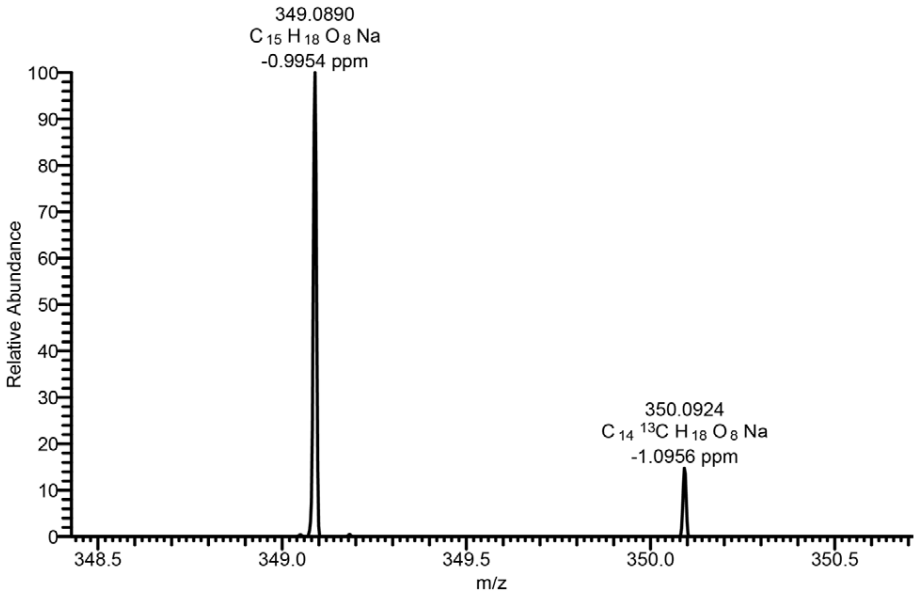

HRMS (+p ESI)
349.0890 $[M+Na]^+$ (100)
350.0924 $[M+Na]^+$ (14.80)
351.0653 $[M+Na]^+$ (4.96)

Figure S10.1 4-(*E*)-*p*-Coumaroyl-D-glucopyranose (**11**), HRESI-MS data

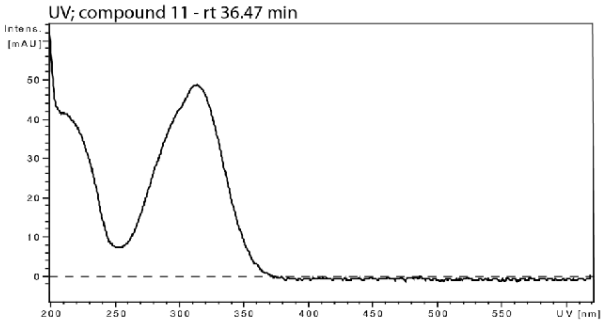

Figure S10.2 4-(*E*)-*p*-Coumaroyl-D-glucopyranose (**11**), UV-Vis data

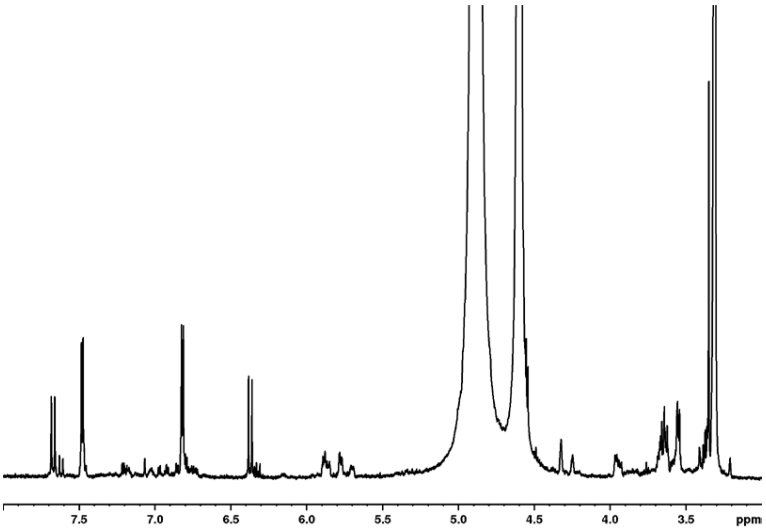

Figure S10.3 4-(*E*)-*p*-Coumaroyl-D-glucopyranose (**11**), ^{1}H-NMR spectrum (700 MHz, MeOH-d_4)

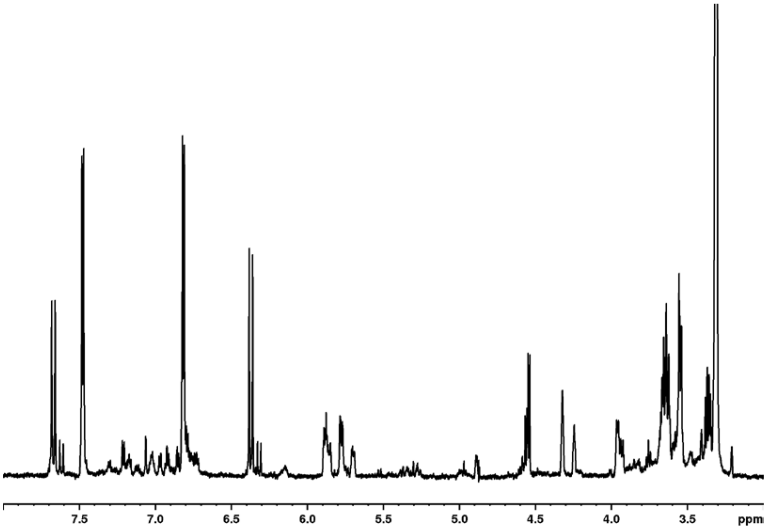

Figure S10.4 4-(*E*)-*p*-Coumaroyl-D-glucopyranose (**11**), 1D NOESY NMR spectrum (700 MHz, MeOH-d_4, o1p = 4.89 ppm)

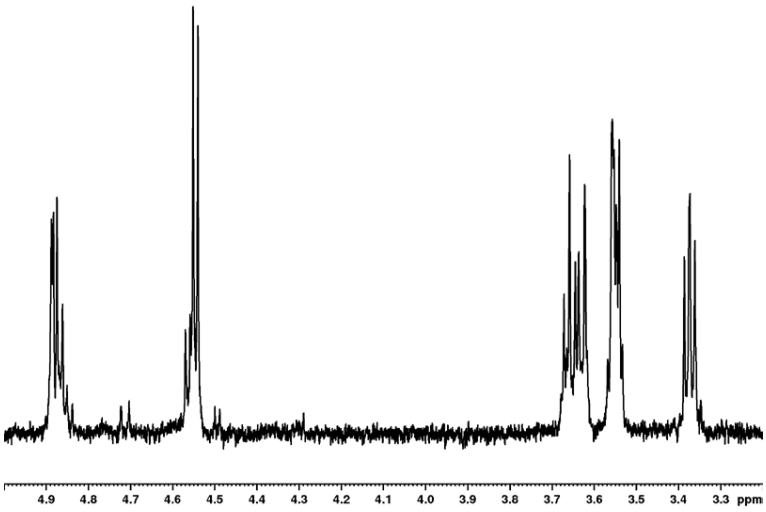

Figure S10.5 4-(*E*)-*p*-Coumaroyl-D-glucopyranose (**11**), selective 1D TOCSY spectrum (700 MHz, MeOH-d_4, o1p = 4.54 ppm)

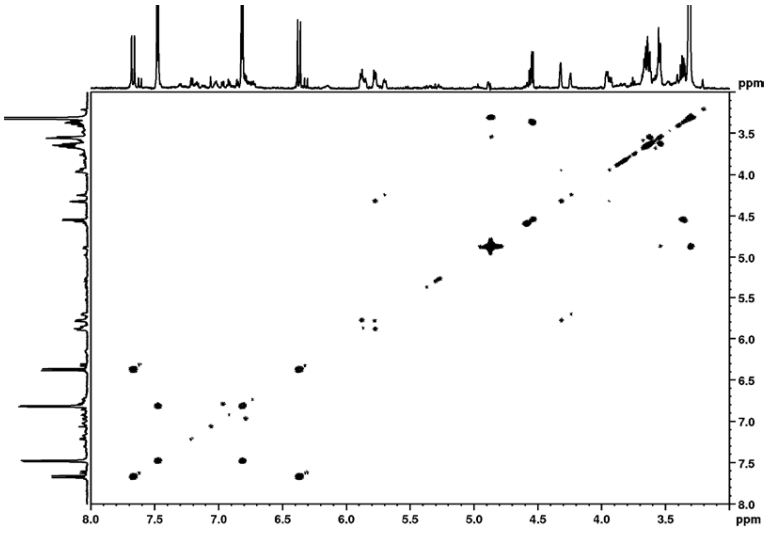

Figure S10.6 4-(*E*)-*p*-Coumaroyl-D-glucopyranose (**11**), ^{1}H-^{1}H COSY spectrum (700 MHz, MeOH-d_4)

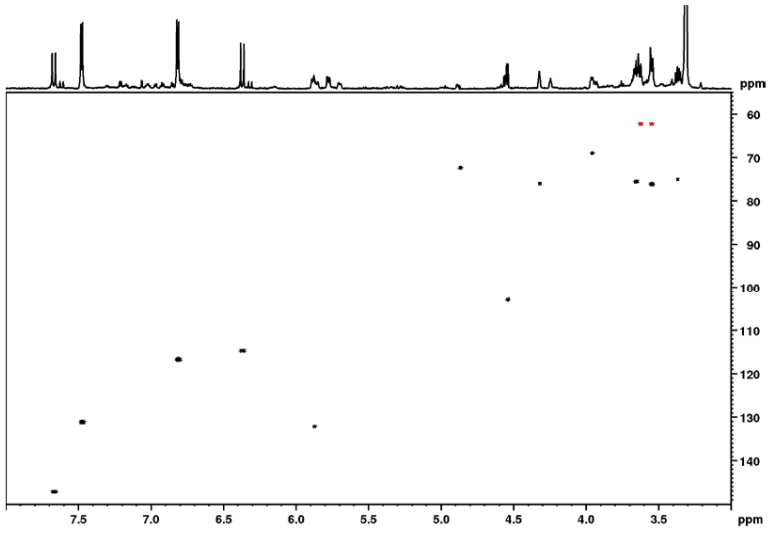

Figure S10.7 4-(*E*)-*p*-Coumaroyl-D-glucopyranose (**11**), ^{1}H-^{13}C HSQC spectrum (700 MHz, MeOH-d_4)

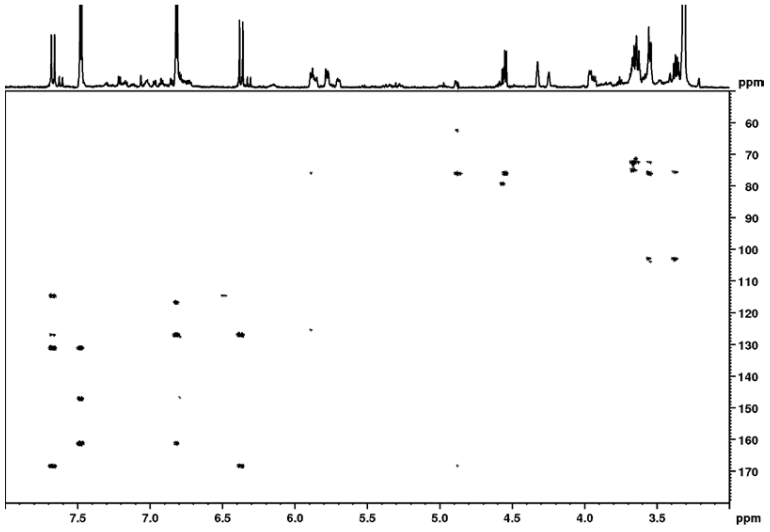

Figure S10.8 4-(*E*)-*p*-Coumaroyl-D-glucopyranose (**11**), ^{1}H-^{13}C HMBC spectrum (700 MHz, MeOH-d_4)

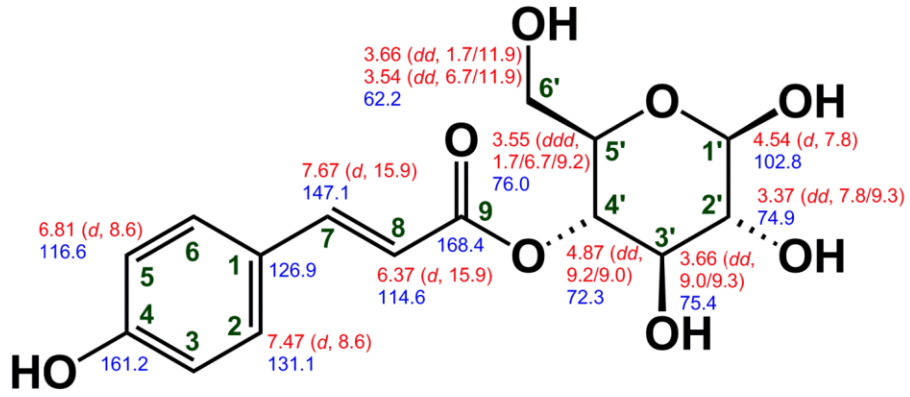

Figure S10.9 4-(*E*)-*p*-Coumaroyl-D-glucopyranose (**11**), structure with chemical shifts

11. Supplementary data of isograndidentatin A (12):

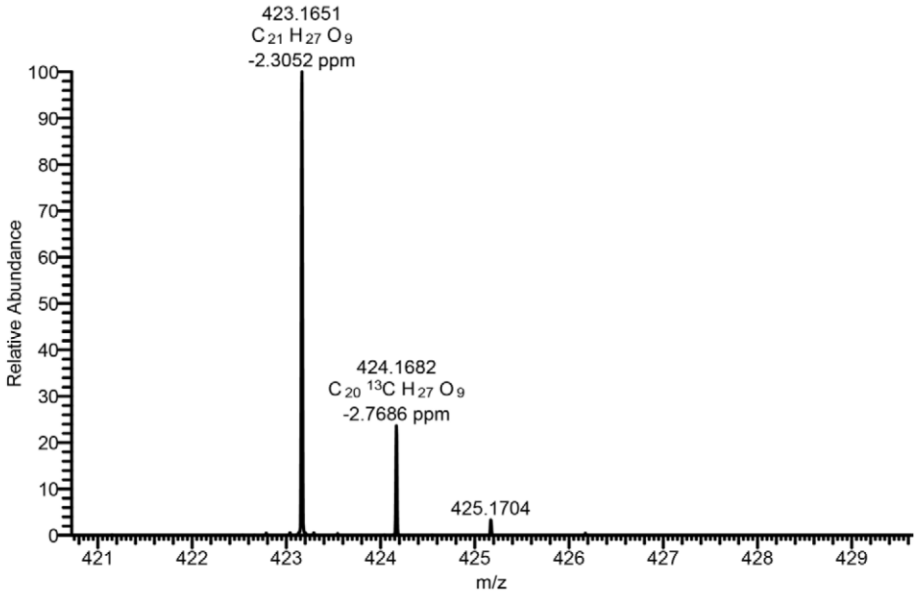

HRMS (-p ESI)

CC

423.1651 [M-H]$^-$ (100)
424.1682 [M-H]$^-$ (23.35)
425.1704 [M-H]$^-$ (3.33)

Figure S11.1 Isograndidentatin A (**12**), HRESI-MS data

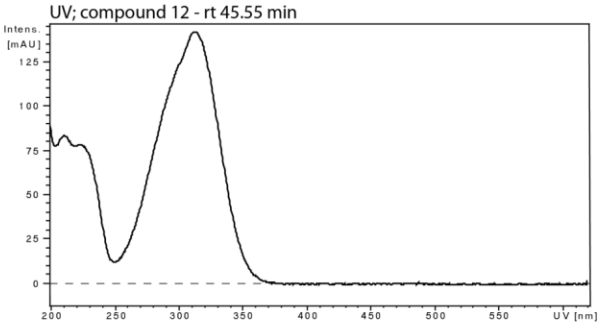

Figure S11.2 Isograndidentatin A (**12**), UV-Vis data

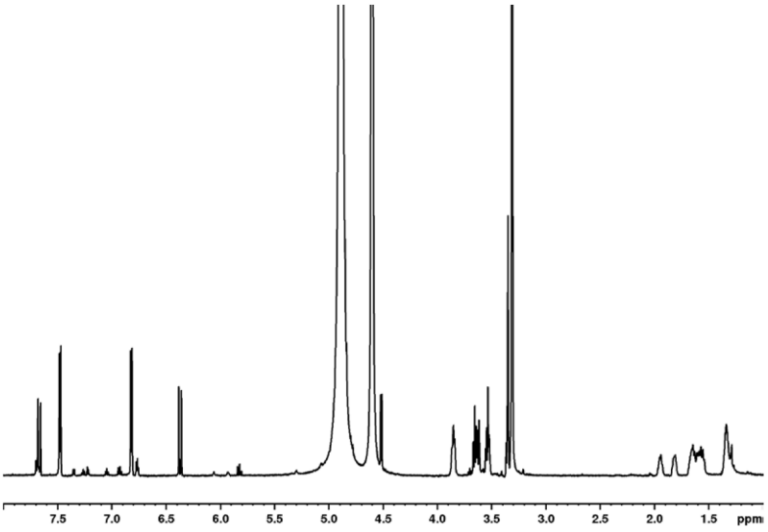

Figure S11.3 Isograndidentatin A (**12**), ^{1}H-NMR spectrum (700 MHz, MeOH-d_4)

CCI

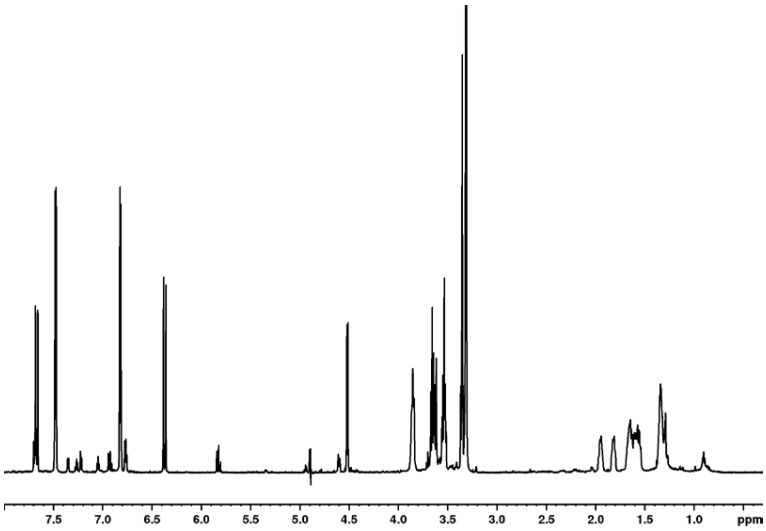

Figure S11.4 Isograndidentatin A (**12**), 1D NOESY NMR spectrum (700 MHz, MeOH-d_4, o1p = 4.89 ppm)

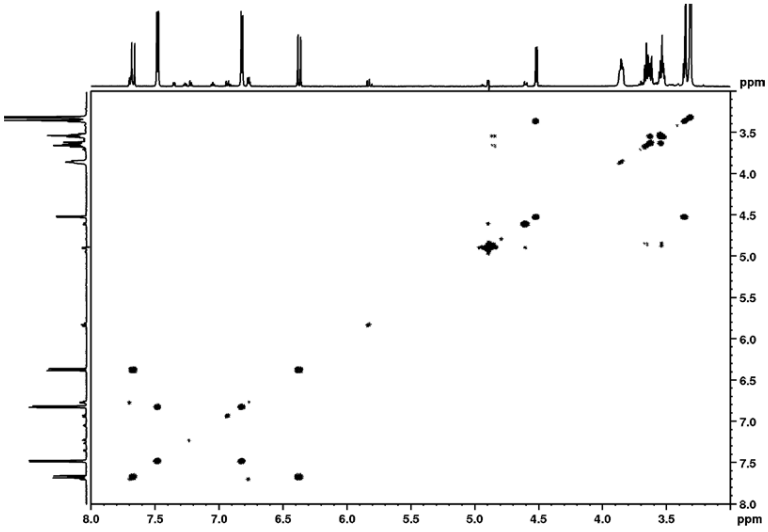

Figure S11.5 Isograndidentatin A (**12**), ^{1}H-^{1}H COSY spectra (700 MHz, MeOH-d_4)

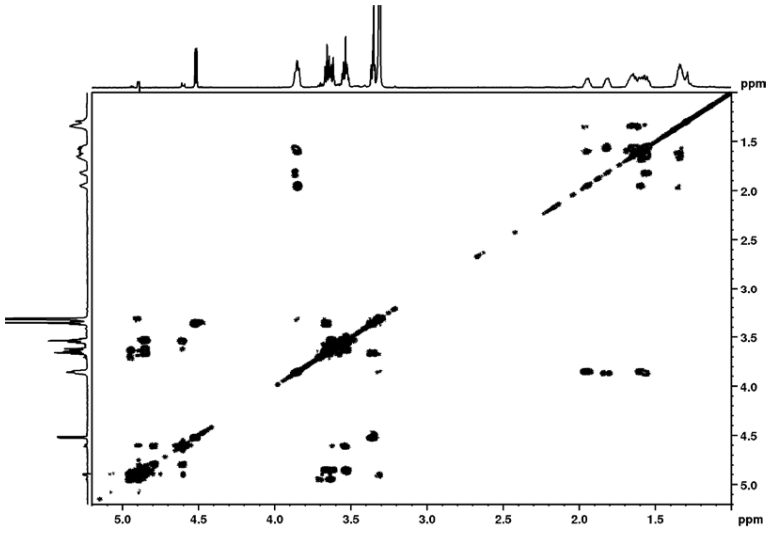

Figure S11.6 Isograndidentatin A (**12**), ^{1}H-^{1}H COSY spectra (700 MHz, MeOH-d_4; 1 to 5.2 ppm)

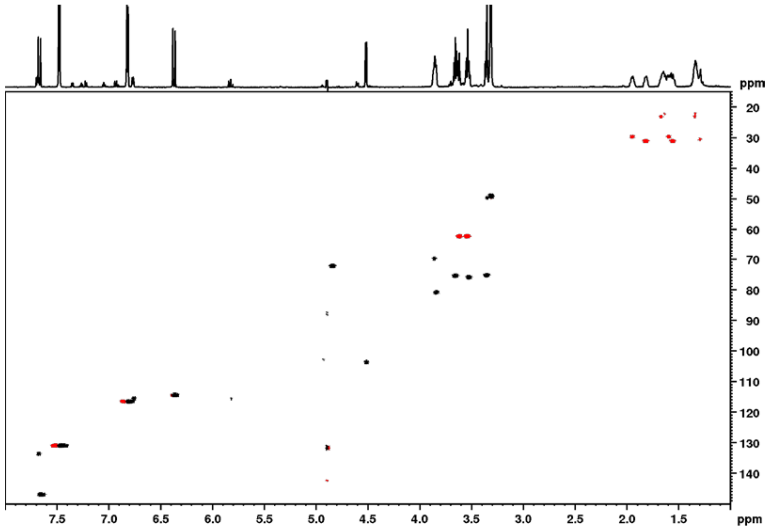

Figure S11.7 Isograndidentatin A (**12**), ^{1}H-^{13}C HSQC spectrum (700 MHz, MeOH-d_4)

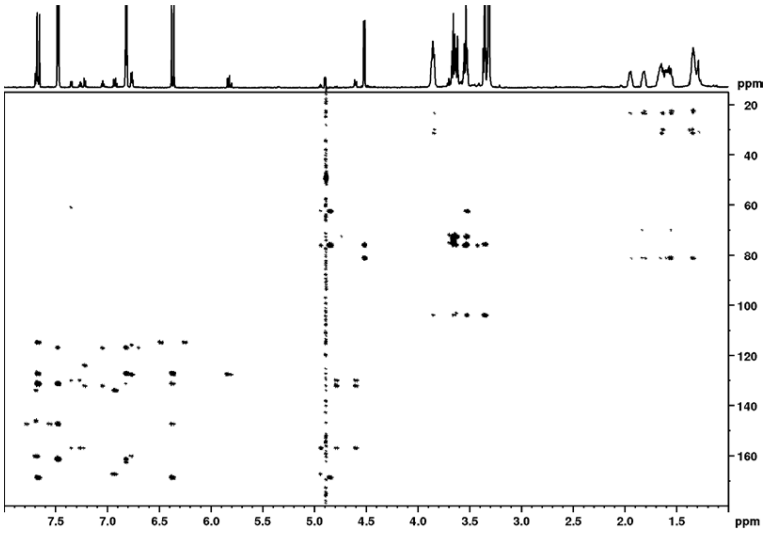

Figure S11.8 Isograndidentatin A (**12**), ^{1}H-^{13}C HMBC spectrum (700 MHz, MeOH-d_4)

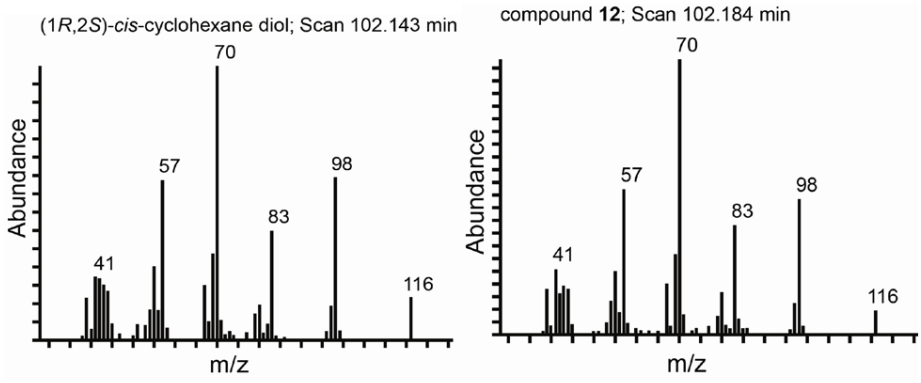

Figure S11.9 GC-MS spectra of (1*R*,2*S*)-*cis*-cyclohexane diol reference (left) and the hydrolysis product of **12** (right)

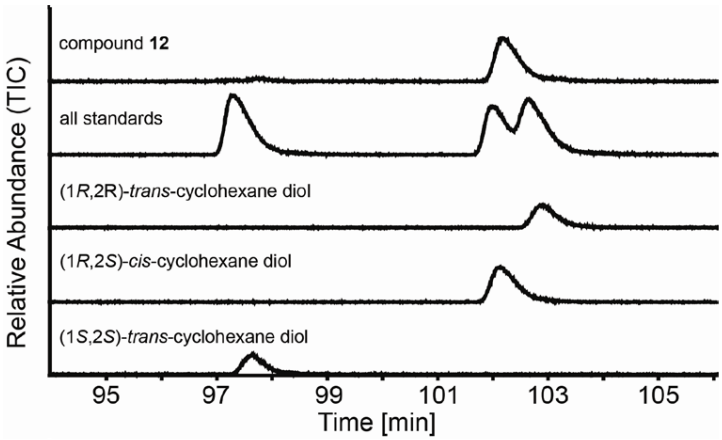

Figure S11.10 Superimposed CG-MS total ion chromatograms of the hydrolysis product of **12** and all references

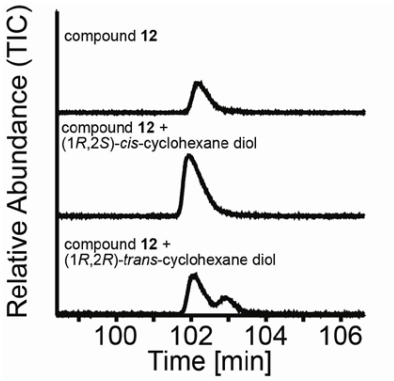

Figure S11.11 Superimposed GC-MS total ion chromatograms of the hydrolysis product of **12** and the reference compounds after standard addition

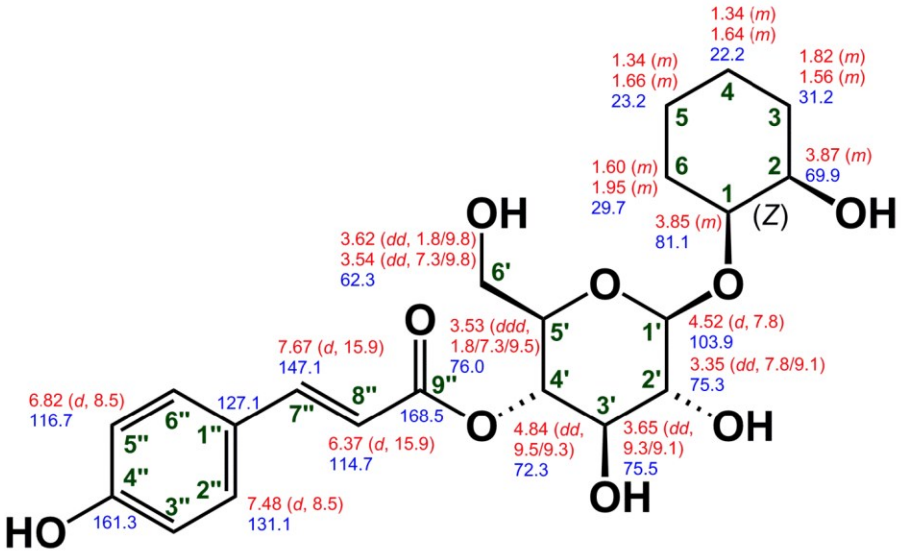

Figure S11.12 Isograndidentatin A (**12**), structure with chemical shifts

12. Supplementary data of 1-*O*-(2-Hydroxyphenyl)-4-*O*-(*E*)-p-coumaroyl-*β*-D-glucopyranose (13):

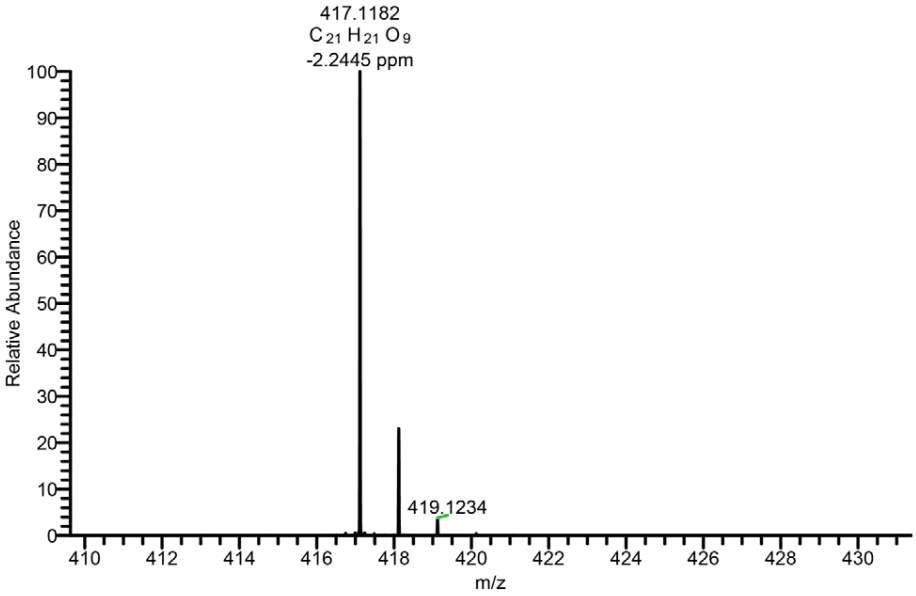

HRMS (-p ESI)
417.1182 $[M-H]^-$ (100)
418.1213 $[M-H]^-$ (22.90)
419.1234 $[M-H]^-$ (3.62)

Figure S12.1 1-*O*-(2-Hydroxyphenyl)-4-*O*-(*E*)-p-coumaroyl-*β*-D-glucopyranose (**13**), HRESI-MS data

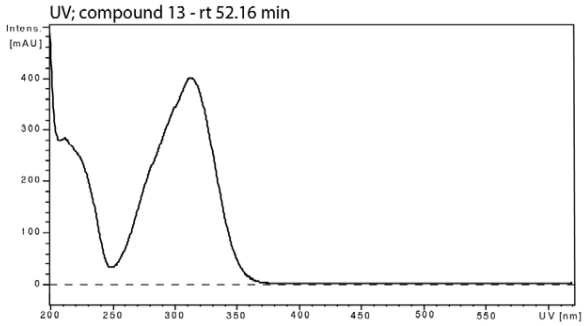

Figure S12.2 1-*O*-(2-Hydroxyphenyl)-4-*O*-(*E*)-p-coumaroyl-*β*-D-glucopyranose (**13**), UV-Vis data

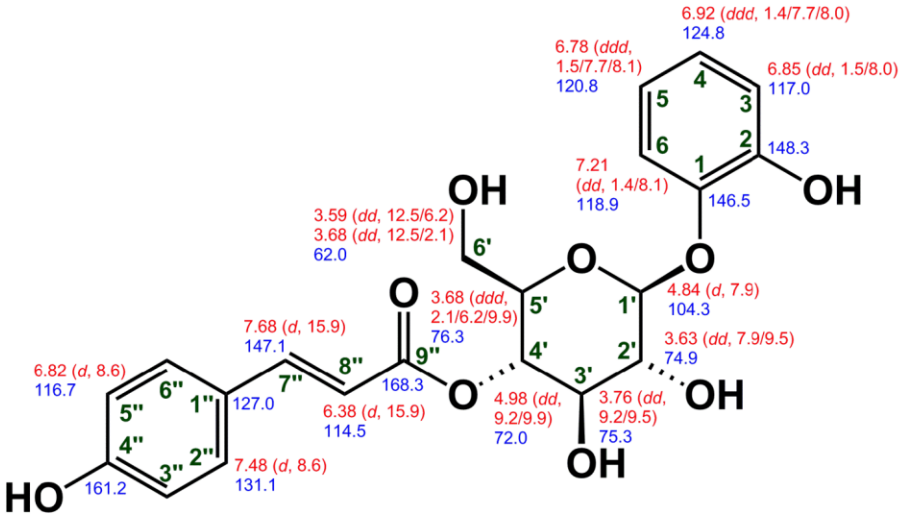

Figure S12.3 1-*O*-(2-Hydroxyphenyl)-4-*O*-(*E*)-p-coumaroyl-*β*-D-glucopyranose (**13**), structure with chemical shifts

Analytical data in accordance with:

Kumar, M., Rawat, P., Khan, M. F., Tamarkar, A. K., Srivastava, A. K., Arya, K. R., Maurya, R., 2010. Phenolic glycosides from *Dodecadenia grandiflora* and their glucose-6-phosphatase inhibitory activity. Fitoterapia 81, 475-479.

13. Supplementary data (-)-idescarparide (14):

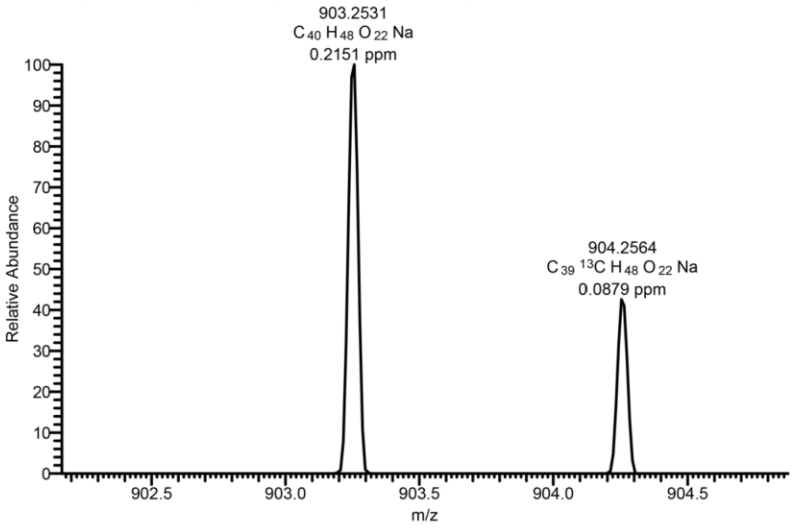

HRMS (+p ESI)
903.2532 $[M+Na]^+$ (100)
904.2564 $[M+Na]^+$ (42.53)
905.2592 $[M+Na]^+$ (12.59)
906.2613 $[M+Na]^+$ (3.14)

Figure S13.1 (-)-Idescarparide (**14**), HRESI-MS data

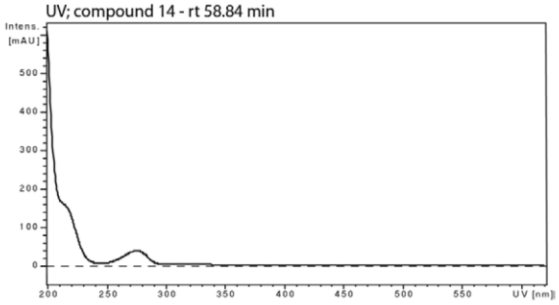

Figure S13.2 (-)-Idescarparide (**14**), UV-Vis data

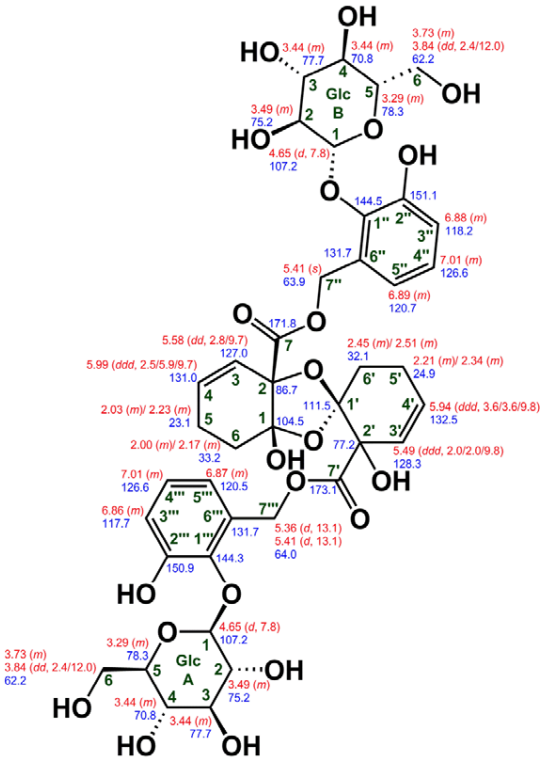

Figure S13.3 (-)-Idescarparide (**14**), structure with chemical shifts

Analytical data in accordance with:

Kim, T. B., Kim, H. W., Lee, M., Lee, H. H., Kim, S. H., Kang, S. K., Sung, S. H., 2014. Isolation and structure elucidation of (−)-idescarparide, a new spiro compound from *Idesia polycarpa*. Tetrahedron Lett. 55, 5447-5449.

14. Supplementary data of idescarpin (15):

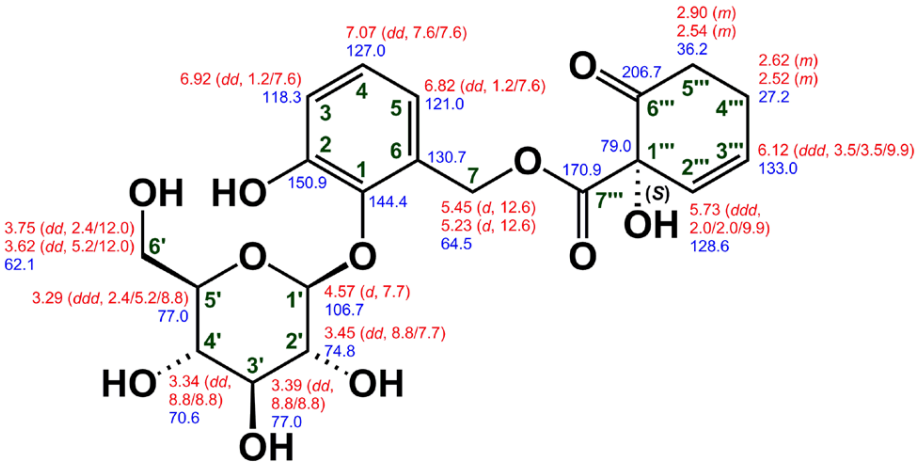

Figure S14.1 Idescarpin (**15**), chemical structure with chemical shifts

Analytical data in accordance with:

Feistel, F., Paetz, C., Lorenz, S., Schneider, B., 2015. The absolute configuration of salicortin, HCH-salicortin and tremulacin from *Populus trichocarpa x deltoides Beaupré*. Molecules 20, 5566-5573.

Supplementary information II – published version of *Manuscript II*

During the submission of this thesis, *Manuscript II* ("Acylated quinic acids are the main salicortin metabolites in the specialist herbivore *Cerura vinula*") was under revision for publication (see pages 30 & 43 et sqq.). The released version, published by the *Journal of Chemical Ecology* in March 2018, is displayed on the next 13 pages.

Journal of Chemical Ecology
https://doi.org/10.1007/s10886-018-0945-1

Acylated Quinic Acids Are the Main Salicortin Metabolites in the Lepidopteran Specialist Herbivore *Cerura vinula*

Felix Feistel[1] · Christian Paetz[1] · Riya C. Menezes[1] · Daniel Veit[1] · Bernd Schneider[1]

Received: 22 December 2017 / Revised: 4 March 2018 / Accepted: 8 March 2018

Abstract
Salicortin is a phenolic glucoside produced in Salicaceae as a chemical defense against herbivory. The specialist lepidopteran herbivorous larvae of *Cerura vinula* are able to overcome this defense. We examined the main frass constituents of *C. vinula* fed on *Populus nigra leaves*, and identified 11 quinic acid derivatives with benzoate and/or salicylate substitution. We asked whether the compounds are a result of salicortin breakdown and sought answers by carrying out feeding experiments with highly ^{13}C-enriched salicortin. Using HRMS and NMR analyses, we were able to confirm that salicortin metabolism in *C. vinula* proceeds through deglucosylation and ester hydrolysis, after which saligenin is oxidatively transformed into salicylic acid and, eventually, conjugated to quinic acid. To the best of our knowledge, this is the first report of a detoxification pathway based on conjugation with quinic acid.

Keywords *Cerura vinula* · *Populus nigra* · Salicortin · Down-stream metabolism · Salicaceae · Stable isotope labeling

Introduction

Salicinoids – glycosides derived from salicyl alcohol (saligenin) – are defensive chemicals of *Populus* species and of other members of the Salicaceae family (Lindroth 1991; Palo 1984). The structural diversity of salicinoids arises from their modular composition, which comprises a saligenin core unit, a glucose moiety and an organic acid. The most representative salicinoid in *Populus* is salicortin (**12**), as so far it has been found in all investigated species (Boeckler et al. 2011; Thieme 1964). Numerous studies have investigated the effect of salicinoids on lepidopteran herbivorous insects, such as *Papilio glaucus* (Lindroth 1991), *Choristoneura conflictica* (Clausen et al. 1989), *Malacosoma disstria* and *Lymantria dispar* (Lindroth and Hemming 1990) or *Operophtera brumata* (Boeckler et al. 2016; Ruuhola et al. 2001). Coleopteran larvae belonging to the Chrysomelidae family can sequester salicinoids and use their host plant's chemical defense to ward off predators (Burse et al. 2009). Recently, a comprehensive study of the generalist herbivore *L. dispar* (Boeckler et al. 2016) provided the first detailed description of how a lepidopteran detoxifies salicinoid compounds. The digestive degradation of salicinoids in the insect gut (Haruta et al. 2001; Lindroth 1988; Ruuhola et al. 2003) results in saligenin and an *o*-quinone (Clausen et al. 1989; Julkunen-Tiitto and Meier 1992; Knuth et al. 2011). Both metabolites are known for their toxic and feeding-deterrent activities (Boeckler et al. 2011; Clausen et al. 1989; Ruuhola et al. 2001).

The larva of the lepidopteran *Cerura vinula* is native to Europe and Asia. In the temperate climate zone of Central Europe, imagines appear from April to August. Females lay eggs on branches and leaves of their host plants. As the insects' nutritional spectrum is limited to plants of the Salicaceae family (*Salix* and *Populus* species), they are regarded as specialist herbivores (Ali and Agrawal 2012; Hintze-Podufal 1970). Numerous metabolic studies (recent examples: Beran et al. 2014; Joussen et al. 2012; Shelomi et al. 2016) have addressed the question whether a specialist herbivore uses a distinct mechanism to cope with the defense of its host plant. In the present publication, we used a double-track strategy: the careful structural identification of metabolic products arising from the diet of the specialist herbivore resulted in an assumption about how the main chemical defense compounds were transformed during digestion. This hypothesis was then supported using stable isotope labeling which eventually allowed us to develop a new salicinoid degradation pathway.

Electronic supplementary material The online version of this article (https://doi.org/10.1007/s10886-018-0945-1) contains supplementary material, which is available to authorized users.

✉ Bernd Schneider
schneider@ice.mpg.de

[1] Max Planck Institute for Chemical Ecology, Hans-Knöll-Straße 8, Beutenberg Campus, D-07745 Jena, Germany

Published online: 17 March 2018

Methods and Materials

General Information In order to address the question of how *C. vinula* is able to deactivate the salicinoid defense of its host plant, several experimental approaches were employed. It was necessary to develop UPLC-MS and NMR protocols for the identification of the main metabolites as well as an HPLC-SPE protocol for the degradation-free workup of the compounds of interest. [^{13}C]-Labeling of salicinoids was accomplished *in planta* by growing plants under a [^{13}C]CO_2-enriched atmosphere in a dedicated growth chamber and subsequent isolation of [U-^{13}C]salicortin from leaf material. Experimental details and procedures can be found in the following section.

NMR spectra for the structure elucidation of acylated quinic acids **1** to **11** were recorded on a Bruker Avance III HD 700 MHz spectrometer, equipped with a 1.7 mm TCI microcryoprobe (Bruker Biospin, Rheinstetten, Germany) using NMR tubes of 1.7 mm outer diameter. NMR spectra of frass extracts from *C. vinula* larvae after [U-^{13}C]salicortin feeding experiments were obtained on a Bruker Avance III HD 500 MHz NMR spectrometer equipped with a 5 mm TCI cryoprobe (Bruker Biospin) using NMR tubes of 5 mm outer diameter. NMR spectra for the characterization of *in vivo*-generated [U-^{13}C]salicortin were recorded on a Bruker Avance III HD 400 MHz NMR spectrometer equipped with a 5 mm BBFO probe (Bruker Biospin) using NMR tubes of 5 mm outer diameter. NMR spectra were recorded using MeOH-d_4 as a solvent. Chemical shifts were referenced to the residual solvent peaks at δ_H 3.31 and δ_C 49.15. Data acquisition and processing were accomplished using TopSpin 3.2. Standard pulse programs as implemented in TopSpin were used for data acquisition.

The ultra-high-performance liquid chromatography–electrospray ionization–tandem mass spectrometry system (UHPLC–ESI–MS/MS) for structure elucidation and analysis of frass compounds after [U-^{13}C]salicortin labeling consisted of an Ultimate 3000 series RSLC (Dionex, Sunnyvale, CA, USA) and a Q Exactive Plus - Orbitrap mass spectrometer (Thermo Fisher Scientific, Bremen, Germany) using heated-electrospray ionization (H-ESI). H-ESI source parameters were set to 4 kV for spray voltage and 35 V for transfer capillary voltage at a capillary temperature of 300 °C. The samples were measured in positive and negative ionization mode in the mass range of m/z 100 to 1000 using 70,000 $m/\Delta m$ resolving power in the Orbitrap mass analyzer.

UHPLC-ESI-MS/MS for hemolymph analysis was performed with an Ultimate 3000 series RSLC (Dionex) and LTQ - Orbitrap XL mass spectrometer (Thermo Fisher Scientific) in which ionization was accomplished using electrospray ionization (ESI). ESI source parameters were set to 4 kV for spray voltage, 35 V for transfer capillary voltage at a capillary temperature 275 °C. The samples were measured in negative ionization mode in the mass range of m/z 100 to 1000 using 30,000 m/Δm resolving power in the Orbitrap mass analyzer. All UHPLC systems used an Acclaim C18 column (150 × 2.1 mm, 2.2 μm, Dionex, Sunnyvale, CA, USA) for chromatographic separation. HRMS data were evaluated and interpreted using Xcalibur software (Thermo Fisher Scientific, Waltham, MA, USA).

HPLC-ESI-MS of acylated quinic acids **1**–**11** was performed on an Agilent 1100 HPLC system, consisting of a degasser, quaternary solvent delivery pump G1311A, an autosampler G1313A (Agilent Technologies, Waldbronn, Germany), a photodiode array detector (detection 200–700 nm; J&M Analytik, Aalen, Germany) and an Esquire 3000 ion trap mass spectrometer (Bruker Daltonik, Bremen, Germany). The column outlet was connected to a Bruker/Spark Holland Prospect 2 solid-phase extraction (SPE) system (Bruker Biospin) for post-column SPE trapping on HySphere resin GP cartridges. To reduce the eluotropic capacity of the HPLC solvent mixture, water was added with a flow rate of 2.5 ml min^{-1} using a make-up pump (Knauer, Berlin, Germany).

[U-^{13}C]Salicortin was chromatographically purified on an Agilent 1100 HPLC system, consisting of a degasser G1322A, a binary pump G1312A, an autosampler G1313A and a photodiode array detector G1315B (Agilent Technologies). The column outlet was connected to an Advantec CHF122SB fraction collector (Jasco, Gross-Umstadt, Germany) triggered by a relay board from the Agilent 1100. HPLC separations were carried out using an Isis RP-18e column (250 × 4.6 mm, 5 μm particle size) (Macherey-Nagel, Düren, Germany). Solvents were evaporated with a rotary evaporator Rotavapor R-114 (Büchi Labortechnik, Flawil, Switzerland) and a Genevac HT-4X vacuum centrifuge (Genevac, Ipswich, UK). Homogenization was carried out with a MINILYS cell disruptor (Bertin Technologies, Montigny-le-Bretonneux, France). Solvents used for extraction and chromatographic separation were purchased from Carl Roth (Karlsruhe, Germany) and VWR International (Darmstadt, Germany), and used without further purification. Acetonitrile and water (hypergrade for LCMS) used for UHPLC-ESI-MS/MS were purchased from Merck (Darmstadt, Germany), and formic acid (eluent additive for LC-MS) was obtained from Sigma Aldrich (Steinheim, Germany). Water used for HPLC was obtained from a Milli-Q Synthesis A 10 purifier (Merck). $^{13}CO_2$ (isotopic purity 99 atom% ^{13}C, <3 atom% ^{18}O) and Phytacon™ vessels (H 140 mm, base diam. 86 mm) used as arenas for the larvae feeding experiments were purchased from Sigma-Aldrich (Taufkirchen, Germany). HR-X SPE cartridges (500 mg sorbent/6 ml volume), folded filters (90 mm) and paper filters (MN 615 ¼, 125 mm) were purchased from Macherey-Nagel. Syringe filters (0.45 μm, PA) were purchased from Carl Roth. (−)-Quinic acid was purchased from Thermo Fisher Kandel (Karlsruhe, Germany).

Plant Material and Insect Larvae Plant samples of black poplar (*P. nigra*) were collected from trees growing in proximity to the Max Planck Institute for Chemical Ecology in Jena, Germany. *P. nigra* is a typical hostplant of *C. vinula* (Hintze-Podufal 1970) in natural habitats and was therefore used to raise the larvae for the experiments. *P. trichocarpa x deltoides* Beaupré were grown in the greenhouse of the Max Planck Institute for Chemical Ecology. The species was thoroughly examined in previous studies regarding its spectrum of salicinoid defense compounds (Feistel et al. 2015). The light period was set from 6:30 to 20:30 (14 h), while temperatures were kept between 21 and 23 °C during the day and between 19 and 21 °C at night. The humidity was regulated between 50 to 60%. Puss moth (*C. vinula*) larvae were hatched from eggs and reared on *P. nigra* leaves in the laboratory.

Extraction and Isolation of *C. vinula* Frass. Frass of *C. vinula* larvae fed on *P. nigra* leaves were collected and lyophilized, resulting in 73 g of dry material. Contaminated material (leaves, petioles and exuviae) was removed manually. Dried frass (20 g) were ground using a ceramic mortar and pestle, and extracted (5 × 200 ml, each 10 min) with MeOH. The extracts were filtered (paper filters and 0.45 μm PA syringe filters), pooled and evaporated under reduced pressure, resulting in 2.5 g dried crude extract. This dry matter (53.8 mg) was suspended in water (20 ml) using ultrasound and subjected to pre-separation on a HR-X SPE (PS/DVB) cartridge. After conditioning with MeOH (2 × 6 ml) and equilibration with water (3 × 6 ml), the cartridge was loaded with the extract suspension and washed with water (3 × 6 ml). After drying in vacuum, the cartridge was eluted with MeOH (3 × 6 ml). The eluate was then dried using a vacuum centrifuge, resulting in 24.7 mg pre-purified extract. For separation, an aliquot dissolved in MeOH (67.4 mg ml^{-1}) was subjected to HPLC-SPE. A binary solvent system of 0.1% formic acid in water (solvent A) and 0.1% formic acid in MeOH (solvent B) was used for HPLC separation, starting with a 5 min isocratic flow of 100% solvent A and decreasing linearly for 90 min to 50% solvent A. Column temperature was set to 35 °C and the solvent flow rate was 0.8 mL min^{-1}. After each run, the column was washed with 100% MeOH for 5 min and equilibrated with 100% H_2O for 10 min. SPE cartridges loaded with metabolites were dried in a stream of N_2 gas before being eluted with MeOH. Eluted compounds were dried by vacuum centrifugation, yielding the following compounds (R_t retention time): **1** (R_t 32.69 min, 2.1 mg g^{-1} dry frass), **4** (R_t 36.69 min, 1.2 mg g^{-1}), **5** (R_t 39.71 min, 1.1 mg g^{-1}), **2** (R_t 41.00 min, 2.6 mg g^{-1}), **3** (R_t 52.59 min, 3.4 mg g^{-1}), **10** (R_t 61.70 min, 1.6 mg g^{-1}), **7** (R_t 64.14 min, 2.1 mg g^{-1}), **9** (R_t 65.52 min, 3.0 mg g^{-1}), **6** (R_t 68.34 min, 2.8 mg g^{-1}), **11** (R_t 70.18 min, 2.1 mg g^{-1}), **8** (R_t 72.73 min, 1.9 mg g^{-1}).

Structure elucidation was carried out using 1D (^{1}H NMR, selective TOCSY) and 2D NMR (^{1}H-^{1}H COSY, ^{1}H-^{13}C HSQC, ^{1}H-^{13}C HMBC) spectra recorded at 700 MHz and UHPLC-ESI-MS/MS measurements (Q Exactive Plus - Orbitrap MS) using a binary solvent system of H_2O (solvent A) and acetonitrile (solvent B), both of which contained 0.1% (v/v) formic acid with a flow rate of 300 μl min^{-1}. The linear gradient used started with 0% B and increased to 100% B within 15 min. Afterwards, the column was washed for 5 min with 100% B and then equilibrated at 0% B for 5 min.

***In Vivo* Generation and Isolation of ^{13}C-Labeled Salicortin** Stable isotope labeling was achieved in a growth chamber resembling a setup described previously (Chen et al. 2011). The greenhouse light system (Philips SON-T Agro 400 W) was used to provide constant light exposure from 6:30 to 22:00 (15.5 h). Temperature and relative humidity were kept between 20 °C to 30 °C and 50% to 80%, respectively. Six *P. trichocarpa x deltoides* Beaupré plants were pruned to a height of about 30 cm, leaving a few basal leaves. After being transferred to the growth chamber, plants were kept in darkness for the first 2 days. At the beginning of day 3, the respired CO_2 (natural abundance isotope ratio) was removed from the chamber's atmosphere and 450 ppm $^{13}CO_2$ was injected into it. This $^{13}CO_2$ level was kept constant during the entire experimental time (26 days). At the end of each day's light period, $^{13}CO_2$ injection was stopped and respired CO_2 was continuously removed during the night. Details about the $^{13}CO_2$ labeling are provided in the supporting information (B.1 and B.2).

The $^{13}CO_2$-labeling experiment was stopped at day 28, and newly grown plant tissue (leaves with petioles) was collected and lyophilized yielding 13 g dry material. The material was manually crushed and filled equally into Falcon tubes (8 × 45 ml) containing steel beads (3 mm). Extraction was accomplished with MeOH (30 ml per tube) in a Skandex S-7 paint shaker (Fluid Management, Wheeling, IL, USA) for 2 × 4 min. Afterwards, the extracts were pooled, filtered, and the solvent was evaporated in vacuo, yielding 4.18 g (32% dw) dry matter. The dry matter was suspended in 500 ml H_2O, divided into 3 parts and subjected to solid-phase extraction on HR-X SPE columns (each 1.5 g sorbent). After loading, columns were washed with H_2O (3 × 20 ml) and eluted with MeOH (20 ml). The combined methanolic fractions were dried in vacuo, yielding 2.26 g pre-purified extract (17.33% dw). An aliquot solution (121 mg ml^{-1}) was subjected to HPLC separation.

[U-^{13}C]Salicortin was separated using a binary solvent system consisting of 0.1% formic acid in H_2O (solvent A) and 0.1% formic acid in MeOH (solvent B). Column temperature was set to 35 °C and the solvent flow rate was 0.8 ml min^{-1}. The HPLC gradient that was used started with a 5 min isocratic flow of 100% solvent A and decreased linearly for 5 min to 85%, 25 min to 70% and finally 50 min to 50% solvent A. Afterwards, the column was washed for 10 min

with 100% MeOH and equilibrated for 10 min with 100% H_2O. The salicortin UV signal peak (λ = 285 nm) appeared at R_t 42.6 min. Unlabeled salicortin (natural abundance ^{13}C) was isolated in the same manner from unlabeled *P. trichocarpa x deltoides* tissue.

Characterization of the salicortin isolated from the ^{13}C-labeled plant tissue and calculation of its ^{13}C-enrichment was done by means of ^{1}H, ^{13}C and ^{1}H-^{13}C HSQC NMR spectra (400 MHz) and HPLC-ESI-MS measurements using the chromatographic method as described above. The *in vivo*-generated salicortin showed uniform ^{13}C-labeling with 82% total ^{13}C-enrichment. Spectroscopic data of the [U-^{13}C]salicortin (82% ^{13}C) and detailed information about the calculation of the ^{13}C-enrichment are presented in the Supplementary data (SI B.2).

[U-^{13}C]Salicortin Larval Feeding Freshly cut leaves of *P. nigra* (LPI 3–10) were used for feeding experiments. The leaf petioles were inserted into 2 ml Eppendorf micro reaction vessels. Lids of the vessels were removed for convenient handling prior to being filled with tap water. The opening of the vessels was sealed with Parafilm® fastening the leaf petioles to prevent the water in the vessel from spilling. An aqueous solution of [U-^{13}C]salicortin (2.5 mg ml^{-1}) was spotted evenly on the surface of 5 poplar leaves (10 × 20 µl droplets per leaf). Control leaves were spotted with water in an analogous fashion. Leaves were left under the fume hood for 3 h, allowing the droplets to dry completely. Subsequently, the [U-^{13}C]salicortin-coated leaves and the control leaves were transferred into arenas for feeding experiments. Each arena contained one leaf and one *C. vinula* larva (late 3rd to early 4th instars), which were placed onto the surface of each leaf. The larvae were kept in the arena until the leaves had been completely consumed. Frass collected from the control experiments and the stable isotope feeding experiments, respectively, were pooled into 2 batches which were subsequently lyophilized.

The freeze-dried frass was then extracted with MeOH (3 × 1 ml) by homogenization in a Minilys cell disruptor (2 ml tubes, 60 s and 4000 rpm), using 1.4 mm o.d. ZrO_2 beads. The supernatants from each sample were pooled and evaporated using N_2 gas and subsequently extracted with H_2O (5 × 1 ml). The aqueous extracts were pooled and dried with N_2 gas. Afterwards, methanolic and aqueous extracts of frass from control and [U-^{13}C]salicortin feeding experiments were subjected to NMR (500 MHz) and UHPLC-ESI-MS/MS (Q Exactive Plus – Orbitrap MS) analysis, using the chromatographic system described above.

Collection of *C. vinula* Hemolymph The question of whether salicinoid metabolites are detectable in the hemolymph of *C. vinula* larvae was addressed as follows: 6 *C. vinula* larvae (3 × control, 3 × fed with [U-^{13}C]salicortin) were immobilized in 15 ml Falcon tubes and kept in the −20 °C freezer for 15 min. A mid-abdominal proleg of an anesthetized larva was pierced with a scalpel, and the emerging hemolymph was transferred by means of a pipette into an ice-cooled 2 ml Eppendorf micro reaction vessel containing MeOH (1 ml). Subsequently, the mixture was centrifuged and the supernatant was evaporated by a stream of N_2 gas, yielding an average amount of 3.07 mg (SD ± 1.51 mg) residue per larva. Each of the 6 dried residues were dissolved in 1 ml MeOH and analyzed independently by UHPLC-ESI-MS/MS (LTQ - Orbitrap XL MS), using a binary solvent system of H_2O (solvent A) and acetonitrile (solvent B), both of which contained 0.1% (*v*/v) formic acid with a flow rate of 300 µl min^{-1}. A linear gradient was used, starting with 5% B to 52% B within 20 min. Afterwards, the column was washed for 5 min with 100% B and then equilibrated at 5% B for another 5 min.

Results

***C. vinula* Frass Analysis** Frass of *C. vinula* larvae fed on *P. nigra* leaves was collected and metabolites extracted as described in the Methods and Materials section. Eleven quinic acid derivatives representing almost 2.5% (23.9 mg g^{-1}) of the frass dry mass were identified (Fig. 1). Among them, 10 compounds (**1**–**3, 5**–**11**) were unknown and only compound **4** had been reported recently (Wan et al. 2016). For an overview about NMR, HR-MS and UV data, see Tables 1, 2, 3 and 4. Spectra of all compounds, including salicortin (**12**) and quinic acid (**13**), are provided in the Supplementary data (SI A.1 to A.13).

The HRESIMS data of compound **1** showed a molecular ion peak at *m/z* 311.0774 $[M\text{-}H]^-$ corresponding to a molecular formula of $C_{14}H_{16}O_8$ (calcd for $C_{14}H_{15}O_8$, *m/z* 311.0772). The ^{1}H NMR spectrum of compound **1** (Table 1) showed signals of 11 protons assignable to 2 different structural units. In the low-field region of the ^{1}H NMR spectra, we observed signals of an asymmetric 4-spin system (ABCD) at δ_H 6.62 ($^{3}J_{HH}$ = 0.8/8.3 Hz; H-3′), δ_H 7.21 ($^{3}J_{HH}$ = 1.5/7.3/8.3 Hz; H-4′), δ_H 6.60 ($^{3}J_{HH}$ = 0.8/6.9/7.3 Hz; H-5′) and δ_H 7.44 ($^{3}J_{HH}$ = 1.4/6.9 Hz; H-6′), characteristic of a 1,2-disubstituted aromatic ring. The corresponding ^{13}C chemical shifts were determined by an ^{1}H-^{13}C hetero-correlation single quantum coherence (HSQC) spectrum as δ_C 118.8 (C-3′), δ_C 135.5 (C-4′), δ_C 119.5 (C-5′) and δ_C 132.5 (C-6′). Further evidence for a 1,2-disubstitution was provided by an ^{1}H-^{13}C heteronuclear multiple-bond correlation (HMBC) spectrum showing $^{3}J_{CH}$ correlations from H-4′ and H-6′ to a quaternary carbon atom at δ_C 159.9 (C-2′) as well as from H-3′ and H-5′ to another quaternary carbon atom at δ_C 115.2 (C-1′). Because of its low-field ^{13}C chemical shift, C-2′ was assigned as oxygenated. Furthermore, H-6′ (δ_H 7.44) showed a long-range CH-correlation to a carboxyl functionality at δ_C 167.7 (C-7′)

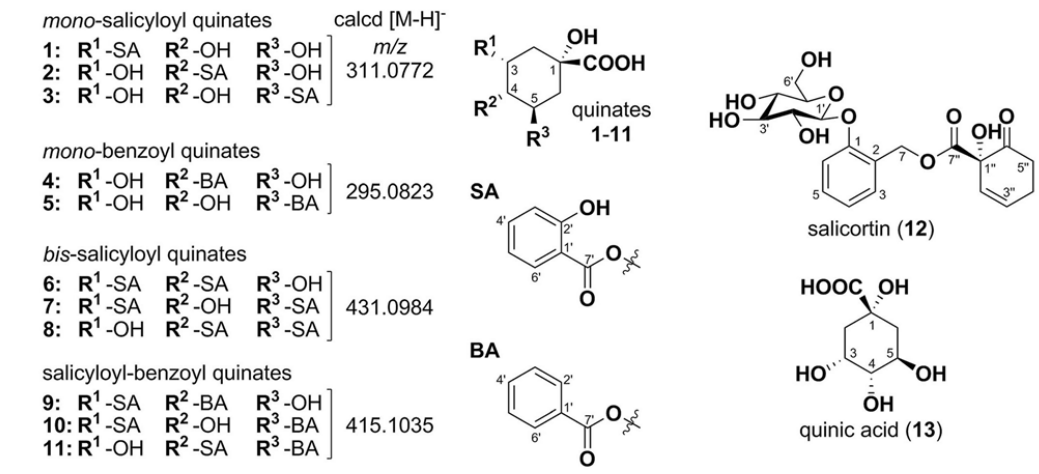

Fig. 1 Metabolites isolated from frass of *C. vinula* larvae fed on *P. nigra* leaves, and the structures of salicortin (**12**) and quinic acid. SA: salicyloyl; BA: benzoyl

tethered to C-1′ (δ_C 115.2). Thus, the data suggest the presence of a salicyloyl moiety (SA). A double-doublet signal of a methine appeared at δ_H 5.70 ($^3J_{HH}$ = 3.1/3.4/3.1; H-3). The corresponding ^{13}C chemical shift was extracted from the ^{1}H-^{13}C HSQC spectrum at δ_C 72.8 (C-3), which is characteristic for a hydroxylated aliphatic carbon atom. Adjacent to H-3, another methine at δ_H 3.60 ($^3J_{HH}$ = 3.4/9.5 Hz; H-4), and a methylene group at δ_H 2.35 ($^3J_{HH}$ = 3.1/14.4 Hz; H-2a) and δ_H 2.11 ($^3J_{HH}$ = 3.1/14.4 Hz; H-2b) were determined from their $^3J_{HH}$ correlations by ^{1}H-^{1}H COSY. Furthermore, consecutive cross-peaks from H-4 to another methine at δ_H 4.06 ($^3J_{HH}$ = 4.6/9.5/12.0 Hz; H-5) and to a second methylene group at δ_H 2.10 ($^3J_{HH}$ = 12.0/12.5 Hz; H-6a) and δ_H 1.95 ($^3J_{HH}$ = 4.6/12.5 Hz; H-2b) were observed. The small $^3J_{HH}$ values (3.4 Hz) for H-3 and H-4 indicated equatorial configuration, whereas the large values (9.5 Hz) for H-4 and H-5 indicated axial configuration. The corresponding ^{13}C-chemical shifts were determined by ^{1}H-^{13}C

Table 1 ^{1}H NMR (700 MHz) and ^{13}C NMR (175 MHz) data of compounds **1**–**4** in MeOH-d_4

Position	**1**		**2**		**3**		**4**	
	δ_H mult. (*J* in Hz)	δ_C	δ_H mult. (*J* in Hz)	δ_C	δ_H mult. (*J* in Hz)	δ_C	δ_H mult. (*J* in Hz)	δ_C
1		80.3		76.4		76.2		76.5
2a	2.35 *dd* (3.1/14.4)	36.8	2.12 *dd* (2.8/14.5)	38.3	2.22 *dd* (2.3/14.1)	38.6	2.19 *dd* (2.6/13.6)	39.1
2b	2.11 *dd* (3.1/14.4)		2.07 *ddd* (2.6/3.8/14.5)		2.06 *dd* (4.4/14.1)		2.06 *dd* (2.7/13.6)	
3	5.70 *ddd* (3.1/3.4/3.1)	72.8	4.35 *ddd* (2.8/2.9/3.8)	69.5	4.19 *ddd* (2.3/3.2/4.4)	71.3	4.37 *ddd* (2.2/2.6/2.7)	68.7
4	3.60 *dd* (3.4/9.5)	75.6	5.02 *dd* (2.9/9.4)	80.0	3.83 *dd* (3.2/8.4)	72.9	5.02 *dd* (2.2/7.8)	79.1
5	4.06 *ddd* (4.6/9.5/12.0)	68.0	4.39 *ddd* (4.7/9.4/10.8)	65.6	5.55 *ddd* (3.6/8.4/9.6)	73.3	4.29 *ddd* (5.4/7.8/9.8)	66.3
6a	2.10 *dd* (12.0/12.5)	42.5	2.20 *ddd* (2.6/4.7/13.3)	42.0	2.28 *dd* (3.6/13.1)	38.6	2.15 *dd* (5.4/14.5)	39.1
6b	1.77 *dd* (4.6/12.5)		1.89 *dd* (10.8/13.3)		2.21 *dd* (9.6/13.1)		2.05 *dd* (9.8/14.5)	
7		182.6		181.8		177.5		179.8
1’		115.2		113.8		113.5		131.5
2’		159.9		162.6		162.7	8.13 *dd* (0.9/8.0)	130.6
3’	6.62 *dd* (0.8/8.3)	118.8	6.95 *d* (8.5)	118.0	6.94 *dd* (0.8/8.4)	118.0	7.49 *dd* (8.0/7.6)	129.2
4’	7.21 *ddd* (1.5/7.3/8.3)	135.5	7.49 *ddd* (1.6/7.4/8.5)	136.8	7.48 *ddd* (1.3/7.2/8.4)	136.6	7.61 *dd* (7.6/7.6)	134.0
5’	6.60 *ddd* (0.8/6.9/7.3)	119.5	6.93 *dd* (7.4/7.4)	120.0	6.91 *ddd* (0.8/7.2/8.0)	120.1	7.49 *dd* (8.0/7.6)	129.2
6’	7.44 *dd* (1.4/6.9)	132.5	8.05 *dd* (1.6/7.4)	131.6	7.88 *dd* (1.3/8.0)	131.1	8.13 *dd* (0.9/8.0)	130.6
7’		167.7		170.8		170.7		167.7

Table 2 ^{1}H NMR (700 MHz) and ^{13}C NMR (175 MHz) data of compounds **5**–**8** in MeOH-d_4

Position	**5**		**6**		**7**		**8**	
	δ_H mult. (*J* in Hz)	δ_C	δ_H mult. (*J* in Hz)	δ_C	δ_H mult. (*J* in Hz)	δ_C	δ_H mult. (*J* in Hz)	δ_C
1		77.3		75.0		79.9		77.3
2a	2.19 *dd* (3.9/13.8)	38.8	2.24 *dd* (2.8/15.1)	42.2	2.26 *dd* (3.2/14.8)	36.6	2.14 *m*	38.4
2b	1.98 *dd* (2.9/13.8)		2.48 *dd* (3.2/15.1)		2.41 *dd* (3.4/14.8)		2.38 *m*	
3	4.15 *ddd* (2.6/2.9/3.9)	72.9	5.95 *ddd* (2.8/3.2/3.4)	70.9	5.71 *ddd* (3.2/3.4/3.4)	74.2	4.49 *ddd* (2.9/3.2/3.6)	69.6
4	3.97 *dd* (2.6/9.4)	74.8	5.28 *dd* (3.4/9.2)	77.3	4.13 *dd* (3.4/8.9)	71.7	5.42 *dd* (2.9/9.4)	76.9
5	5.52 *ddd* (4.9/9.4/11.1)	73.3	4.48 *ddd* (6.6/9.2/10.9)	65.6	5.71 *ddd* (4.8/8.9/11.7)	73.3	5.95 *ddd* (6.7/8.3/9.4)	70.3
6a	2.19 *dd* (11.1/14.9)	40.1	2.13 *dd* (10.9/13.7)	42.2	2.30 *dd* (11.7/12.8)	39.9	2.37 *m*	39.4
6b	2.11 *dd* (4.9/14.9)		2.31 *dd* (6.6/13.7)		2.33 *dd* (4.8/12.8)		2.37 *m*	
7		176.2		177.5		182.3		178.8
1'		131.6		133.8		113.9		113.0
2'	8.06 *dd* (1.2/8.3)	130.5		161.9		162.1		162.1
3'	7.47 *dd* (7.4/8.3)	129.4	6.92 *d* (8.5)	118.5	6.94 *d* (8.5)	118.2	6.88 *d* (8.5)	118.1
4'	7.59 *dd* (7.4/7.4)	134.1	7.48 *ddd* (1.5/7.3/8.5)	136.7	7.47 *ddd* (1.2/6.9/8.5)	136.3	7.42 *ddd* (1.2/8.2/8.5)	137.1
5'	7.47 *dd* (7.4/8.3)	129.4	6.90 *dd* (7.3/7.9)	120.2	6.94 *dd* (6.9/8.0)	120.1	6.85 *dd* (8.0/8.2)	120.4
6'	8.06 *dd* (1.2/8.3)	130.5	7.91 *dd* (1.5/7.9)	131.8	8.04 *dd* (1.2/8.0)	132.2	7.88 *dd* (1.2/8.0)	131.1
7'		168.1		169.3		169.8		170.5
1"				113.4		113.9		113.0
2"				162.4		162.9		162.4
3"			6.93 *d* (8.5)	118.0	6.93 *d* (8.3)	118.1	6.87 *d* (8.5)	118.1
4"			7.44 *ddd* (1.5/7.1/8.5)	136.7	7.49 *ddd* (1.5/6.9/8.3)	136.7	7.43 *ddd* (1.3/7.8/8.5)	137.1
5"			6.74 *dd* (7.1/7.9)	120.0	6.93 *dd* (6.9/8.1)	120.1	6.83 *dd* (7.8/7.8)	120.4
6"			7.62 *dd* (1.5/7.9)	130.9	7.92 *dd* (1.5/8.1)	131.0	7.75 *dd* (1.3/7.8)	130.7
7"				170.6		170.3		170.4

HSQC as δ_C 36.8 (C-2), δ_C 75.6 (C-4), δ_C 68.0 (C-5) and δ_C 42.5 (C-6). As for C-3 (δ_C 72.8), large ^{13}C NMR chemical shift values indicated oxygenation for C-4 and C-5. The ^{1}H-^{13}C HMBC spectrum revealed a $^{3}J_{CH}$ correlation of H-3 with an oxygenated quaternary carbon atom at δ_C 80.3 (C-1). Furthermore, both methylene groups (H-2ab and H-6ab) showed weak long-range CH correlations to C-1, as a result of which the entire aliphatic structure can be characterized as a cyclohexane ring system. Another HMBC correlation from H-6b to a quaternary carbon at δ_C 182.6 (C-7) tethered to C-1 revealed quinic acid. The characteristic low-field shift of H-3 indicated substitution in this position. This assumption was further supported by an ^{1}H-^{13}C HMBC correlation from H-3 to the carboxyl carbon C-7′ (δ_C 167.7) of the salicyloyl moiety. Accordingly, the structure of compound **1** was assigned as 3-*O*-salicyloyl quinic acid.

Similar to **1**, the HRESIMS spectra of compounds **2** and **3** showed a molecular ion peak of *m/z* 311.0773 [M-H]$^-$, again corresponding to a molecular formula of $C_{14}H_{16}O_8$ (calcd for $C_{14}H_{15}O_8$, *m/z* 311.0772). The data from ^{1}H NMR, ^{1}H-^{1}H COSY, ^{1}H-^{13}C HSQC and the ^{1}H-^{13}C HMBC spectra resembled those of compound **1** (Table 1). Signals of the salicyloyl moiety and the quinic acid subunit were present, but the substitution patterns differed at C-3, C-4 and C-5 of the quinic acid moieties. Acylation of the hydroxyl groups in (−)-quinic acid (**13**) leads to low-field shifts of the signals of H-3, H-4 and H-5 (Pauli et al. 1998). However, the multiplicities and coupling constants remain unaffected. Thus, the shift of a characteristic multiplet to the low field indicates the substitution site (Fig. 2). The multiplets of H-4 (δ_H 5.02) in the ^{1}H NMR spectrum of compound **2** and H-5 (δ_H 5.55) in the spectrum of compound **3** – which in comparison with the corresponding signals of quinic acid (**13**) appeared at the low field – revealed esterification with salicyloyl units at the hydroxyl groups in positions 4 and 5, respectively.

The structures of **2** and **3** were further characterized by ^{1}H-^{13}C HMBC correlations of H-4 (**2**; δ_H 5.02) and H-5 (**3**; δ_H 5.55) with the carboxylic carbon atoms of their salicyloyl moieties at δ_C 170.8 (**2**; C-7′) and 170.7 (**3**; C-7′), respectively. Accordingly, compound **2** was identified as 4-*O*-salicyloyl quinic acid and compound **3** was identified as 5-*O*-salicyloyl quinic acid.

The analytical data of compound **4** were in accordance with previously reported 4-*O*-benzoyl quinic acid (Wan et al. 2016). The HRESIMS spectra of compound **5** showed a molecular ion peak of *m/z* 295.0819 [M-H]$^-$, corresponding to a

Table 3 ^{1}H NMR (700 MHz) and ^{13}C NMR (175 MHz) data of compounds **9**–**11** in MeOH-d_4

Position	**9**		**10**		**11**	
	δ_H mult. (*J* in Hz)	δ_C	δ_H mult. (*J* in Hz)	δ_C	δ_H mult. (*J* in Hz)	δ_C
1		75.2		75.1		72.9
2a	2.22 *dd* (3.7/14.8)	37.2	2.26 *dd* (5.3/14.8)	36.6	2.11 *dd* (3.7/14.7)	38.7
2b	2.47 *dd* (3.2/14.8)		2.40 *dd* (4.6/14.8)		2.38 *dd* (3.6/14.7)	
3	5.93 *ddd* (3.2/3.3/3.7)	71.0	5.71 *ddd* (2.9/4.9/5.3)	74.4	4.47 *ddd* (3.1/3.6/3.7)	70.0
4	5.22 *dd* (3.3/9.2)	77.0	4.12 *dd* (2.9/8.3)	71.8	5.41 *dd* (3.1/9.5)	77.6
5	4.46 *ddd* (3.7/9.2/9.2)	65.8	5.56 *ddd* (5.6/8.3/10.0)	72.9	5.91 *ddd* (4.2/9.5/11.2)	69.8
6a	2.12 *dd* (9.2/14.4)	42.0	2.29 *dd* (10.0/13.5)	39.2	2.36 *m*	40.0
6b	2.30 *dd* (3.7/14.4)		2.29 *dd* (5.6/13.5)		2.36 *m*	
7		178.5		177.6		178.3
1’		113.8		114.1		113.2
2’		161.9		162.0		162.9
3’	6.92 *dd* (0.7/8.5)	118.3	6.93 *d* (8.2)	118.3	6.87 *dd* (0.5/8.7)	118.1
4’	7.48 *ddd* (1.1/7.5/8.5)	136.6	7.47 *dd* (7.4/8.2)	136.5	7.42 *ddd* (1.9/7.5/8.7)	136.8
5’	6.90 *ddd* (0.7/7.5/7.9)	120.1	6.94 *dd* (7.4/7.5)	120.0	6.83 *ddd* (0.5/7.5/7.9)	120.1
6’	7.88 *dd* (1.1/7.9)	131.8	8.04 *d* (7.5)	132.1	7.88 *dd* (1.9/7.9)	131.2
7’		169.5		169.7		170.9
1”		131.1		131.0		131.2
2”	7.91 *dd* (1.1/8.2)	130.4	8.06 *d* (8.5)	130.5	7.92 *dd* (1.0/8.1)	130.3
3”	7.39 *dd* (7.5/8.2)	129.2	7.49 *dd* (7.4/8.5)	129.2	7.40 *dd* (7.6/8.1)	129.3
4”	7.57 *dd* (7.5/7.5)	134.1	7.61 *dd* (7.4/7.4)	134.1	7.54 *dd* (7.6/7.6)	134.2
5”	7.39 *dd* (7.5/8.2)	129.2	7.49 *dd* (7.4/8.5)	129.2	7.40 *dd* (7.6/8.1)	129.3
6”	7.91 *dd* (1.1/8.2)	130.4	8.06 *d* (8.5)	130.5	7.92 *dd* (1.0/8.1)	130.3
7”		167.2		167.1		167.0

molecular formula of $C_{14}H_{16}O_7$ (calcd for $C_{14}H_{15}O_7$, *m/z* 295.0823) and indicating an isomer of compound **4**. In accordance with this suggestion, the ^{1}H NMR, ^{1}H-^{1}H COSY, ^{1}H-^{13}C HSQC and the ^{1}H-^{13}C HMBC spectra of compound **5** (Table 2) showed very similar signals in comparison to compound **4**. Thus, both compounds are constitutional isomers consisting of a quinic acid moiety substituted with a benzoyl moiety. Accordingly, the ^{1}H NMR data of compound

Table 4 UV and HRESIMS data of compounds **9**–**11**

Compound		**UV (MeOH/H_2O)**	**HRESIMS**	
	No. **Calcd for, *m/z* [M-H]$^-$**	**Name**	**λ_{max} (nm)**	***m/z* [M-H]$^-$**
1	3-*O*-Salicyloyl quinic acid	203.5, 237.5, 303.9	311.0774	$C_{14}H_{15}O_8$, 311.0772
2	4-*O*-Salicyloyl quinic acid	203.5, 237.5, 303.9	311.0773	$C_{14}H_{15}O_8$, 311.0772
3	5-*O*-Salicyloyl quinic acid	203.5, 237.0, 305.9	311.0773	$C_{14}H_{15}O_8$, 311.0772
4	4-*O*-Benzoyl quinic acid*	279.4	295.0820	$C_{14}H_{15}O_7$, 295.0823
5	5-*O*-Benzoyl quinic acid	276.4	295.0819	$C_{14}H_{15}O_7$, 295.0823
6	3-*O*,4-*O*-Disalicyloyl quinic acid	204.5, 235.0, 305.4	431.0986	$C_{21}H_{19}O_{10}$, 431.0984
7	3-*O*,5-*O*-Disalicyloyl quinic acid	204.0, 236.0, 304.9	431.0985	$C_{21}H_{19}O_{10}$, 431.0984
8	4-*O*,5-*O*-Disalicyloyl quinic acid	208.0, 306.9	431.0987	$C_{21}H_{19}O_{10}$, 431.0984
9	3-*O*-Salicyloyl-4-*O*-benzoyl quinic acid	302.4	415.1038	$C_{21}H_{19}O_9$, 415.1035
10	3-*O*-Salicyloyl-5-*O*-benzoyl quinic acid	210.0, 309.9	415.1038	$C_{21}H_{19}O_9$, 415.1035
11	4-*O*-Salicyloyl-5-*O*-benzoyl quinic acid	217.5, 283.4	415.1038	$C_{21}H_{19}O_9$, 415.1035

*Reported by Wan et al. 2016

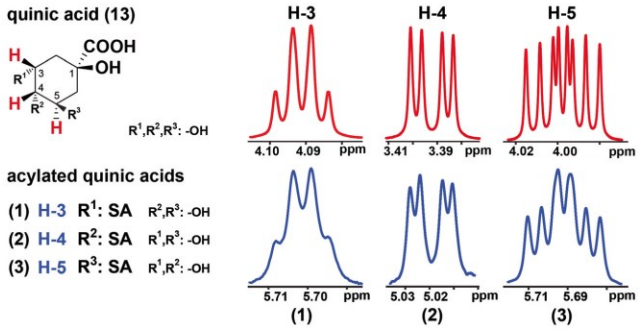

Fig. 2 ^{1}H NMR signals illustrating identical multiplicities and coupling constants of H-3, H-4 and H-5 of (−)-quinic acid (**13**) (red) compared to the corresponding ^{1}H NMR signals of acylated compounds **1**–**3** (blue), shifted to the low field. Full spectra are given in the Supplementary data.

5 showed signals assignable to a symmetrical 5-spin system (AA'XX'Y) at δ_H 8.06 ($^3J_{HH}$ = 1.2/8.3 Hz, H-2′/6′), δ_H 7.47 ($^3J_{HH}$ = 7.4/8.3 Hz, H-3′/5′) and δ_H 7.59 ($^3J_{HH}$ = 7.4/7.4 Hz, H-4′); these signals are characteristic of a mono-substituted aromatic ring. Corresponding ^{13}C chemicals shifts were extracted from the ^{1}H-^{13}C HSQC spectrum at δ_C 130.5 (C-2′/6′), δ_C 129.4 (C-3′/5′) and δ_C 134.1 (C-4′). The aromatic ring structure was further determined by $^3J_{CH}$ correlations in the ^{1}H-^{13}C HMBC spectrum from H-3′/5′ (δ_H 7.47) to a quaternary carbon atom at δ_C 131.6 (C-1′). Another long-range CH-correlation of H-2′/6′ (δ_H 8.06) to a carboxyl carbon atom at δ_C 168.1 (C-7′) tethered to the C-1′ position of the aromatic ring was observed in the HMBC spectrum, confirming the benzoyl moiety. Substitution to the quinic acid moiety was determined by the characteristic low-field shift of the signal of H-5 (δ_H 5.52), indicating substitution at the hydroxyl group at position 5 (δ_C 73.3; δ_H 5.52). Accordingly, the structure of compound **5** was assigned as 5-*O*-benzoyl quinic acid.

The HRESIMS data of compound **6** showed a molecular ion peak of *m/z* 431.0986 [M-H]$^-$, corresponding to a molecular formula of $C_{21}H_{20}O_{10}$ (calcd for $C_{21}H_{19}O_{10}$, *m/z* 431.0984). The ^{1}H NMR, ^{1}H-^{1}H COSY, ^{1}H-^{13}C HSQC and the ^{1}H-^{13}C HMBC spectra of compound **6** (Table 2) showed signals of a quinic acid as well as 2 salicyloyl moieties. The ^{1}H NMR spectra showed characteristic low-field shifts for H-3 (δ_H 5.95) and H-4 (δ_H 5.28), suggesting a bis-substituted quinate. Due to overlapping signals, selective TOCSY together with ^{1}H-^{1}H COSY and ^{1}H-^{13}C HSQC were employed to extract the chemical shifts of both salicyloyl moieties. Connectivities between quinate and salicyloyl moieties were established by ^{1}H-^{13}C long-range correlations of H-3 to δ_C 169.3 (C-7′) and of H-4 to δ_C 170.6 (C-7″), both characterized as carboxyl carbons of the respective salicyloyl units. Accordingly, the structure of compound **6** was assigned as 3-*O*,4-*O*-disalicyloyl quinic acid.

The HRESIMS spectra of compounds **7** and **8** showed molecular ion peaks of *m/z* 431.0985 [M-H]$^-$ and 431.0987 [M-H]$^-$, respectively. As in compound **6**, both values corresponded to a molecular formula of $C_{21}H_{20}O_{10}$ (calcd for $C_{21}H_{19}O_{10}$, *m/z* 431.0984). ^{1}H NMR, ^{1}H-^{1}H COSY, ^{1}H-^{13}C HSQC and the ^{1}H-^{13}C HMBC spectra showed almost the same signals (Table 2), indicating quinic acid esters with salicyloyl moieties as substituents. The structures were characterized by ^{1}H-^{13}C long-range correlations as well as the characteristic chemical shifts of ^{1}H NMR signals for H-3, H-4 and H-5. For compound **7**, we observed low-field shifts for H-3 (δ_H 5.708) and H-5 (δ_H 5.712), suggesting acylation at this positions. The assumption was proven by $^3J_{CH}$ correlations of H-3 to δ_C 169.8 (C-7′) and of H-5 to δ_C 170.3 (C-7″), indicating C-7′ and C-7″ as carboxyl carbons of 2 different salicyloyl moieties. Likewise, for compound **8**, we observed low-field shifts for H-4 at δ_H 5.42, which further showed a $^3J_{CH}$ correlation to δ_C 170.5 (C-7′). The ^{1}H NMR signal of H-5 appeared at δ_H 5.95 with a $^3J_{CH}$ correlation to δ_C 170.4 (C-7″). Accordingly, the structures of the compounds **7** and **8** were assigned as 3-*O*,5-*O*-disalicyloyl quinic acid and 4-*O*,5-*O*-disalicyloyl quinic acid, respectively.

The HRESIMS spectra of compound **9** showed a molecular ion peak of *m/z* 415.1038 [M-H]$^-$ corresponding to a molecular formula of $C_{21}H_{20}O_9$ (calcd for $C_{21}H_{19}O_9$, *m/z* 415.1035). The NMR data (Table 3) extracted from the ^{1}H NMR, ^{1}H-^{1}H COSY, ^{1}H-^{13}C HSQC and the ^{1}H-^{13}C HMBC spectra were very similar to those of compounds **1** and **6**. Accordingly, the presence of a salicyloyl quinate unit was suggested. Furthermore, signals of a benzoyl moiety as described for compound **4** were observed as a substituent of quinic acid. The ^{1}H NMR spectra showed characteristic low-field shifts for H-3 (δ_H 5.93) and H-4 (δ_H 5.22), suggesting substitution at those positions. Cross-signals observed in the ^{1}H-^{13}C HMBC between H-3 and the carboxylic carbon atom C-7′ (δ_C 169.5) of the salicyloyl moiety proved the substitution in position C-3 of the quinic acid via an ester bond. An additional $^3J_{CH}$ correlation of H-4 to the carboxylic carbon atom C-7″ (δ_C 167.2) of the benzoyl moiety revealed another esterification. Accordingly, the structure of compound **9** was assigned as 3-*O*-salicyloyl-4-*O*-benzoyl quinic acid.

Like the data for compound **9**, the HRESIMS data for compounds **10** and **11** showed a molecular ion peak of 415.1038 $[M\text{-}H]^-$ corresponding to a molecular formula of $C_{21}H_{20}O_9$ (calcd for $C_{21}H_{19}O_9$, *m/z* 415.1035). The NMR data for both compounds (Table 3) were very similar to those of **9**, suggesting acylated quinic acid derivatives with mixed salicyloyl and benzoyl substituents. The structures of compounds **10** and **11** were elucidated by characteristic ^{1}H NMR chemical shifts and ^{1}H-^{13}C long-range correlations as described for compounds **6**–**8**. For compound **10**, substitution with a salicyloyl group in position 3 (δ_C 74.4; δ_H 5.71) and with the benzoyl unit in position 5 (δ_C 72.9; δ_H 5.56) of the quinic acid was observed. For compound **11**, salicyloyl substitution was observed at position 4 (δ_C 77.6; δ_H 5.41), and benzoylation was found at position 5 (δ_C 69.8; δ_H 5.91) of the quinic acid moiety. Accordingly, the structures were assigned as 3-*O*-salicyloyl-5-*O*-benzoyl quinic acid (**10**) and 4-*O*-salicyloyl-5-*O*-benzoyl quinic acid (**11**).

Hemolymph Analysis Hemolymph samples of 6 *C. vinula* larvae were analyzed by UHPLC-ESI-MS/MS. Mass spectra were scanned for the presence of the molecular ions of compounds **1**–**11** (*m/z* 311, 295, 431, 415 ± 0.5 $[M\text{-}H]^-$) as well as for the molecular ions of salicortin (**12**, *m/z* 424 ± 0.5 $[M\text{-}H]^-$) and salicin (*m/z* 285 ± 0.5 $[M\text{-}H]^-$). None of these compounds were detected. Data are provided in Supplementary data (SI D.1 and D.2).

^{13}C-Labeling Study In order to investigate a possible precursor-product relationship of salicortin with the metabolites **1**–**11**, leaves of *P. nigra* were spotted with [U-^{13}C]salicortin (82% ^{13}C), as described in the Methods and Materials section (2.5), and subsequently fed to *C. vinula* larvae. The frass of larvae were extracted and analyzed by NMR and UHPLC-HRMS (see Supplementary data, C.2 and C.3). All larvae survived the feeding experiment without exhibiting negative effects arising from an elevated salicortin intake.

The ^{13}C NMR spectrum of the frass extract from the [U-^{13}C]salicortin feeding experiment showed signals characteristic for compounds **1**–**11**. Pronounced ^{13}C satellites appeared for signals of salicylates around δ_C 170, δ_C 165 and δ_C 135–130. No ^{13}C enrichment was found for glucosyl or quinate moieties (SI C.2–1 to C.2–5). Further structure elucidation was accomplished by 2D ^{1}H-^{13}C correlation spectroscopy. ^{1}H-^{13}C HSQC allowed for the identification of protons attached to the ^{13}C-enriched positions. The associated spin systems were assigned by selective TOCSY experiments to δ_H 7.93 (dd, $^3J_{HH}$ = 1.8/8.0 Hz)/δ_C 131.0, δ_H 7.98 (dd, $^3J_{HH}$ = 1.9/8.0 Hz)/δ_C 131.7 and δ_H 8.04 ($^3J_{HH}$ = 1.8/8.0 Hz)/δ_C 131.3, corresponding to salicylic acid moieties such as those observed for compounds **1**–**3** and **6**–**11**. The ^{1}H-^{13}C HMBC spectrum showed correlations of the salicylic acid moiety protons at δ_H 7.93 (δ_C 131.0; C-6), δ_H 7.98 (δ_C 131.6; C-6) and δ_H 8.04 (δ_C 131.3; C-6), with carbon atoms resonating at δ_C 136.7/136.5/136.2 (C-4), δ_C 162.1/162.8 (C-2) and δ_C 171.0/171.2/171.5 (C-7; COOH). ^{13}C-^{13}C Satellite signals for all those carbon signals indicated multiple ^{13}C enrichment of the salicyloyl moieties.

No ^{13}C-^{13}C satellites were observed in the ^{13}C NMR spectra and thus no ^{13}C enrichment occurred in the benzoyl units. The low intensity of the ^{1}H-^{13}C HMBC correlations of the benzoyl protons at δ_H 8.09 (δ_C 130.5; C-2/6) and δ_H 8.13 (δ_C 130.6; C-2/6) with δ_C 134.0 (C-4) and δ_C 168.1 (C-7; COOH) (Fig. 3 and SI C.2–6 to C.2–17) confirmed that the benzoyl units remained unlabeled.

Furthermore, UHPLC-HRMS spectra of the frass extract of *C. vinula* larvae fed with [U-^{13}C]salicortin showed ^{13}C-isotopologue patterns from $[M\text{-}H + 3]^-$ up to $[M\text{-}H + 7]^-$ (Fig. 4; C.3–1 to C.3–23). Remarkably, only salicylate-containing quinate esters, mono-salicyloyl quinates **1**–**3**, di-salicyloyl quinates **6**–**8** and salicyloyl-benzoyl quinates **9**–**11**, were labeled, and benzoyl quinates **4** and **5** showed no ^{13}C enrichment. The incorporation of ^{13}C from [U-^{13}C]salicortin into the salicyloyl moiety of the acylated quinic acids **1**–**3** and **6**–**11** clearly indicated a substrate-product relationship. Accordingly, we concluded that the acylated quinic acids were downstream products of the salicortin metabolism in *C. vinula*.

Another 7 (up to $[M\text{-}H + 14]^-$) isotopologue peaks are present in the spectra of di-salicyloyl quinates **6**–**8**. The $[M\text{-}H + 8]^-$ peak may be due to the presence of a natural abundance $^{13}C_1$ quinate or a $^{13}C_1$ salicyloyl substituent, in addition to the $^{13}C_7$-labeled first salicyloyl unit.

Discussion

The chemical defense of poplar includes abundant phenolic glycosides, such as salicortin and tremulacin, which can make up to 4% of the leaf dry mass (Boeckler et al. 2011; Donaldson et al. 2006). It is widely accepted that the digestive activation of salicinoids leads to toxic products warding off non-adapted herbivores. For salicortin, it has been proposed that activation proceeds through deglucosylation by β-glucosidases (Clausen et al. 1990; Lindroth 1988; Pentzold et al. 2014). The aglycon is either hydrolyzed spontaneously in the alkaline gut environment or degraded enzymatically by insect esterases (Lindroth et al. 1988; Lindroth 1989) to saligenin and a 1-hydroxy-6-oxocyclohex-2-en-1-oyl (HCH) fragment (Haruta et al. 2001; Julkunen-Tiitto and Meier 1992). The latter is believed to be oxidized to pyrocatechol and finally to *o*-quinone (Appel 1993; Barbehenn et al. 2010; Knuth et al. 2011; Ruuhola et al. 2003). *o*-Quinones have a high potential to bind to a variety of biomolecules, including amino acids and proteins (Haruta et al. 2001; Smith 1985). Generalist lepidopteran

species, such as the gypsy moth (*L. dispar*), have developed a strategy of detoxification (Boeckler et al. 2016) where the major salicinoids in *P. nigra*, salicortin and tremulacin, are transformed into typical metabolic phase II conjugates (Grant 1991), with salicin as the major metabolite (Boeckler et al. 2016).

The compounds **1**–**11** described in the present work are new quinic acid derivatives, isolated from the frass of *C. vinula*. The quinic acid moiety is substituted with either 1 or 2 salicylate units (**1**–**3**, **6**–**8**), benzoate units (**4**, **5**) or one of each unit (**9**–**11**). Compound **4** is the only compound that has been previously reported, namely as a constituent of fruits of *Ficus hirta* (Wan 2016). The results show that conjugation with quinic acid plays a decisive role in the transformation of salicinoids by *C. vinula*. The conjugation with quinic acids is described here for the first time as part of a detoxification pathway. Quinic acid has been reported to play a role in response to herbivory (Wang et al. 2016), and quinic acids were detected in the gut of insects (Crecelius et al. 2017). It was also suggested that quinic acid conjugates like chlorogenic acid produce feeding-deterrent compounds after cleavage and oxidative transformation of the phenylpropanoic part (Stevenson et al. 1993). The latter aspect needs to be clarified in the present example, and experiments addressing the question are ongoing.

Unlike in *L. dispar*, deglycosylation is an important feature of the metabolism in *C. vinula*, as glycosidic compounds or free sugars are absent in the frass extract. Generally, the salicinoid breakdown follows reported routes like deglucosylation, ester cleavage and conjugation (Clausen et al. 1990; Lindroth 1988; Pentzold et al. 2014). The structural diversity of the compounds – namely, the differential substitution of quinic acid with salicylate or benzoate – can be rationalized by acyl migration under basic conditions as present in the insect gut (Appel and Martin 1990). An enzymatic and hence stereospecific conjugation with quinic acid may take place at first, but those products rapidly isomerize later on. Another metabolite present after salicinoid degradation in *L. dispar*, hippuric acid, was absent in the [^{13}C]-metabolite spectrum of *C. vinula*. We can therefore conclude that hippuric acid is not a degradation product of salicortin, but arises likely from benzoyl-substituted structures like tremulacin.

The question of whether the source of salicyloyl units in quinic acid derivatives **1**–**11** were indeed salicinoid glycosides was tackled by stable isotope labeling experiments. *C. vinula* larvae were allowed to feed on leaves of *P. nigra* spotted with [U-^{13}C]salicortin (82% ^{13}C). Frass extracts were analyzed by means of NMR and HRMS. The resulting data were screened for isotopic incorporation into **1**–**11**. The isotopologue pattern of both NMR and HRMS spectra indicated differences in the incorporation of labeled salicortin into mono-salicyloyl quinic acids (**1**–**3**), mono-benzoyl quinic acids (**4**, **5**), bis-salicyloyl quinic acids (**6**–**8**) and salicyloyl-benzoyl quinic acids (**9**–**11**). NMR data showed enrichment of ^{13}C only in the salicyloyl moiety of quinic acid derivatives (Fig. 3). ^{13}C enrichment was further supported by HRMS data (Fig. 4) which showed a specific isotopologue pattern spanning from $[M\text{-}H]^-$ to $[M\text{-}H+7]^-$ for **1**–**3**. The HRMS spectra of **4** and **5** did not show additional ^{13}C-isotopologue signals. Thus, neither quinic acid nor benzoyl moieties is thought to represent a downstream product of the [U-^{13}C]salicortin precursor. This suggestion was further reflected in the HRMS data of **6**–**11**. Whereas mixed salicyloyl-benzoyl

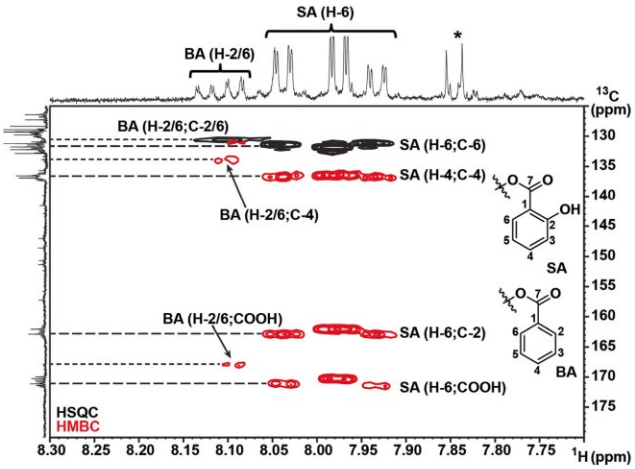

Fig. 3 Superimposed ^{1}H-^{13}C HSQC (black) and HMBC spectra (red) (500 MHz, MeOH-d_4) of *C. vinula* frass extract demonstrating ^{13}C enrichment of salicyloyl (SA) units but not of benzoyl (BA) units from [U-^{13}C]salicortin feeding. Top: Partial ^{1}H NMR spectrum showing signals of BA and SA. In the ^{13}C NMR spectrum (125 MHz) on the left, resonances of salicyloyl substituents show coupling patterns indicative of ^{13}C-enrichment. Cross-signals of * are not shown

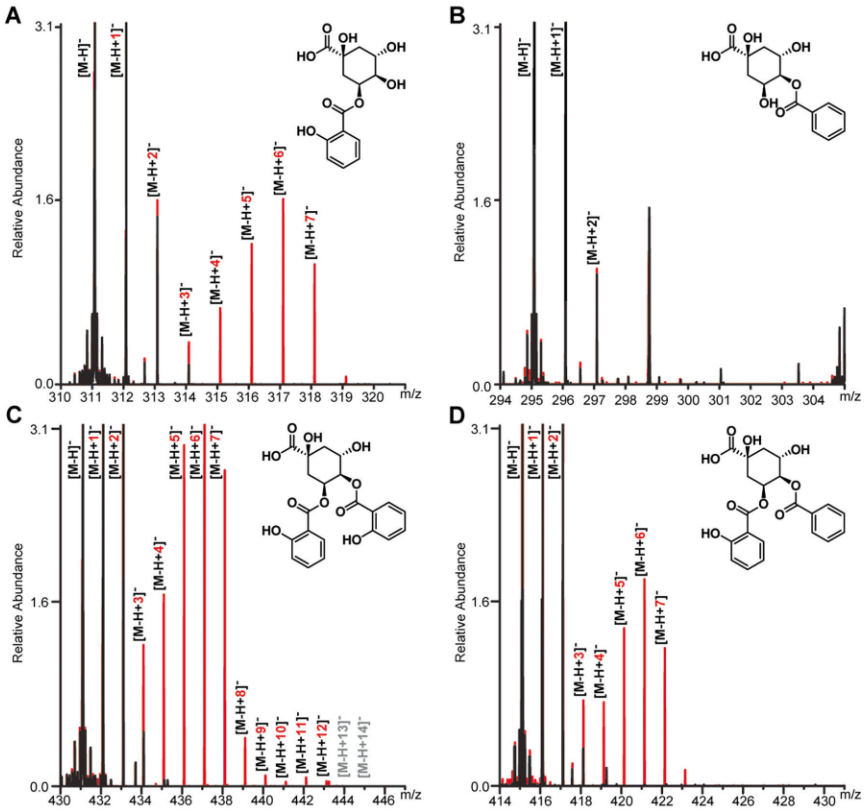

Fig. 4 Superimposed extracted ion HRMS spectra of the 4 acylated quinic acid groups – mono-salicyloyl quinates, mono-benzoyl quinates, di-salicyloyl quinates and salicyloyl-benzoyl quinates – isolated from the frass of *C. vinula* larva reared on [U-^{13}C]salicortin-coated *P. nigra* leaves (red) and unlabeled leaves (black). The groups are represented by compounds **1** (**A**), **4** (**B**), **6** (**C**) and **9** (**D**). The gray labeled isotopologue signals in panel **C** are very weak and thus not visible in this magnification

substituted compounds show only isotopologue signals up to $[M\text{-}H + 7]^-$, the bis-salicyloyl derivatives show signals up to $[M\text{-}H + 14]^-$.

Accordingly, this finding is a clear evidence that saligenin is transformed into salicylic acid. We assume that structurally similar salicinoids are transformed in an analogous manner. No ^{13}C incorporation was detected in the quinic acid moieties of **1–11**. Therefore, quinic acids likely originate from chlorogenic acids (caffeoyl quinates), which have already been described as leaf constituents of the Salicaceae (Caseys et al. 2015; Glynn et al. 2004). Considering the metabolic scheme in Fig. 5, it is important to note that there seems to be only one specific oxidative transformation of saligenin into salicylic acid in *C. vinula*. Likely, this specificity prevents the caffeoyl moiety of chlorogenic acid to be transformed into a toxic species (Felton et al. 1989) and facilitates quinic acids to scavenge the phenolic degradation products.

In our search for break-down products related to the HCH-moiety of salicortin, we did not find any further ^{13}C-labeled compound. Therefore, we speculate that there is a mechanism by which HCH degradation yields salicylic acid (Fig. 5). Under basic conditions, the HCH fragment could rearrange to an HCH-enolate followed by a spontaneous dehydration to form salicylic acid. The feasibility of such a transformation was observed in synthetic studies (Nagasawa et al. 2010). The origin of benzoyl substituents in **4**, **5**, **9**, **10** and **11** are likely common Salicaceae leaf constituents, such as chaenomeloidin, nigracin, populin, salireposid, tremulacin or tremuloidin (Boeckler et al. 2011).

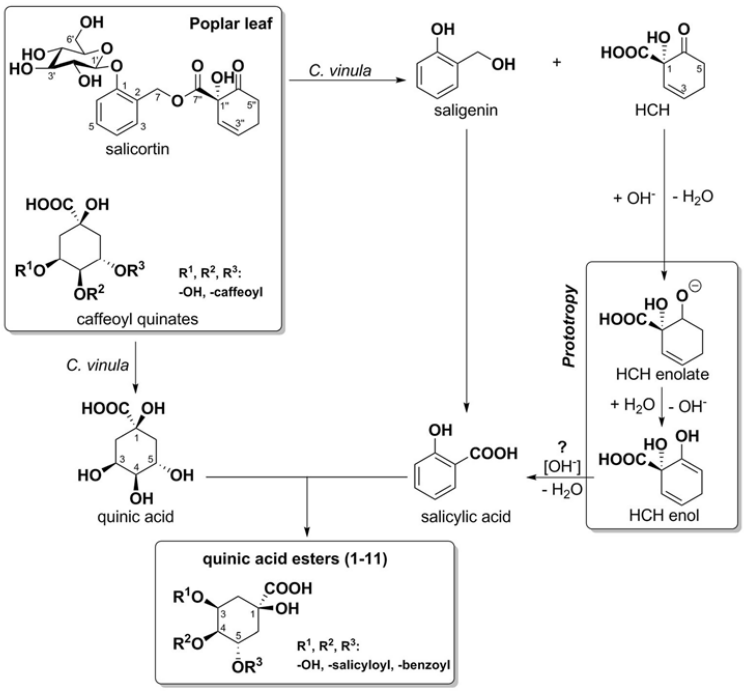

Fig. 5 Conversion of *Populus* leaf constituents to acylated quinic acid derivatives in the *C. vinula* larval gut

Acknowledgements Open access funding provided by Max Planck Society. The authors thank the workshop and IT-teams of the Max Planck Institute for Chemical Ecology for constructive cooperation, the greenhouse team for rearing the *Populus beaupré* trees, Regina Seibt for establishing the *C. vinula* breeding at our institute and Emily Wheeler for polishing the language.

References

Ali JG, Agrawal AA (2012) Specialist versus generalist insect herbivores and plant defense. Trends Plant Sci 17:293–302

Appel HM (1993) Phenolics in ecological interactions: the importance of oxidation. J Chem Ecol 19:1521–1552

Appel HM, Martin MM (1990) Gut redox conditions in herbivorous lepidopteran larvae. J Chem Ecol 16:3277–3290

Barbehenn R, Dukatz C, Holt C, Reese A, Martiskainen O, Salminen J-P, Yip L, Tran L, Constabel CP (2010) Feeding on poplar leaves by caterpillars potentiates foliar peroxidase action in their guts and increases plant resistance. Oecologia 164:993–1004

Beran F, Pauchet Y, Kunert G, Reichelt M, Wielsch N, Vogel H, Reinecke A, Svatoš A, Mewis I, Schmid D, Ramasamy S, Ulrichs C, Hansson BS, Gershenzon J, Heckel DG (2014) *Phyllotreta striolata* flea beetles utilize host plant defense compounds to create their own glucosinolate-myrosinase system. Proc Natl Acad Sci U S A 111:7349–7354

Boeckler GA, Gershenzon J, Unsicker SB (2011) Phenolic glycosides of the salicaceae and their role as anti-herbivore defenses. Phytochemistry 72:1497–1509

Boeckler GA, Paetz C, Feibicke P, Gershenzon J, Unsicker SB (2016) Metabolism of poplar salicinoids by the generalist herbivore *Lymantria dispar* (Lepidoptera). Insect Biochem Mol Biol 78:39–49

Burse A, Frick S, Discher S, Tolzin-Banasch K, Kirsch R, Strauß A, Kunert M, Boland W (2009) Always being well prepared for defense: the production of deterrents by juvenile *Chrysomelina* beetles (Chrysomelidae). Phytochemistry 70:1899–1909

Caseys C, Stritt C, Glauser G, Blanchard T, Lexer C (2015) Effects of hybridization and evolutionary constraints on secondary metabolites: the genetic architecture of phenylpropanoids in European *Populus* species. PLoS One 10:23

Chen W-P, Yang X-Y, Harms GL, Gray WM, Hegeman AD, Cohen JD (2011) An automated growth enclosure for metabolic labeling of *Arabidopsis thaliana* with ^{13}C-carbon dioxide - an *in vivo* labeling system for proteomics and metabolomics research. Proteome Sci 9:9

Clausen TP, Reichardt PB, Bryant JP, Werner RA, Post K, Frisby K (1989) Chemical model for short-term induction in quaking aspen (*Populus tremuloides*) foliage against herbivores. J Chem Ecol 15:2335–2346

Clausen TP, Koller JW, Reichardt PB (1990) Aglycone fragmentation accompanies β-glucosidase catalyzed hydrolysis of salicortin, a

Curriculum vitae

Dipl. Chem. Felix Feistel

Biosynthesis/NMR Research Group

Max Planck Institute for Chemical Ecology, Hans-Knöll-Straße 8, 07745 Jena

Education

Okt. 2007 − Apr. 2014	studies Dipl. Chemie/ Umweltchemie, Friedrich-Schiller-Universität Jena, Jena, Germany degree: Diploma Chemist, 17.04.2014
since Mai 2014	Ph.D student, Friedrich-Schiller-Universität Jena, Jena, Germany

Research experience

Diploma thesis	"Generation and Chemical Characterization of ^{13}C-enriched Salicinoids from Poplar (*Populus trichocarpa x deltoides*)" Supervisors: Prof. Georg Pohnert, Dr. Bernd Schneider, Dr. Christian Paetz
Ph.D thesis	*"*Structural investigations on Salicaceae derived salicylates and their metabolic transformation in the lepidopteran herbivore *Cerura vinula"* Supervisors: Prof. Georg Pohnert, Dr. Bernd Schneider, Dr. Christian Paetz

Publications record

1. **Feistel, F.**, Paetz, C., Menezes R.C., Veit D., Schneider, B. (2017). Acylated quinic acids are the main salicortin metabolites in the specialist herbivore *Cerura vinula*. Submitted to Journal of Chemical Ecology December 2017
2. **Feistel, F.**, Paetz, C., Lorenz, S., Beran, F., Kunert, G., Schneider, B. (2017). Idesia polycarpa (Salicaceae) leaf constituents and their toxic effect on Cerura vinula and Lymantria dispar (Lepidoptera) larvae. Phytochemistry, 143, 170-179.
3. Paetz, C., Hammerbacher, A., Menezes, R. C., **Feistel, F.**, Weigel, C., Voigt, K., Schneider, B. (2016). Chemical composition and antimicrobial activity of *Populus nigra* shoot resin. Natural Product Communications, 11(7), 989-992.
4. **Feistel, F.**, Paetz, C., Lorenz, S., Schneider, B. (2015). The absolute configuration of salicortin, HCH-salicortin and tremulacin from Populus trichocarpa × deltoides Beaupré. Molecules, 20, 5566-5573

Oral presentations

1. **Feistel F.** (2017). Detoxification of salicortin in the specialist herbivore *Cerura vinula*. Talk presented at 16th IMPRS Symposium, International Max Planck Research School, Dornburg, Germany
2. **Feistel. F.** (2016). The detoxification strategy of the puss moth (Cerura vinula). Talk presented at Postgraduate workshop of the section „ Natural Products “, German Society for Plant Sciences (DBG), Meisdorf, Germany

Poster presentations

1. **Feistel F.**, Paetz C., Schneider B., Veit D., Seibt R., Menezes R.C. (2016). Detoxification of salicortin in the specialist herbivore Cerura vinula. Poster presented at SAB Meeting 2016, MPI for Chemical Ecology, Jena, Germany

2. **Feistel F.**, Paetz C., Schneider B., Seibt R., Menezes R.C. (2015). Detoxification of 6-HCH-salicinoids in the specialist herbivore Cerura vinula. Poster presented at ICE Symposium, MPI for Chemical Ecology, Jena, Germany
3. **Feistel F.**, Paetz C., Lorenz S., Schneider B. (2015). The absolute configuration of salicortin, HCH-salicortin and tremulacin from *Populus trichocarpa x deltoides* Beaupré. Poster presented at 14th IMPRS Symposium, MPI for Chemical Ecology, Dornburg, Germany
4. **Feistel F.**, Paetz C., Schneider B. (2013). Isolation and Characterization of 13C-enriched Salicinoids from Poplar. Poster presented at ICE Symposium, MPI for Chemical Ecology, Jena, Germany
5. **Feistel F.**, Paetz C., Schneider B., Boeckler A., Unsicker S., Gershenzon J. (2012). A mobile low-cost setup for isotopic carbon labeling experiments. Poster presented at SAB Meeting 2012, MPI for Chemical Ecology, Jena, Germany

Erklärung zu den Eigenanteilen an den Publikationen

Publication: Feistel, F., Paetz, C., Lorenz, S. Schneider, B. , The absolute configuration of salicortin, HCH-salicortin and tremulacin from *Populus trichocarpa x deltoides* Beaupre. Molecules, 2015. **20**(4): p. 5566-73.				
Participation				
	Author 1: Felix Feistel	**Author 2**: Christian Paetz	**Author 3:** Sybille Lorenz	**Author 4:** Bernd Schneider
Conception & Strategy	x	x		
Extraction & Isolation	x			
Collection of Data **CD** **NMR** **HRESIMS**	x	x	x	
Data Assessment and Discussion	x	x		
Manuscript	x	x		x
Proposed Publication Äquivalents	**1.0**			

Publication: Feistel, F., Paetz, C., Lorenz, S., Beran, F., Kunert, G., Schneider, B. , *Idesia polycarpa* (Salicaceae) leaf constituents and their toxic effect on *Cerura vinula* and *Lymantria dispar* (Lepidoptera) larvae. Phytochemistry, 2017. **143**: p. 170-179.						
Participation						
	Author 1: Felix Feistel	**Author 2**: Christian Paetz	**Author 3:** Sybille Lorenz	**Author 4:** Franziska Beran	**Author 5:** Grit Kunert	**Author 6:** Bernd Schneider
Conception & Strategy	x	x				
Extraction & Isolation	x					
Collection of Data **CD** **NMR** **HRESIMS** **GCMS** **Feeding Assays**	x x x x x	x	x	x		
Structrue elucidation	x	x				
Statistics					x	
Data Assessment and Discussion	x	x				
Manuscript	x	x				x
Proposed Publication Äquivalents	**1.0**					

Publication: Feistel, F., Patz, C., Menezes, R.C. Veit, D., Schneider, B. , Acylated quinic acid esters are the main salicortin metabolites in the specialist herbivore *C. vinula*. Submitted to Journal of Chemical Ecology December 2017					
Participation					
	Author 1: Felix Feistel	**Author 2:** Christian Paetz	**Author 3:** Riya C. Menezes	**Author 4:** Daniel Veit	**Author 5:** Bernd Schneider
Conception & Strategy	x	x			
Extraction & Isolation	x				
Collection of Data **NMR** **ESIMS** **HRESIMS**	 x x	x	 x		
Development and Construction of the $^{13}CO_2$ labeling Setup	x			x	
^{13}C precursor Generation, Isolation and Feeding	x				
Data Assessment and Discussion	x	x			
Manuscript	x	x			x
Proposed Publication Äquivalents	**1.0**				

Erklärung zu den Eigenanteilen des Promovenden/ der Promovendin sowie der weiteren Doktoranden/Doktorandinnen als Koautoren an den Publikationen und Zweitpublikationsrechten bei einer kumulativen Dissertation

Für alle in dieser kumulativen Dissertation verwendeten Manuskripte liegen die notwendigen Genehmigungen der Verlage („Reprint permissions“) für die Zweitpublikation vor.

Die Co-Autoren der in dieser kumulativen Dissertation verwendeten Manuskripte sind sowohl über die Nutzung, als auch über die oben angegebenen Eigenanteile der weiteren Doktoranden/ Doktorandinnen als Koautoren an den Publikationen und Zweitpublikationsrechten bei einer kumulativen Dissertation informiert und stimmen dem zu.

Die Anteile des Promovenden sowie der Doktoranden/ Doktorandinnen als Koautoren an den Publikationen und Zweitpublikationsrechten bei einer kumulativen Dissertation sind in der Anlage aufgeführt.

Name des Promovenden Datum Ort Unterschrift

Ich bin mit der Abfassung der Dissertation als publikationsbasiert, d.h. kumulativ, einverstanden und bestätige die vorstehenden Angaben. Eine entsprechend begründete Befürwortung mit Angabe des wissenschaftlichen Anteils des Doktoranden an den verwendeten Publikationen werde ich parallel an den Rat der Fakultät der Chemisch-Geowissenschaftlichen Fakultät richten.

Name Erstbetreuer Datum Ort Unterschrift

Name Zweitbetreuer Datum Ort Unterschrift

Erklärung der Promotionsordnung

Ich erkläre,

dass mir die geltende Promotionsordnung der Fakultät bekannt ist;

dass ich die Dissertation selbst angefertigt, keine Textabschnitte eines Dritten oder eigener Prüfungsarbeiten ohne Kennzeichnung übernommen und alle von mir benutzten Hilfsmittel, persönlichen Mitteilungen und Quellen in meiner Arbeit angegeben habe;

dass mich folgende Personen bei der Auswahl und Auswertung des Materials sowie bei der Herstellung des Manuskripts unterstützt haben: Dr. Bernd Schneider, Dr. Christian Paetz, Sybille Lorenz, Dr. Grit Kunert, Dr. Franziska Beran, Daniel Veit, Dr. Riya C. Menezes, Theresa Sporer, Regina Seibt, Dr. Sybille Unsicker, Emily Wheeler, Linda Maak

dass die Hilfe eines Promotionsberaters nicht in Anspruch genommen wurde und dass Dritte weder unmittelbar noch mittelbar geldwerte Leistungen von mir für Arbeiten erhalten haben, die im Zusammenhang mit dem Inhalt der vorgelegten Dissertation stehen;

dass ich die Dissertation noch nicht als Prüfungsarbeit für eine staatliche oder andere wissenschaftliche Prüfung eingereicht habe,

dass ich nicht die gleiche, eine in wesentlichen Teilen ähnliche oder eine andere Abhandlung bei einer anderen Hochschule als Dissertation eingereicht habe.

Ort, Datum, Unterschrift

Danksagung

An erster Stelle gilt mein besonderer Dank meinen Gutachtern Prof. Dr. Georg Pohnert und PD Dr. Bernd Schneider für ihre ausgezeichnete wissenschaftliche Betreuung und Diskussionsbereitschaft.

Ich danke der Max-Planck-Gesellschaft für die finanzielle Unterstützung meines Projektes in der Arbeitsgruppe NMR/ Biosynthese am Max-Planck-Institut für chemische Ökologie.

Ganz besonders möchte ich mich bei Dr. Christian Paetz für die intenisve wissentschaftliche Betreuung mit vielen guten Ratschlägen sowie die fruchtbare Zusammenarbeit über die letzten Jahre hinweg bedanken.

Desweiteren bedanke ich mich bei ...

... den Koorperationspartnern, die bei der Durchführung, Auswertung oder Messung an den einzelnen Manuskripten mitgewirkt haben: Dr. Grit Kunert, Dr. Franziska Beran, Dr. Riya C. Menezes, Sybille Lorenz

... allen ehemaligen und jetztigen Mitgliedern der Arbeitsgruppe NMR/ Biosynthese am Max-Planck-Institut für chemische Ökologie, darunter Dr. William F. H. Buchelli, Dr. Monica Scognamiglio, Dr. Fernanda M. M. Ocampus, Bettina Dudek, Dr. Jima Chandran, Dr. Yu Chen, Dr. Renate Ellinger, Kati Barthold für ihre Unterstützung und die angenehme Arbeitsatmosphäre. Einen besonderen Dank möchte ich gegenüber Dr. Anne-Christin Warskulat für die vielen anregenden Diskussionen, die mir seit 2011 bis hin zur Fertigstellung dieser Arbeit sehr geholfen haben.

... dem Gewächshausteam des Max-Planck-Institutes für chemische Ökologie, insbesondere Dr. Tamara Krügel, Dr. Danny Kessler, Birgit Arnold und Andreas Weber für die gute Zusammenarbeit sowie die ständige Pflege der Pappel- und Idesiabäume, ohne die dieses Projekt nicht möglich gewesen wäre.

... dem Werkstattteam des Max-Planck-Institutes für chemische Ökologie ohne deren Know-How die technische Konstruktion der Labelingkammer nicht möglich gewesen wäre. Besonderer dank gilt hierbei Daniel Veit für seinen außerordentlichen Einsatzwillen sowie die unkomplizierte und fruchtbare Zusammenabeit.

... Regina Seibt für ihre Untersützung bei der Etablierung der *C. vinula* Zucht.

... Dr. Sybille Unsicker für das Überlassen der *L. dispar* Raupen für die Fütterungsversuche.

... Theresa Sporer für die Sektion der *C. vinula* Raupen sowie Verena Jeschke für die hilfreichen Tipps zum Sammeln der Hemolymphe.

... Emily Wheeler für die Sprachkorrekturarbeiten an den Manskripten und der Dissertation.

... Linda Maack für ihre Hilfe bei der Beschaffung von Literaturstellen und der Beratung berzüglich der Verwalten meiner Literaturbibliothek.

... den Mitgliedern der Arbeitsgruppe Mass Spectrometry/ Proteomics für angenehme und hilfreiche wissenschaftliche Diskussionen.

Abschließend danke ich ausdrücklich meiner Familie und meinen Freunden, die mich während der gesamten Promotionsphase sowie darüber hinaus auf vielfältige Weise unterstützt haben.

Eigenständigkeitserklärung

Ich erkläre, dass ich die vorliegende Arbeit selbständig und unter Verwendung der angegebenen Hilfsmittel, persönlichen Mitteilungen und Quellen angefertigt habe.

Ort, Datum Unterschrift des Verfassers